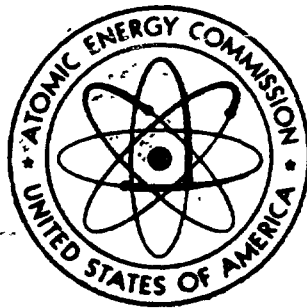


NVO-140  
VOLUME III

5287

# ENEWETAK RADIOLOGICAL SURVEY



OCTOBER 1973

UNITED STATES ATOMIC ENERGY COMMISSION  
NEVADA OPERATIONS OFFICE  
LAS VEGAS, NEVADA

ERDA/ERSP Mgr. EA



NVO-140  
VOLUME III

# ENEWETAK RADIOLOGICAL SURVEY



OCTOBER 1973

UNITED STATES ATOMIC ENERGY COMMISSION  
NEVADA OPERATIONS OFFICE  
LAS VEGAS, NEVADA

## Appendix II - Survey Results by Island

Introduction . . . . .	iii
Map of Enewetak Atoll . . . . .	iv
Cross-reference list of island names . . . . .	v
Individual photomap scale factors . . . . .	vi
Contour map key for use with the EG&G aerial radiological survey figures . . . . .	vii
Survey results, Volume II	B.
ALICE . . . . .	B. 1. 1
BELLE . . . . .	B. 2. 1
CLARA . . . . .	B. 3. 1
DAISY . . . . .	B. 4. 1
EDNA . . . . .	B. 5. 1
IRENE A . . . . .	B. 6. 1
IRENE B . . . . .	B. 7. 1
JANET . . . . .	B. 8. 1
KATE . . . . .	B. 9. 1
LUCY . . . . .	B. 10. 1
PERCY . . . . .	B. 11. 1
MARY . . . . .	B. 12. 1
NANCY . . . . .	B. 13. 1
OLIVE . . . . .	B. 14. 1
PEARL . . . . .	B. 15. 1
RUBY . . . . .	B. 16. 1
SALLY . . . . .	B. 17. 1
TILDA . . . . .	B. 18. 1
URSULA . . . . .	B. 19. 1
VERA . . . . .	B. 20. 1
WILMA . . . . .	B. 21. 1
YVONNE A . . . . .	B. 22. 1
Survey results, Volume III	
YVONNE B . . . . .	B. 23. 1
YVONNE C . . . . .	B. 24. 1
YVONNE D . . . . .	B. 25. 1
YVONNE E . . . . .	B. 26. 1
YVONNE F . . . . .	B. 27. 1

Survey results (continued)

SAM . . . . .	. B. 28. 1
TOM . . . . .	. B. 29. 1
URIAH . . . . .	. B. 30. 1
VAN . . . . .	. B. 31. 1
ALVIN . . . . .	. B. 32. 1
BRUCE . . . . .	. B. 33. 1
CLYDE . . . . .	. B. 34. 1
DAVID . . . . .	. B. 35. 1
REX . . . . .	. B. 36. 1
ELMER A . . . . .	. B. 37. 1
ELMER B . . . . .	. B. 38. 1
ELMER C . . . . .	. B. 39. 1
ELMER D . . . . .	. B. 40. 1
WALT . . . . .	. B. 41. 1
FRED A . . . . .	. B. 42. 1
FRED B . . . . .	. B. 43. 1
FRED C . . . . .	. B. 44. 1
FRED D . . . . .	. B. 45. 1
FRED E . . . . .	. B. 46. 1
FRED F . . . . .	. B. 47. 1
GLENN . . . . .	. B. 48. 1
HENRY . . . . .	. B. 49. 1
IRWIN A . . . . .	. B. 50. 1
IRWIN B . . . . .	. B. 51. 1
JAMES . . . . .	. B. 52. 1
KEITH . . . . .	. B. 53. 1
LEROY . . . . .	. B. 54. 1
Summary of Experimental Data . . . . .	. C.

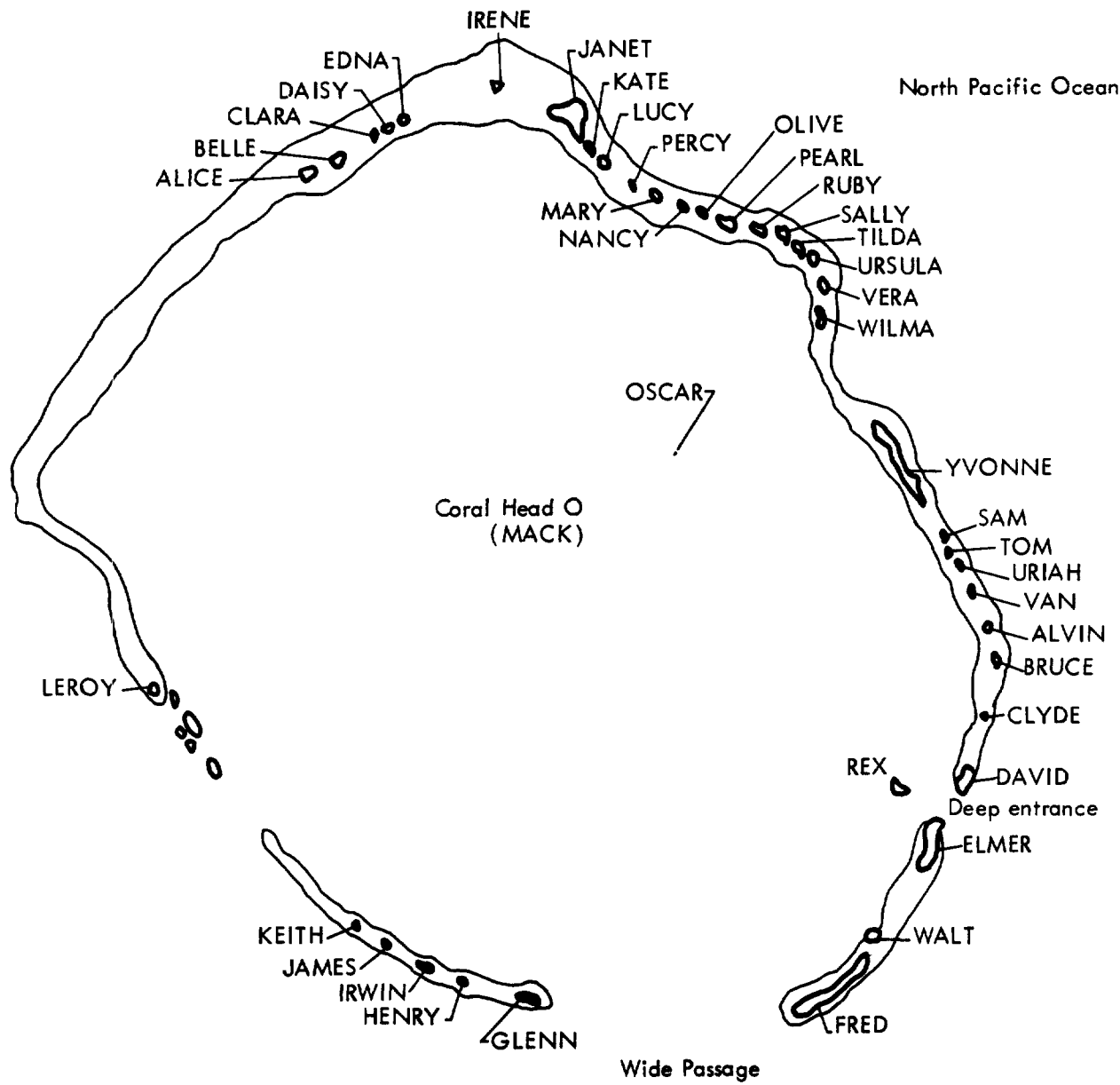
## INTRODUCTION

This appendix is a compilation of radiological survey results for each of the islands in Enewetak Atoll. The information for each island includes a color aerial photograph, a series of photographs overprinted with survey data, and a set of analytical data. It should be noted that several islands (i.e., IRENE, YVONNE, ELMER, FRED, and IRWIN) have been subdivided into sections (e.g., IRENE A and IRENE B) because of their relatively large size. In addition, it should be pointed out that the sets of overprints are not necessarily the same for all islands. Thermoluminescent detectors (TLD's), for example, were not used on all islands. For ease of comparison and clarity, the same data parameter for each island is overprinted on the same color of photograph.

For a discussion of the techniques used in collecting the data presented on the photographic overprints, the reader is referred to the appropriate section in Vol. I of this document.

A typical set of survey results is outlined below for ALICE, together with the page and figure designation scheme used.

	<u>Fig. No.</u>
Current condition . . . . .	
a. Color photograph . . . . .	B. 1. 1a
b. 0-3 MeV EG&G isopleth . . . . .	B. 1. 1b
c. 0-300 keV EG&G isopleth . . . . .	B. 1. 1c
d. Ground measurements with Baird Atomic . . . . .	B. 1. 1d
f. Soil-sampling locations . . . . .	B. 1. 1f
g. Vegetation sampling locations . . . . .	B. 1. 1g
h. TLD locations . . . . .	B. 1. 1h
i. <sup>239</sup> Pu soil content isopleths . . . . .	B. 1. 1i
j. <sup>90</sup> Sr soil content isopleths . . . . .	B. 1. 1j
k. <sup>137</sup> Cs EG&G isopleths . . . . .	B. 1. 1k
l. <sup>137</sup> Cs soil data . . . . .	B. 1. 1l
m. <sup>60</sup> Co EG&G isopleths . . . . .	B. 1. 1m
n. <sup>60</sup> Co soil data . . . . .	B. 1. 1n
o. Animal sampling location . . . . .	B. 1. 1o
Analytical data for soils . . . . .	
a. through m. Soil profile data plots . . . . .	B. 1. 2a through B. 1. 2m



Map of Enewetak Atoll

At the end of Volume III, after the section on LEROY, is a section containing microfiche transparencies reproducing all of the analytical data obtained in this survey. Instructions on the use of microfiche film are also included in that section.

Table B.1. Cross-reference list of island names.

Site	Native names from U. S. Hydrographic Office charts		Native names from Dr. Jack A. Tobin
	1946	1968	
ALICE	Bogallua	Bogallua	BOKOLUO
BELLE	Bogombogo	Bogombogo	BOKOMBAKO
CLARA	Ruchi	Eybbiyae	__ <sup>a</sup>
DAISY	__ <sup>a</sup>	Lidilbut	LOUJ
EDNA	__ <sup>a</sup>	__ <sup>a</sup>	__ <sup>a</sup>
HELEN	Bogairikk	Bogeirik	BOKAIDRIK
IRENE	Bogon	Bogon	BOKEN
JANET	Engebi	Engebi	ENJEBI
KATE	Muzinbaarikku	Mujinkarikku	MIJIKADREK
LUCY	Kirinian	Billee	KIDRINEN
PERCY	__ <sup>a</sup>	__ <sup>a</sup>	__ <sup>a</sup>
MARY	Bokonaarappu	Bokonarppu	BOKENELAB
NANCY	Yeiri	Yeiri	ELLE
OLIVE	Aitsu	Aitsu	AEJ
PEARL	Rujoru	Rujiyoru	LUJOR
RUBY	Eberiru	Eberiru	ELELERON
SALLY	Aomon	Aomon	AOMON
TILDA	Bijjiri	Bijjiri	BIKILE
URSULA	Rojoa	Rojoa	LOJWA
VERA	Aaraanbiru	Arambiru	ALEMBEL
WILMA	Piirai	Piirai	BILLAE
YVONNE	Runit	Runit	RUNIT
SAM	__ <sup>a</sup>	__ <sup>a</sup>	__ <sup>a</sup>
TOM	__ <sup>a</sup>	__ <sup>a</sup>	ANEROWIJ
URIAH	__ <sup>a</sup>	__ <sup>a</sup>	__ <sup>a</sup>
VAN	__ <sup>a</sup>	__ <sup>a</sup>	__ <sup>a</sup>
ALVIN	Chinieero	__ <sup>a</sup>	JINEDROL
BRUCE	Aniyaanii	Japtan	ANANIJ
CLYDE	Chinimi	Chinimi	JINIMI
DAVID	Japtan	Muti	JAPTAN
ELMER	Parry	Parry	MEDREN
WALT	__ <sup>a</sup>	__ <sup>a</sup>	__ <sup>a</sup>
FRED	Eniwetok	Eniwetok	ENEWETAK

Table B.1 (Continued)

Site	Native names from U. S. Hydrographic Office Charts		Native names from Dr. Jack A. Tobin
	1946	1968	
GLENN	Igurin	Igurin	IKUREN
HENRY	Mui	Buganegan	MUT
IRWIN	Pokon	Bogan	BOKEN
JAMES	Ribaion	Libiron	RIBEWON
KEITH	Giriinien	Grinem	KIDRENEN
LEROY	Rigili	Rigili	BIKEN
REX	Jieroru	Bogen	JEDROL
OSCAR	— <sup>a</sup>	— <sup>a</sup>	DREKATIMON
MACK	— <sup>a</sup>	— <sup>a</sup>	UNIBOR

<sup>a</sup>No native name.

Table B.2. Enewetak Atoll individual photomap scale factors.

Island	Altitude flown, ft	Scale
ALICE	5000	1 cm = 37 m
BELLE	5000	34
CLARA	3000	23
DAISY	3000	25
EDNA	5000	38
IRENE A, B	5000	51
JANET	10000	87
KATE	3000	24
LUCY	3000	26
PERCY	3000	21
MARY	3000	24
NANCY	5000	33
OLIVE	5000	38
PEARL	5000	44
RUBY	3000	17
SALLY	8000	67
TILDA	5000	36
URSULA	5000	33
VERA	5000	31
WILMA	3000	27
YVONNE A, B, C, D	5000	51
SAM	1000	13

Table B.2 (Continued)

Island	Altitude flown, ft	Scale
TOM	2000	1 cm = 8 m
URIAH	2000	17
VAN	4000	20
ALVIN	2000	15
BRUCE	5000	42
CLYDE	2000	12
DAVID	5000	44
REX	2000	18
ELMER A, B, C, D	5000	47
WALT	2000	15
FRED A, B, C, D, E, F	5000	48
GLENN	9000	77
HENRY	6000	55
IRWIN A, B	3000	29
JAMES	3000	16
KEITH	3000	26
LEROY	3000	20
YVONNE E, F	10000	95

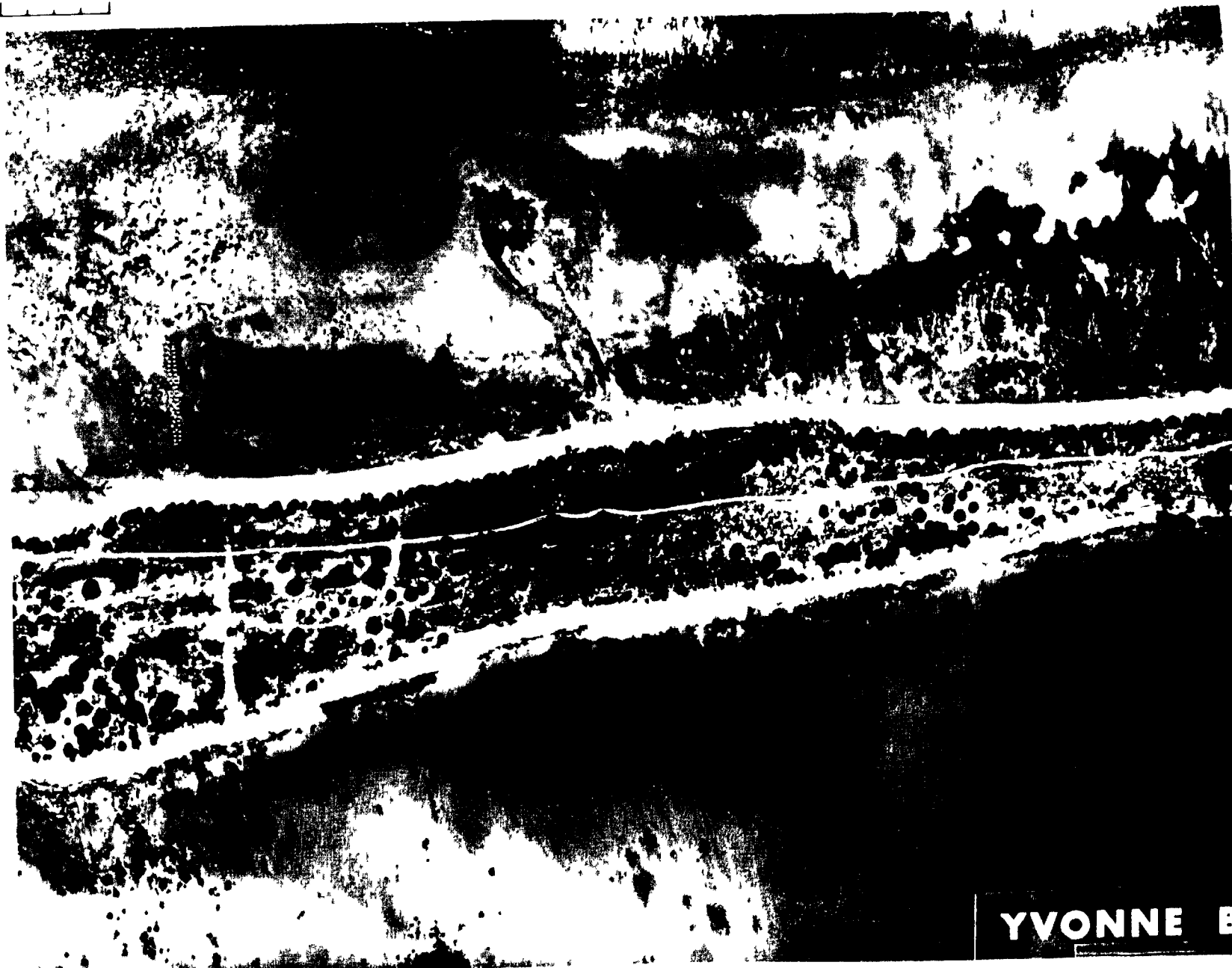
Table B.3. Contour map key for use with the EG&G aerial radiological survey figures in Appendix II. <sup>a</sup>

Sym- bol	<sup>241</sup> Am concentration <sup>b</sup> (assumed 10-cm relaxation depth)		<sup>137</sup> Cs <sup>c</sup>		<sup>60</sup> Co <sup>d</sup>		Gross count exposure rate, <sup>e</sup> μR/hr
	Total μCi/m <sup>2</sup>	averaged over top 10 cm, pCi/g	Concentration ±50% for 1 cm (relaxation depth < 10 cm), μCi/m <sup>2</sup>	Exposure rate, μR/hr	Concentration ±50% for 1 cm (relaxation depth < 10 cm), μCi/m <sup>2</sup>	Exposure rate, μR/hr	
A <sup>-</sup>			0-0.1	0-0.34			
A <sup>-</sup>			0.1-0.2	0.34-0.68	0-0.04	0-0.59	
A	0-21	0-9	0.2-0.4	0.68-1.36	0.04-0.08	0.59-1.14	0-1.0
B	21-30	9-13	0.4-0.6	1.36-2.0	0.08-0.12	1.14-1.7	1.0-1.5
C	30-45	13-19	0.6-0.8	2.0-2.7	0.12-0.16	1.70-2.3	1.5-2.0
D	45-66	19-28	0.8-1.6	2.7-5.4	0.16-0.32	2.3-4.6	2.0-4
E	66-100	28-42	1.6-3.1	5.4-11	0.32-0.64	4.6-0.9	4-8
F	100-145	42-61	3.1-6.2	11-22	0.64-1.3	9.2-18	8-16
G	145-210	61-89	6.2-12	22-44	1.3-2.5	18-36	16-33
H	210-300	89-130	12-25	44-88	2.5-5.0	36-72	33-66
I	300-450	130-190	25-50	88-170	5-10	72-140	66-130
J			50-100	170-340	10-20	140-290	130-260
K			100-200	340-700	20-40	290-580	260-520
L			200-400	700-1400	40-80	580-1200	520-1050

<sup>a</sup>See chapter on the EG&G aerial radiological survey in Vol. 1.<sup>b</sup>Shown in "c" figures in this Appendix.<sup>c</sup>Shown in "k" figures in this Appendix.<sup>d</sup>Shown in "m" figures in this Appendix.<sup>e</sup>Shown in "b" figures in this Appendix.



100 METERS



YVONNE B

Fig. B.23.1.a.

100 METERS



Fig. B.23.1.b. Gross count isosexposure contours. (Refer to alphabetic symbol key in this appendix.)

100 METERS

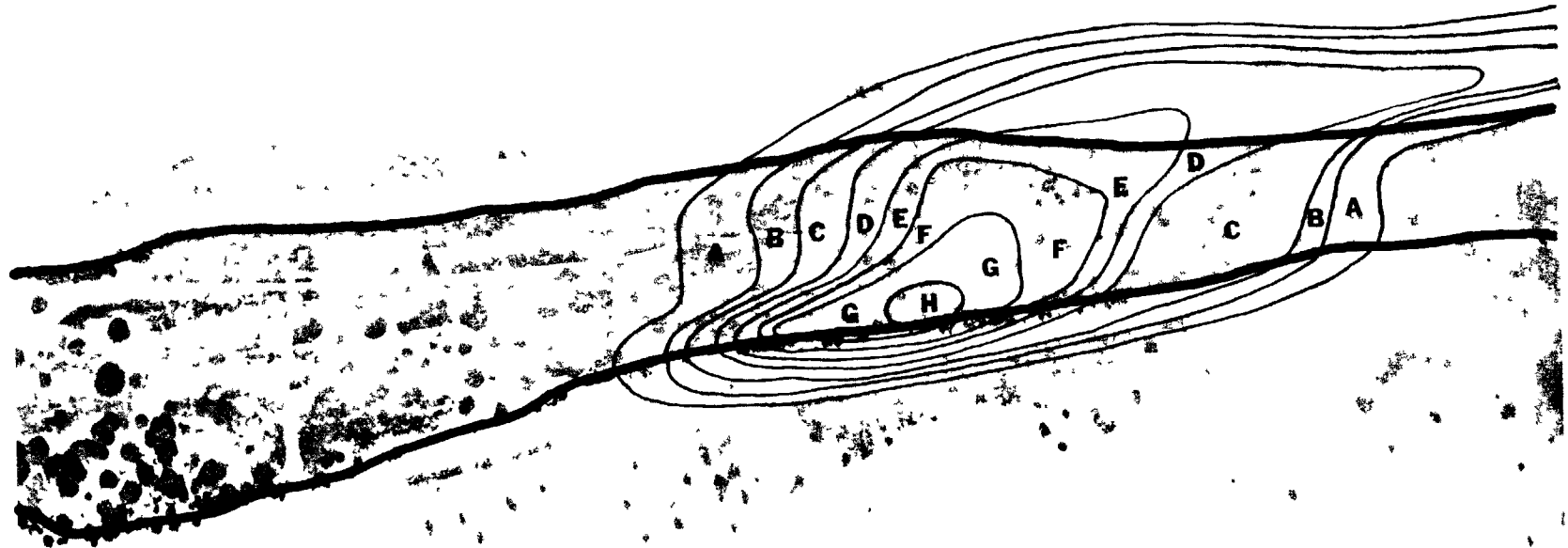
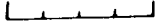
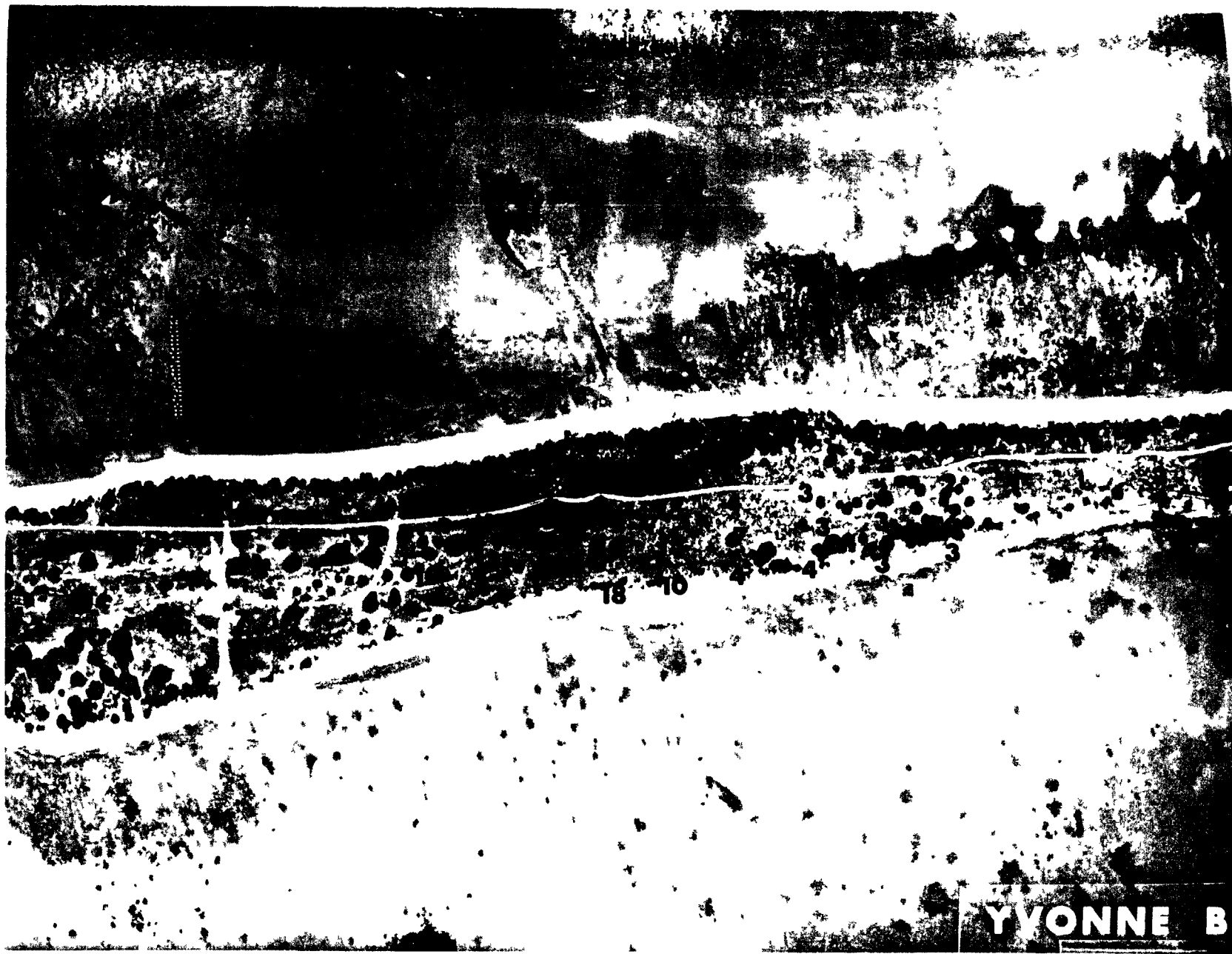


Fig. B.23.1.c.  $^{241}\text{Am}$  isoconcentration contours. (Refer to alphabetic symbol key in this appendix.)

100 METERS



B.23.1.d. The gamma background exposure rate ( $\mu\text{R/hr}$ ) at 1 m above the ground, measured with a portable NaI scintillation counter.

100 METERS



B.23.1.f. Soil-sample locations.

100 METERS



Fig. B.23.1.g. Vegetation sample locations.

100 METERS



B.23.1.i.1. The average  $^{239}\text{Pu}$  activities (pCi/gm) in soil samples collected between depths of 0 and 10 cm.

100 METERS



B.23.1.1.2. The average  $^{239}\text{Pu}$  activities (pCi/gm) in soil samples collected between depths of 10 and 20 cm.





100 METERS

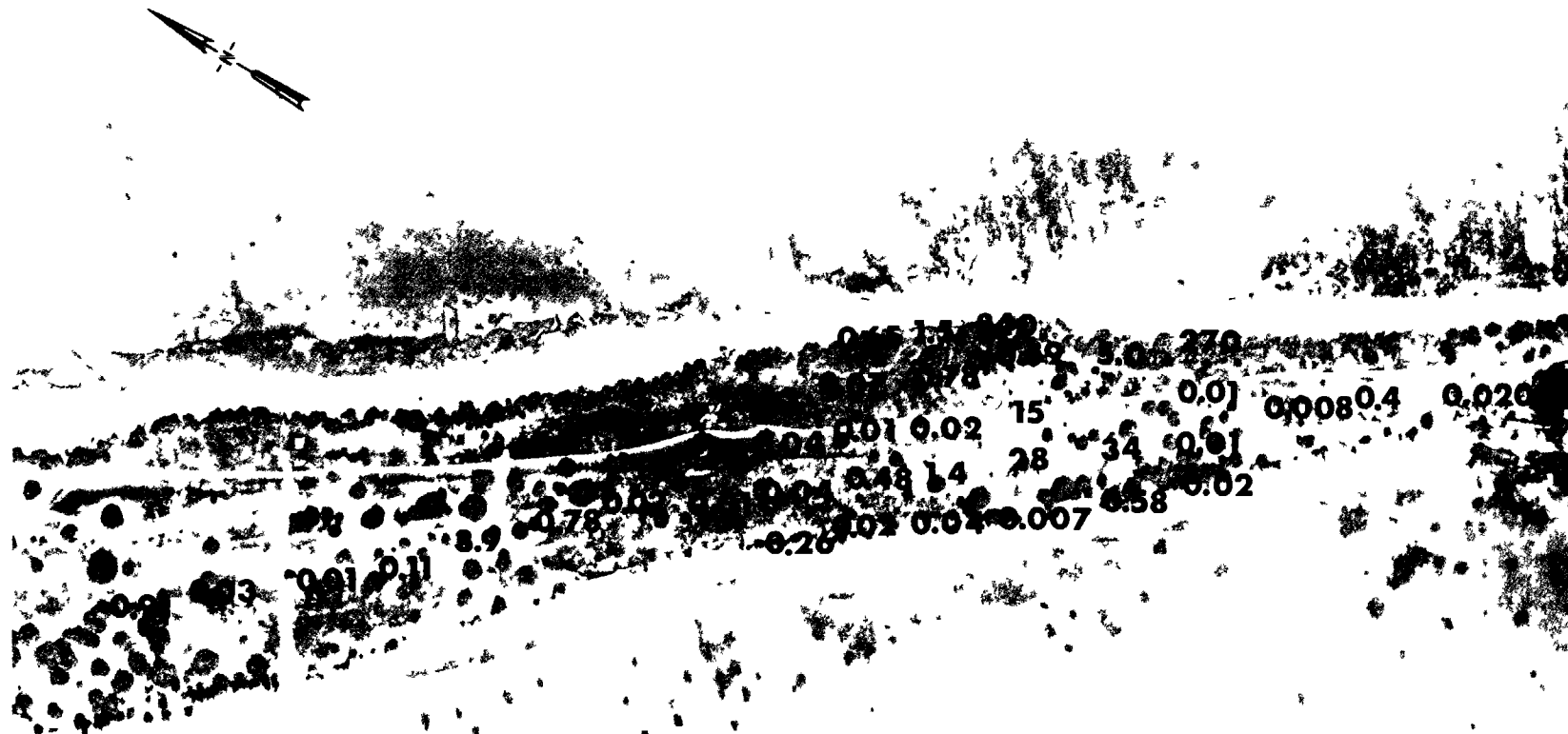


B.23.1.i.4. The average  $^{239}\text{Pu}$  activities (pCi/gm) in soil samples collected between depths of 30 and 40 cm.





100 METERS



B.23.1.i.7. The average  $^{239}\text{Pu}$  activities (pCi/gm) in soil samples collected between depths of 60 and 70 cm.



□ PROFILE SAMPLES (0-35 cm)

● CORE SAMPLES (15 cm)

Fig. B.29.1.f. Soil-sample locations.

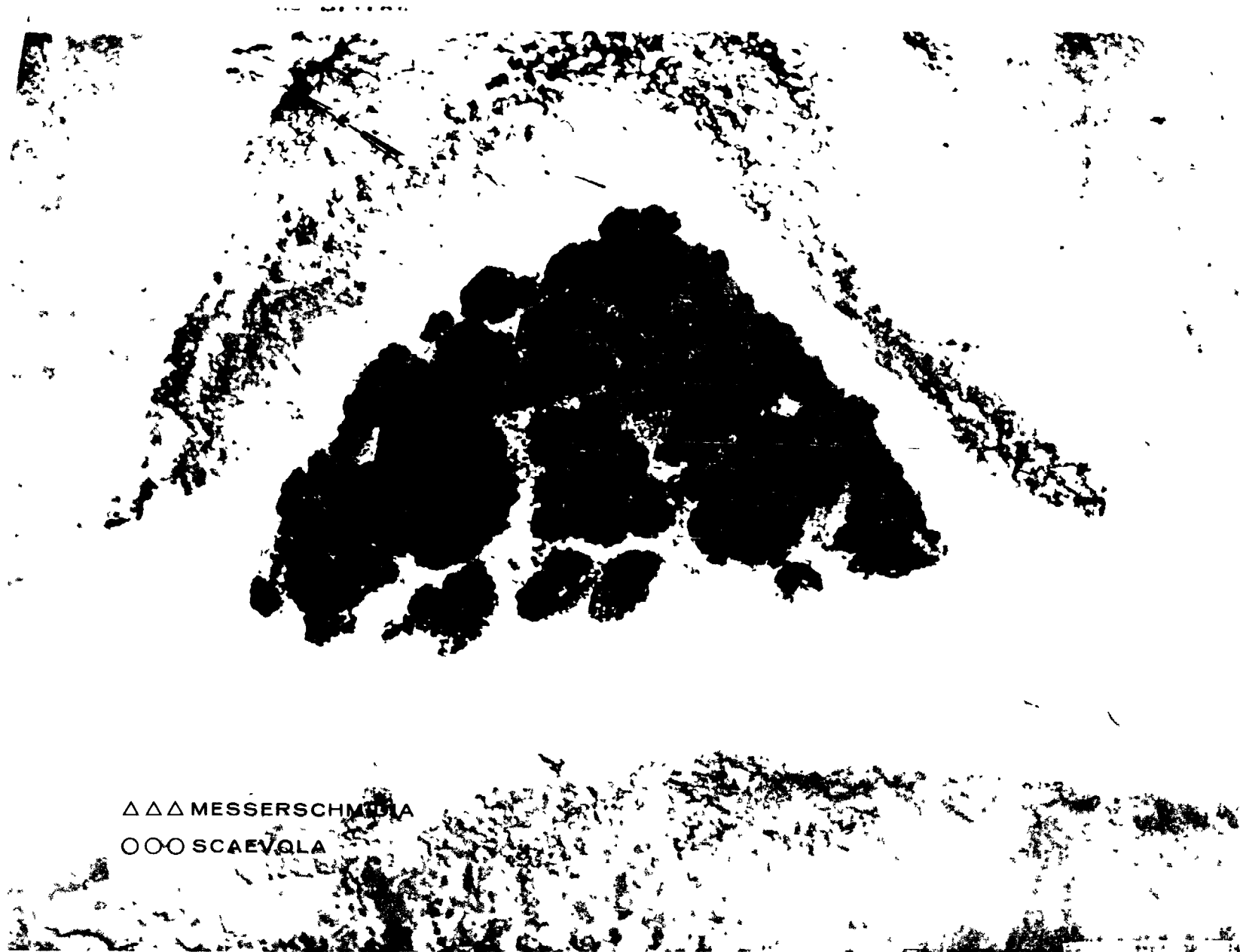


Fig. B.29.1.g. Vegetation sample locations.

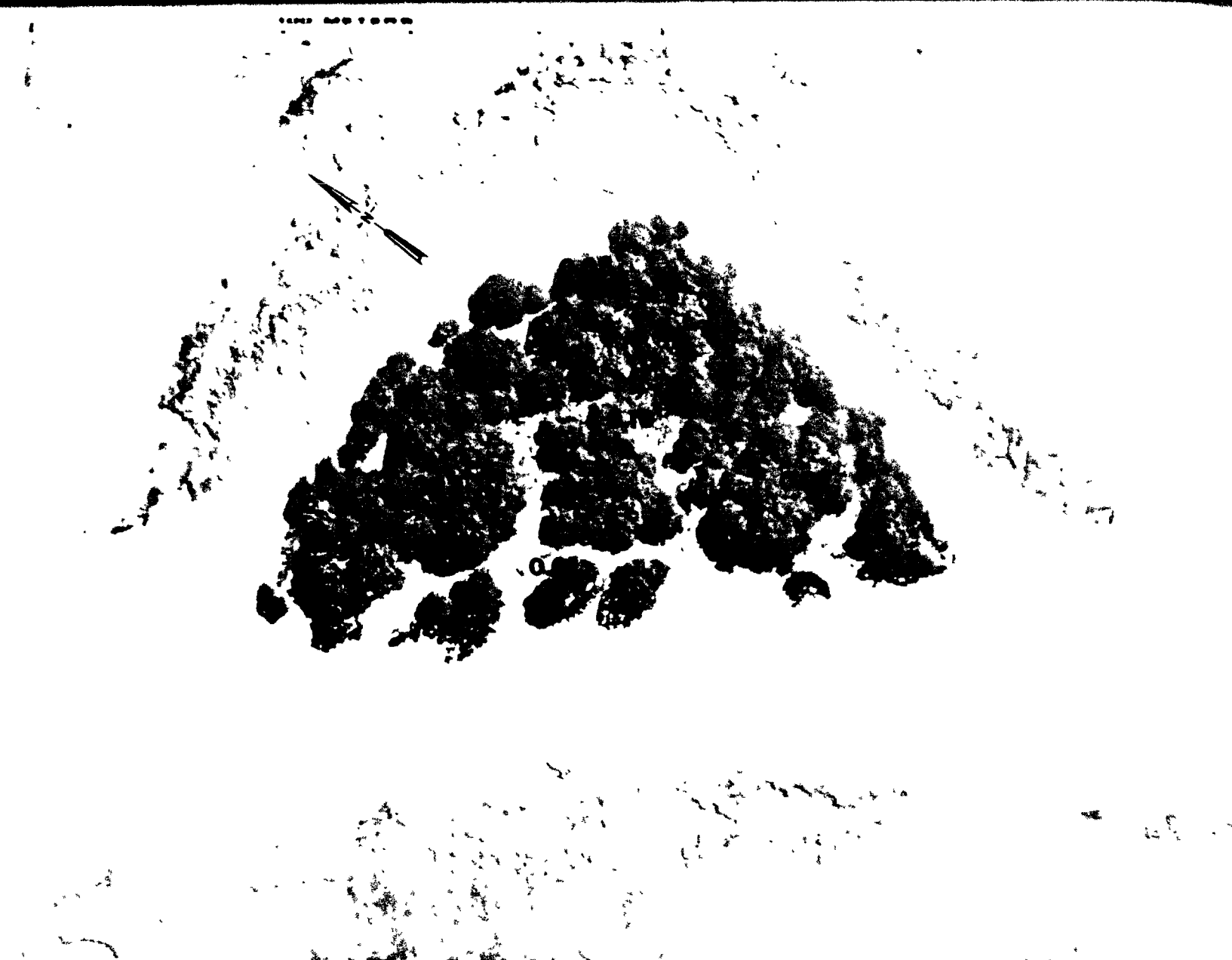


Fig. B.29.1.i. The average  $^{239}\text{Pu}$  activities (pCi/g) in soil samples collected to a depth of 15 cm.



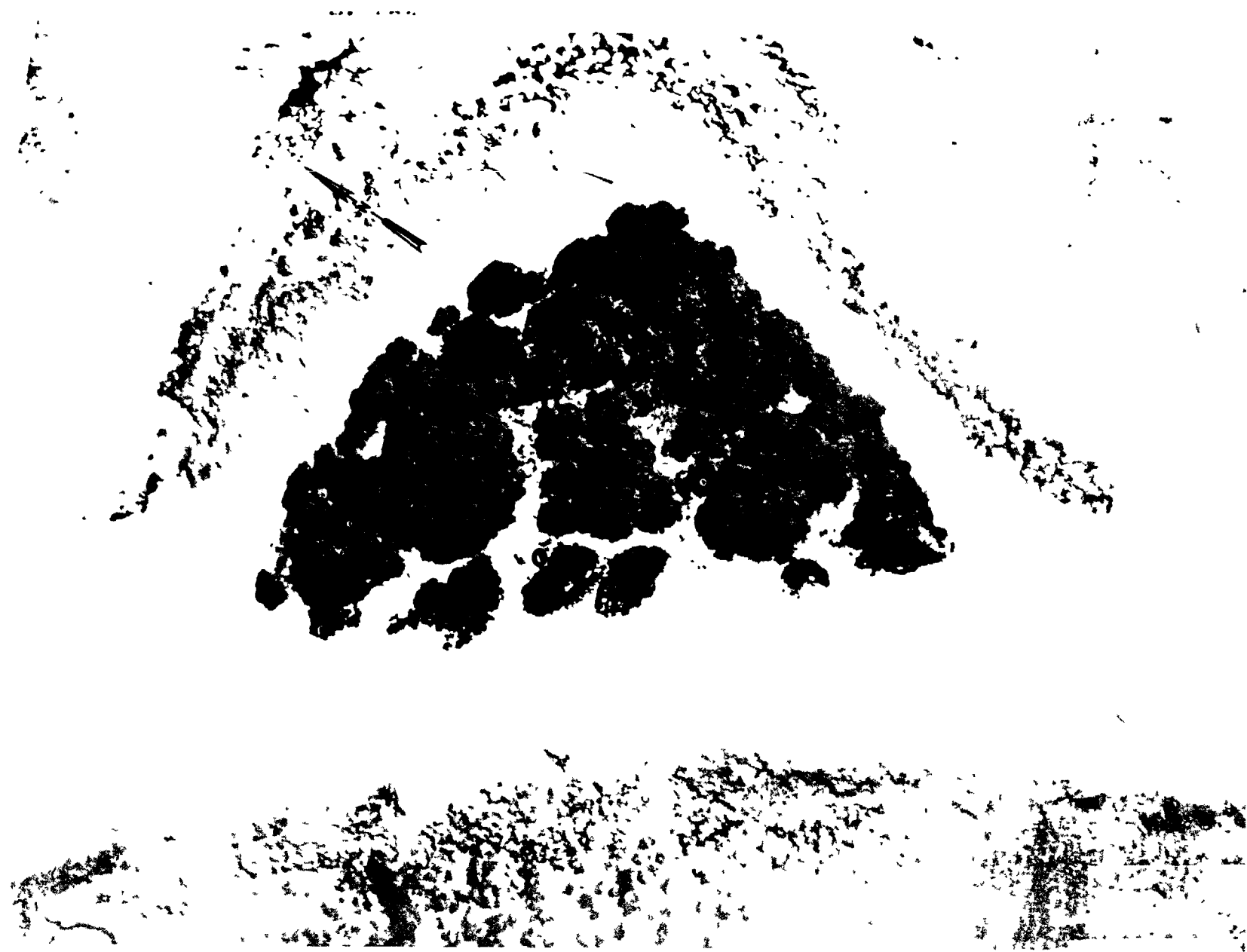


Fig. B.29.1.j. The average  $^{90}\text{Sr}$  activities (pCi/g) in soil samples collected to a depth of 15 cm.



Fig. B.29.1.k.  $^{137}\text{Cs}$  isoexposure and isoconcentration contours. (Refer to alphabetic symbol key in this appendix.)

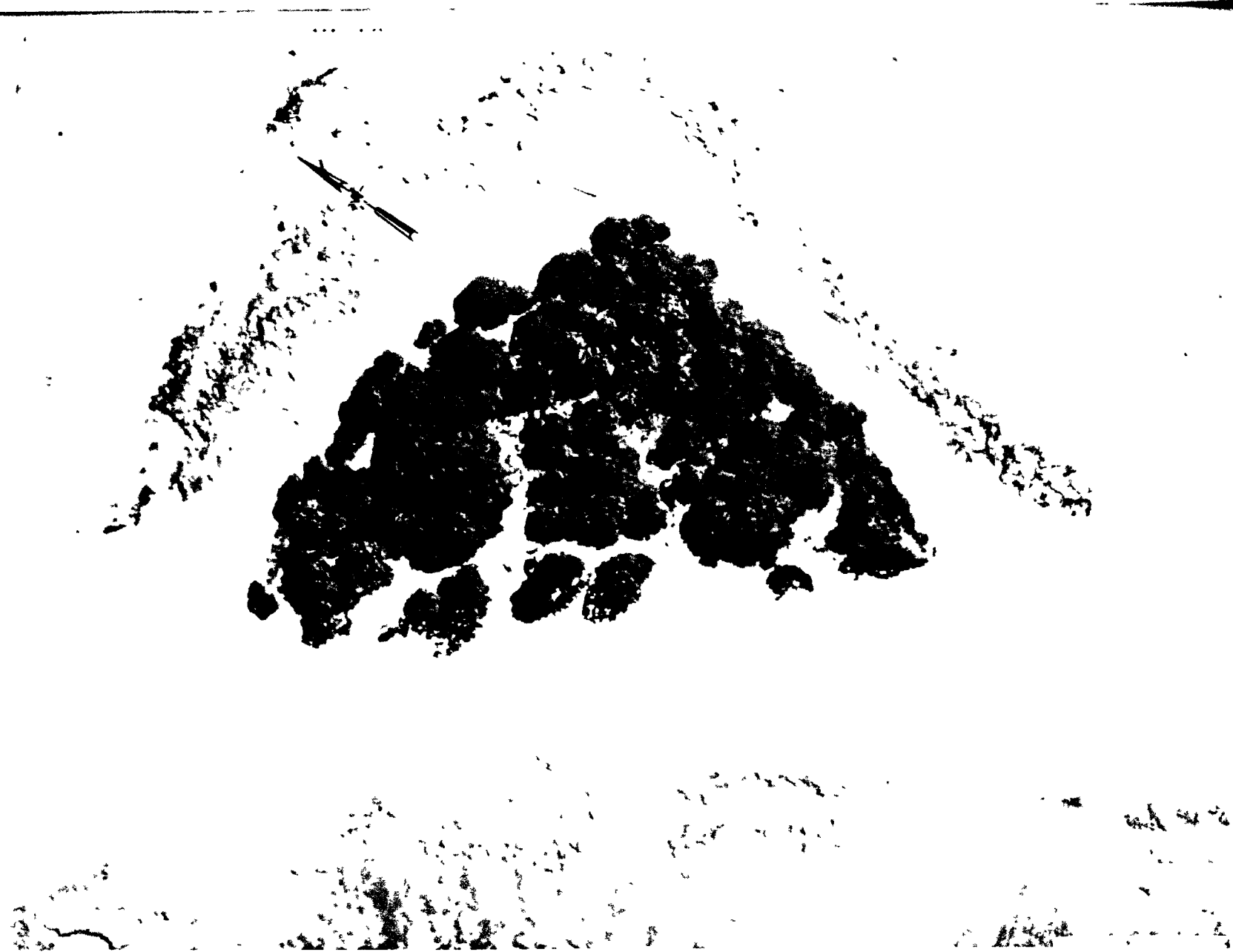


Fig. B.29.1.1. The average  $^{137}\text{Cs}$  activities (pCi/g) in soil samples collected to a depth of 15 cm.



Fig. B. 29. 1. m.  $^{60}\text{Co}$  isoeposure and isoconcentration contours. (Refer to alphabetic symbol key in this appendix.)



Fig. B.29.1.n. The average  $^{60}\text{Co}$  activities (pCi/g) in soil samples collected to a depth of 15 cm.

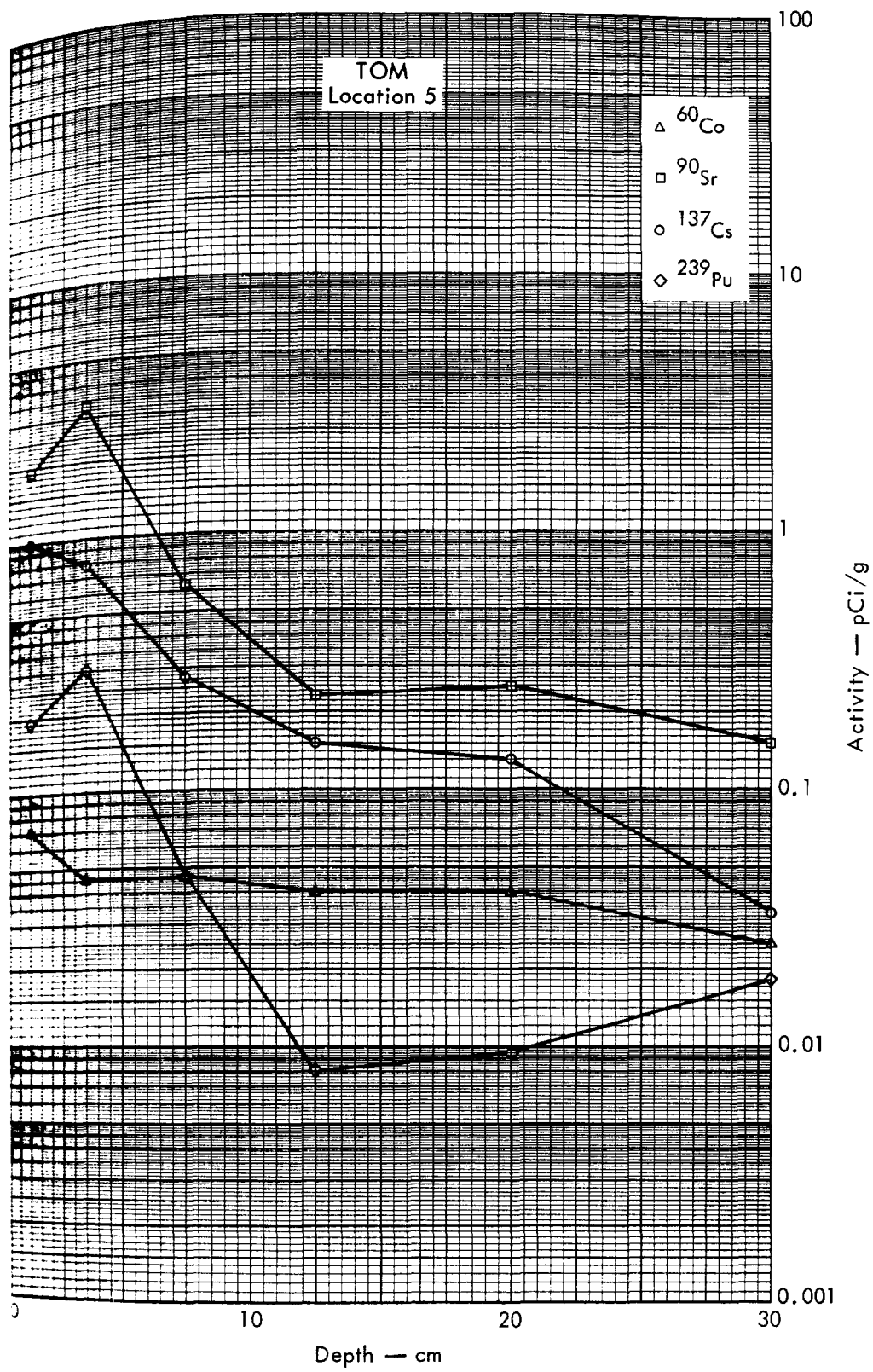


Fig. B.29.2a. Activities of selected radionuclides as a function of soil depth.



URIAH

Fig. B. 30. 1. a.



Fig. B.30.1.b. Gross count isoexposure contours. (Refer to alphabetic symbol key in this appendix.)





Fig. B.30.1.d. The gamma background exposure rate ( $\mu\text{R/hr}$ ) at 1 m above the ground, measured with a portable NaI scintillation counter.

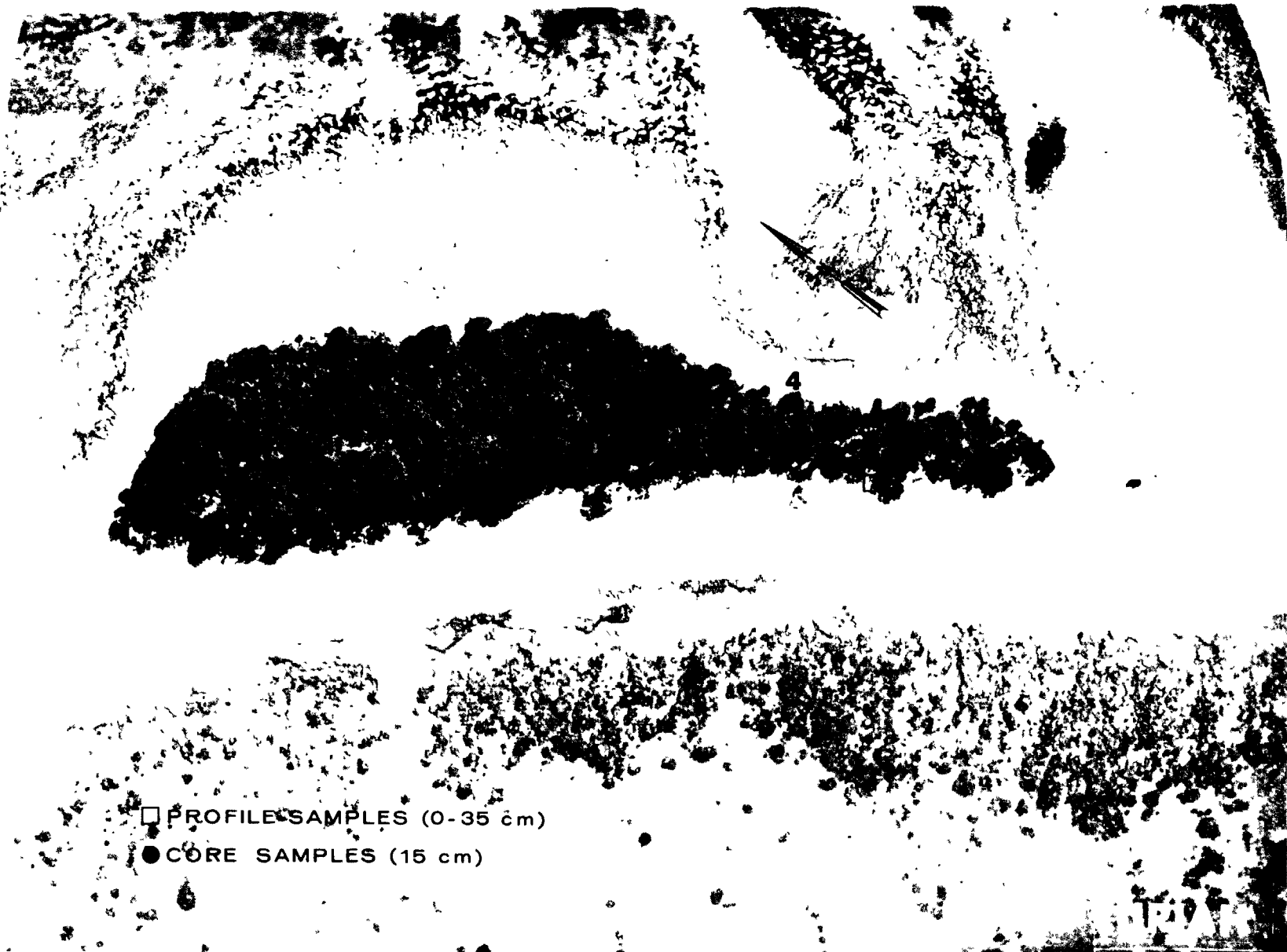


Fig. B.30.1.f. Soil-sample locations.



△ △ △ MESSERSCHMIDIA  
○ ○ ○ SCAEVOLA

Fig. B.30.1.g. Vegetation sample locations.

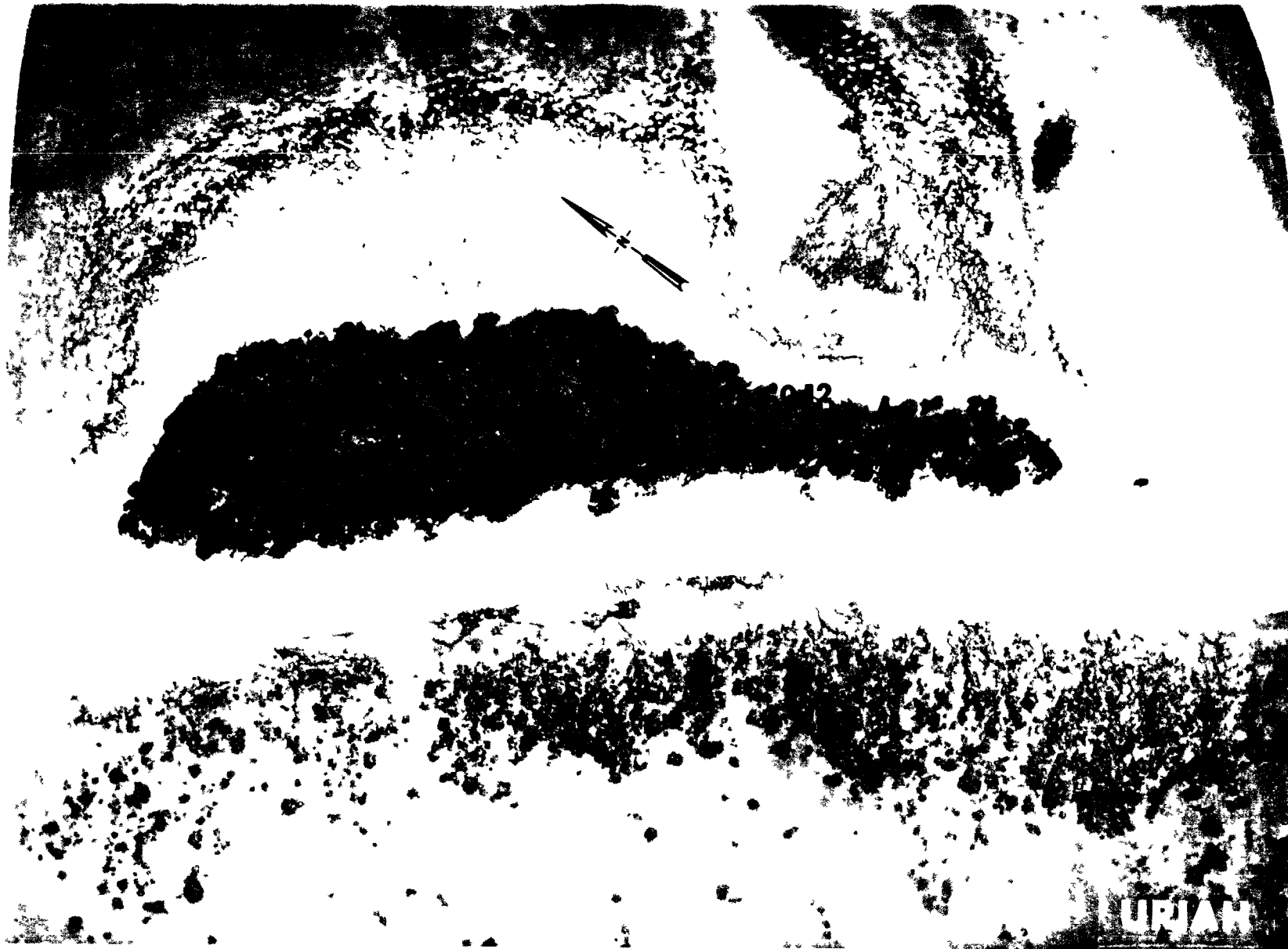


Fig. B.30.1.i. The average  $^{239}\text{Pu}$  activities (pCi/g) in soil samples collected to a depth of 15 cm.



Fig. B.30.1.j. The average  $^{90}\text{Sr}$  activities (pCi/g) in soil samples collected to a depth of 15 cm.



Fig. B.30.1.k.  $^{137}\text{Cs}$  isoexposure and isoconcentration contours. (Refer to alphabetic symbol key in this appendix.)



Fig. B.30.1.1. The average  $^{137}\text{Cs}$  activities (pCi/g) in soil samples collected to a depth of 15 cm.



Fig. B.30.1.m.  $^{60}\text{Co}$  isoexposure and isoconcentration contours. (Refer to alphabetic symbol key in this appendix.)



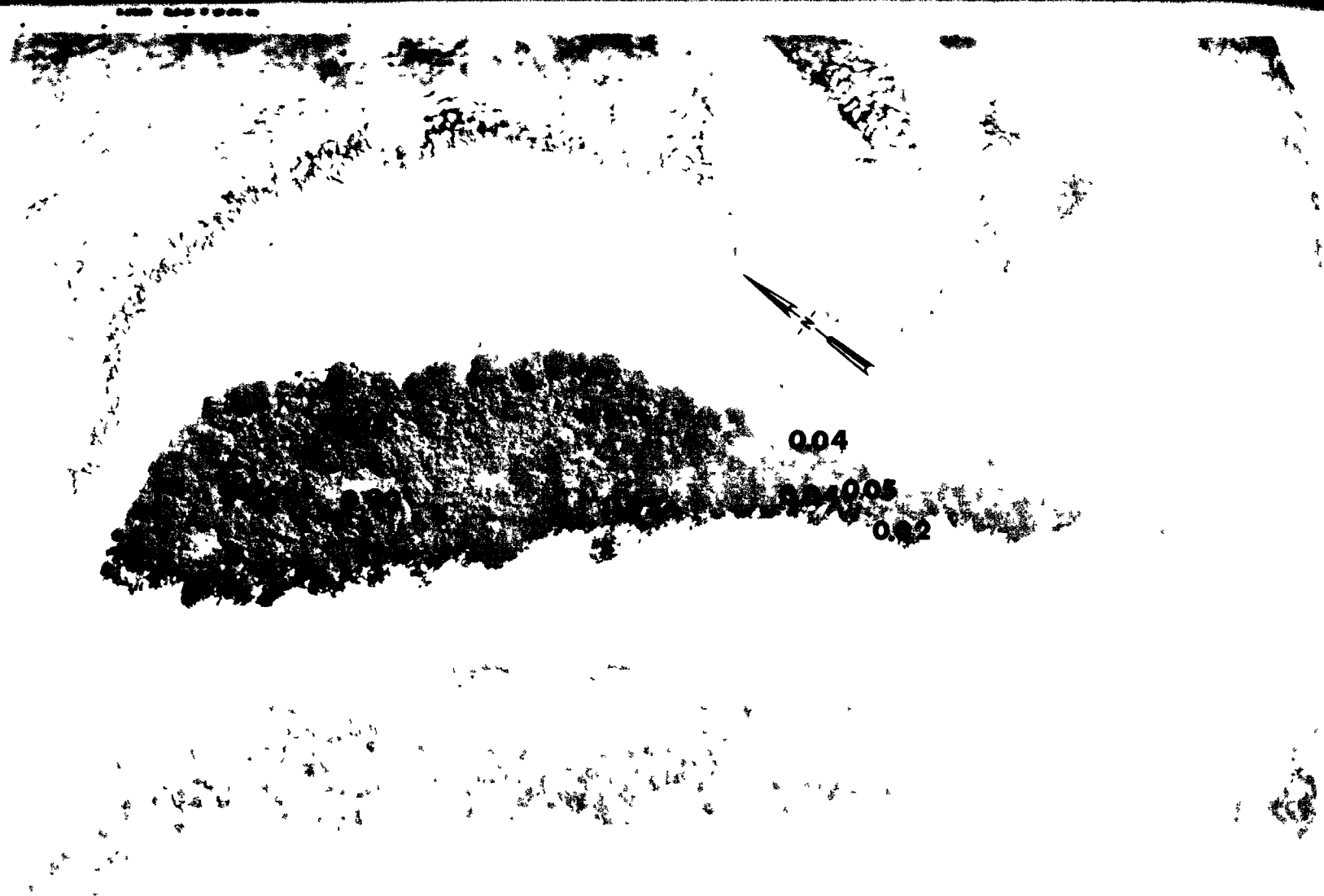


Fig. B.30.1.n. The average  $^{60}\text{Co}$  activities (pCi/g) in soil samples collected to a depth of 15 cm.

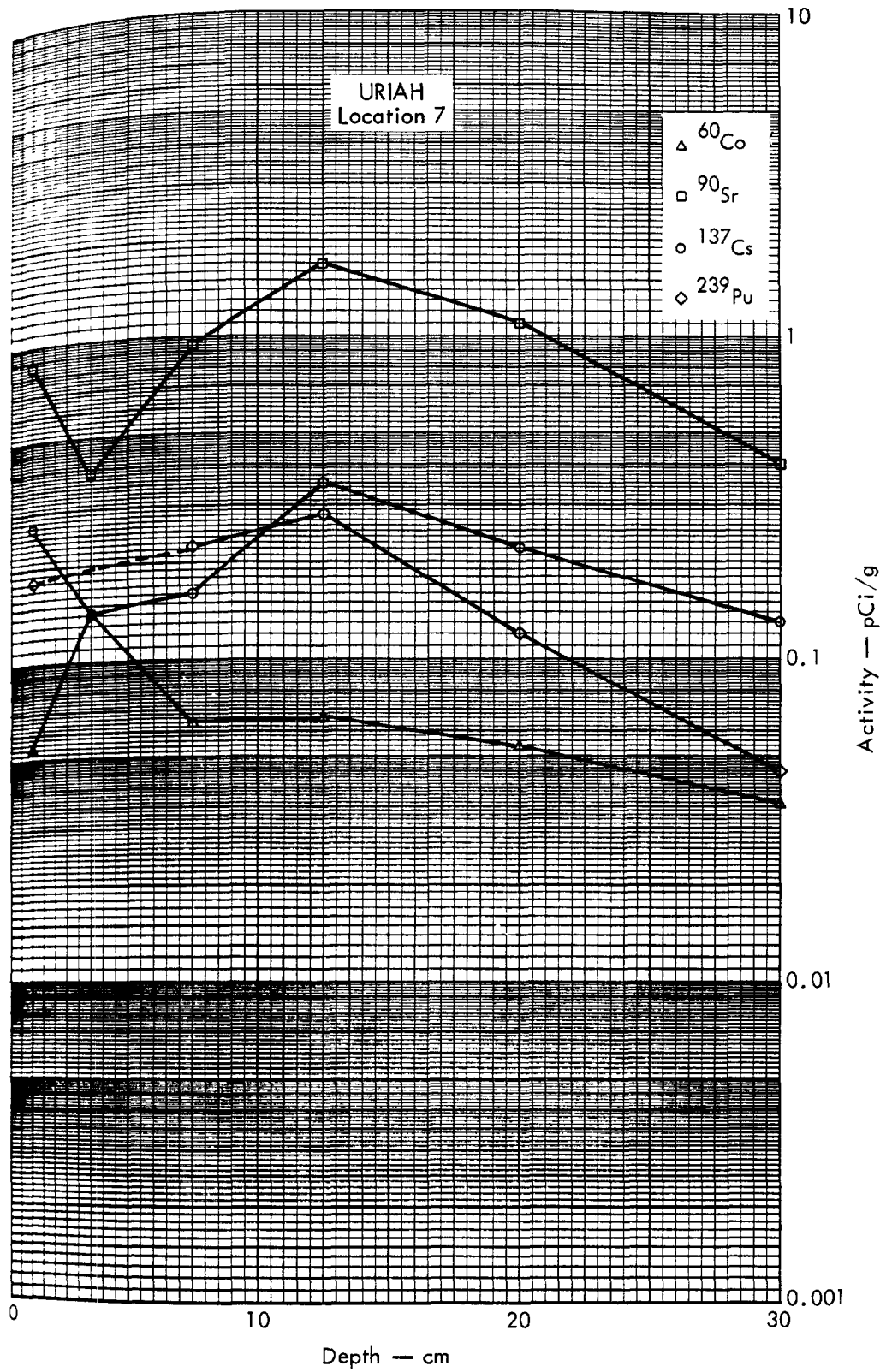


Fig. B. 30. 2a. Activities of selected radionuclides as a function of soil depth.

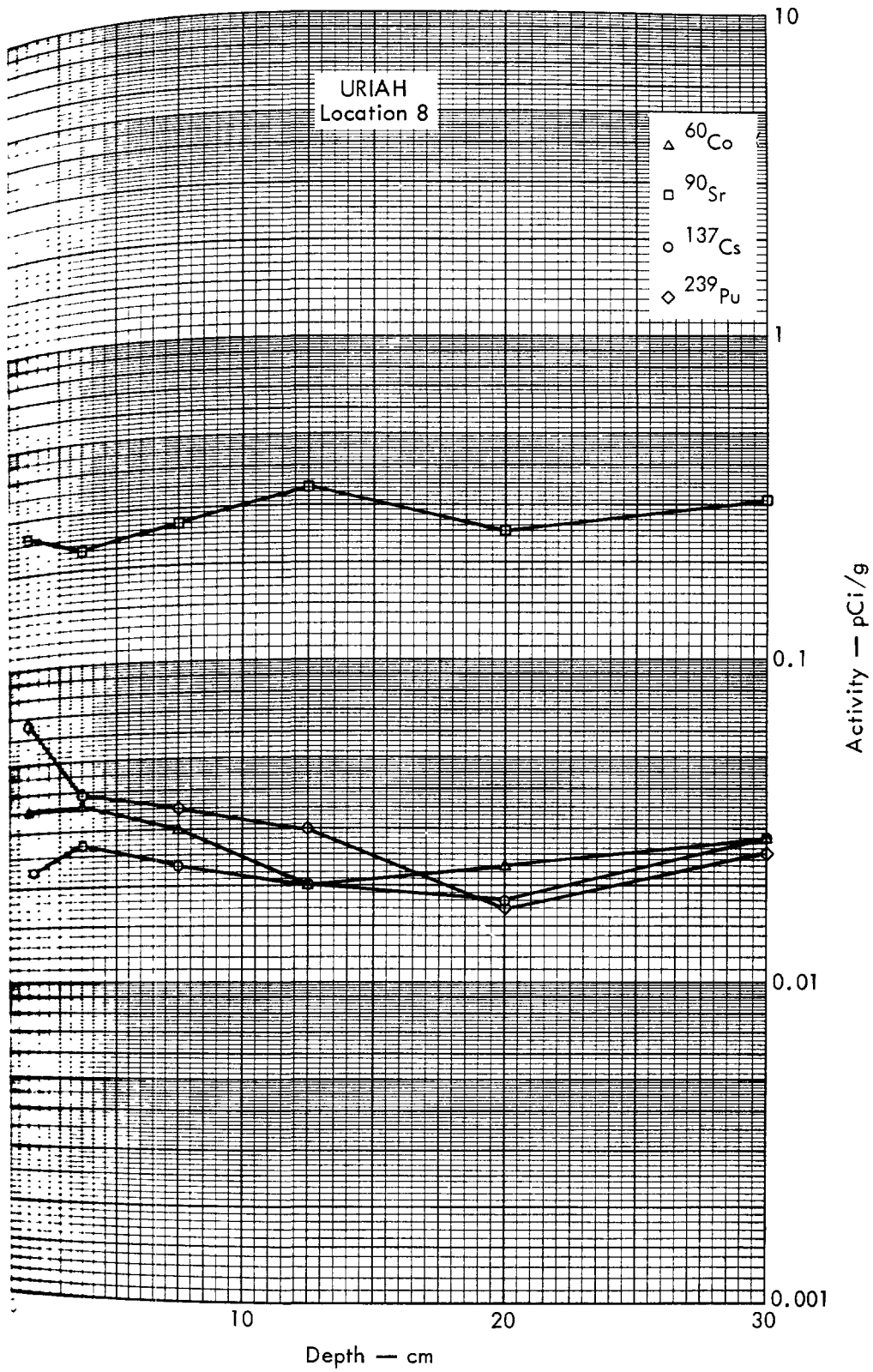


Fig. B 30.2b. Activities of selected radionuclides as a function of soil depth.

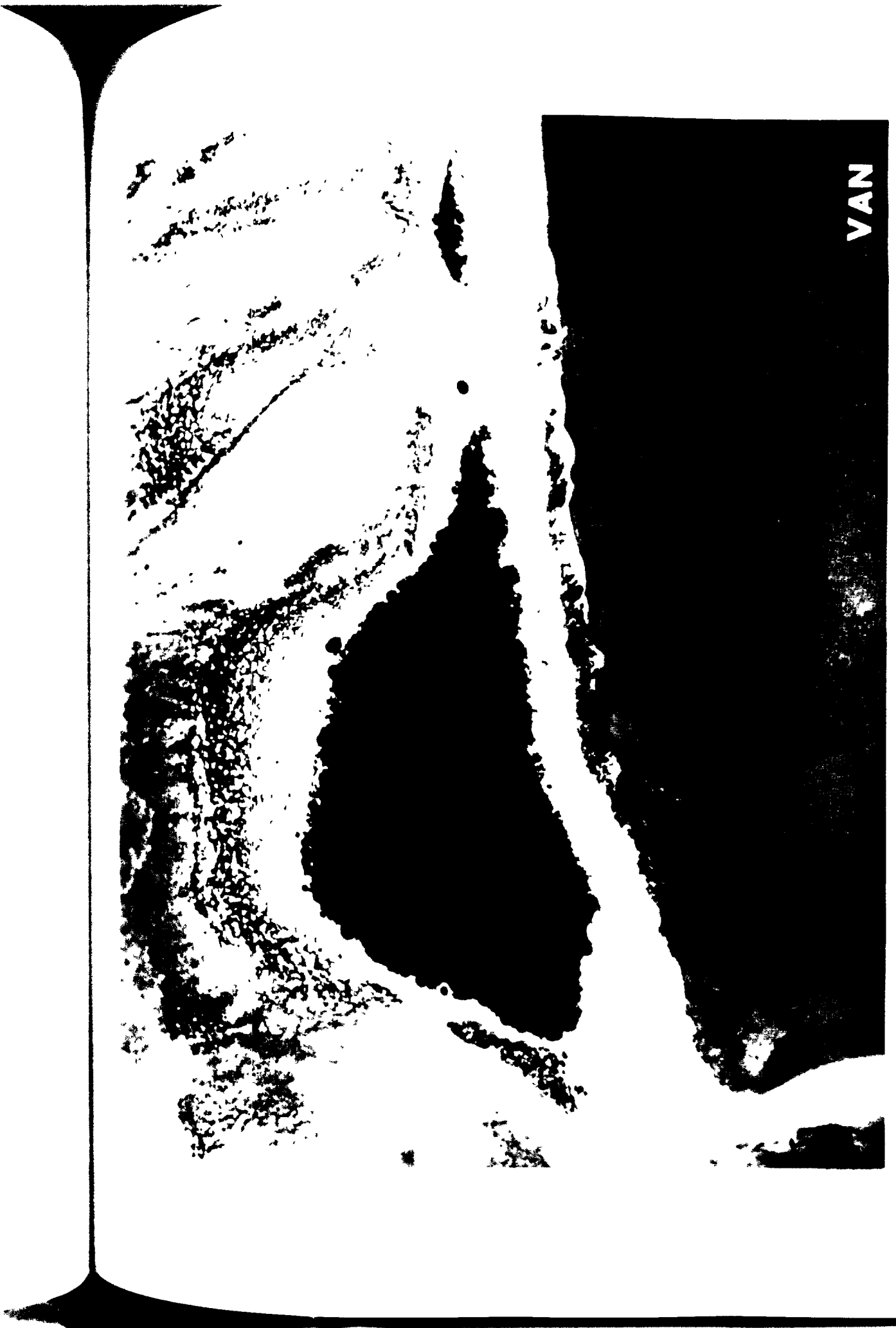


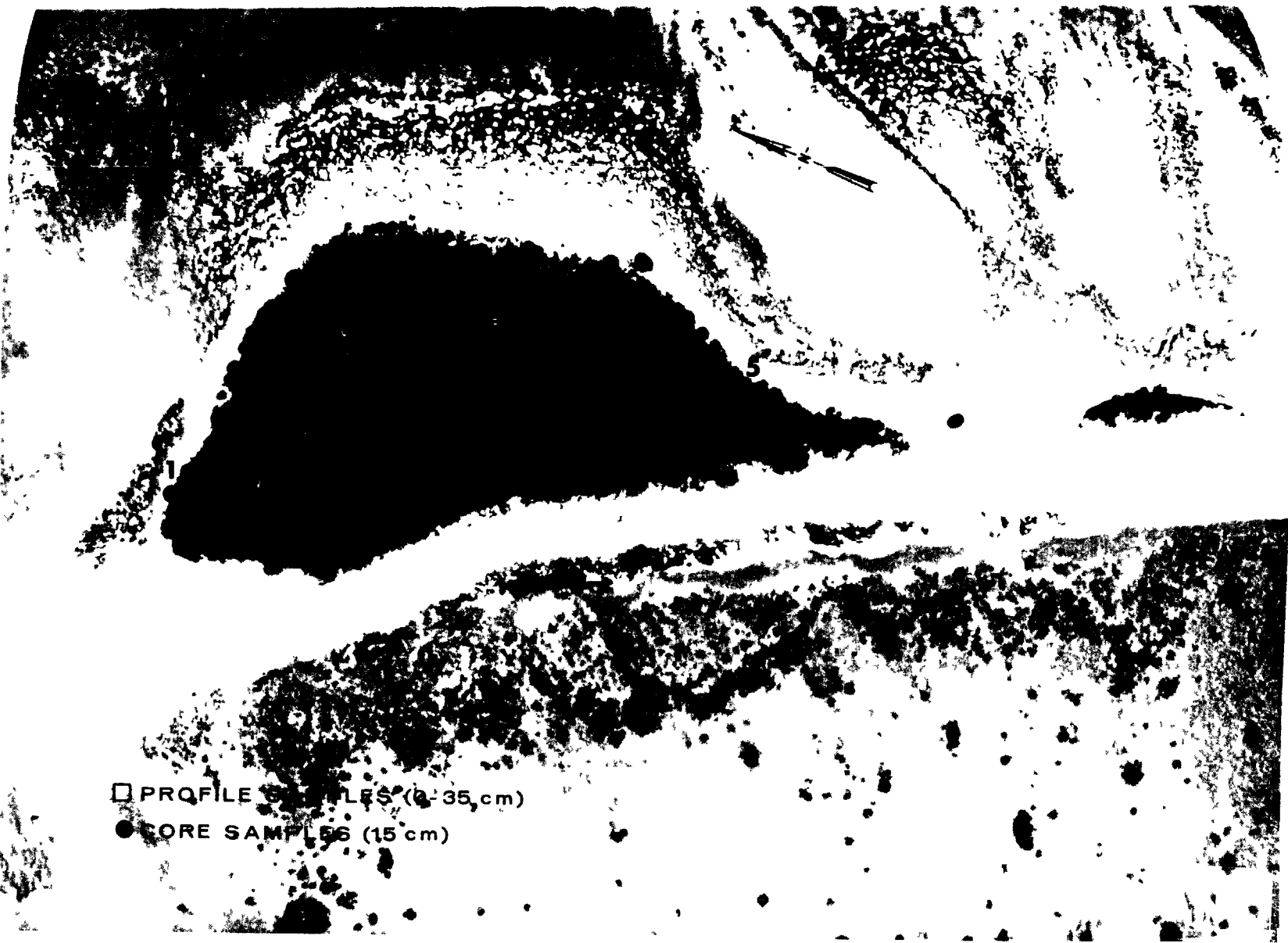
Fig. B.31.1.a.



Fig. B.31.1.b. Gross count isosexposure contours. (Refer to alphabetic symbol key in this appendix.)



Fig. B.31.1.d. The gamma background exposure rate ( $\mu\text{R/hr}$ ) at 1 m above the ground, measured with a portable NaI scintillation counter.



□ PROFILE SAMPLES (0-35 cm)

● CORE SAMPLES (15 cm)

Fig. B.31.1.f. Soil-sample locations.



Fig. B.31.1.g. Vegetation sample locations.





Fig. B.31.1.i. The average  $^{239}\text{Pu}$  activities (pCi/g) in soil samples collected to a depth of 15 cm.



Fig. B.31.1.j. The average  $^{90}\text{Sr}$  activities (pCi/g) in soil samples collected to a depth of 15 cm.



Fig. B.31.1.k.  $^{137}\text{Cs}$  isoexposure and isoconcentration contours. (Refer to alphabetic symbol key in this appendix.)

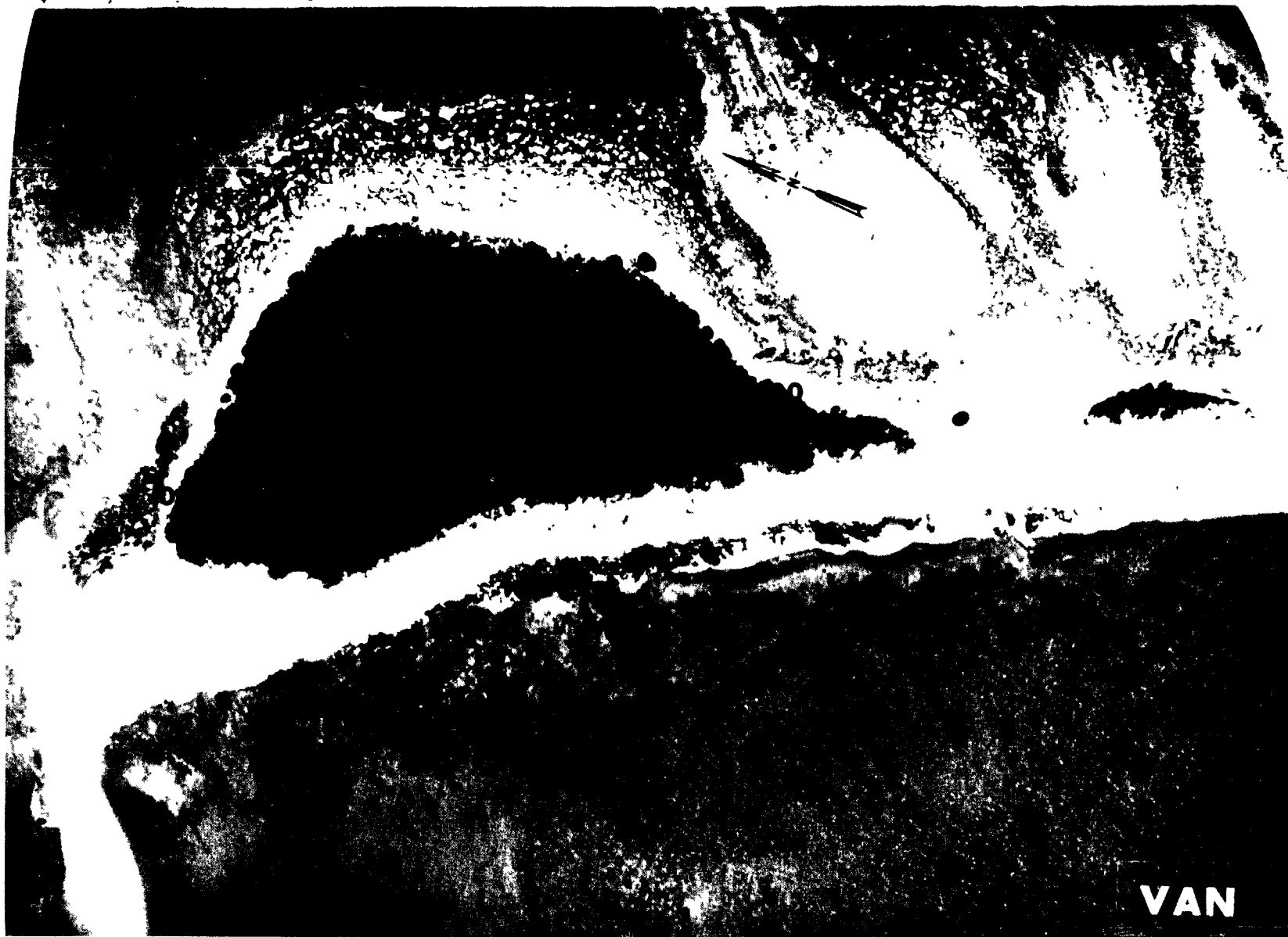


Fig. B.31.1.1. The average  $^{137}\text{Cs}$  activities (pCi/g) in soil samples collected to a depth of 15 cm.



Fig. B.31.1.m.  $^{60}\text{Co}$  isoexposure and isoconcentration contours. (Refer to alphabetic symbol key in this appendix.)

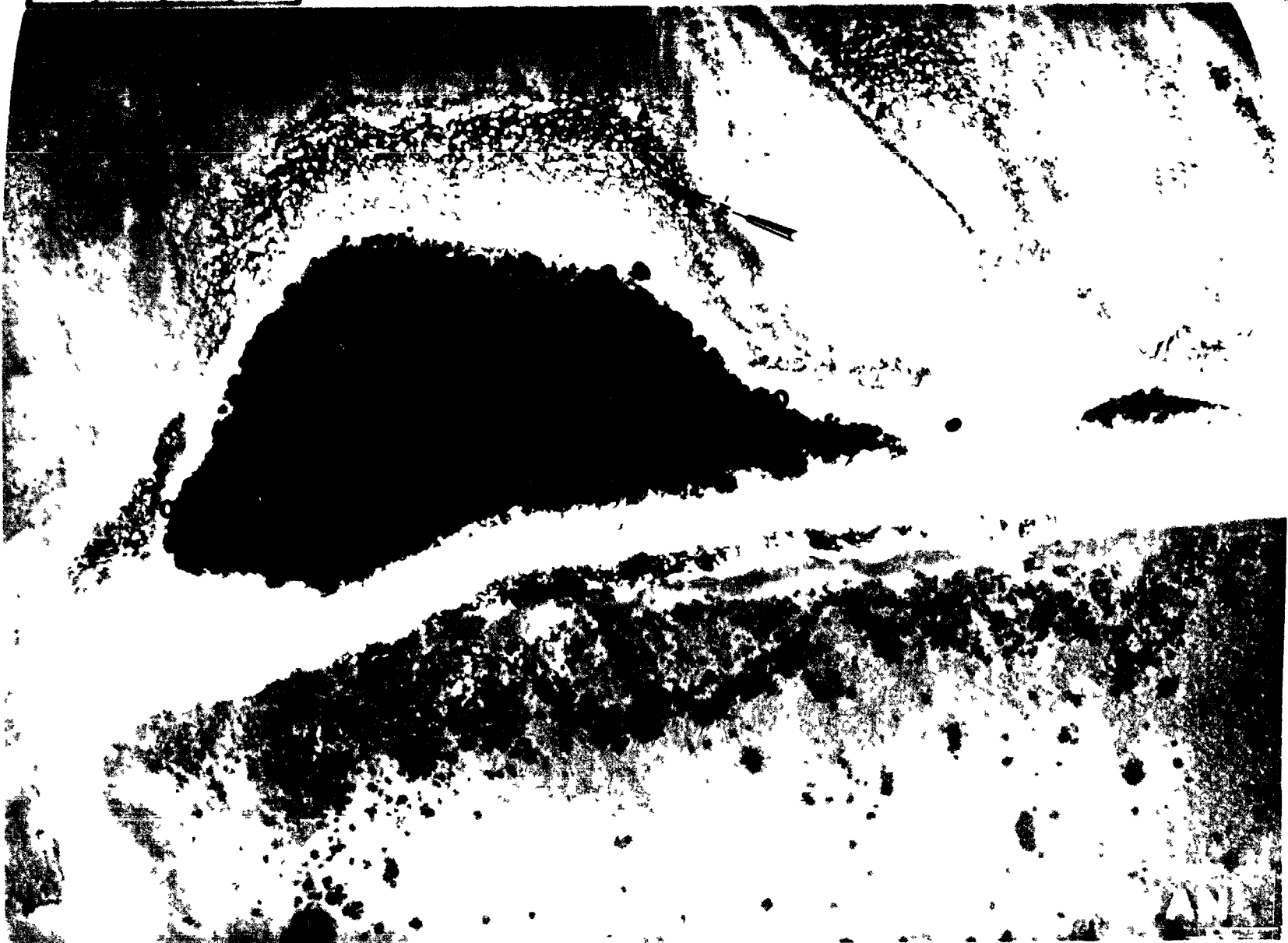


Fig. B.31.1.n. The average <sup>60</sup>Co activities (pCi/g) in soil samples collected to a depth of 15 cm.



Fig. B.31.1.o. Terrestrial animal sample locations.

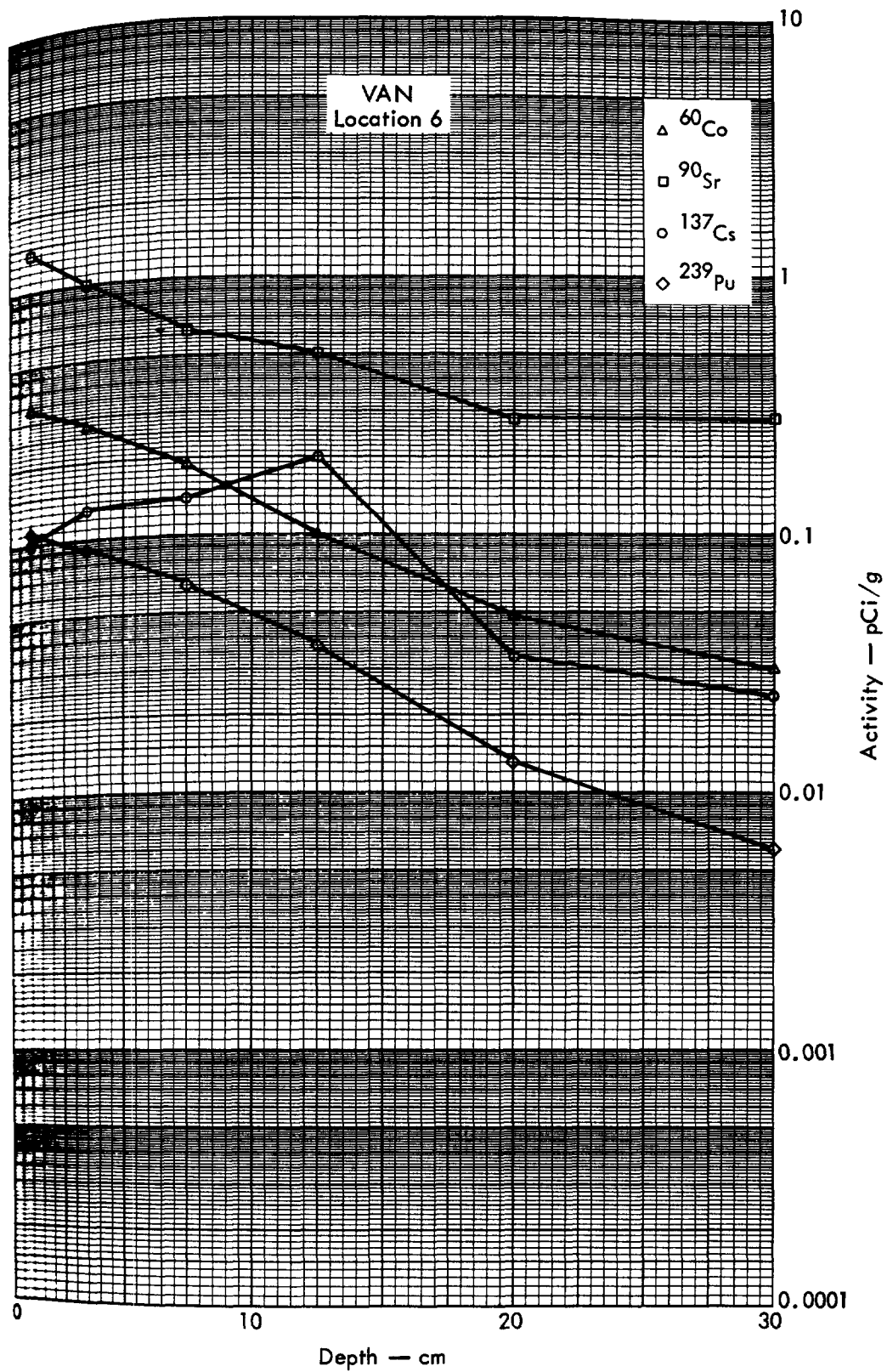


Fig. B. 31. 2a. Activities of selected radionuclides as a function of soil depth.





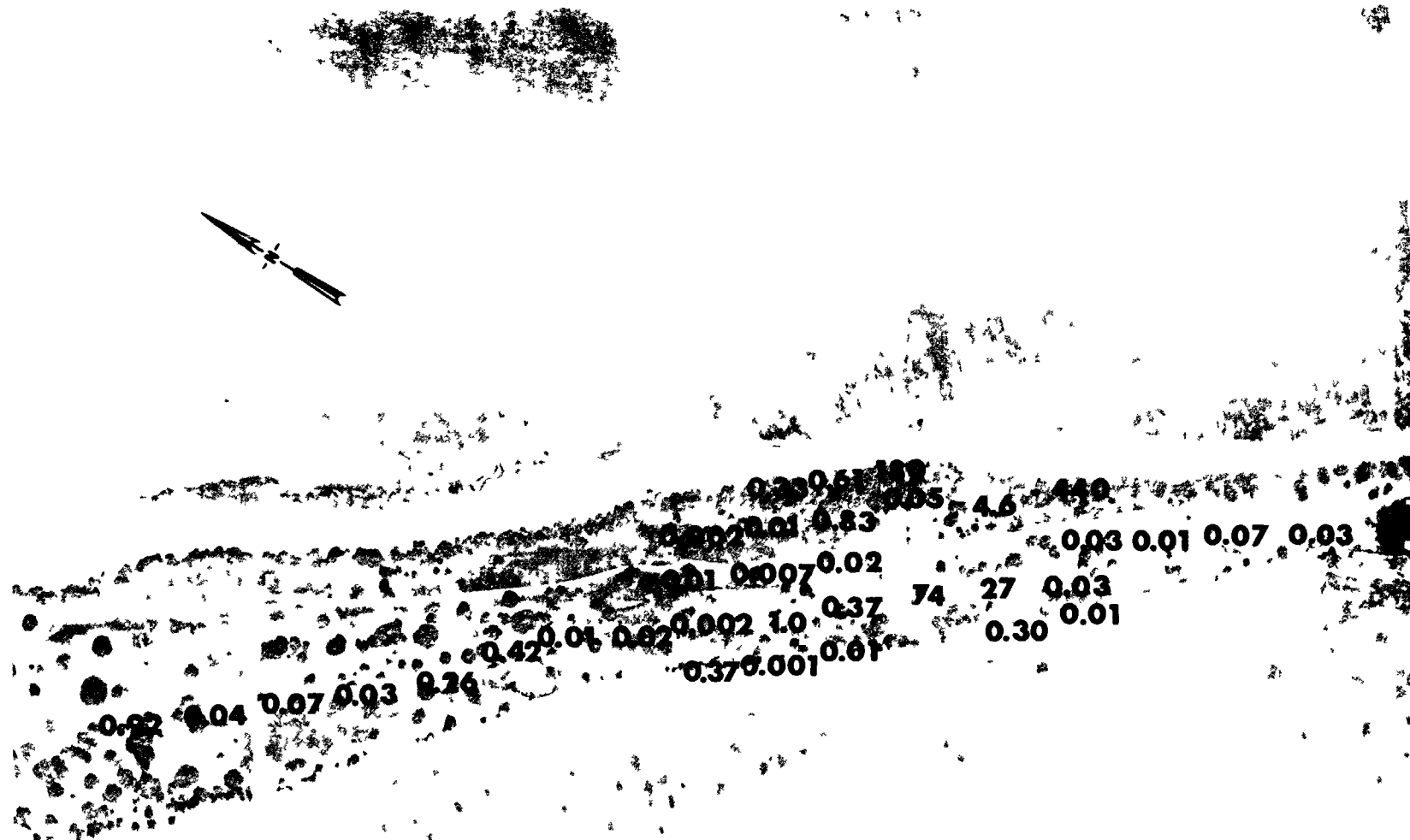
ALVIN

Fig. B.32.1.a.



Fig. B.32.1.b. Gross count isoeposure contours. (Refer to alphabetic symbol key in this appendix.)

100 METERS



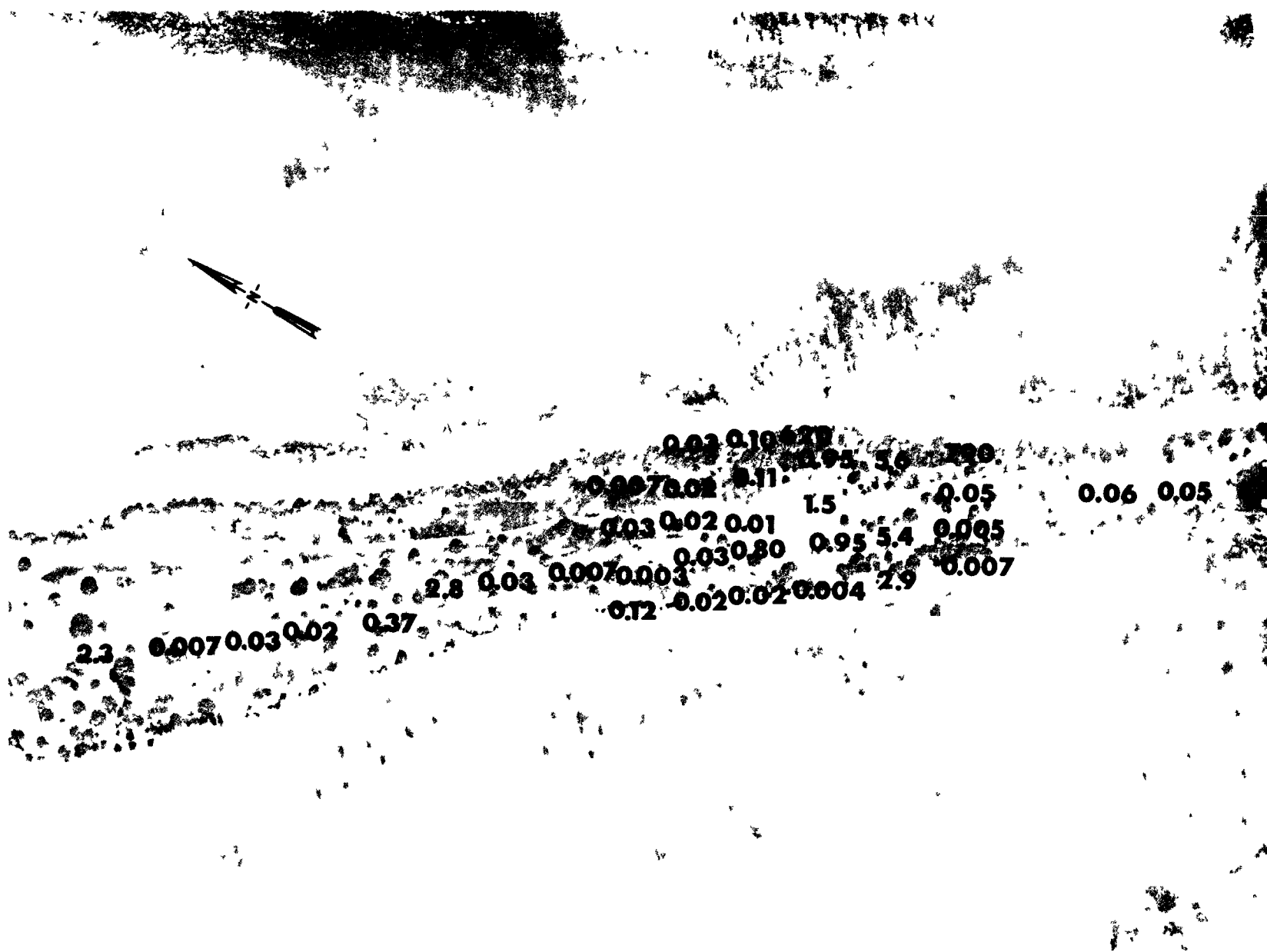
B.23.1.i.8. The average  $^{239}\text{Pu}$  activities (pCi/gm) in soil samples collected between depths of 70 and 80 cm.

100 METERS



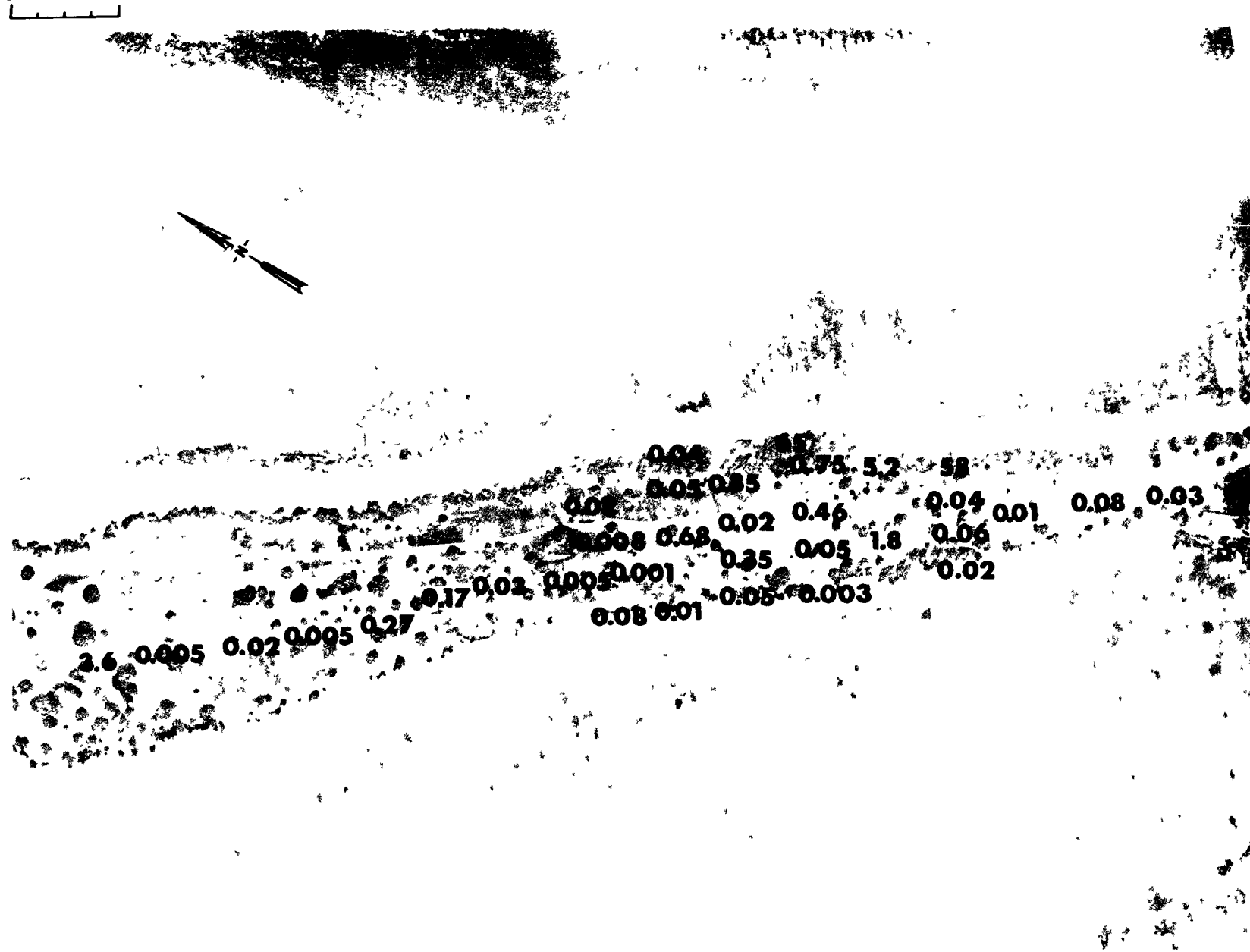
B.23.1.i.9. The average  $^{239}\text{Pu}$  activities (pCi/gm) in soil samples collected between depths of 80 and 90 cm.

100 METERS



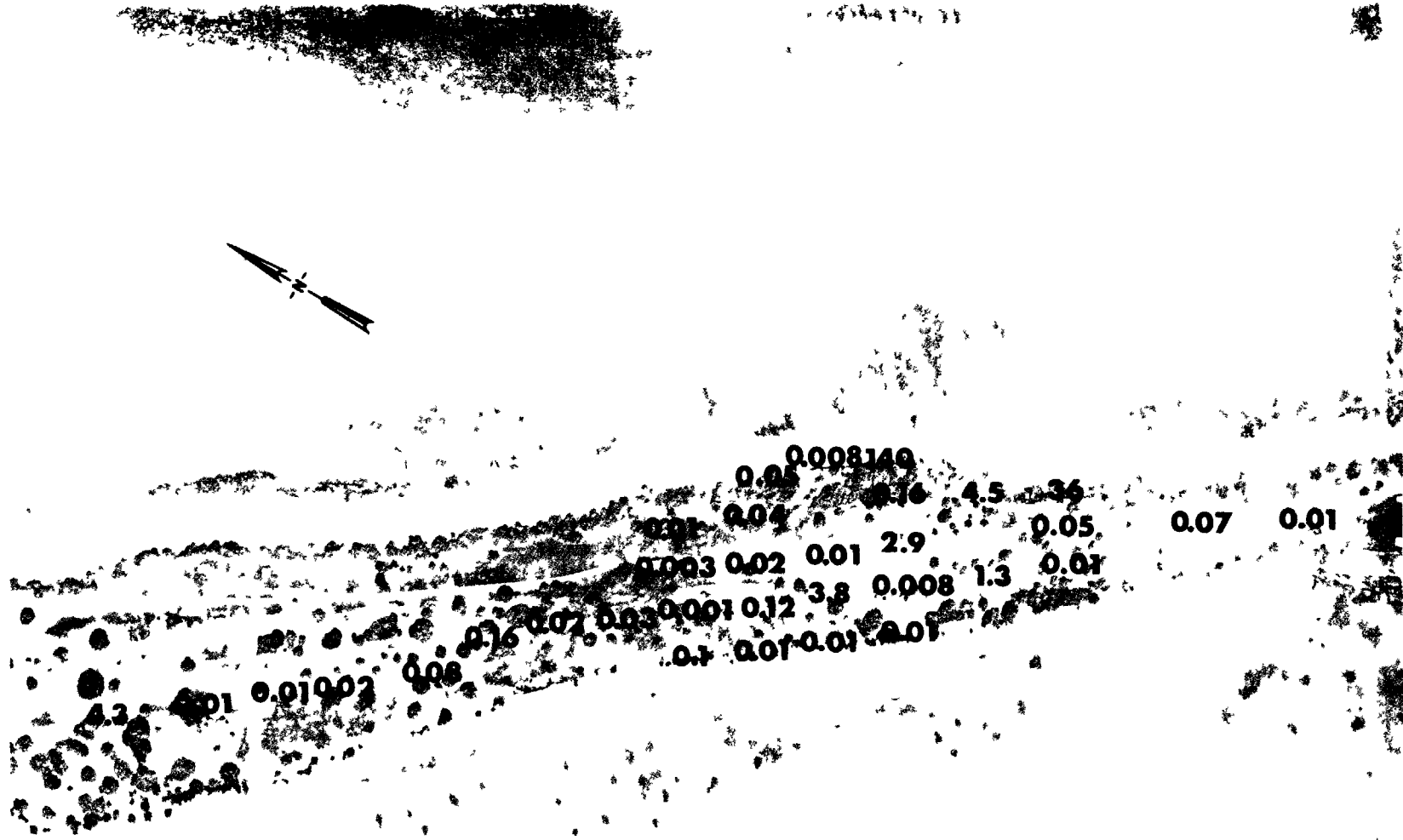
B.23.1.i.10. The average  $^{239}\text{Pu}$  activities (pCi/gm) in soil samples collected between depths of 90 and 100 cm.

100 METERS



B.23.1.i.11. The average  $^{239}\text{Pu}$  activities (pCi/gm) in soil samples collected between depths of 100 and 110 cm.

100 METERS



B.23.1.i.12. The average <sup>239</sup>Pu activities (pCi/gm) in soil samples collected between depths of 110 and 120 cm.

100 METERS



Fig. B.23.1.k. <sup>137</sup>Cs isoexposure and isoconcentration contours. (Refer to alphabetic symbol key in this appendix.)



100 METERS

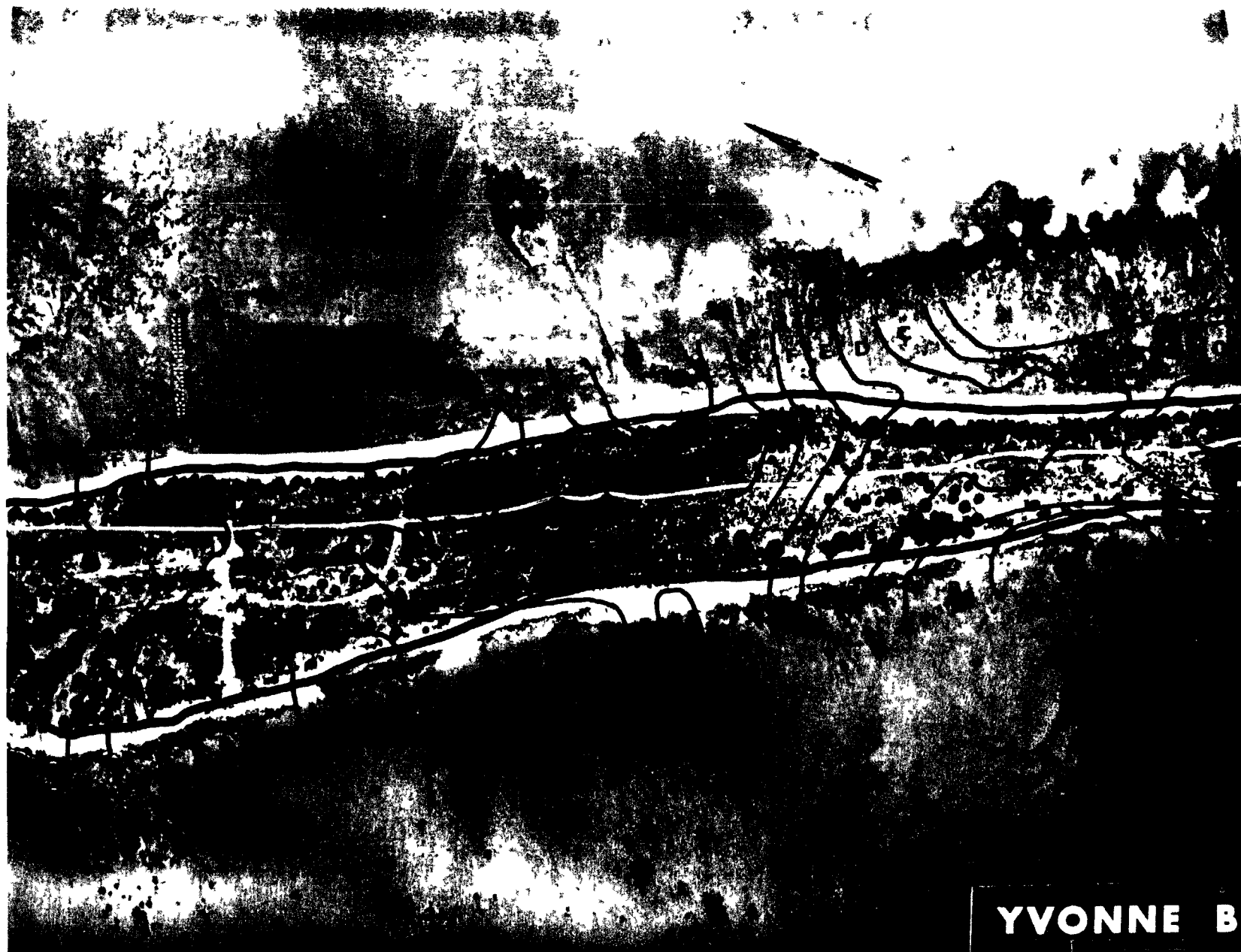
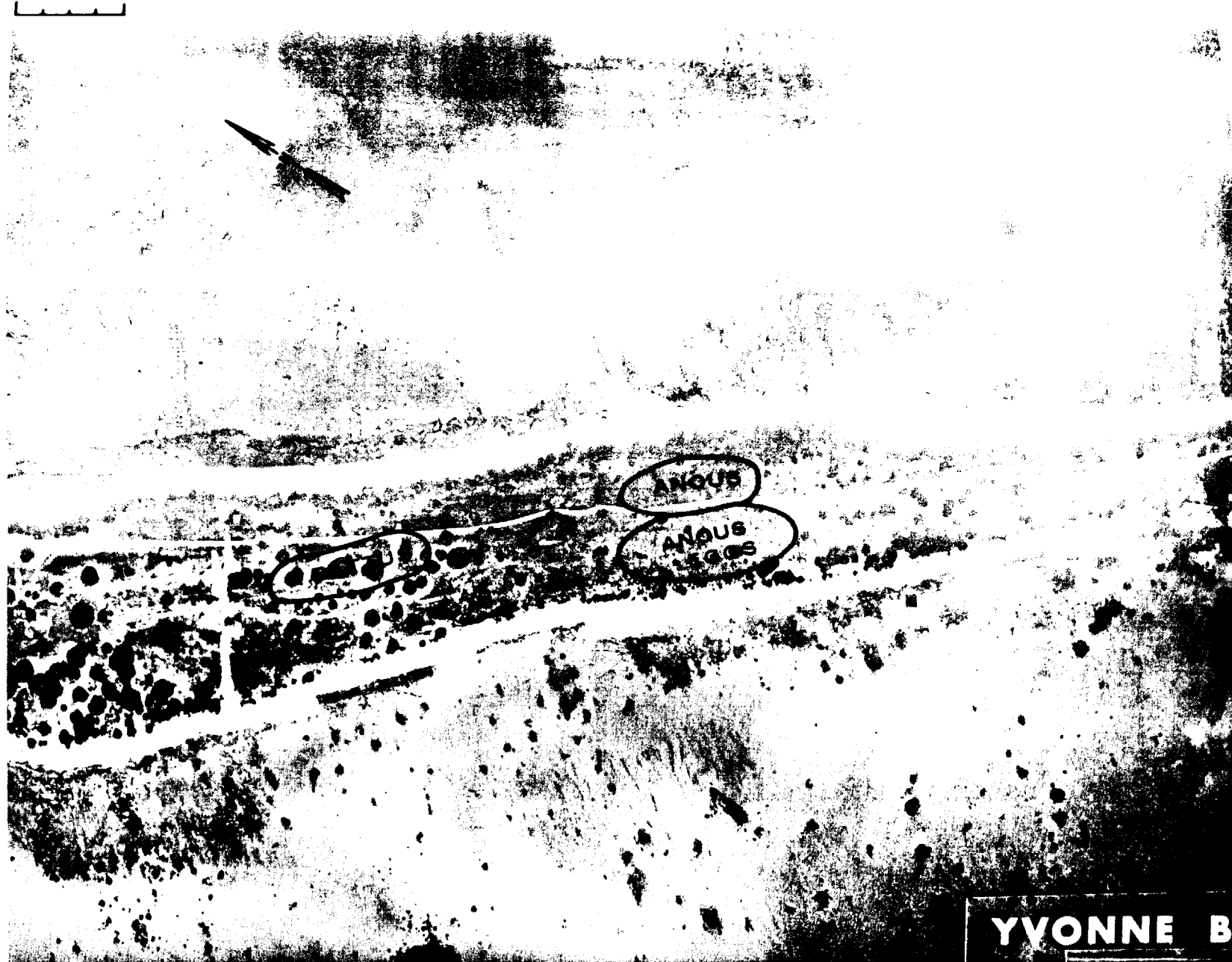


Fig. B.23.1.m.  $^{60}\text{Co}$  isoexposure and isoconcentration contours. (Refer to alphabetic symbol key in this appendix.)

100 METERS



YVONNE B

Fig. B.23.1.o. Terrestrial animal sample locations.

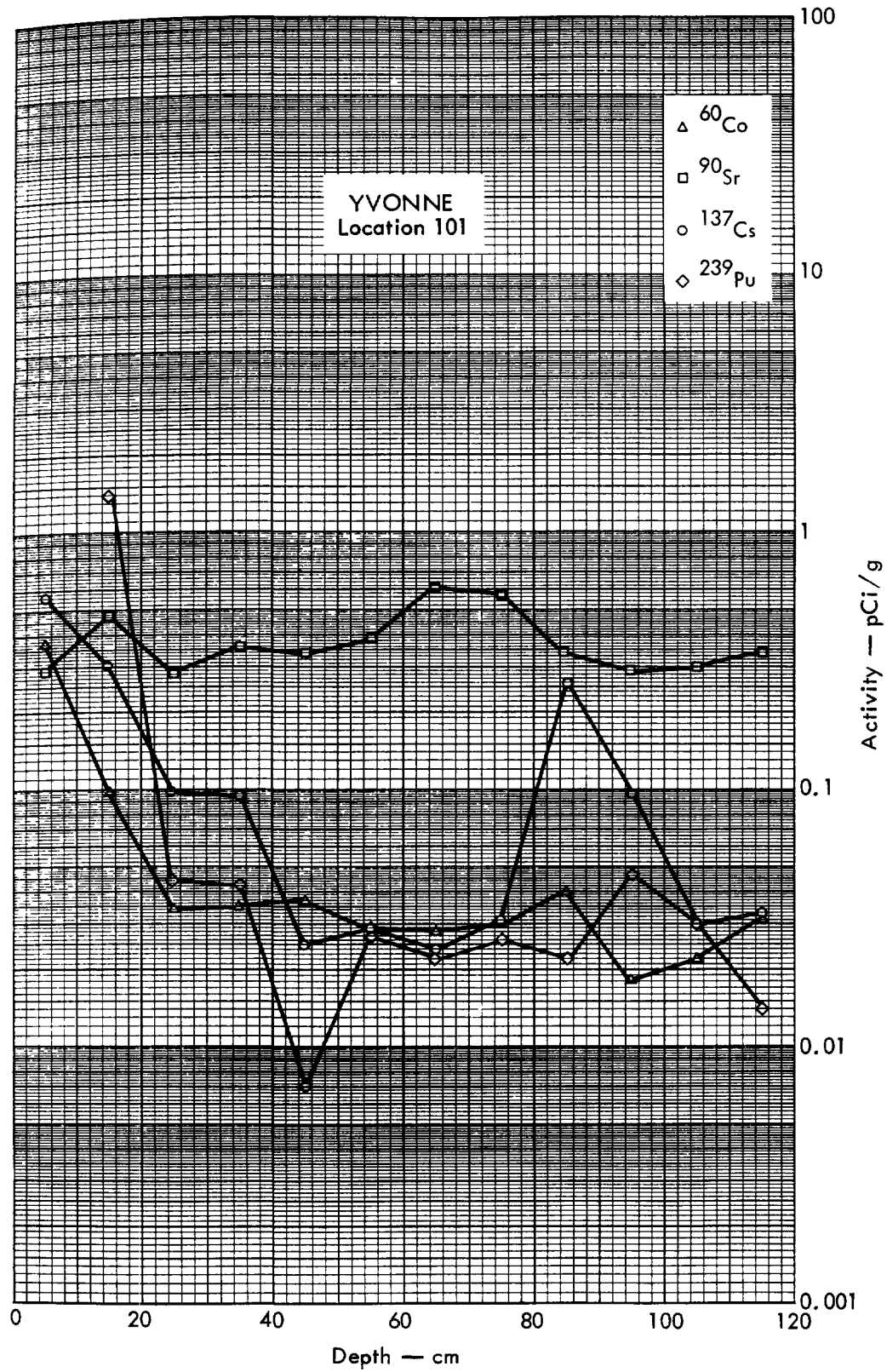


Fig. B. 23.2a. Activities of selected radionuclides as a function of soil depth.

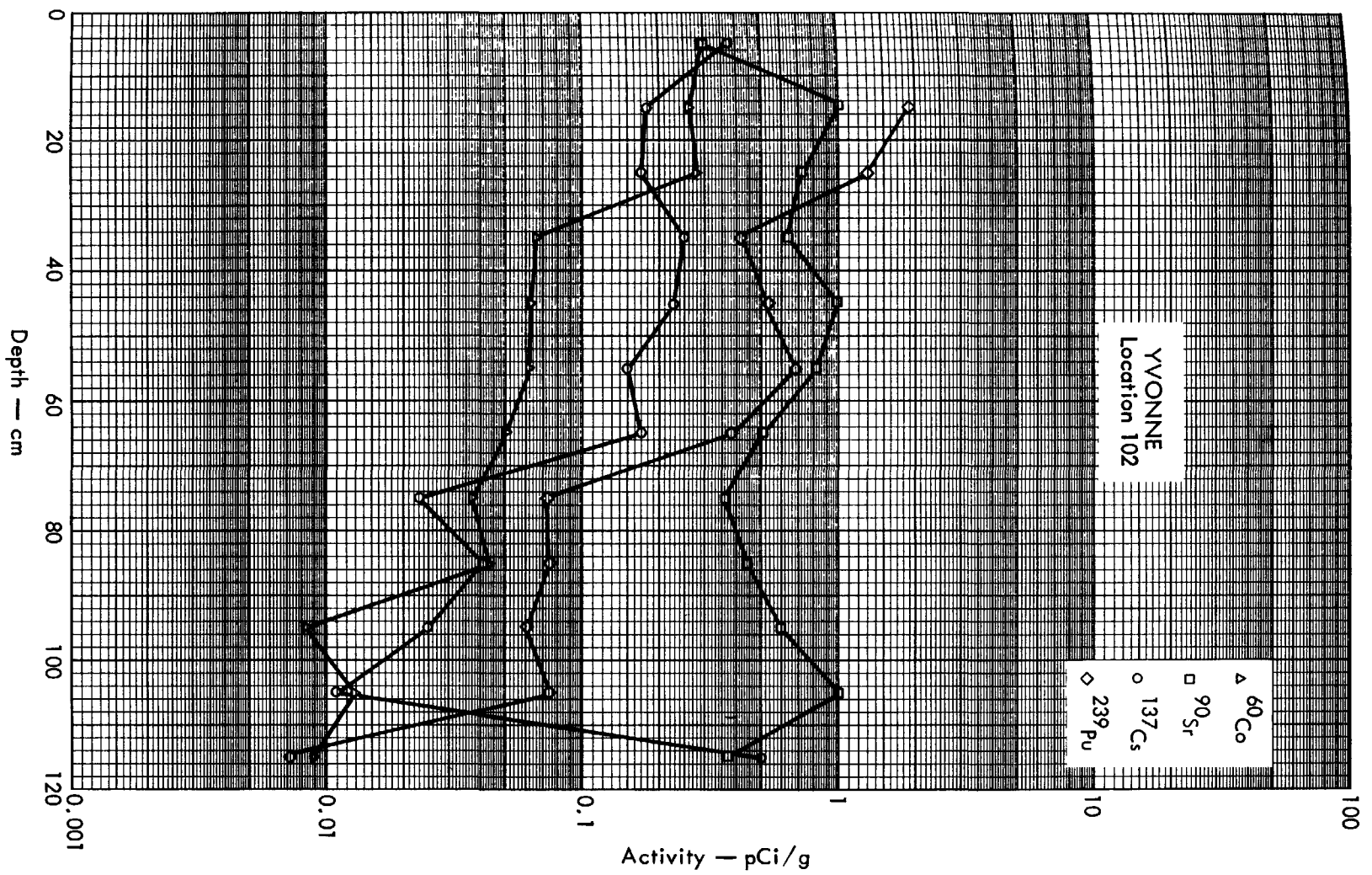


Fig. B. 23.2b. Activities of selected radionuclides as a function of soil depth.

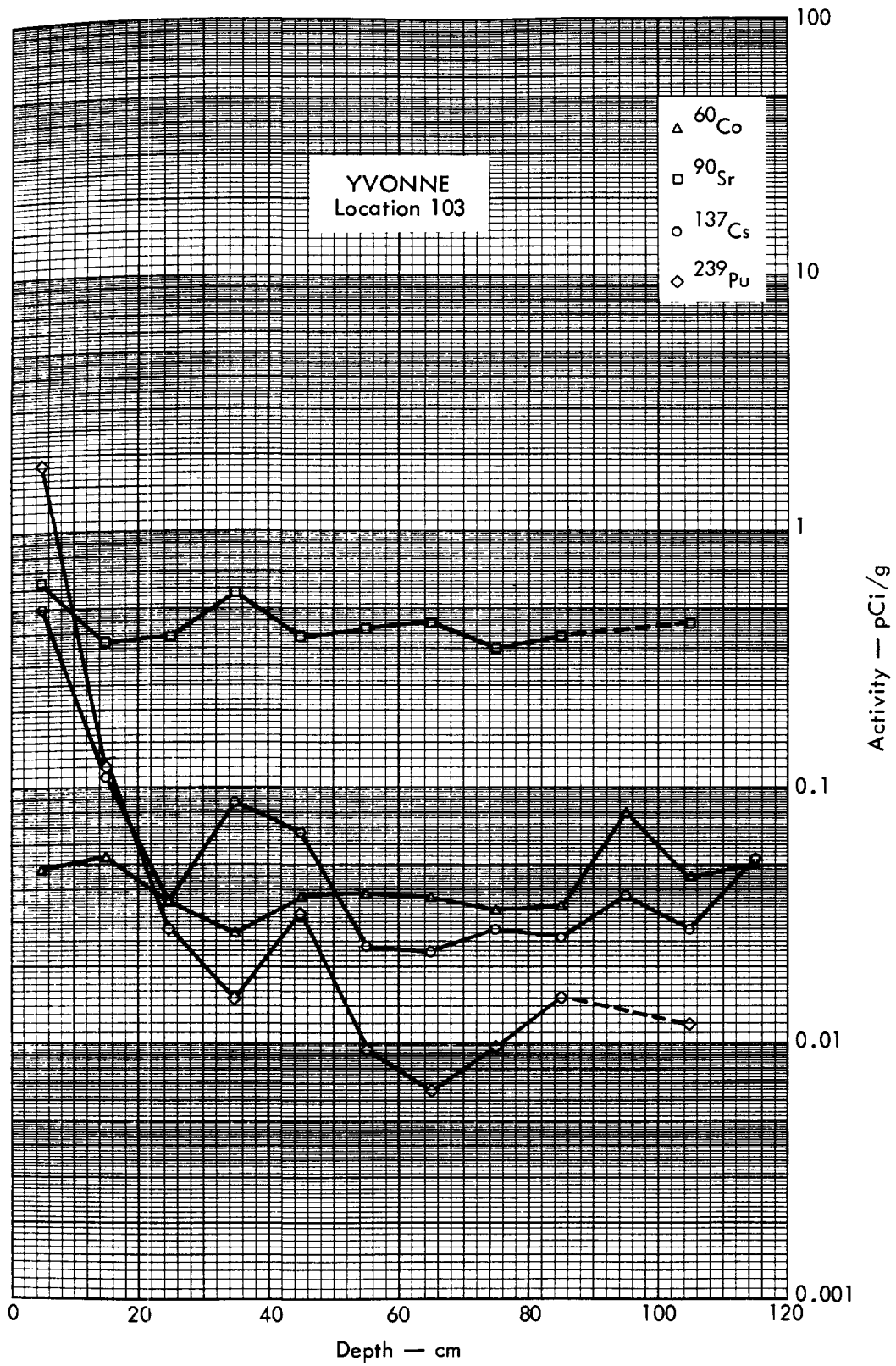


Fig. B. 23.2c. Activities of selected radionuclides as a function of soil depth.

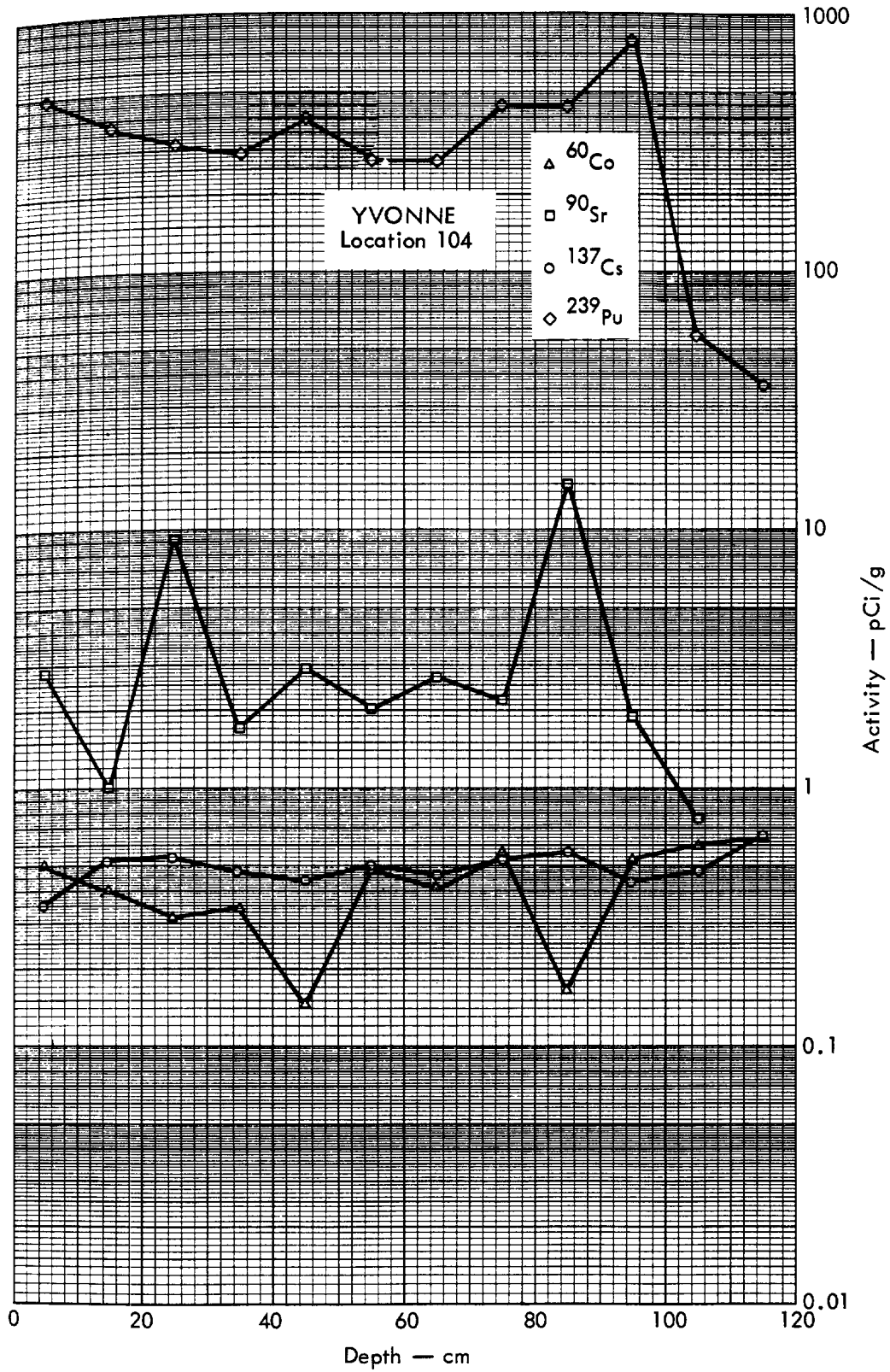


Fig. B. 23.2d. Activities of selected radionuclides as a function of soil depth.

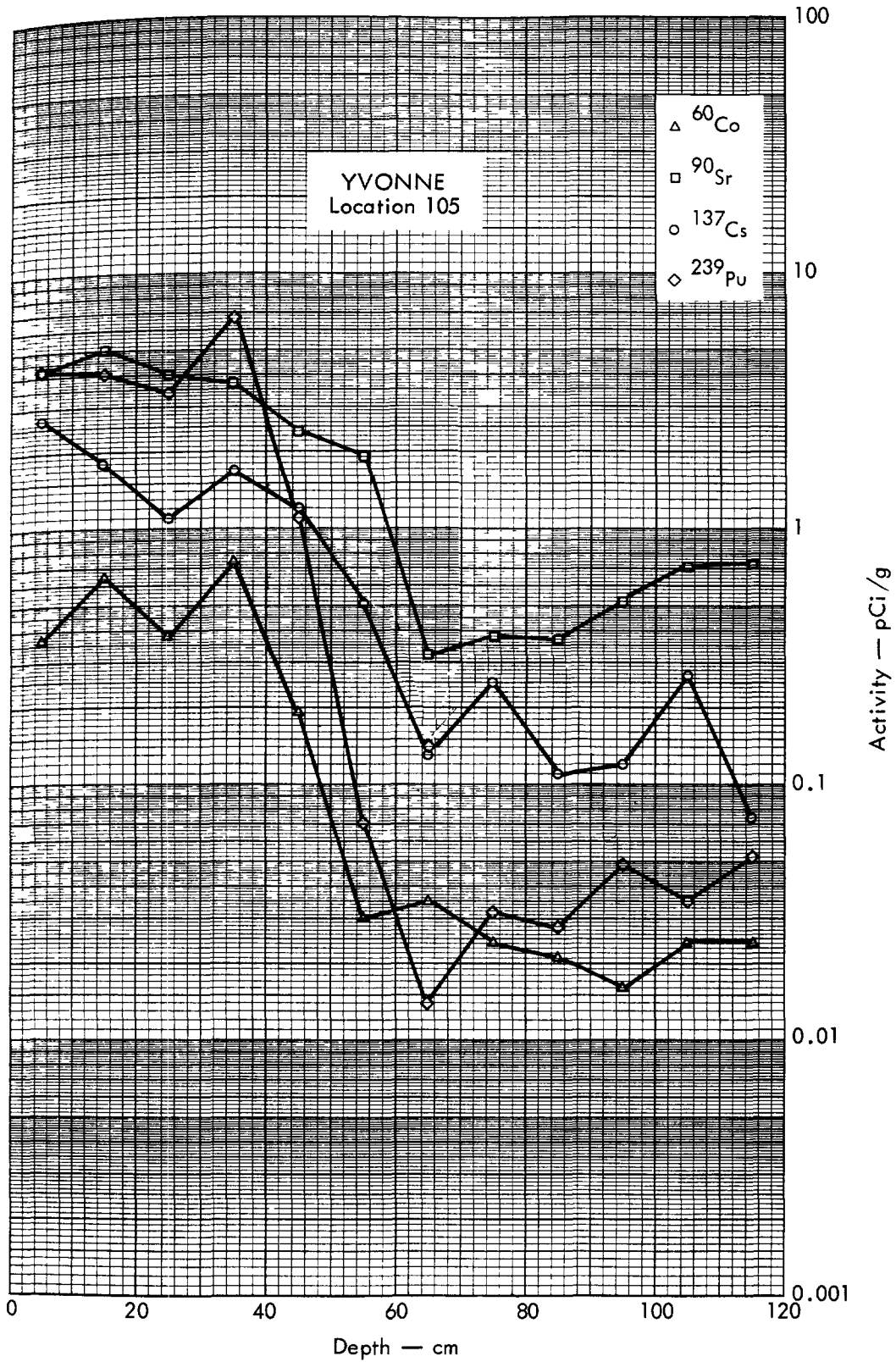


Fig. B. 23.2e. Activities of selected radionuclides as a function of soil depth.



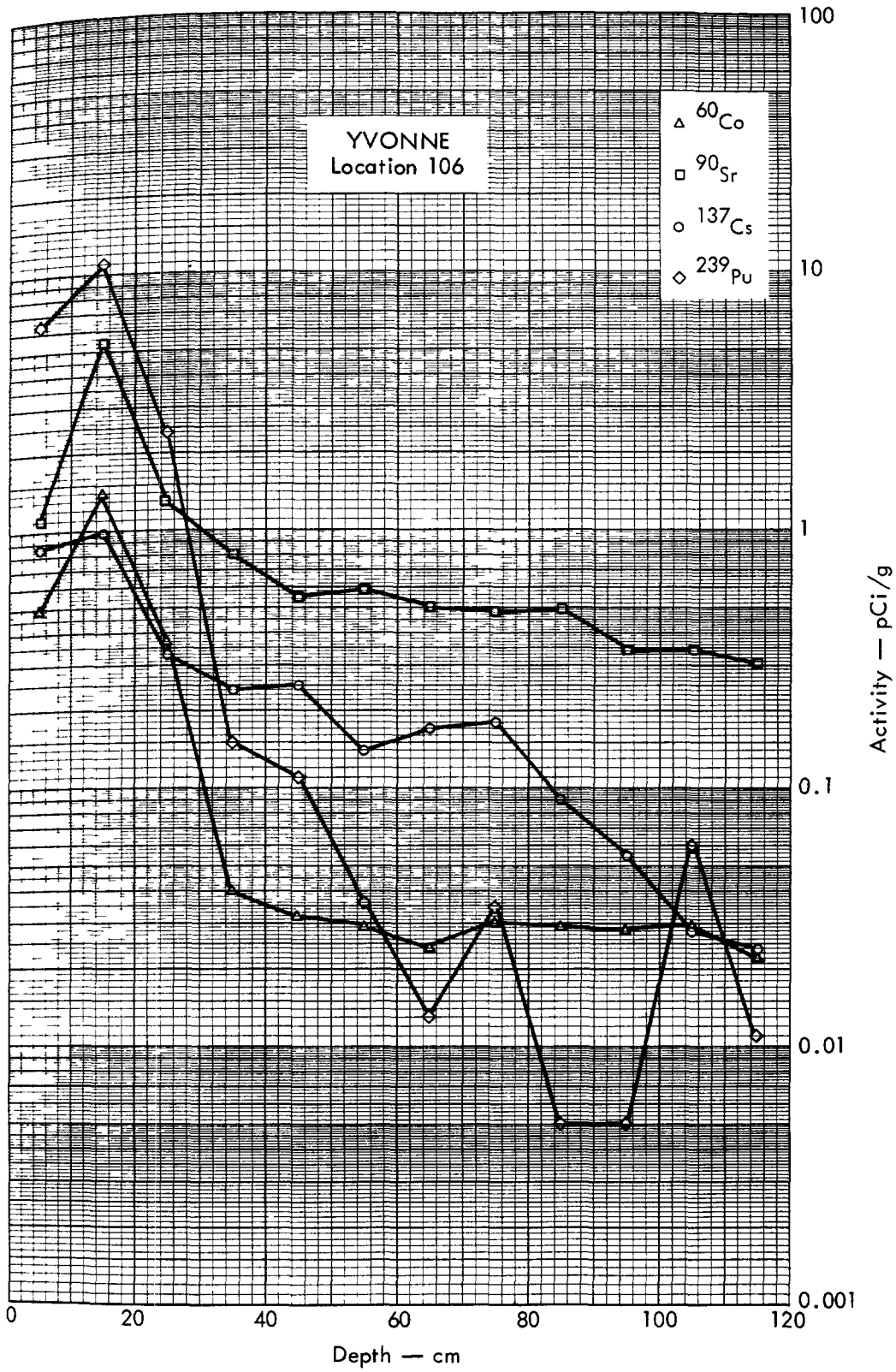


Fig. B. 23.2f. Activities of selected radionuclides as a function of soil depth.



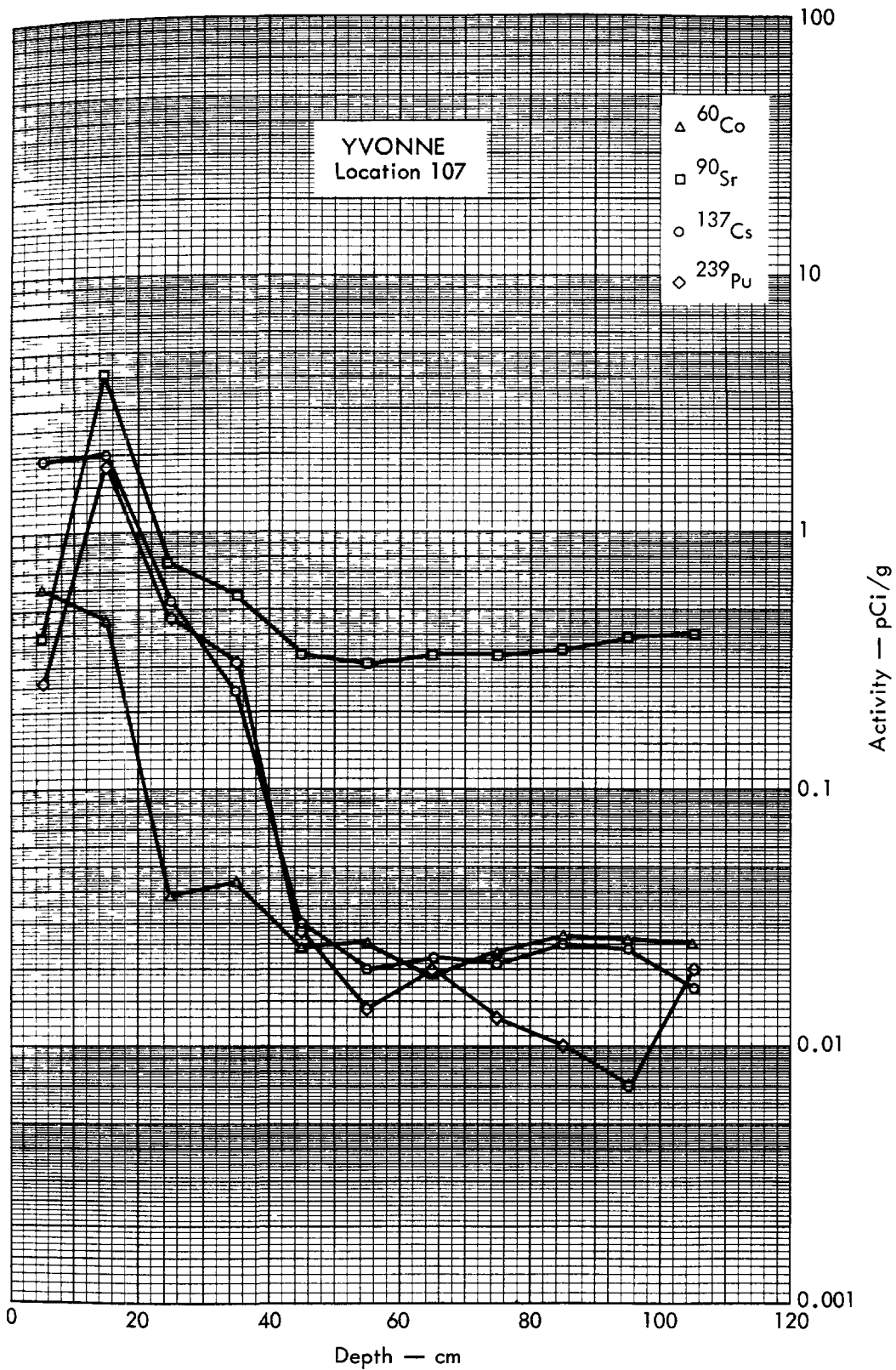


Fig. B. 23.2g. Activities of selected radionuclides as a function of soil depth.

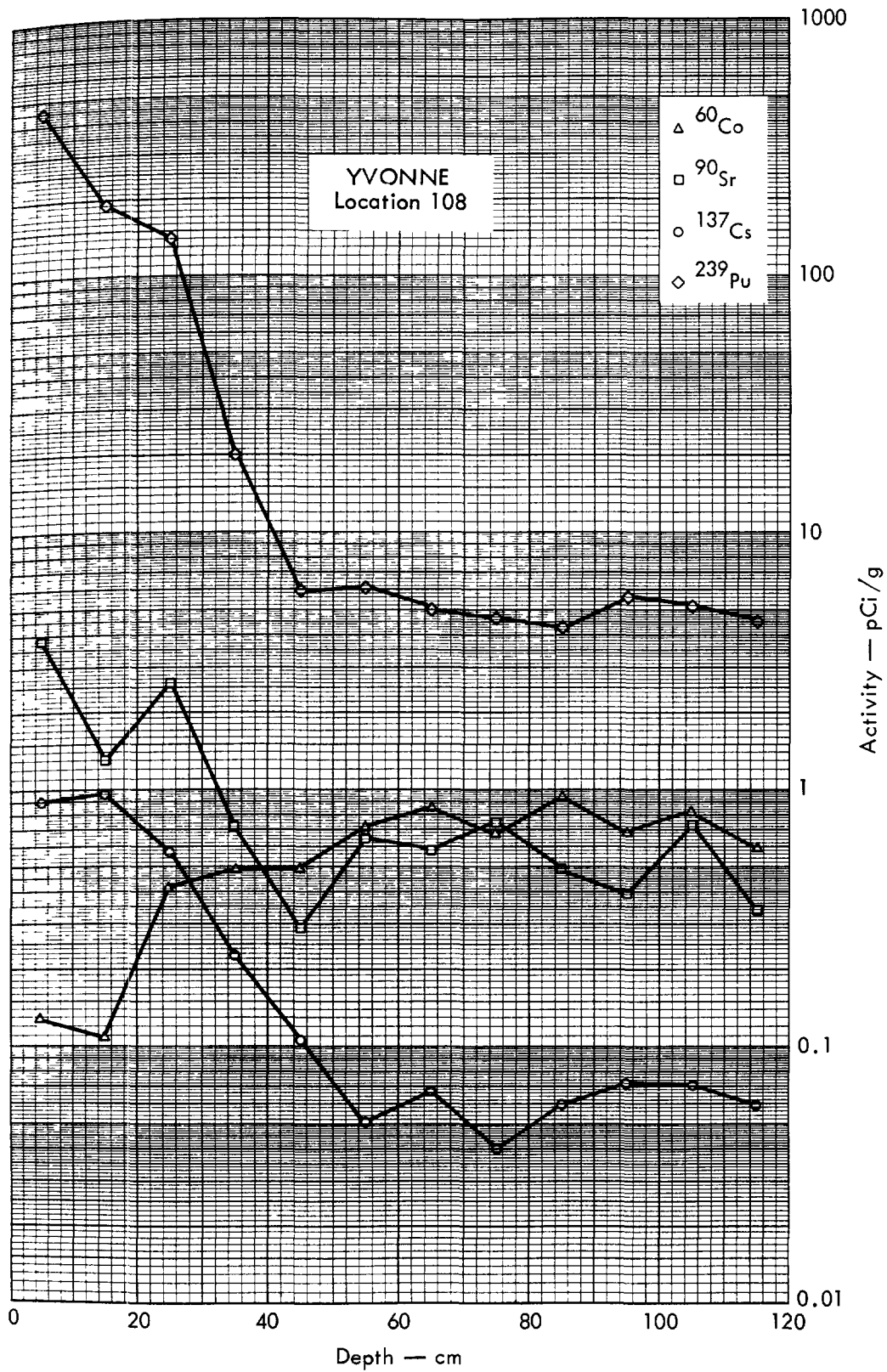


Fig. B. 23.2h. Activities of selected radionuclides as a function of soil depth.

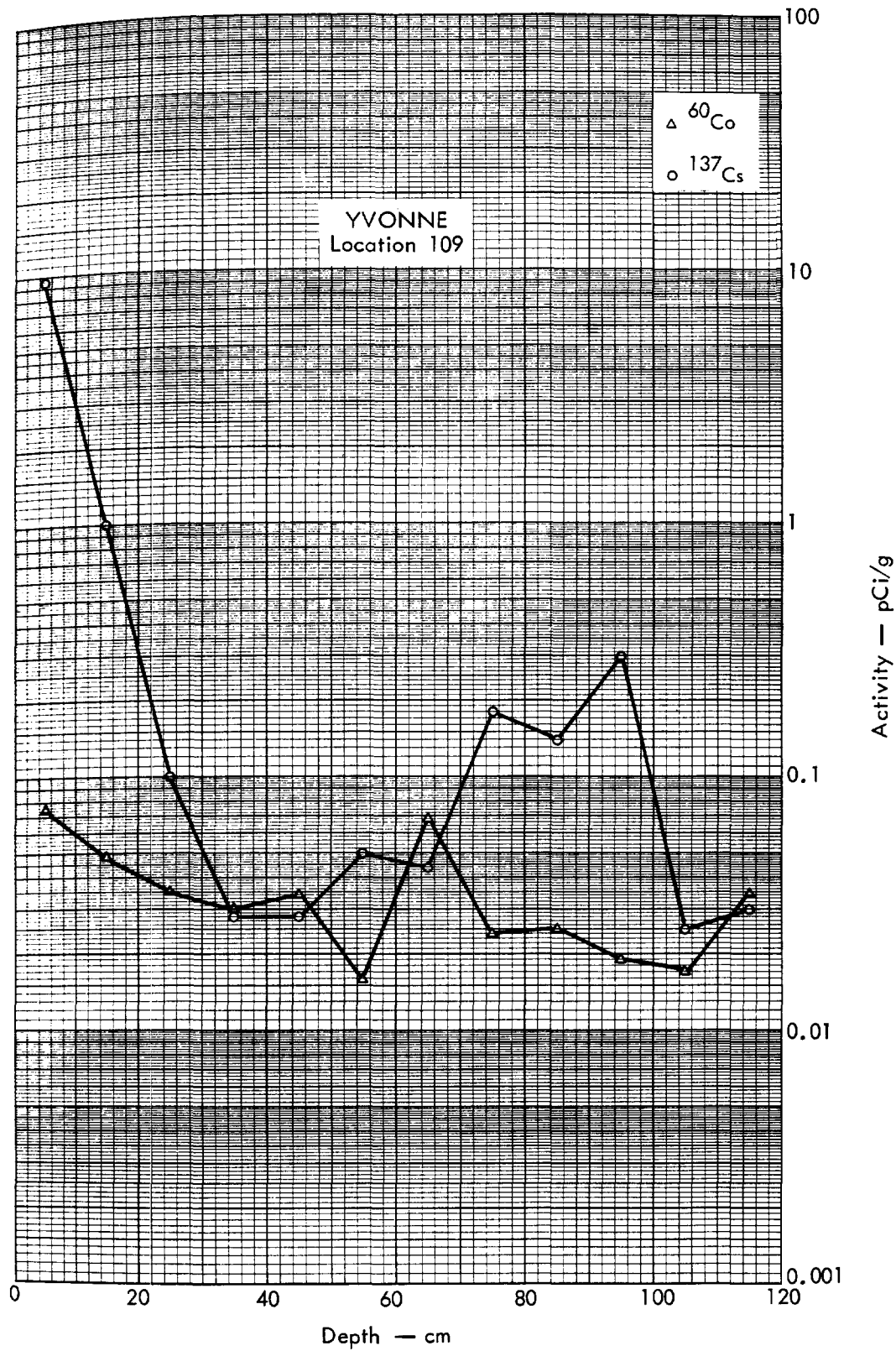


Fig. B. 23.2i. Activities of selected radionuclides as a function of soil depth.

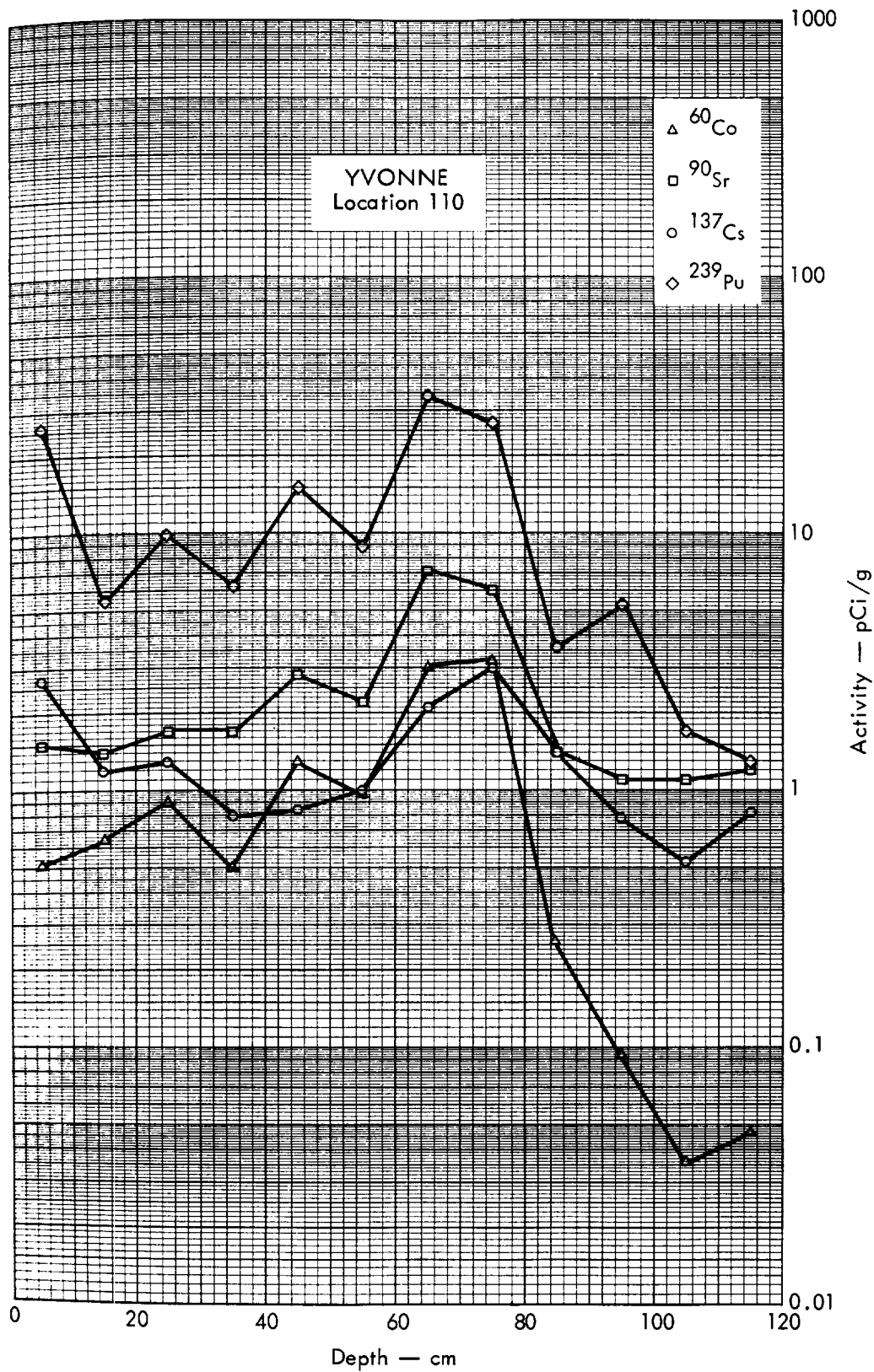


Fig. B. 23.2j. Activities of selected radionuclides as a function of soil depth.

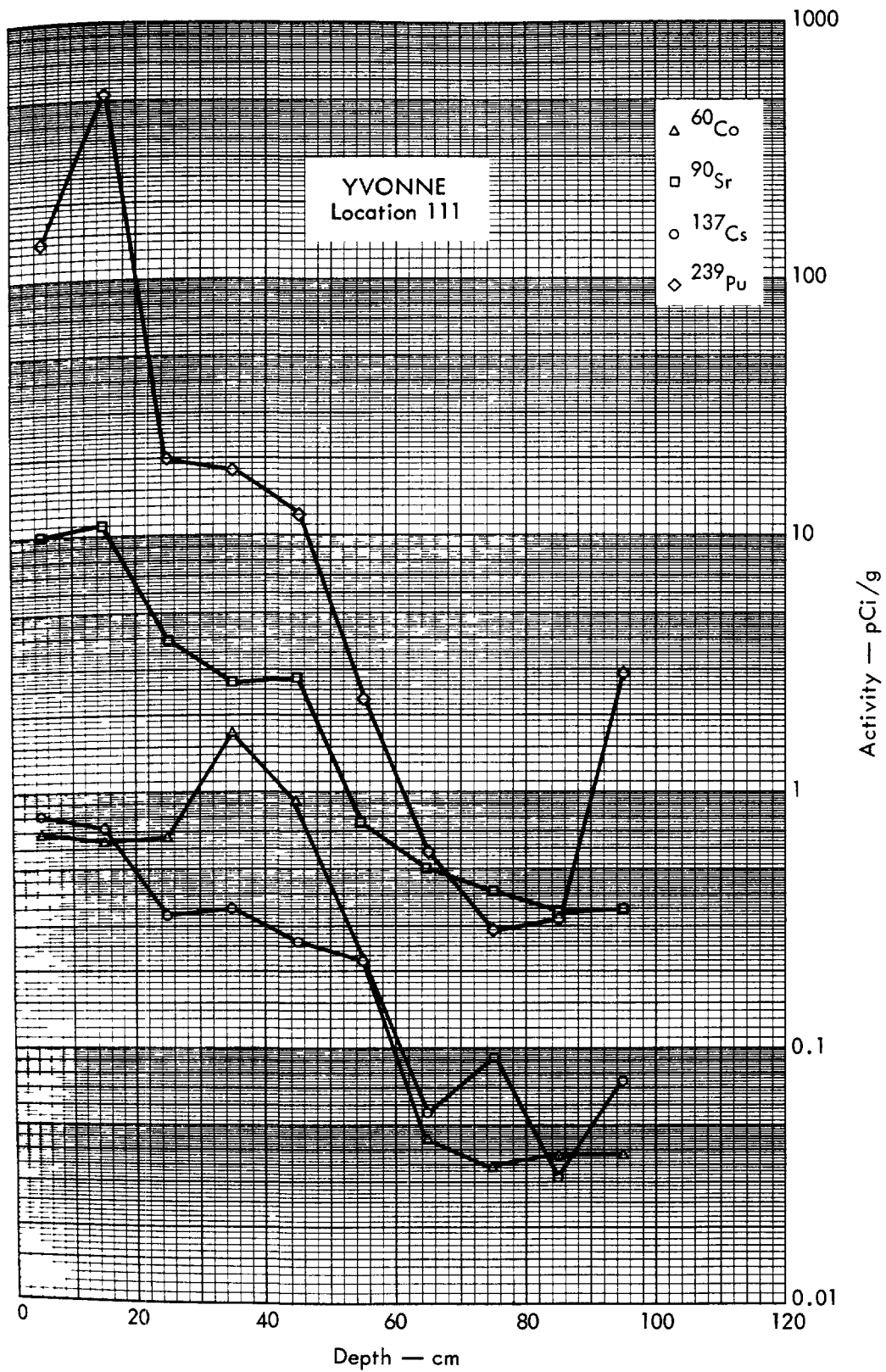


Fig. B. 23.2k. Activities of selected radionuclides as a function of soil depth.

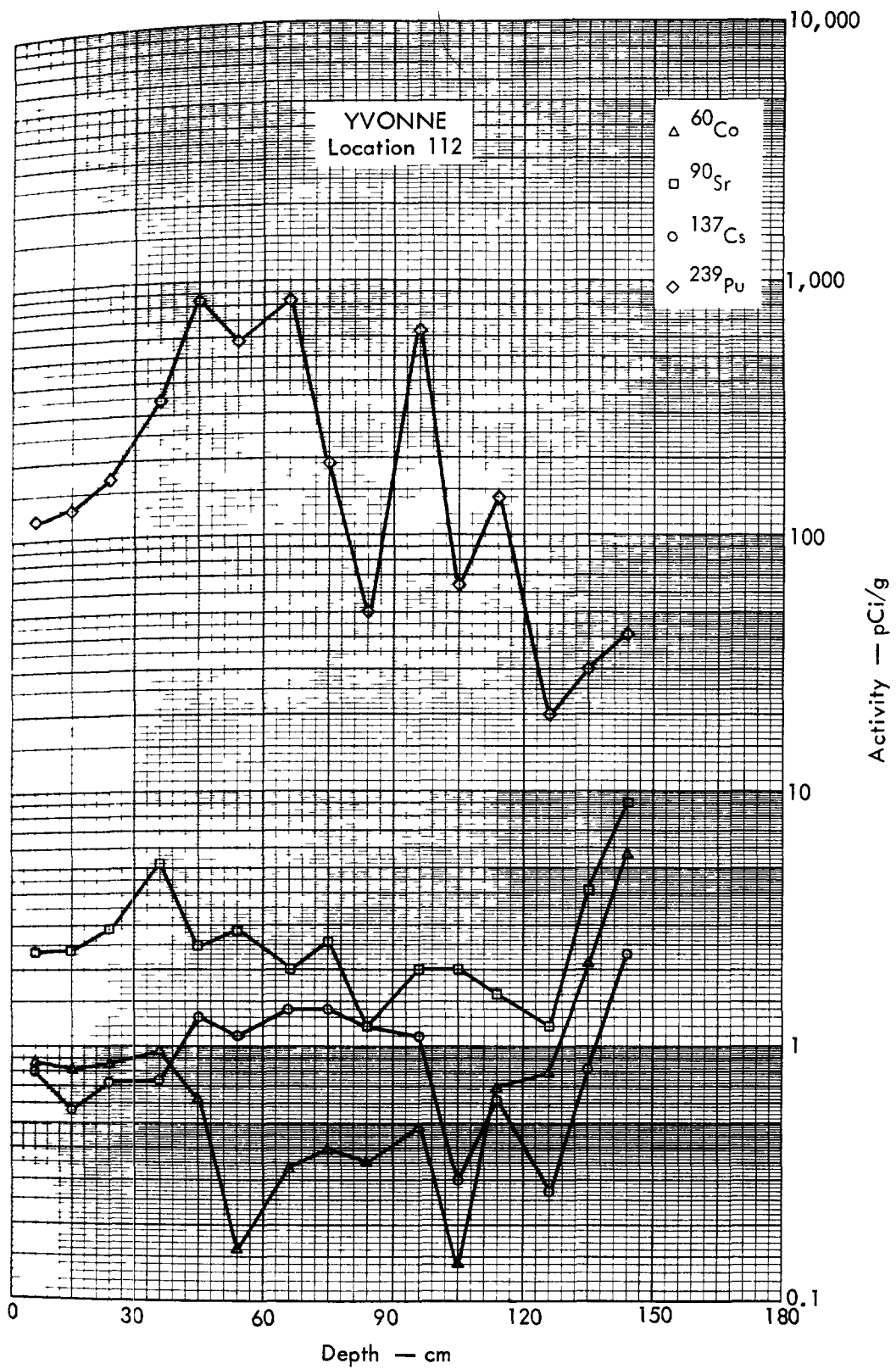


Fig. B. 23.21. Activities of selected radionuclides as a function of soil depth.

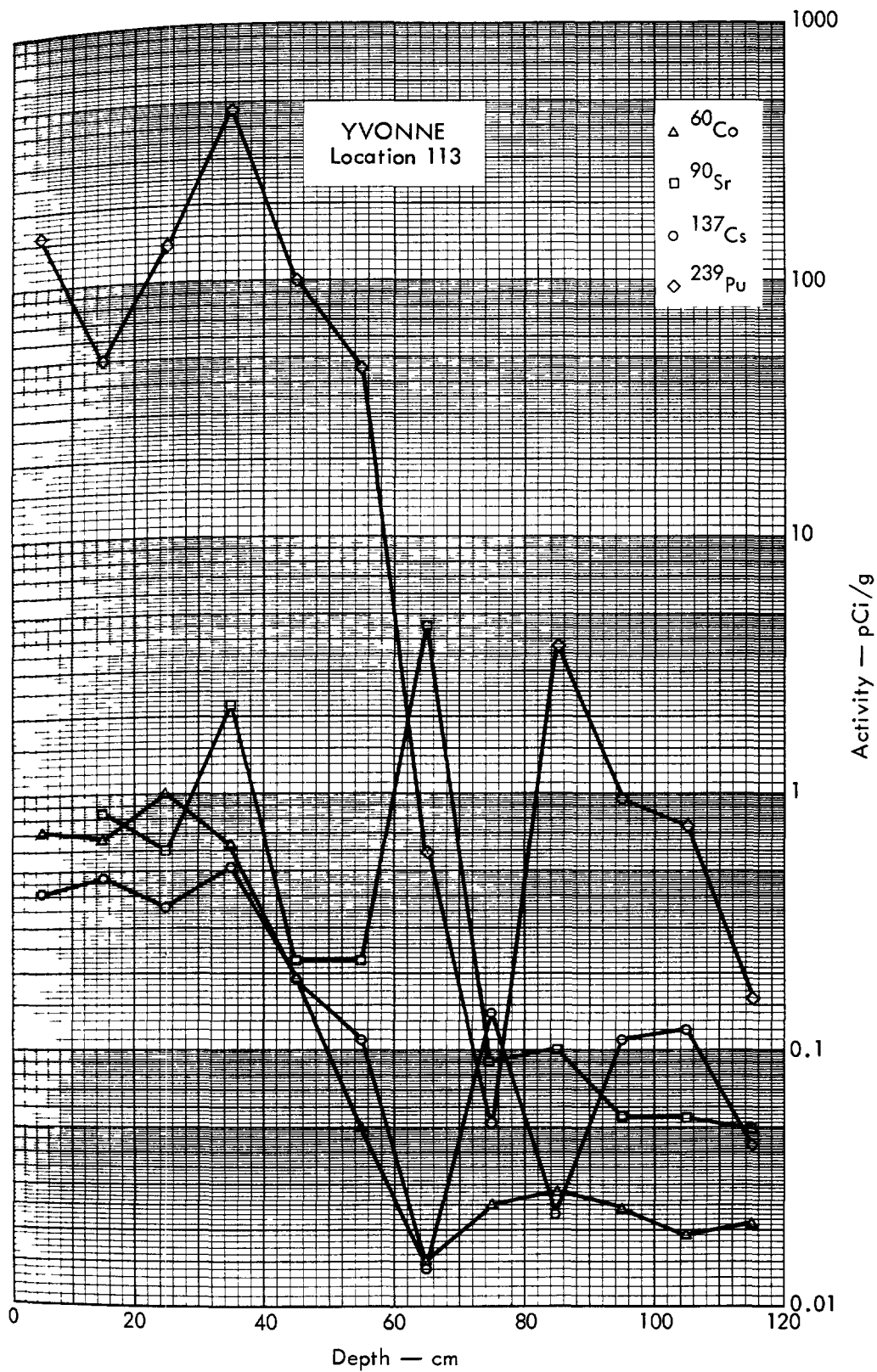


Fig. B. 23.2m. Activities of selected radionuclides as a function of soil depth.

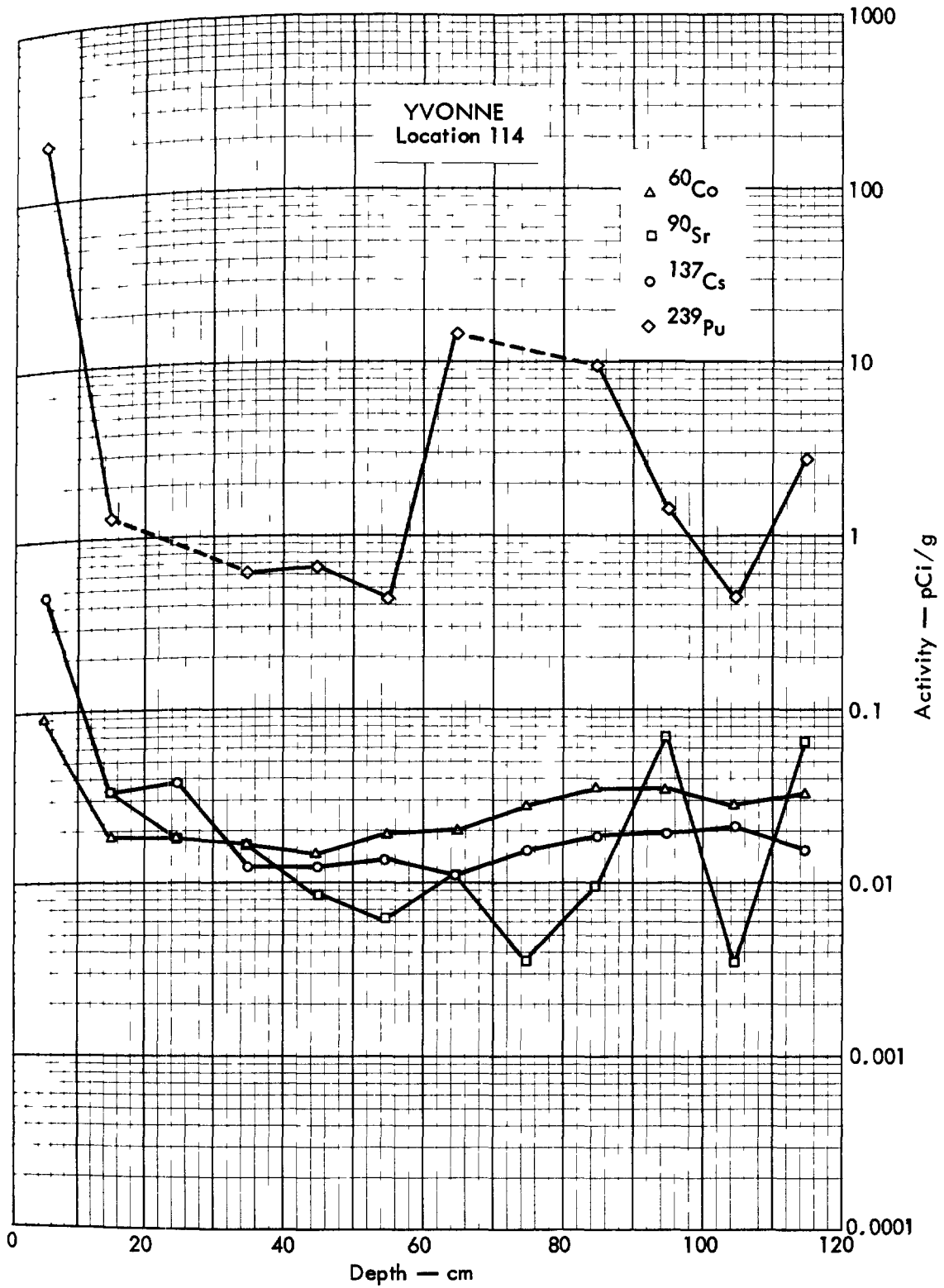


Fig. B. 23.2n. Activities of selected radionuclides as a function of soil depth.



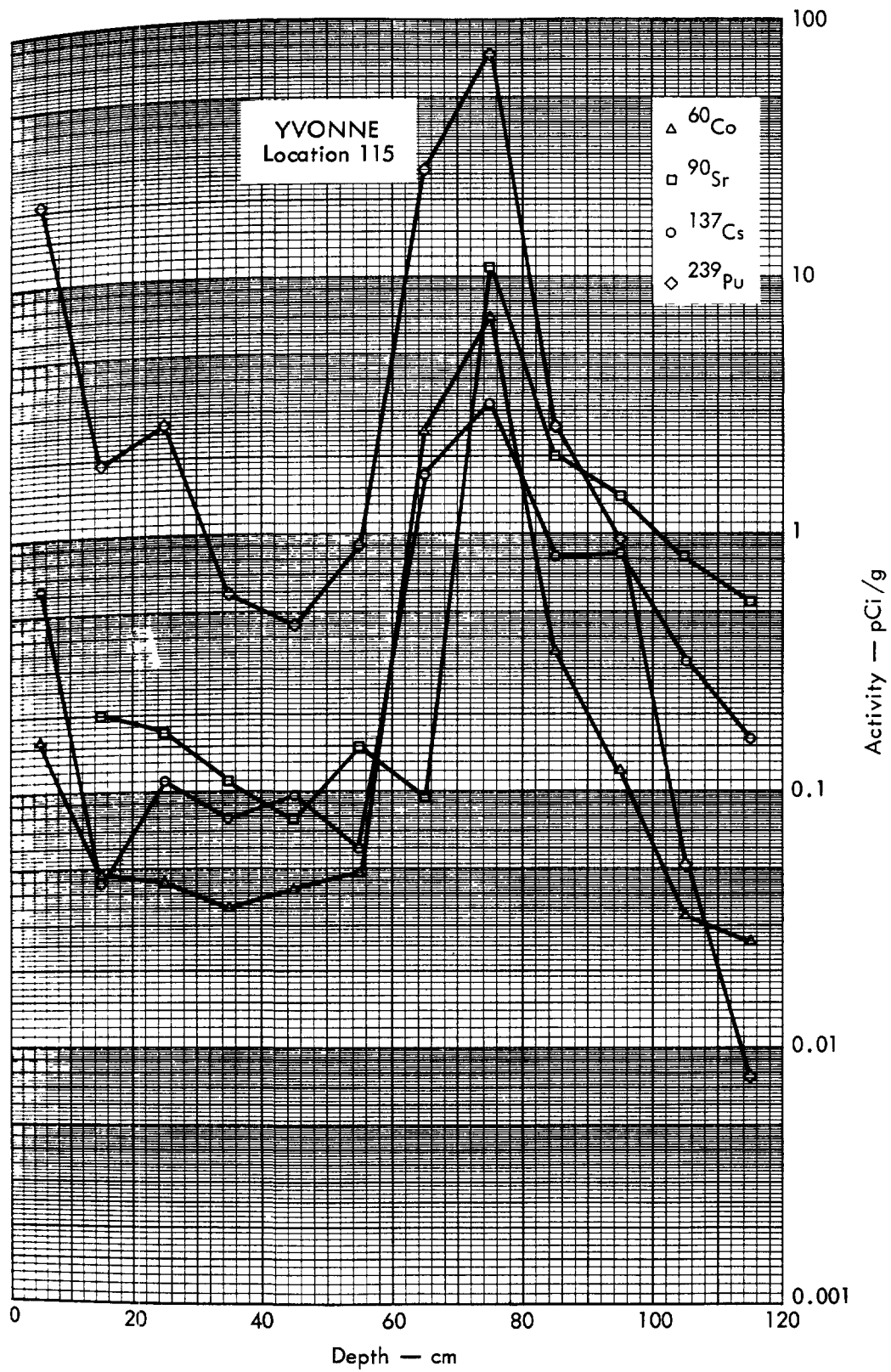


Fig. B.23.20. Activities of selected radionuclides as a function of soil depth.

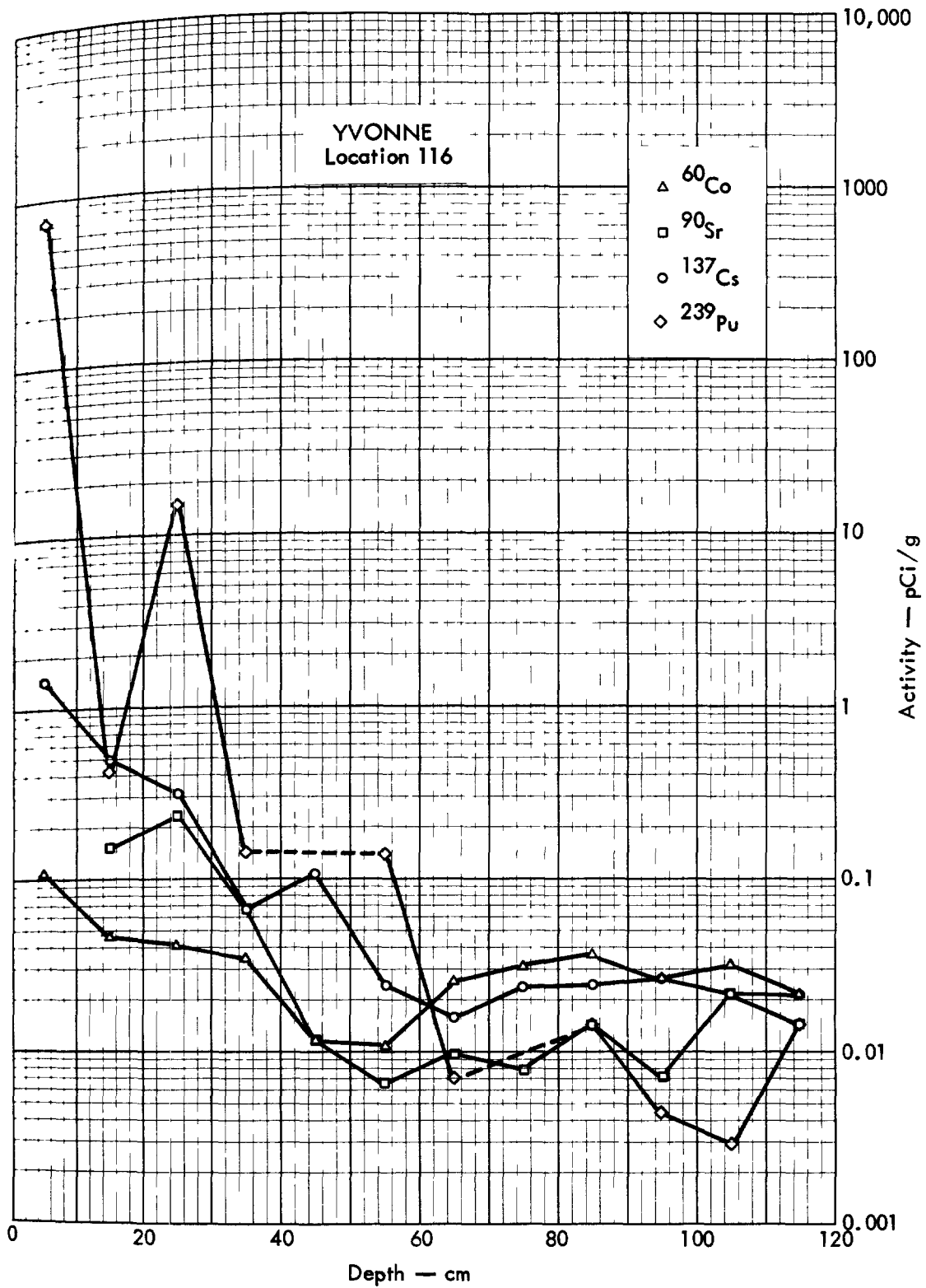


Fig. B. 23.2p. Activities of selected radionuclides as a function of soil depth.

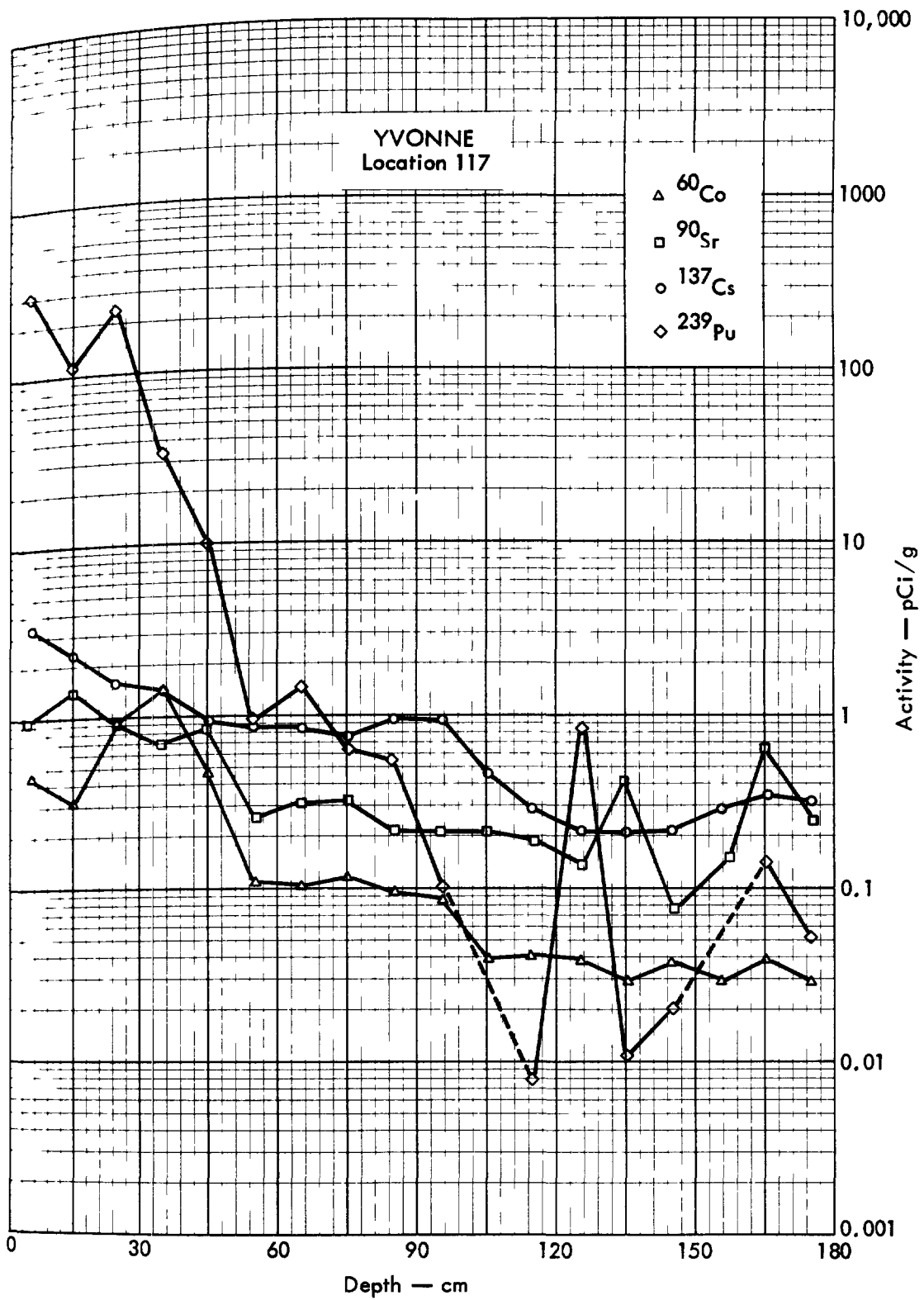


Fig. B. 23.2q. Activities of selected radionuclides as a function of soil depth.

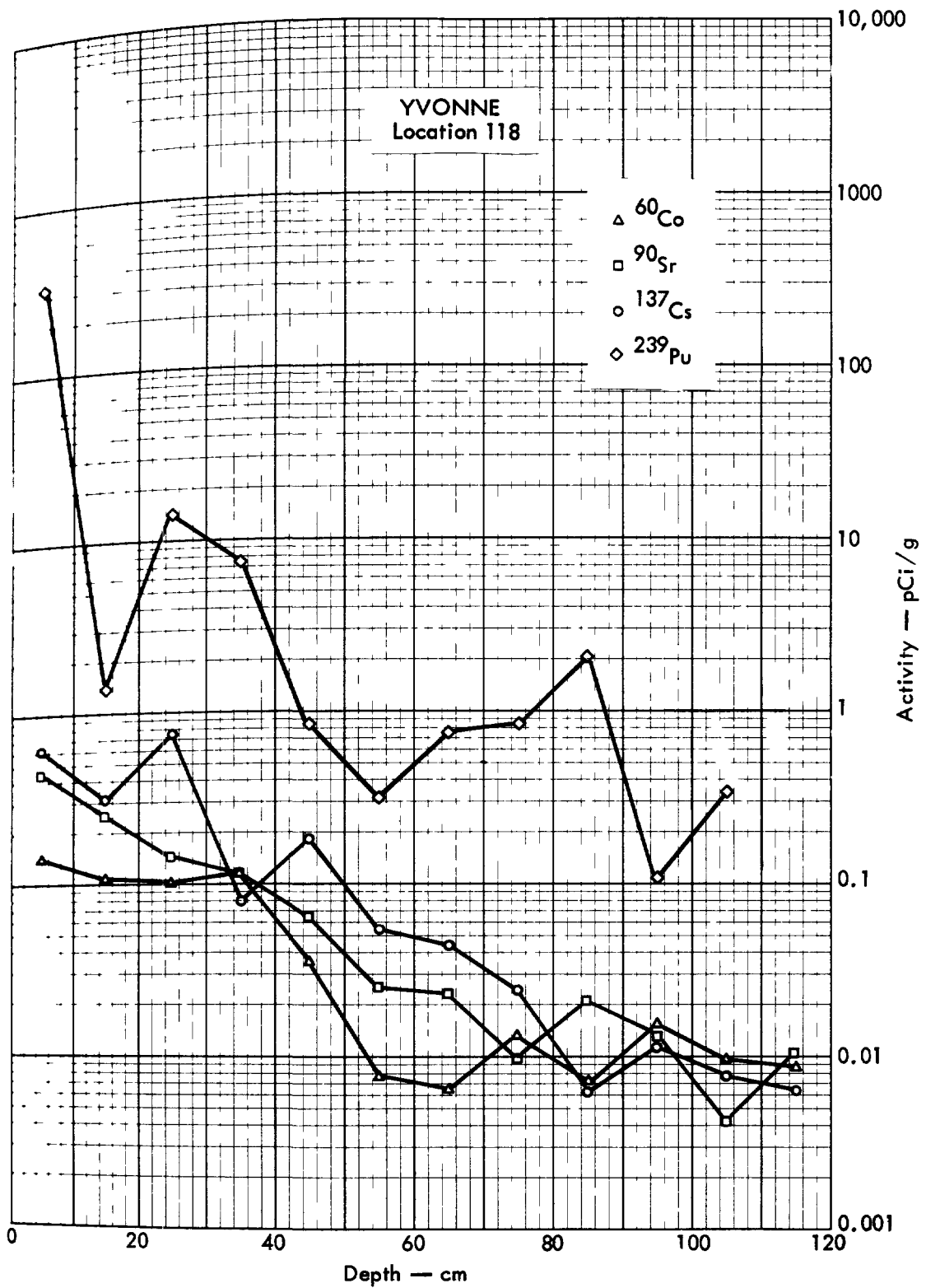


Fig. B. 23.2r. Activities of selected radionuclides as a function of soil depth.

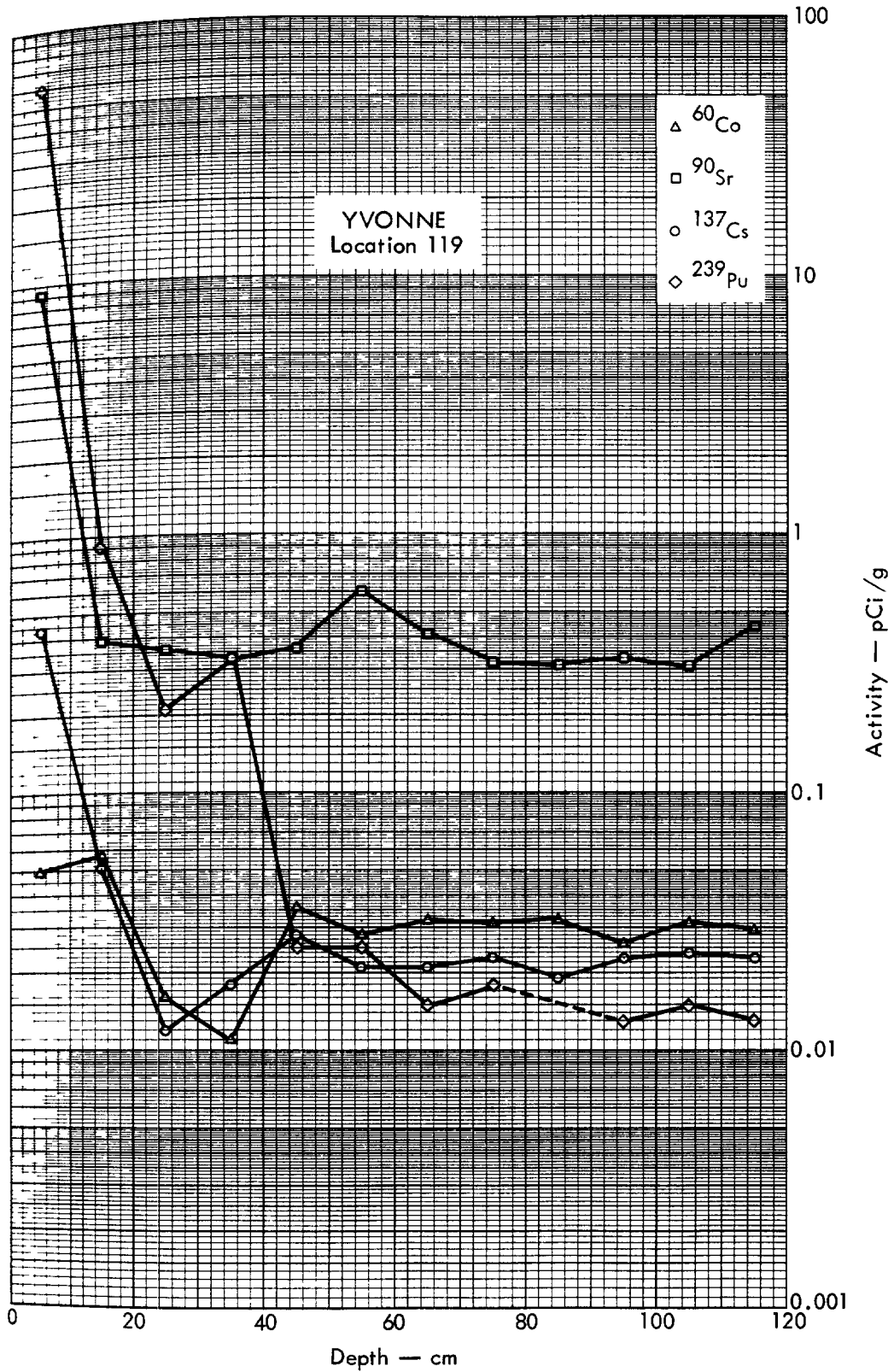


Fig. B. 23.2s. Activities of selected radionuclides as a function of soil depth.

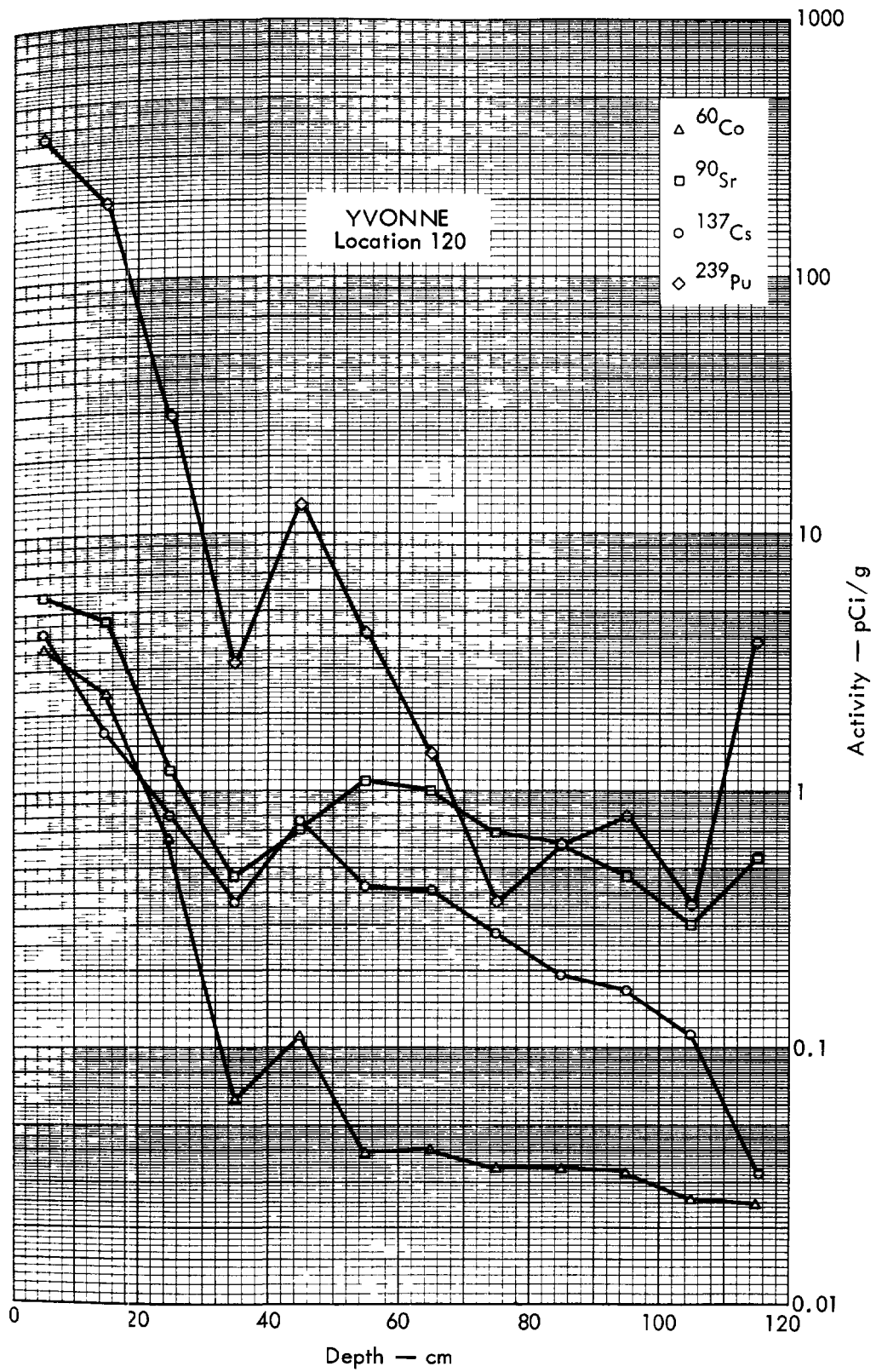


Fig. B. 23.2t. Activities of selected radionuclides as a function of soil depth.

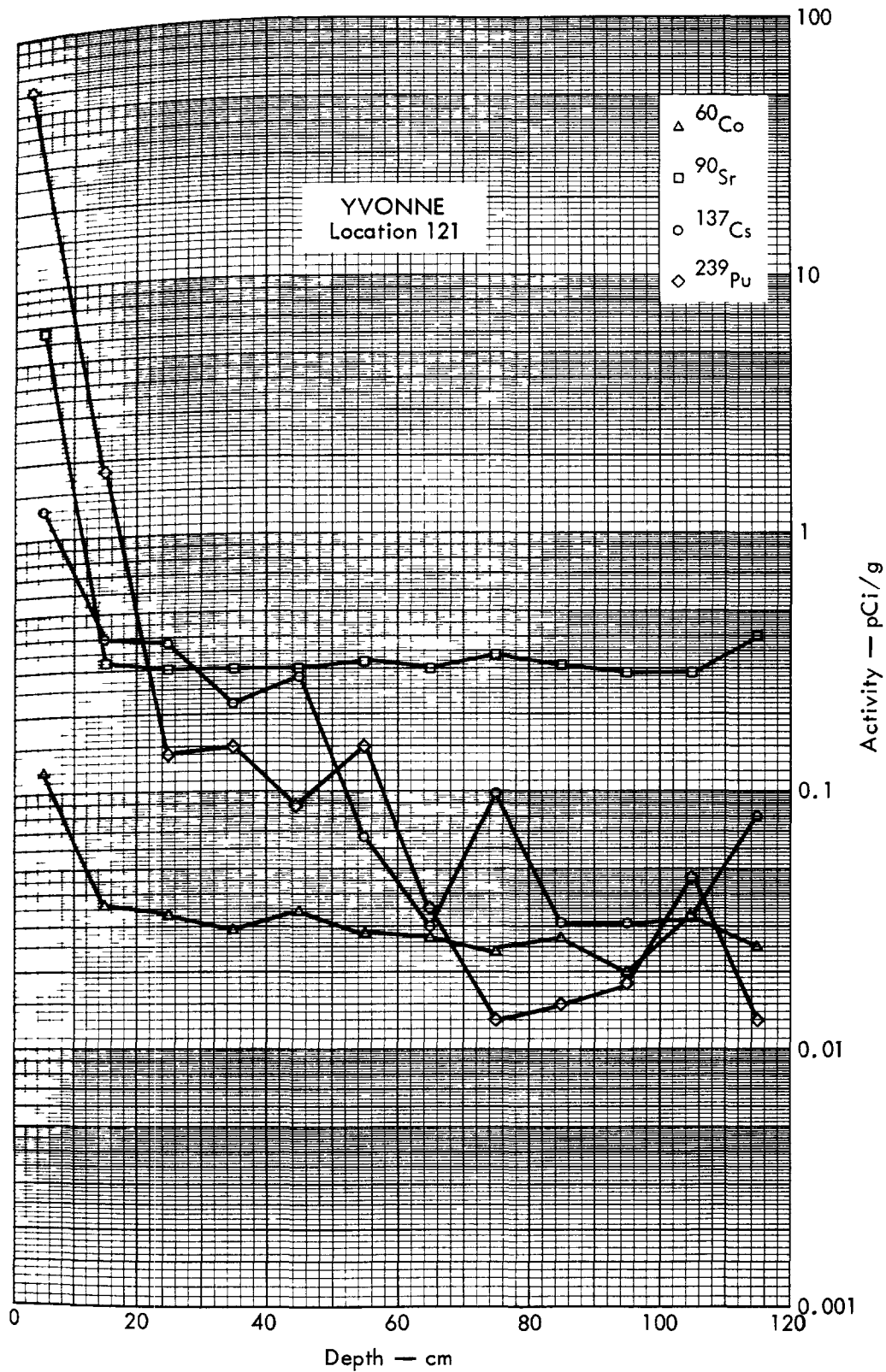


Fig. B. 23.2u. Activities of selected radionuclides as a function of soil depth.

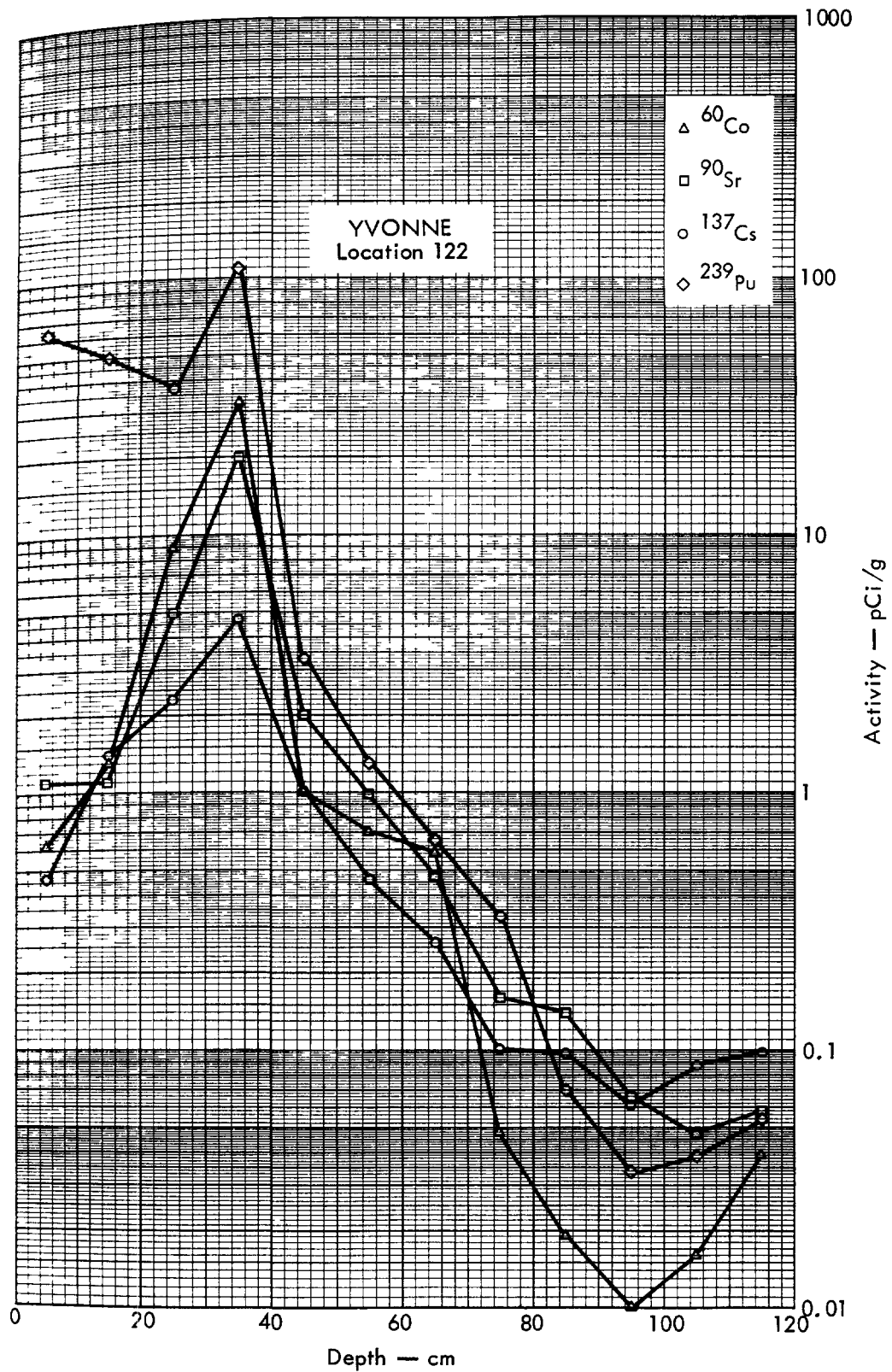


Fig. B. 23.2v. Activities of selected radionuclides as a function of soil depth.



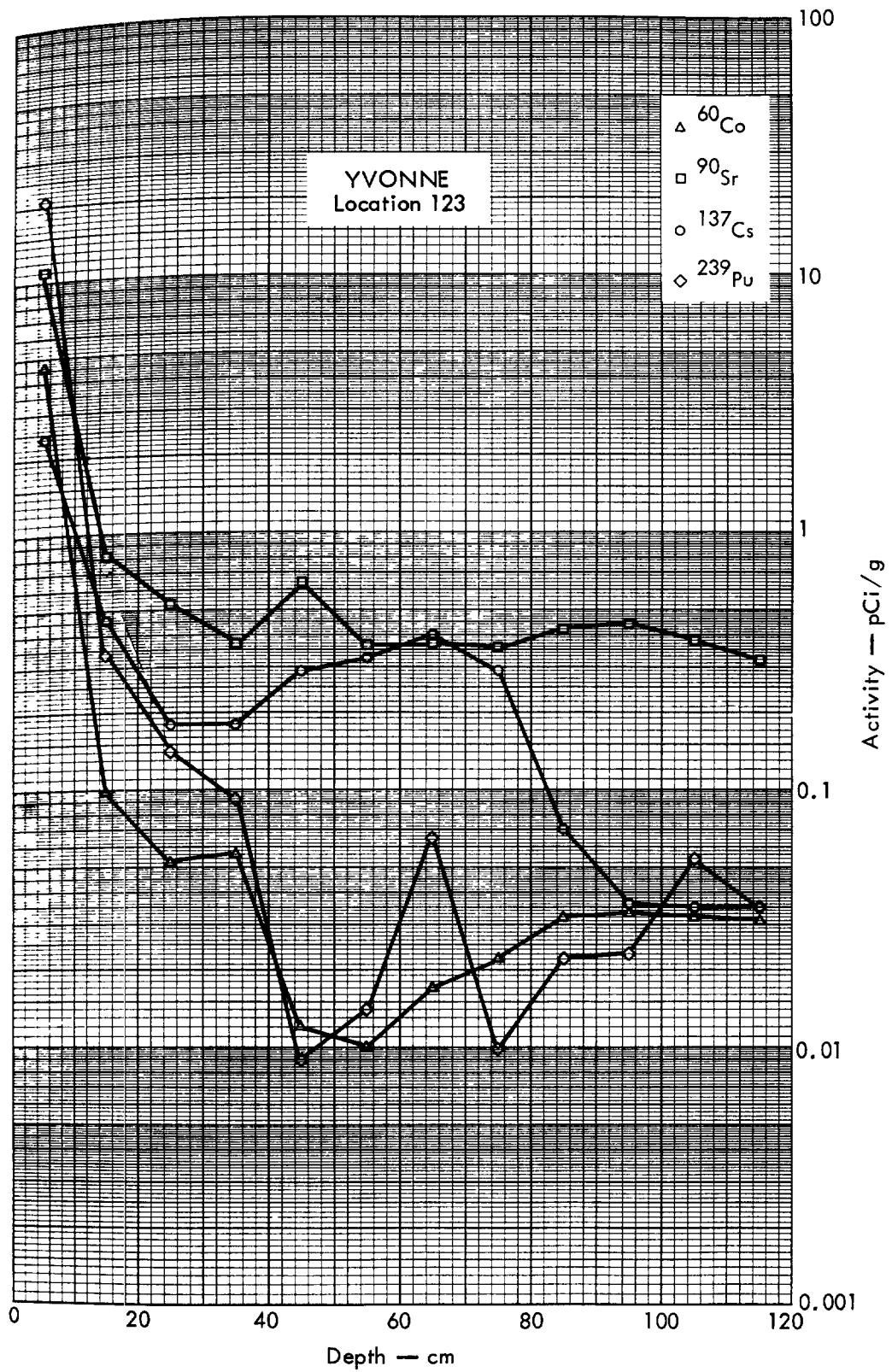


Fig. B. 23.2w. Activities of selected radionuclides as a function of soil depth.

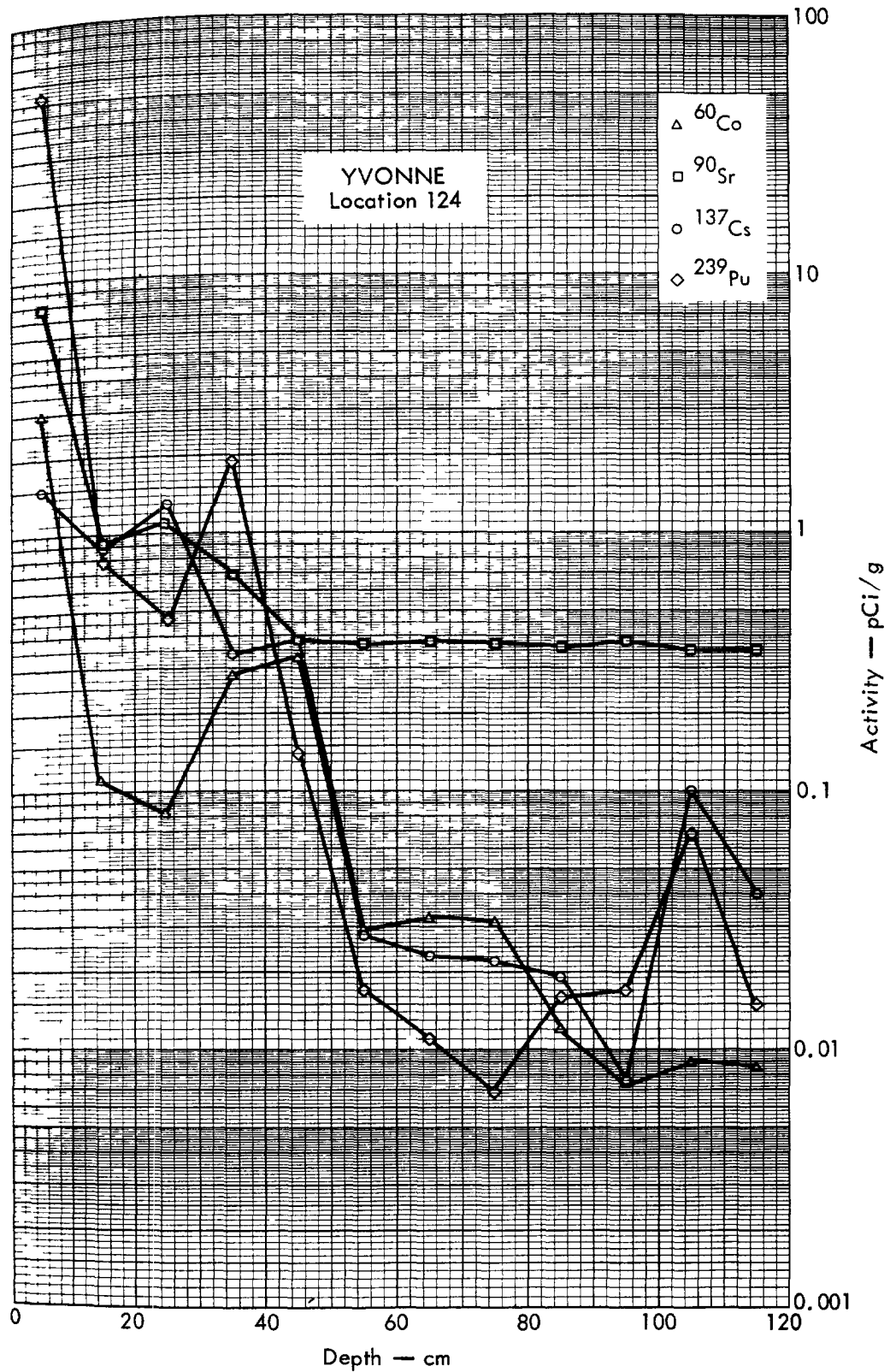


Fig. B. 23.2x. Activities of selected radionuclides as a function of soil depth.

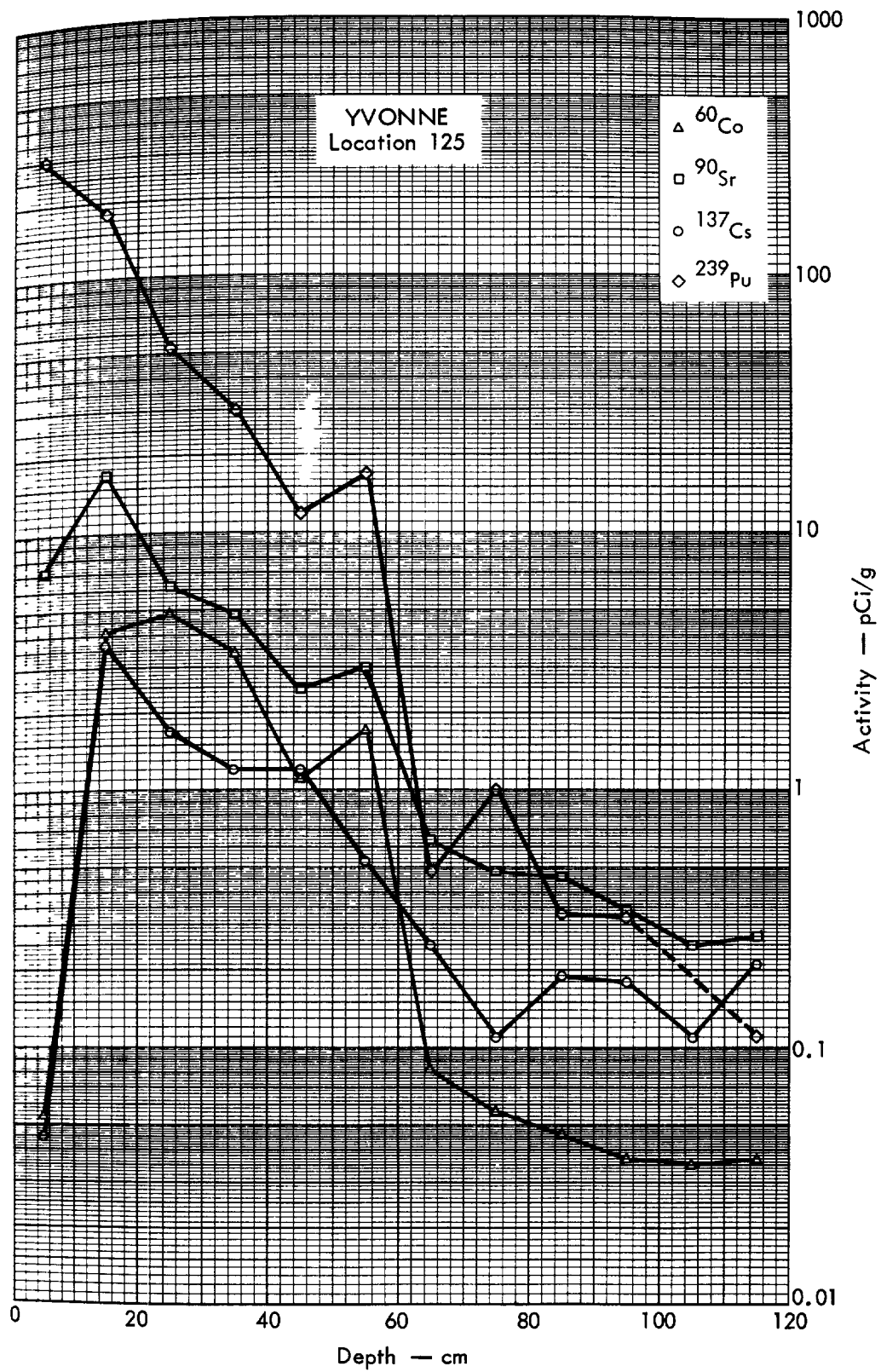


Fig. B. 23.2y. Activities of selected radionuclides as a function of soil depth.

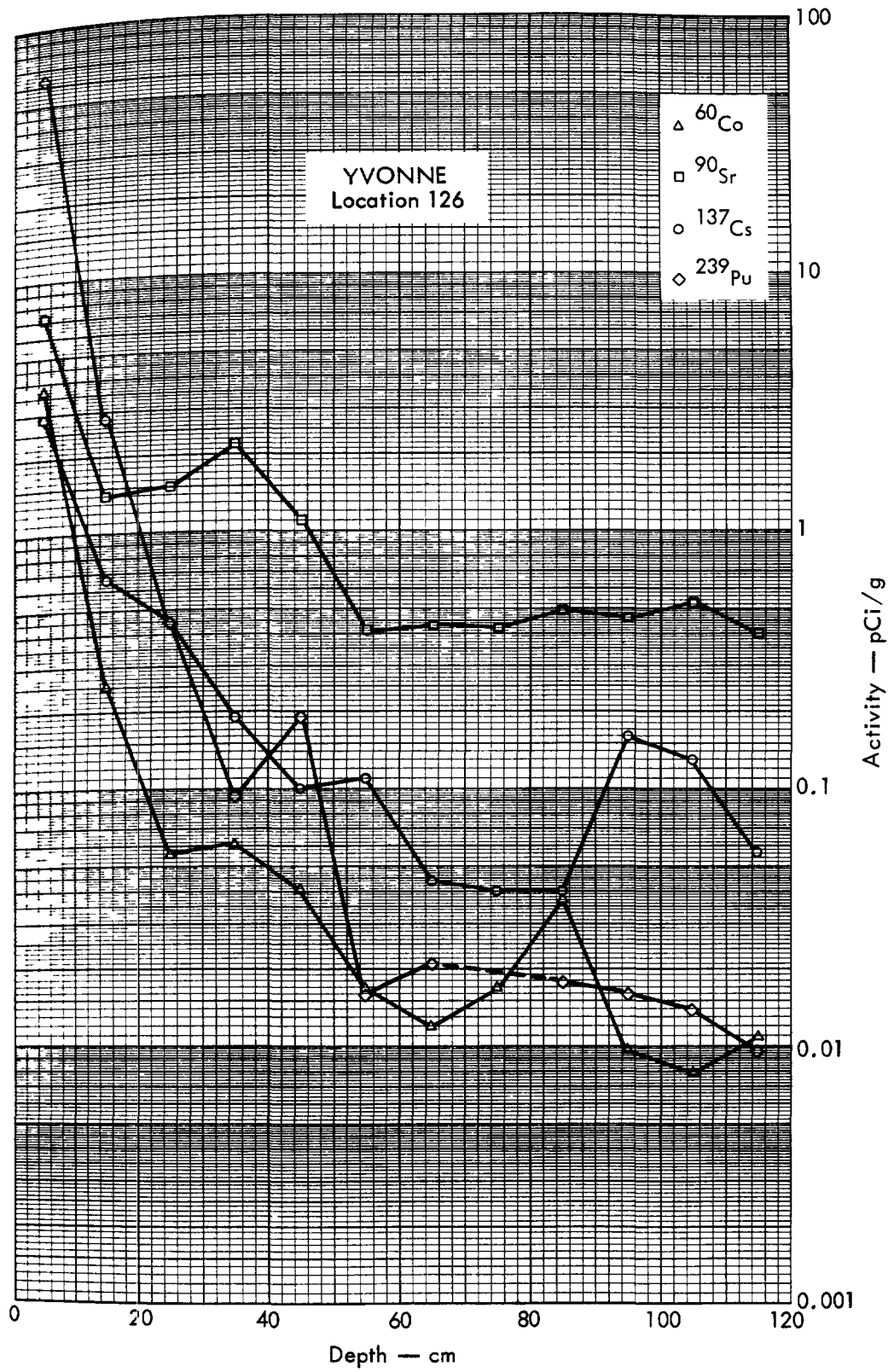


Fig. B. 23.2z. Activities of selected radionuclides as a function of soil depth.

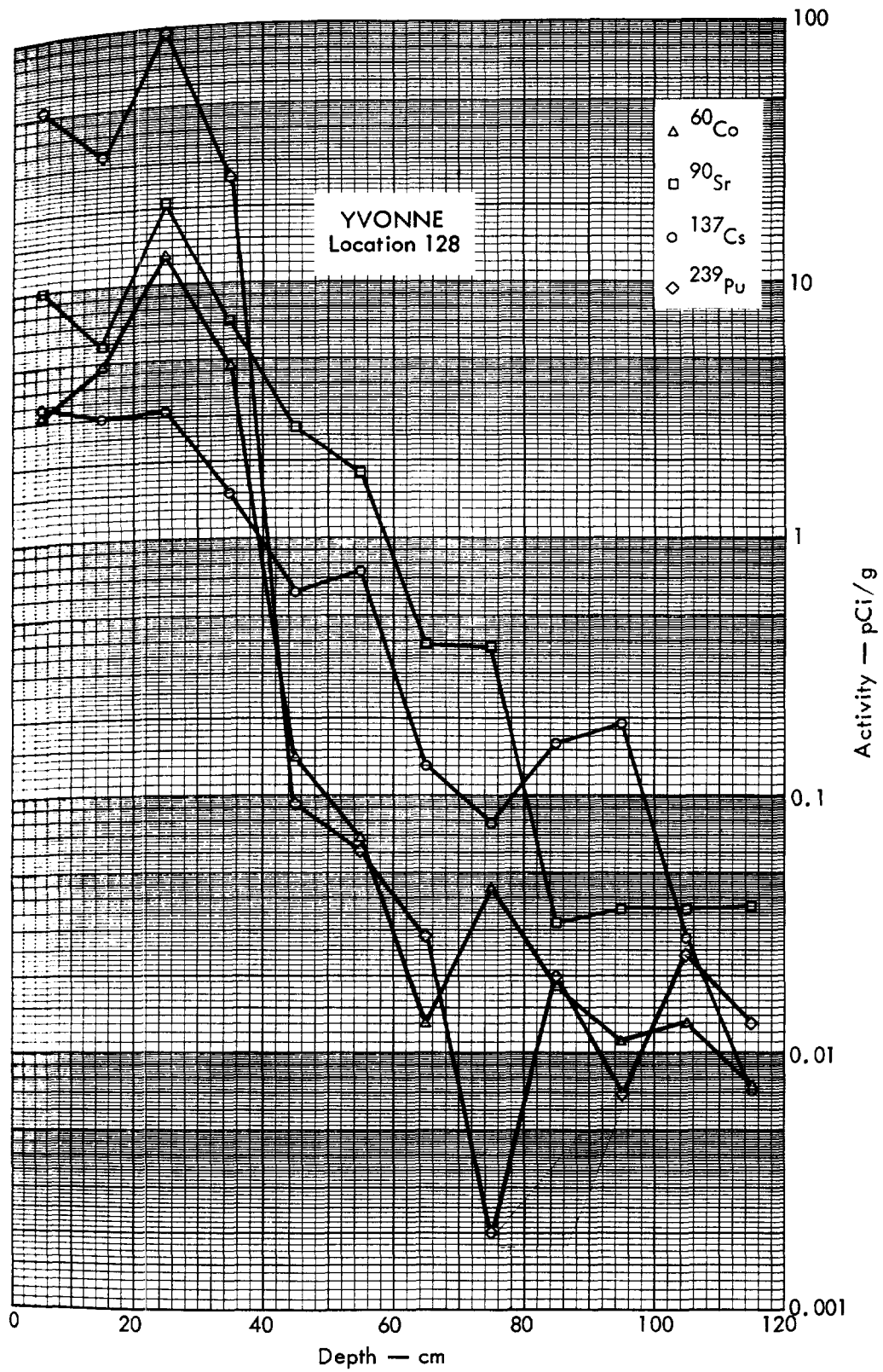


Fig. B. 23.2aa. Activities of selected radionuclides as a function of soil depth.

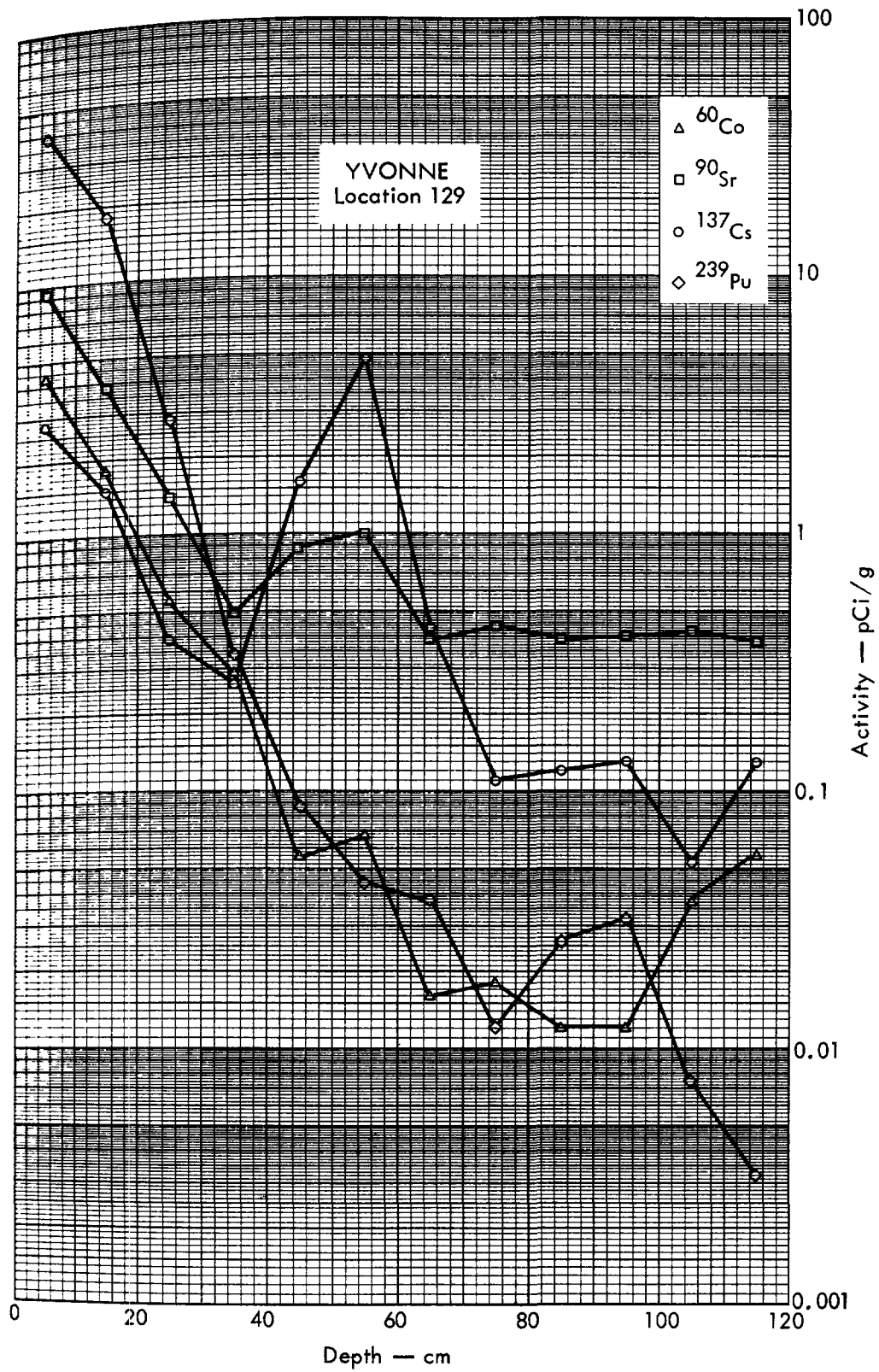


Fig. B. 23.2bb. Activities of selected radionuclides as a function of soil depth.

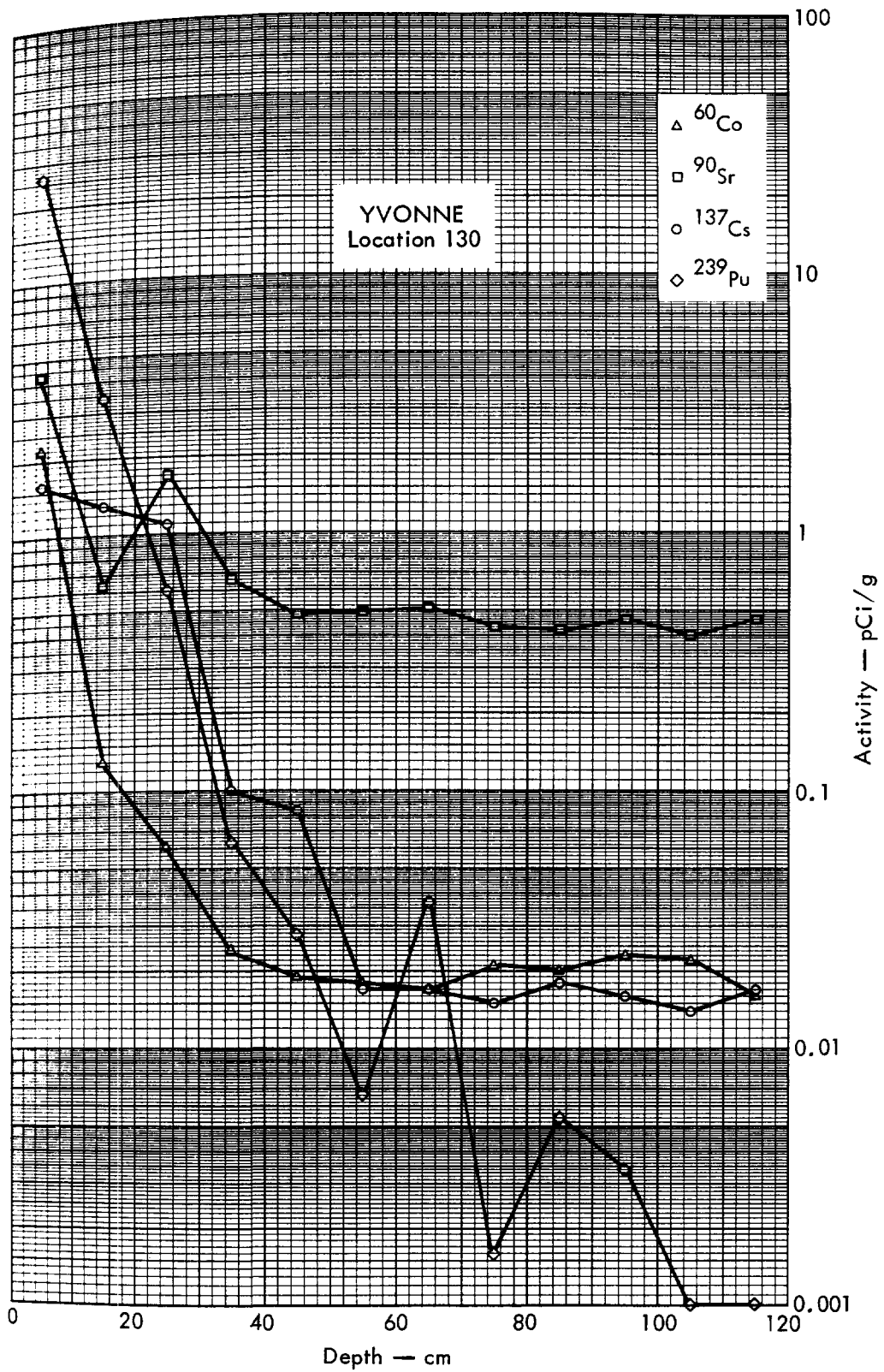


Fig. B. 23.2cc. Activities of selected radionuclides as a function of soil depth.



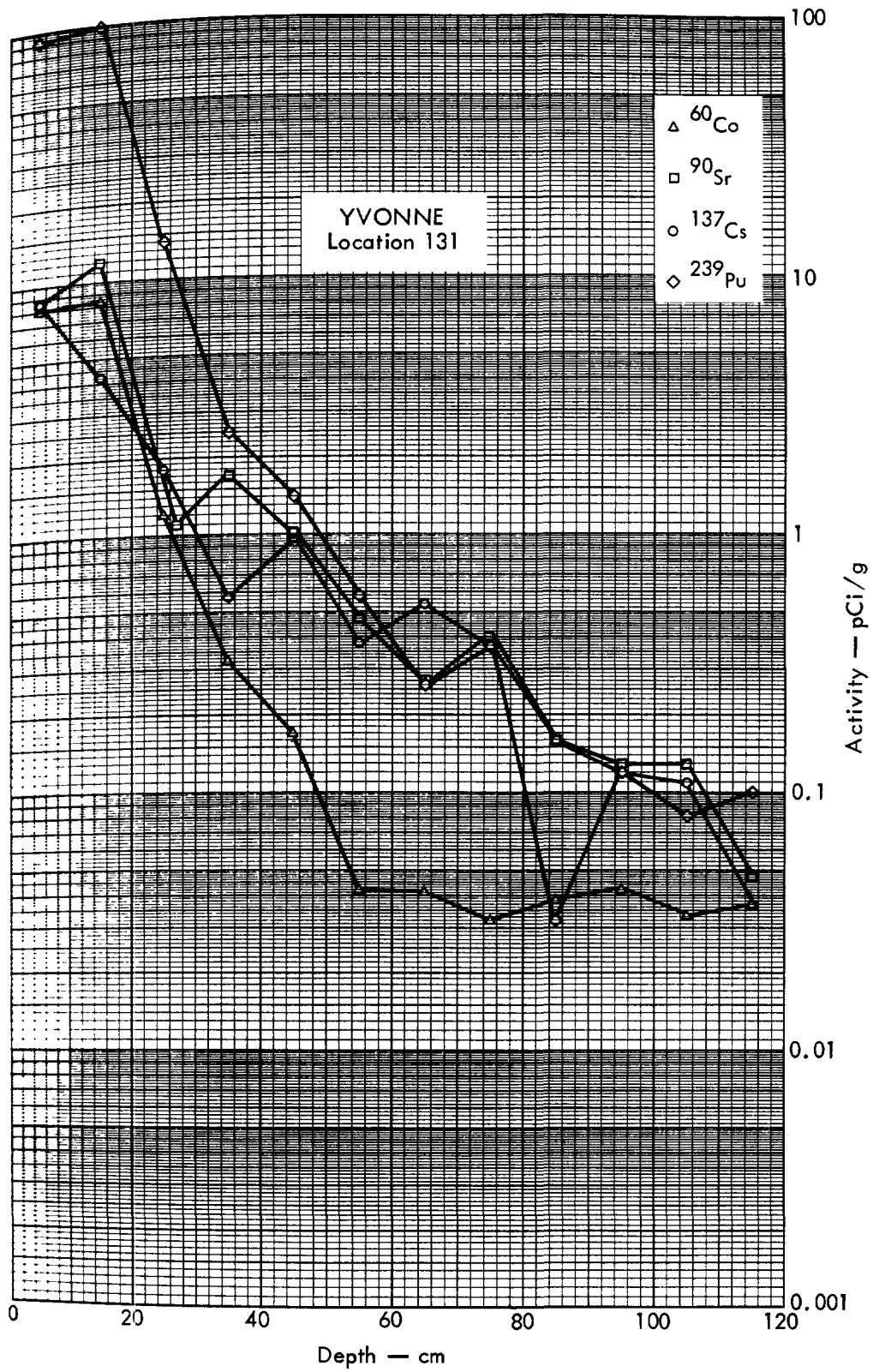


Fig. B. 23.2dd. Activities of selected radionuclides as a function of soil depth.



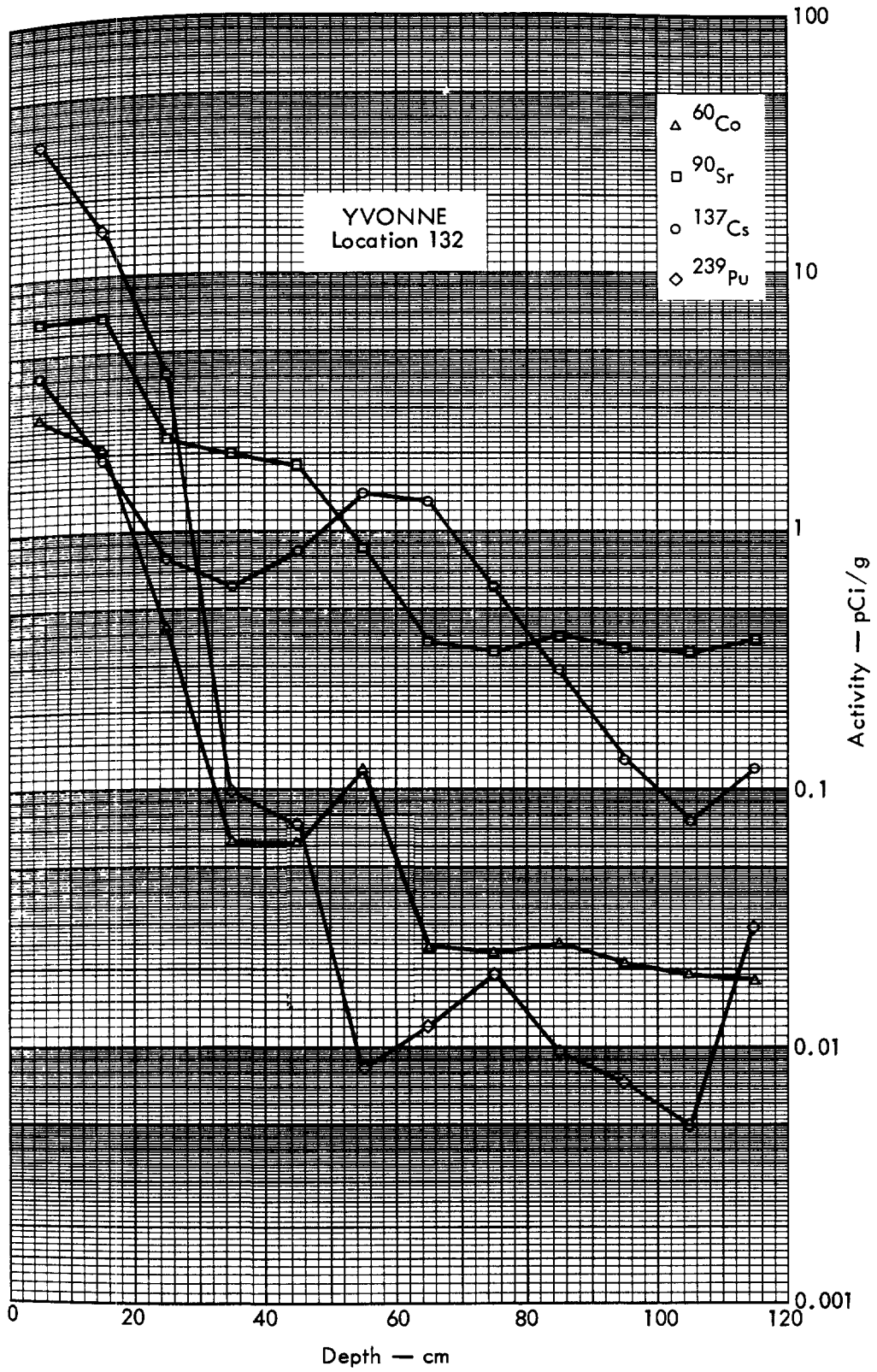


Fig. B. 23.2ee. Activities of selected radionuclides as a function of soil depth.

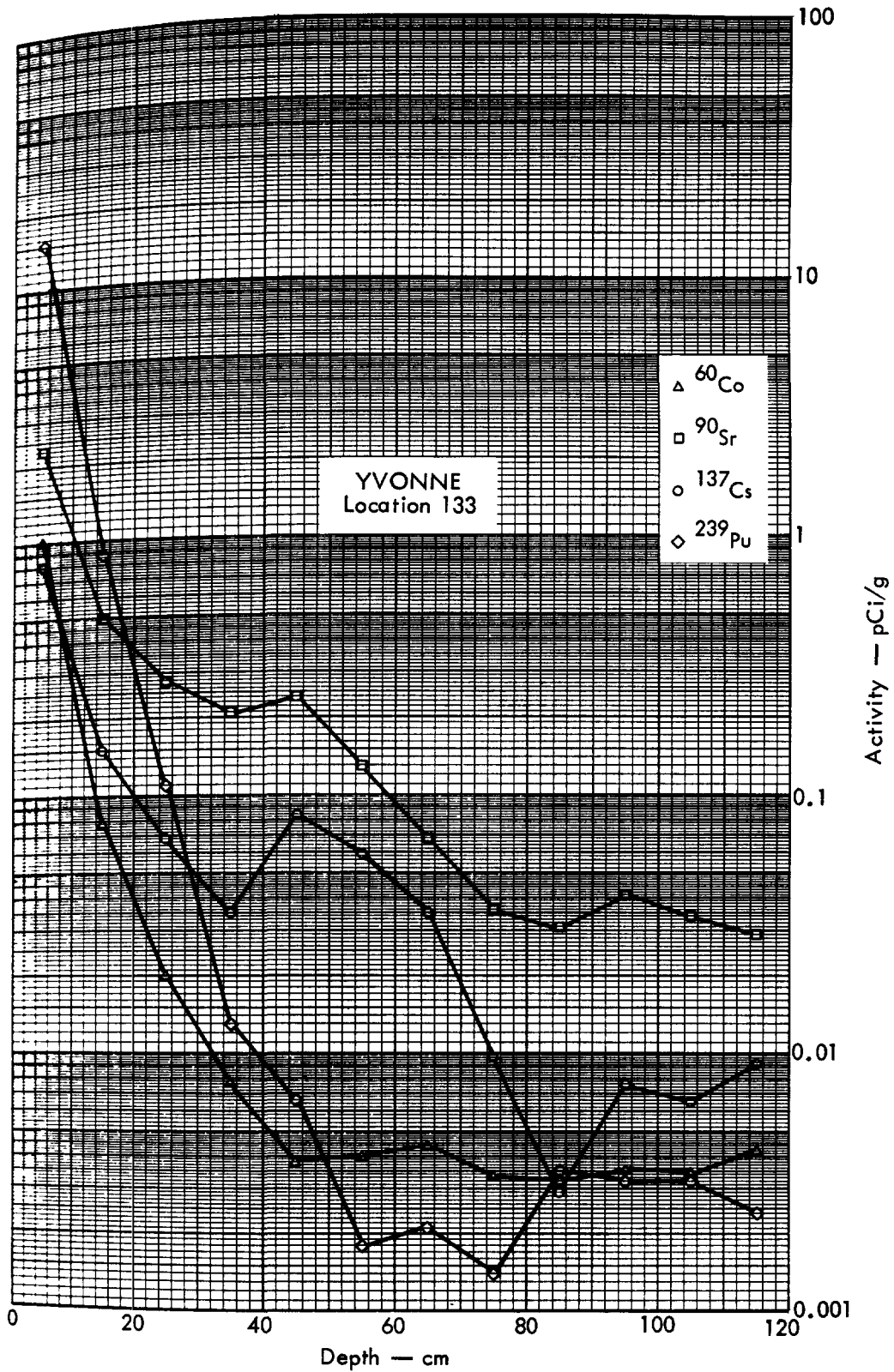


Fig. B. 23.2ff. Activities of selected radionuclides as a function of soil depth.

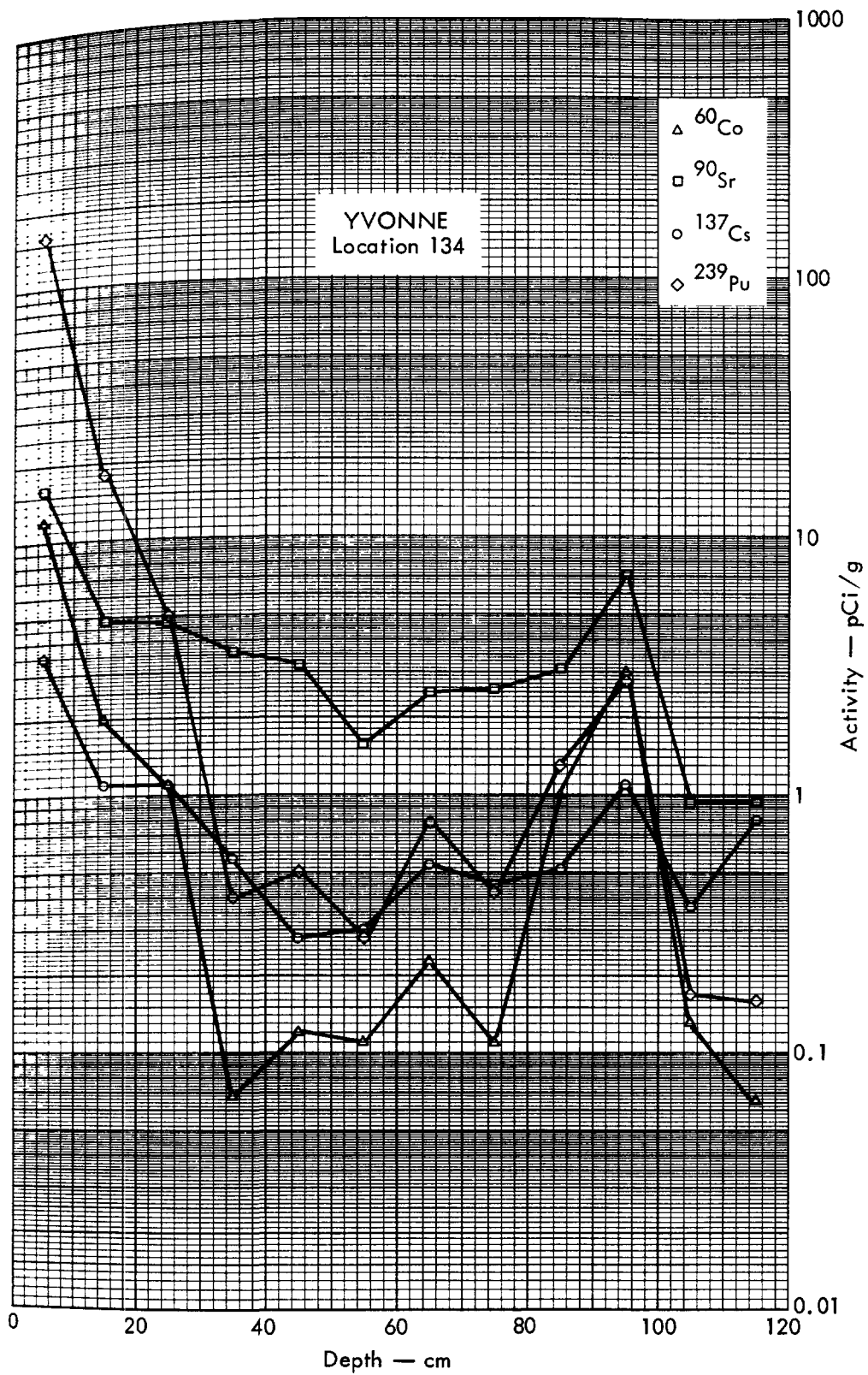


Fig. B. 23.2gg. Activities of selected radionuclides as a function of soil depth.

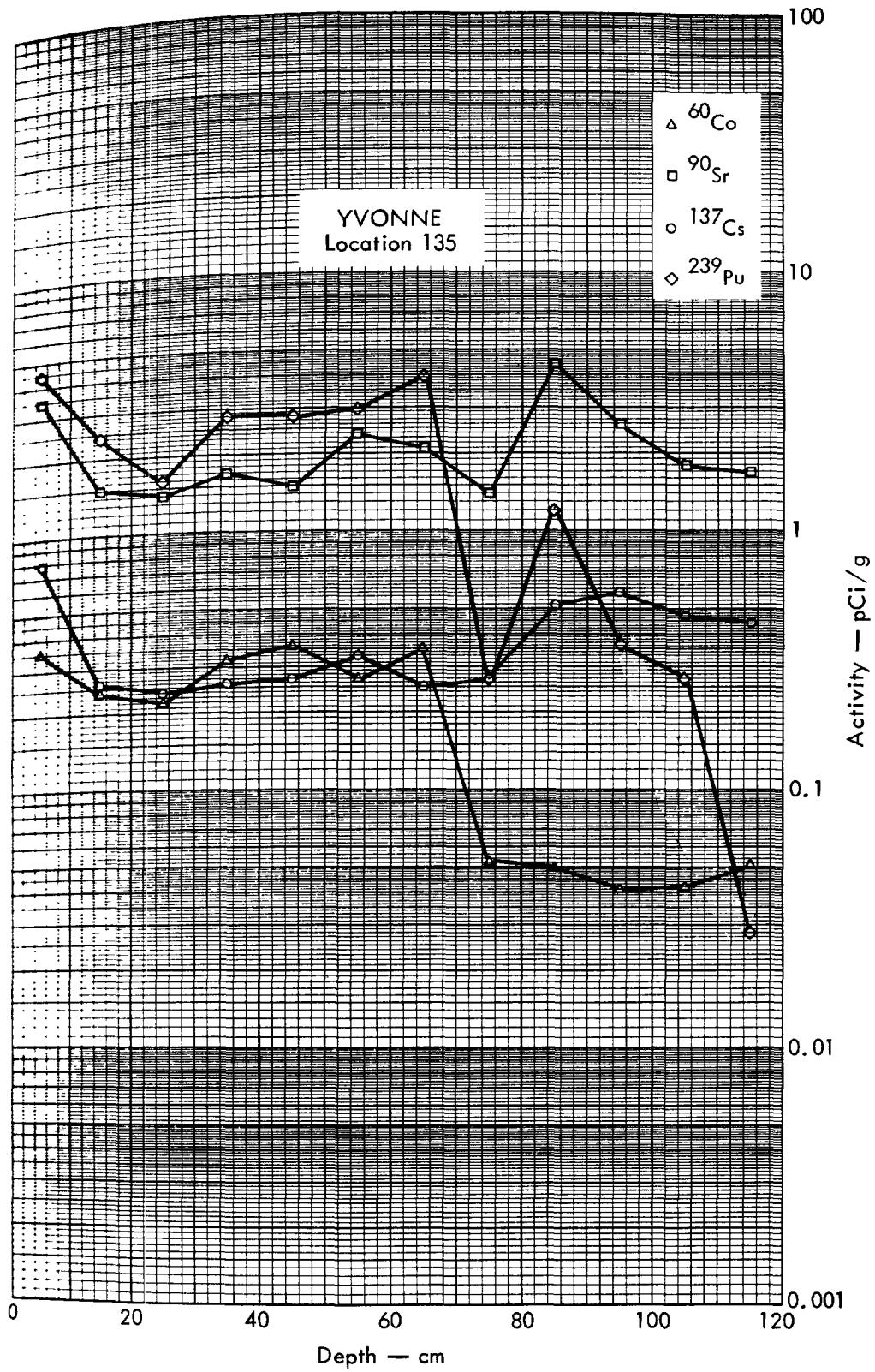


Fig. B.23.2hh. Activities of selected radionuclides as a function of soil depth.

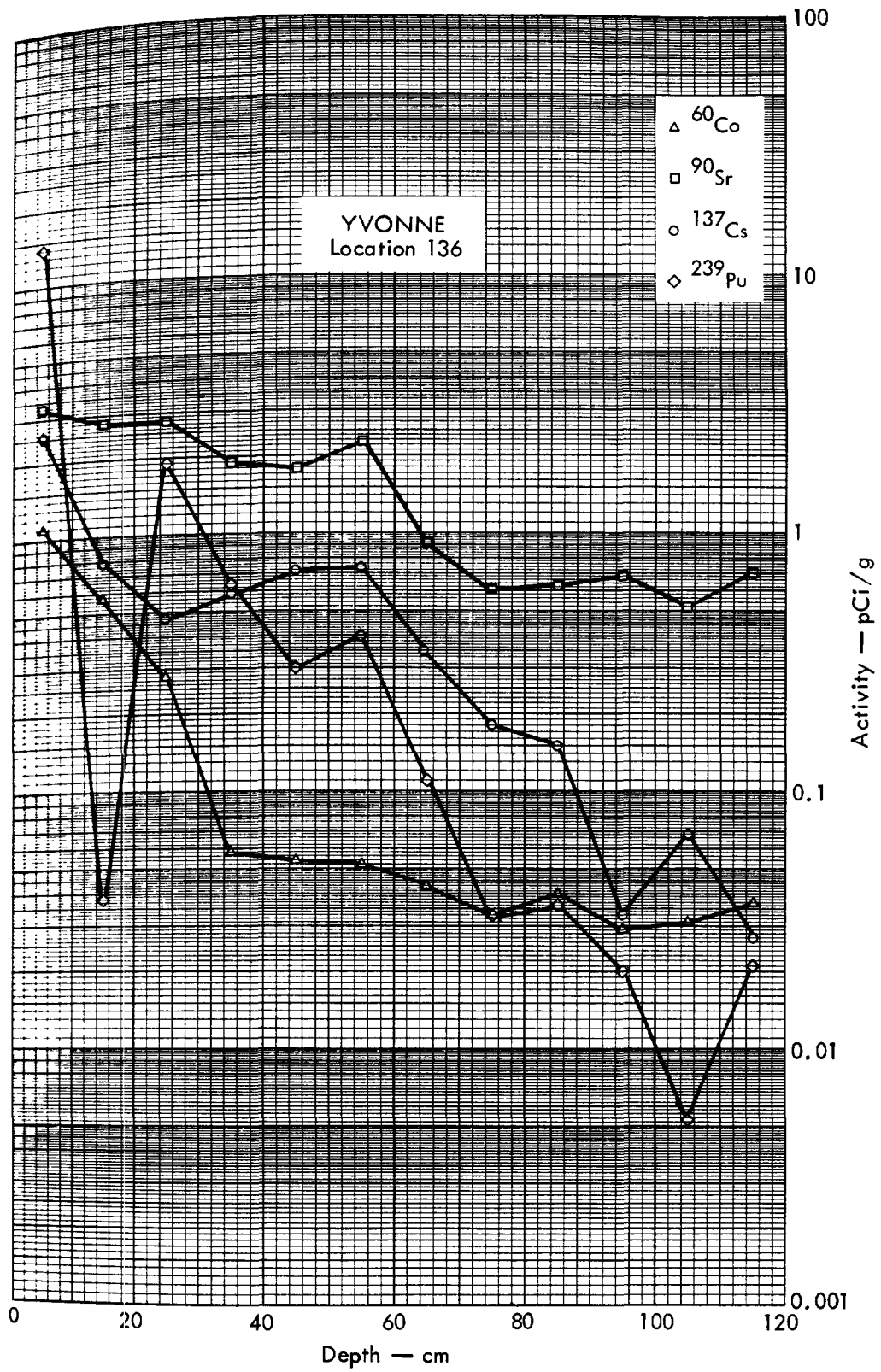


Fig. B. 23.2ii. Activities of selected radionuclides as a function of soil depth.

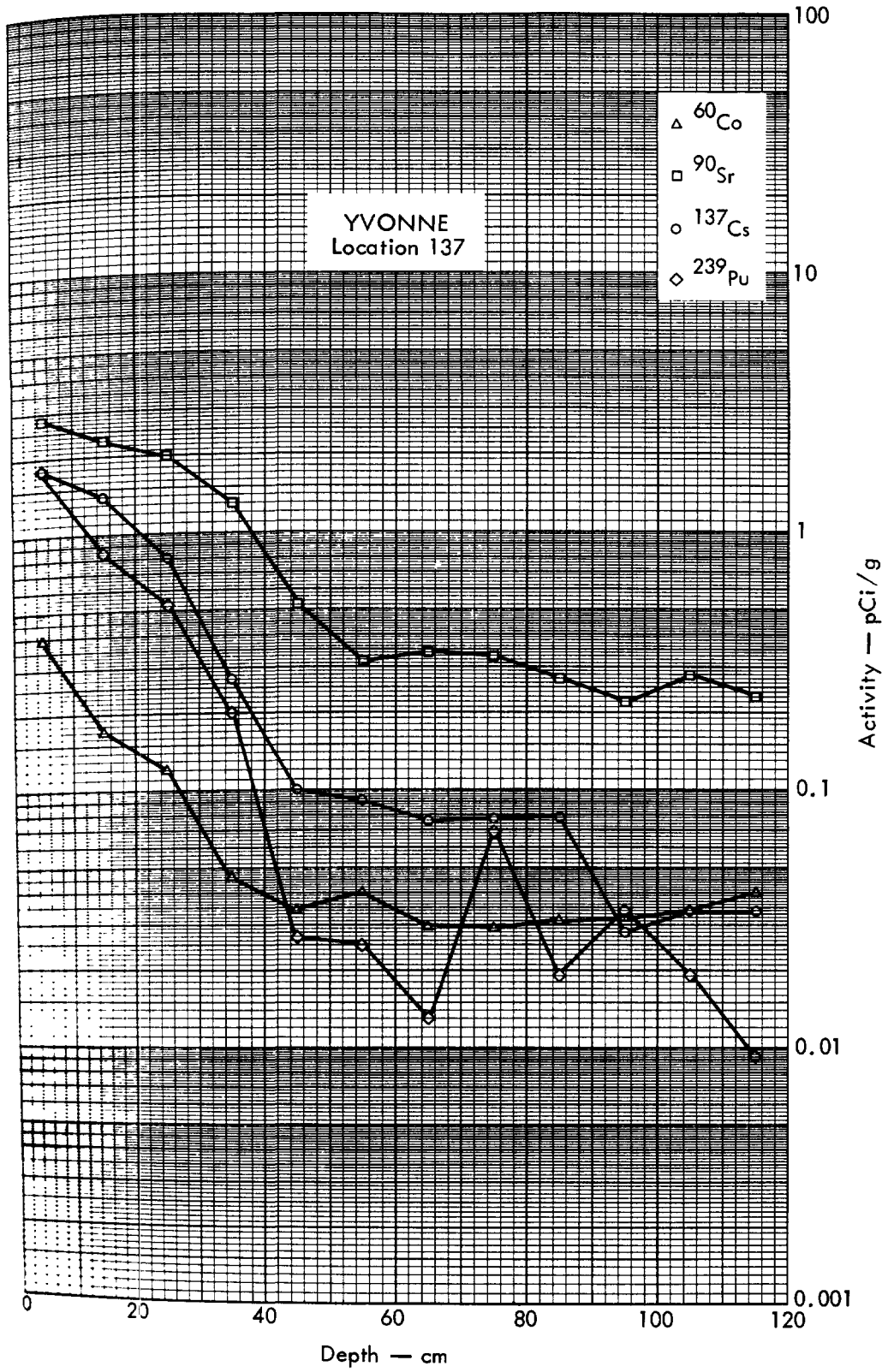


Fig. B. 23.2JJ. Activities of selected radionuclides as a function of soil depth.

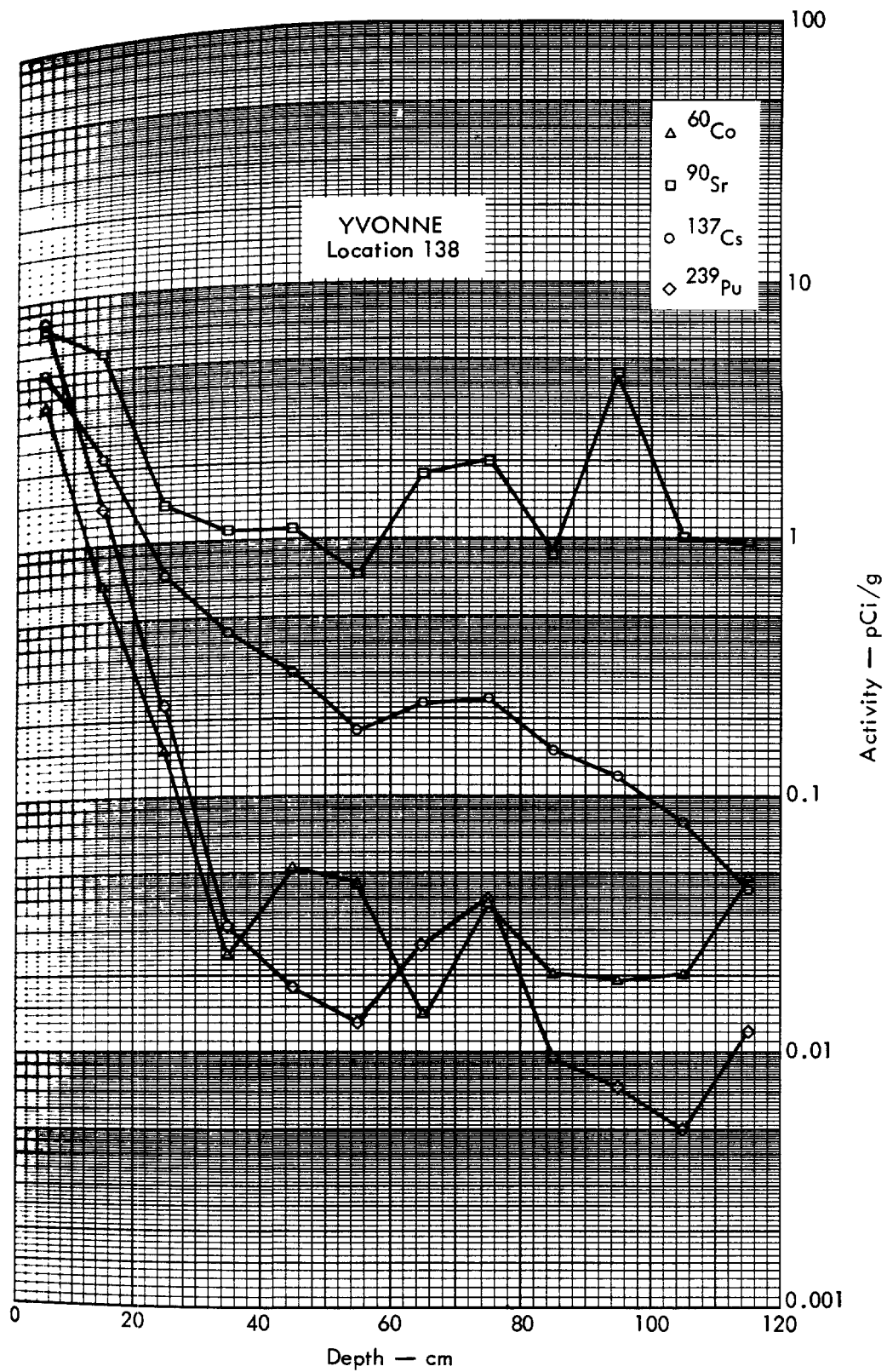


Fig. B. 23.2kk. Activities of selected radionuclides as a function of soil depth.



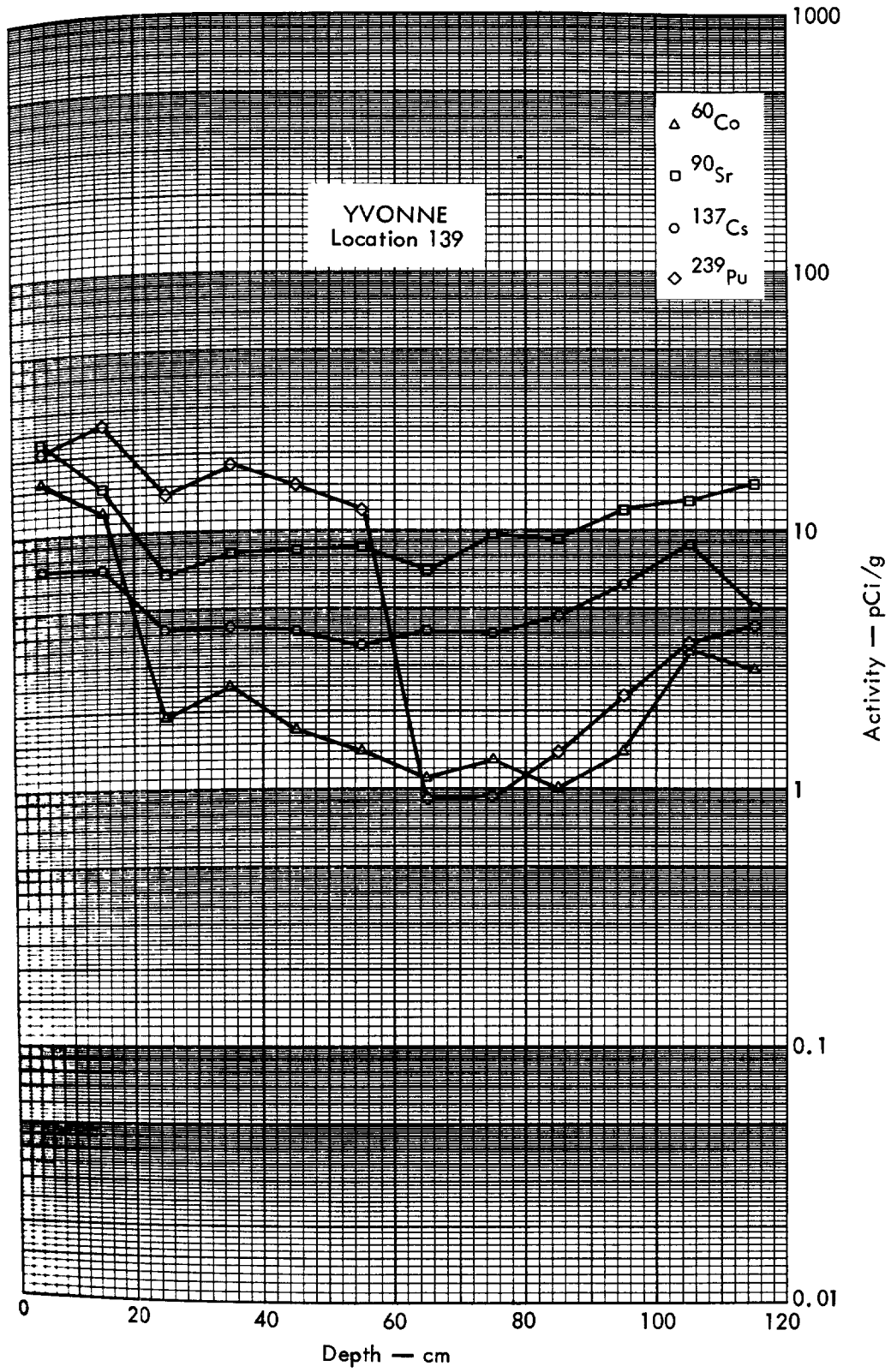


Fig. B. 23.211. Activities of selected radionuclides as a function of soil depth.





YVONNE C

Fig. B.24.1.a.

100 METERS  
L A S T

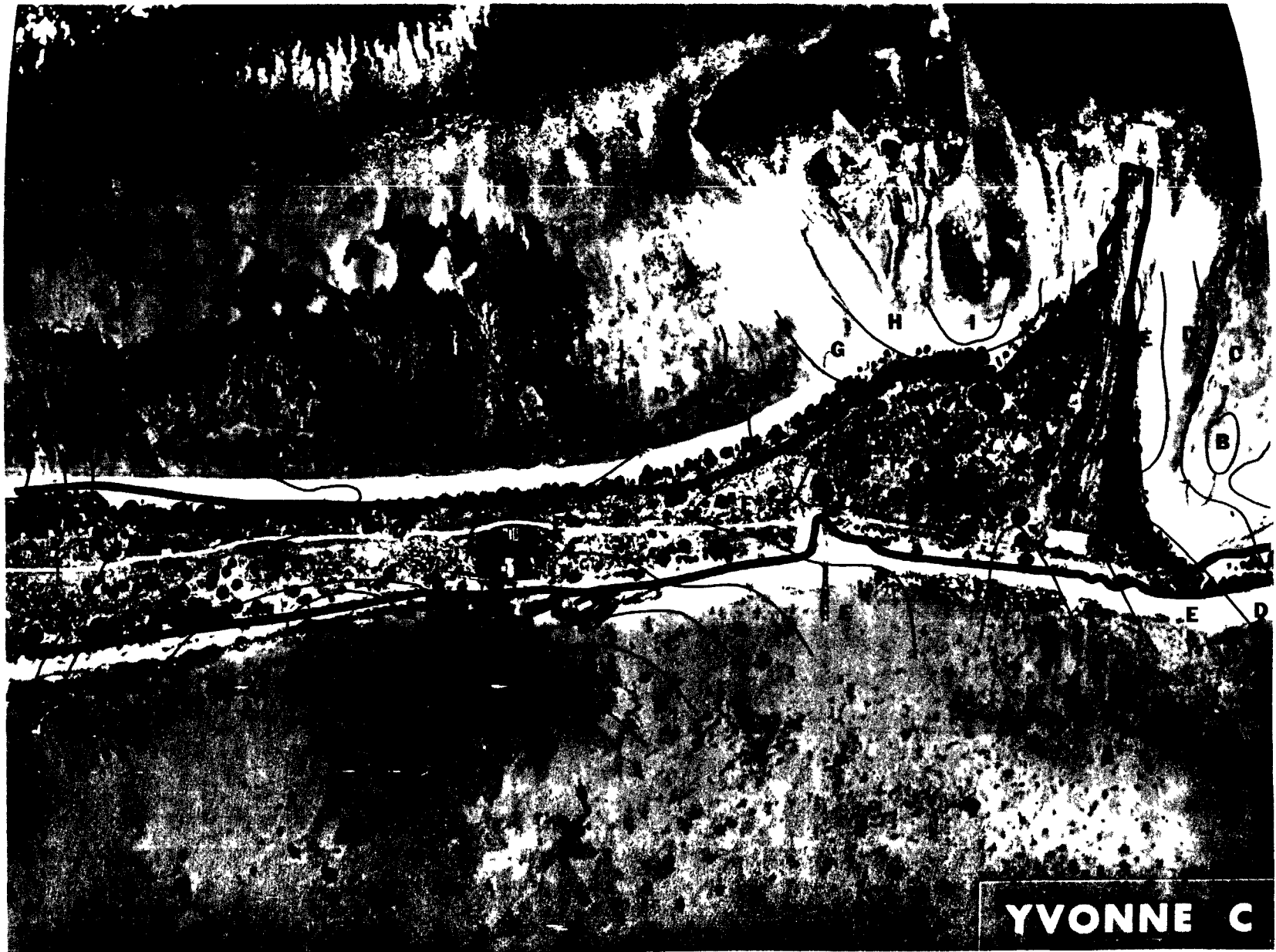


Fig. B.24.1.b. Gross count isosexposure contours. (Refer to alphabetic symbol key in this appendix.)



Fig. B.24.1.c.  $^{241}\text{Am}$  isoconcentration contours. (Refer to alphabetic symbol key in this appendix.)

100 METERS  
(A.A.A.A.)

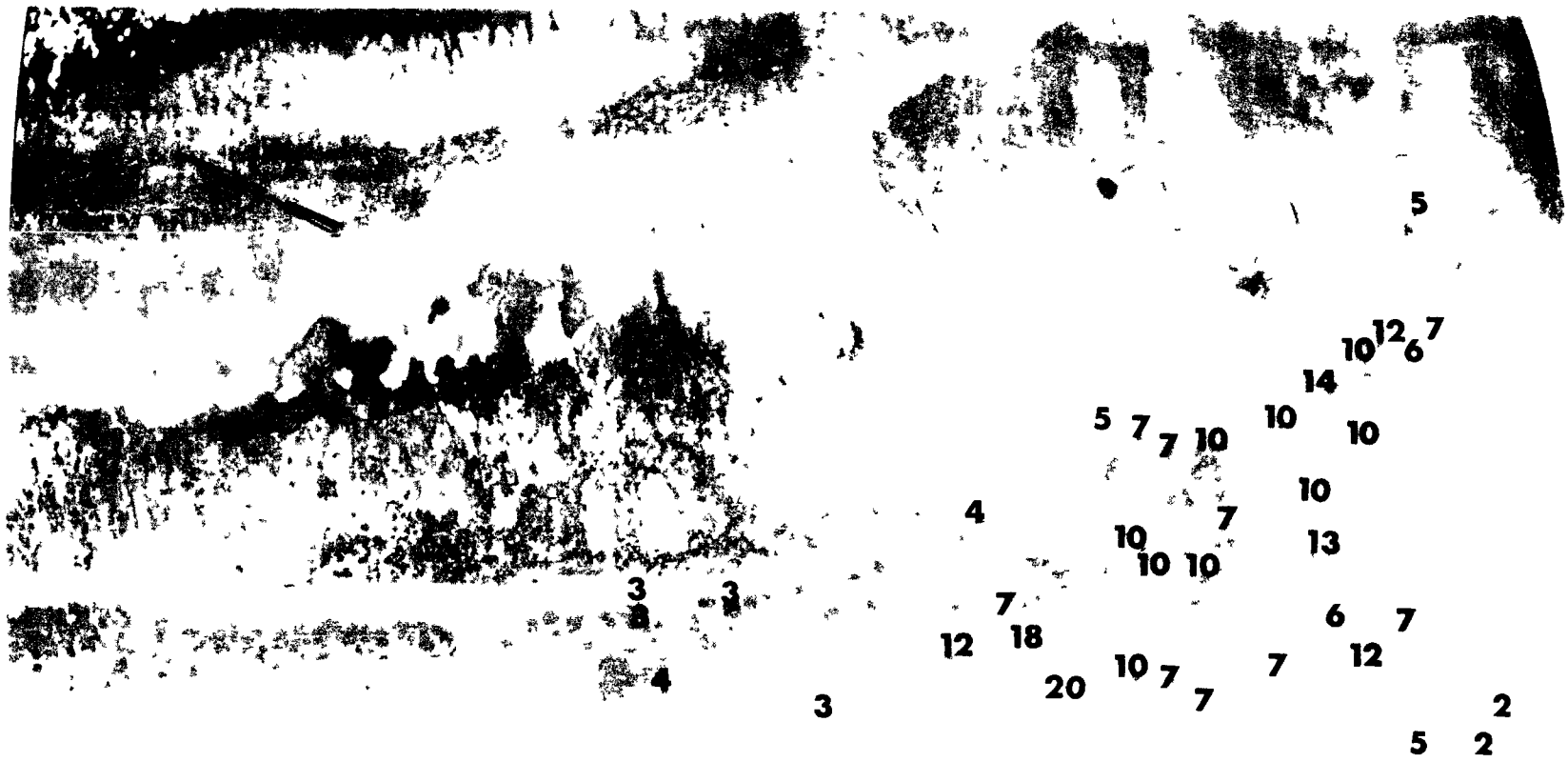


Fig. B.24.1.d. The gamma background exposure rate ( $\mu\text{R/hr}$ ) at 1 m above the ground, measured with a portable NaI scintillation counter.

1000 0000000



Fig. B.24.1.f. Soil-sample locations.



△ △ △ MESSERSCHMIDIA

○ ○ ○ SCAEVOLA

WONNI C

Fig. B.24.1.g. Vegetation sample locations.

100 METERS



Fig. B.24.1.1. The average  $^{239}\text{Pu}$  activities (pCi/gm) in soil samples collected to a depth of 15 cm.

100 METERS

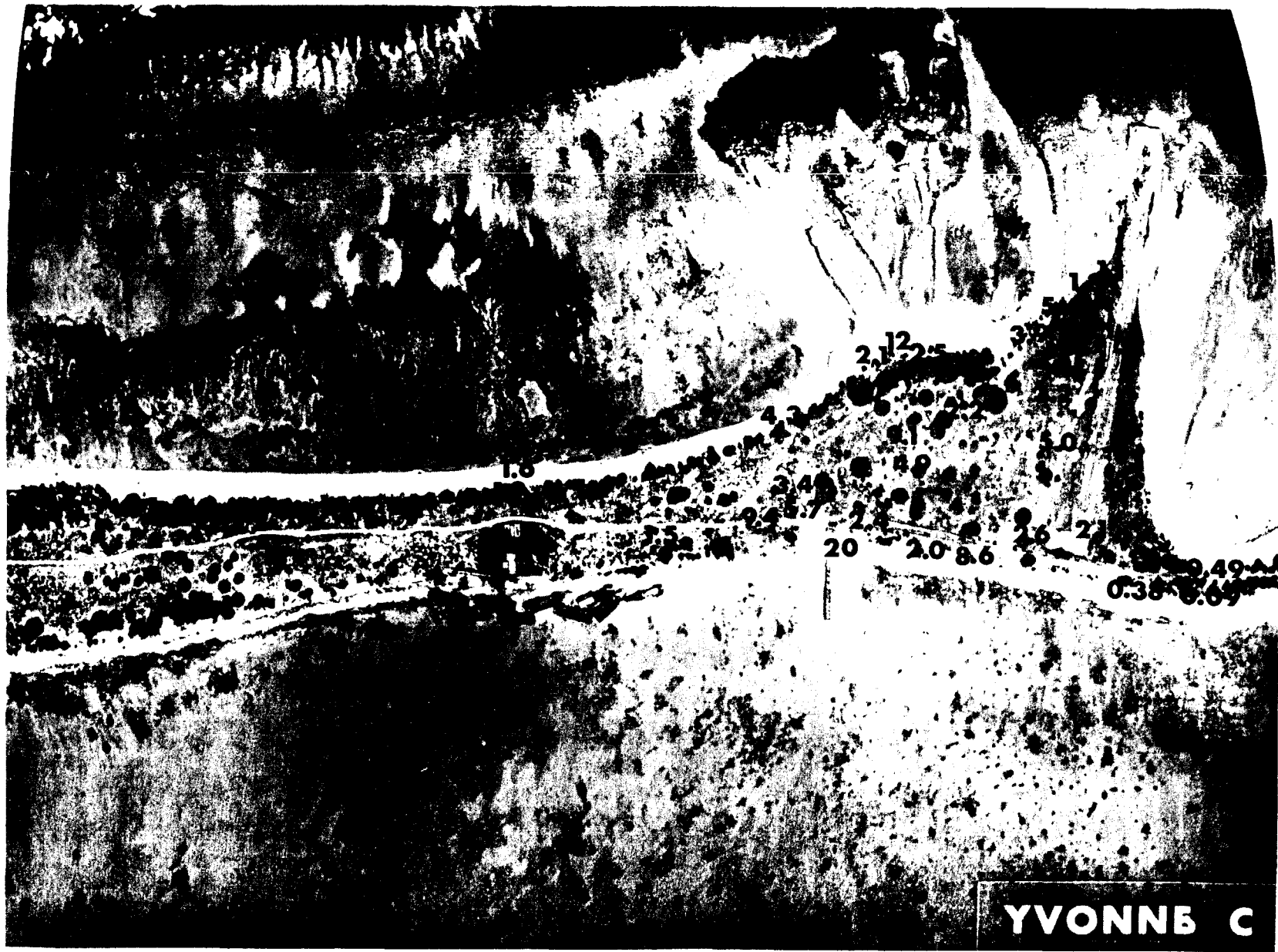


Fig. B.24.1.j. The average  $^{90}\text{Sr}$  activities (pCi/gm) in soil samples collected to a depth of 15 cm.





Fig. B. 24. 1. k.  $^{137}\text{Cs}$  isoexposure and isoconcentration contours. (Refer to alphabetic symbol key in this appendix.)



Fig. B.24.1.1. The average <sup>137</sup>Cs activities (pCi/gm) in soil samples collected to a depth of 15 cm.

100 METERS  
1:10,000

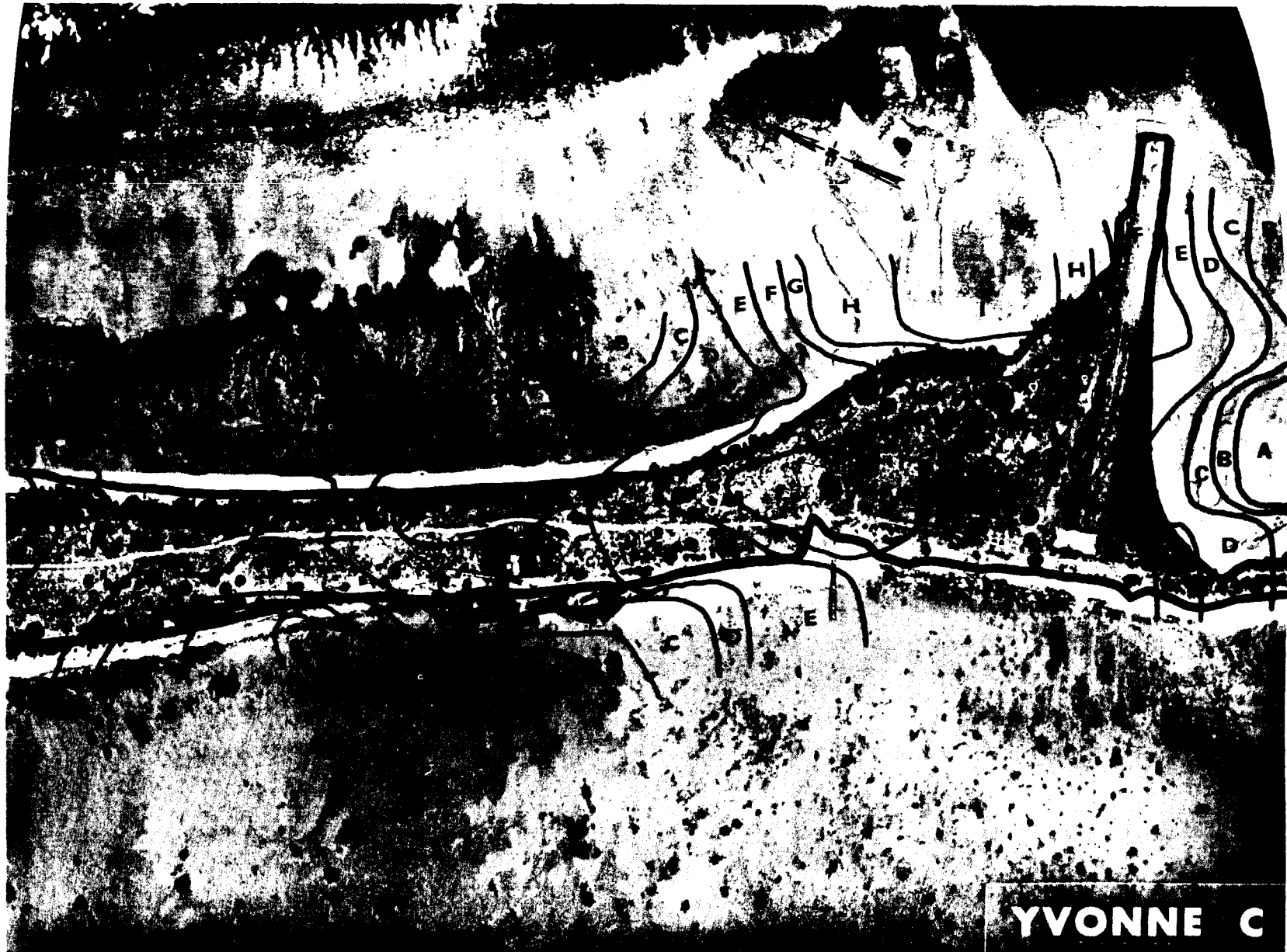


Fig. B.24.1.m.  $^{60}\text{Co}$  isoexposure and isoconcentration contours. (Refer to alphabetic symbol key in this appendix.)

100 METERS

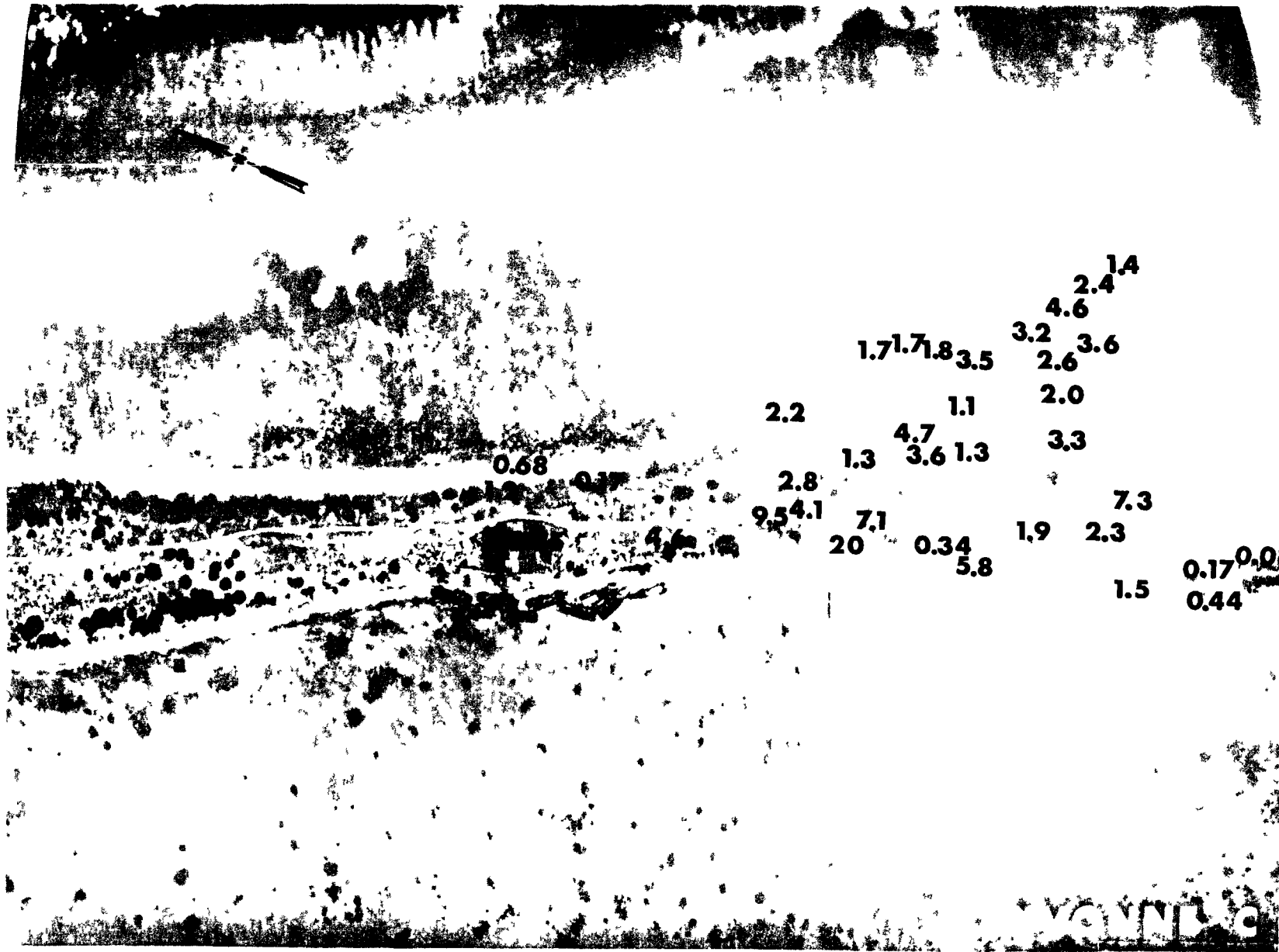


Fig. B.24.1.n. The average  $^{60}\text{Co}$  activities (pCi/gm) in soil samples collected to a depth of 15 cm.

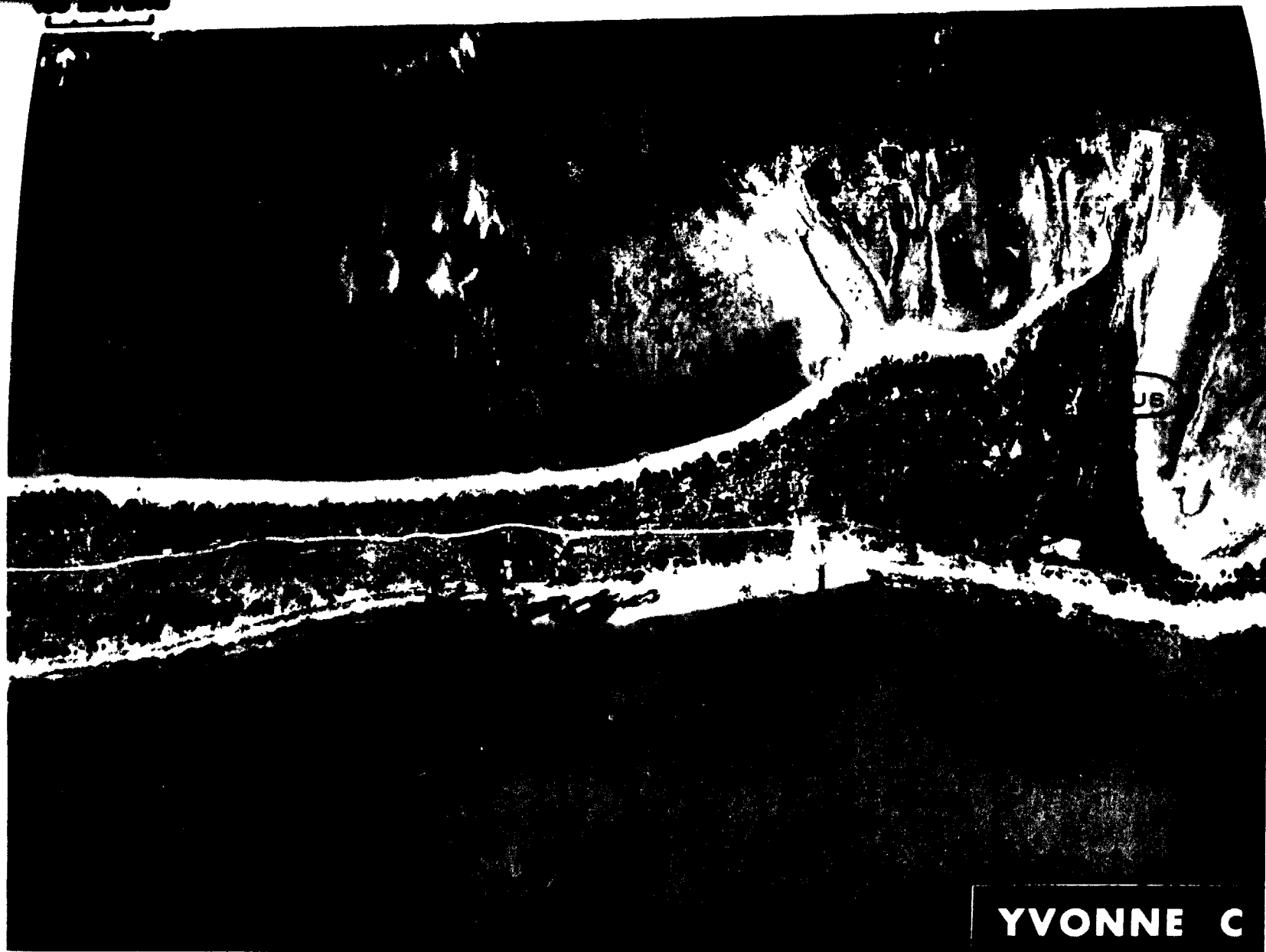


Fig. B.24.1.o. Terrestrial animal sample locations.

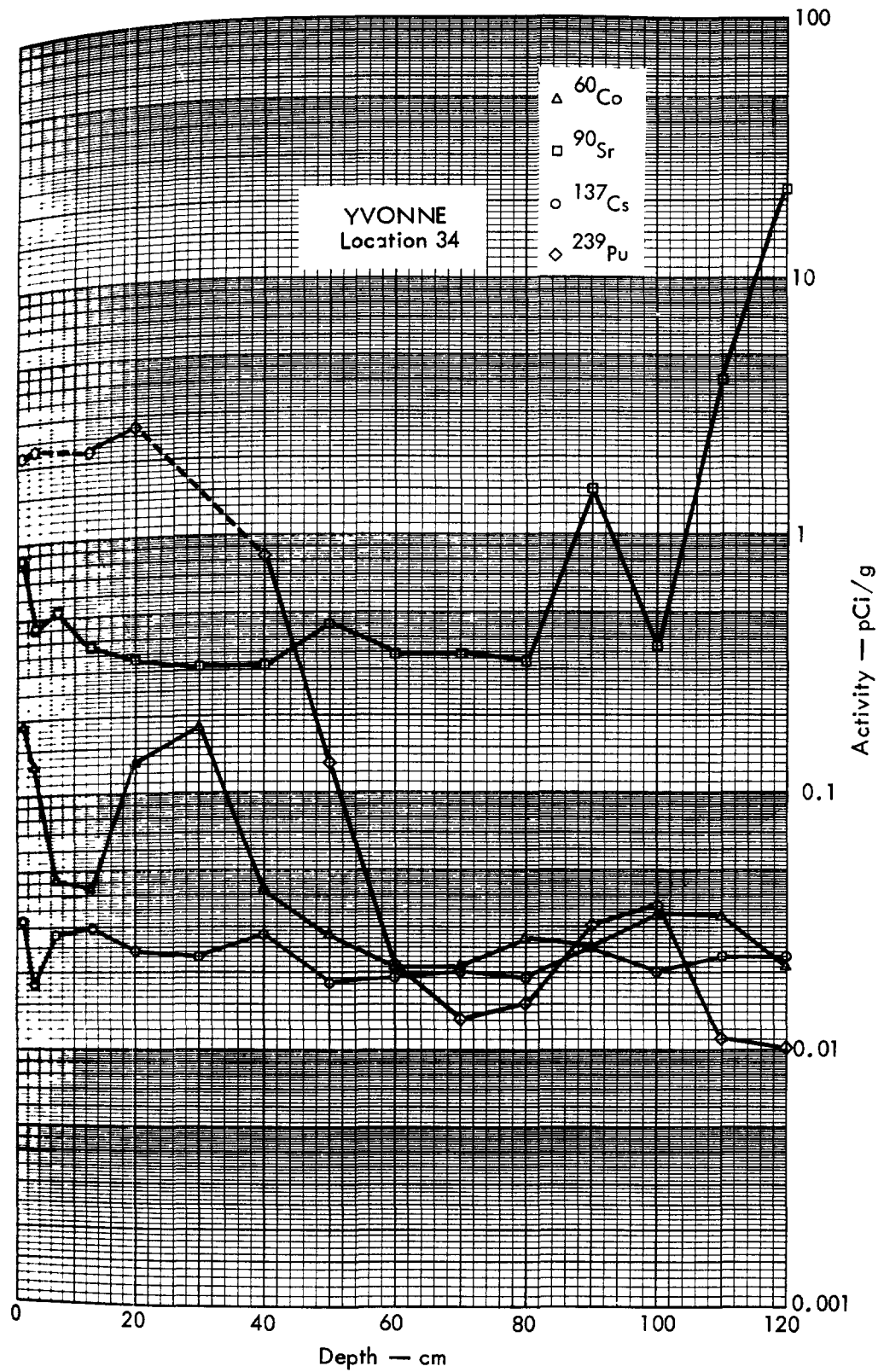


Fig. B. 24.2a. Activities of selected radionuclides as a function of soil depth.

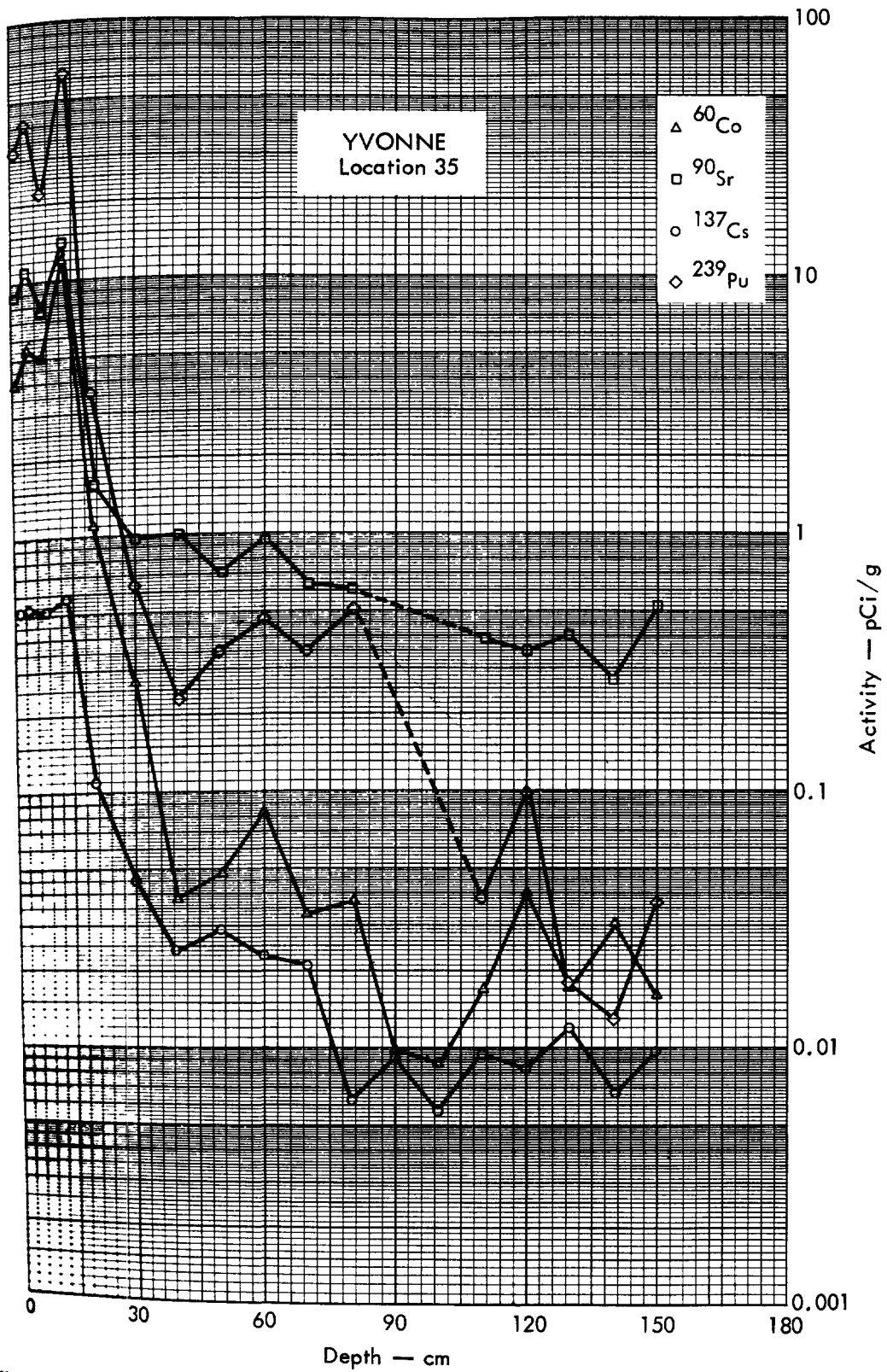


Fig. B.24.2b. Activities of selected radionuclides as a function of soil depth.

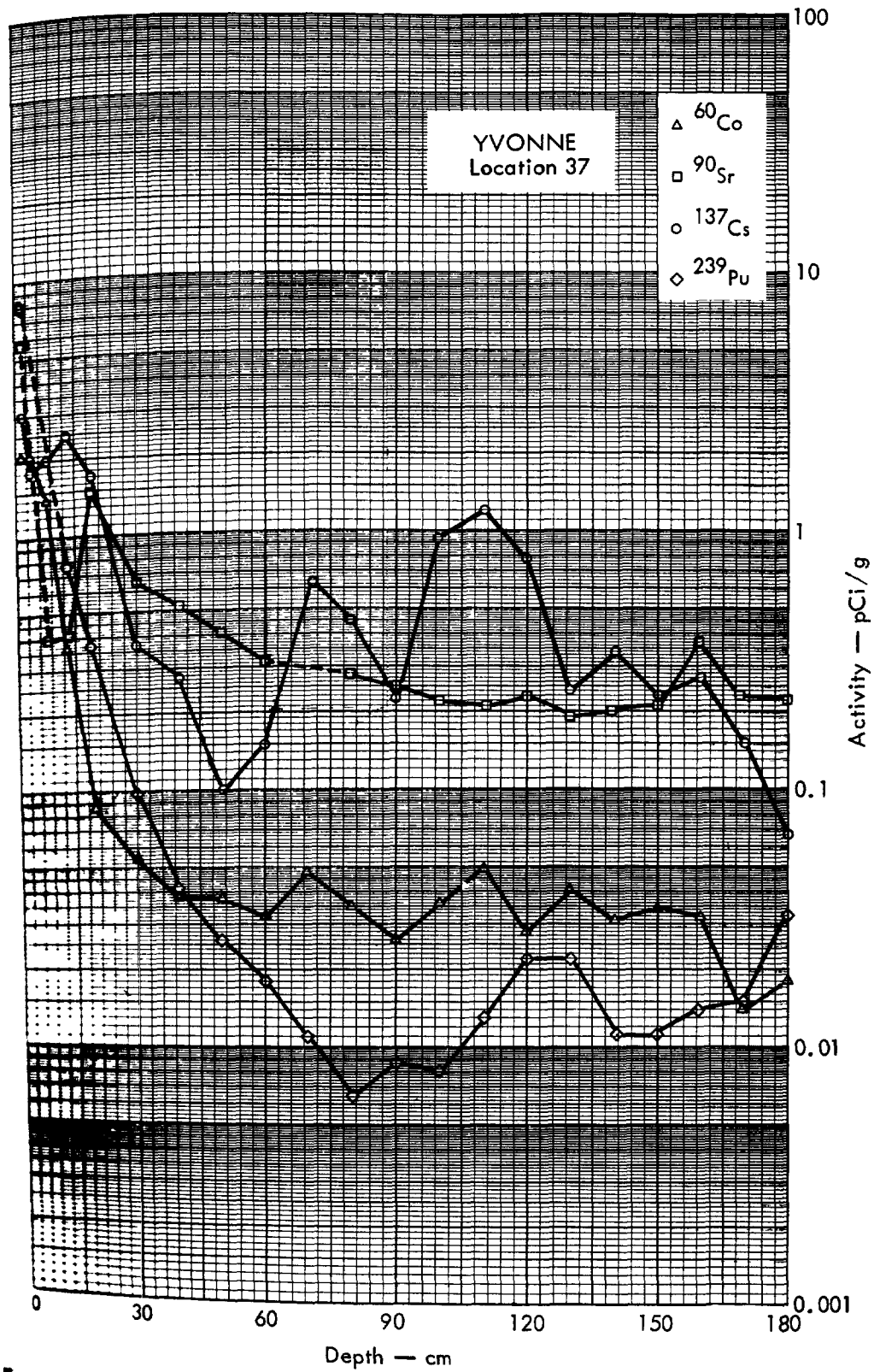


Fig. B.24.2c. Activities of selected radionuclides as a function of soil depth.



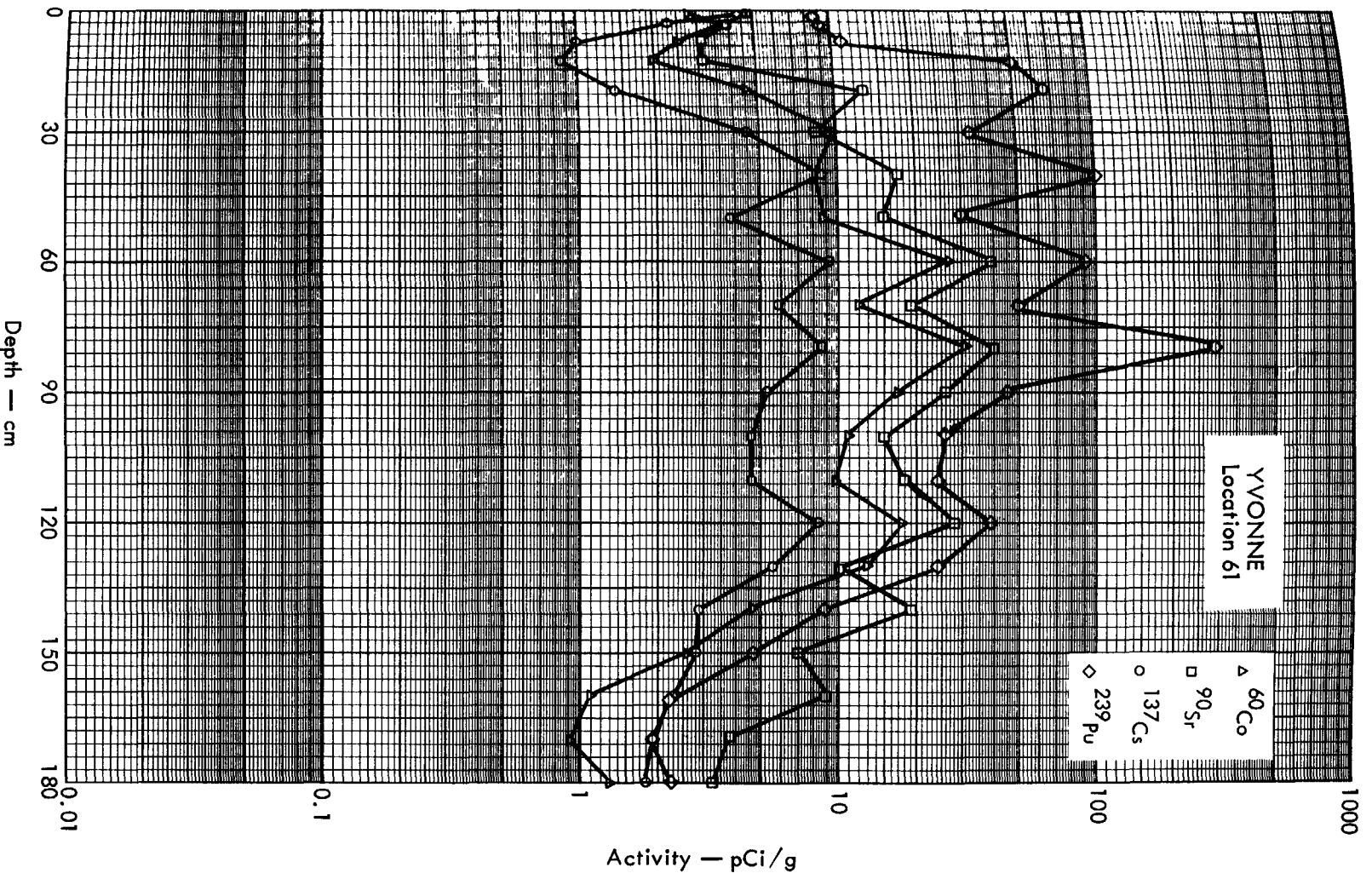


Fig. B. 24. 2d. Activities of selected radionuclides as a function of soil depth.



YVONNE D

Fig. B.25.1.a.



Fig. B.25.1.b. Gross count isoexposure contours. (Refer to alphabetic symbol key in this appendix.)

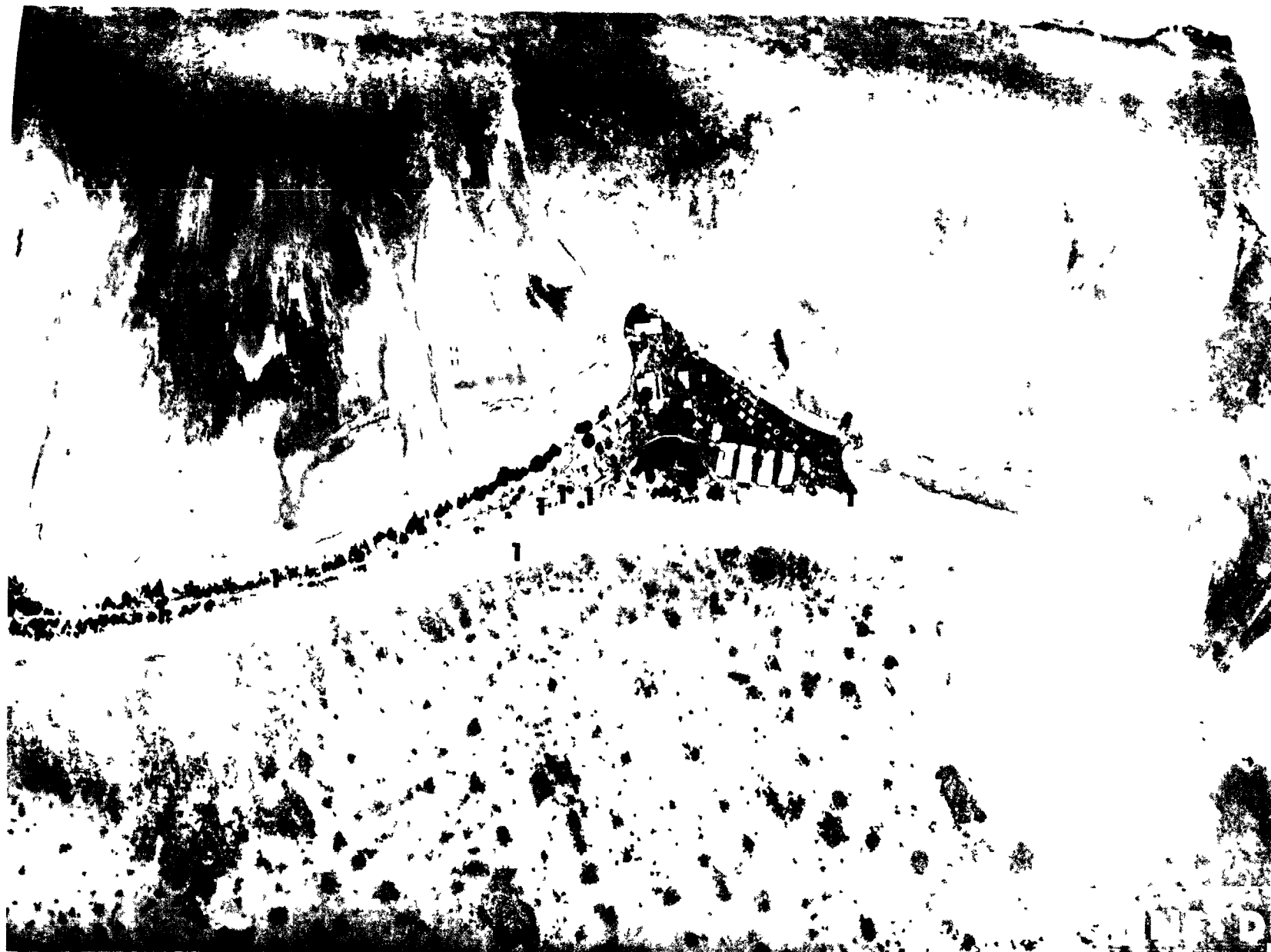


Fig. B.25.1.d. The gamma background exposure rate ( $\mu\text{R/hr}$ ) at 1 m above the ground, measured with a portable NaI scintillation counter.



Fig. B.25.1.f. Soil-sample locations.

1951 06 15 1951  
1 2 3 4 5



Fig. B.25.1.g. Vegetation sample locations.



Fig. B.25.1.i. The average  $^{239}\text{Pu}$  activities (pCi/gm) in soil samples collected to a depth of 15 cm.

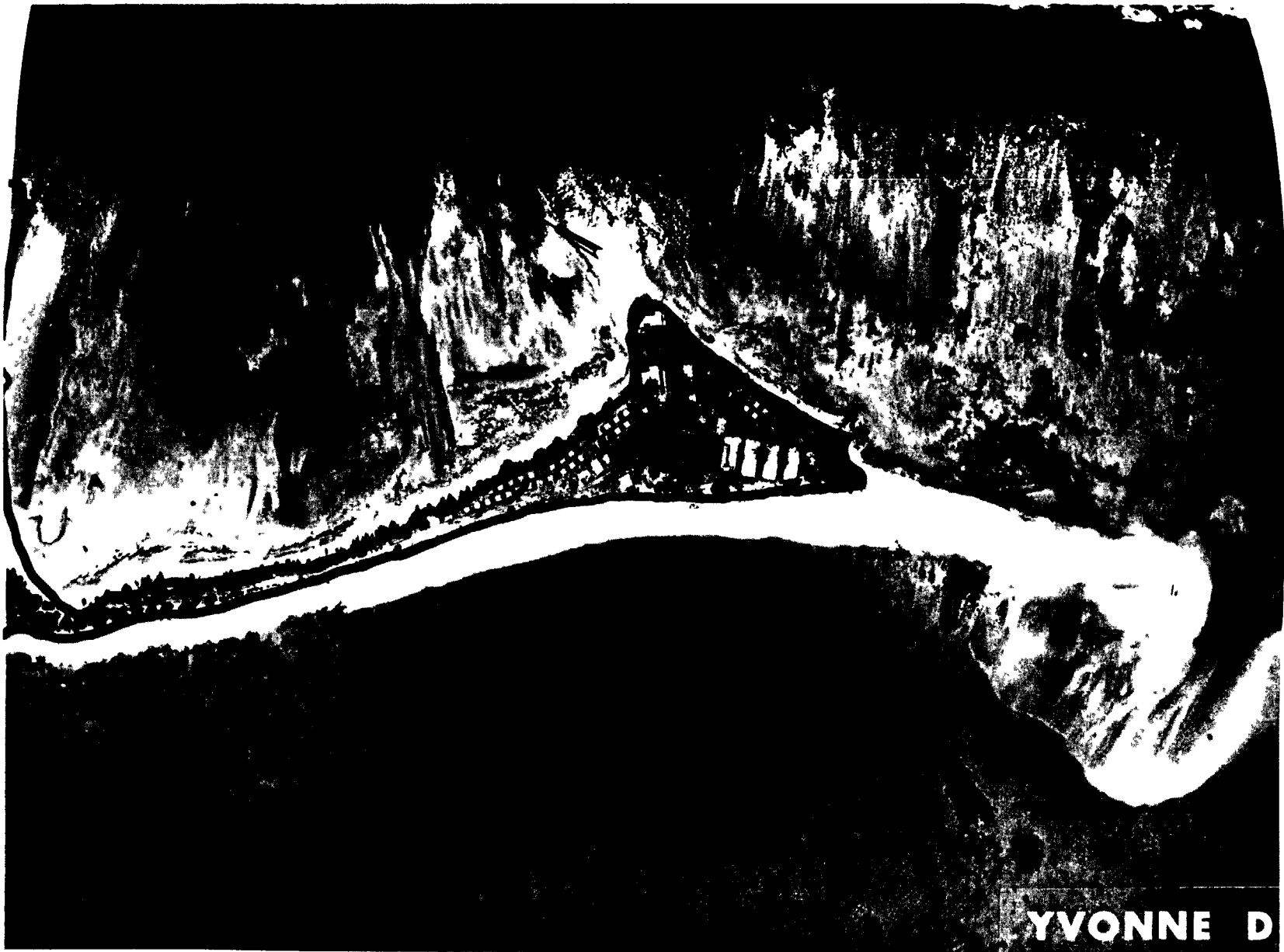
100 METERS



Fig. B.25.1.j. The average  $^{90}\text{Sr}$  activities (pCi/gm) in soil samples collected to a depth of 15 cm.



400 YVONNE  
L. 2. 2. 2.



YVONNE D

Fig. B.25.1.k.  $^{137}\text{Cs}$  isoexposure and isoconcentration contours. (Refer to alphabetic symbol key in this appendix.)

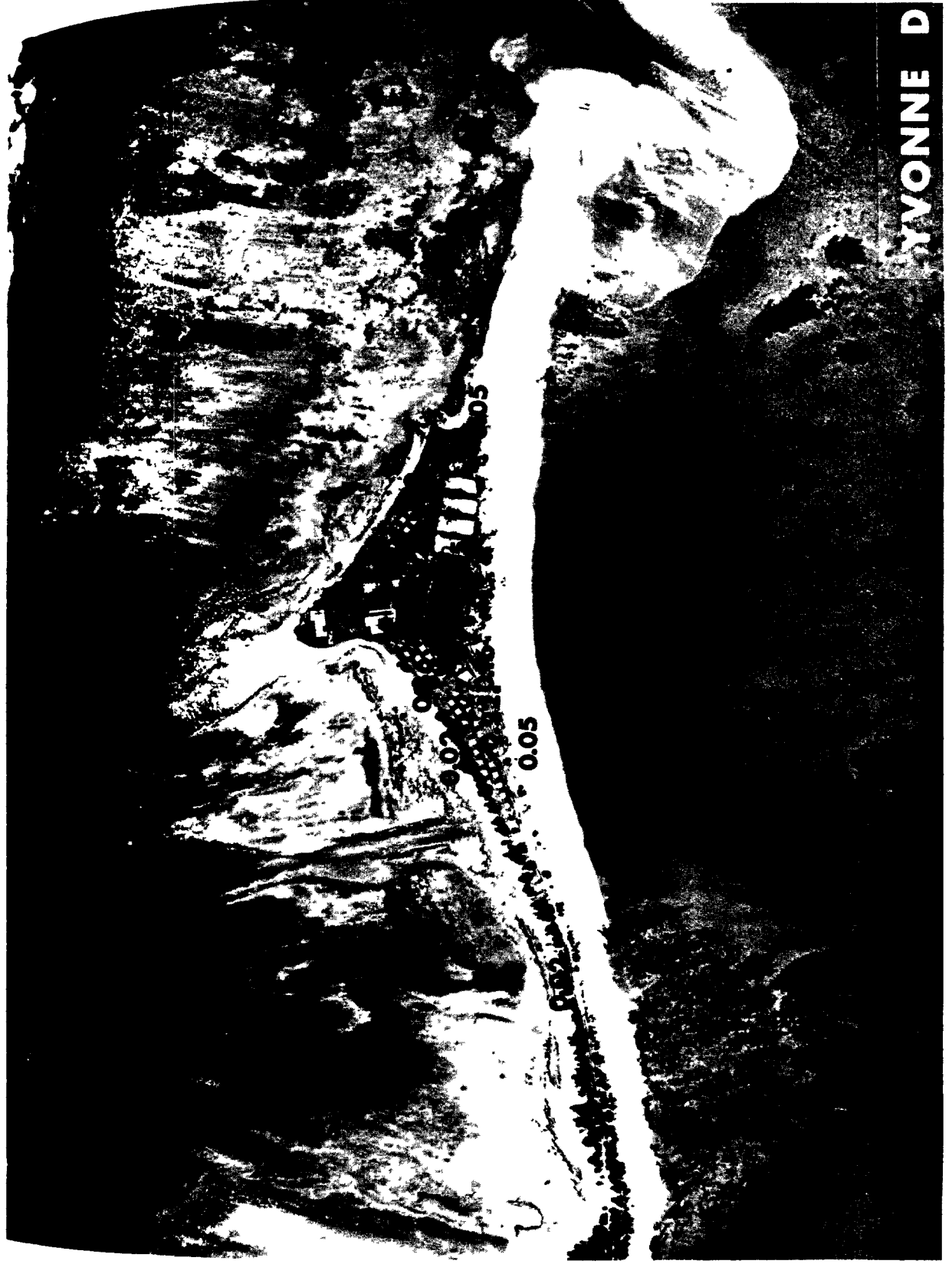


Fig. B.25.1.1. The average  $^{137}\text{Cs}$  activities ( $\mu\text{Ci}/\text{gm}$ ) in soil samples collected to a depth of 15 cm.



Fig. B.25.1.m.  $^{60}\text{Co}$  isoexposure and isoconcentration contours. (Refer to alphabetic symbol key in this appendix.)

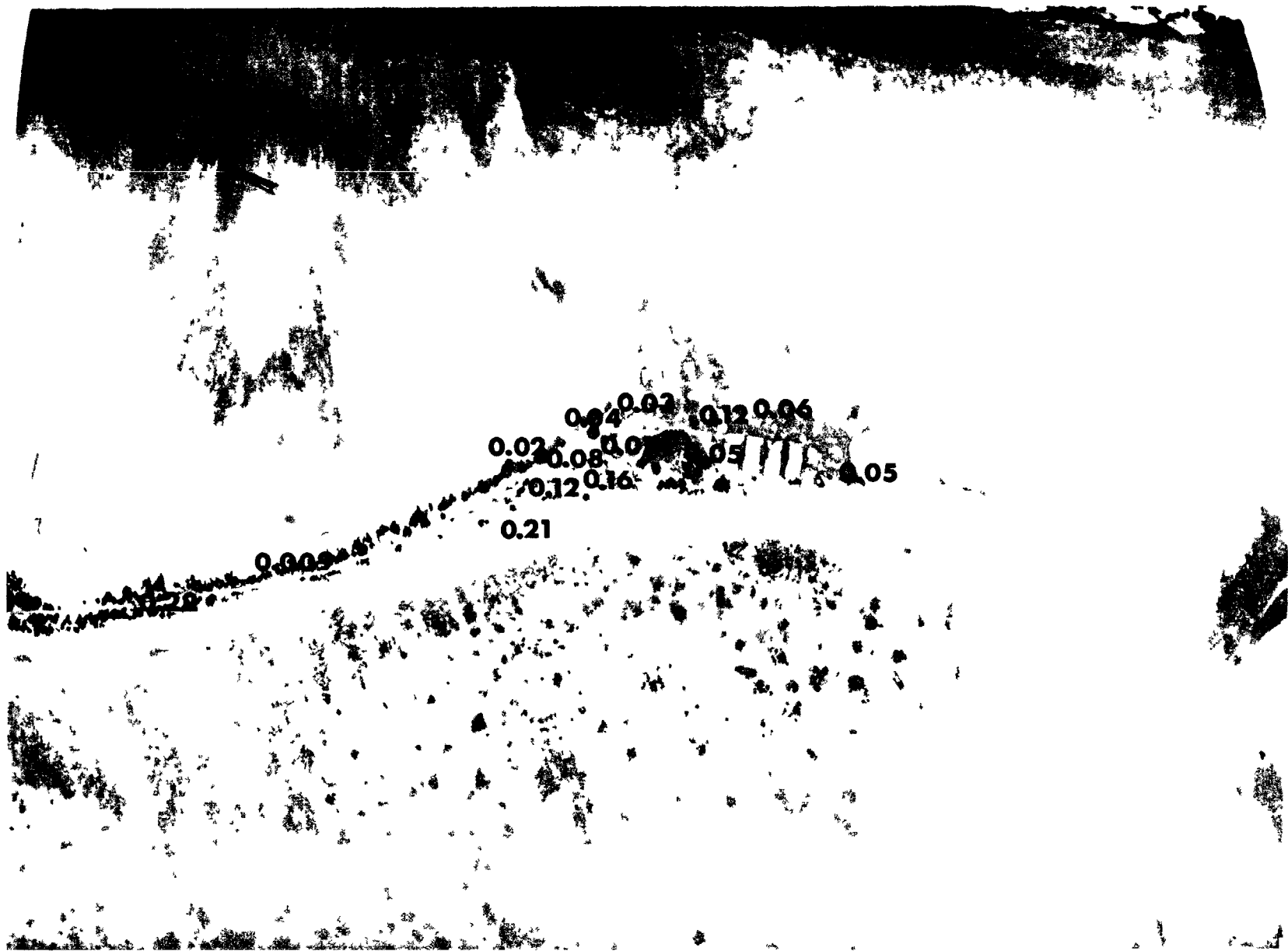


Fig. B.25.1.n. The average  $^{60}\text{Co}$  activities (pCi/gm) in soil samples collected to a depth of 15 cm.



Fig. B.25.1.o. Terrestrial animal sample locations.

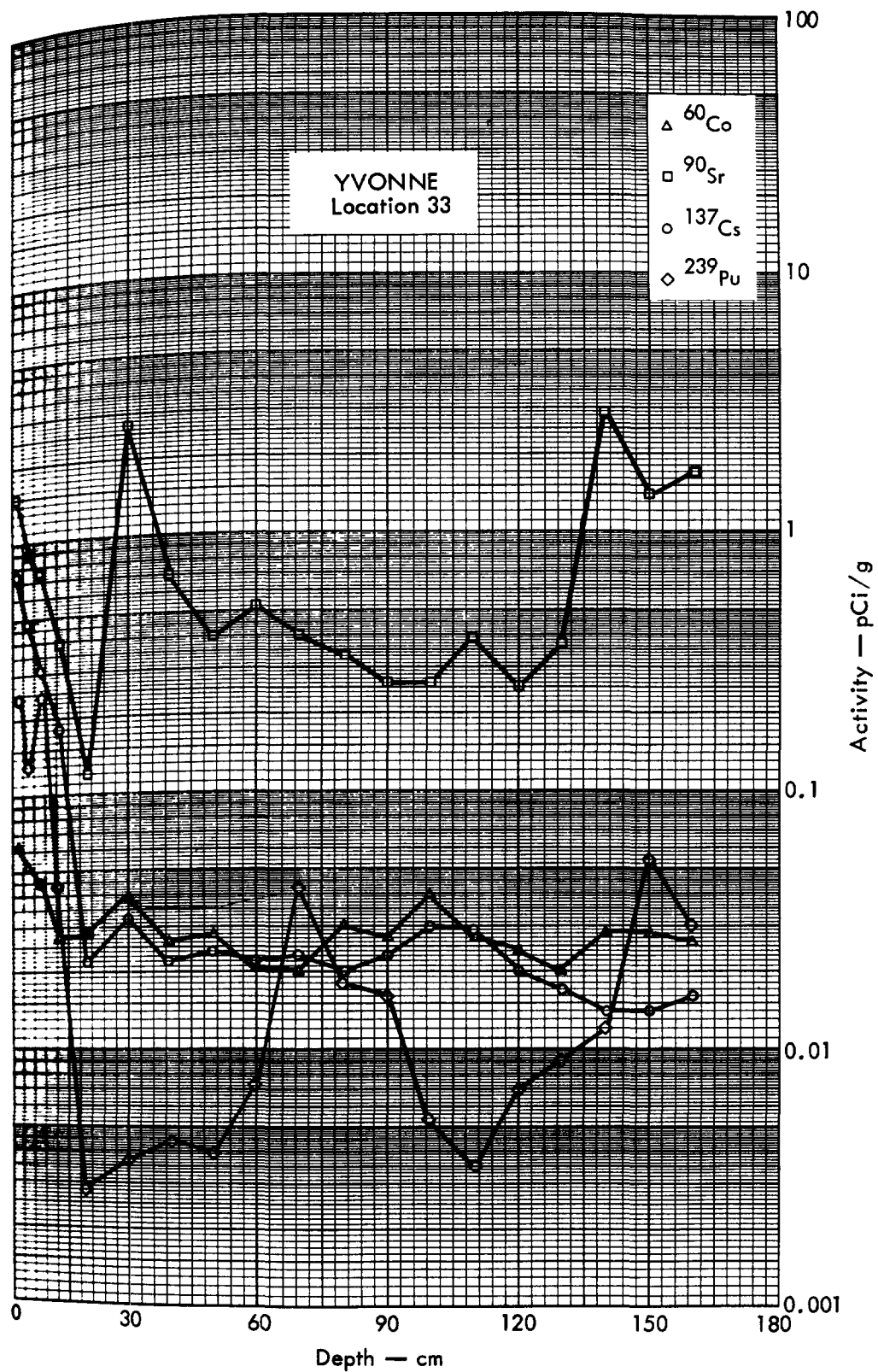


Fig. B. 25.2a. Activities of selected radionuclides as a function of soil depth.



YVONNE E

Fig. B.26. L. a.



YVONNE F

Fig. B.27.1.





Fig. B.28.1.a.



Fig. B.28.1.b. Gross count isoeexposure contours. (Refer to alphabetic symbol key in this appendix.)



Fig. B.28.1.d. The gamma background exposure rate ( $\mu\text{R}/\text{hr}$ ) at 1 m above the ground, measured with a portable NaI scintillation counter.



Fig. B.28.1.f. Soil-sample locations.



Fig. B.28.1.g. Vegetation sample locations.



Fig. B.28.1.i. The average  $^{239}\text{Pu}$  activities (pCi/g) in soil samples collected to a depth of 15 cm.

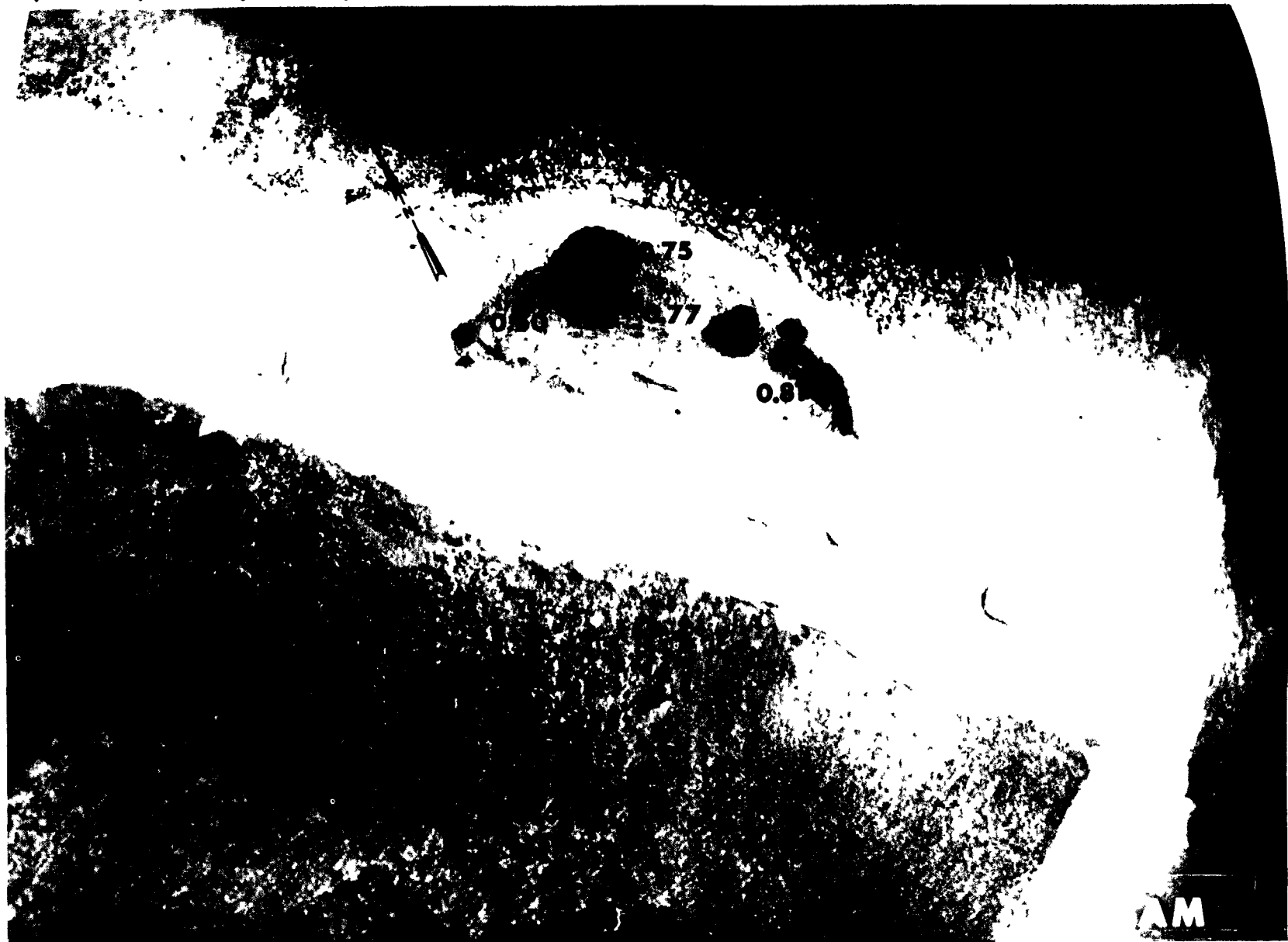


Fig. B.28.1.j. The average  $^{90}\text{Sr}$  activities (pCi/g) in soil samples collected to a depth of 15 cm.



Fig. B.28.1.k.  $^{137}\text{Cs}$  isoexposure and isoconcentration contours. (Refer to alphabetic symbol key in this appendix.)





Fig. B.28.1.1. The average  $^{137}\text{Cs}$  activities (pCi/g) in soil samples collected to a depth of 15 cm.



Fig. B.28.1.m.  $^{60}\text{Co}$  isoexposure and isoconcentration contours. (Refer to alphabetic symbol key in this appendix.)



Fig. B.28.1.n. The average  $^{60}\text{Co}$  activities (pCi/g) in soil samples collected to a depth of 15 cm.

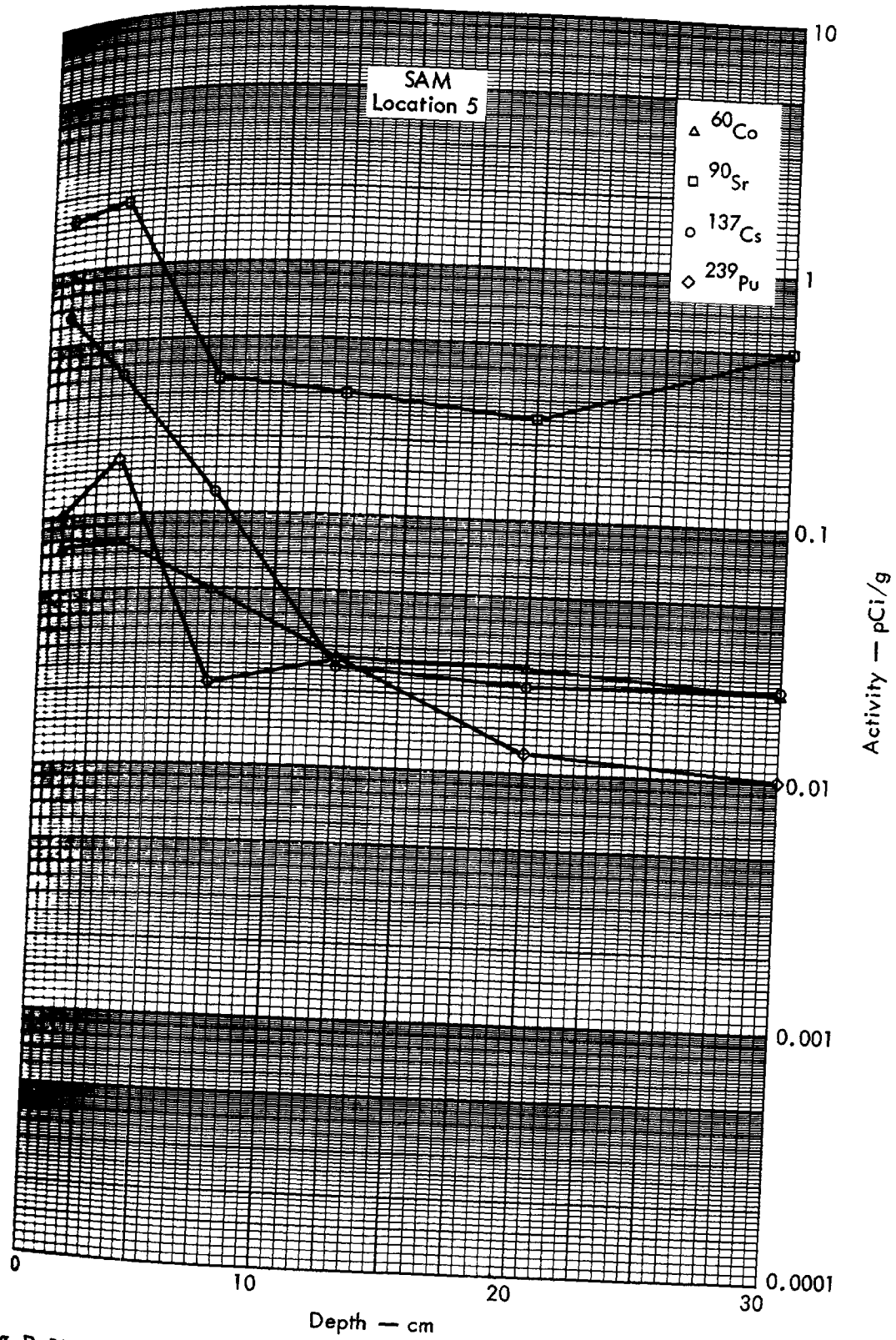


Fig. B. 28. 2a. Activities of selected radionuclides as a function of soil depth.



TOM

Fig. B.29.1.a.

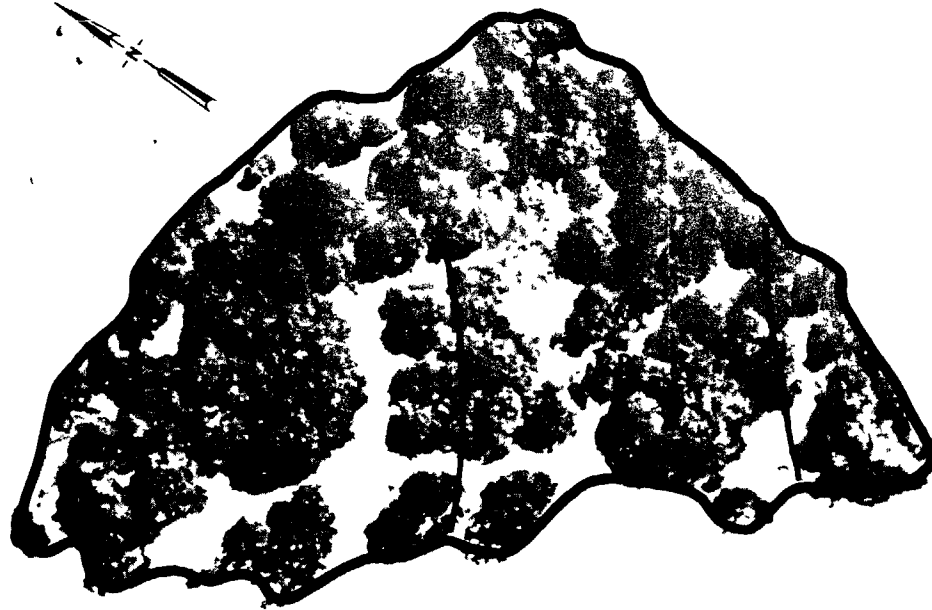


Fig. B.29.1.b. Gross count isoexposure contours. (Refer to alphabetic symbol key in this appendix.)

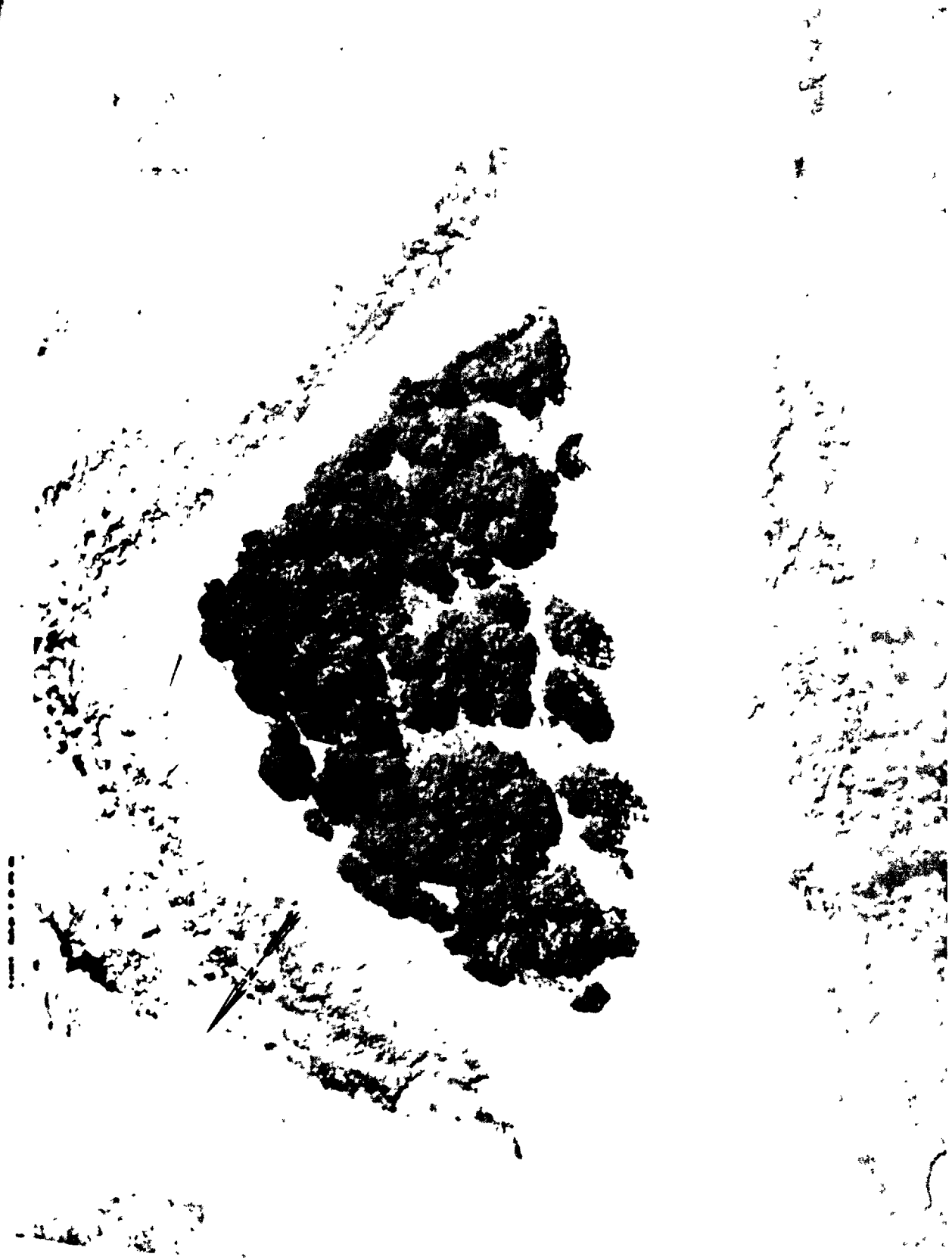


Fig. B.29.1.d. The gamma background exposure rate ( $\mu\text{R}/\text{hr}$ ) at 1 m above the ground, measured with a portable NaI scintillation counter.

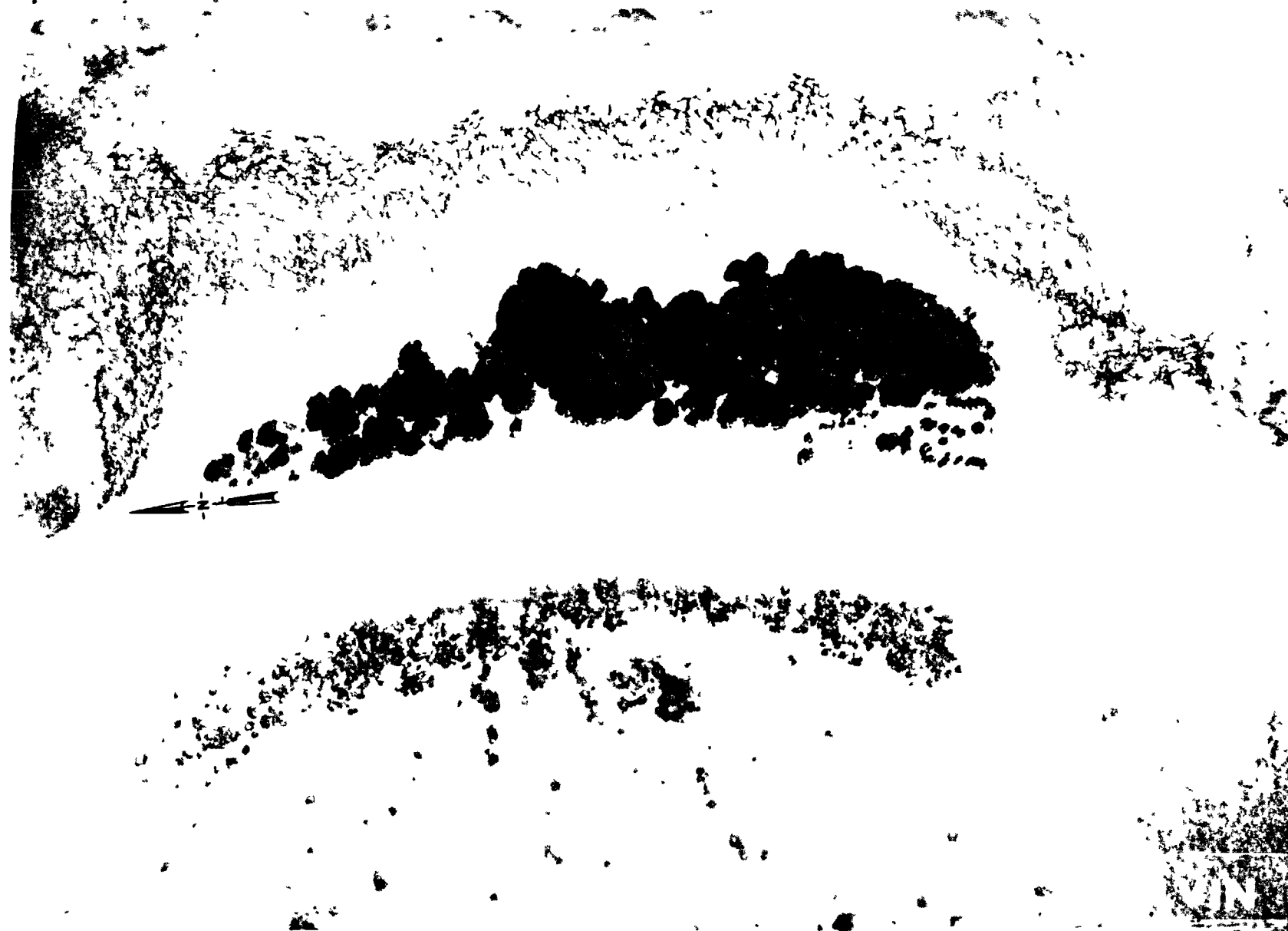
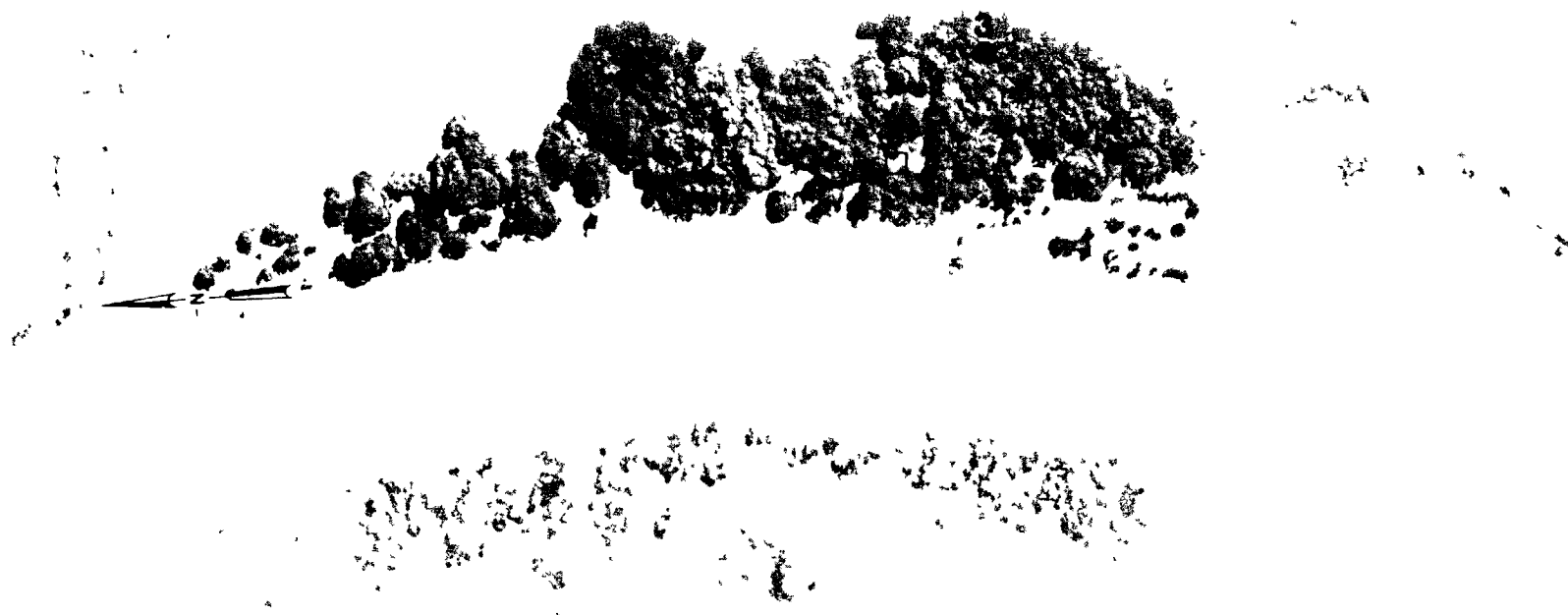


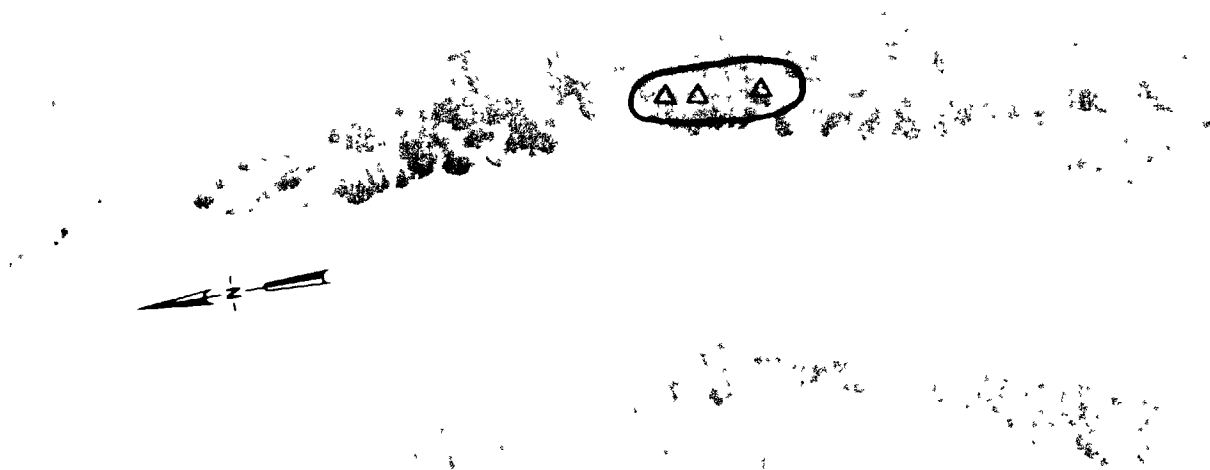
Fig. B.32.1.d. The gamma background exposure rate ( $\mu\text{R/hr}$ ) at 1 m above the ground, measured with a portable NaI scintillation counter.





- PROFILE SAMPLES (0-35 cm)
- CORE SAMPLES (15 cm)

Fig. B.32.1.1. Soil-sample locations.



△△△ MESSERSCHMIDIA

Fig. B.32.1.g. Vegetation sample locations.

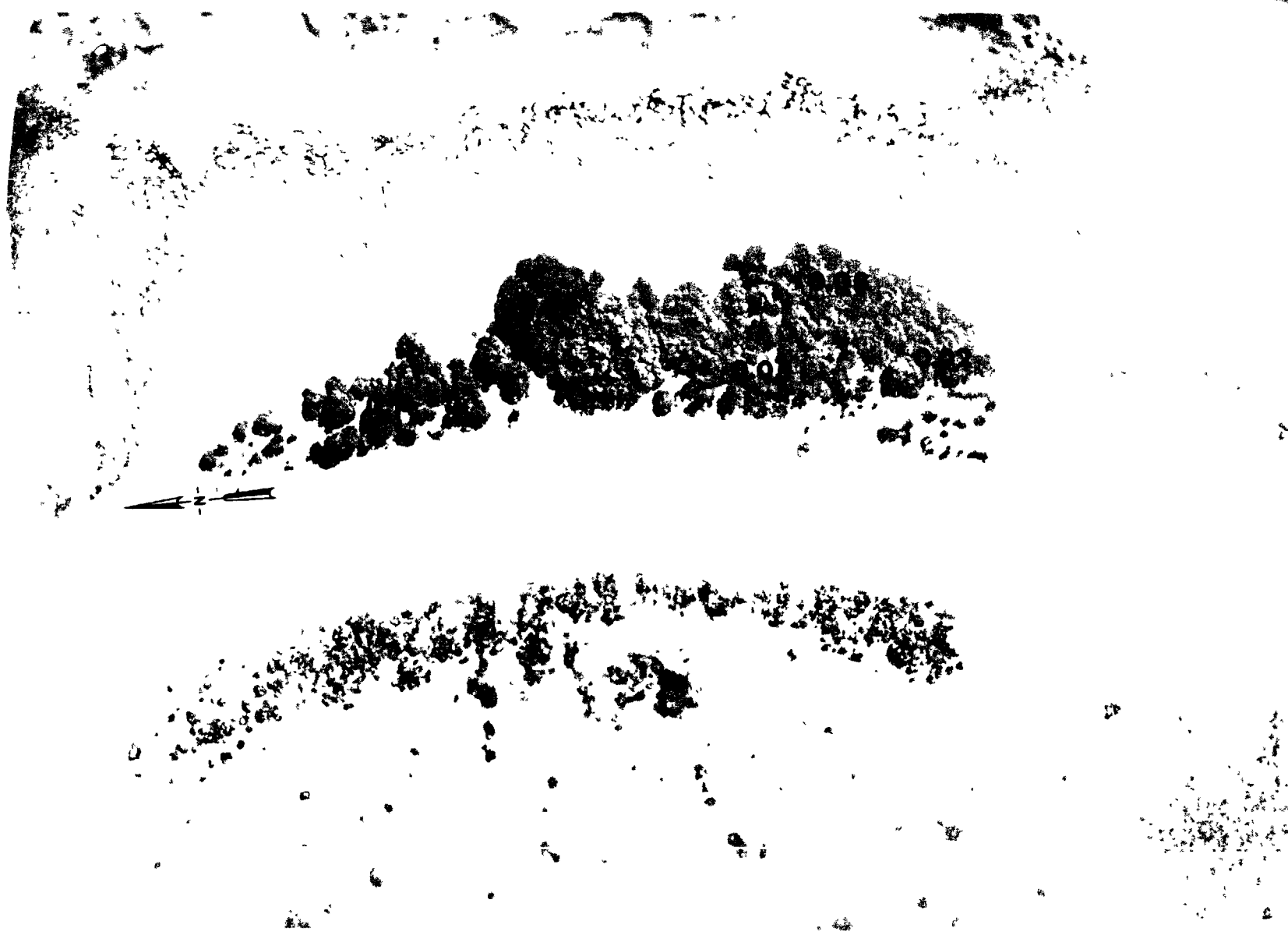


Fig. B.32.1.i. The average  $^{239}\text{Pu}$  activities (pCi/gm) in soil samples collected to a depth of 15 cm.

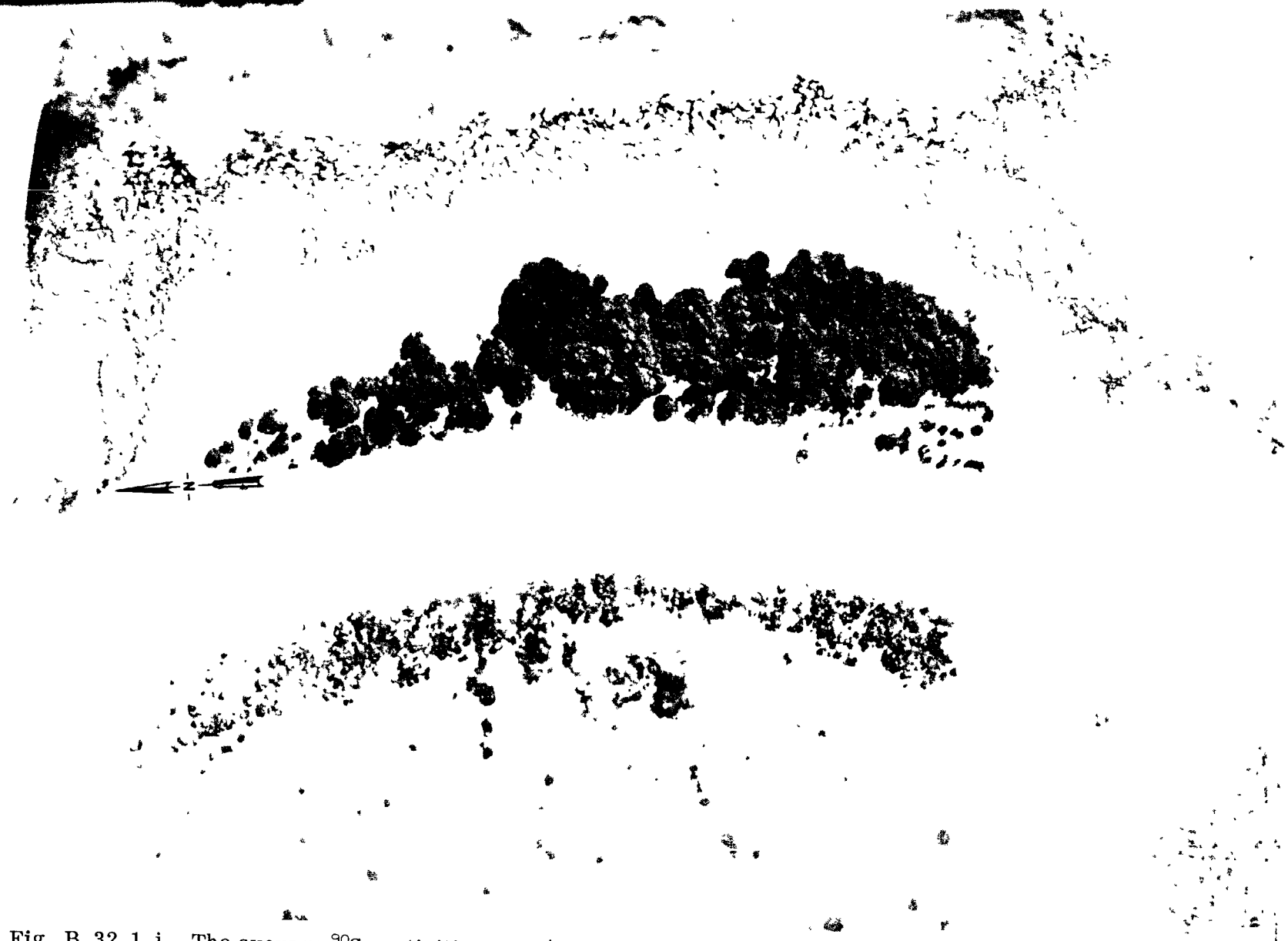


Fig. B.32.1.j. The average  $^{90}\text{Sr}$  activities (pCi/gm) in soil samples collected to a depth of 15 cm.

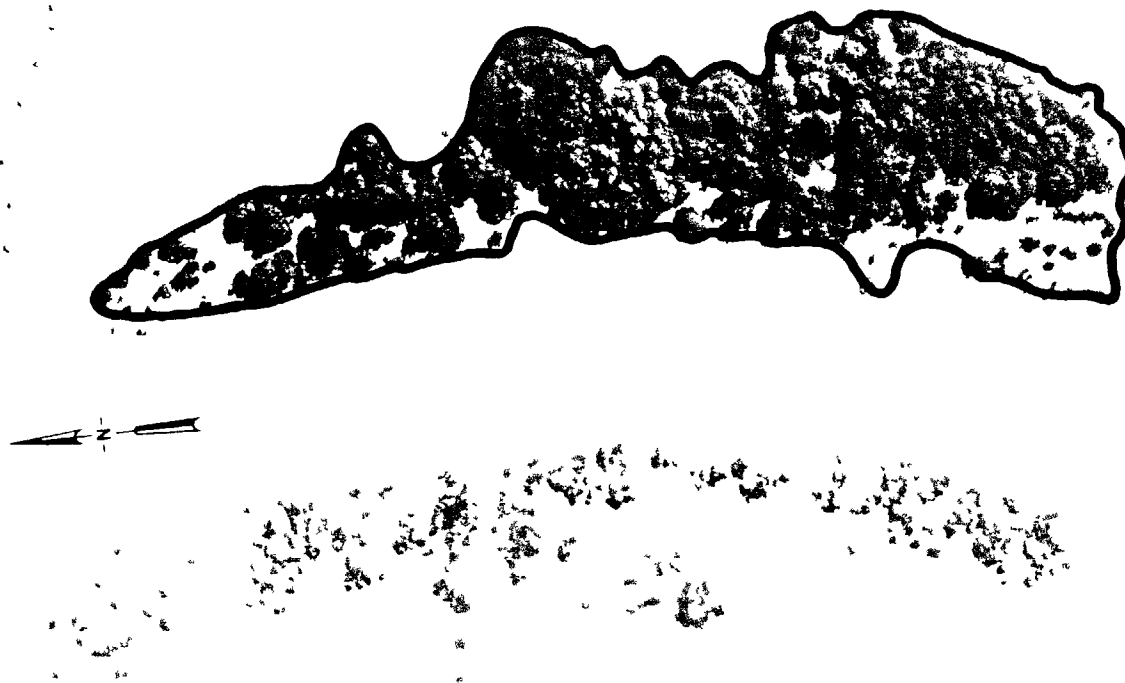


Fig. B.32.1.k.  $^{137}\text{Cs}$  isosexposure and isoconcentration contours. (Refer to alphabetic symbol key in this appendix.)

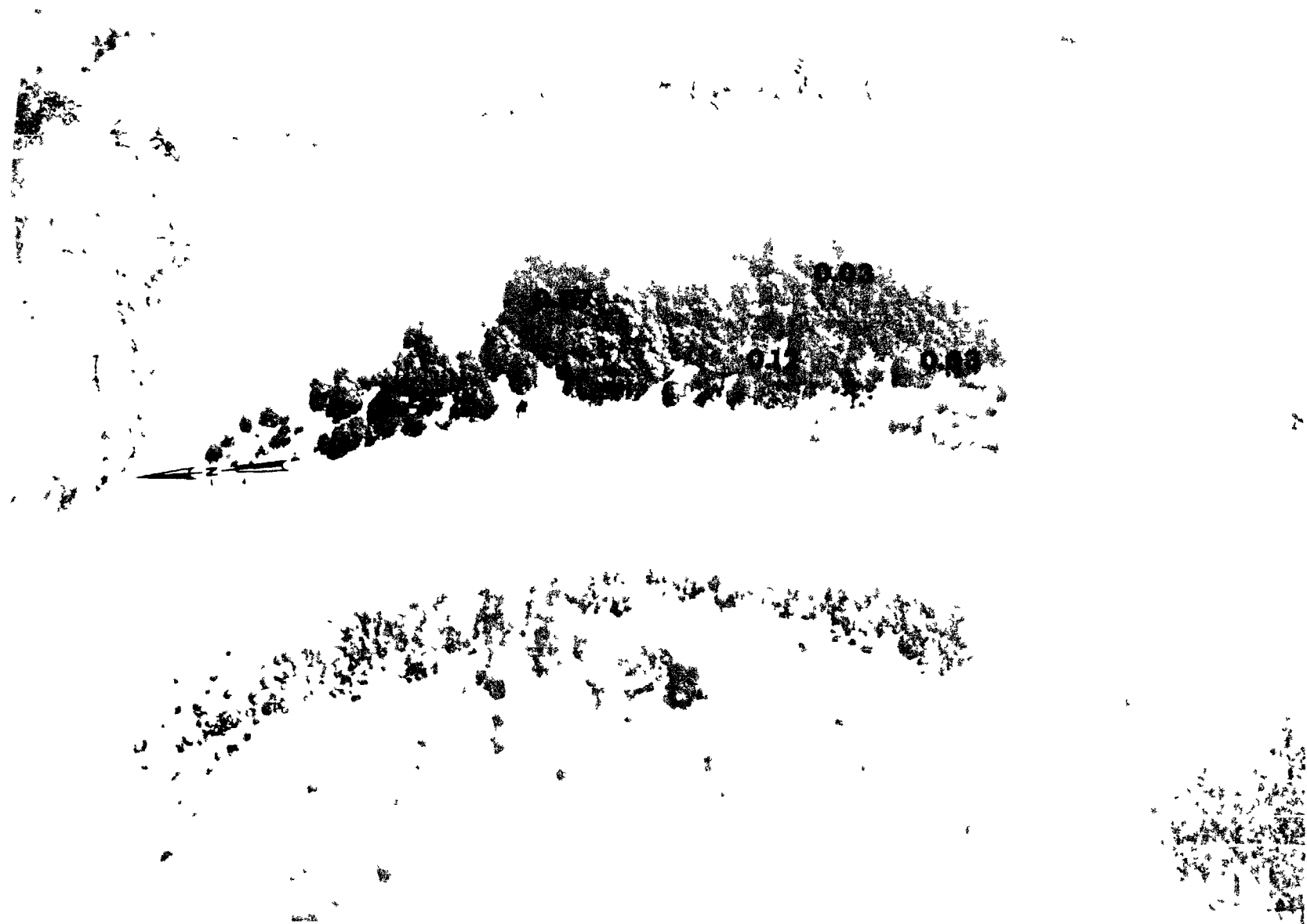


Fig. B.32.1.1. The average  $^{137}\text{Cs}$  activities (pCi/gm) in soil samples collected to a depth of 15 cm.



Fig. B.32.1.m.  $^{60}\text{Co}$  isoexposure and isoconcentration contours. (Refer to alphabetic symbol key in this appendix.)

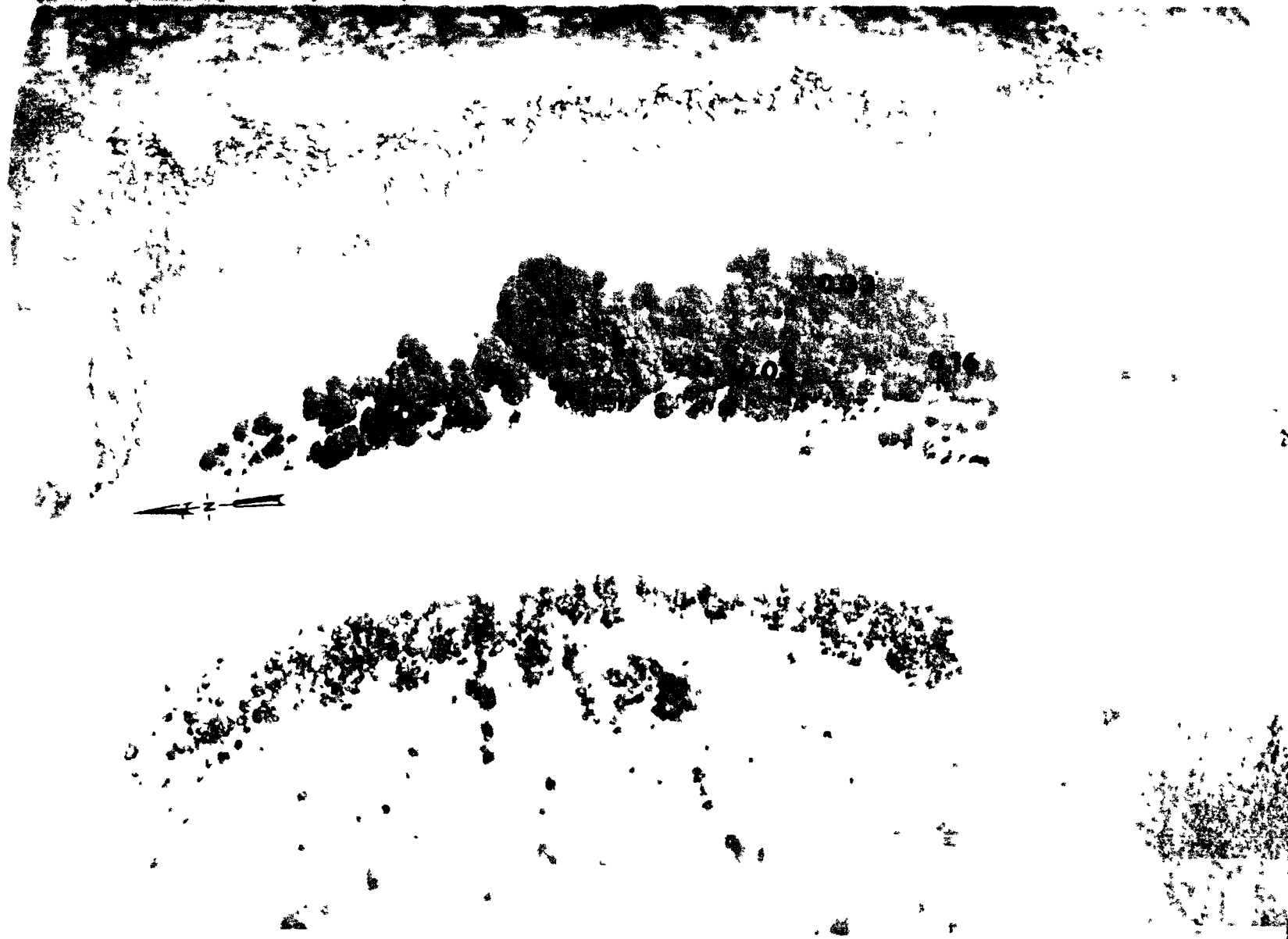


Fig. B.32.1.n. The average  $^{60}\text{Co}$  activities (pCi/gm) in soil samples collected to a depth of 15 cm.



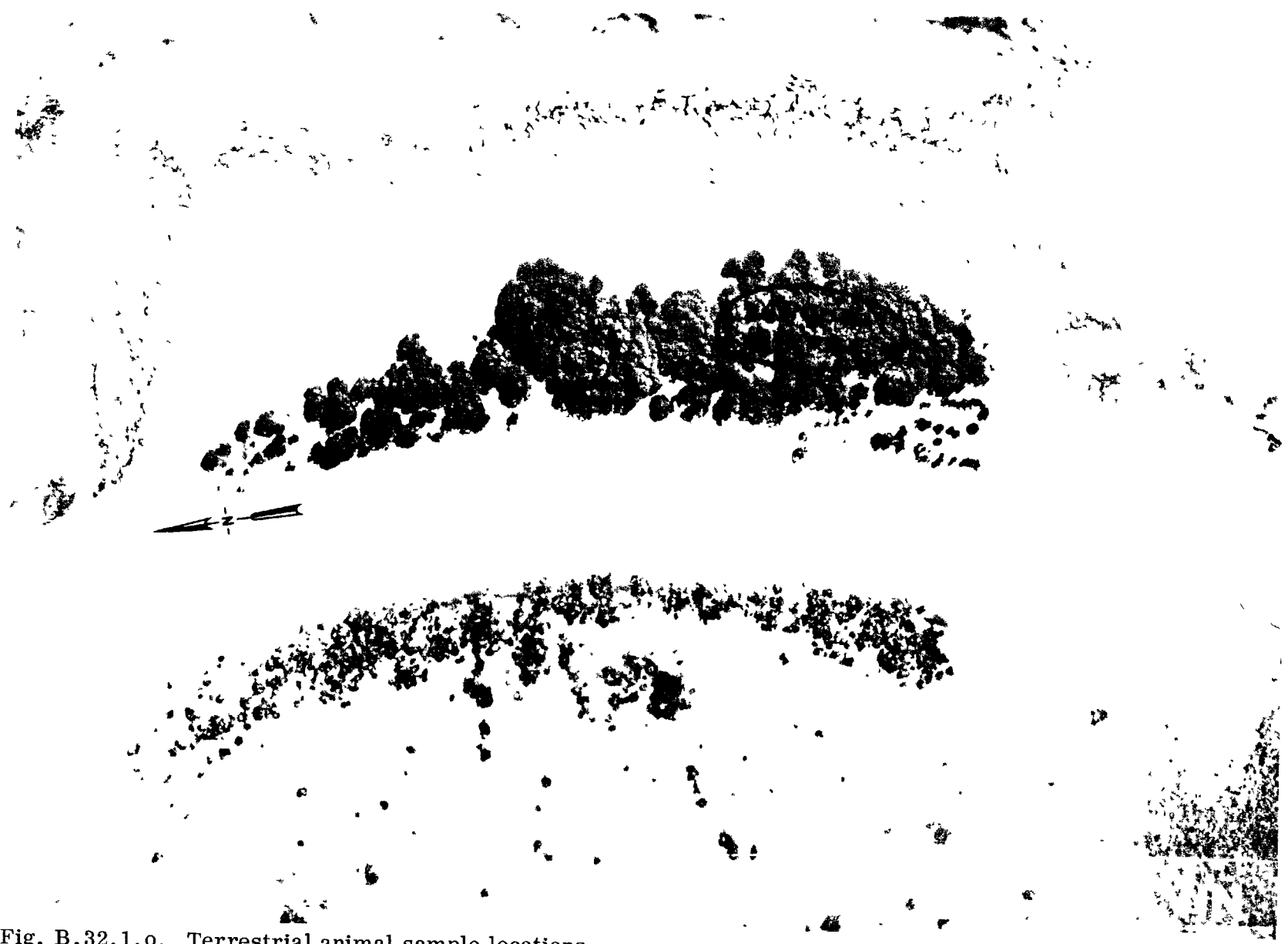


Fig. B.32.1.o. Terrestrial animal sample locations.

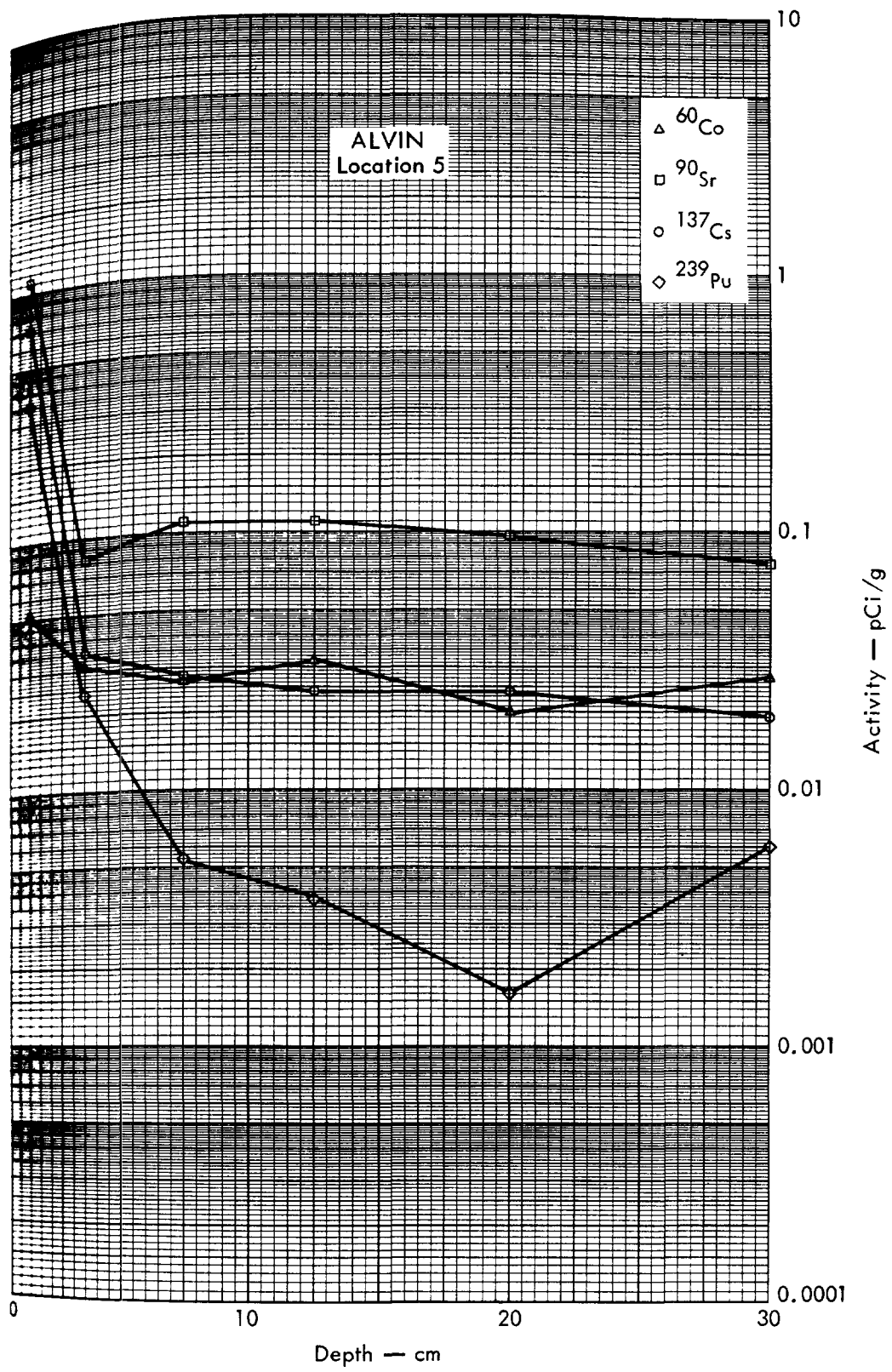


Fig. B.32.2a. Activities of selected radionuclides as a function of soil depth.



**BRUCE**

Fig. B.33.1.a.



Fig. B.33.1.b. Gross count isocount contours. (Refer to alphabetic symbol key in this appendix.)

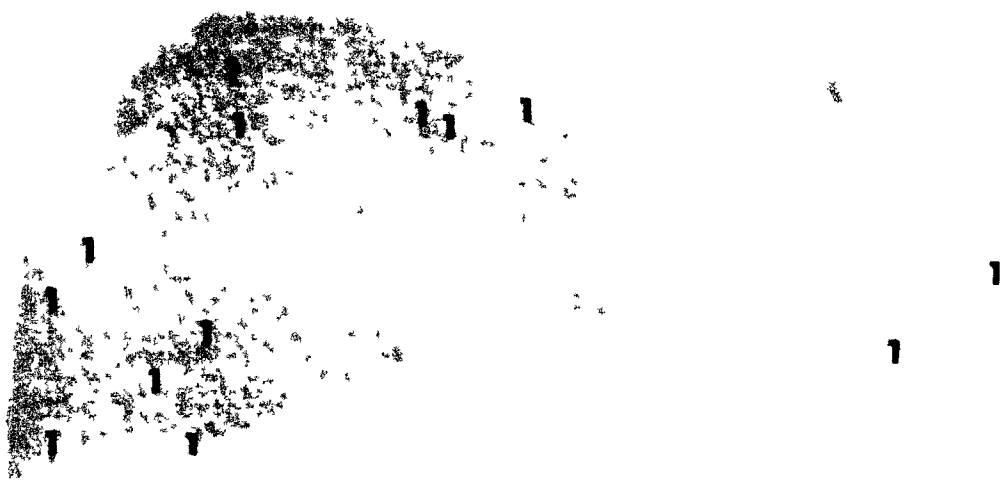


Fig. B.33.1.d. The gamma background exposure rate ( $\mu\text{R/hr}$ ) at 1 m above the ground, measured with a portable NaI scintillation counter.

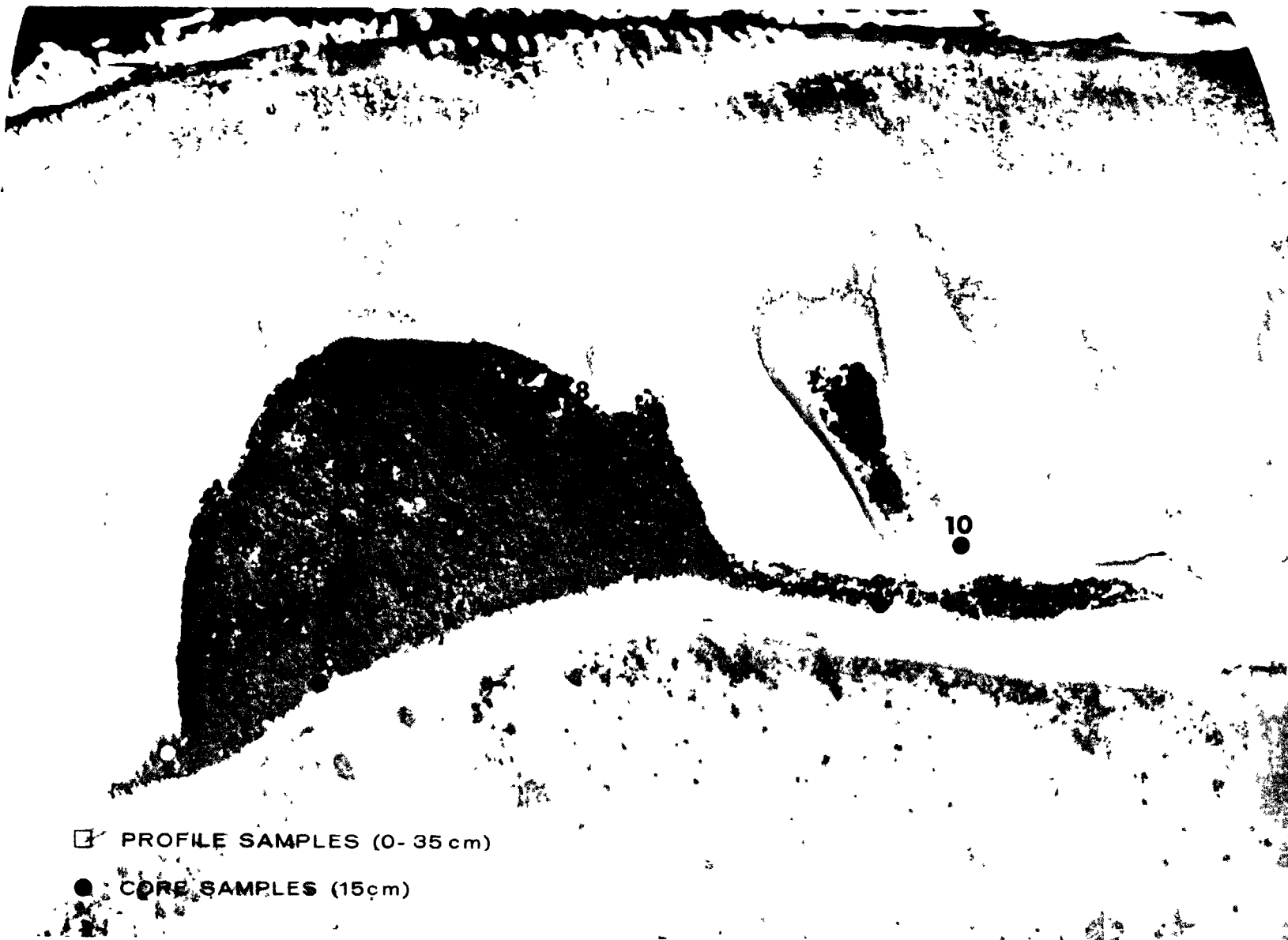


Fig. B.33.1.f. Soil-sample locations.



△ △ △ MESSERSCHMIDIA

○ ○ ○ SCAEVOLA

● COCONUT

◇ PISONIA

Fig. B.33.1.g. Vegetation sample locations.

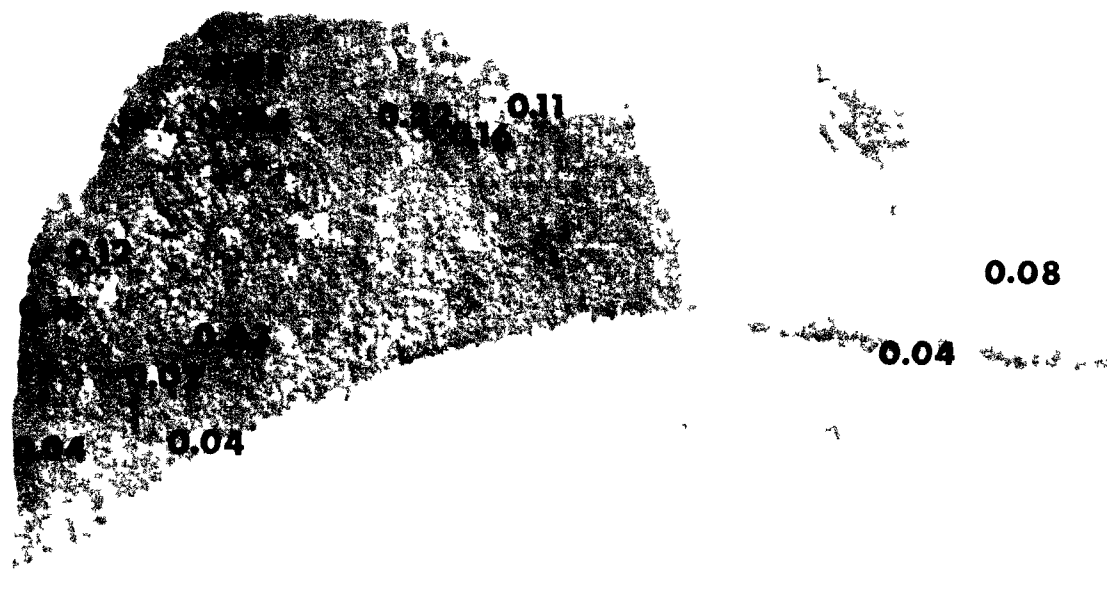


Fig. B.33.1.i. The average  $^{239}\text{Pu}$  activities (pCi/g) in soil samples collected to a depth of 15 cm.





Fig. B.33.1.j. The average <sup>90</sup>Sr activities (pCi/g) in soil samples collected to a depth of 15 cm.



Fig. B.33.1.k.  $^{137}\text{Cs}$  isoexposure and isoconcentration contours. (Refer to alphabetic symbol key in this appendix.)



Fig. B.33.1.1. The average <sup>137</sup>Cs activities (pCi/g) in soil samples collected to a depth of 15 cm.



Fig. B.33.1.m.  $^{60}\text{Co}$  isoexposure and isoconcentration contours. (Refer to alphabetic symbol key in this appendix.)

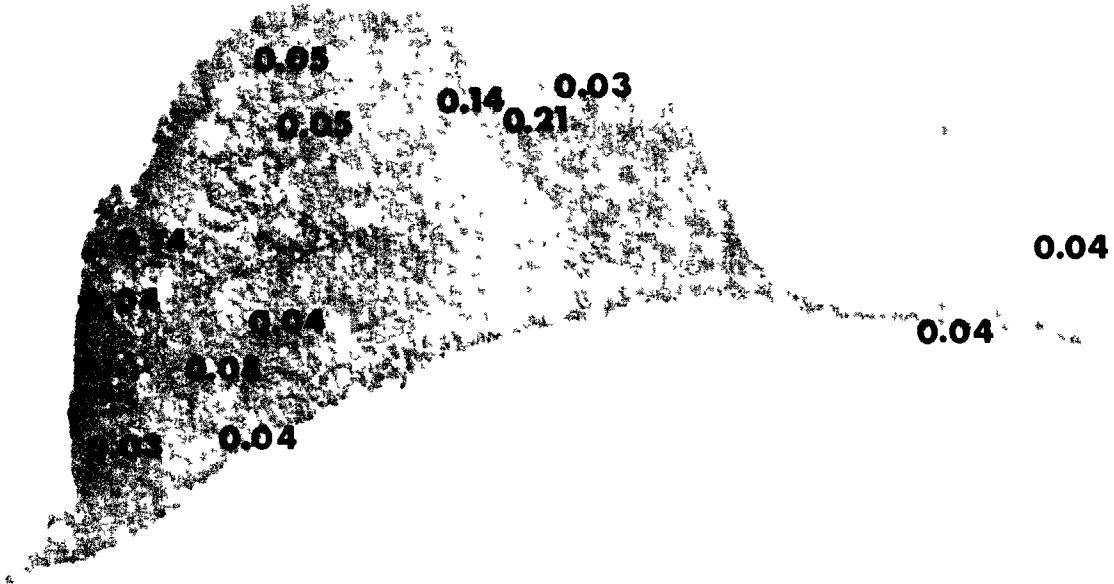


Fig. B.33.1.n. The average  $^{60}\text{Co}$  activities (pCi/g) in soil samples collected to a depth of 15 cm.



Fig. B.33.1.o. Terrestrial animal sample locations.

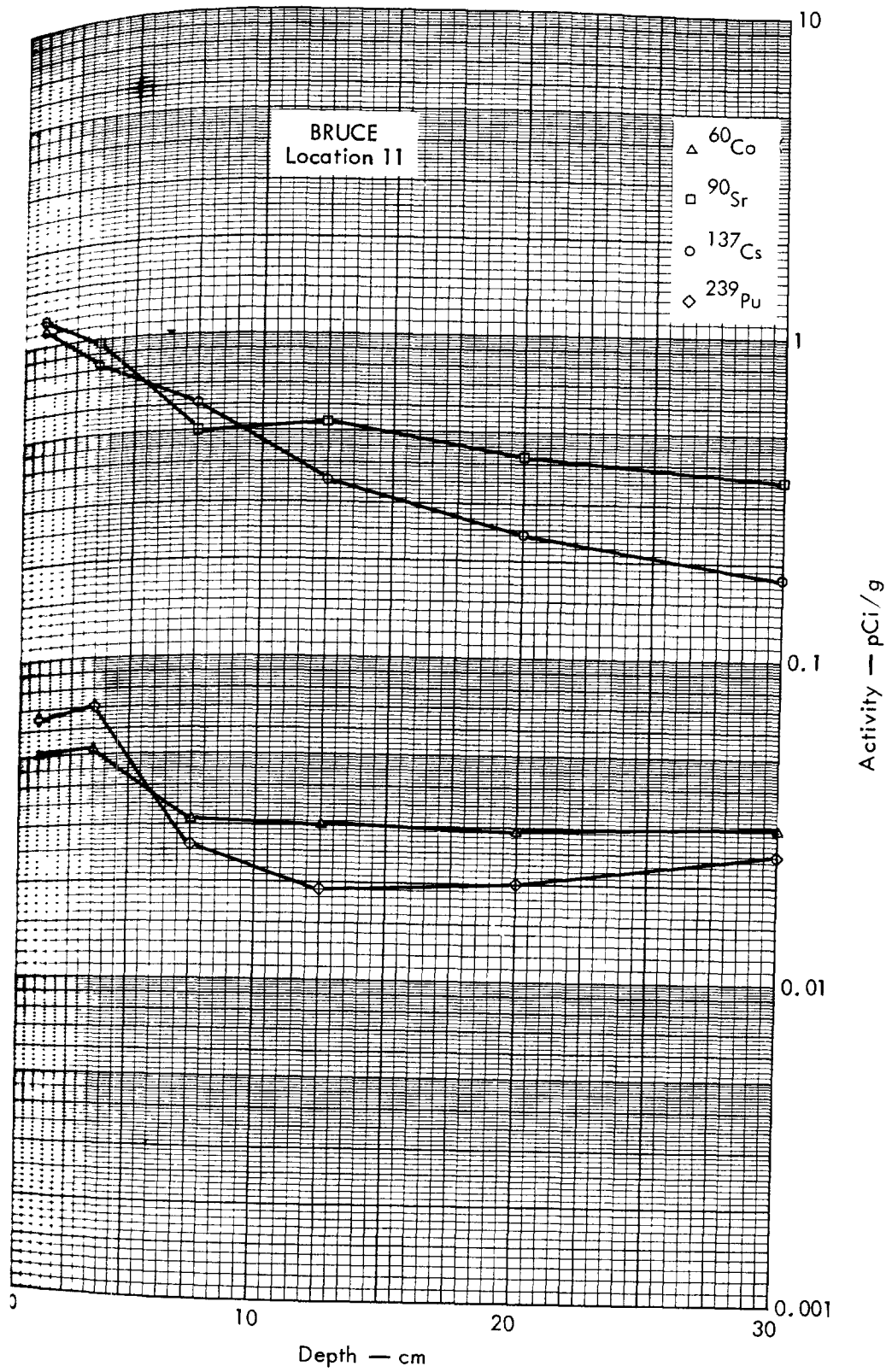


Fig. B.33.2a. Activities of selected radionuclides as a function of soil depth.

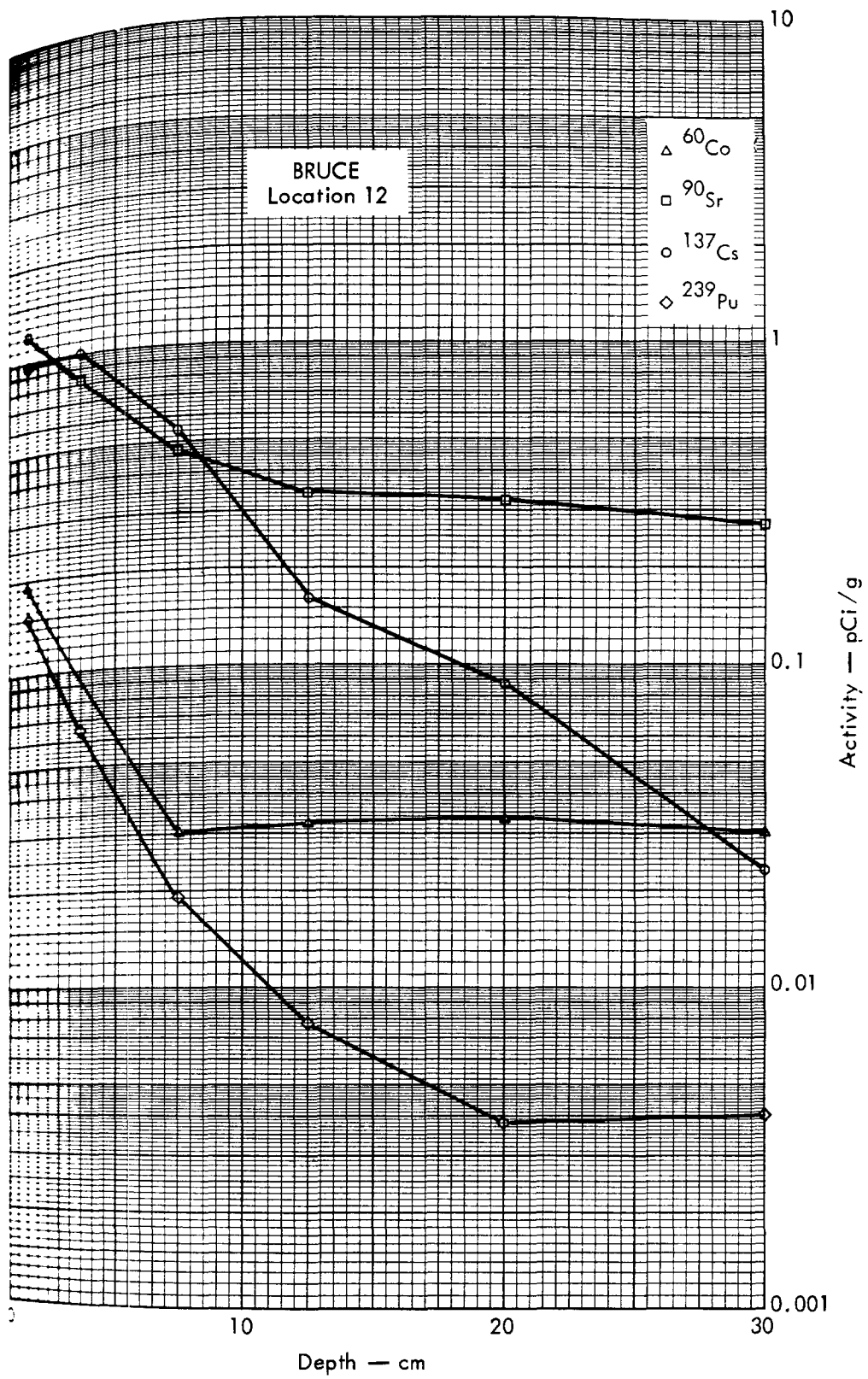


Fig. B.33.2b. Activities of selected radionuclides as a function of soil depth.



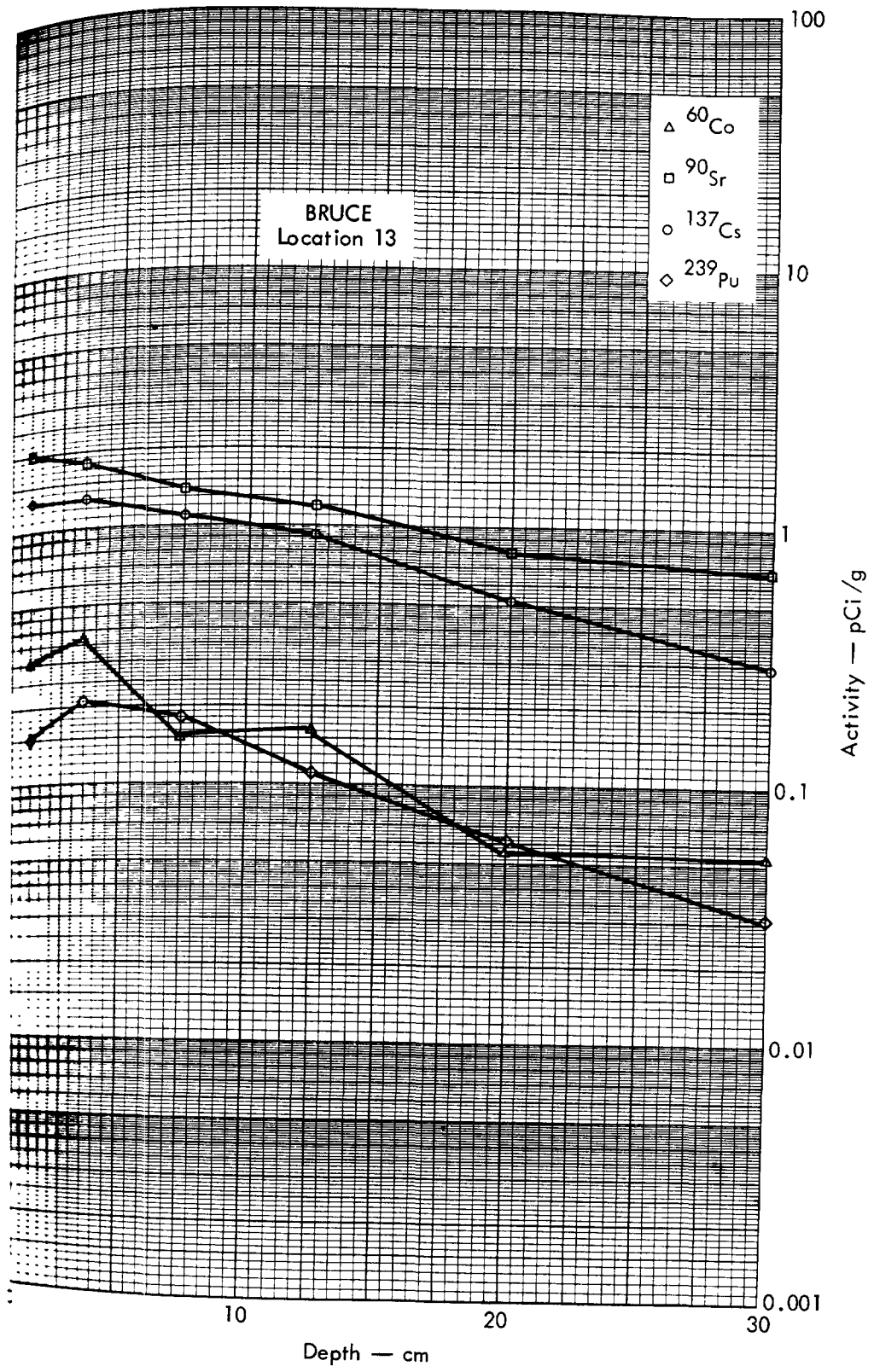


Fig. B.33.2c. Activities of selected radionuclides as a function of soil depth.



Fig. B.34.1.a.



Fig. B.34.1.b. Gross count isosexposure contours. (Refer to alphabetic symbol key in this appendix.)



Fig. B.34.1.d. The gamma background exposure rate ( $\mu\text{R}/\text{hr}$ ) at 1 m above the ground, measured with a portable NaI scintillation counter.



Fig. B.34.1.f. Soil-sample locations.

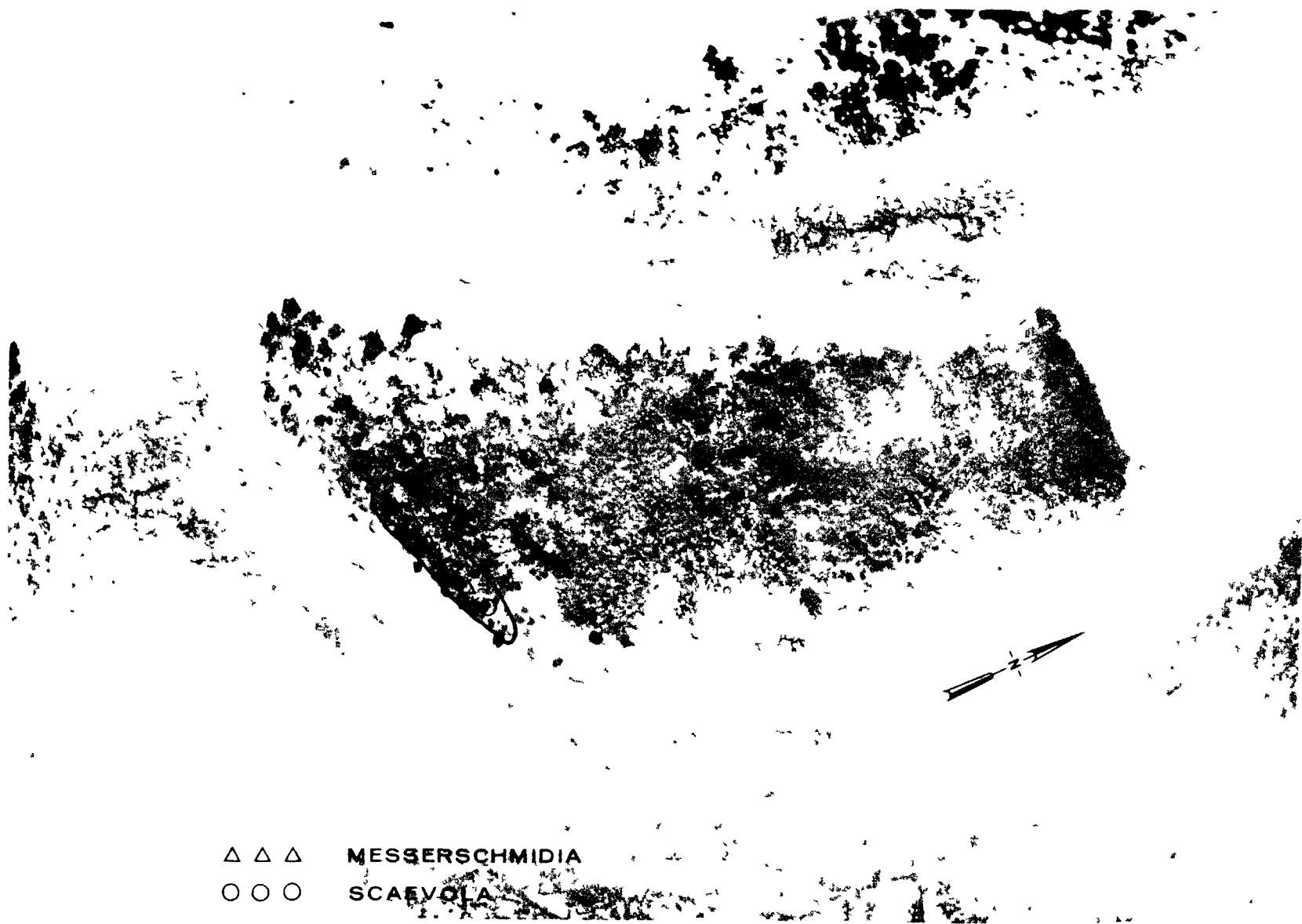


Fig. B.34.1.g. Vegetation sample locations.

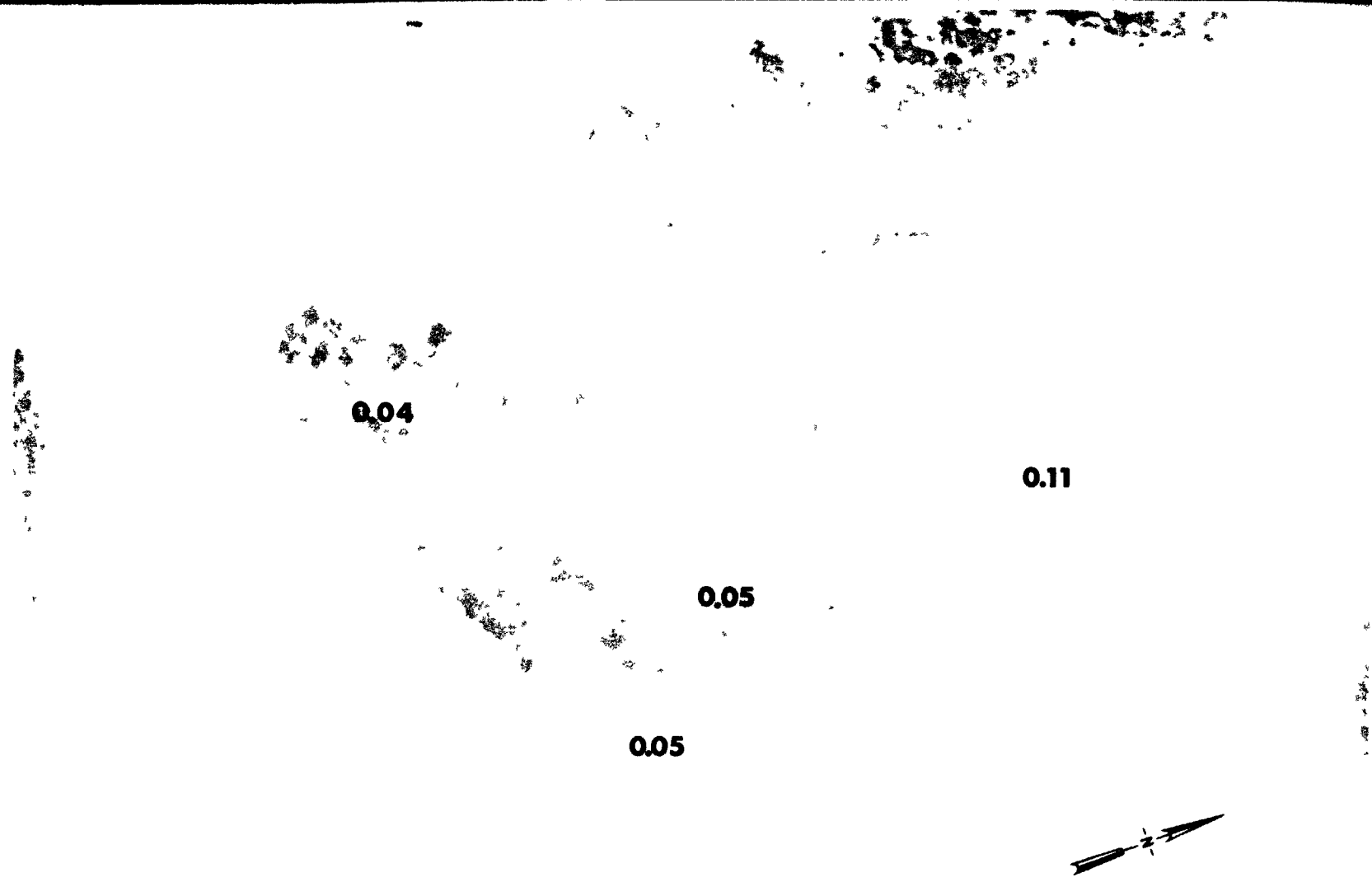


Fig. B.34.1.i. The average  $^{239}\text{Pu}$  activities (pCi/gm) in soil samples collected to a depth of 15 cm.



Fig. B.34.1.j. The average <sup>90</sup>Sr activities (pCi/gm) in soil samples collected to a depth of 15 cm.





Fig. B.34, 1.k.  $^{137}\text{Cs}$  isosexposure and isoconcentration contours. (Refer to alphabetic symbol key in this appendix.)



Fig. B.34.1.1. The average  $^{137}\text{Cs}$  activities (pCi/gm) in soil samples collected to a depth of 15 cm.



Fig. B.34.1.m.  $^{60}\text{Co}$  isoexposure and isoconcentration contours. (Refer to alphabetic symbol key in this appendix.)



Fig. B.34.1.n. The average  $^{60}\text{Co}$  activities (pCi/gm) in soil samples collected to a depth of 15 cm.



Fig. B.34.1.o. Terrestrial animal sample locations.

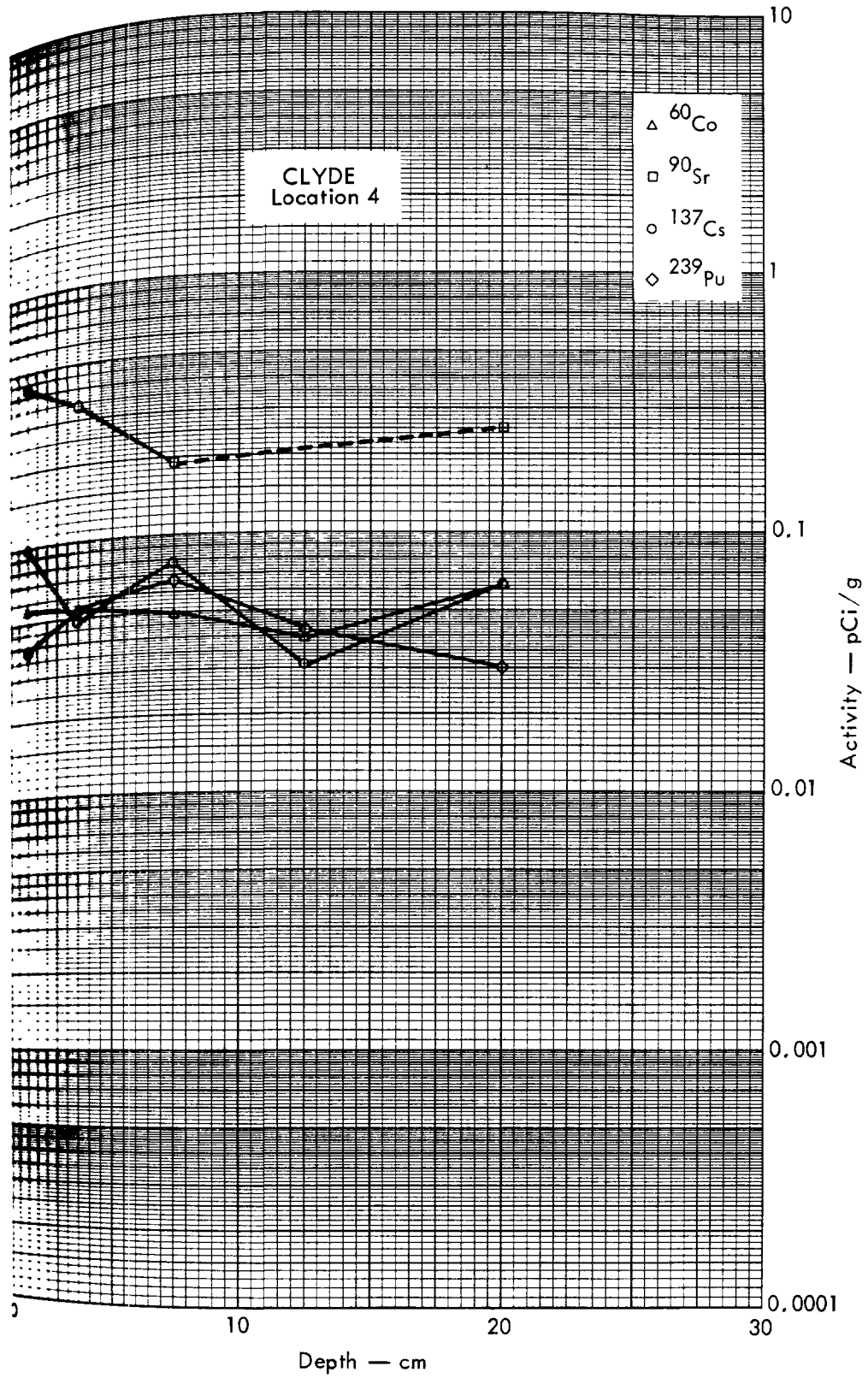


Fig. B. 34. 2a. Activities of selected radionuclides as a function of soil depth.



Fig. B.35. I. a.



Fig. B.35.1.b. Gross count isocounting contours. (Refer to alphabetic symbol key in this appendix.)





Fig. B.35.1.d. The gamma background exposure rate ( $\mu\text{R/hr}$ ) at 1 m above the ground, measured with a portable NaI scintillation counter.



Fig. B.35.1.f. Soil-sample locations.



Fig. B. 35. 1.g. Vegetation sample locations.

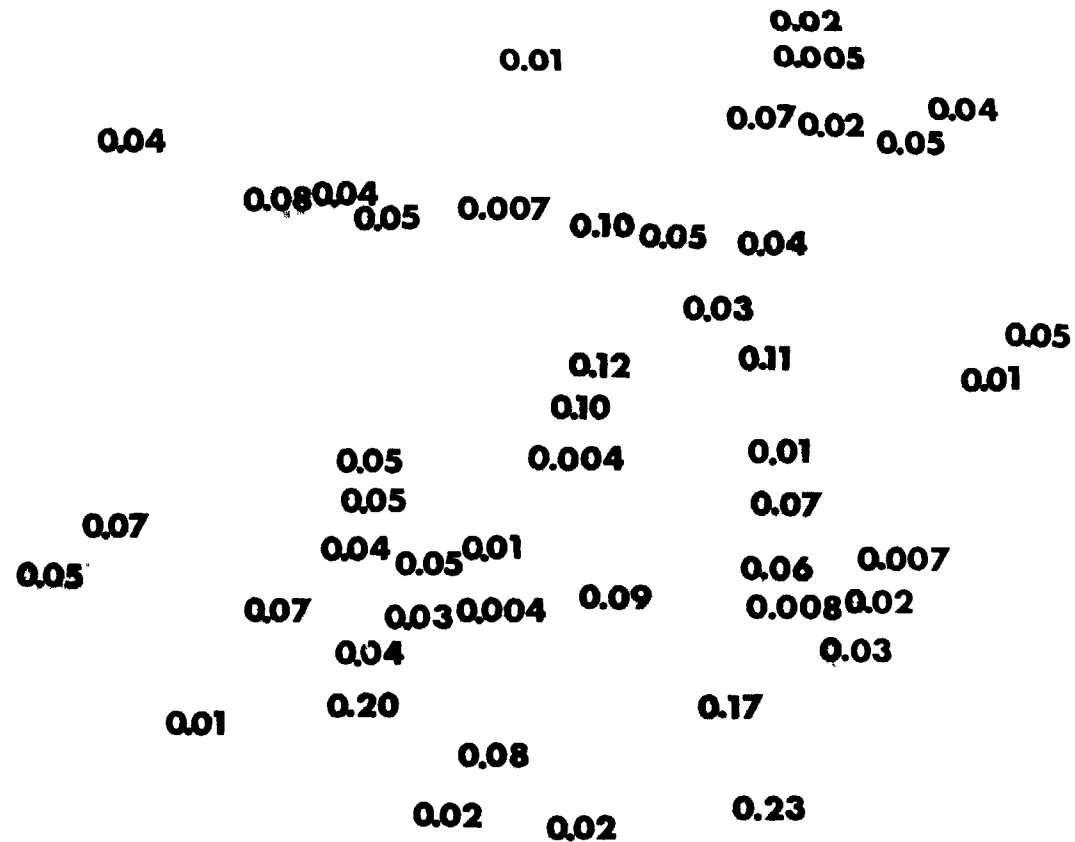


Fig. B.35.1.i. The average  $^{239}\text{Pu}$  activities (pCi/gm) in soil samples collected to a depth of 15 cm.



Fig. B.35.1.J. The average  $^{90}\text{Sr}$  activities (pCi/gm) in soil samples collected to a depth of 15 cm.



Fig. B.35.1.1. The average  $^{137}\text{Cs}$  activities (pCi/gm) in soil samples collected to a depth of 15 cm.





Fig. B.35.1.o. Terrestrial animal sample locations.



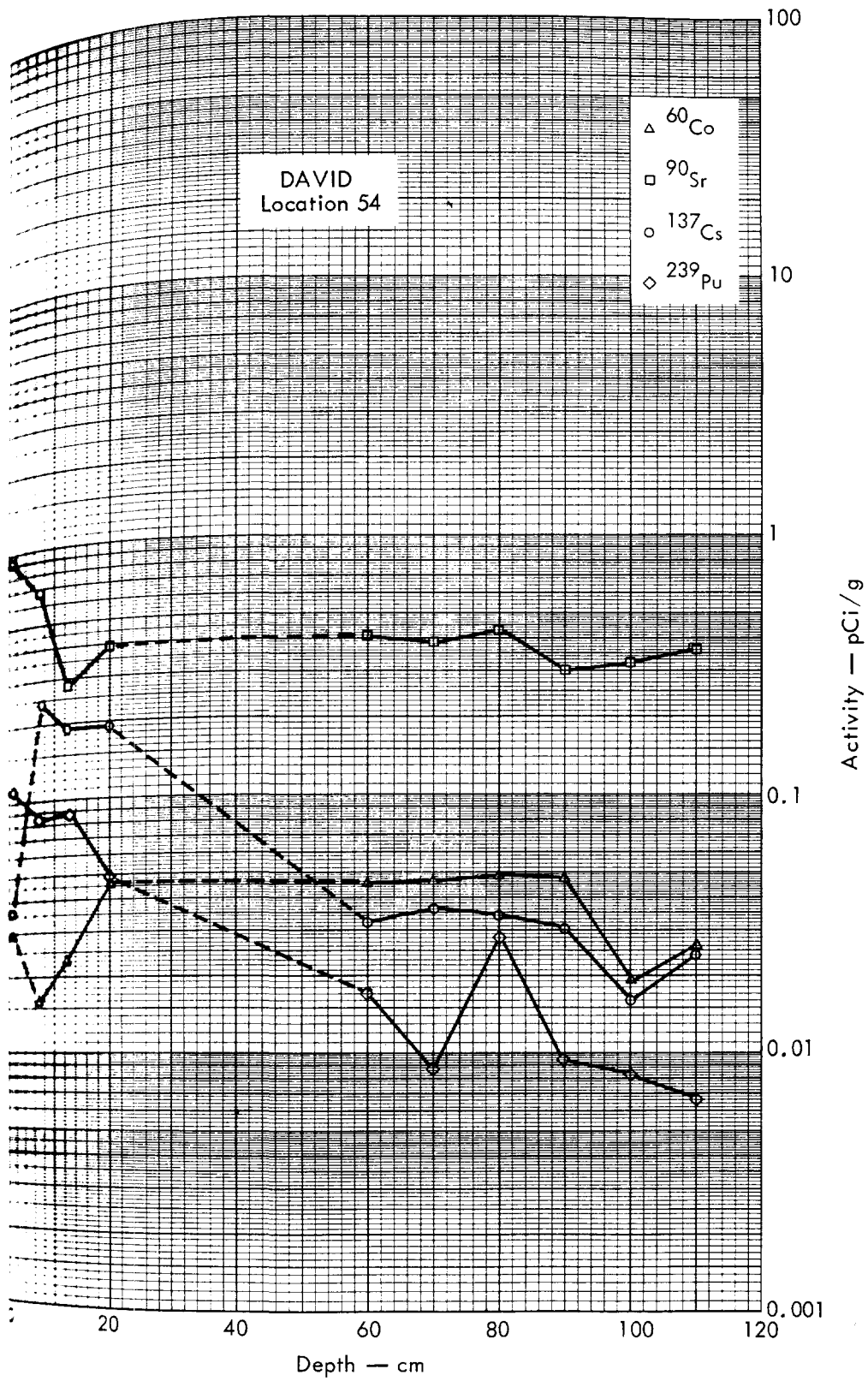


Fig. B.35.2a. Activities of selected radionuclides as a function of soil depth.

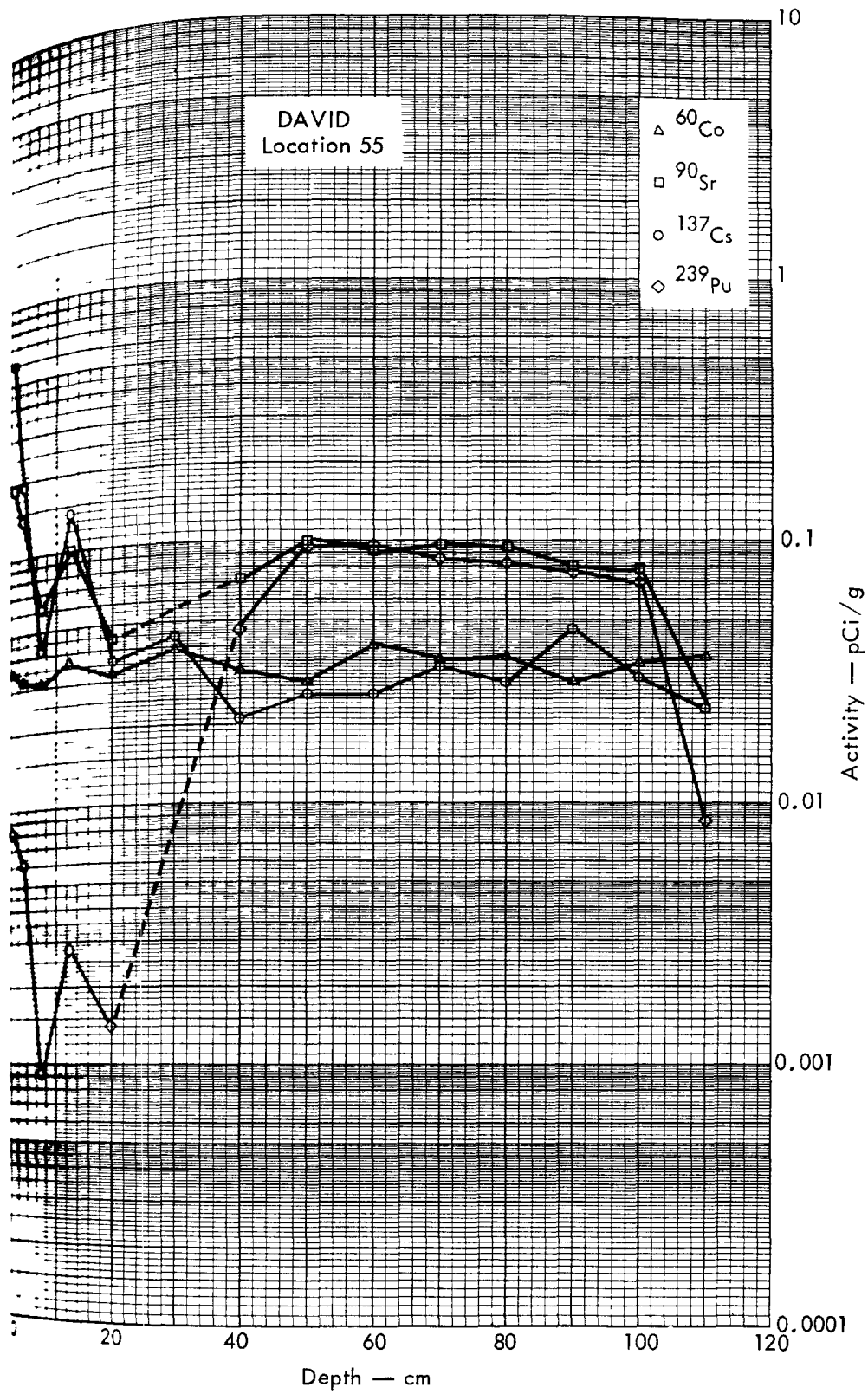


Fig. B.35.2b. Activities of selected radionuclides as a function of soil depth.

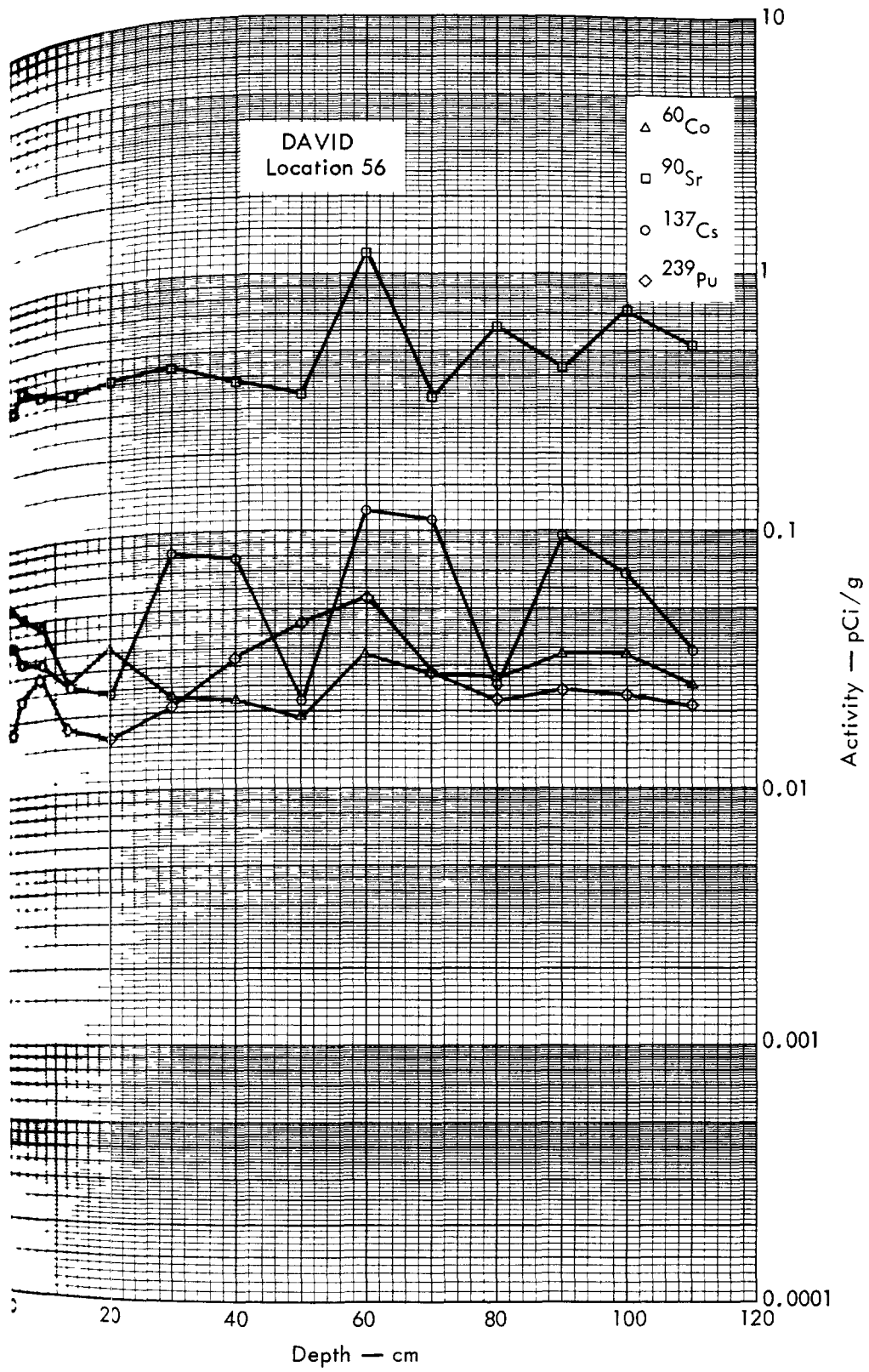


Fig. B 35.2c. Activities of selected radionuclides as a function of soil depth.

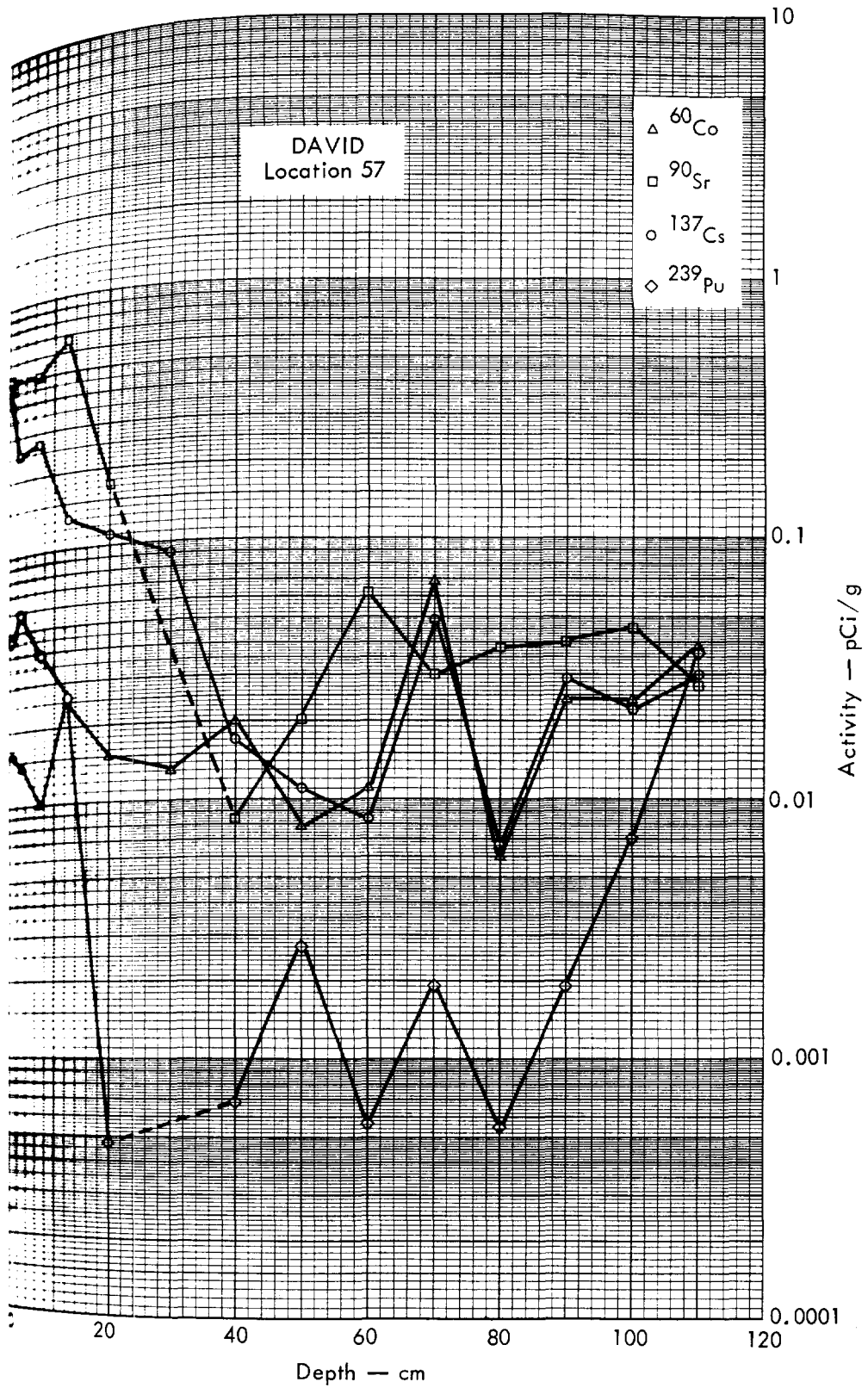


Fig. B.35.2d. Activities of selected radionuclides as a function of soil depth.

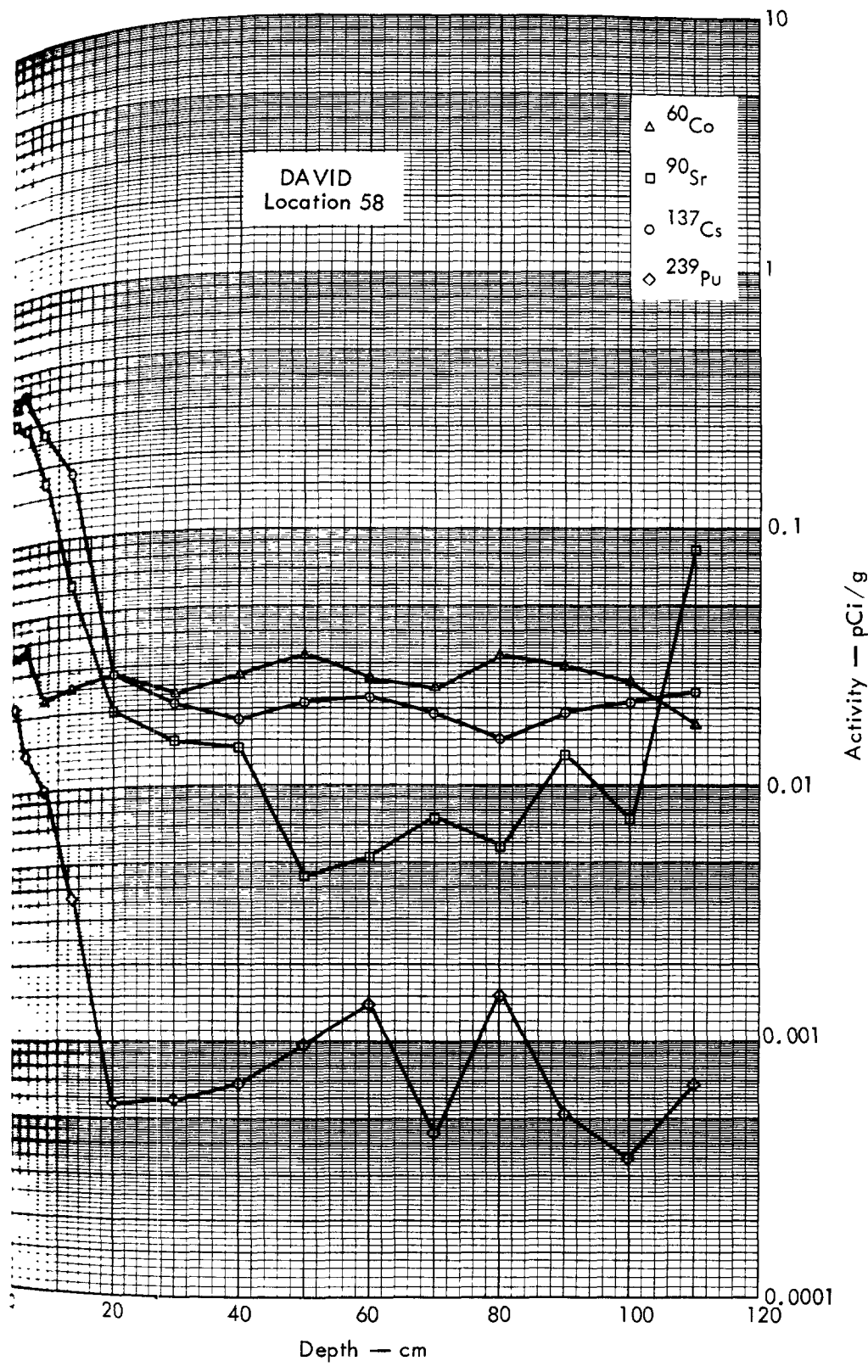


Fig. B.35.2e. Activities of selected radionuclides as a function of soil depth.

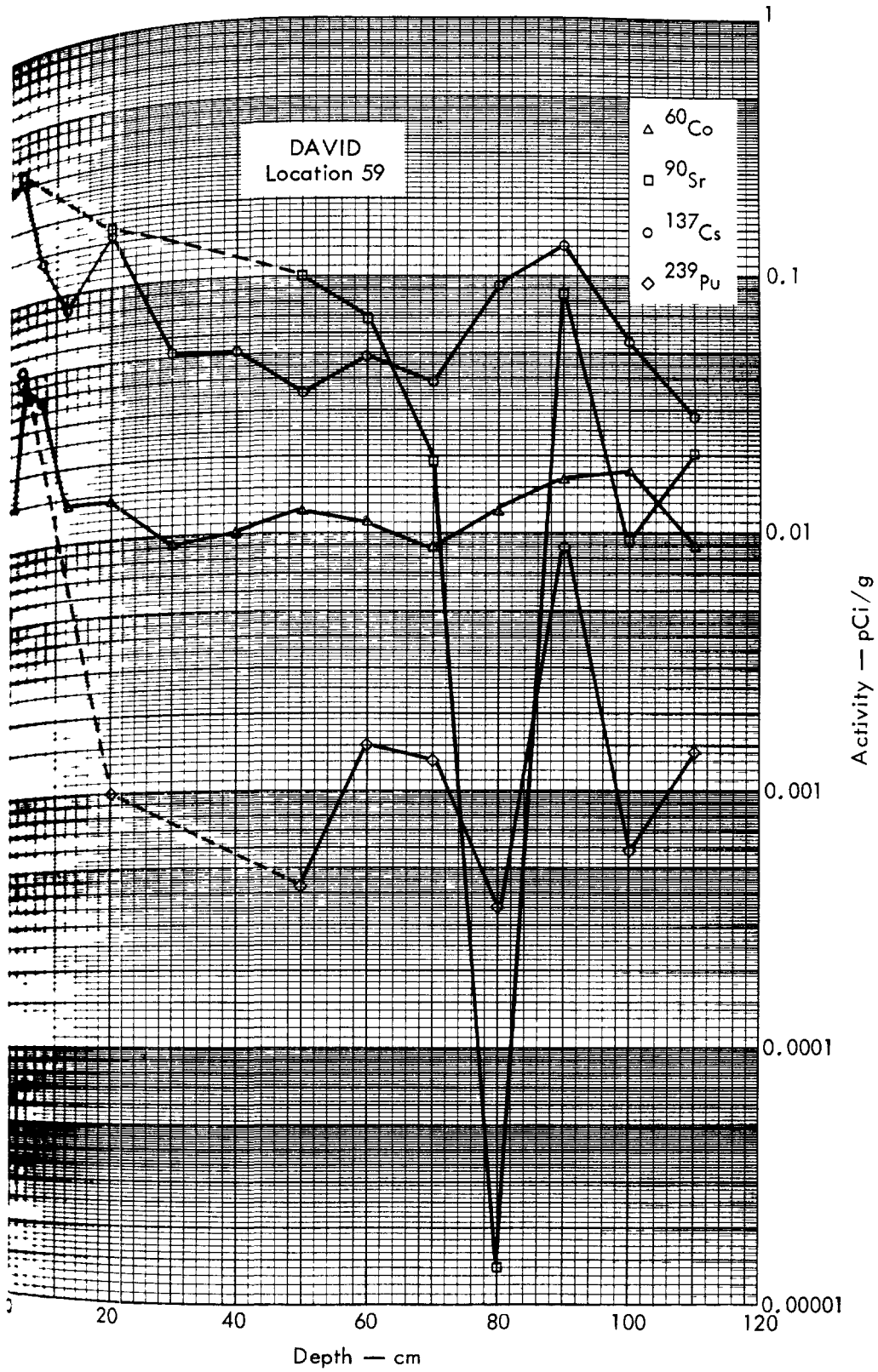
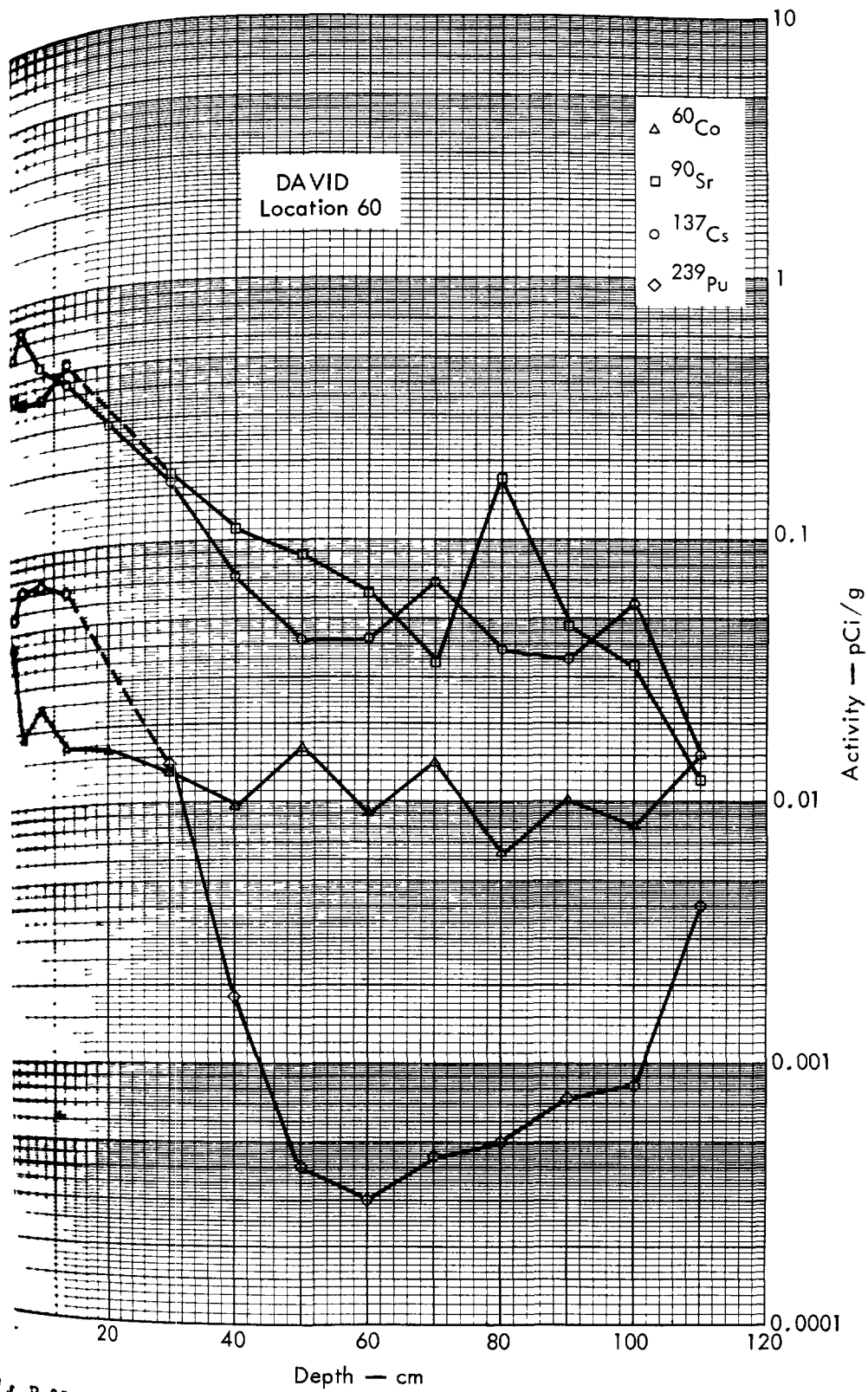


Fig. B. 35.2f. Activities of selected radionuclides as a function of soil depth.



B.35.2g. Activities of selected radionuclides as a function of soil depth.





Fig. B.36.1.a.





Fig. B. 36. 1. b. Gross count isosexposure contours. (Refer to alphabetic symbol key in this appendix.)



Fig. B.36.1.d. The gamma background exposure rate ( $\mu\text{R/hr}$ ) at 1 m above the ground, measured with a portable NaI scintillation counter.



□ PROFILE SAMPLES (0-35 cm)

● CORE SAMPLES (15 cm)

Fig. B.36.1.f. Soil-sample locations.

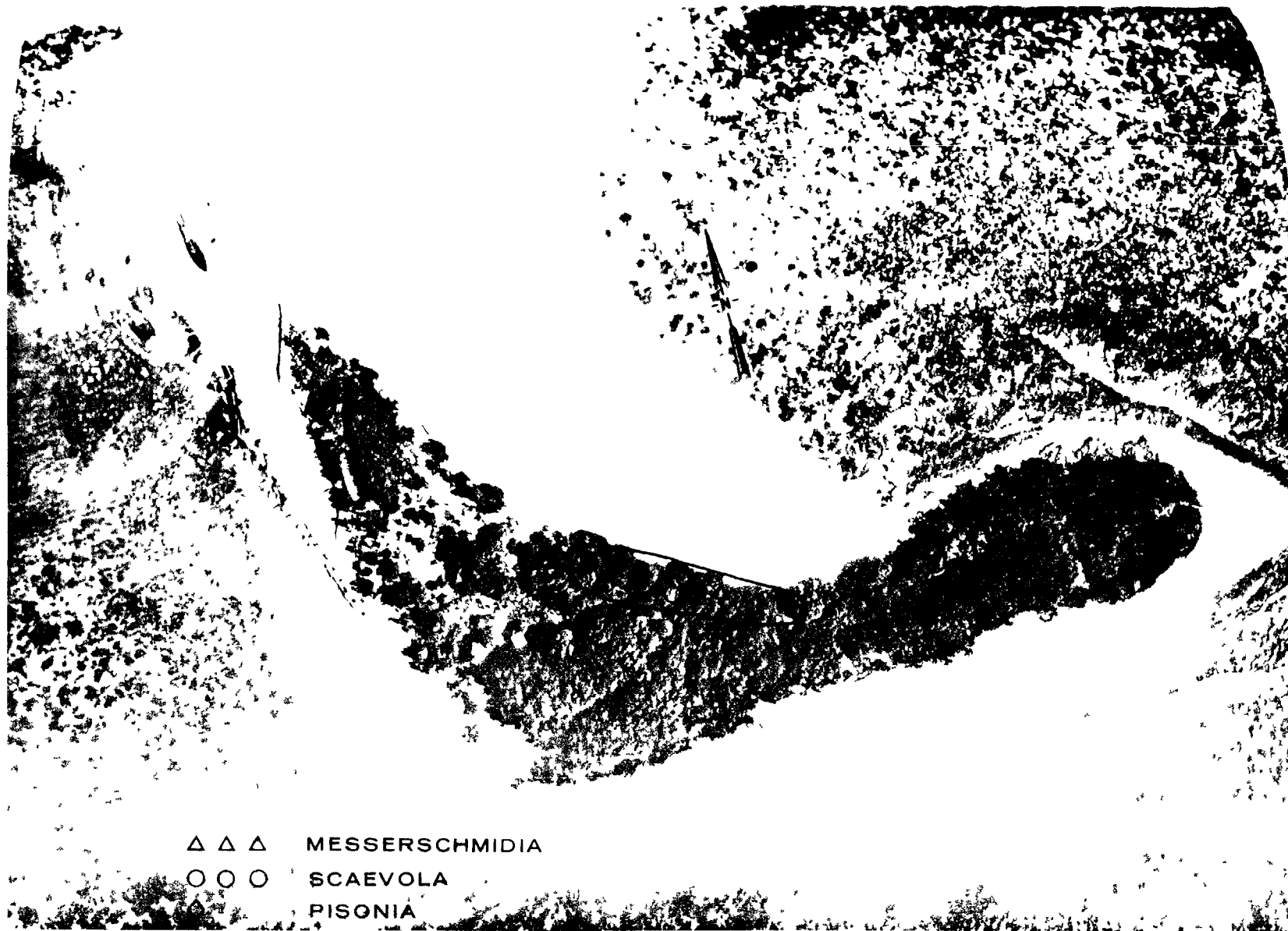


Fig. B.36.1.g. Vegetation sample locations.

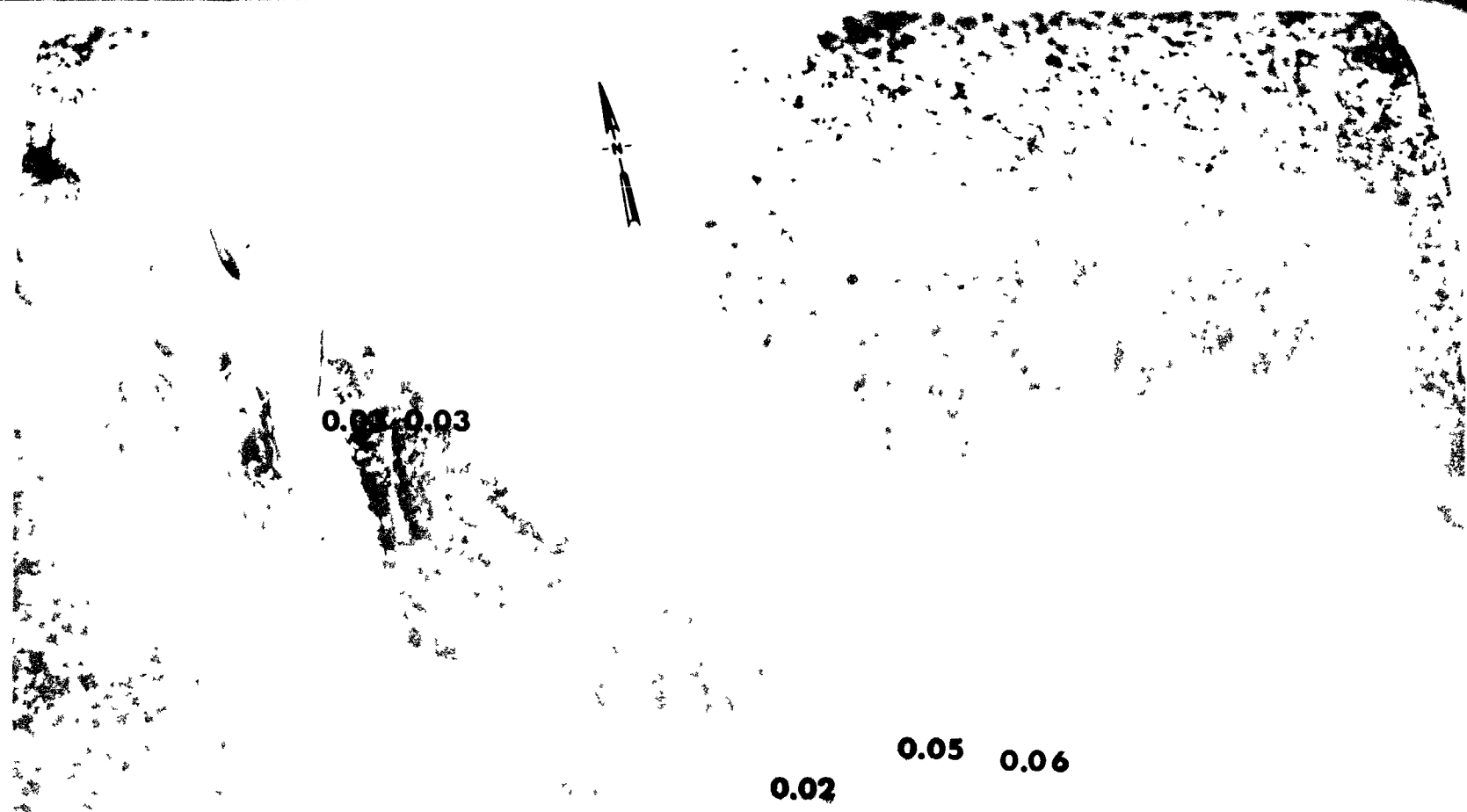


Fig. B.36.1.i. The average  $^{239}\text{Pu}$  activities (pCi/gm) in soil samples collected to a depth of 15 cm.



Fig. B.36.1.J. The average  $^{90}\text{Sr}$  activities (pCi/gm) in soil samples collected to a depth of 15 cm.



Fig. B.36.1.k.  $^{137}\text{Cs}$  isoexposure and isoconcentration contours. (Refer to alphabetic symbol key in this appendix.)



Fig. B.36.1.1. The average <sup>137</sup>Cs activities (pCi/gm) in soil samples collected to a depth of 15 cm.





Fig. B.36.1.m.  $^{60}\text{Co}$  isoexposure and isoconcentration contours. (Refer to alphabetic symbol key in this appendix.)

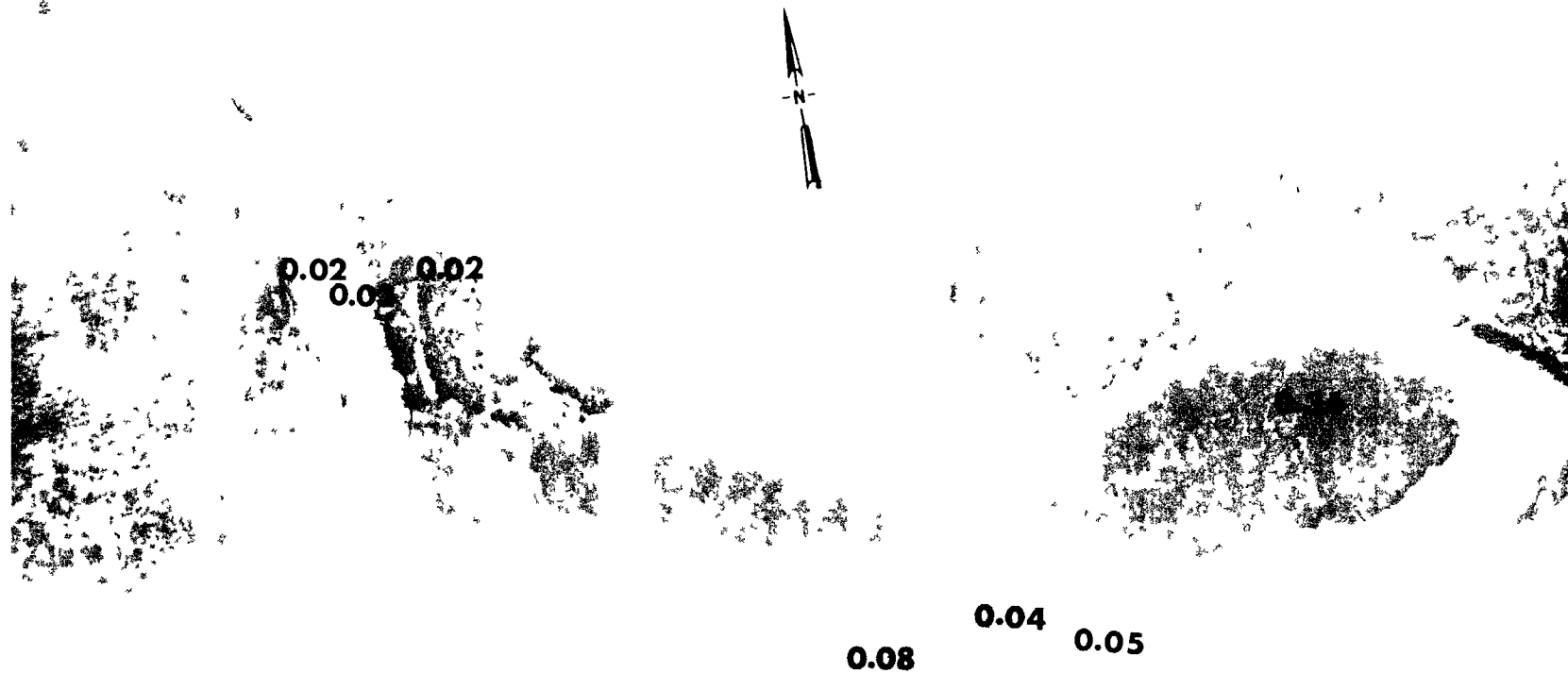


Fig. B.36.1.n. The average  $^{60}\text{Co}$  activities (pCi/gm) in soil samples collected to a depth of 15 cm.

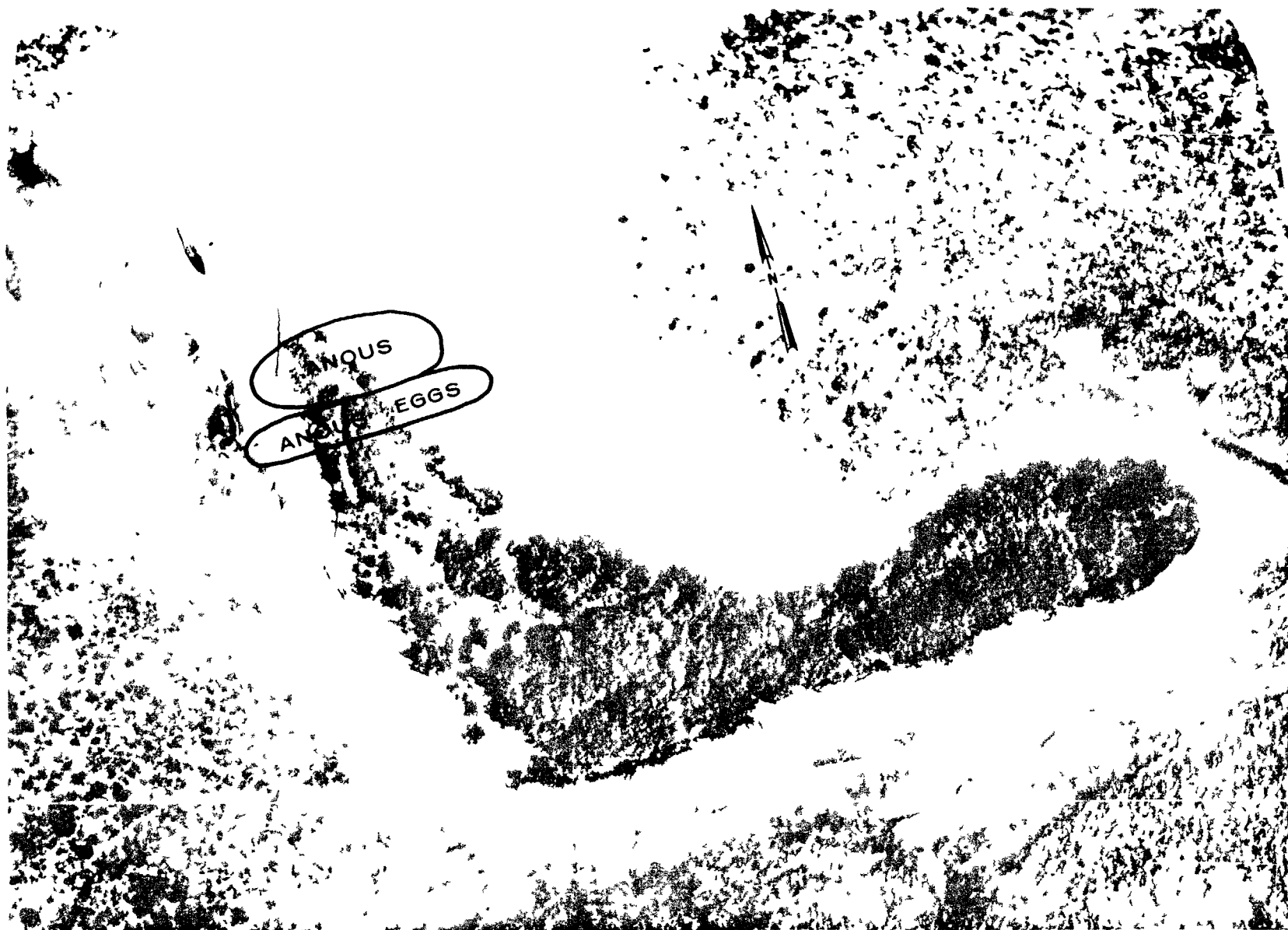
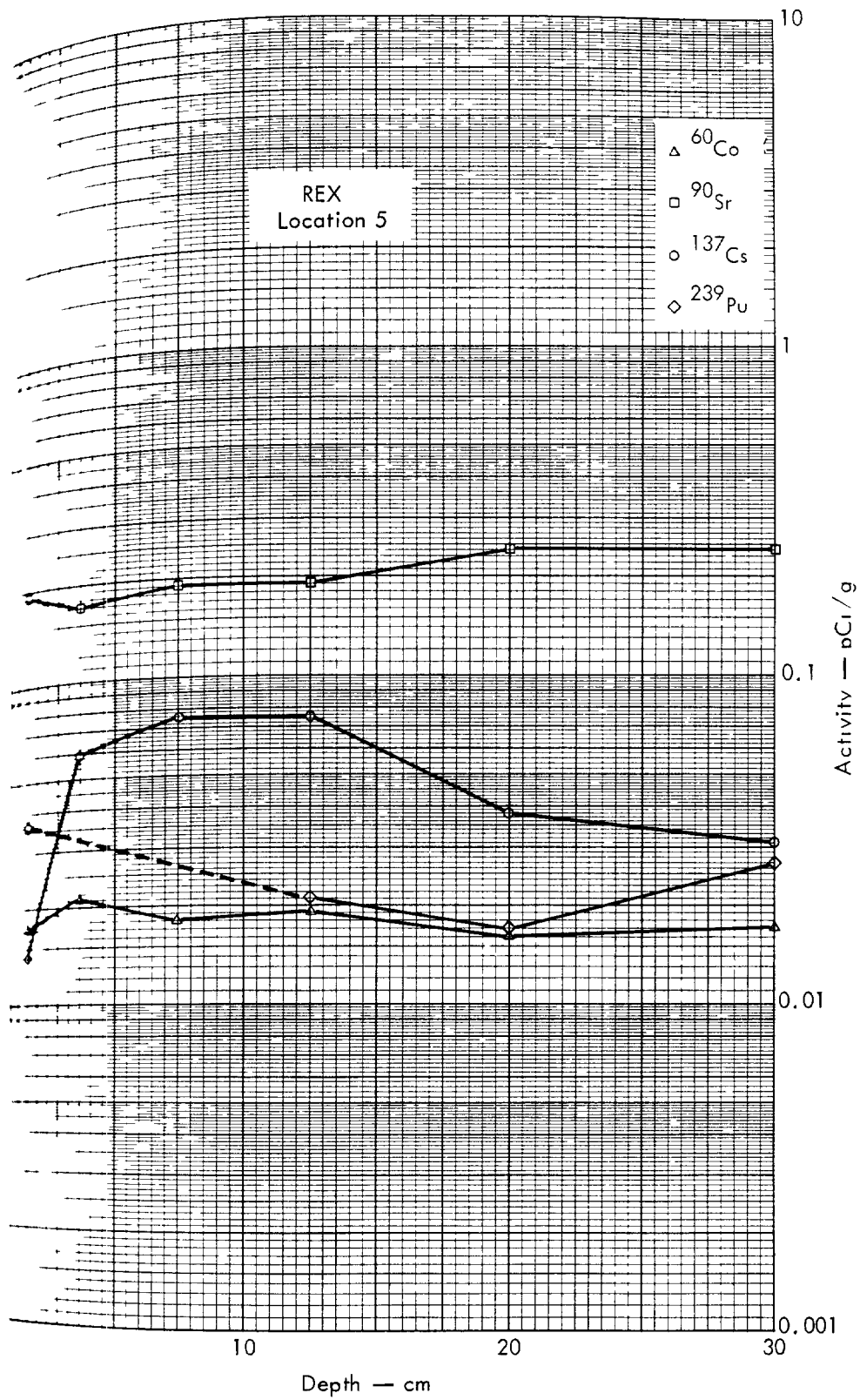
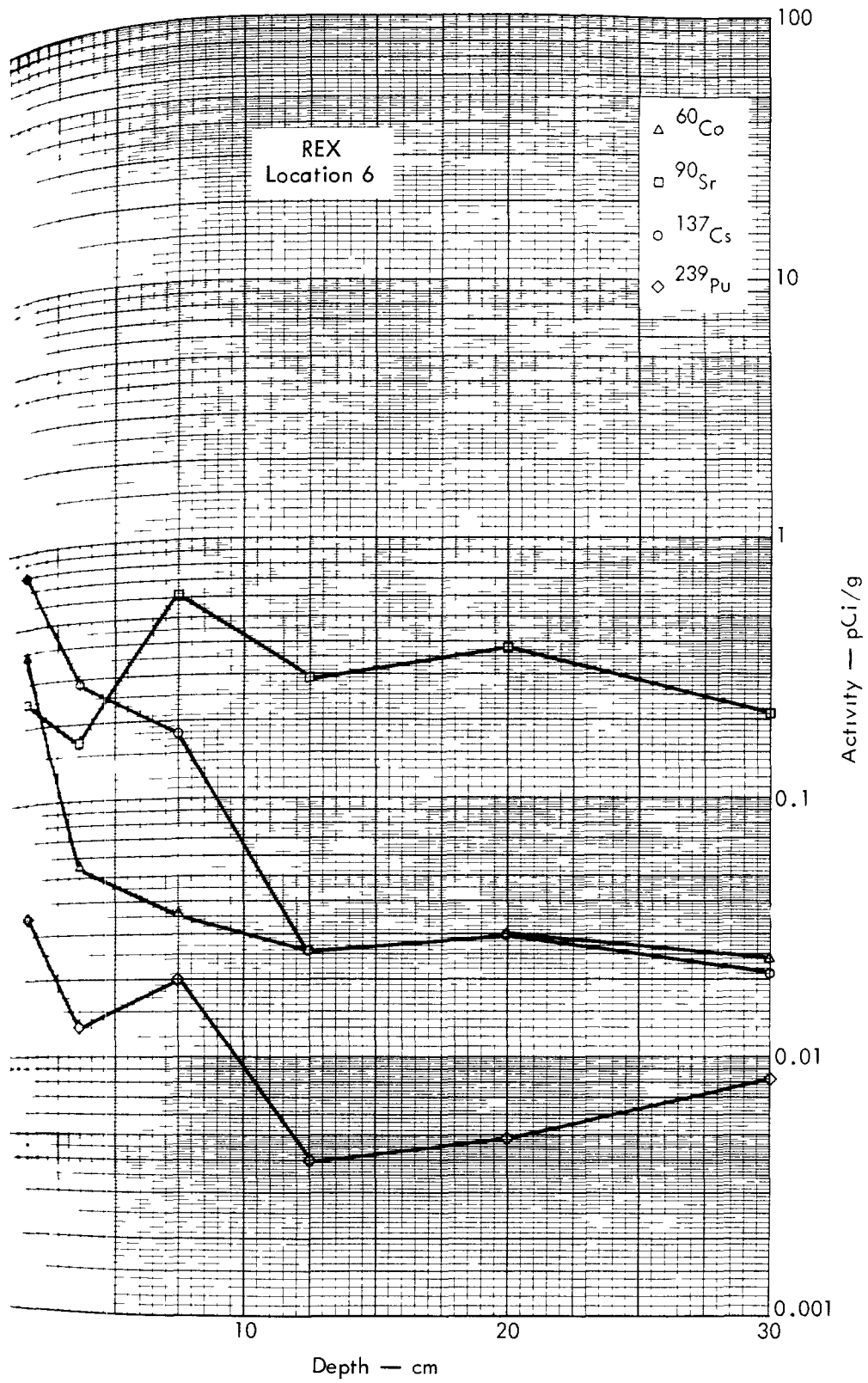


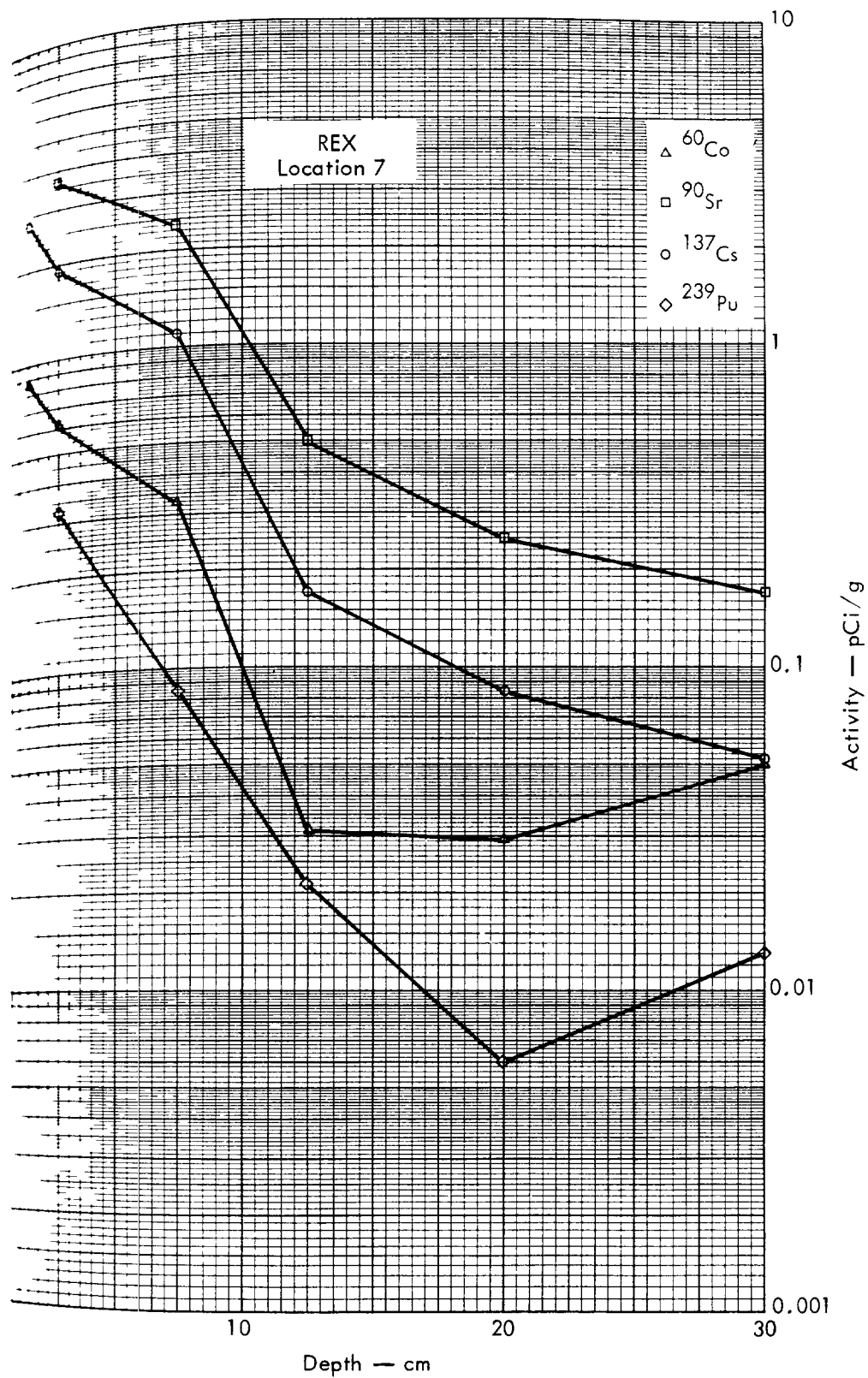
Fig. B.36.1.o. Terrestrial animal sample locations.



36 2a Activities of selected radionuclides as a function of soil depth.



36.2b. Activities of selected radionuclides as a function of soil depth.



B 36 2c Activities of selected radionuclides as a function of soil depth.



ELMER A

Fig. B.37.1.a.

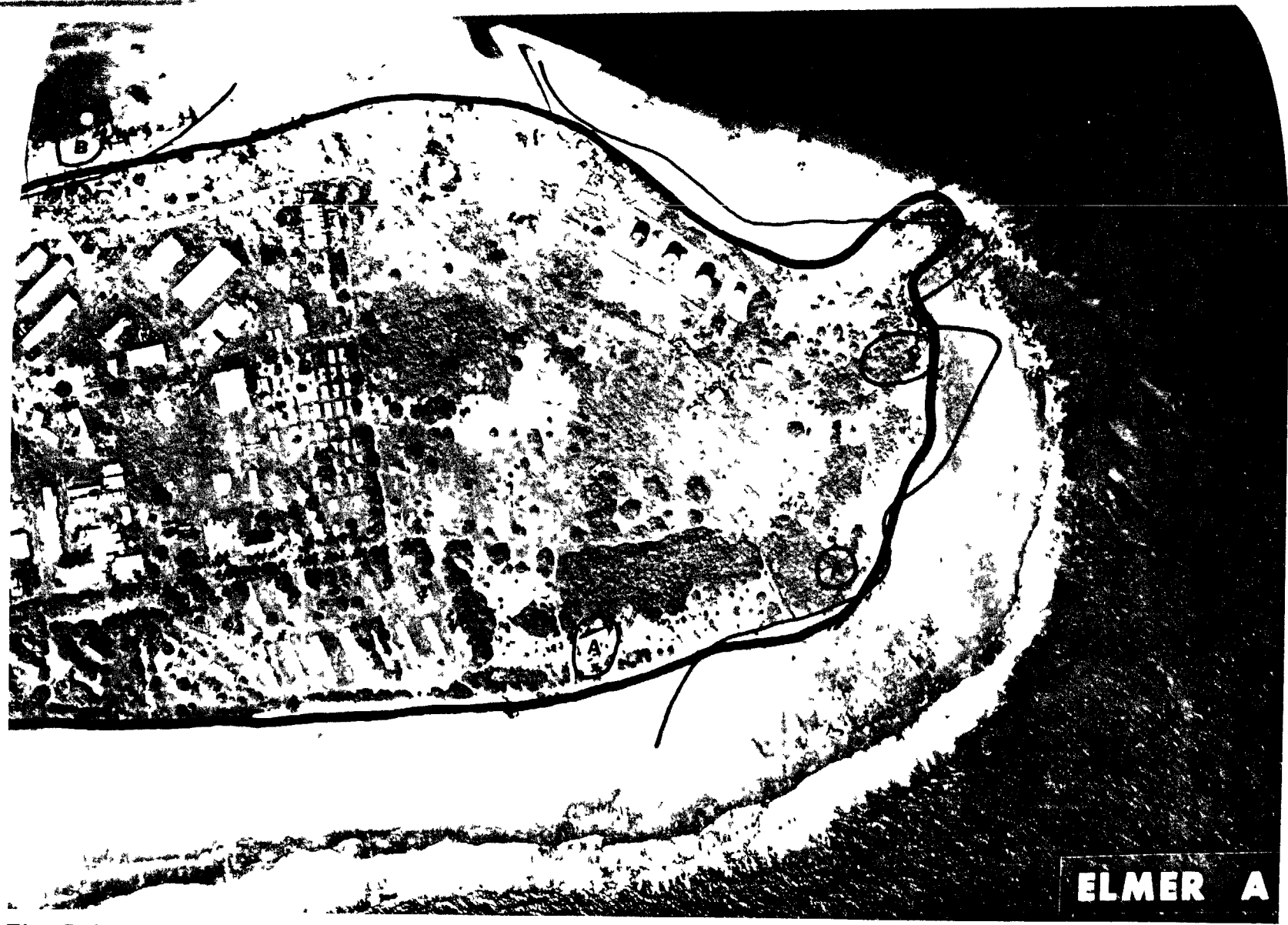


Fig. B.37.1.b. Gross count isosexposure contours. (Refer to alphabetic symbol key in this appendix.)



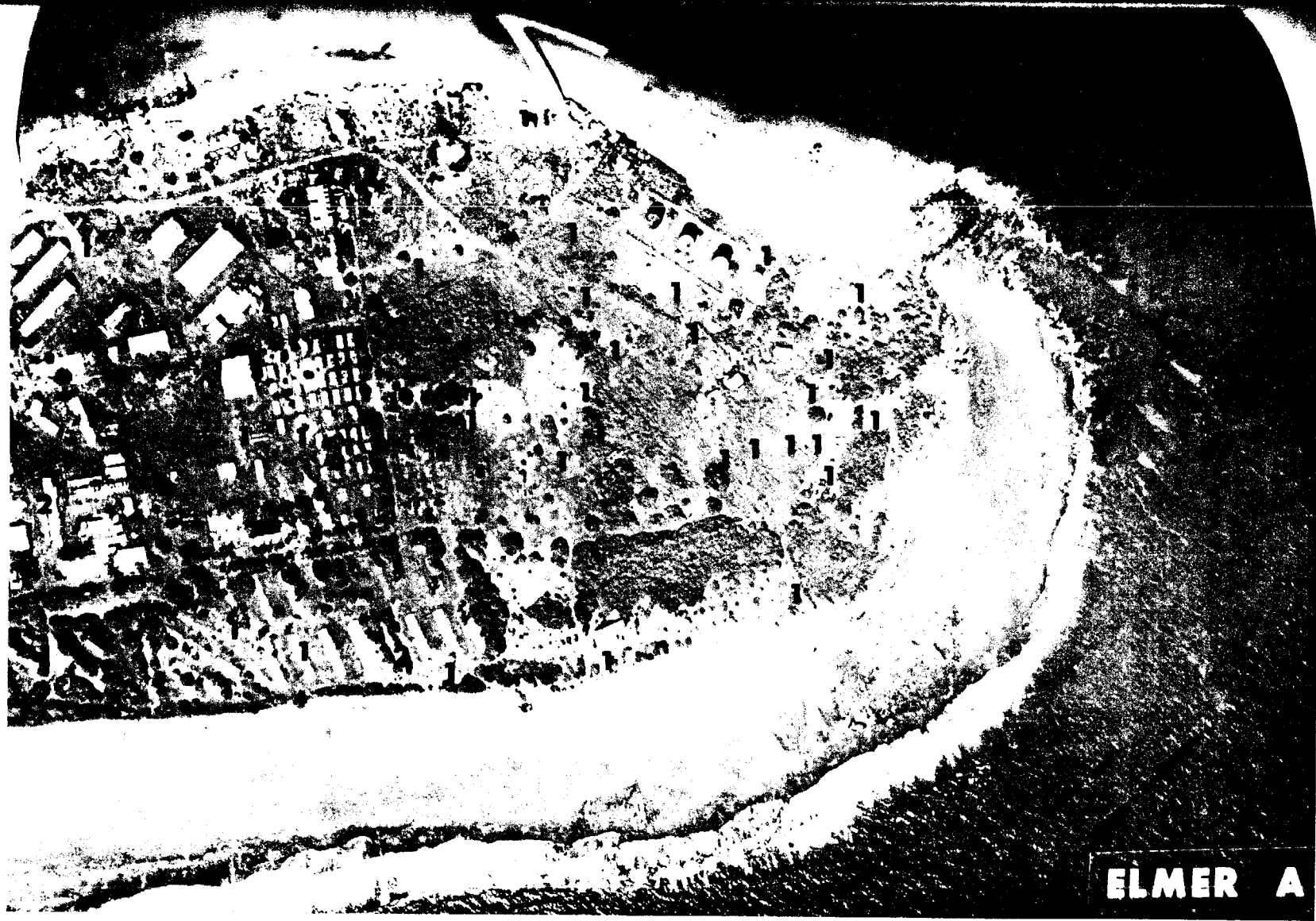


Fig. B.37.1.d. The gamma background exposure rate ( $\mu\text{R/hr}$ ) at 1 m above the ground, measured with a portable NaI scintillation counter.



Fig. B.37.1.f. Soil-sample locations.

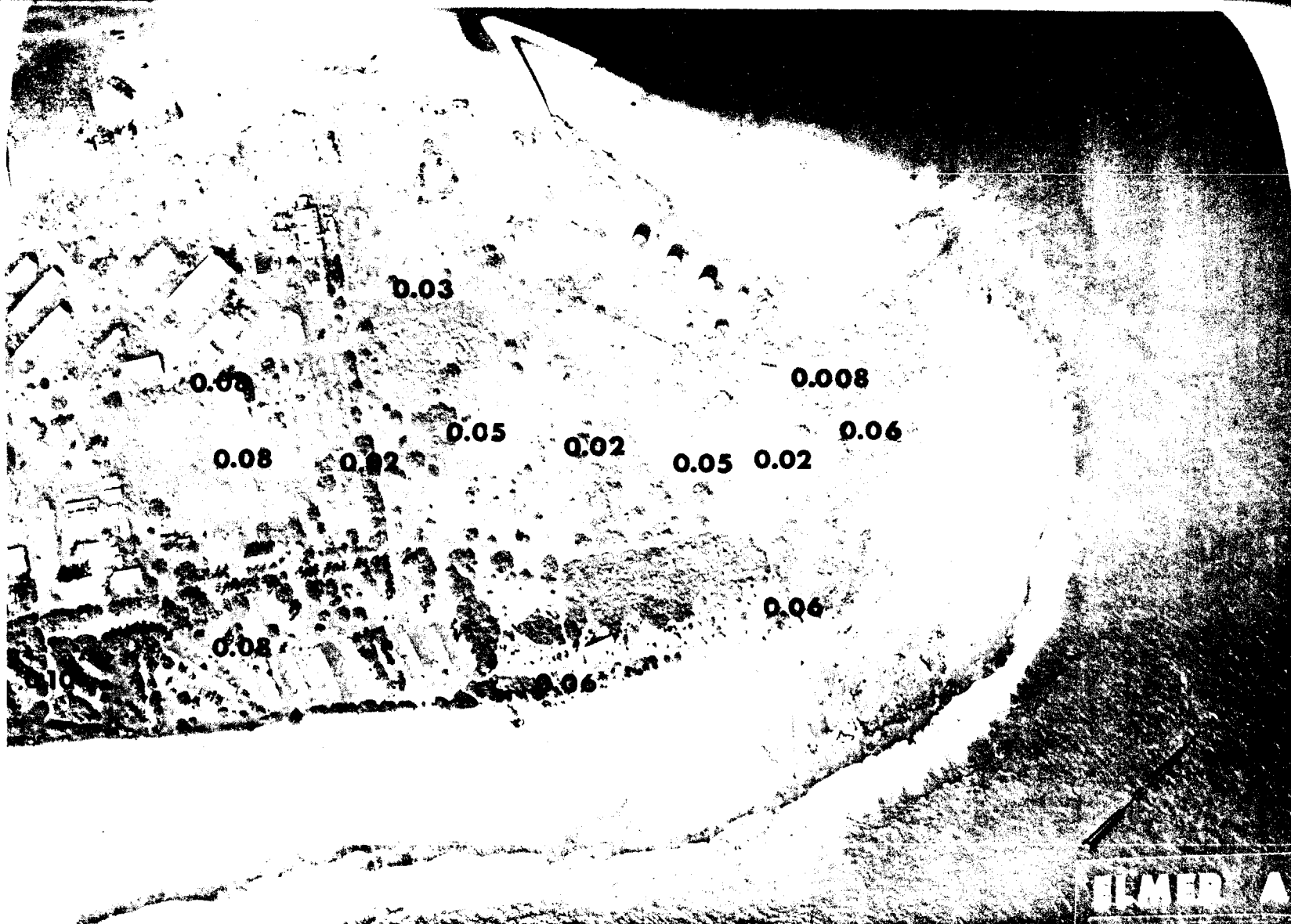


Fig. B.37.1.i. The average  $^{239}\text{Pu}$  activities (pCi/g) in soil samples collected to a depth of 15 cm.



Fig. B.37.1.j. The average <sup>90</sup>Sr activities (pCi/g) in soil samples collected to a depth of 15 cm.



Fig. B.37.1.1. The average  $^{137}\text{Cs}$  activities (pCi/g) in soil samples collected to a depth of 15 cm.

**ELMER A**



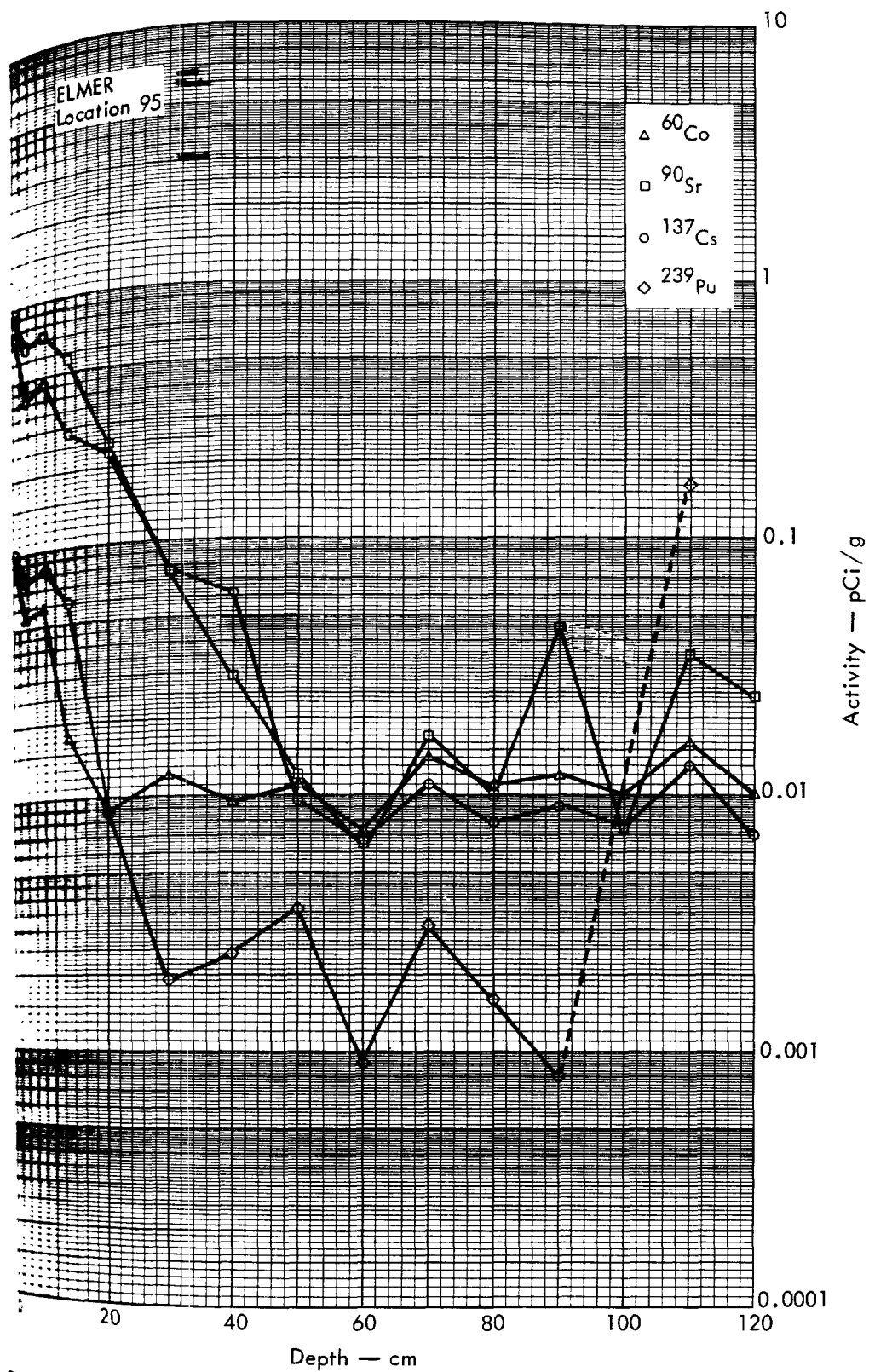


Fig. B.37.2a. Activities of selected radionuclides as a function of soil depth.



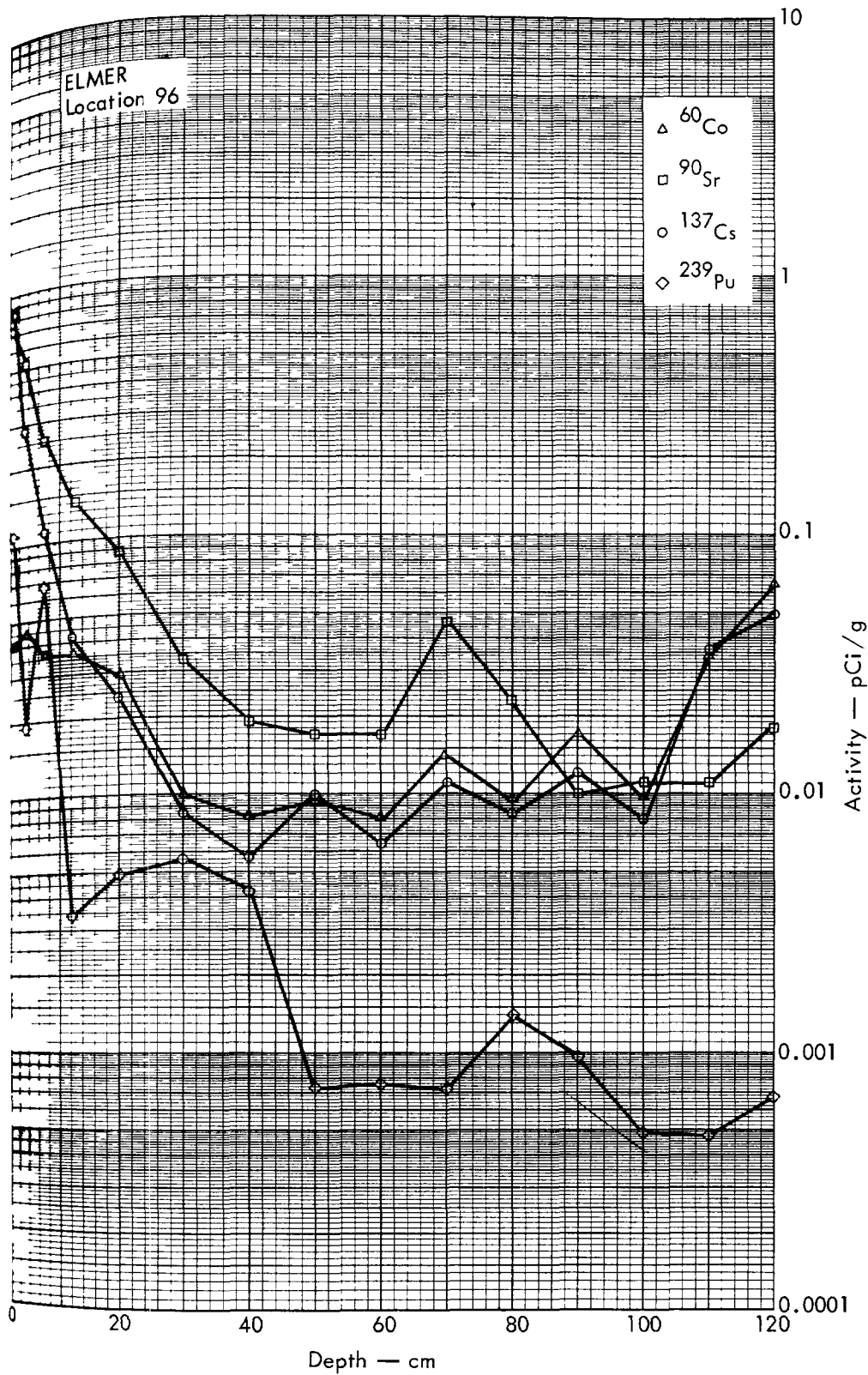
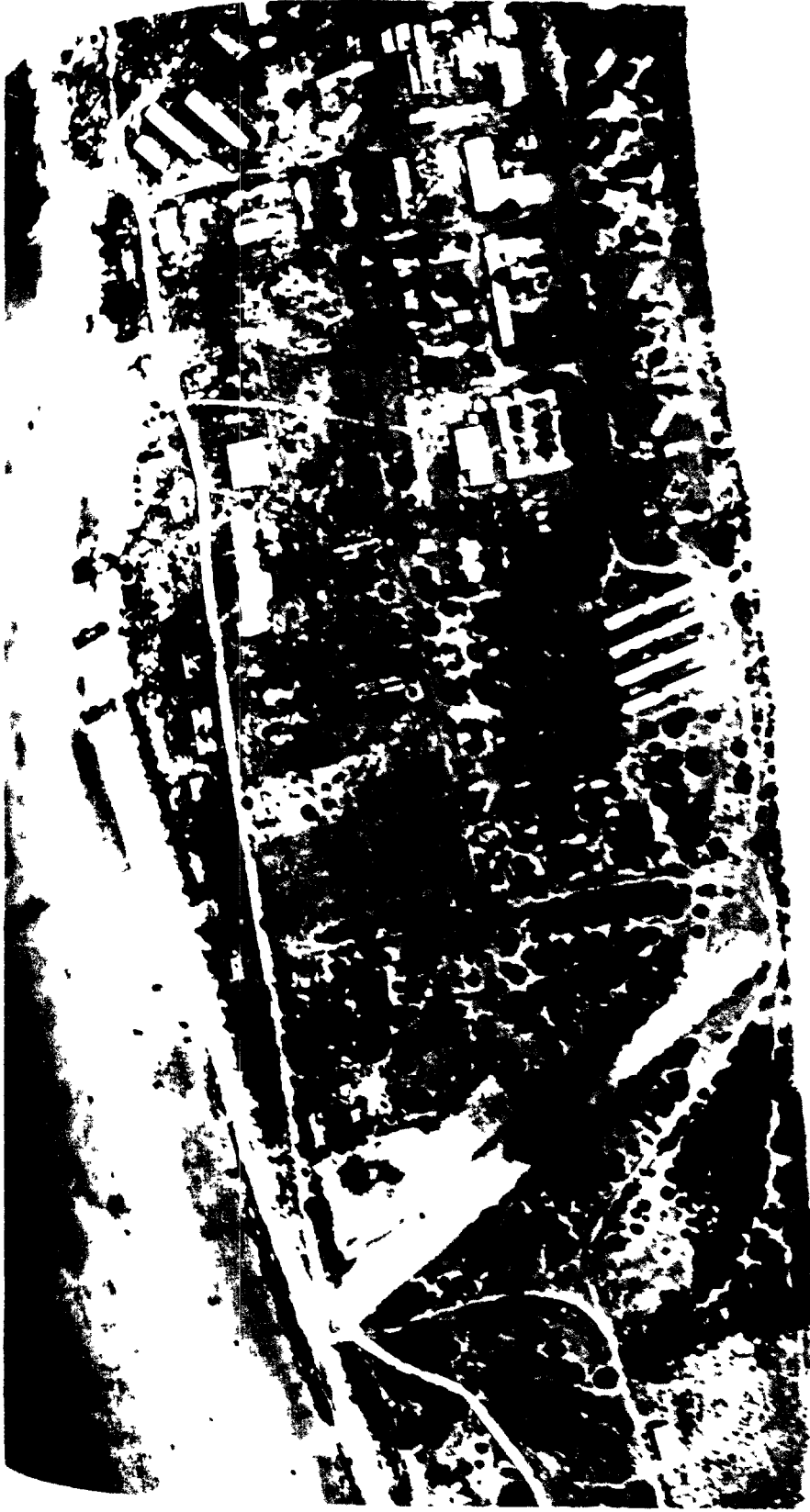


Fig. B.37.2b. Activities of selected radionuclides as a function of soil depth





ELMER B

FIG. B. (S.)

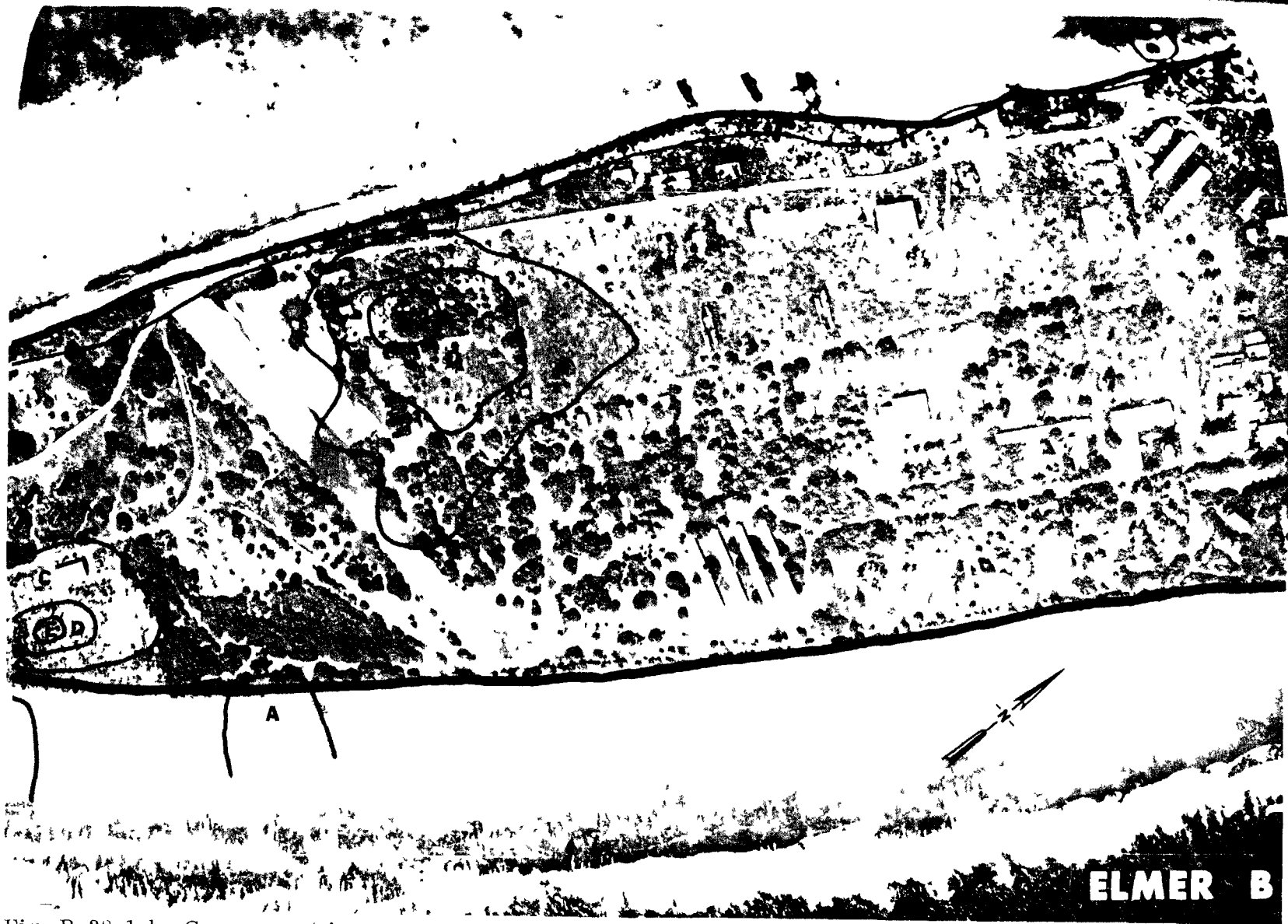


Fig. B.38.1.b. Gross count isosexposure contours. (Refer to alphabetic symbol key in this appendix.)



Fig. B.38.1.d. The gamma background exposure rate ( $\mu\text{R/hr}$ ) at 1 m above the ground, measured with a portable NaI scintillation counter.

\*Elevated levels may be due to nearby  $^{60}\text{Co}$  source which was subsequently removed.



□ PROFILE SAMPLES (0-125 cm)  
 ● CORE SAMPLES (0-5 cm)

**ELMER B**

Fig. B.38.1.f. Soil-sample locations.



▲▲▲ MESSERSCHMIDIA

■ PANDANUS

○○○ SCAEVOLA

● COCONUT

ELMER B

Fig. B.38.1.g. Vegetation sample locations.

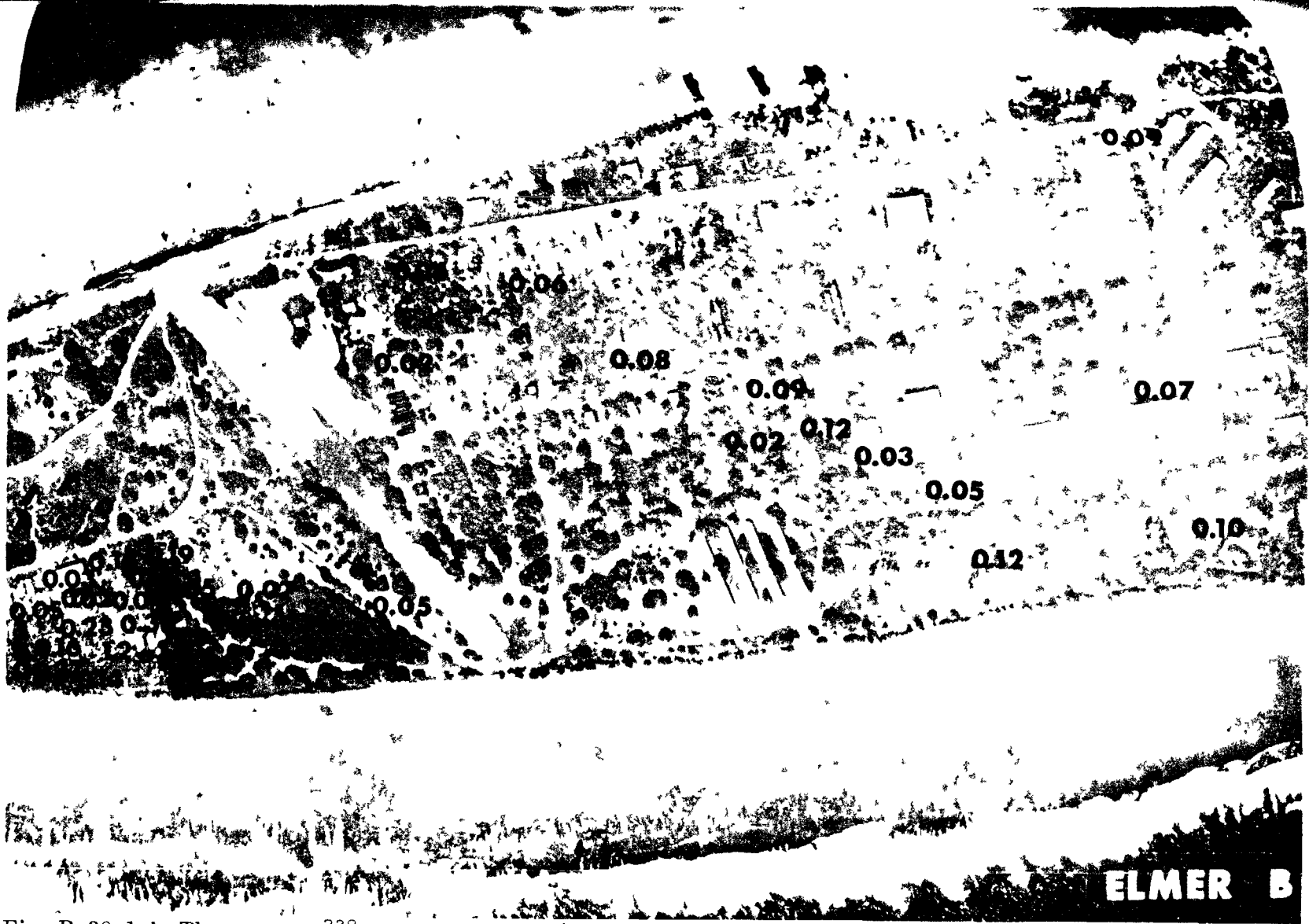


Fig. B.38.1.i. The average  $^{239}\text{Pu}$  activities (pCi/g) in soil samples collected to a depth of 15 cm.

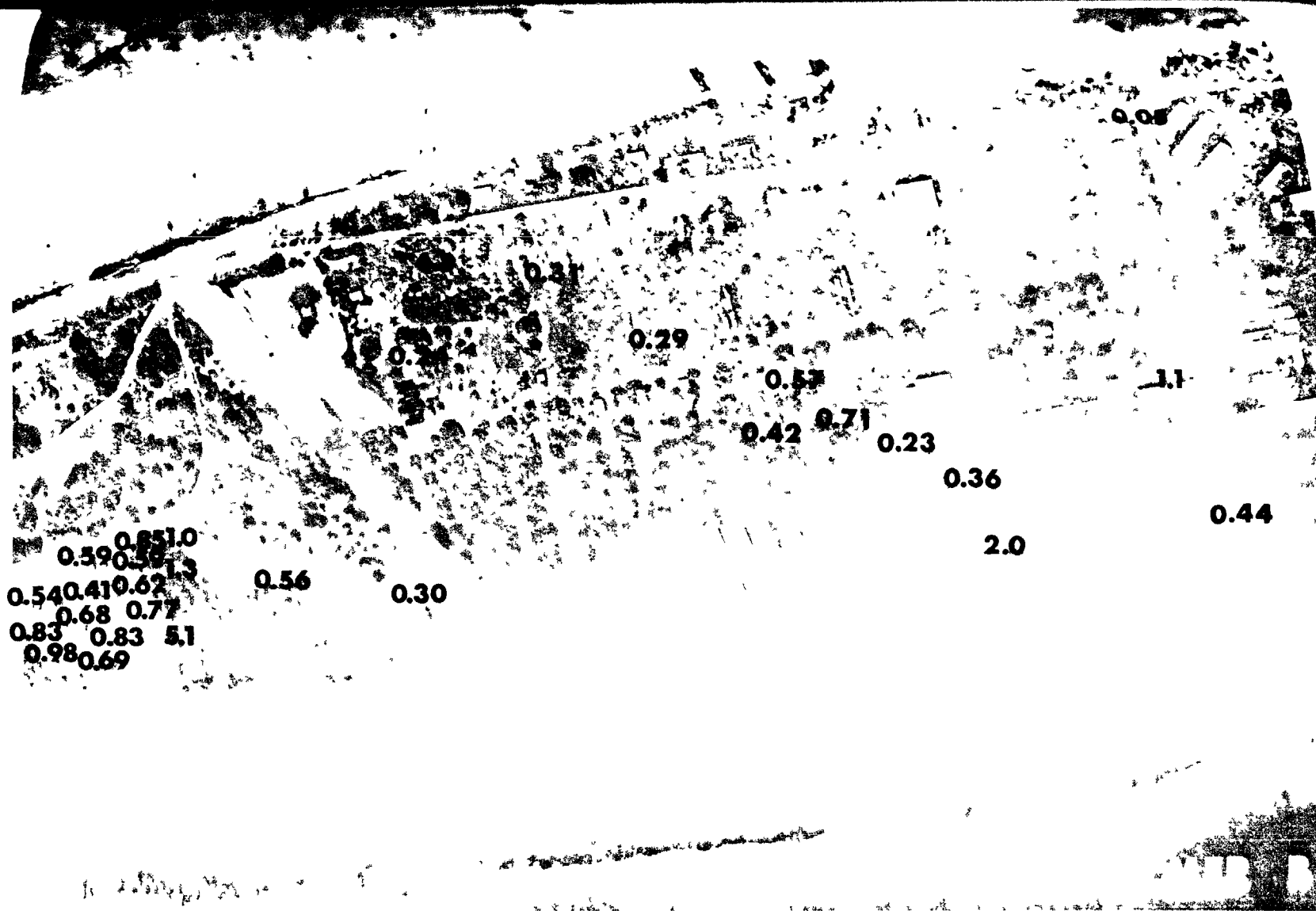


Fig. B.38.1.j. The average  $^{90}\text{Sr}$  activities (pCi/g) in soil samples collected to a depth of 15 cm.







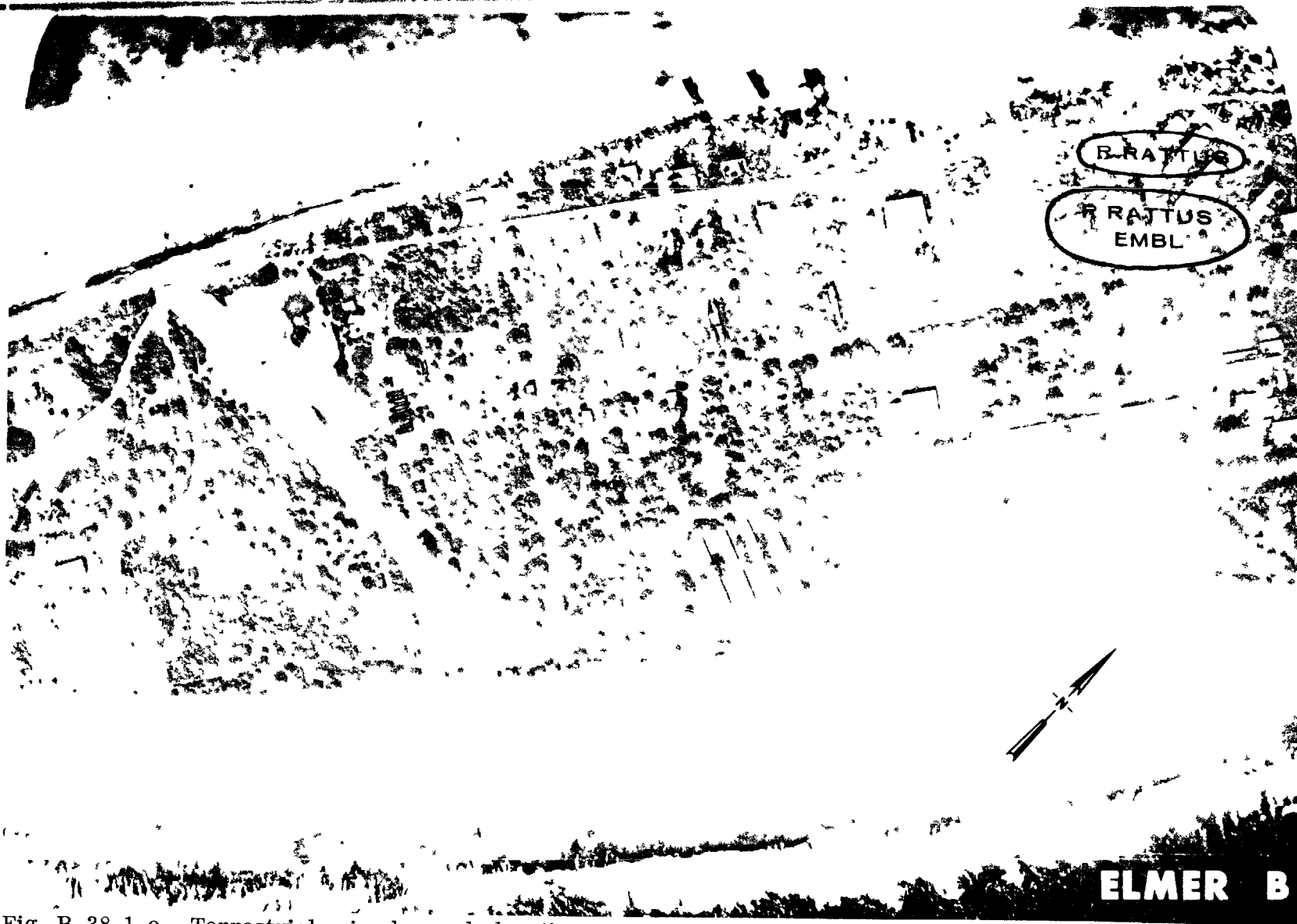
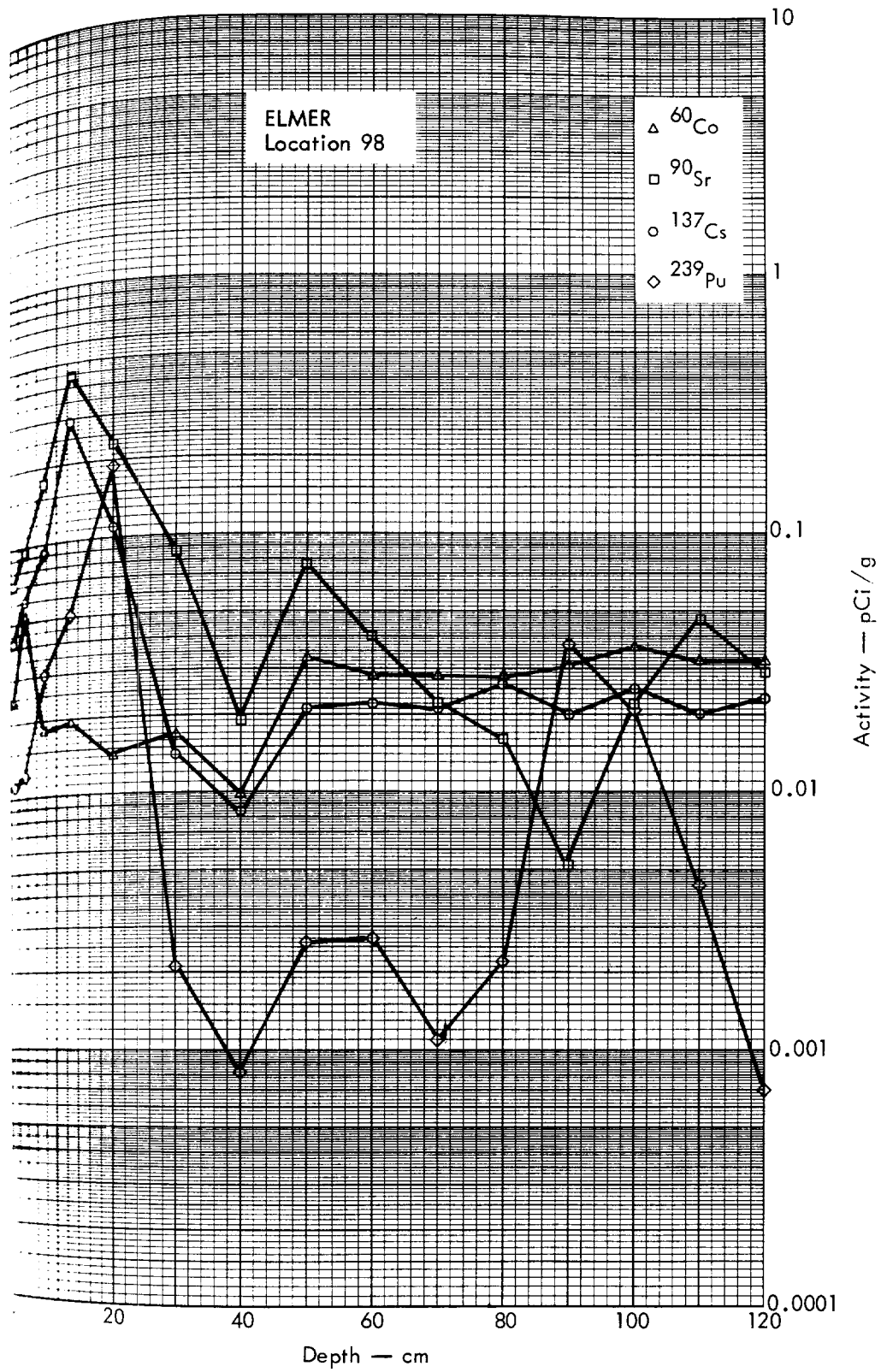
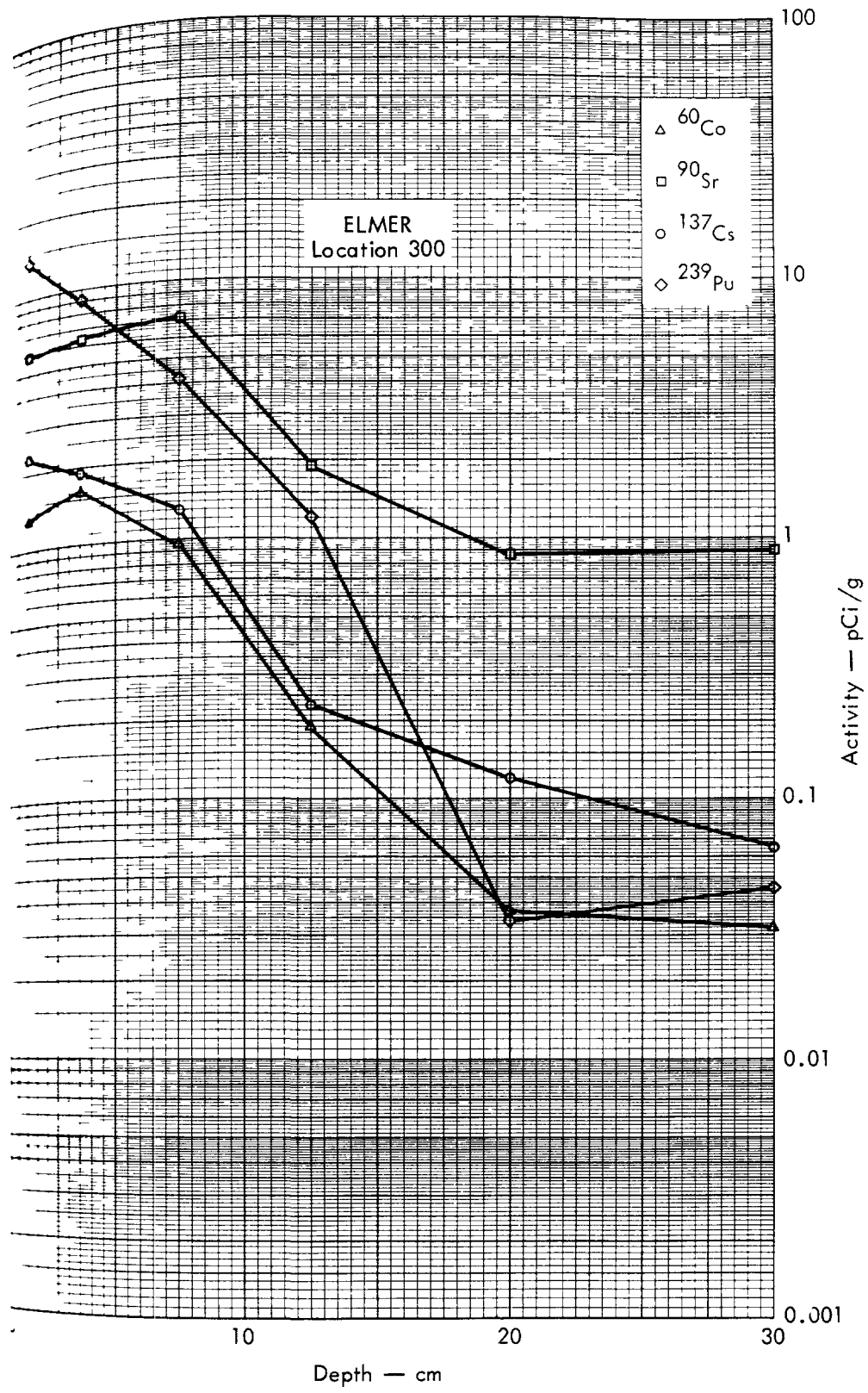


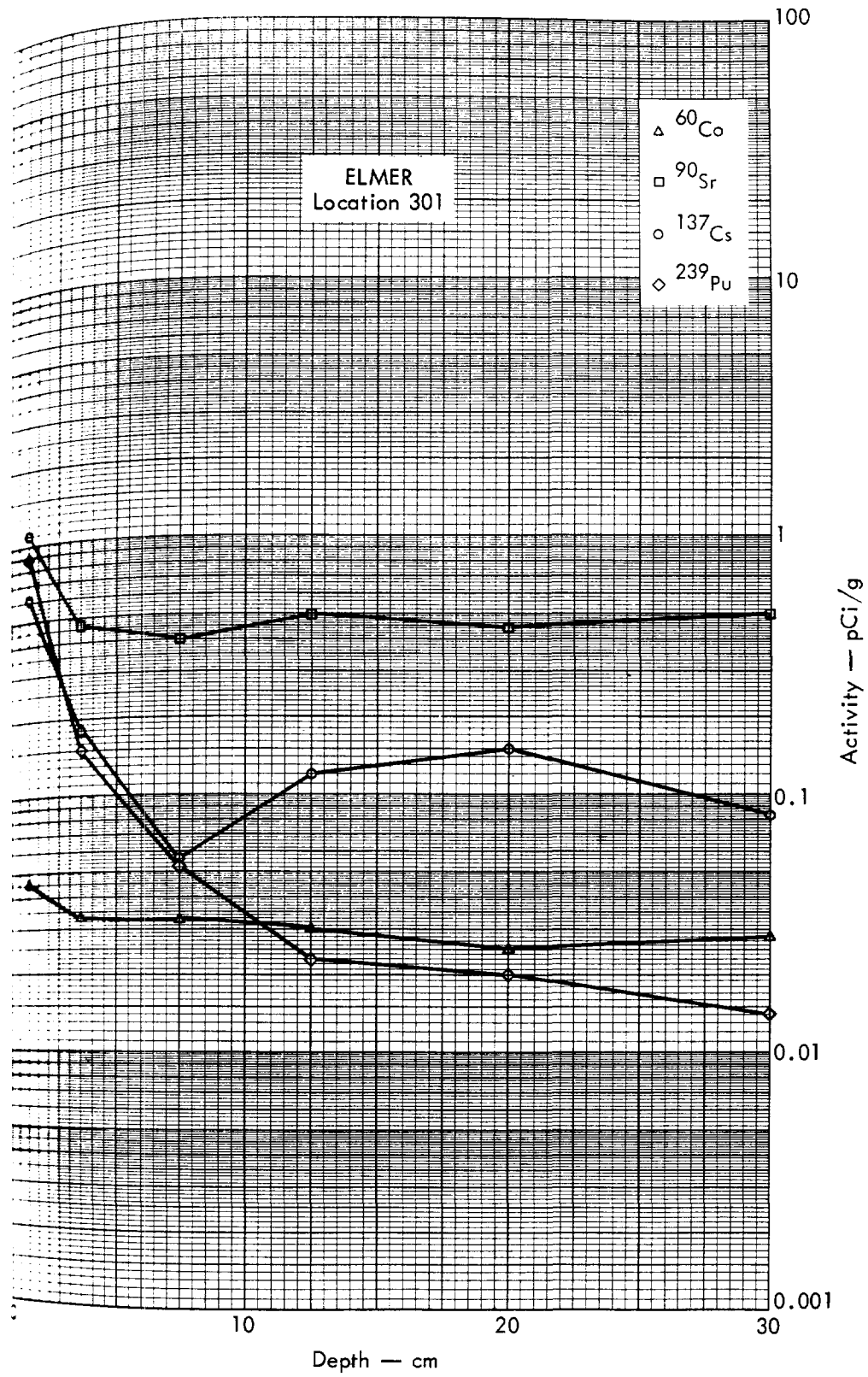
Fig. B.38.1.o. Terrestrial animal sample locations.



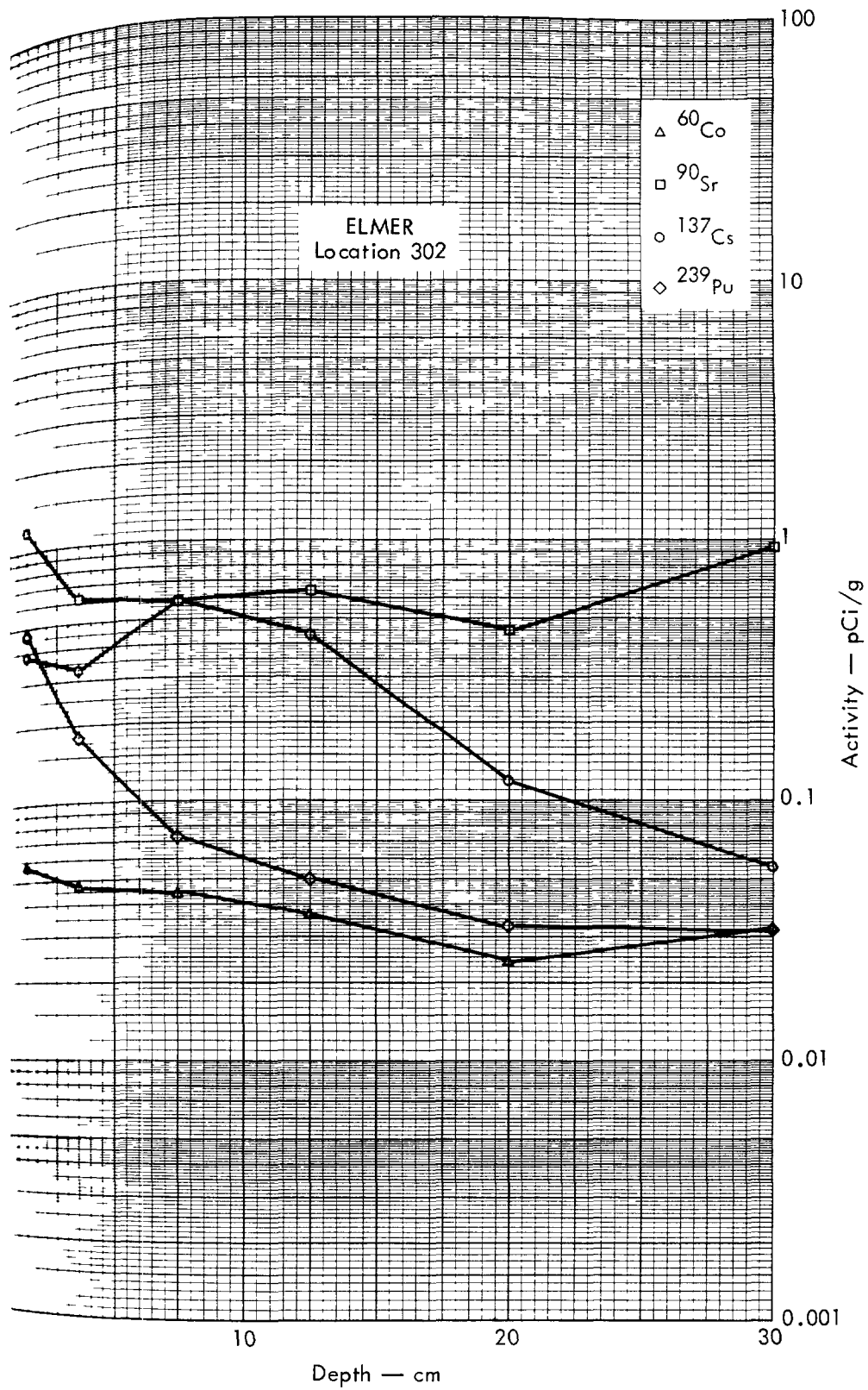
B.38. 2a. Activities of selected radionuclides as a function of soil depth.



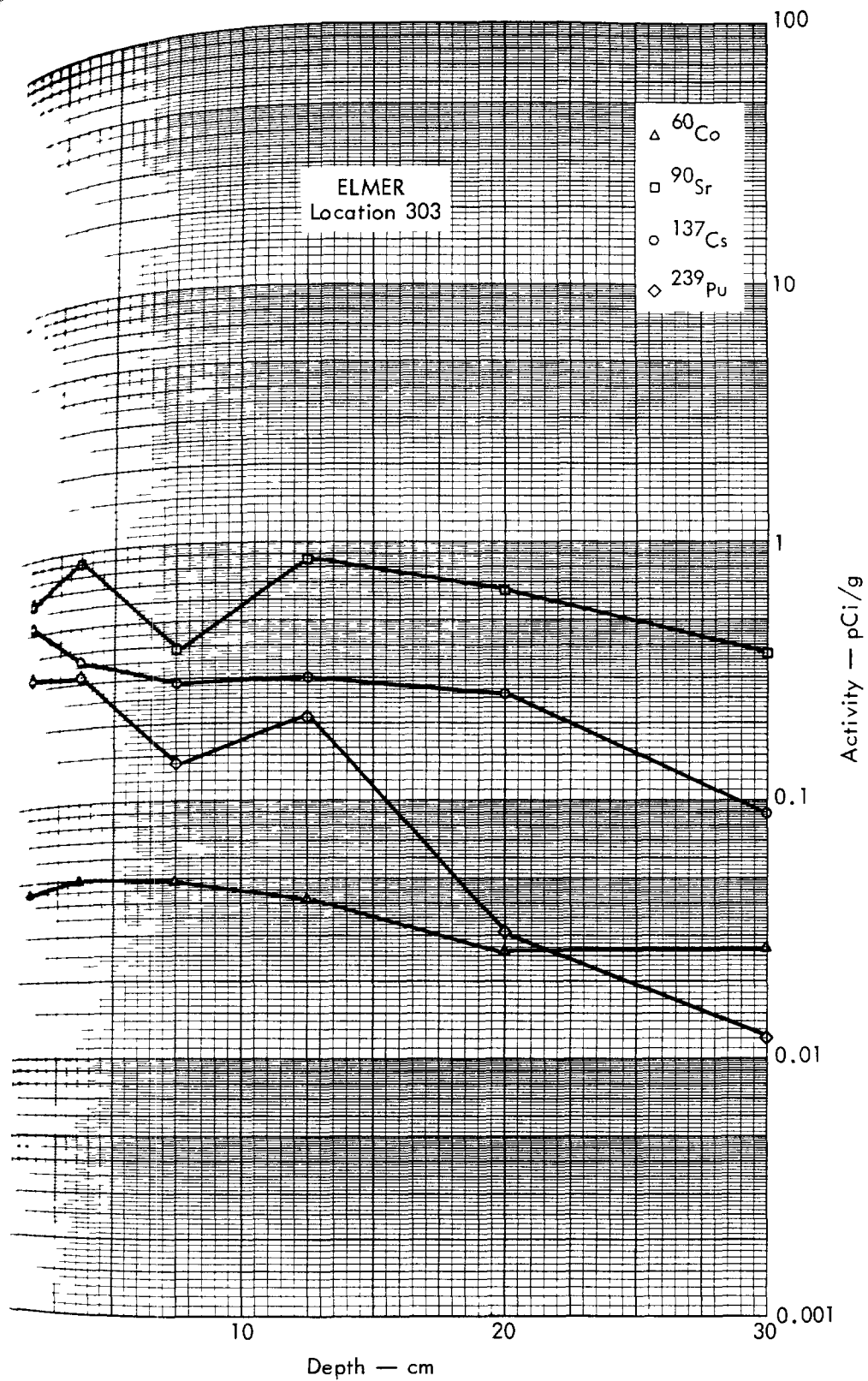
z B. 38. 2b. Activities of selected radionuclides as a function of soil depth.



B.38.2c. Activities of selected radionuclides as a function of soil depth.



• B 38.2d. Activities of selected radionuclides as a function of soil depth.



B. 38. 2e. Activities of selected radionuclides as a function of soil depth.



Fig. B. 39, 1. a.





Fig. B. 39. 1. b. Gross count isoexposure contours. (Refer to alphabetic symbol key in this appendix.)



Fig. B.39.1.d. The gamma background exposure rate ( $\mu\text{R/hr}$ ) at 1 m above the ground, measured with a portable NaI scintillation counter.

\*Elevated levels may be due to nearby  $^{60}\text{Co}$  source which was subsequently removed.

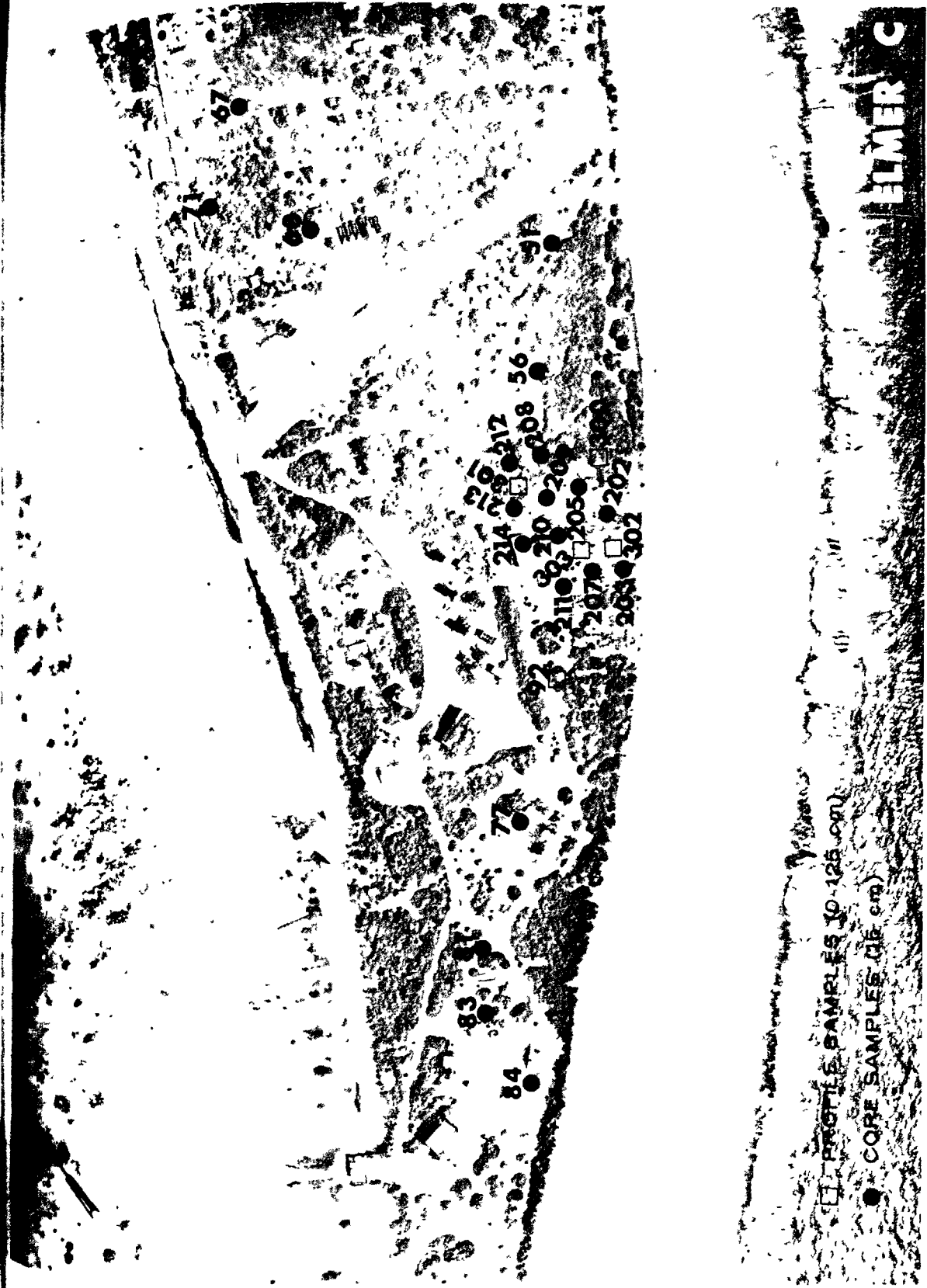


Fig. B.39. 1.f. Soil-sample locations.





Fig. B.39.1.j. The average  $^{90}\text{Sr}$  activities (pCi/g) in soil samples collected to a depth of 15 cm.



Fig. B.39.1.1. The average  $^{137}\text{Cs}$  activities (pCi/g) in soil samples collected to a depth of 15 cm.

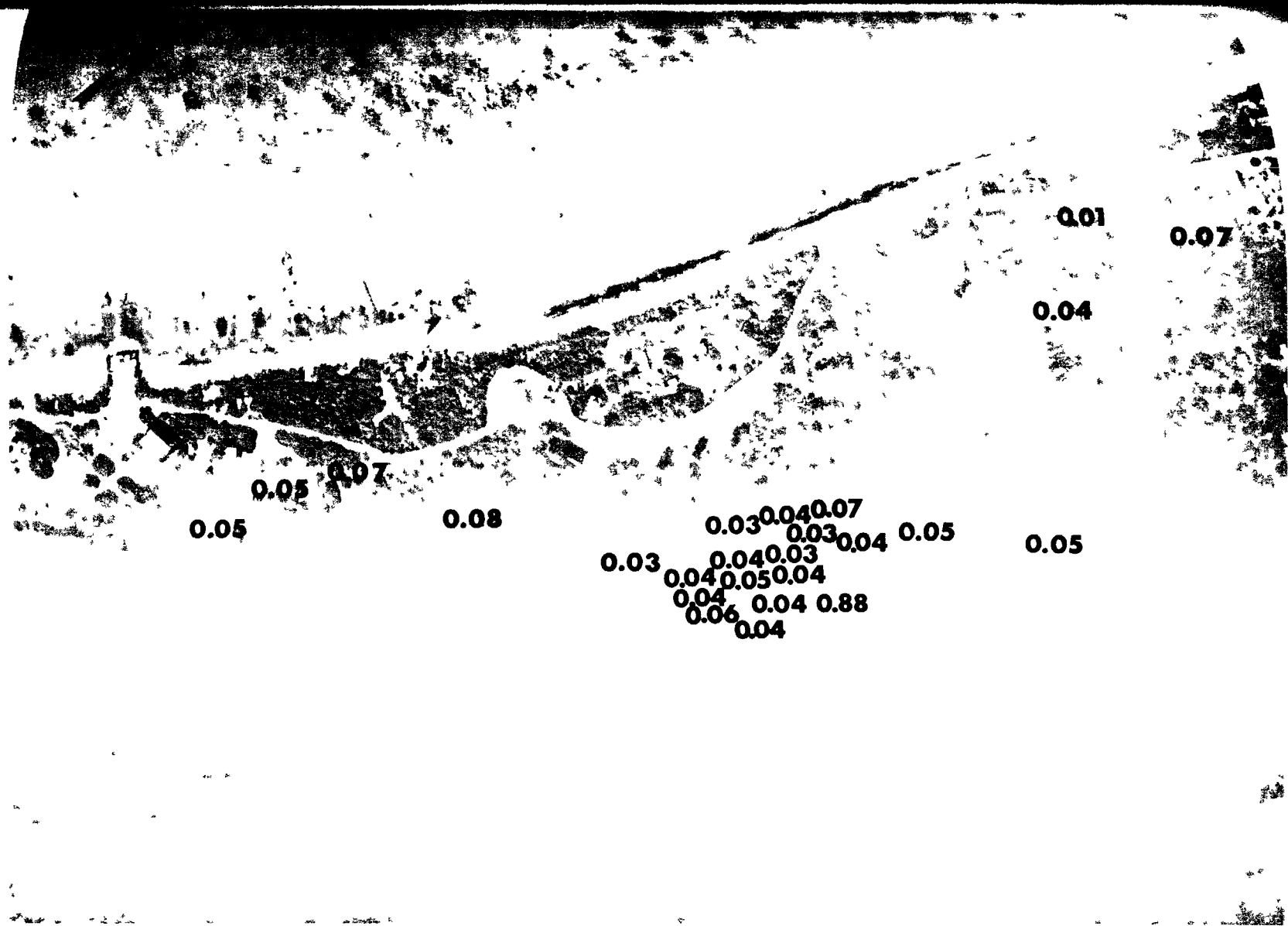


Fig. B.39.1.n. The average  $^{60}\text{Co}$  activities (pCi/g) in soil samples collected to a depth of 15 cm.

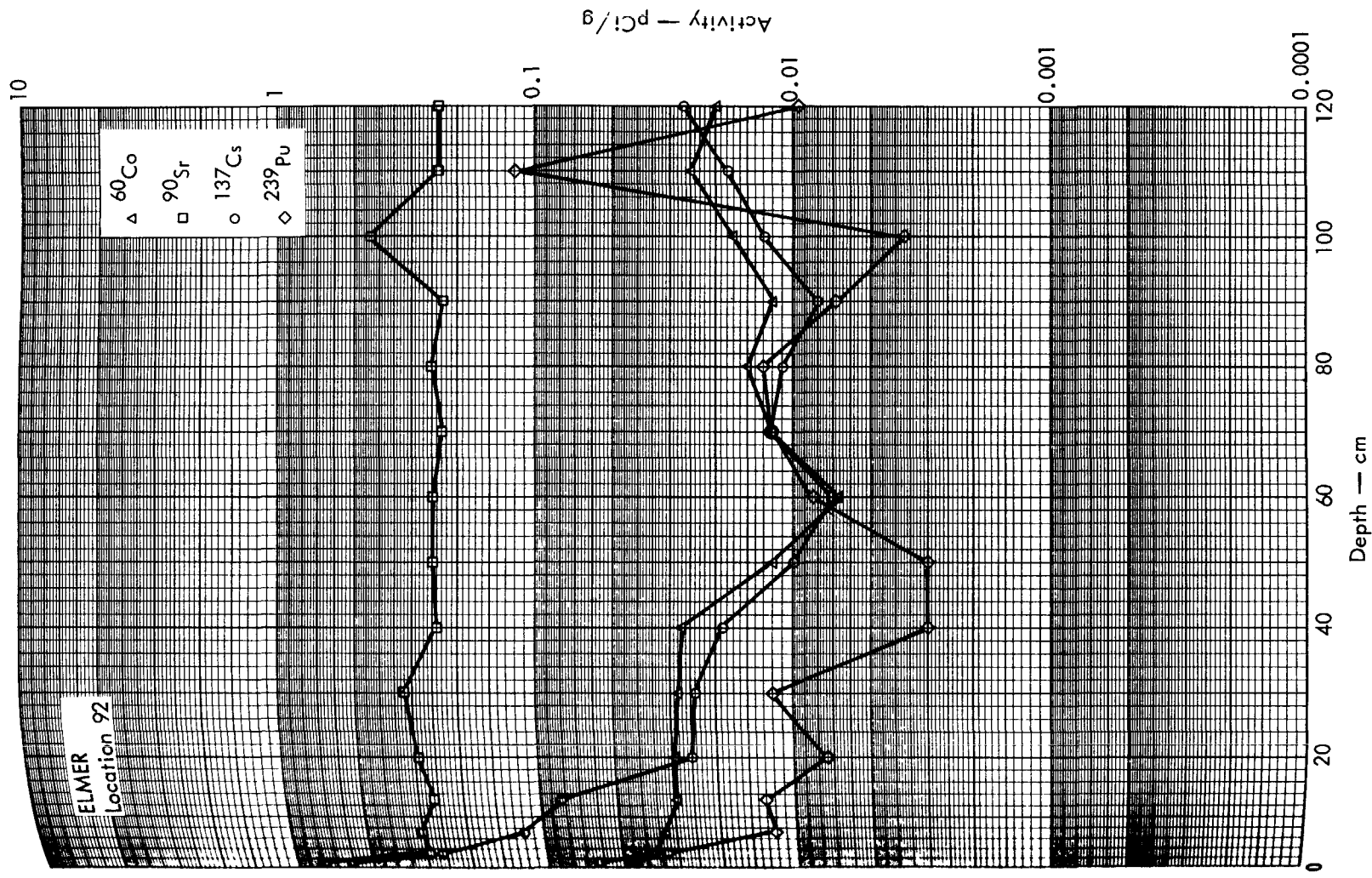


Fig. B.39. 2a. Activities of selected radionuclides as a function of soil depth.





ELMER D

Fig. B.40.1.a.



**ELMER D**

Fig. B.40.1.b. Gross count isoeposure contours. (Refer to alphabetic symbol key in this appendix.)



Fig. B.40.1.d. The gamma background exposure rate ( $\mu\text{R/hr}$ ) at 1 m above the ground, measured with a portable NaI scintillation counter.



B.40.1.f. Soil-sample locations.

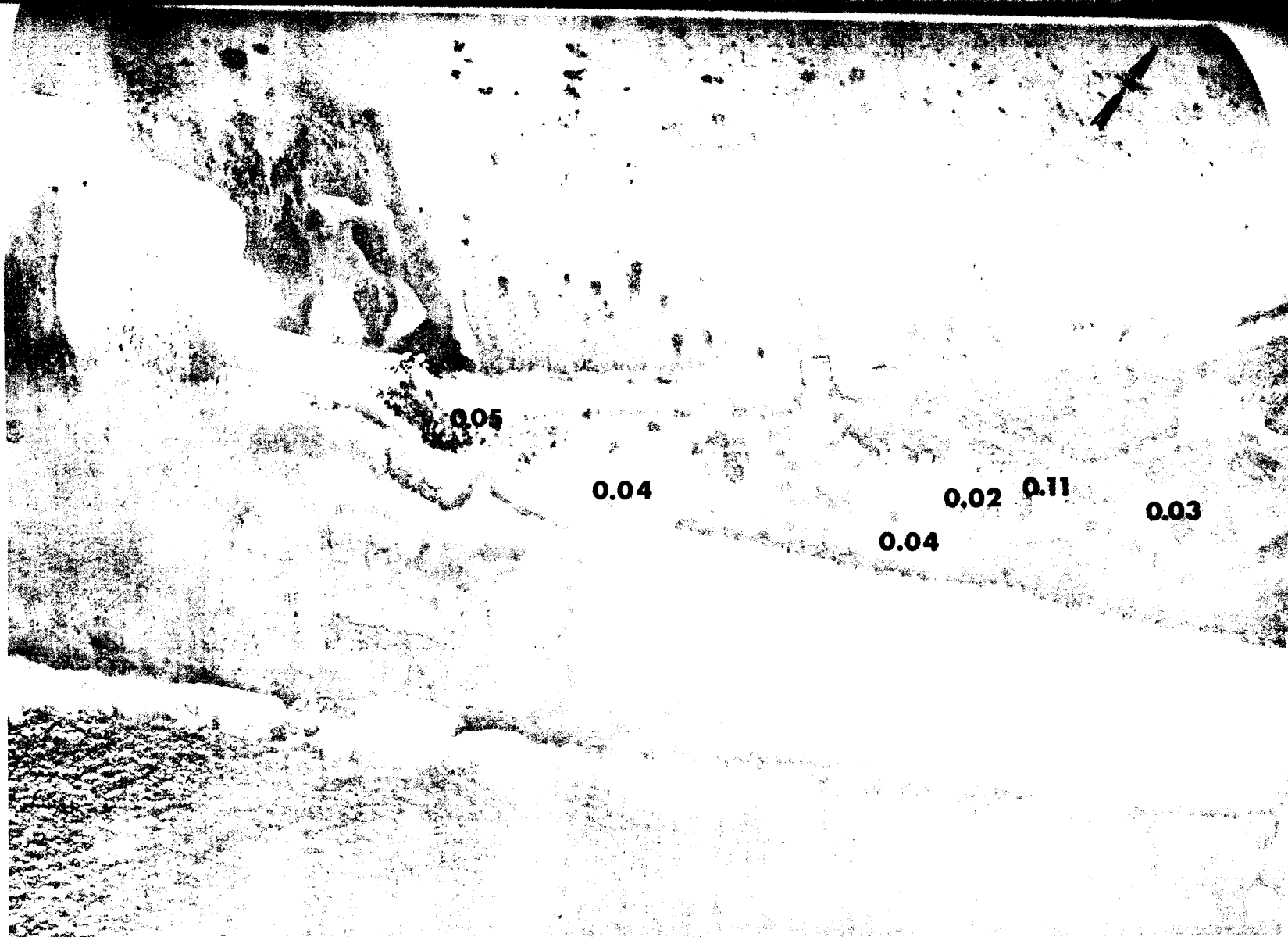


Fig. B.40.1.i. The average  $^{239}\text{Pu}$  activities (pCi/g) in soil samples collected to a depth of 15 cm.



Fig. B.40.1.j. The average  $^{90}\text{Sr}$  activities (pCi/g) in soil samples collected to a depth of 15 cm.

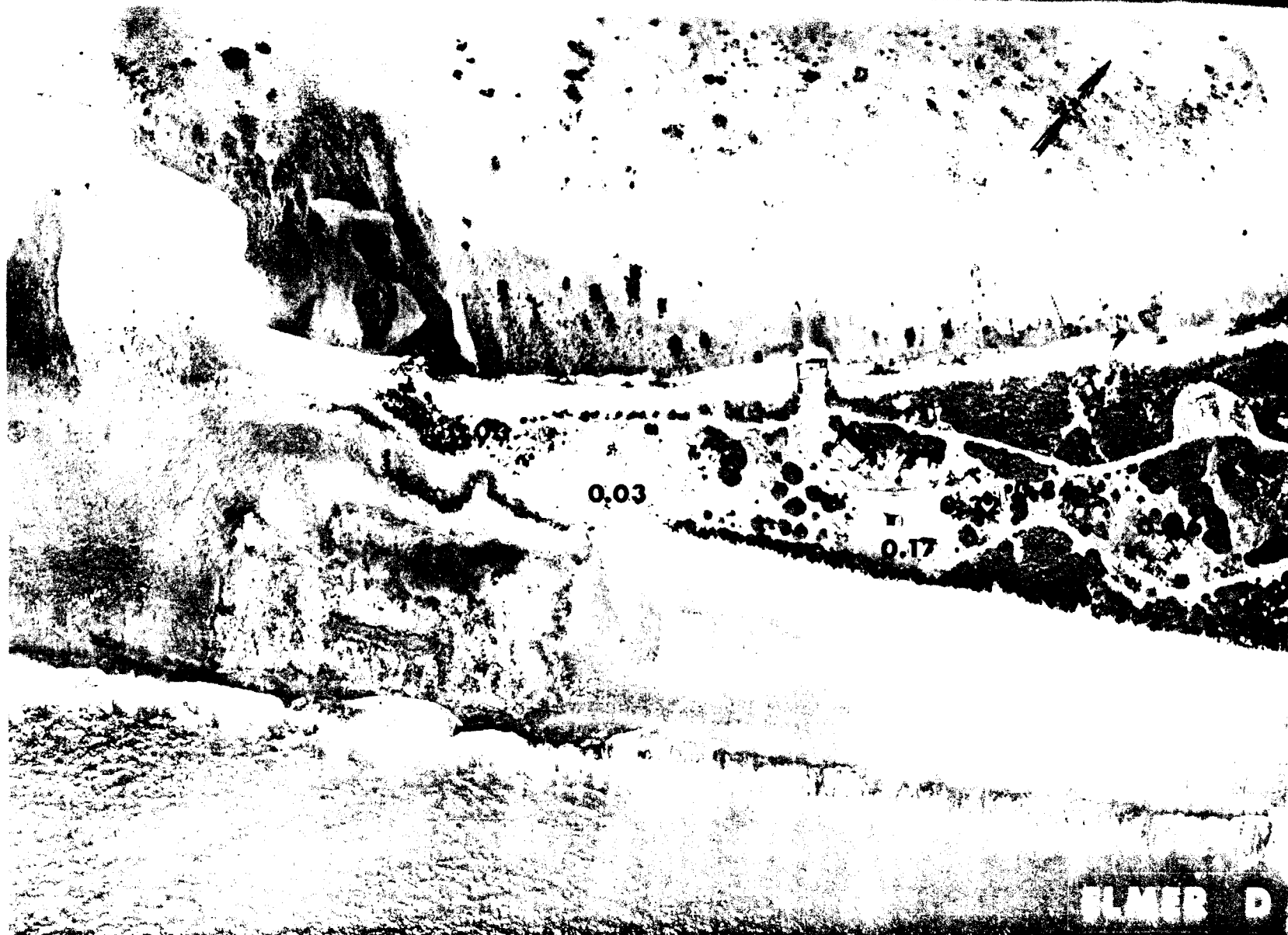


Fig. B.40.1.1. The average  $^{137}\text{Cs}$  activities (pCi/g) in soil samples collected to a depth of 15 cm.

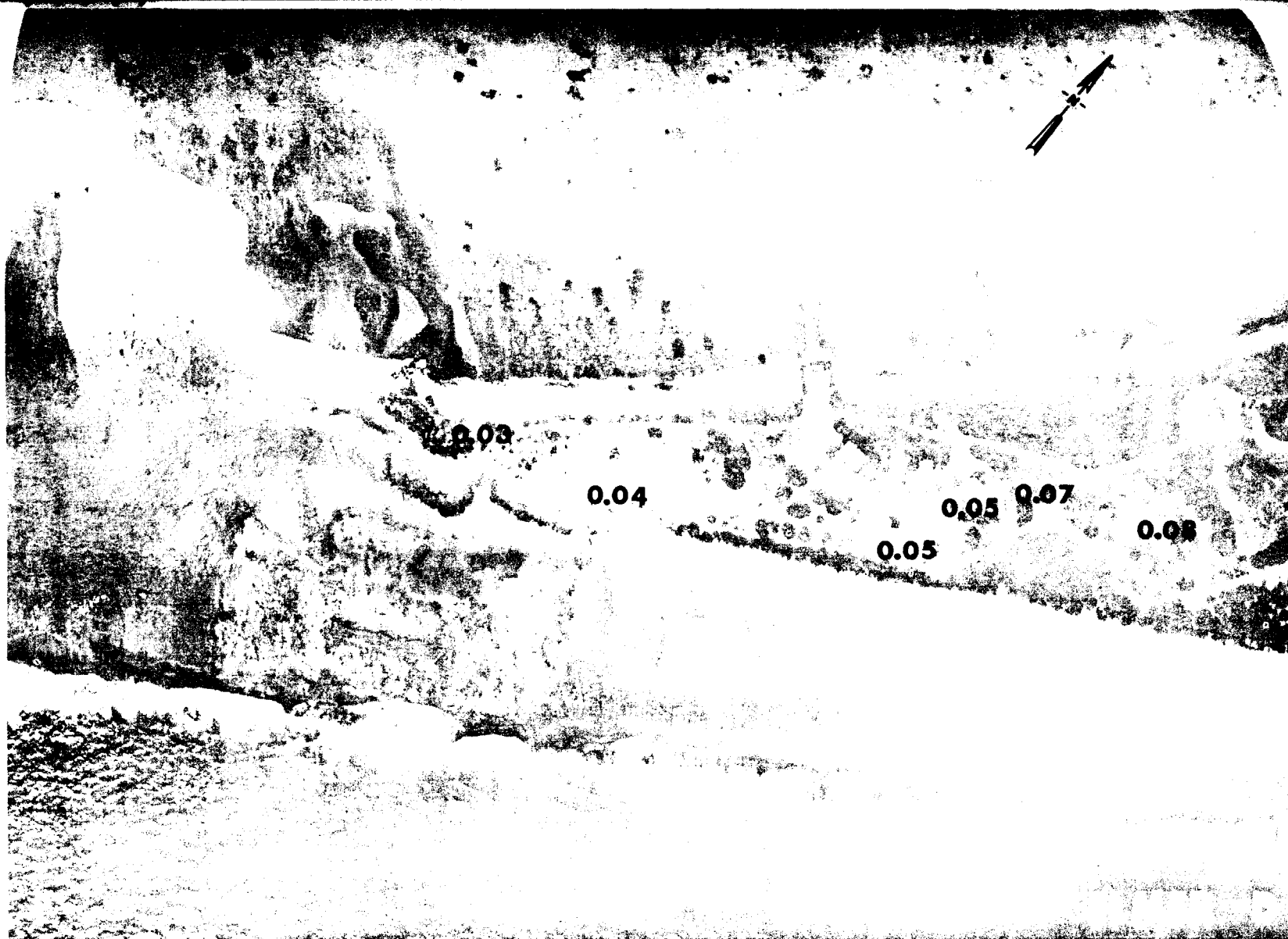


Fig. B.40.1.n. The average  $^{60}\text{Co}$  activities (pCi/g) in soil samples collected to a depth of 15 cm.





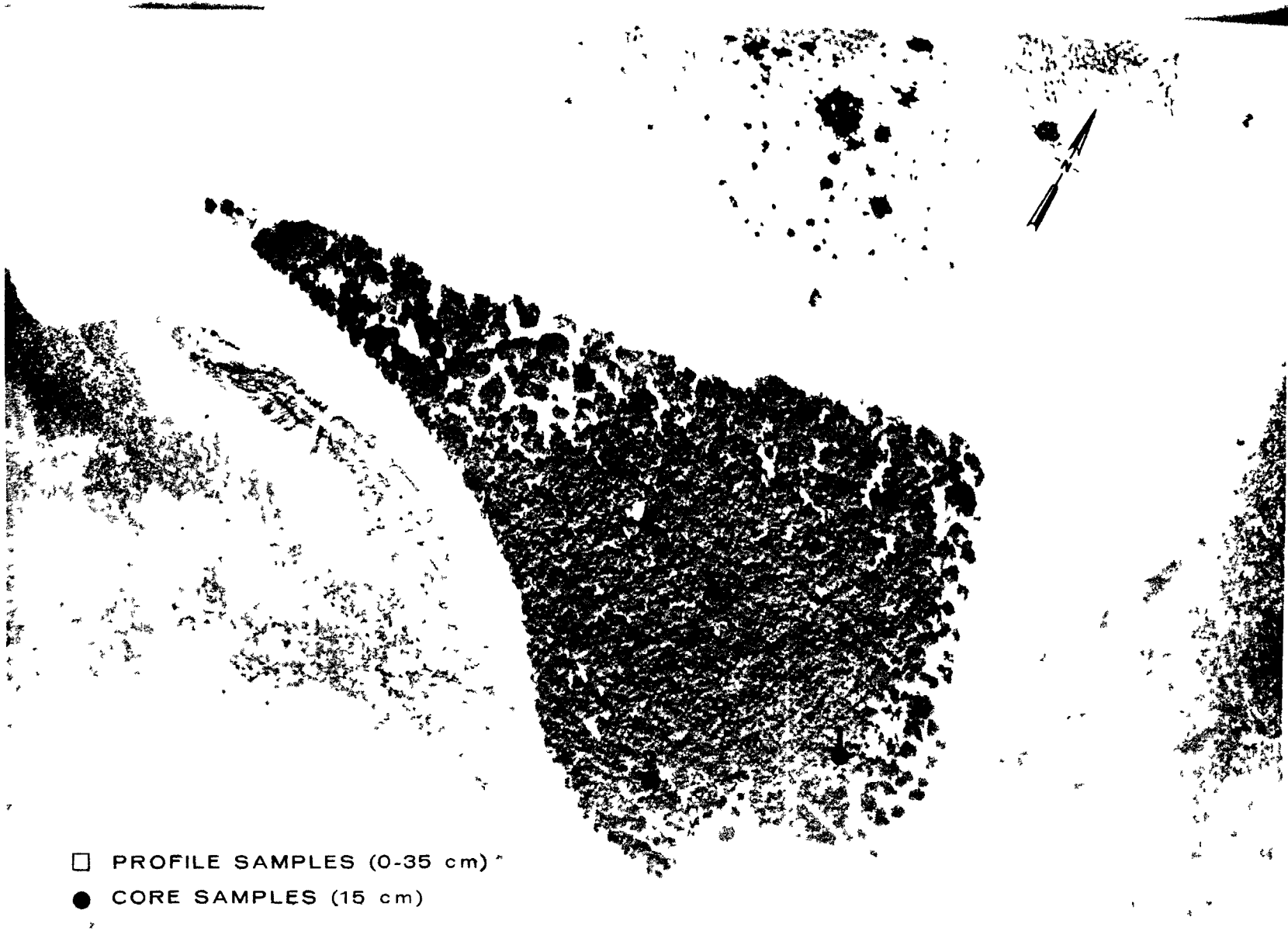
Fig. B.41.1.a.



Fig. B.41.1.b. Gross count isoeposure contours. (Refer to alphabetic symbol key in this appendix.)



Fig. B.41.1.d. The gamma background exposure rate ( $\mu\text{R}/\text{hr}$ ) at 1 m above the ground, measured with a portable NaI scintillation counter.



□ PROFILE SAMPLES (0-35 cm)  
● CORE SAMPLES (15 cm)

Fig. B.41.1.f. Soil-sample locations.

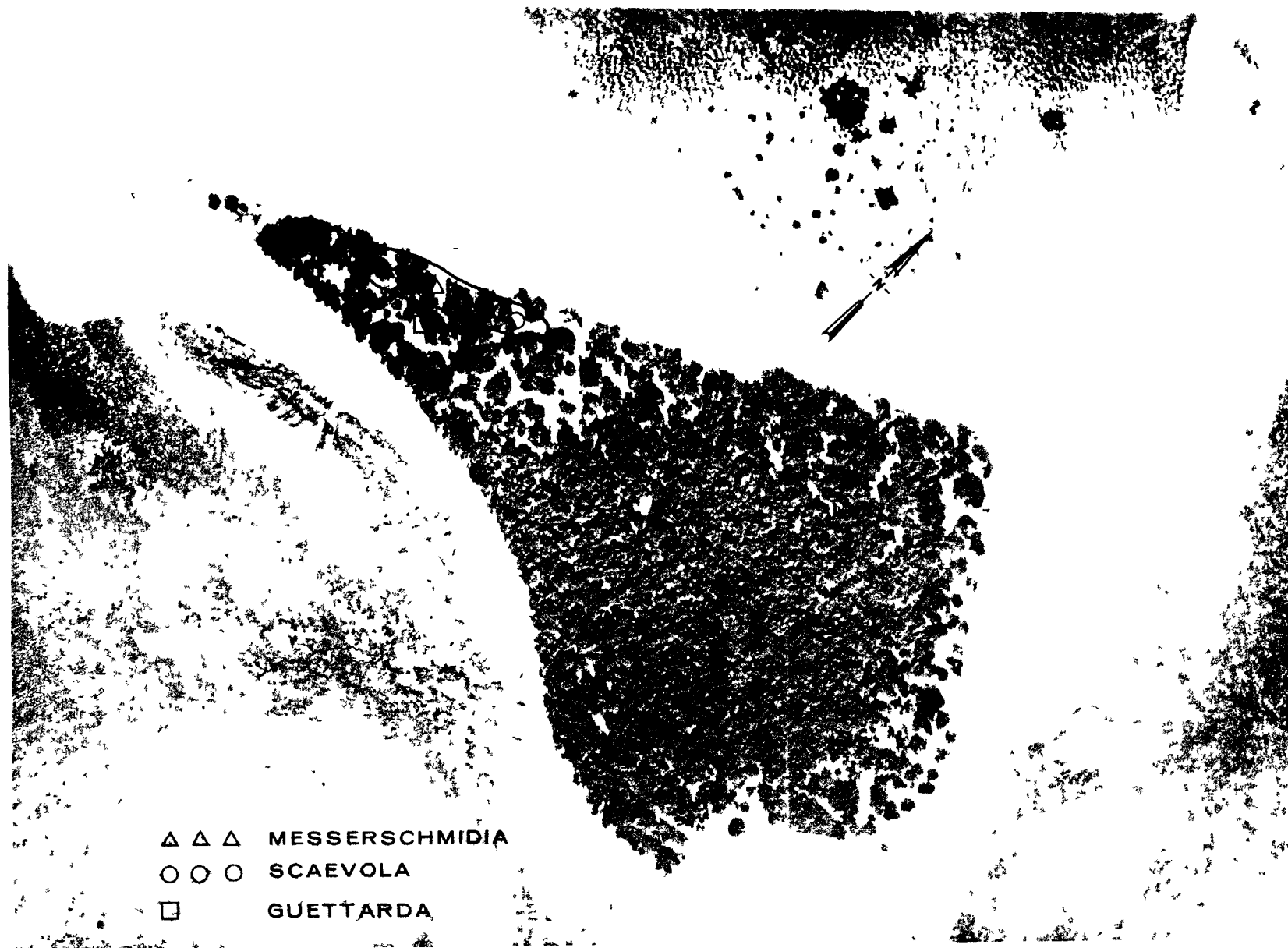


Fig. B.41.1.g. Vegetation sample locations.



Fig. B.41.1.i. The average  $^{239}\text{Pu}$  activities (pCi/gm) in soil samples collected to a depth of 15 cm.

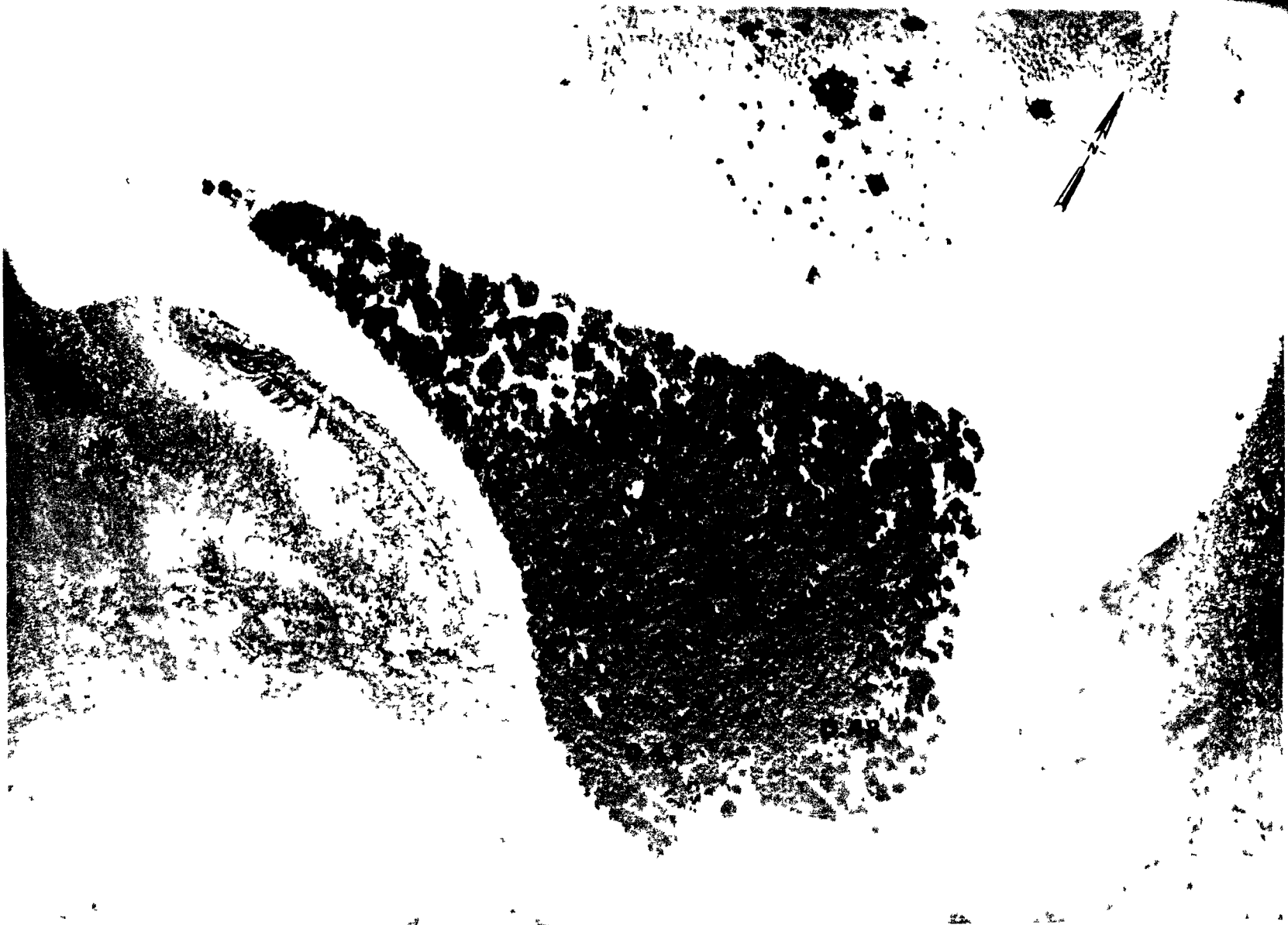


Fig. B.41.1.j. The average  $^{90}\text{Sr}$  activities (pCi/gm) in soil samples collected to a depth of 15 cm.



Fig. B.41.1.k.  $^{137}\text{Cs}$  isoexposure and isoconcentration contours. (Refer to alphabetic symbol key in this appendix.)





Fig. B.41.1.1. The average  $^{137}\text{Cs}$  activities (pCi/gm) in soil samples collected to a depth of 15 cm.



Fig. B.41.1.m.  $^{60}\text{Co}$  isoexposure and isoconcentration contours. (Refer to alphabetic symbol key in this appendix.)



Fig. B.41.1.n. The average <sup>60</sup>Co activities (pCi/gm) in soil samples collected to a depth of 15 cm.

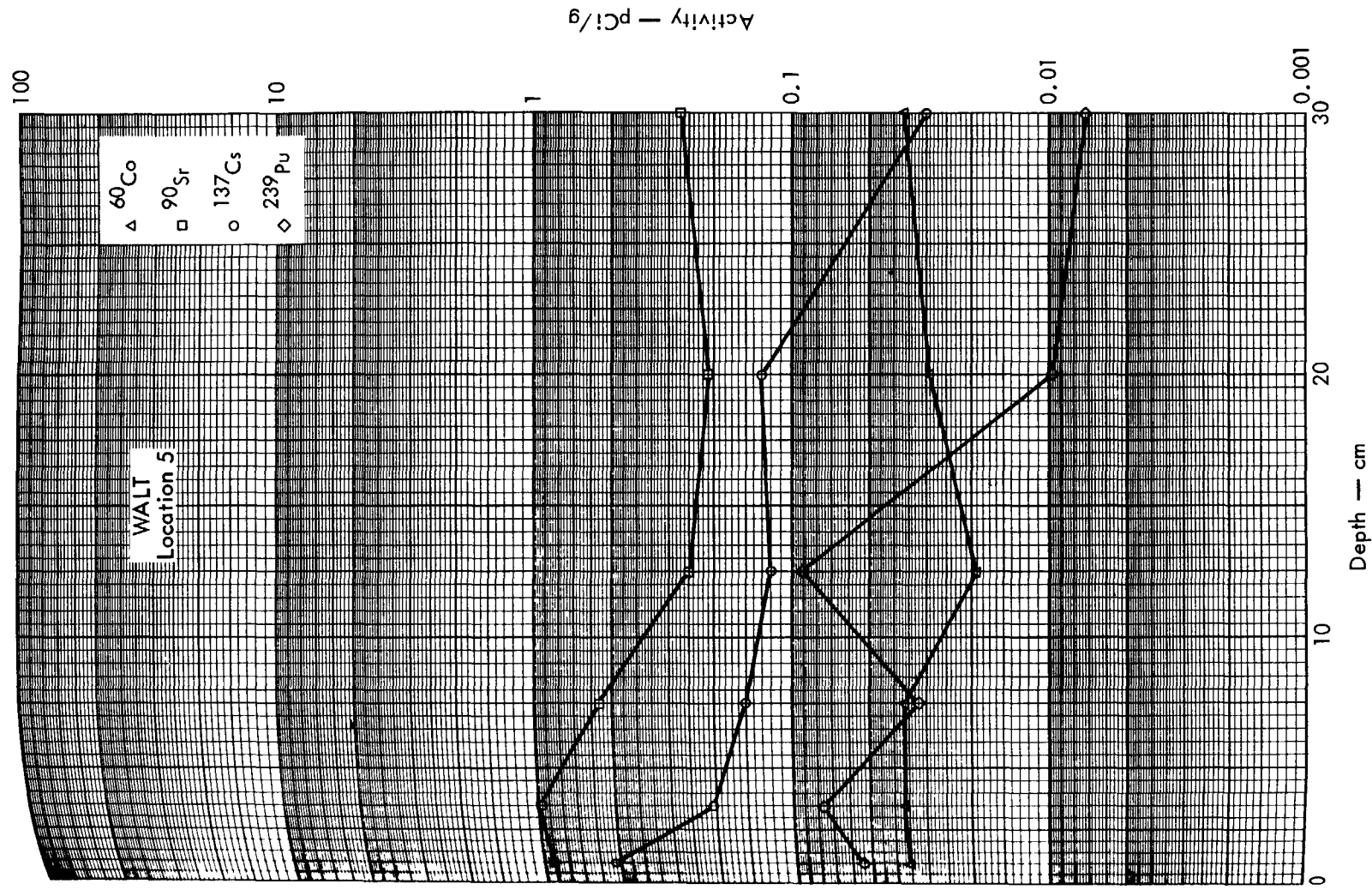


Fig. B.41.2a. Activities of selected radionuclides as a function of soil depth.



FRED A

Fig. B.42.1.a.



Fig. B.42.1.b. Gross count isoexposure contours. (Refer to alphabetic symbol key in this appendix.)

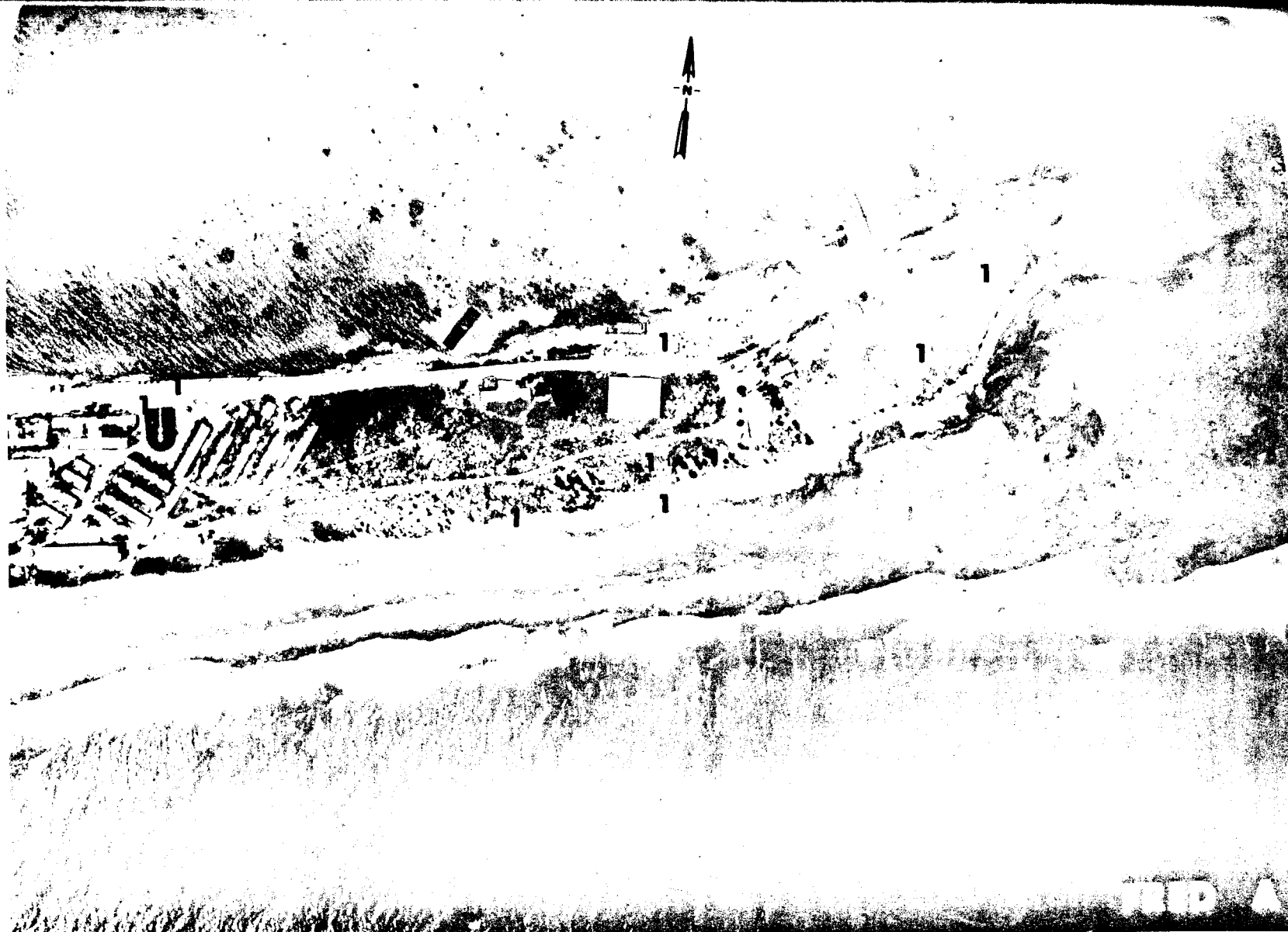


Fig. B.42.1.d. The gamma background exposure rate ( $\mu\text{R}/\text{hr}$ ) at 1 m above the ground, measured with a portable NaI scintillation counter.



● CORE SAMPLES (15cm)

Fig. B.42.1.f. Soil-sample locations.



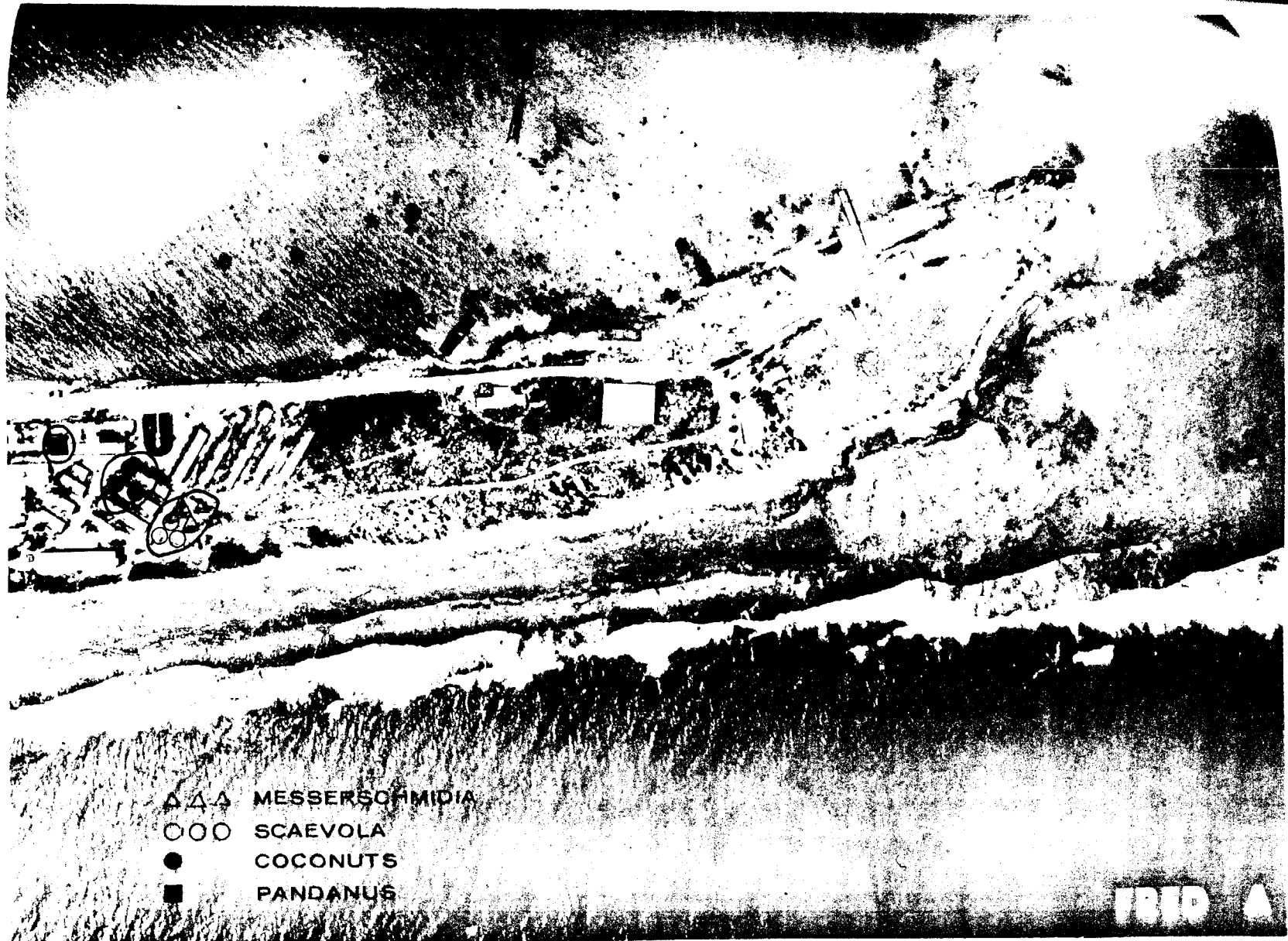


Fig. B.42.1.g. Vegetation sample locations.



Fig. B.42.1.i. The average  $^{239}\text{Pu}$  activities (pCi/g) in soil samples collected to a depth of 15 cm.



Fig. B.42.1.j. The average  $^{90}\text{Sr}$  activities (pCi/g) in soil samples collected to a depth of 15 cm.

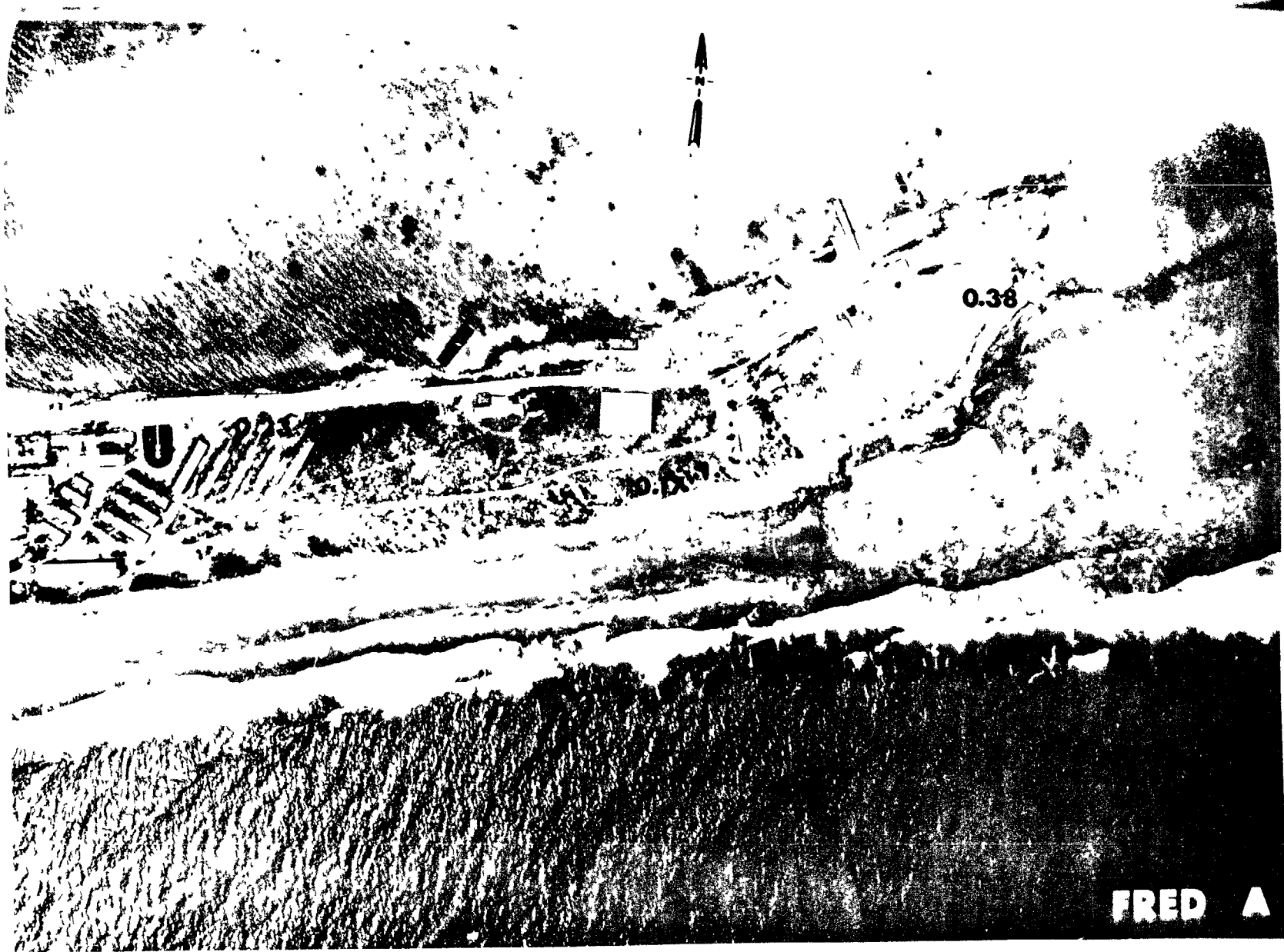


Fig. B.42.1.1. The average  $^{137}\text{Cs}$  activities (pCi/g) in soil samples collected to a depth of 15 cm.

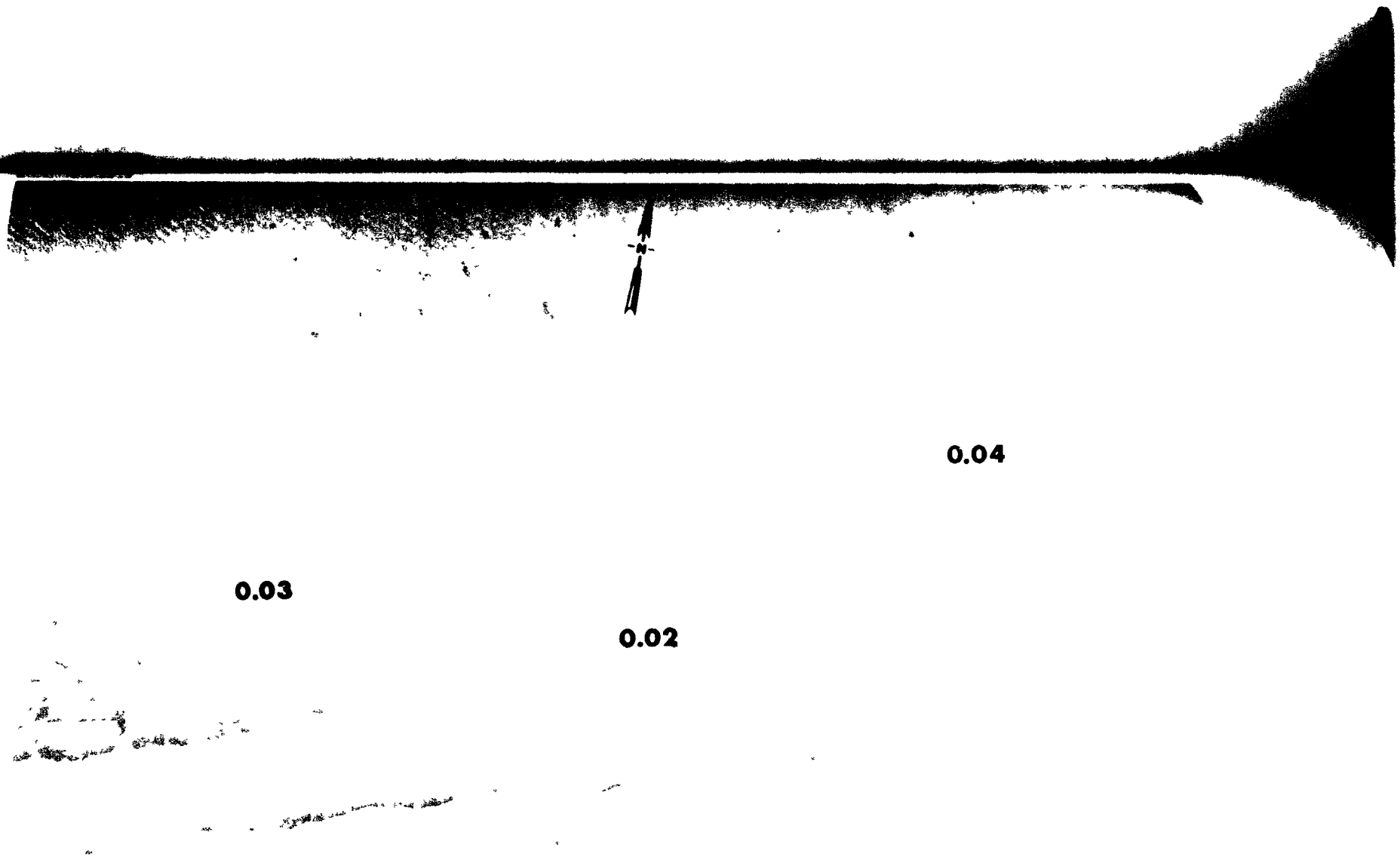
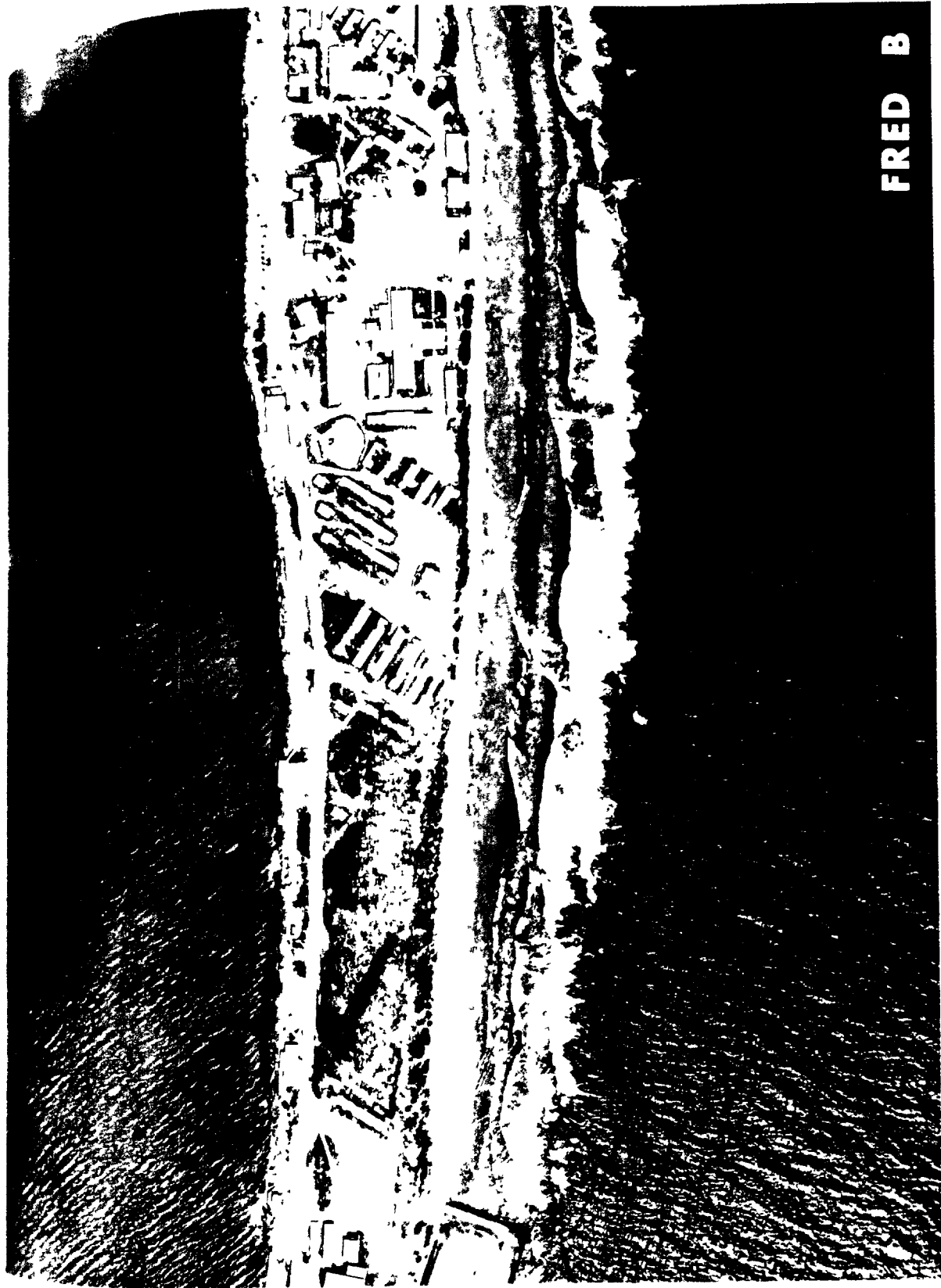
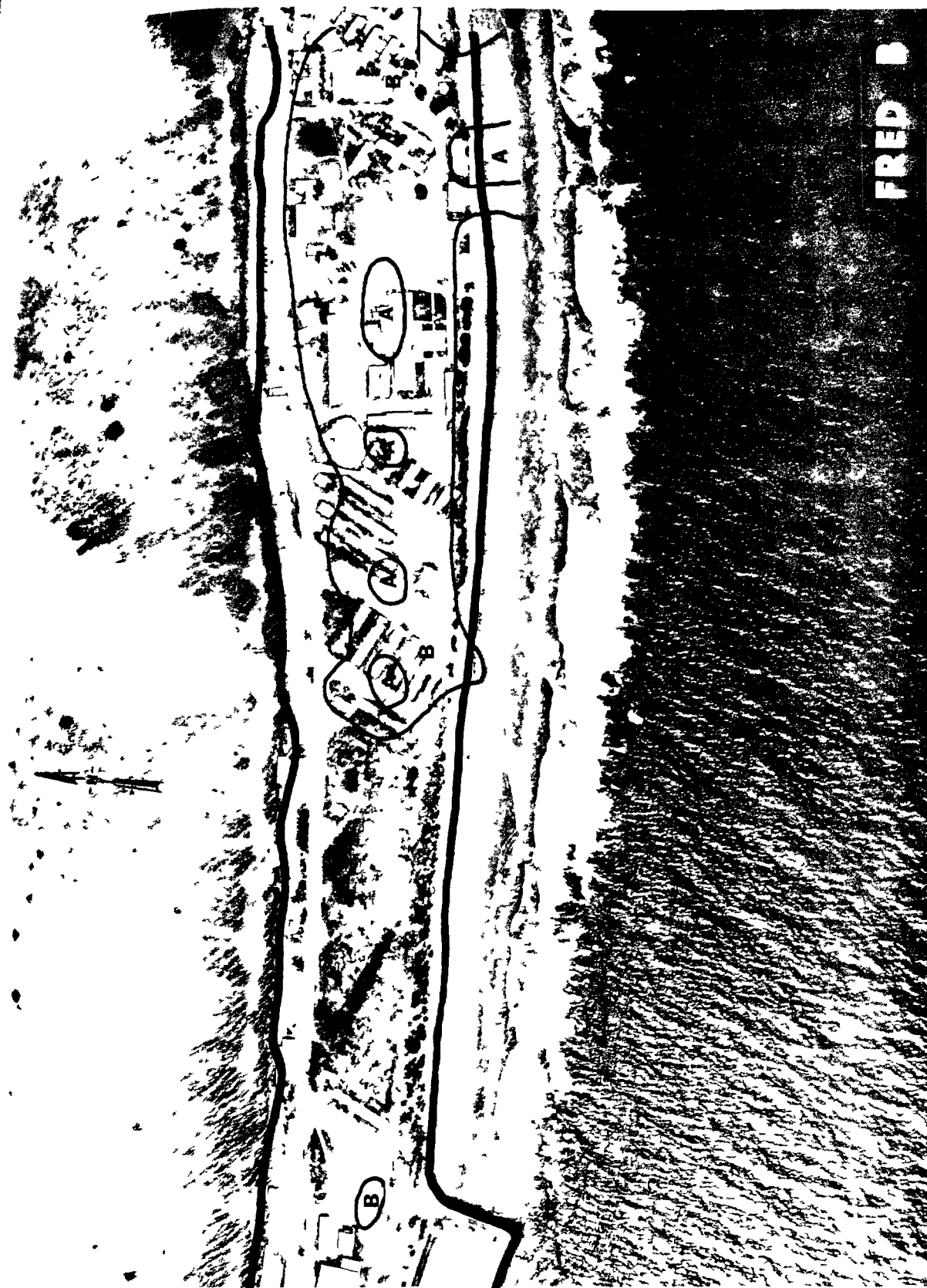


Fig. B.42.1.n. The average  $^{60}\text{Co}$  activities (pCi/g) in soil samples collected to a depth of 15 cm.



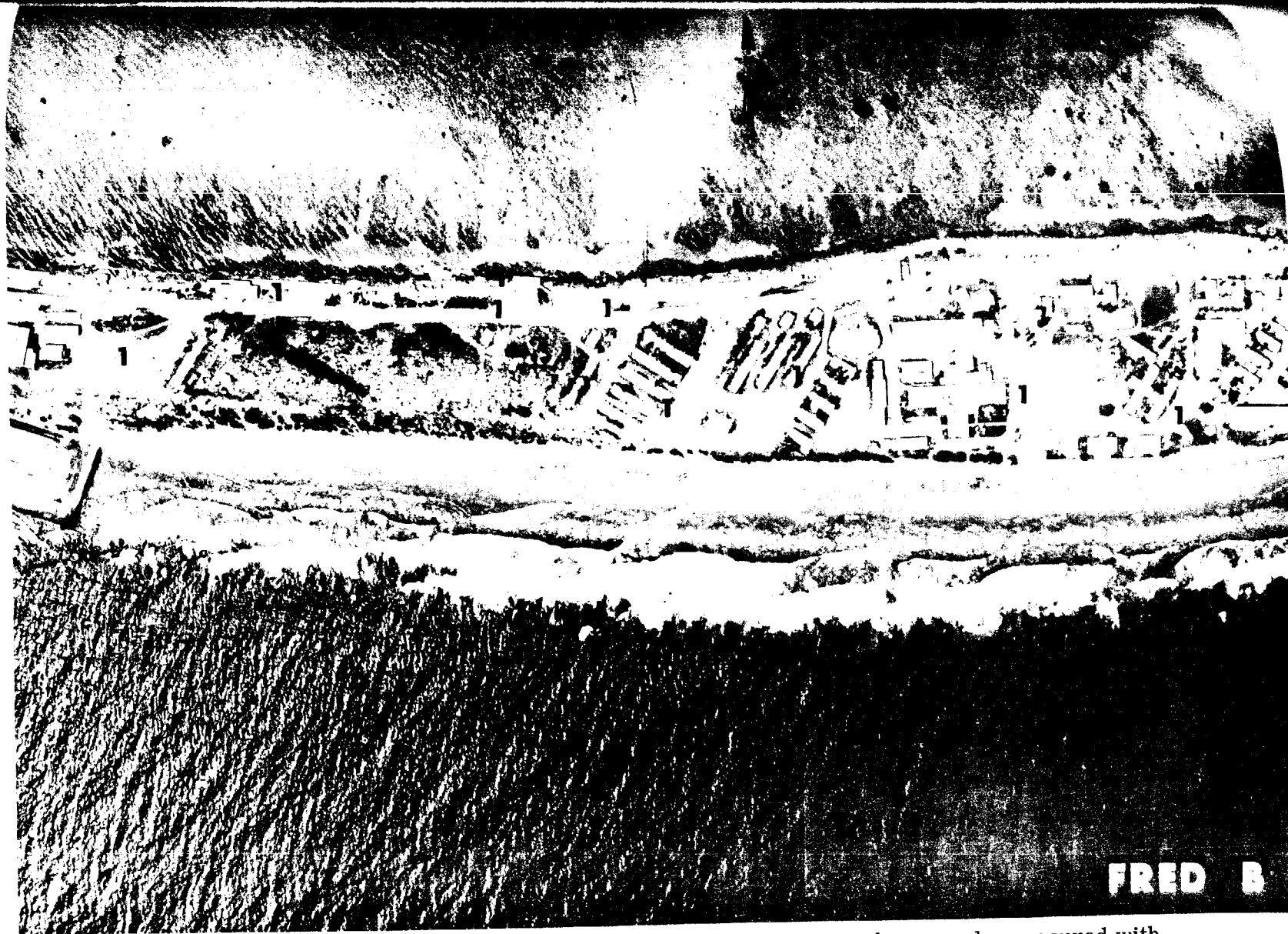
FRED B

Fig. B.43.1.a.



FRED B

Fig. B-43.1.b. Gross count isoeexposure contours. (Refer to alphabetic symbol key in this appendix.)



FRED B

Fig. B.43.1.d. The gamma background exposure rate ( $\mu\text{R/hr}$ ) at 1 m above the ground, measured with a portable NaI scintillation counter.



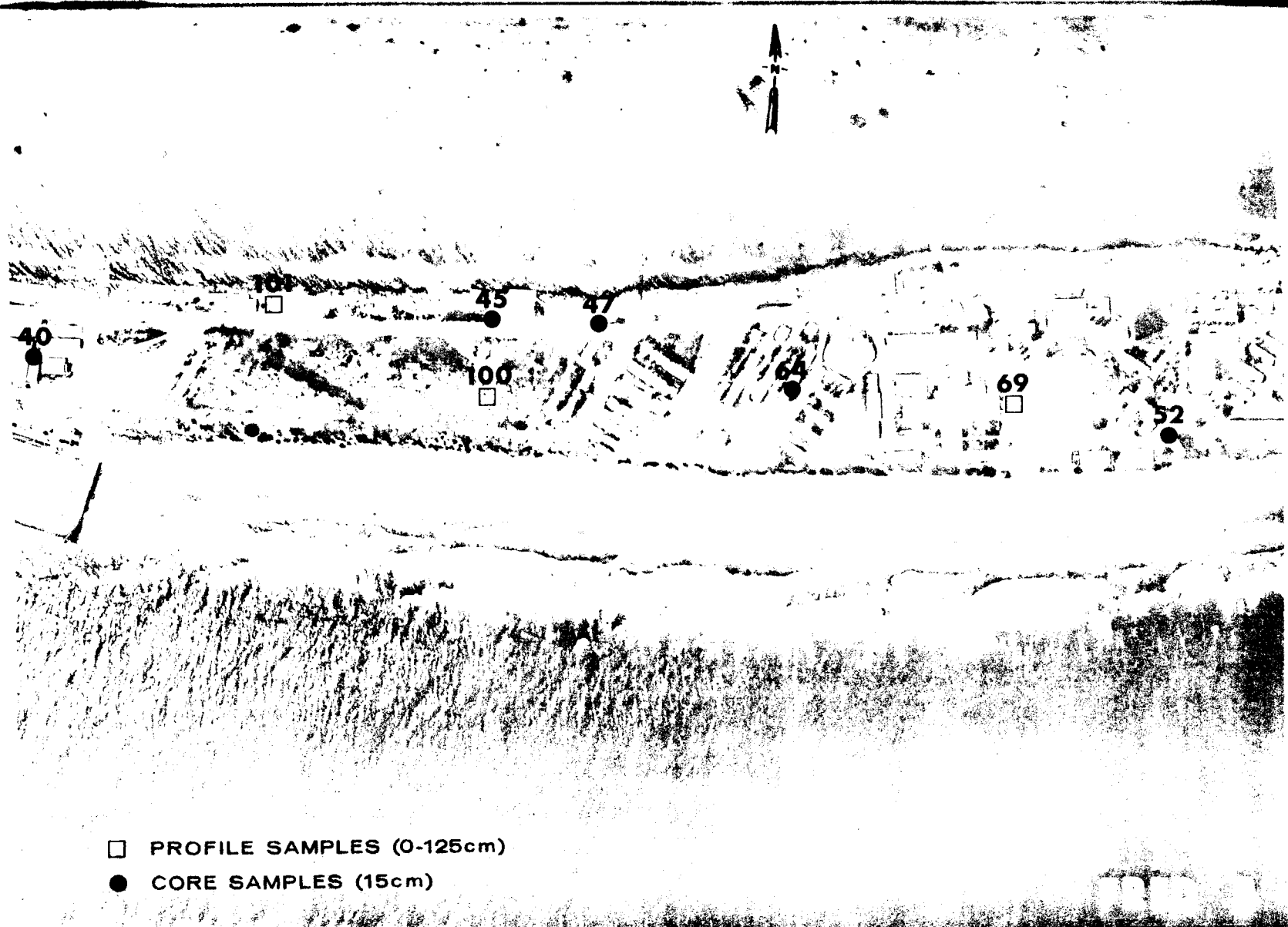


Fig. B.43.1.f. Soil-sample locations.

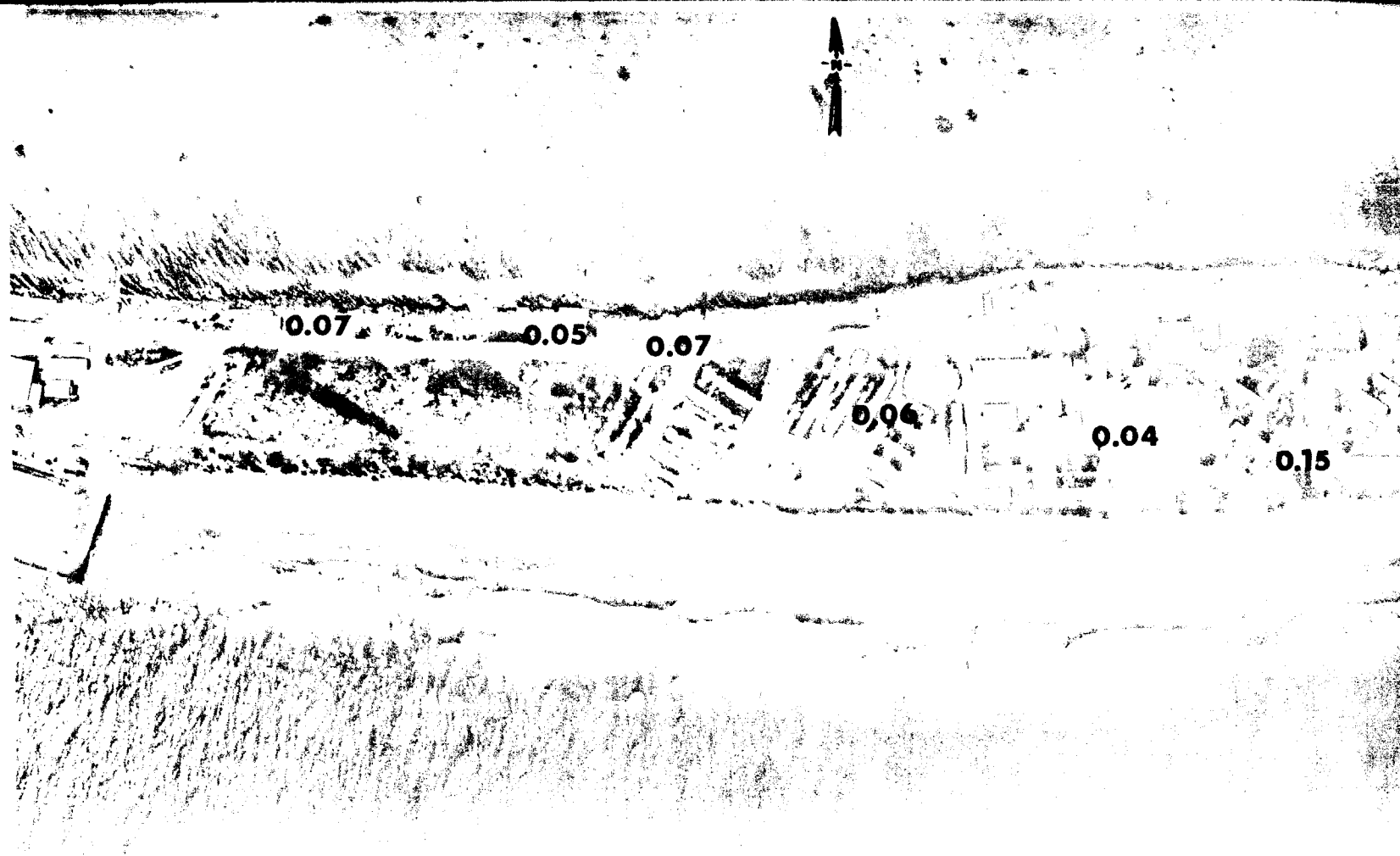


Fig. B.43.1.i. The average  $^{239}\text{Pu}$  activities (pCi/g) in soil samples collected to a depth of 15 cm.

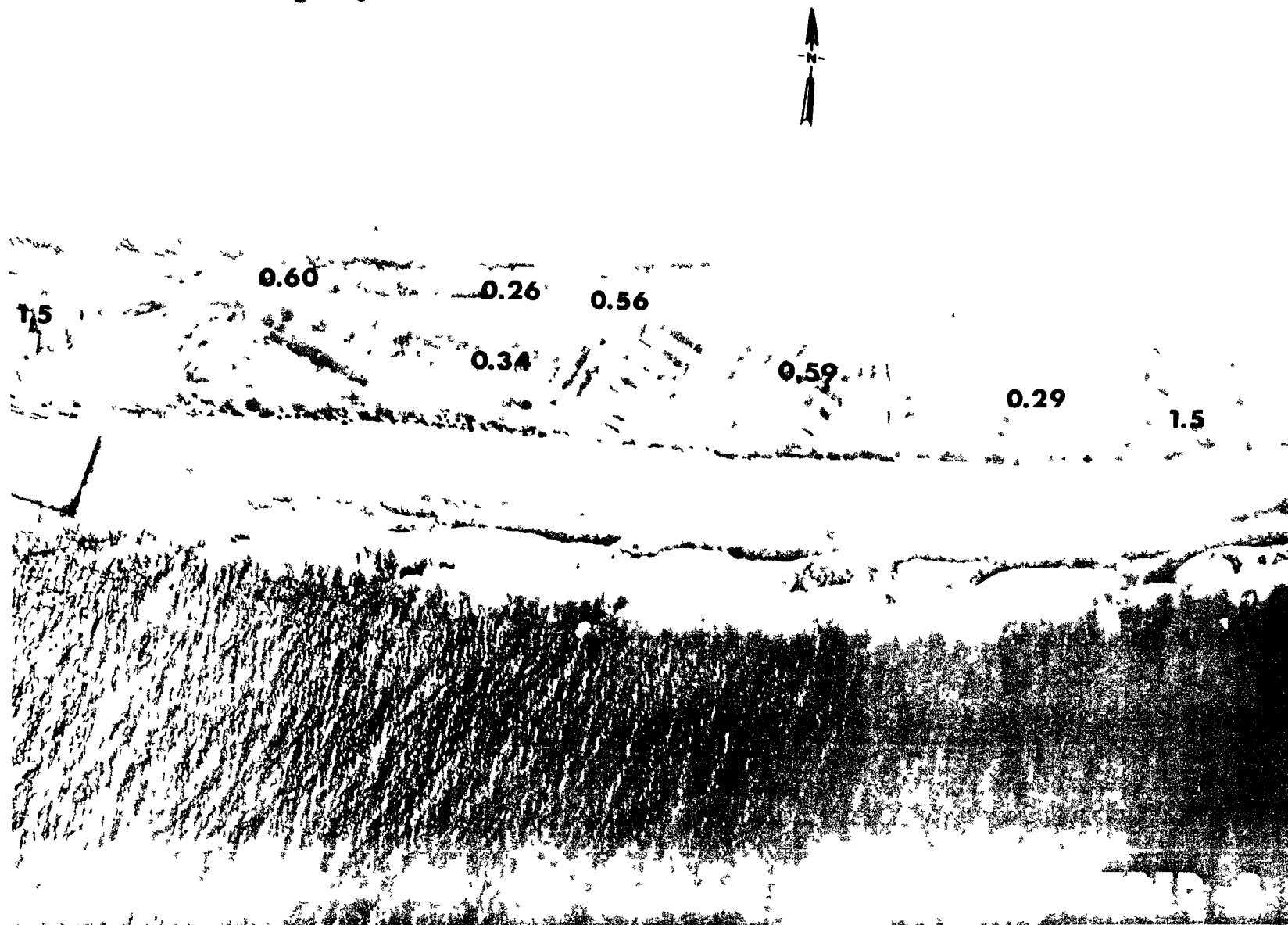


Fig. B.43.1.j). The average  $^{90}\text{Sr}$  activities (pCi/g) in soil samples collected to a depth of 15 cm.

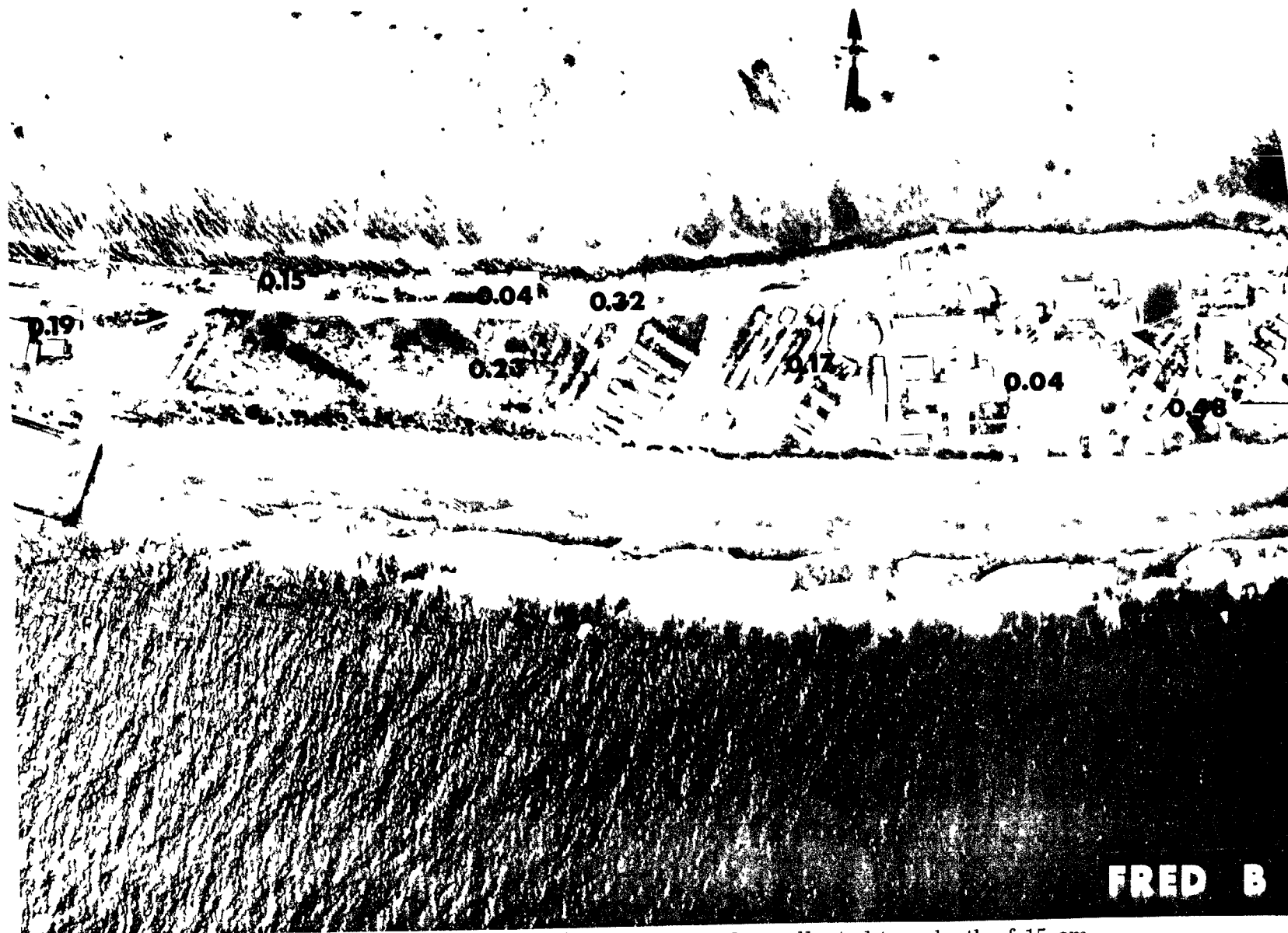


Fig. B.43.1.1. The average <sup>137</sup>Cs activities (pCi/g) in soil samples collected to a depth of 15 cm.

FRED B

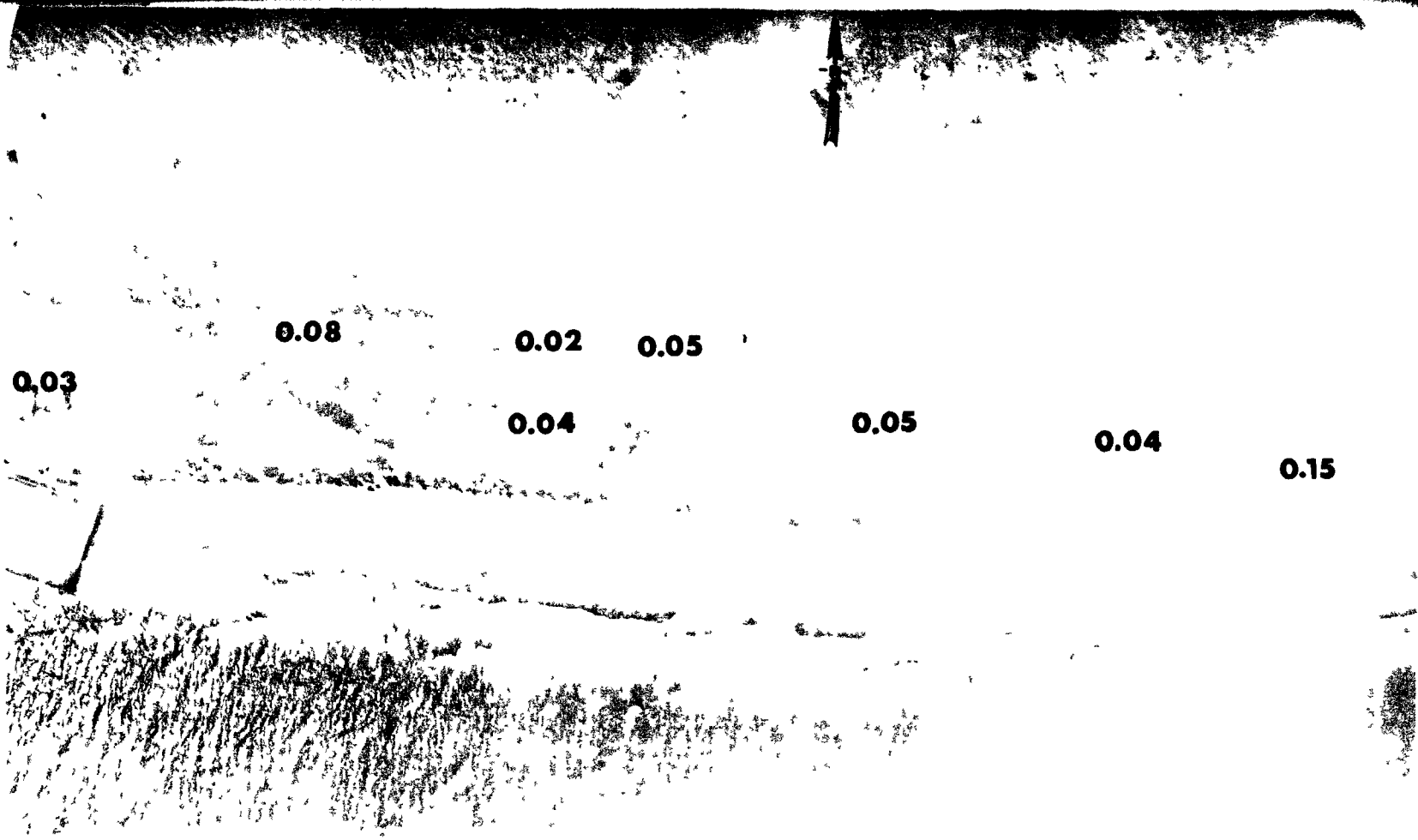


Fig. B.43.1.n. The average  $^{60}\text{Co}$  activities (pCi/g) in soil samples collected to a depth of 15 cm.

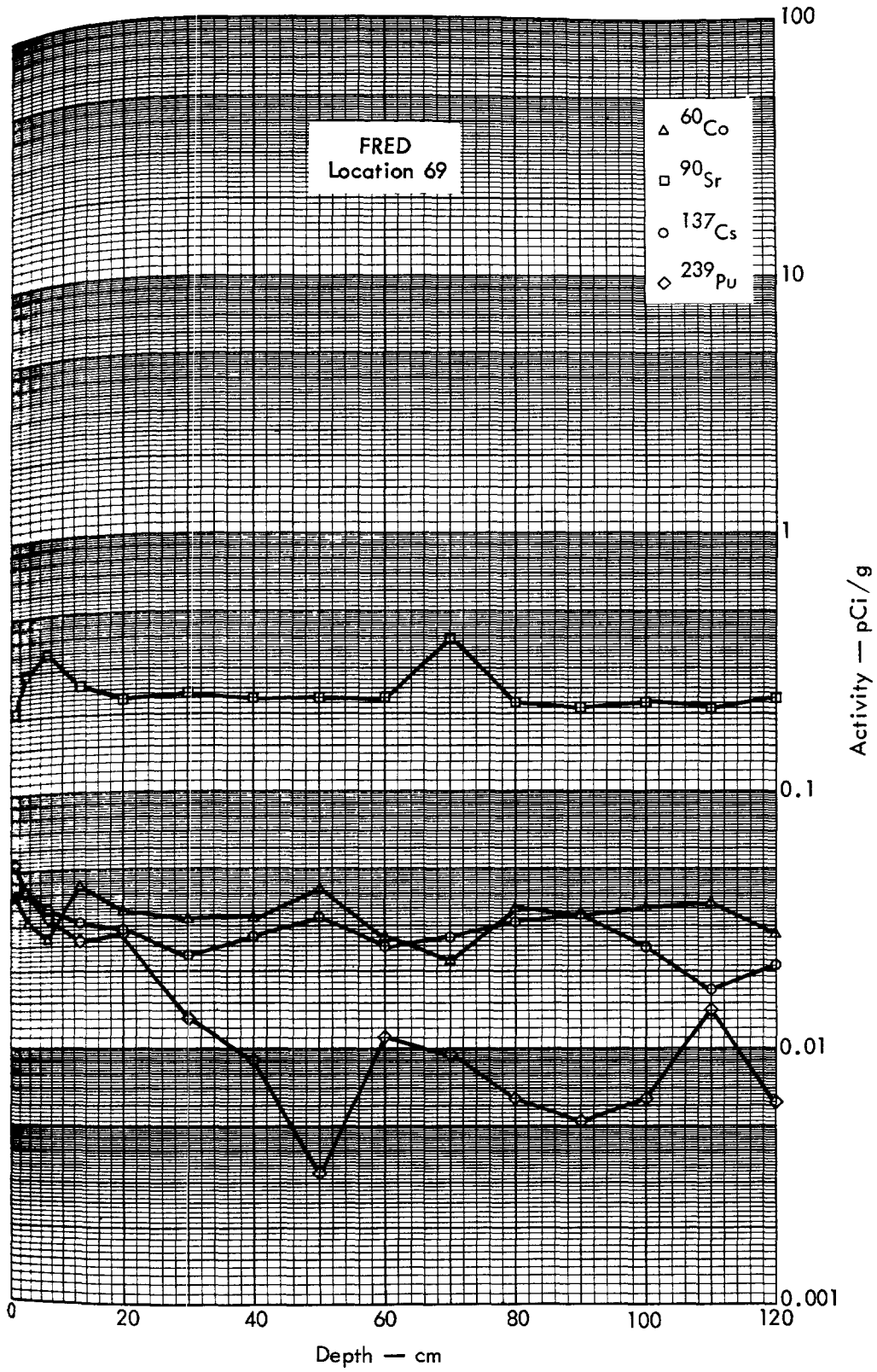


Fig. B.43.2a Activities of selected radionuclides as a function of soil depth.

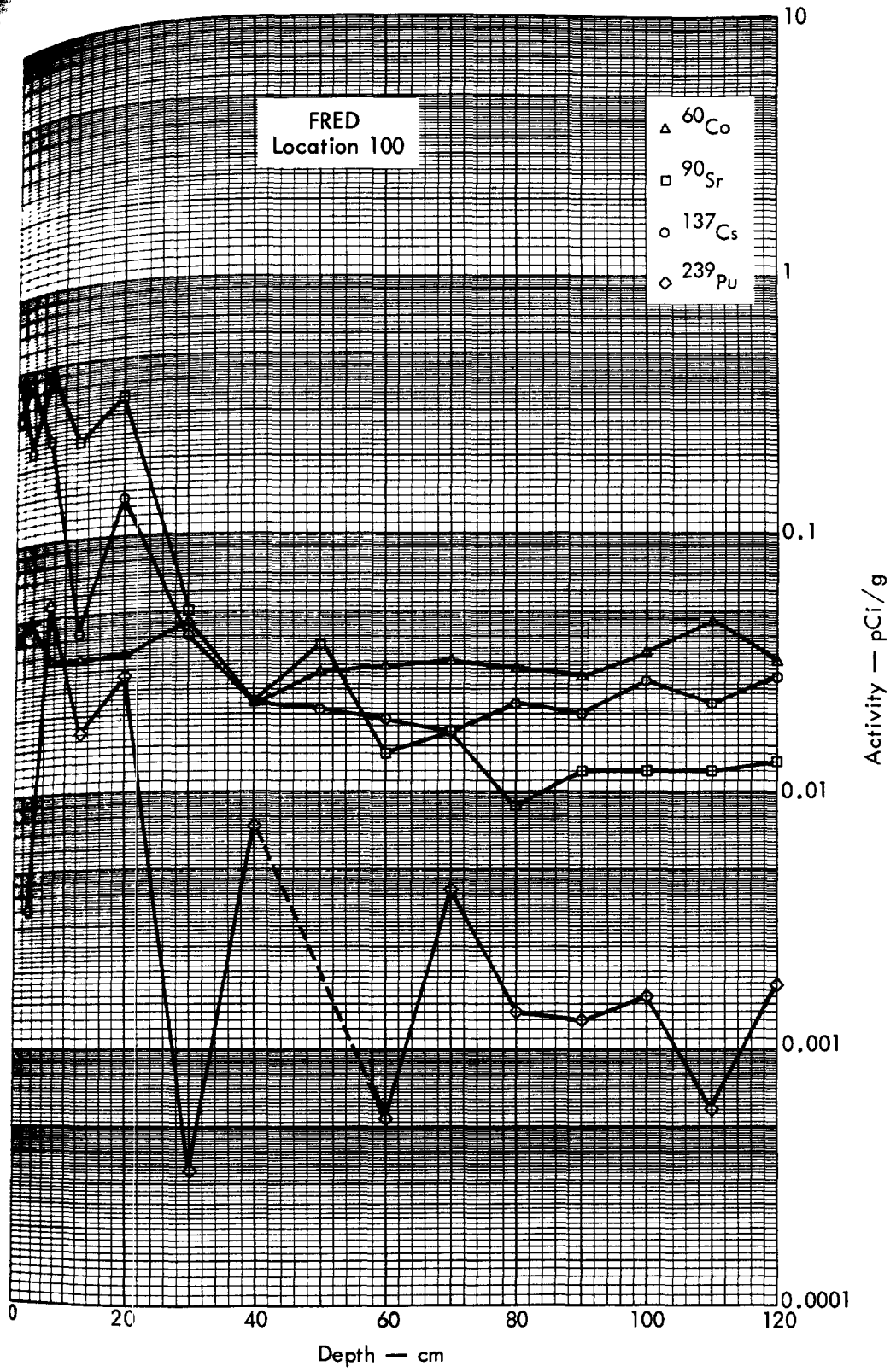


Fig. B.43.2b. Activities of selected radionuclides as a function of soil depth.

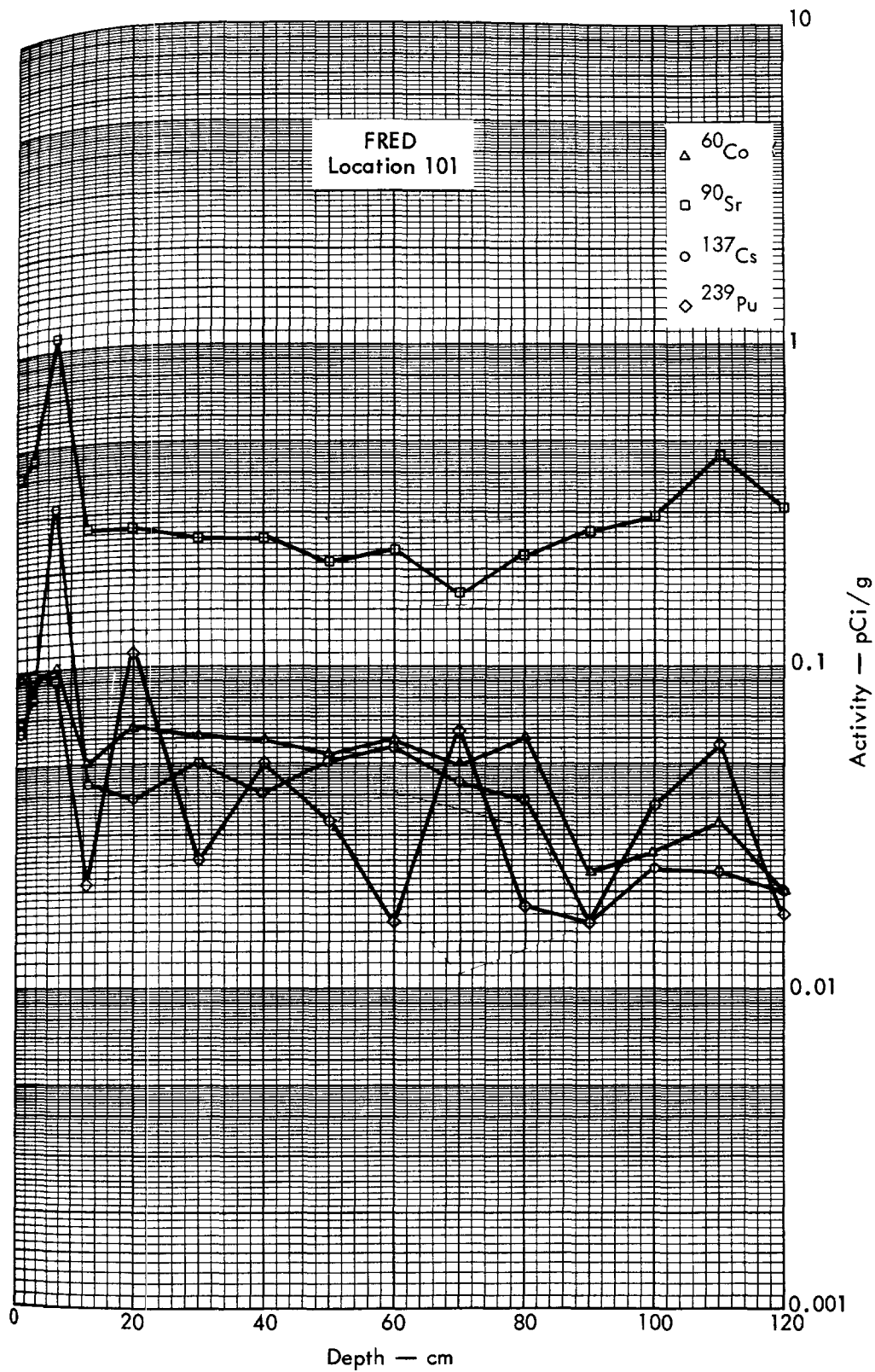
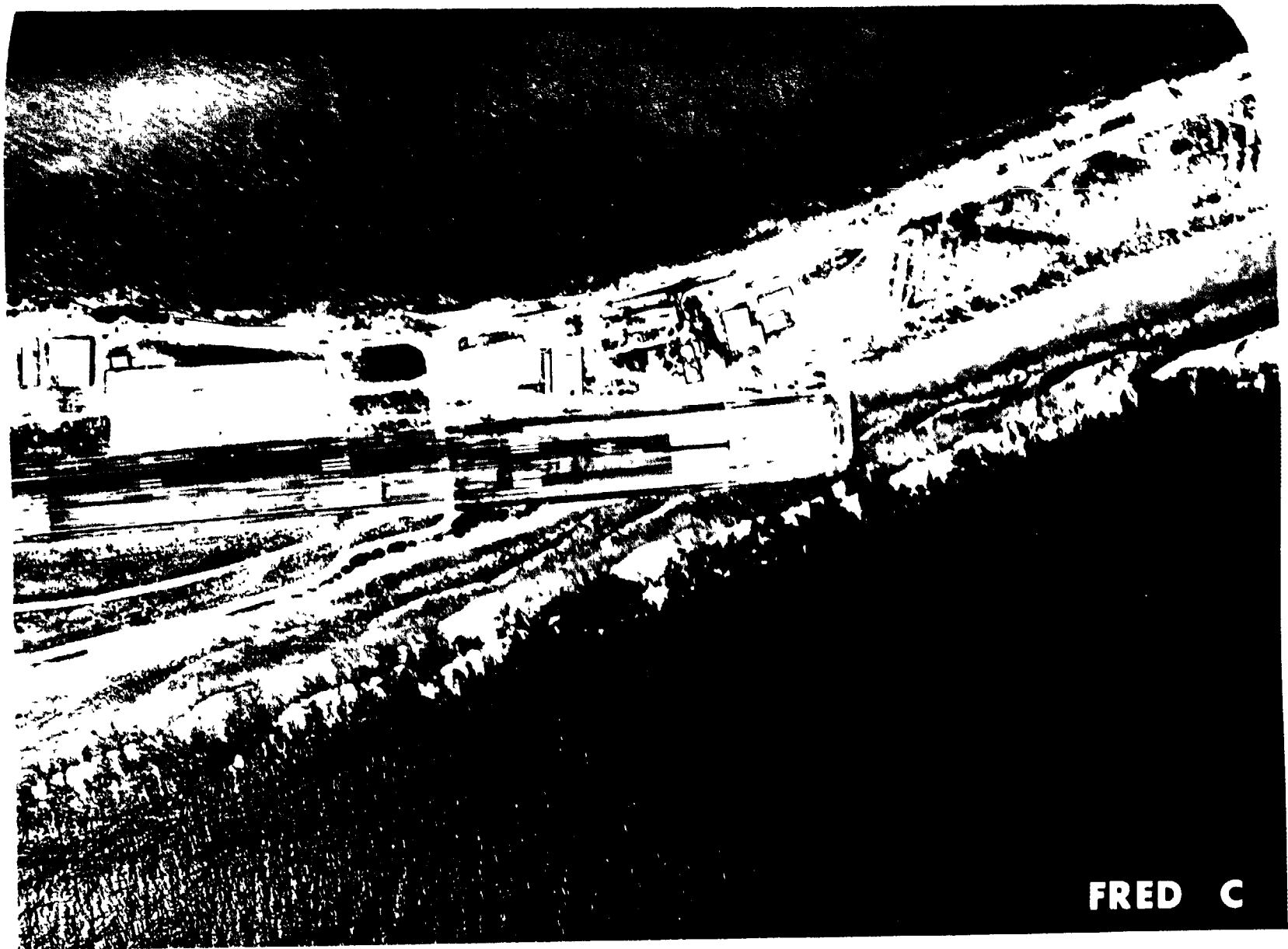


Fig. B.43.2c. Activities of selected radionuclides as a function of soil depth.





FRED C

Fig. B.44.1.a.

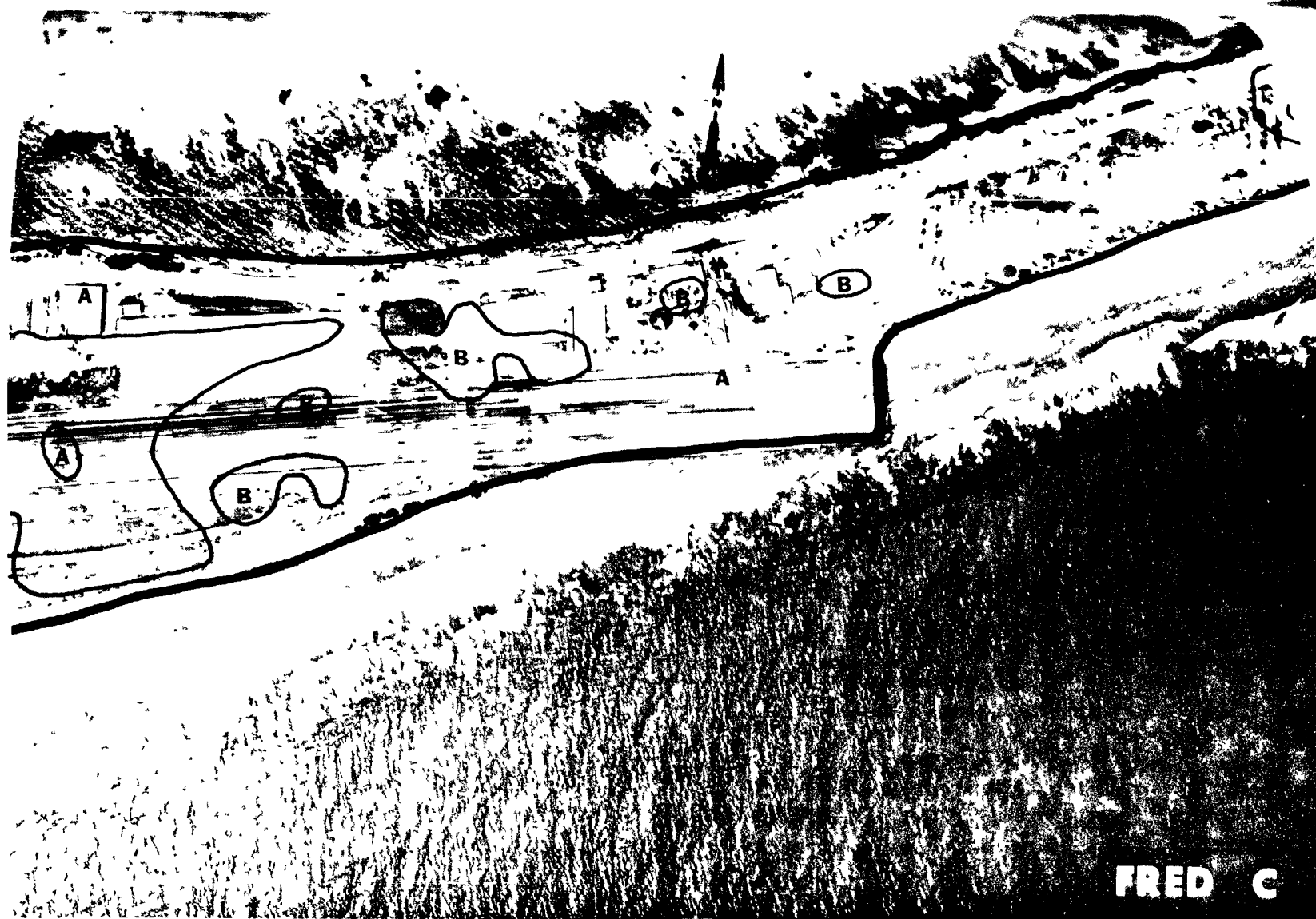


Fig. B.44.1.b. Gross count isoexposure contours. (Refer to alphabetic symbol key in this appendix.)



Fig. B.44.1.d. The gamma background exposure rate ( $\mu\text{R}/\text{hr}$ ) at 1 m above the ground, measured with a portable NaI scintillation counter.



Fig. B.44.1.f. Soil-sample locations.



Fig. B.44.1.i. The average  $^{239}\text{Pu}$  activities (pCi/g) in soil samples collected to a depth of 15 cm.



Fig. B.44.1.j. The average  $^{90}\text{Sr}$  activities (pCi/g) in soil samples collected to a depth of 15 cm.

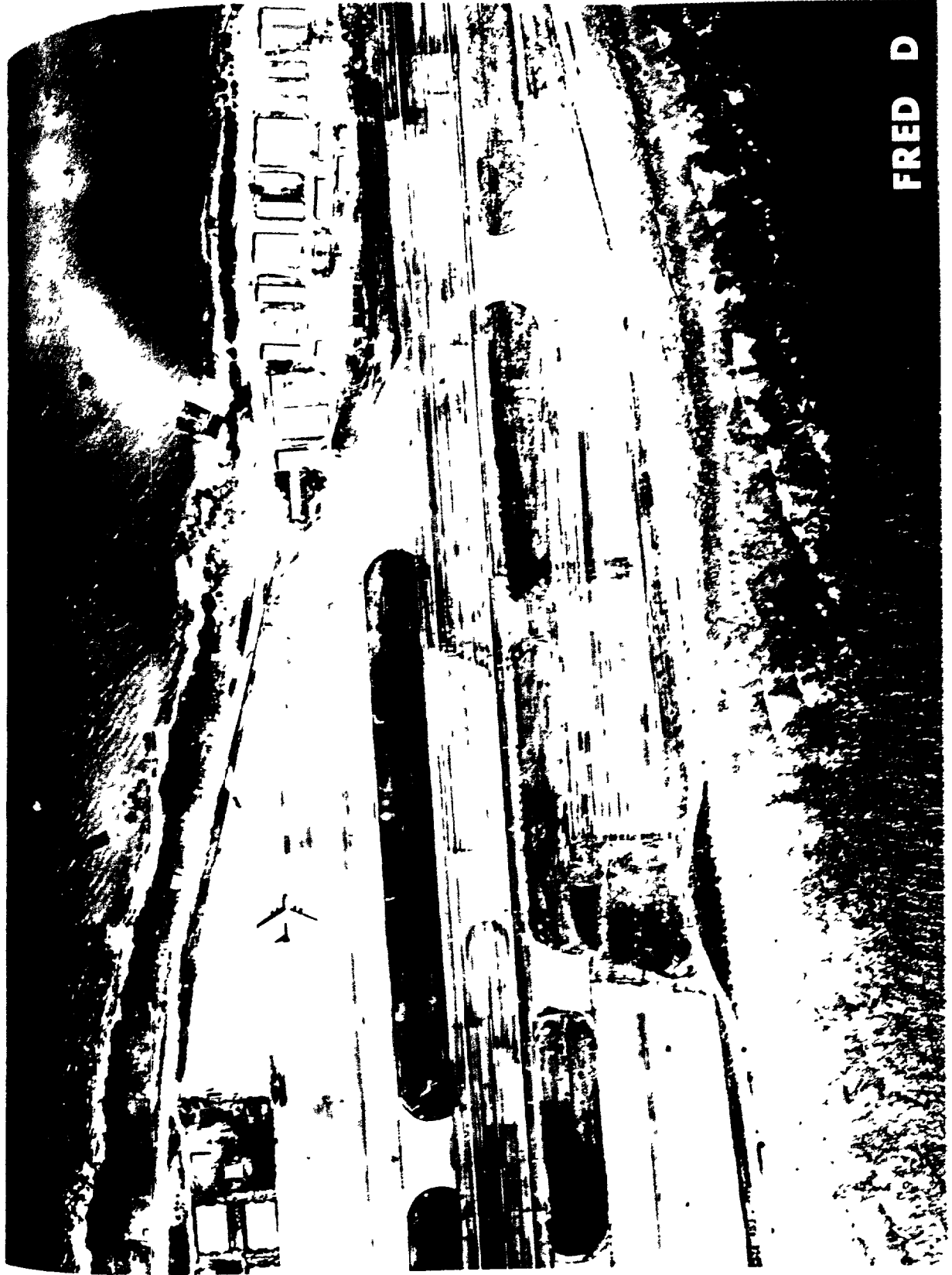


Fig. B.44.1.1. The average  $^{137}\text{Cs}$  activities ( $\text{pCi/g}$ ) in soil samples collected to a depth of 15 cm.



Fig. B.44.1.n. The average  $^{60}\text{Co}$  activities (pCi/g) in soil samples collected to a depth of 15 cm.





FRED D

Fig. B.45. I.a.



Fig. B.45.1.b. Gross count isoexposure contours. (Refer to alphabetic symbol key in this appendix.)



Fig. B.45.1.d. The gamma background exposure rate ( $\mu\text{R}/\text{hr}$ ) at 1 m above the ground, measured with a portable NaI scintillation counter.

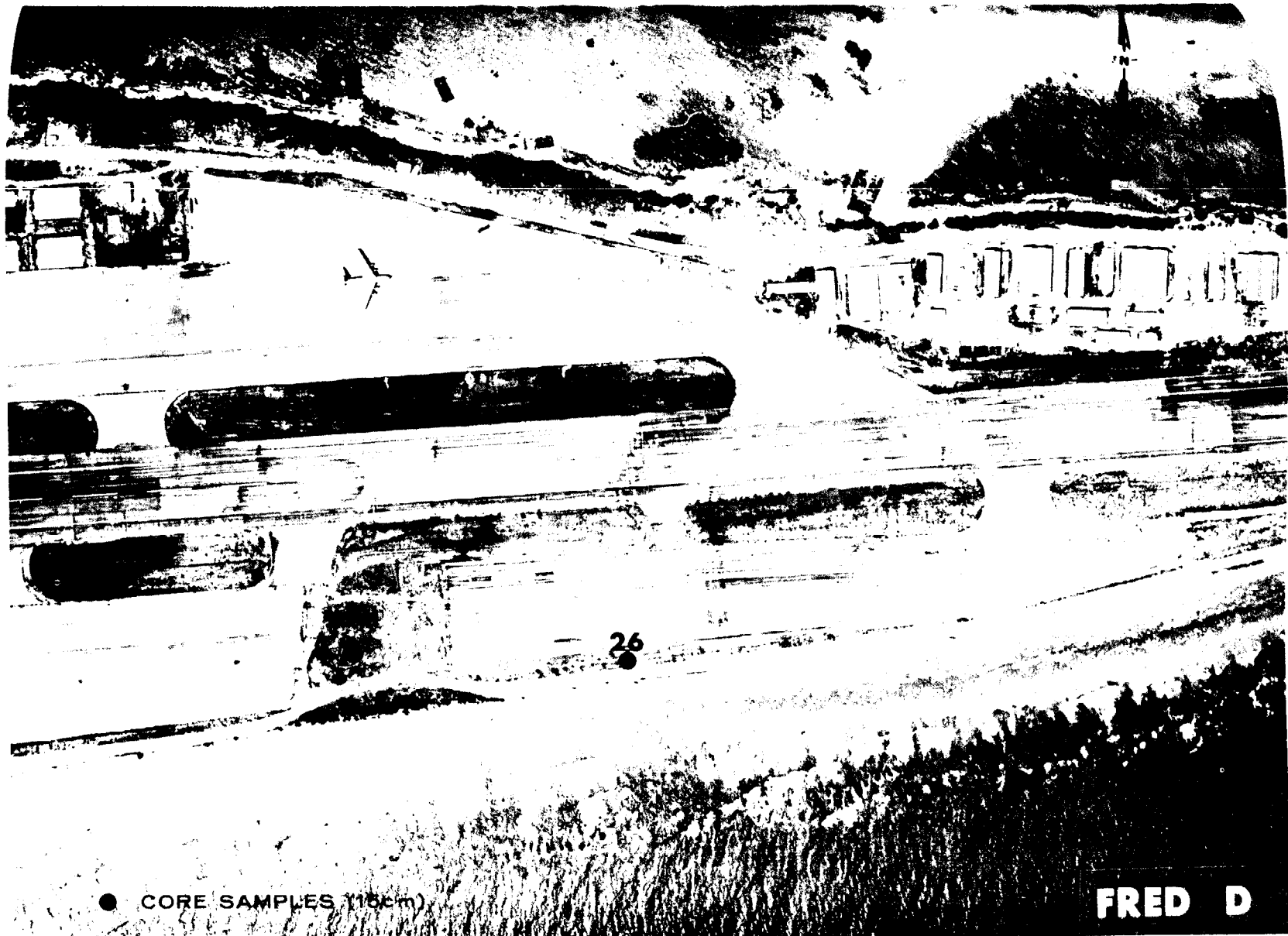


Fig. B.45.1.f. Soil-sample locations.

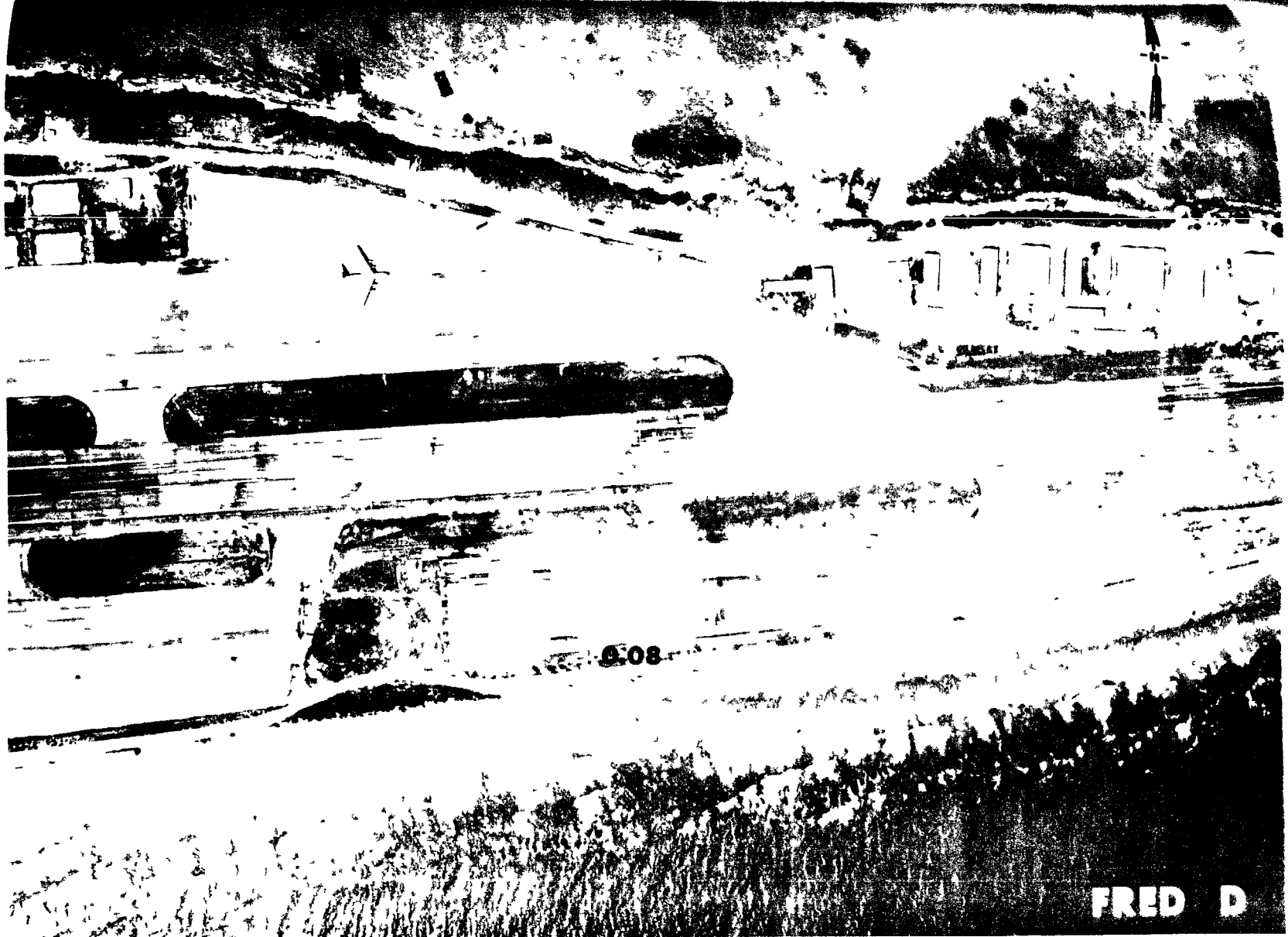
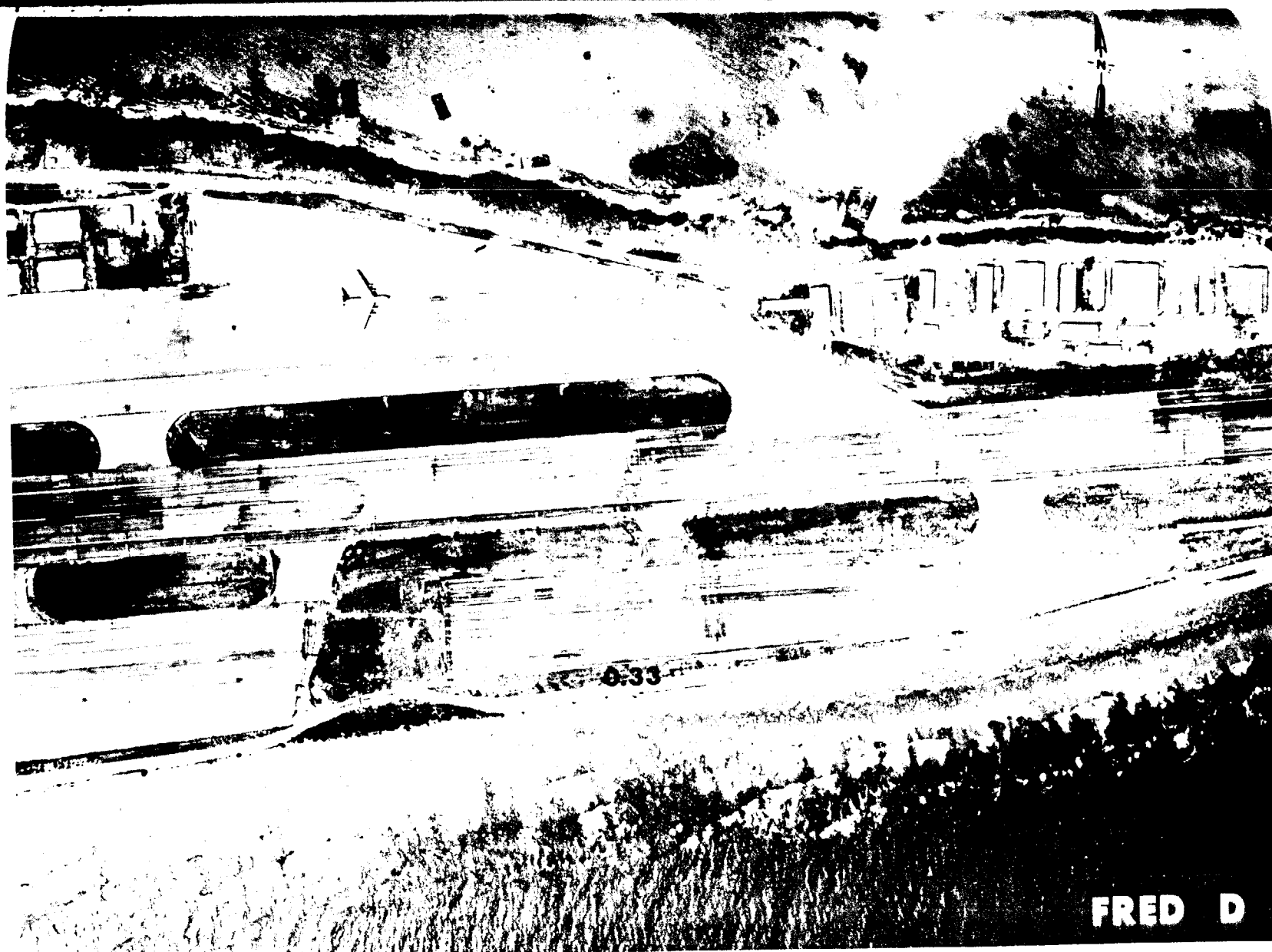


Fig. B.45.1.1. The average  $^{239}\text{Pu}$  activities (pCi/g) in soil samples collected to a depth of 15 cm.



FRED D

Fig. B.45.1.j. The average  $^{90}\text{Sr}$  activities (pCi/g) in soil samples collected to a depth of 15 cm.

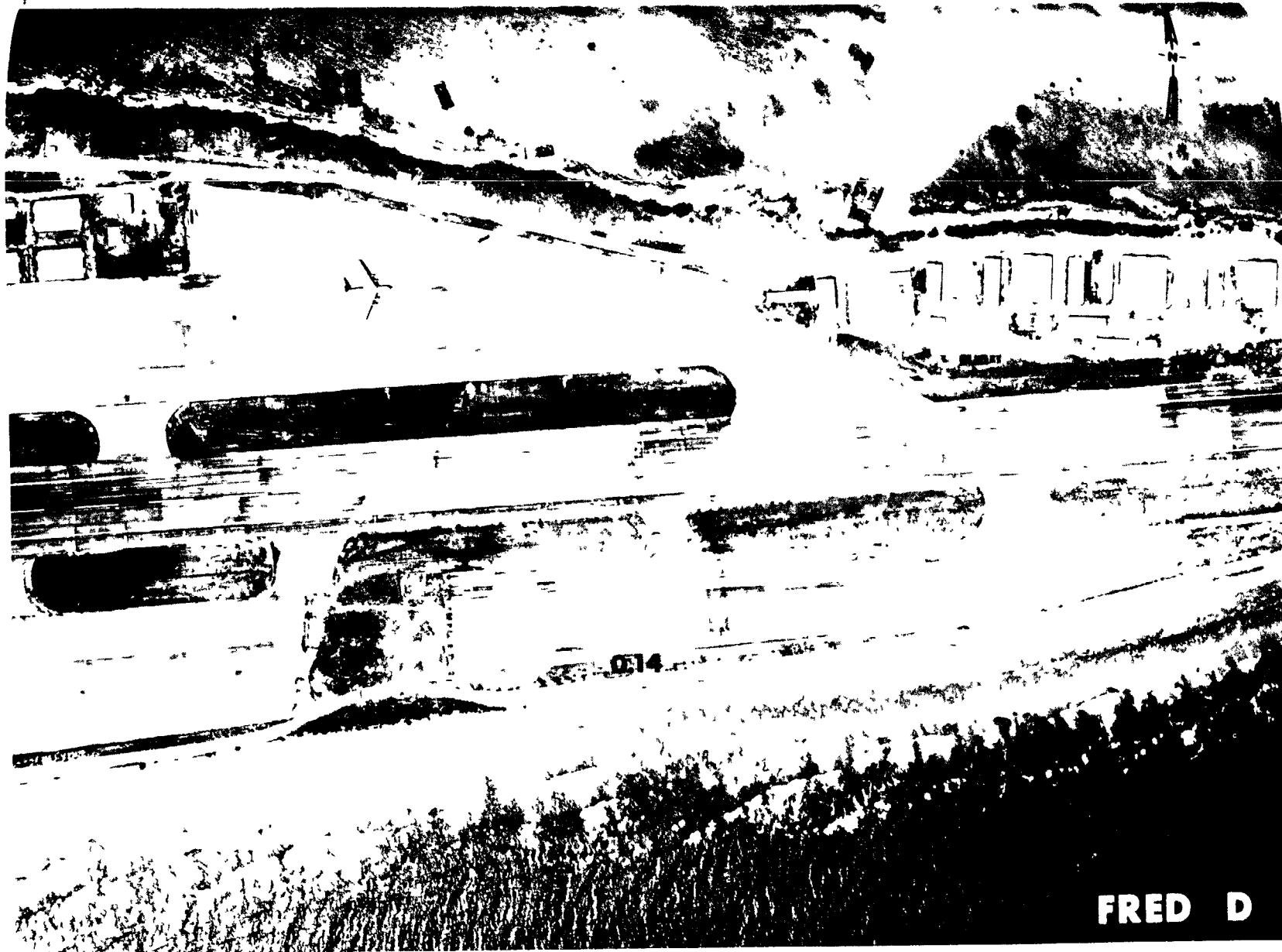


Fig. B.45.1.1. The average  $^{137}\text{Cs}$  activities (pCi/g) in soil samples collected to a depth of 15 cm.



Fig. B.45.1.n. The average  $^{60}\text{Co}$  activities (pCi/g) in soil samples collected to a depth of 15 cm.



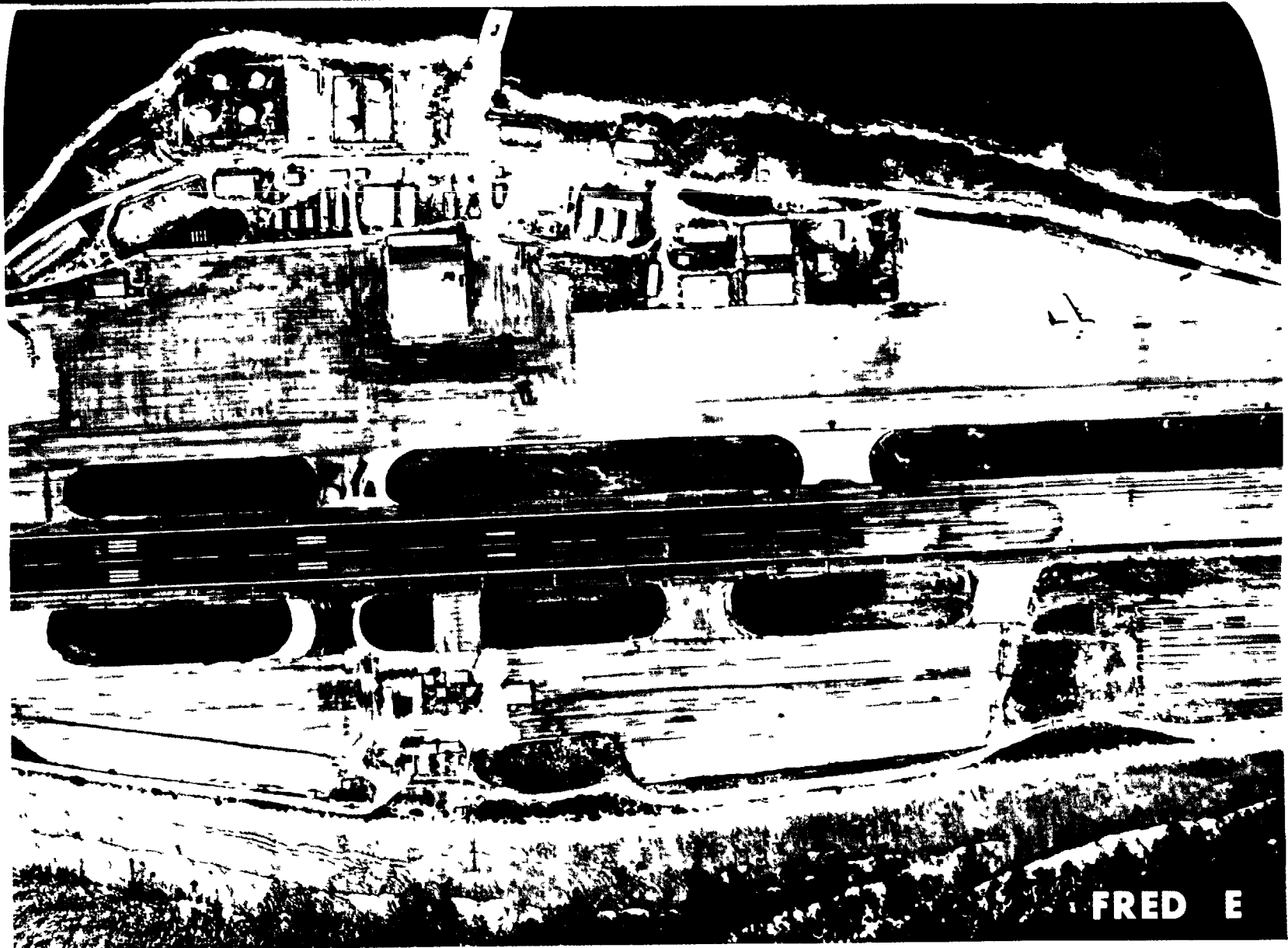


Fig. B.46.1.a.

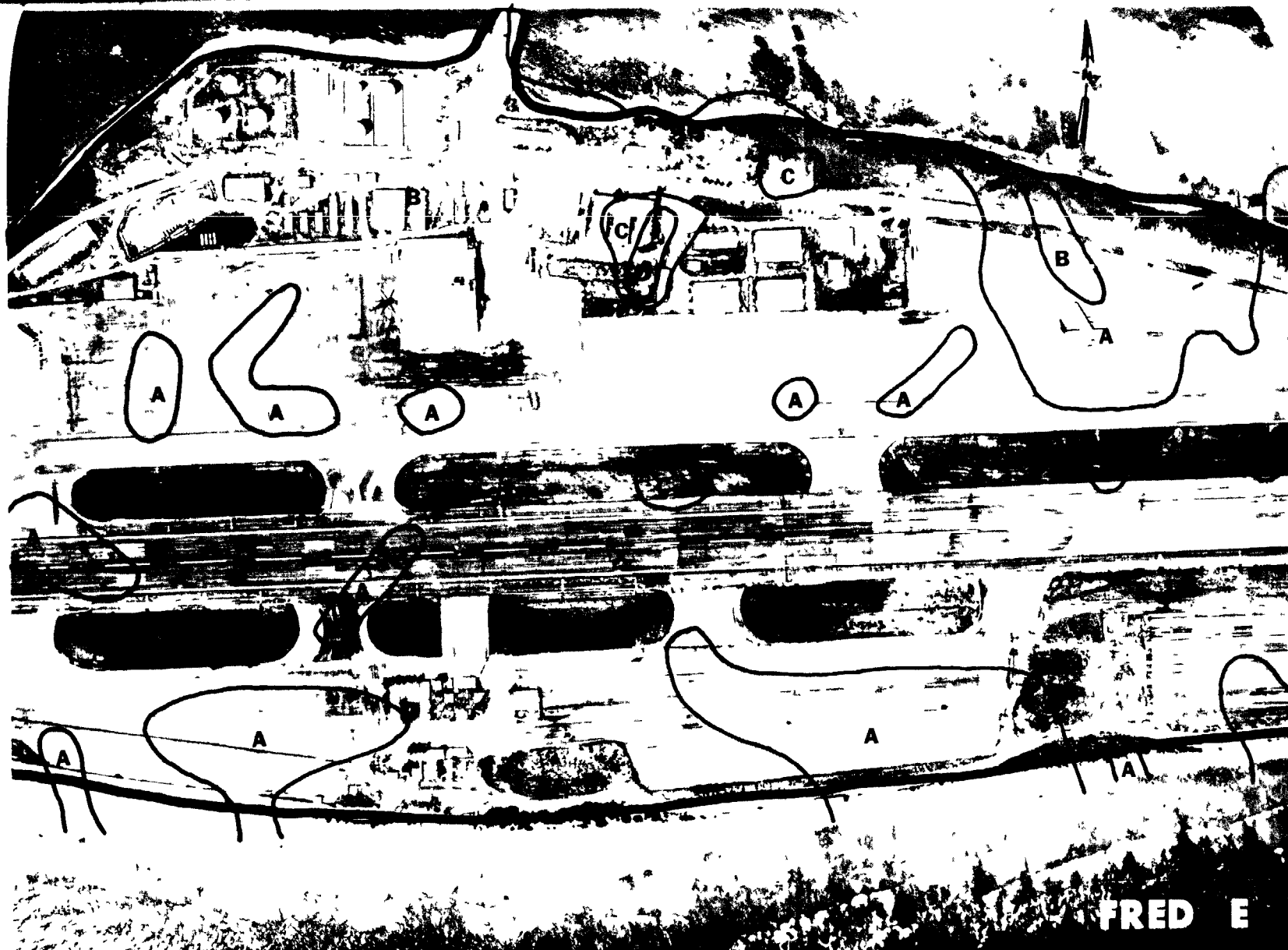


Fig. B.46.1.b. Gross count isoexposure contours. (Refer to alphabetic symbol key in this appendix.)

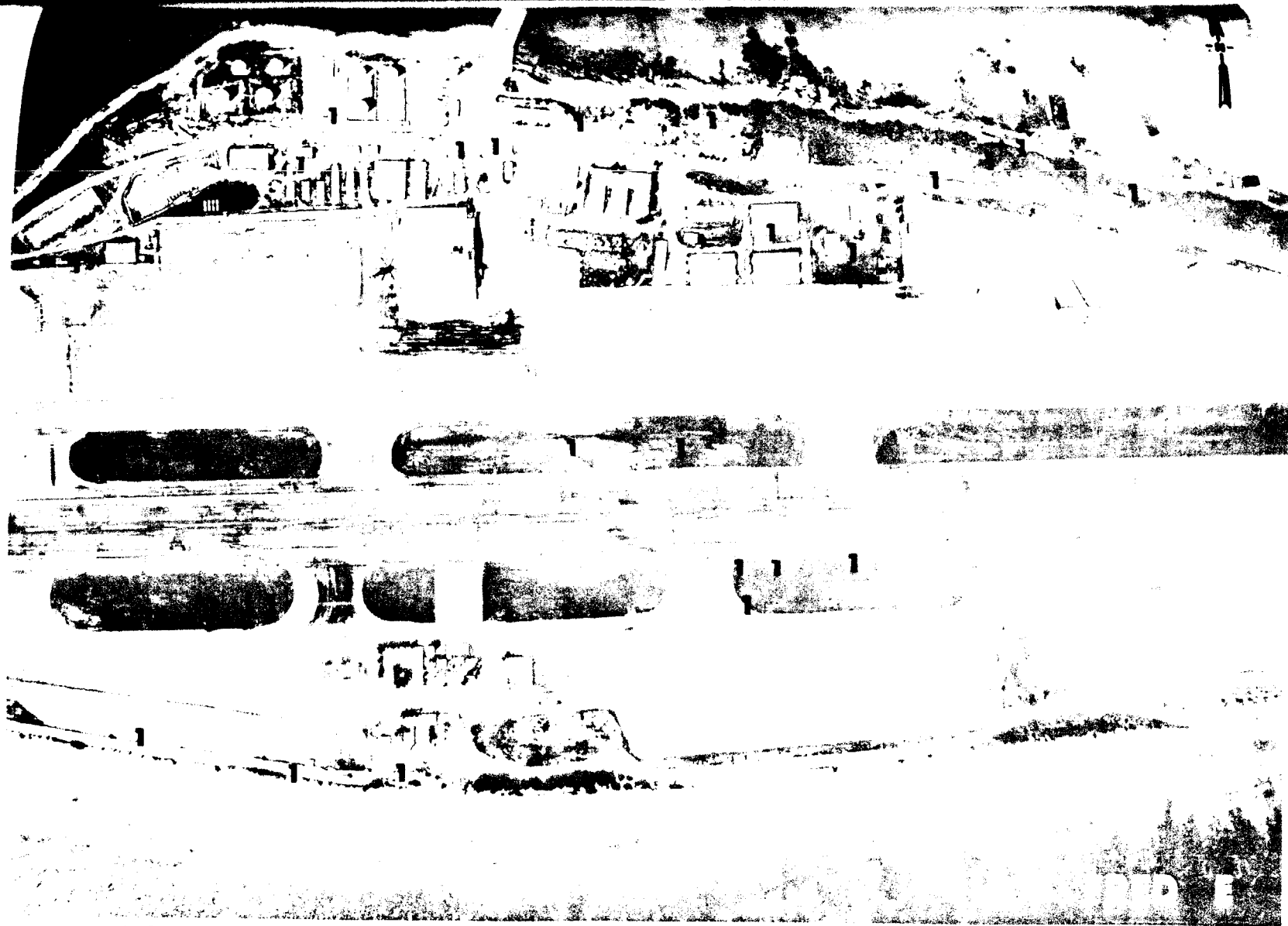


Fig. B.46.1.d. The gamma background exposure rate ( $\mu\text{R/hr}$ ) at 1 m above the ground, measured with a portable NaI scintillation counter.

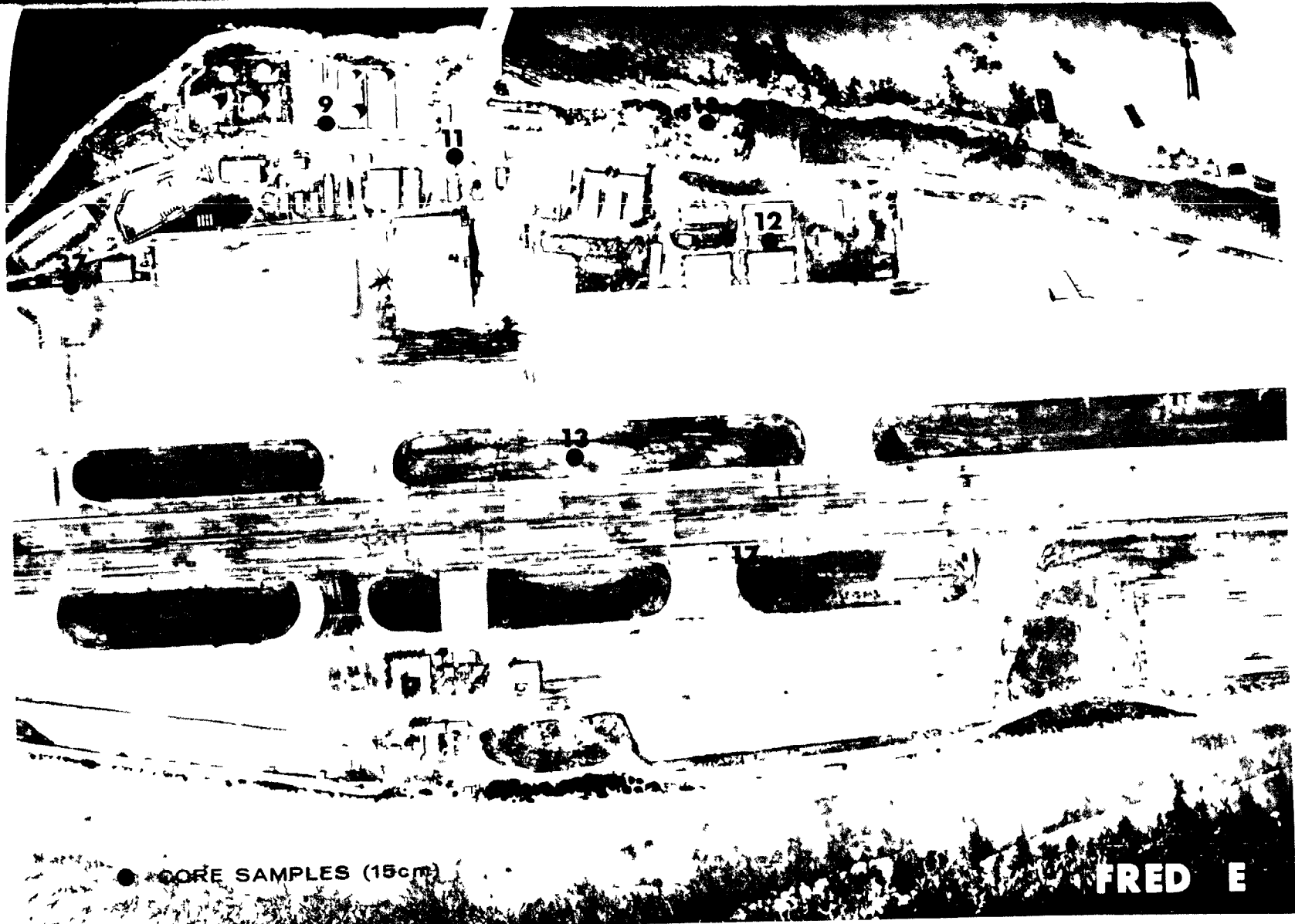
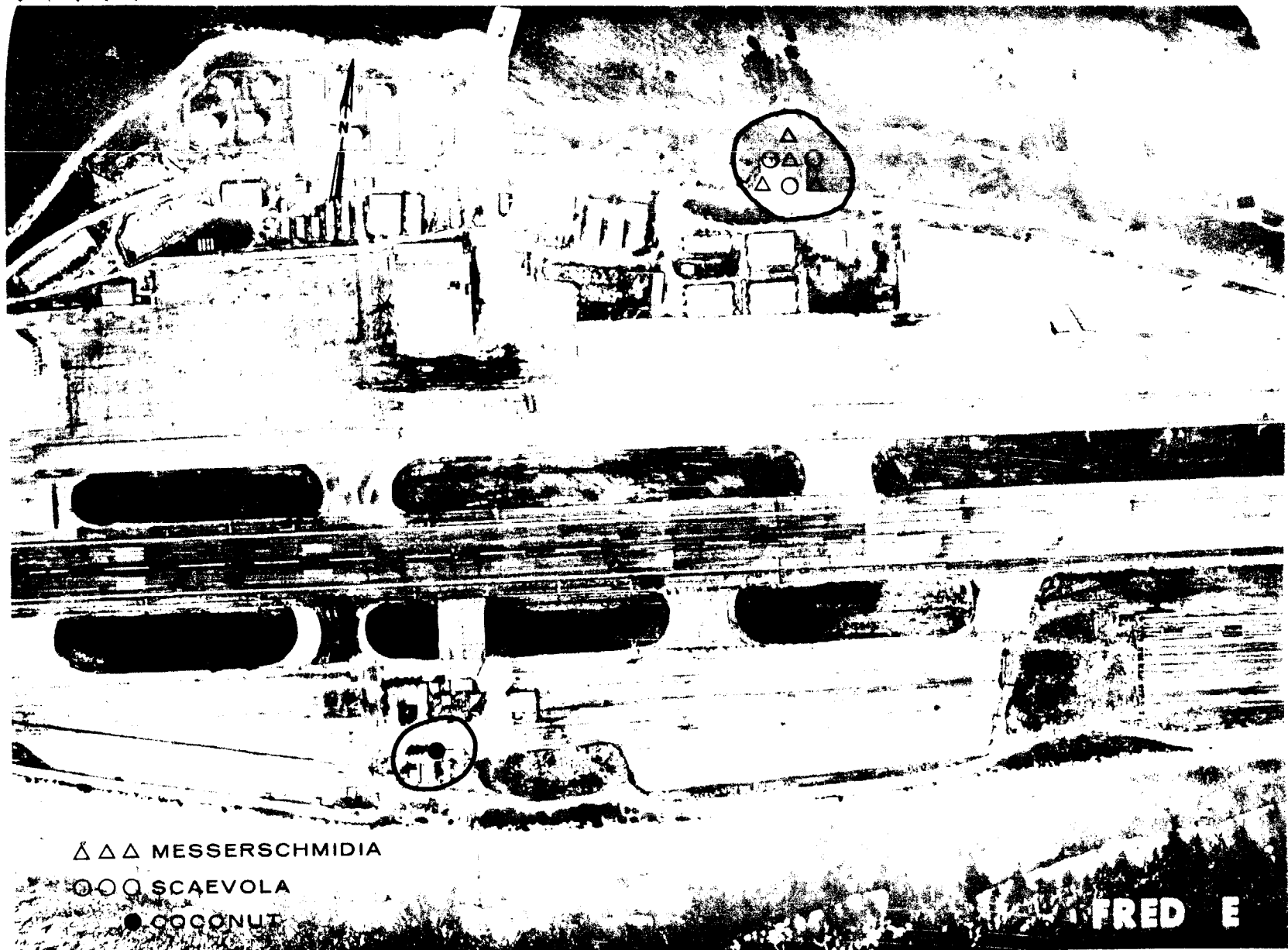


Fig. B.46. 1.f. Soil-sample locations.



△△△ MESSERSCHMIDIA

○○○ SCAEVOLA

● COCONUT

FRED E

Fig. B.46.1.g. Vegetation sample locations.

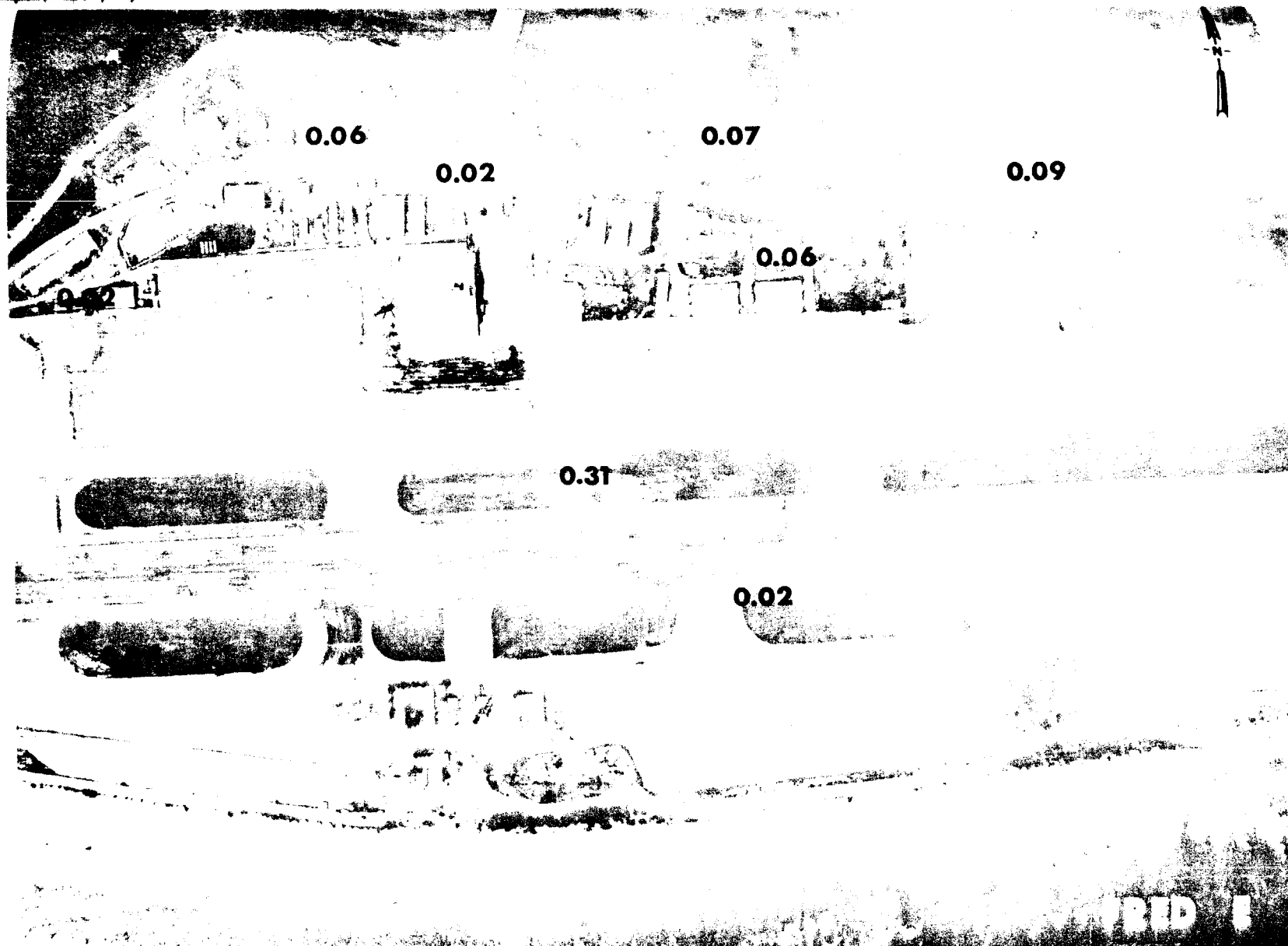


Fig. B.46.1.i. The average  $^{239}\text{Pu}$  activities (pCi/g) in soil samples collected to a depth of 15 cm.

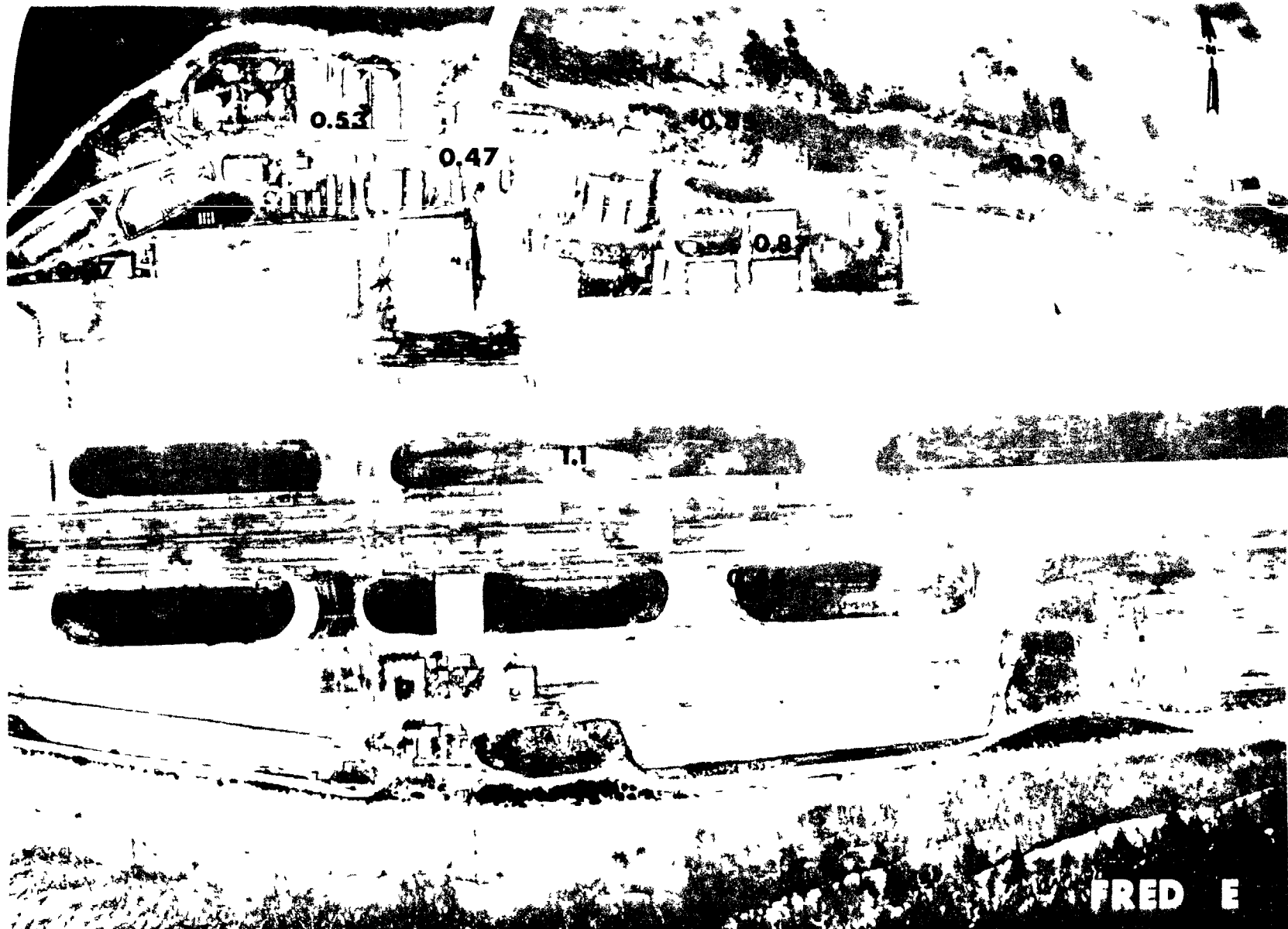


Fig. B.46.1.j. The average  $^{90}\text{Sr}$  activities (pCi/g) in soil samples collected to a depth of 15 cm.



Fig. B.46.1.1. The average <sup>137</sup>Cs activities (pCi/g) in soil samples collected to a depth of 15 cm.



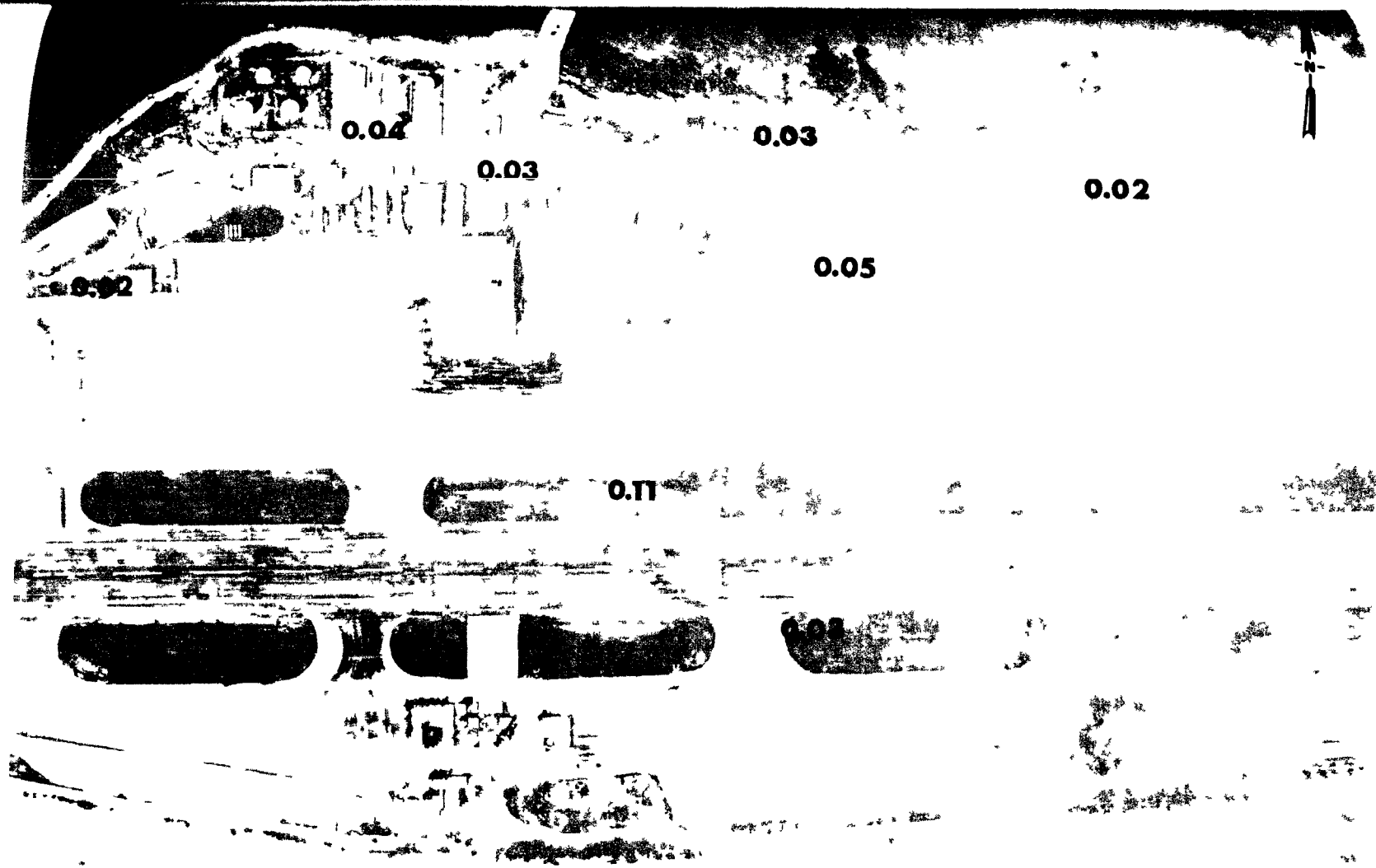


Fig. B.46.1.n. The average <sup>60</sup>Co activities (pCi/g) in soil samples collected to a depth of 15 cm.

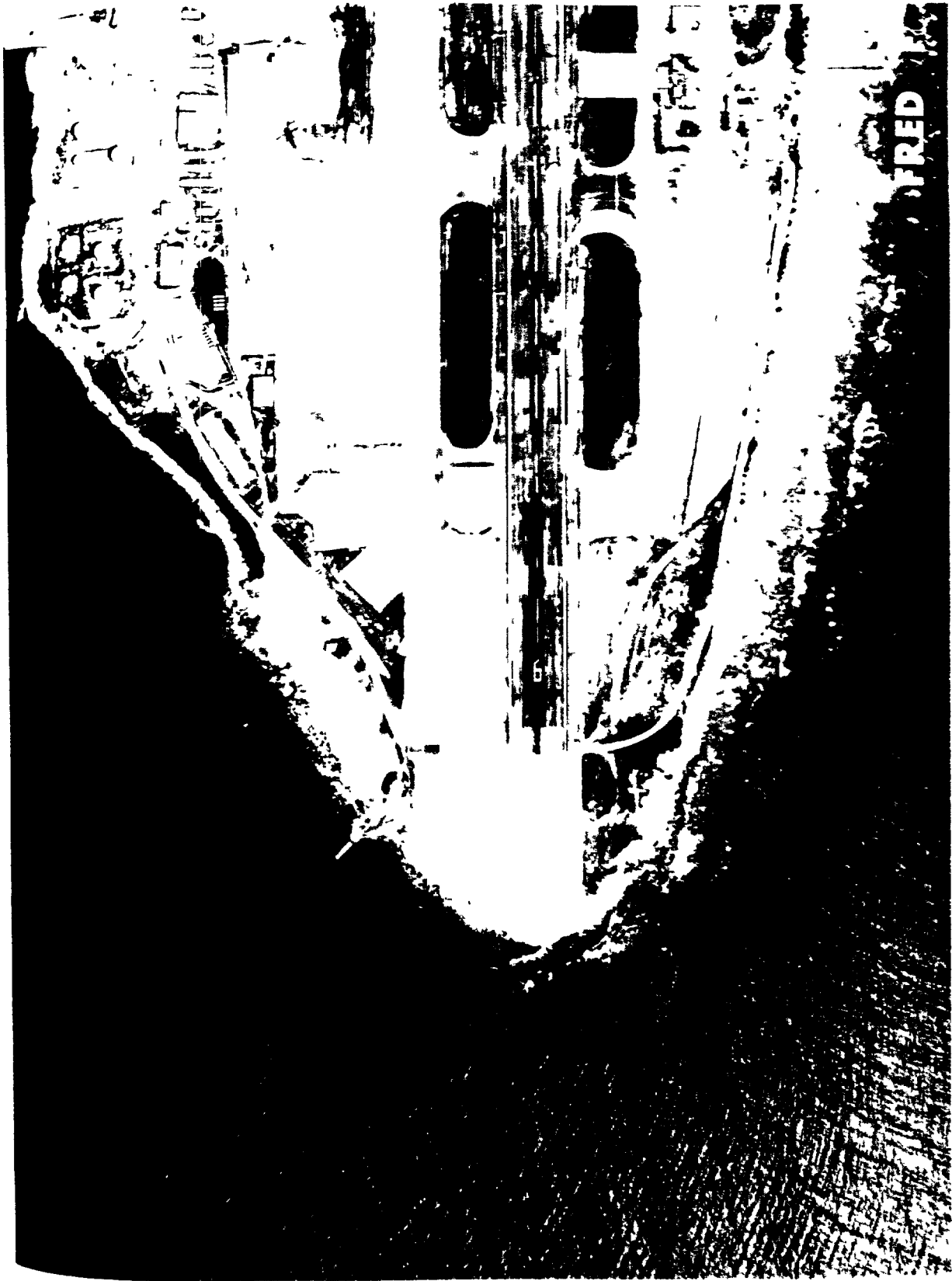


Fig. B.47.1.a.

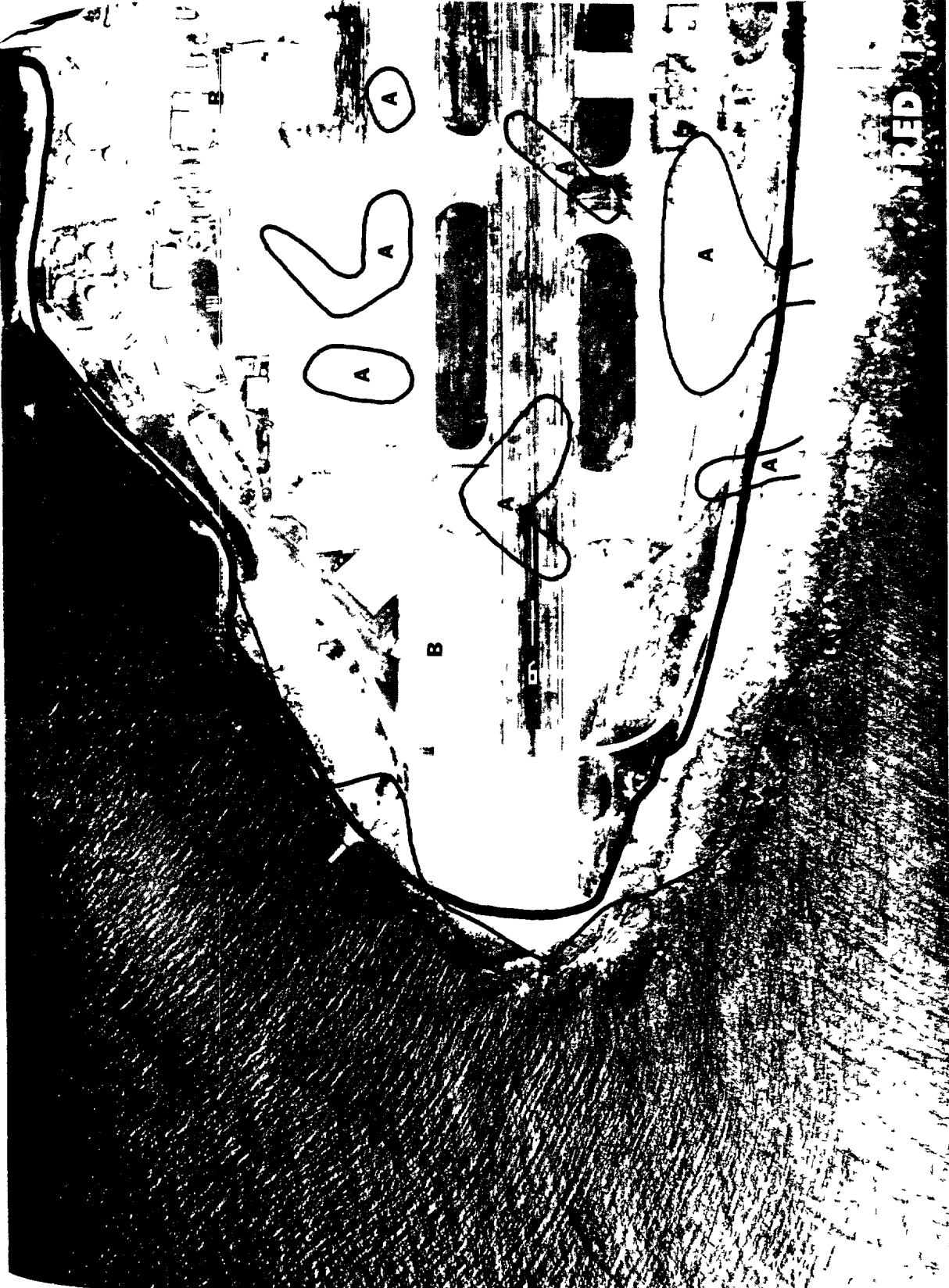


Fig. B.47.1.b. Gross count isoexposure contours. (Refer to alphabetic symbol key in this appendix.)



Fig. B.47.1.d. The gamma background exposure rate ( $\mu\text{R/hr}$ ) at 1 m above the ground, measured with a portable NaI scintillation counter.

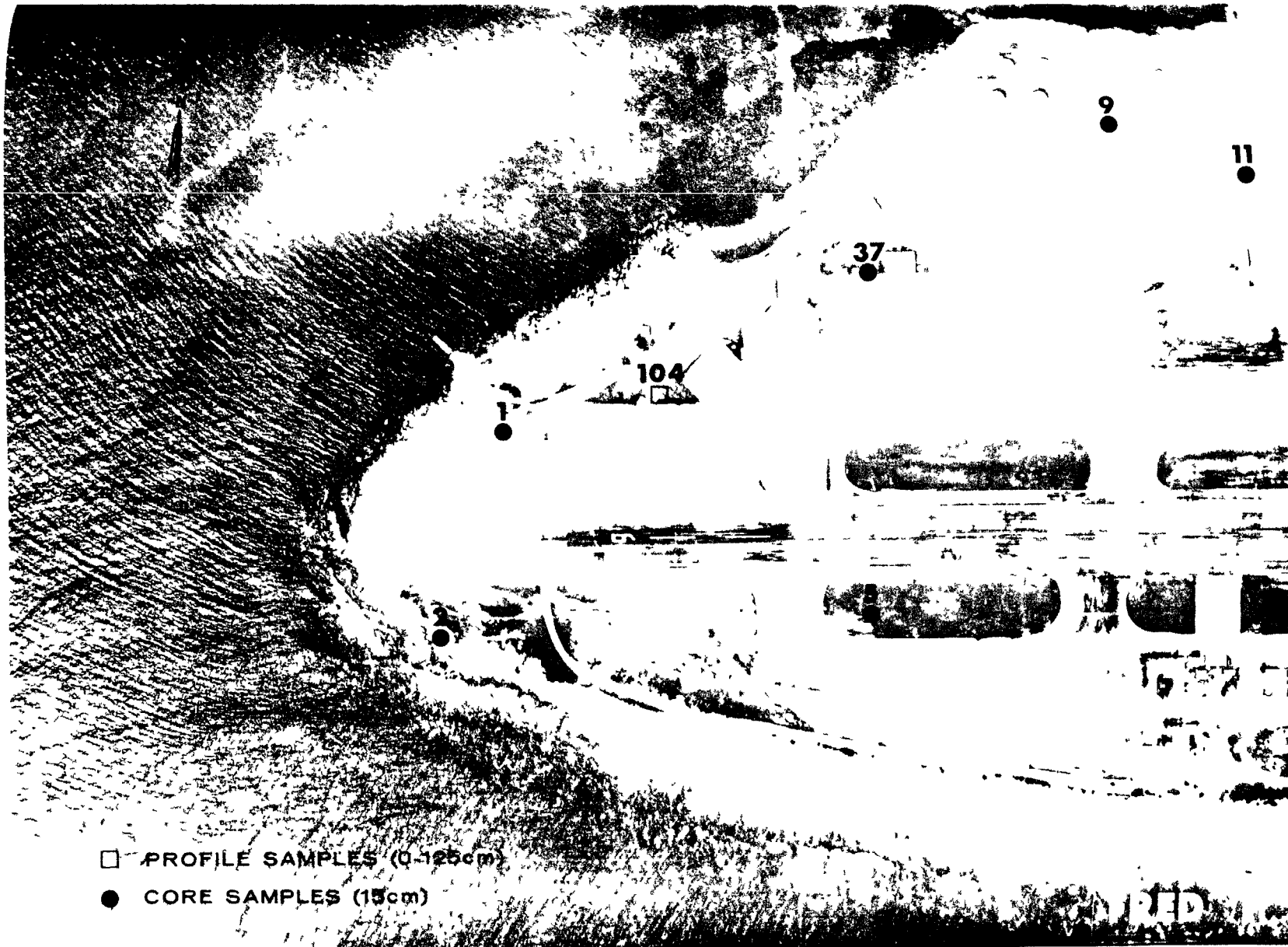


Fig. B.47.1.f. Soil-sample locations.

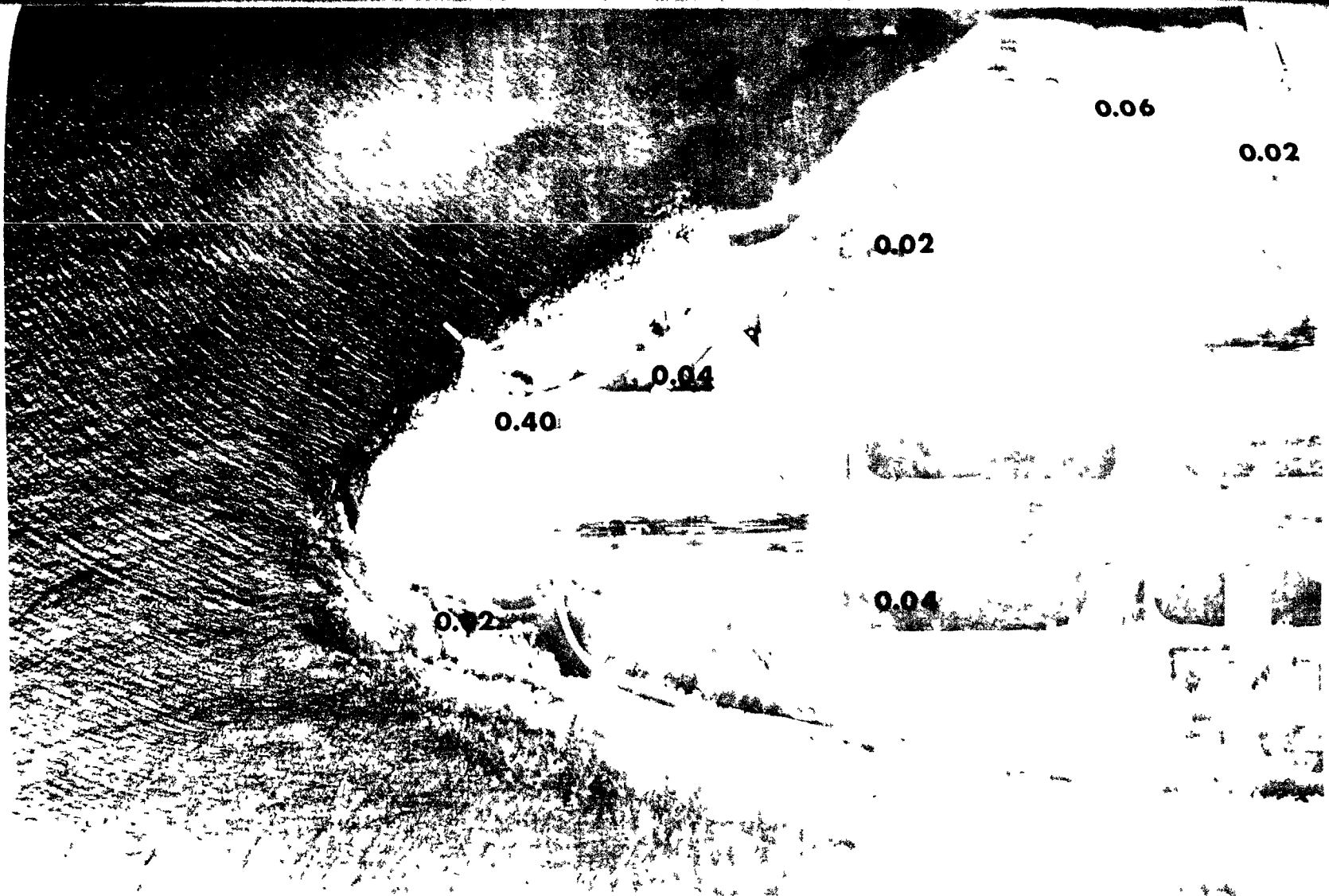


Fig. B.47.1.i. The average  $^{239}\text{Pu}$  activities (pCi/g) in soil samples collected to a depth of 15 cm.

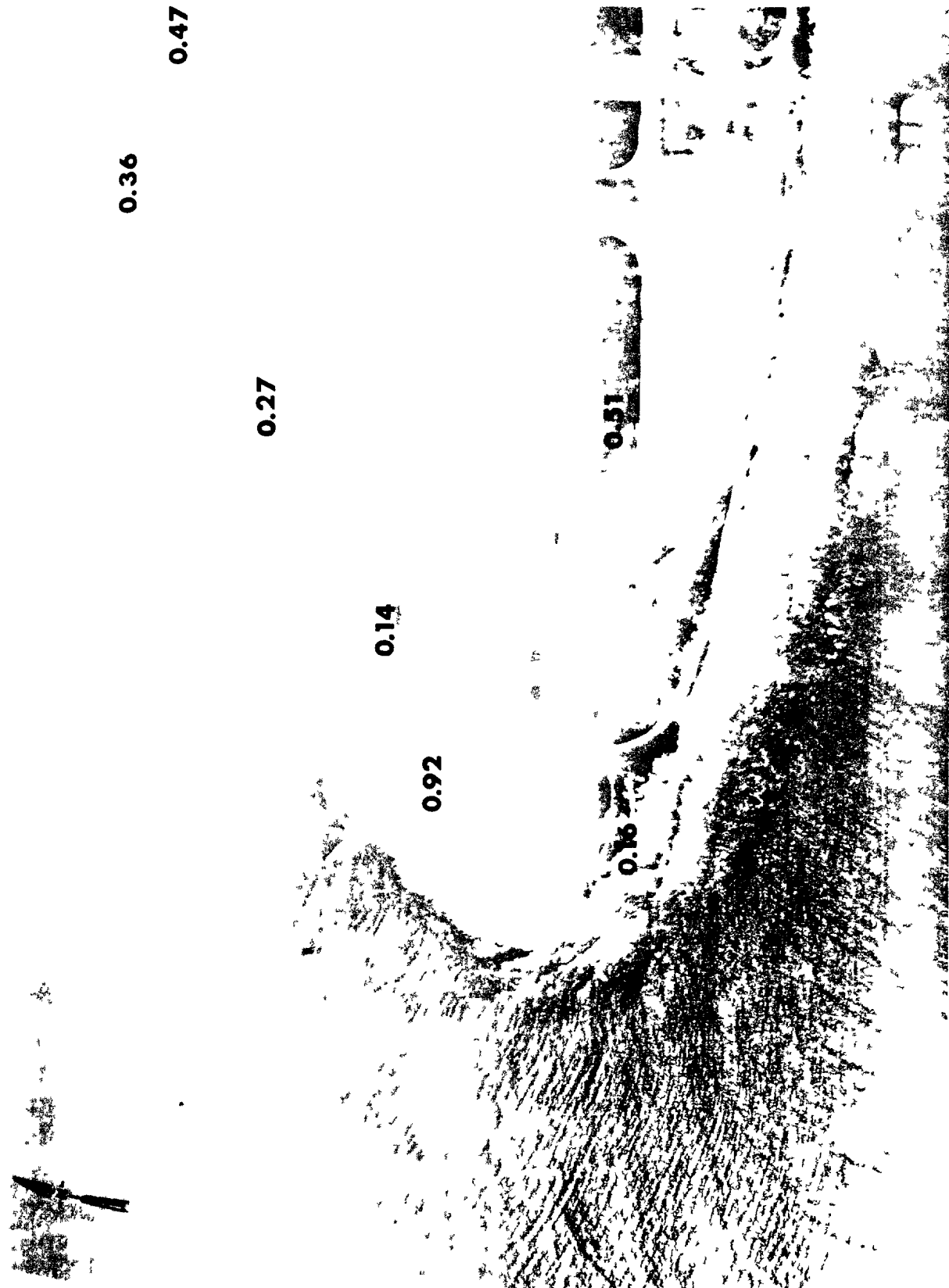


Fig. B.47.1.J. The average  $^{90}\text{Sr}$  activities (pCi/g) in soil samples collected to a depth of 15 cm.

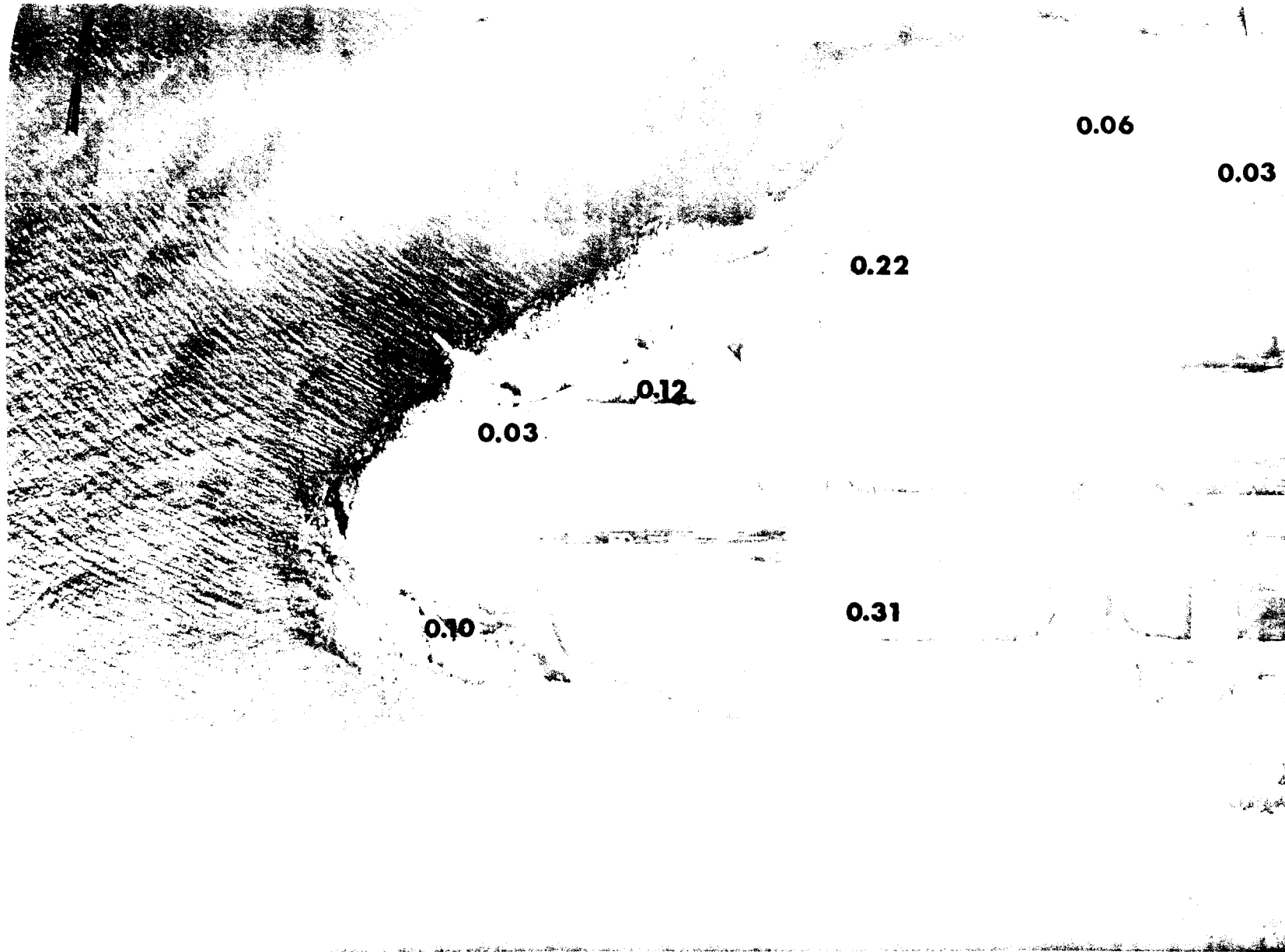


Fig. B.47.1.1. The average  $^{137}\text{Cs}$  activities (pCi/g) in soil samples collected to a depth of 15 cm.,



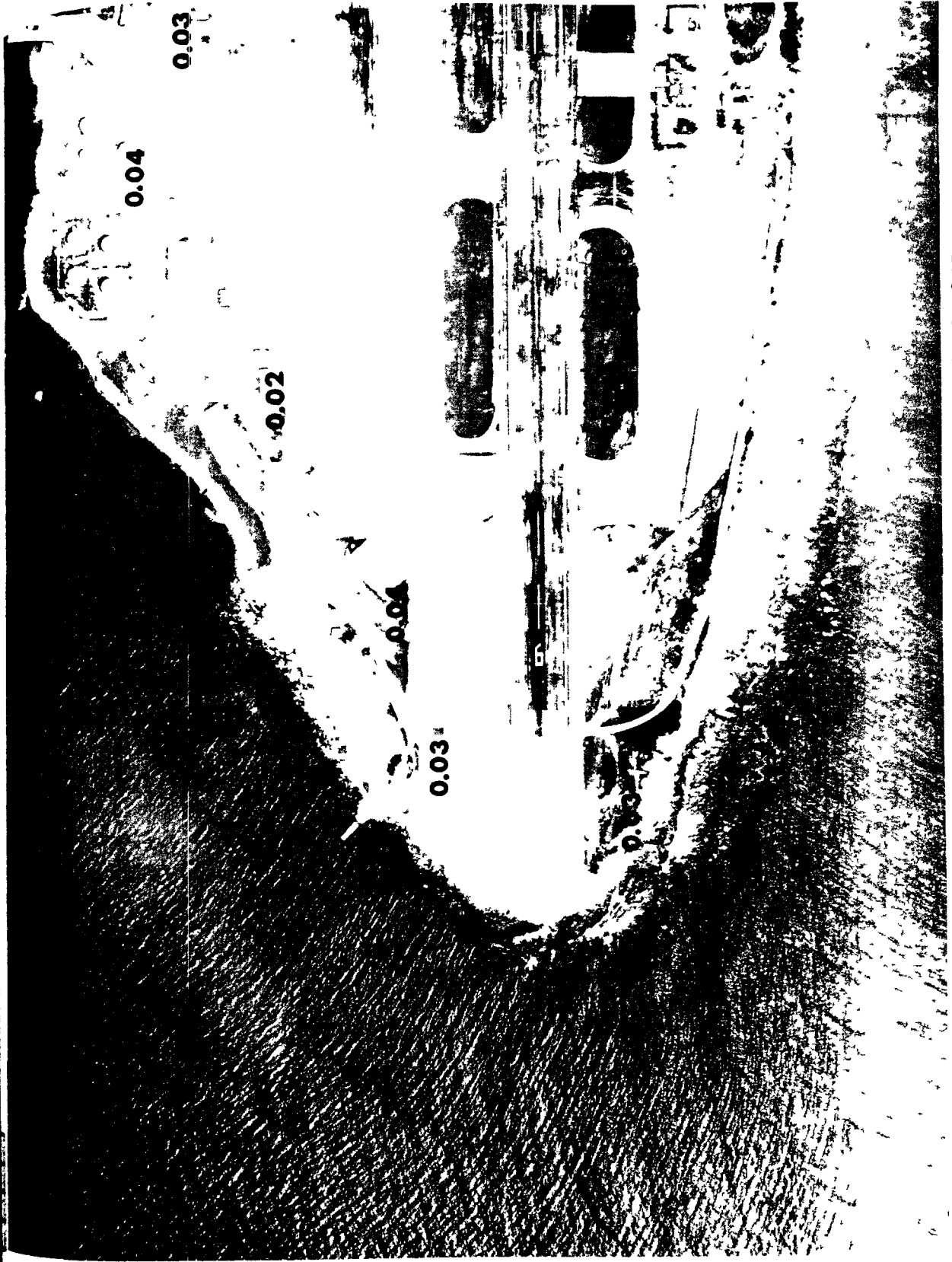


Fig. B.47.1.n. The average  $^{60}\text{Co}$  activities (pCi/g) in soil samples collected to a depth of 15 cm.

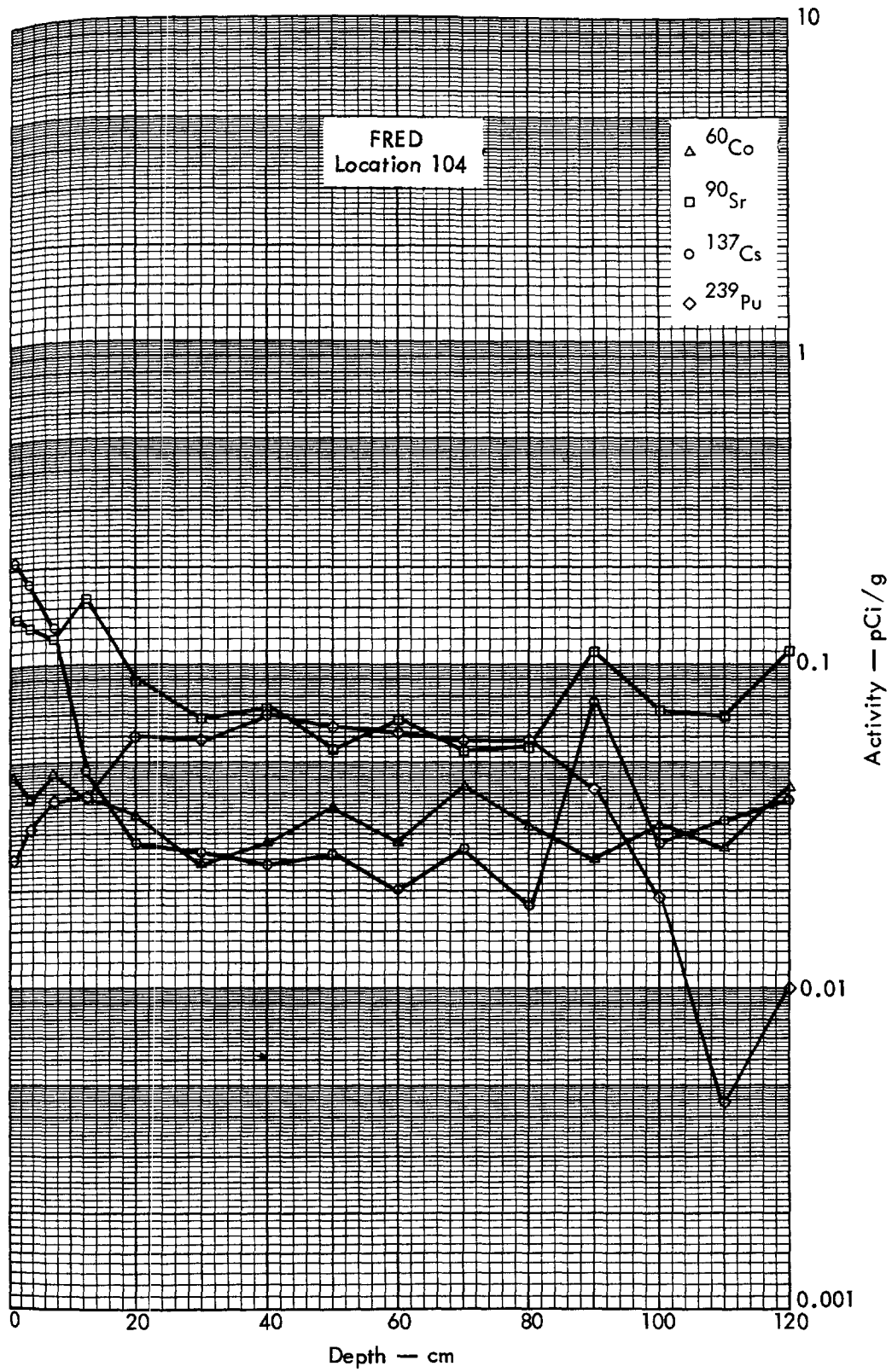


Fig. B. 47. 2a. Activities of selected radionuclides as a function of soil depth.



**GLENN**

Fig. B.48.1.a.

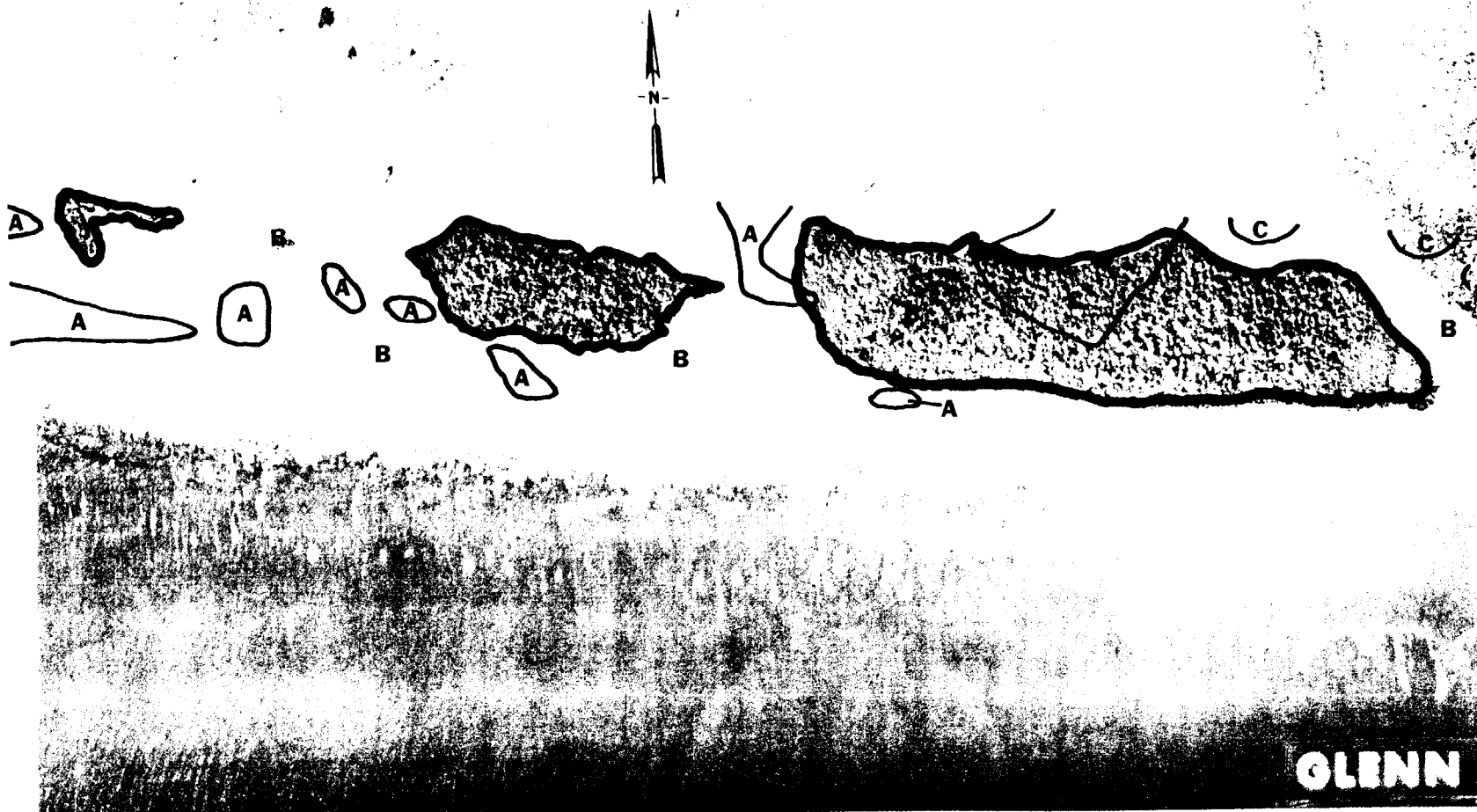


Fig. B.48.1.b. Gross count isosexposure contours. (Refer to alphabetic symbol key in this appendix.)

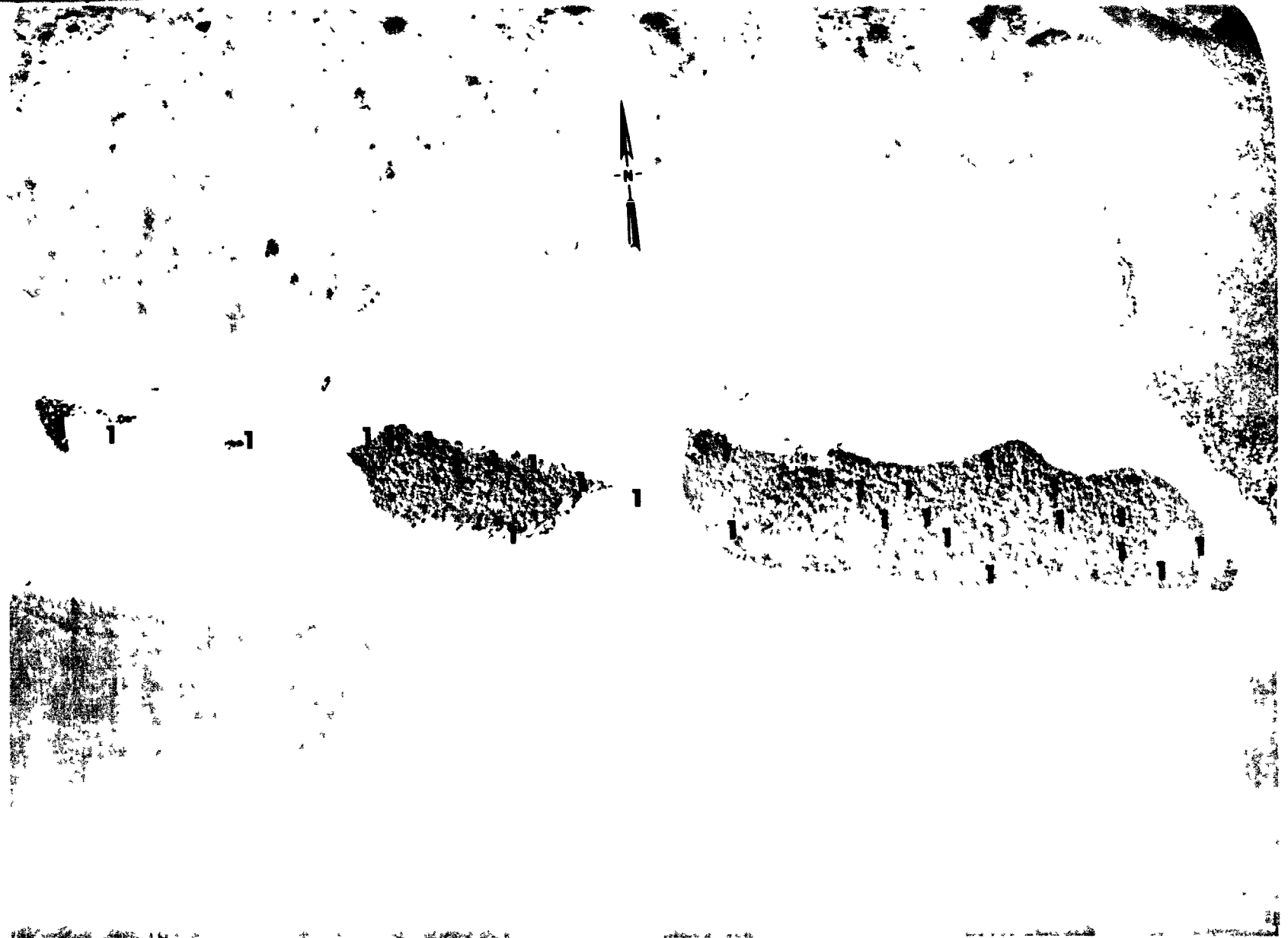


Fig. B.48.1.d The gamma background exposure rate ( $\mu\text{R/hr}$ ) at 1 m above the ground, measured with a portable NaI scintillation counter.

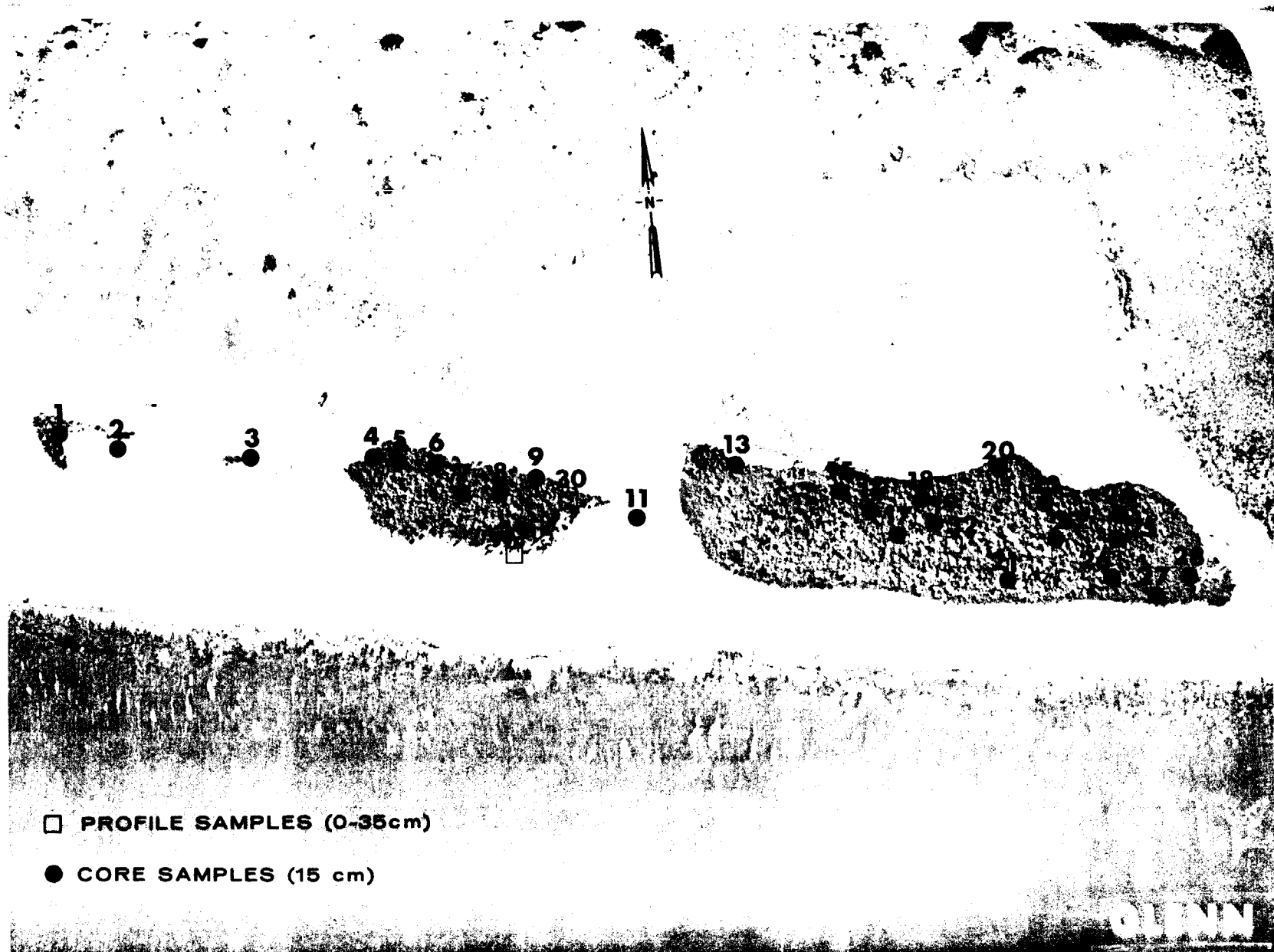


Fig. B.48.1.f. Soil-sample locations.

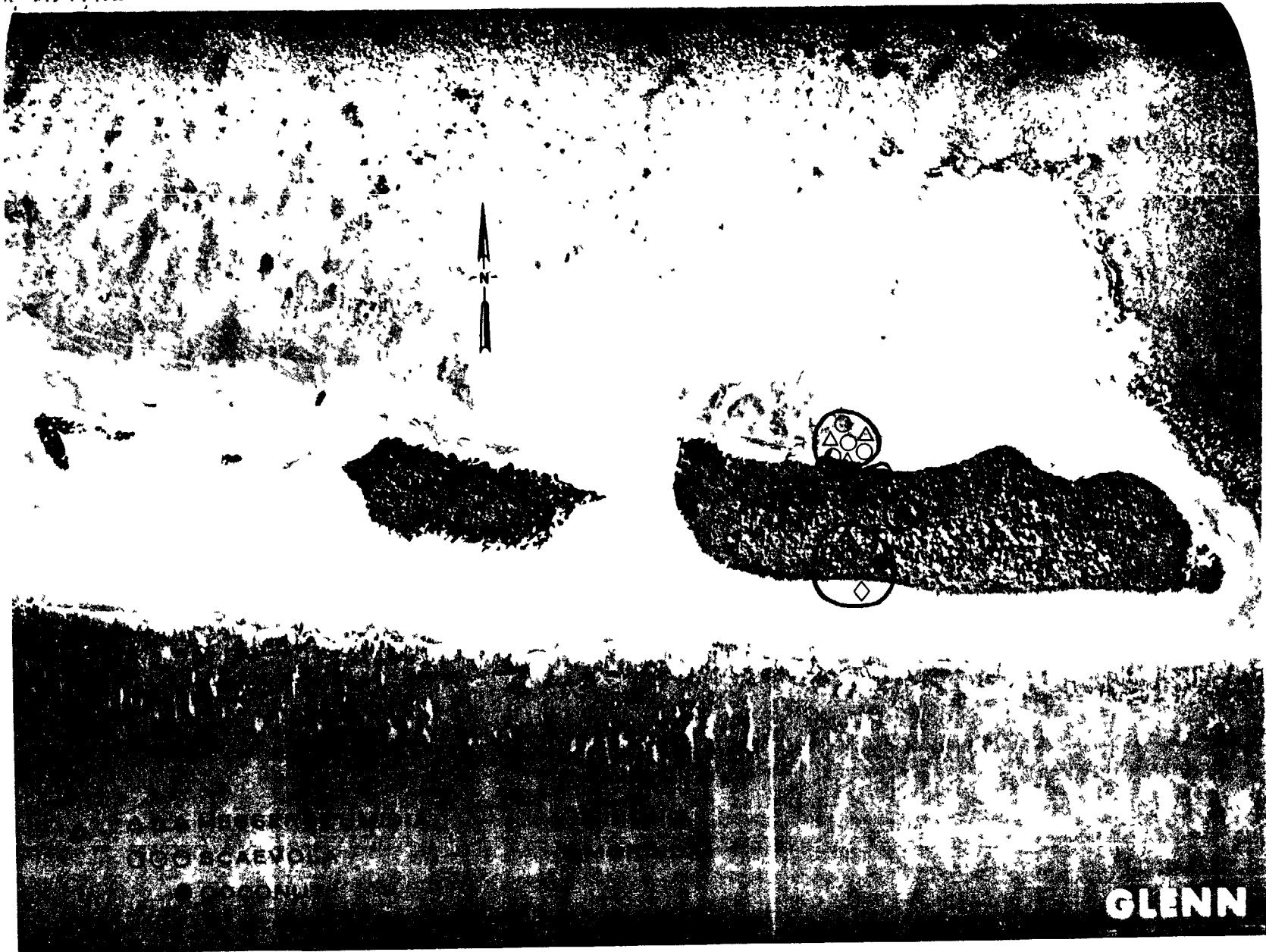


Fig. B.48.1.g. Vegetation sample locations.



Fig. B.48.1.i. The average  $^{239}\text{Pu}$  activities (pCi/g) in soil samples collected to a depth of 15 cm.

**GLENN**



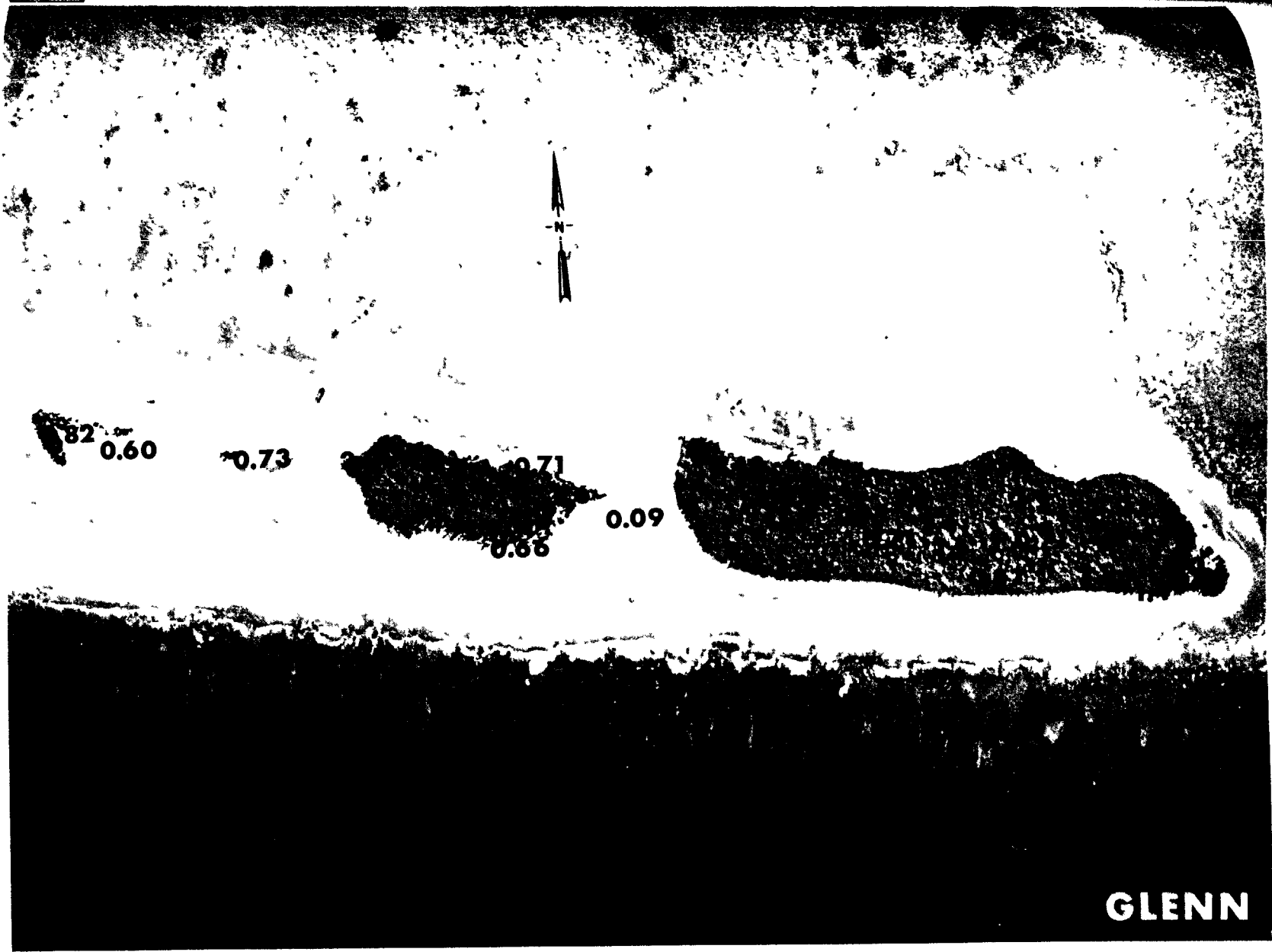


Fig. B.48.1.j. The average  $^{90}\text{Sr}$  activities (pCi/g) in soil samples collected to a depth of 15 cm.

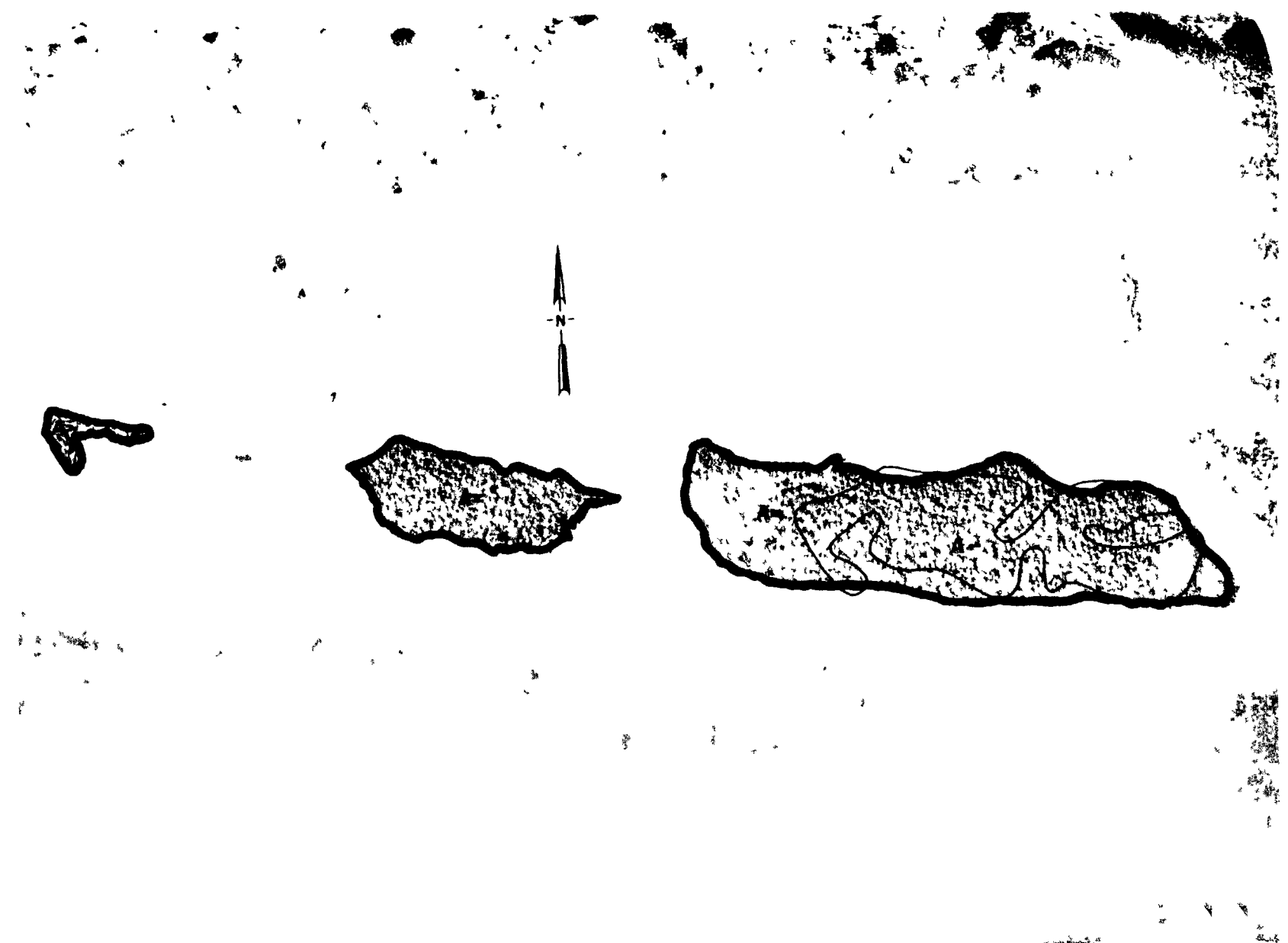


Fig. B.18.1.k. <sup>137</sup>Cs isoexposure and isoconcentration contours. (Refer to alphabetic symbol key in this appendix.)



Fig. B.48.1.1. The average  $^{137}\text{Cs}$  activities (pCi/g) in soil samples collected to a depth of 15 cm.



Fig. B.48.1.m. <sup>60</sup>Co isoexposure and isoconcentration contours. (Refer to alphabetic symbol key in this appendix.)

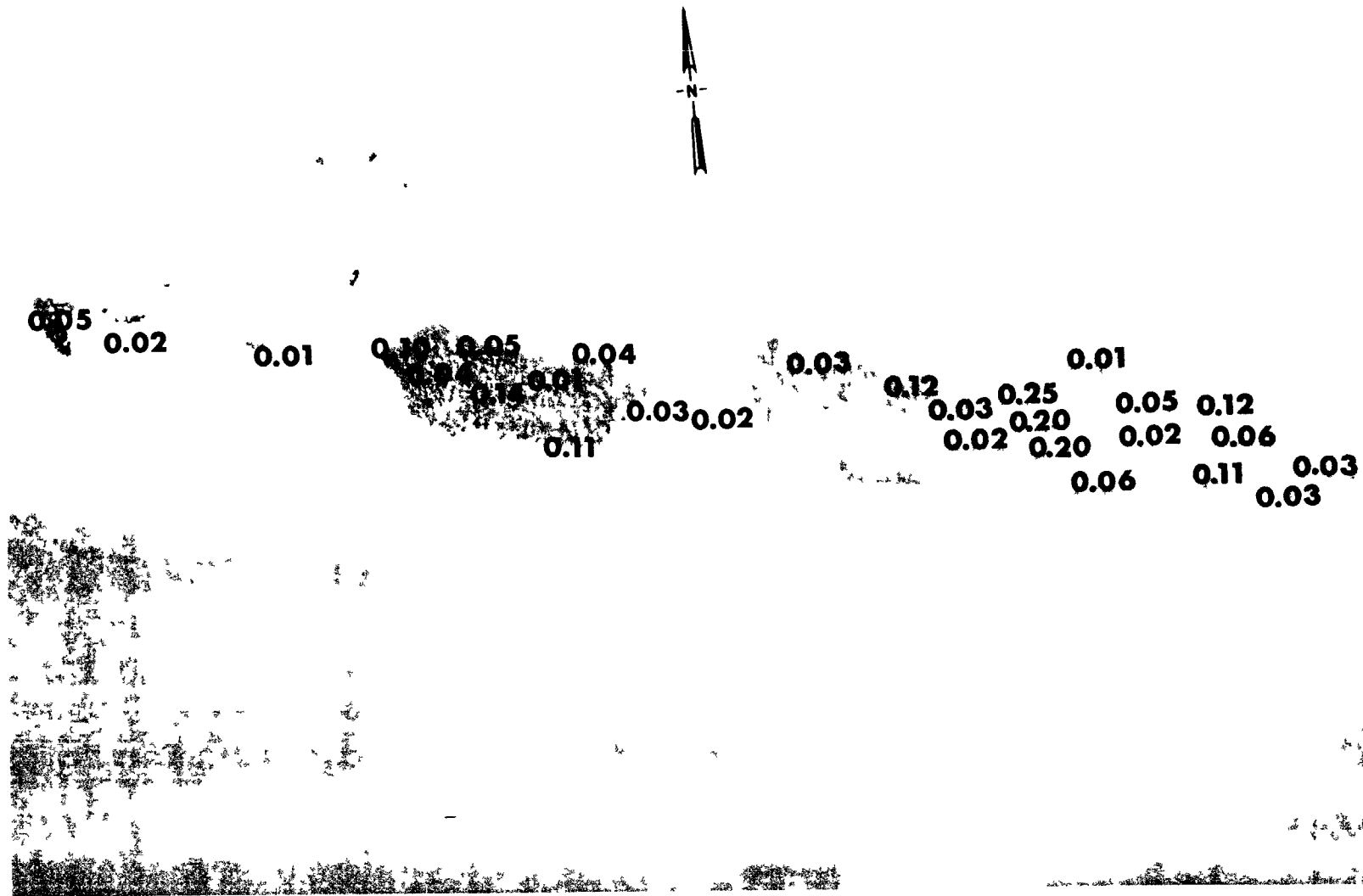


Fig. B.48.1.n. The average  $^{60}\text{Co}$  activities (pCi/g) in soil samples collected to a depth of 15 cm.

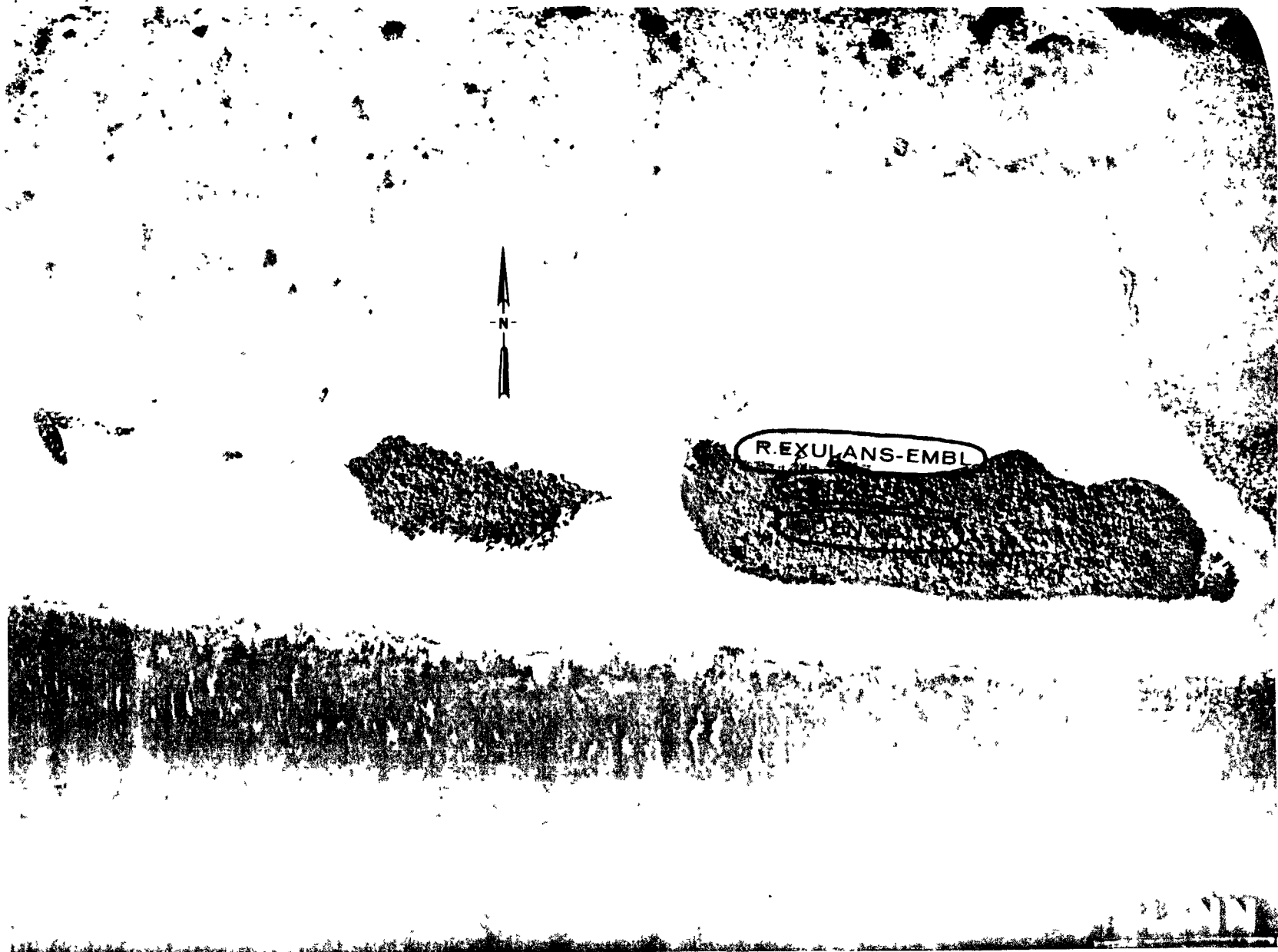


Fig. B.48.1.o. Terrestrial animal sample locations.

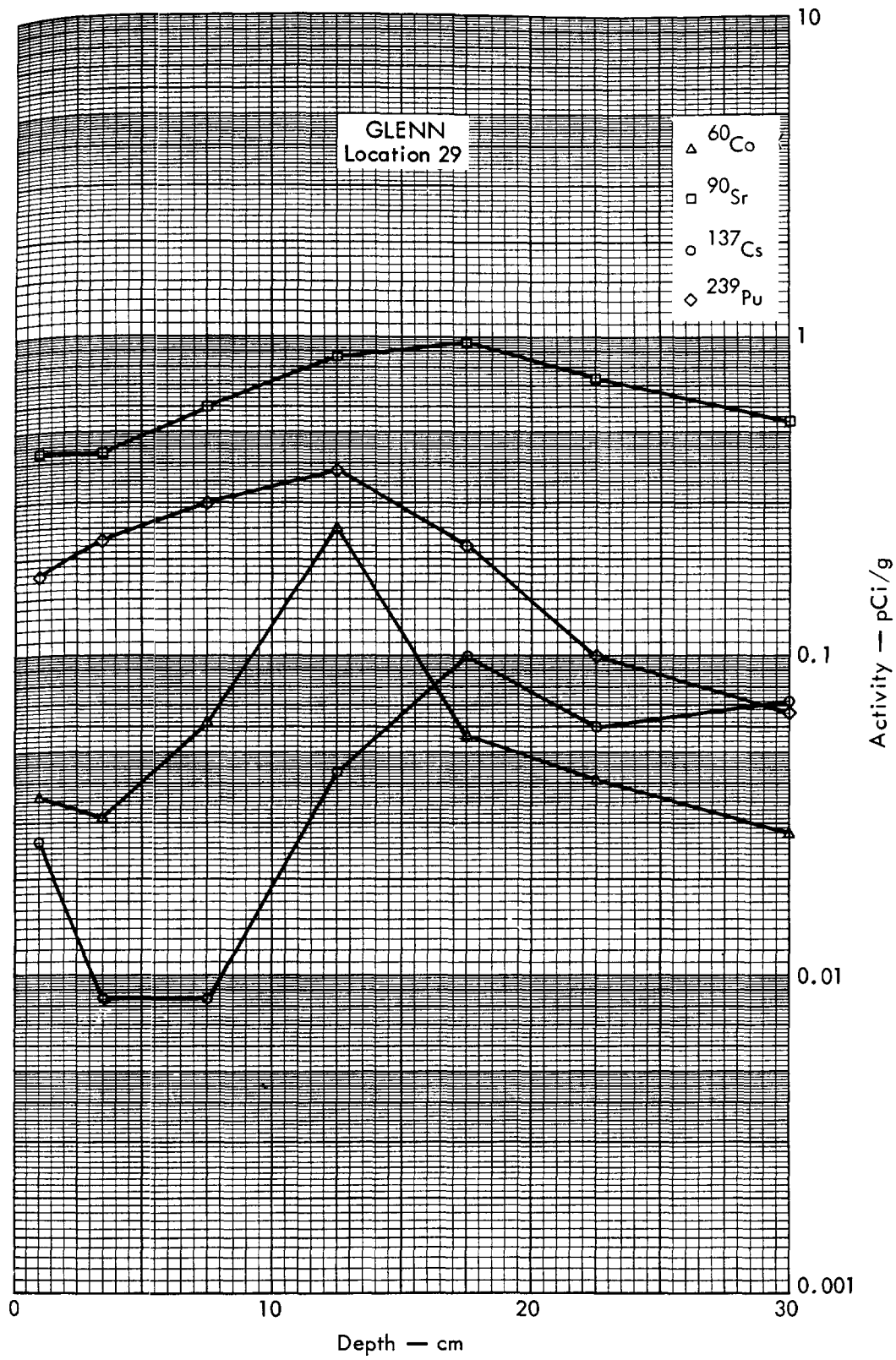


Fig. B.48.2a. Activities of selected radionuclides as a function of soil depth.

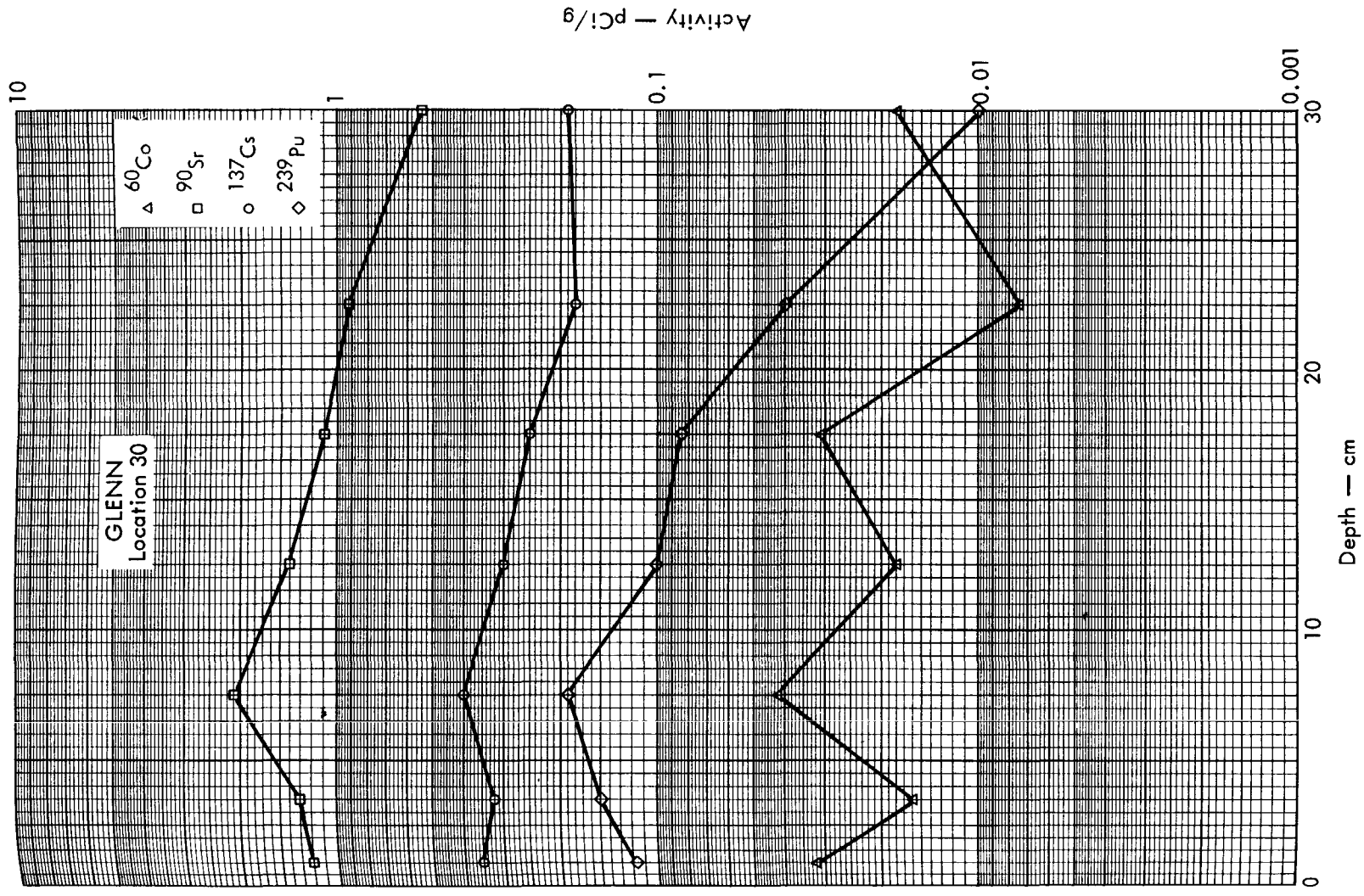


Fig. B. 48. 2b. Activities of selected radionuclides as a function of soil depth.



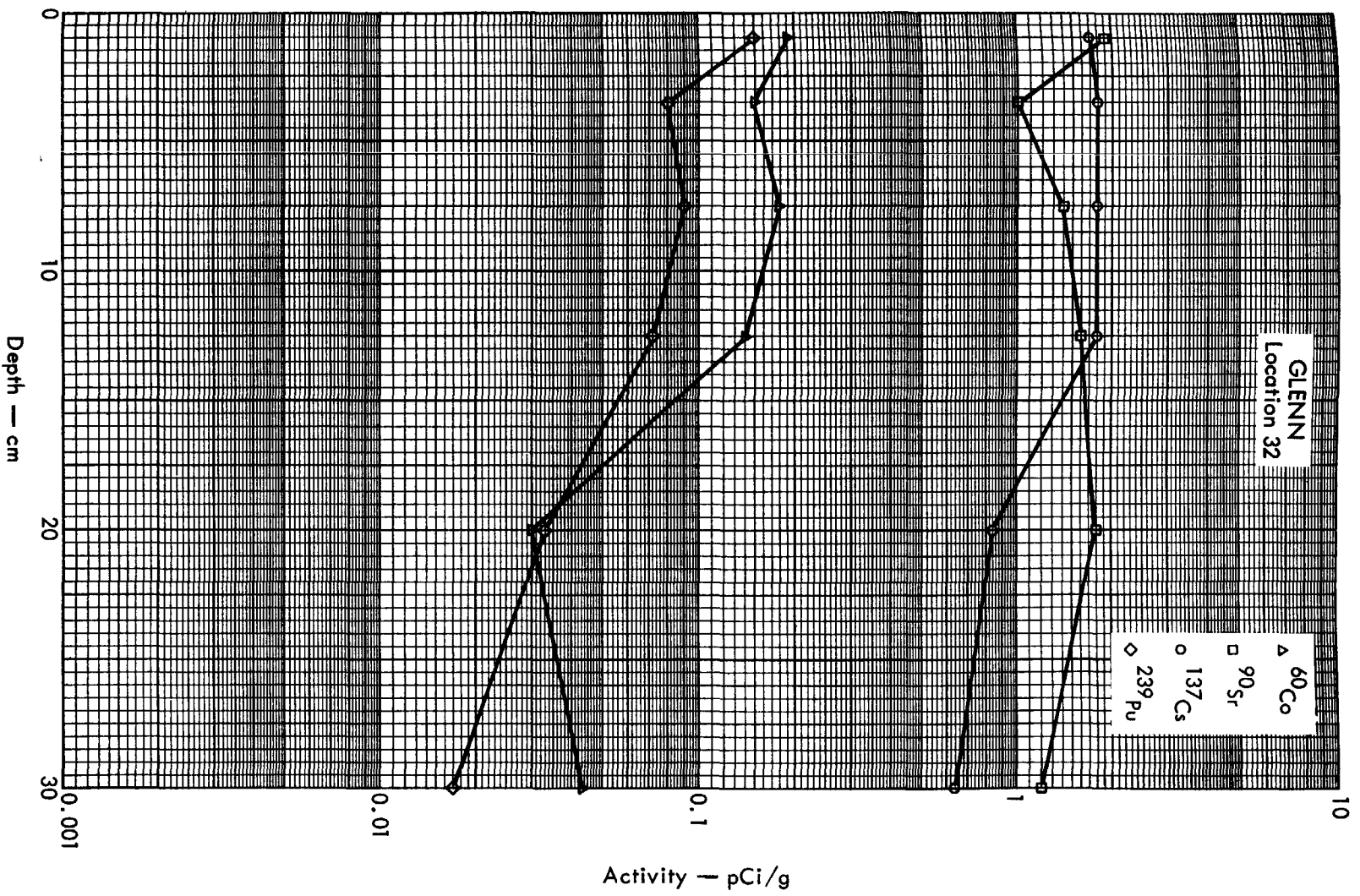
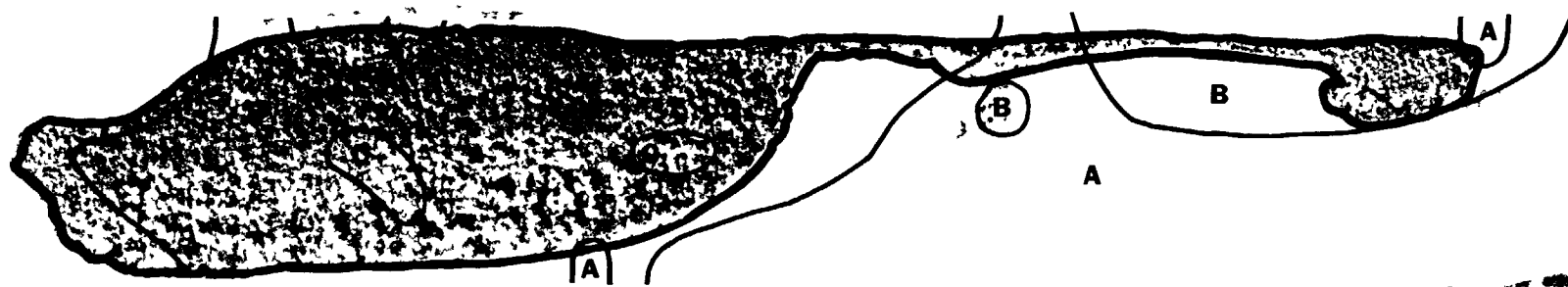


Fig. B. 48. 2c. Activities of selected radionuclides as a function of soil depth.



HENRY

Fig. B.49.1.a.



**HENRY**

Fig. B.49.1.b. Gross count isosexposure contours. (Refer to alphabetic symbol key in this appendix.)



Fig. B.49.1.d. The gamma background exposure rate ( $\mu\text{R/hr}$ ) at 1 m above the ground, measured with a portable NaI scintillation counter.

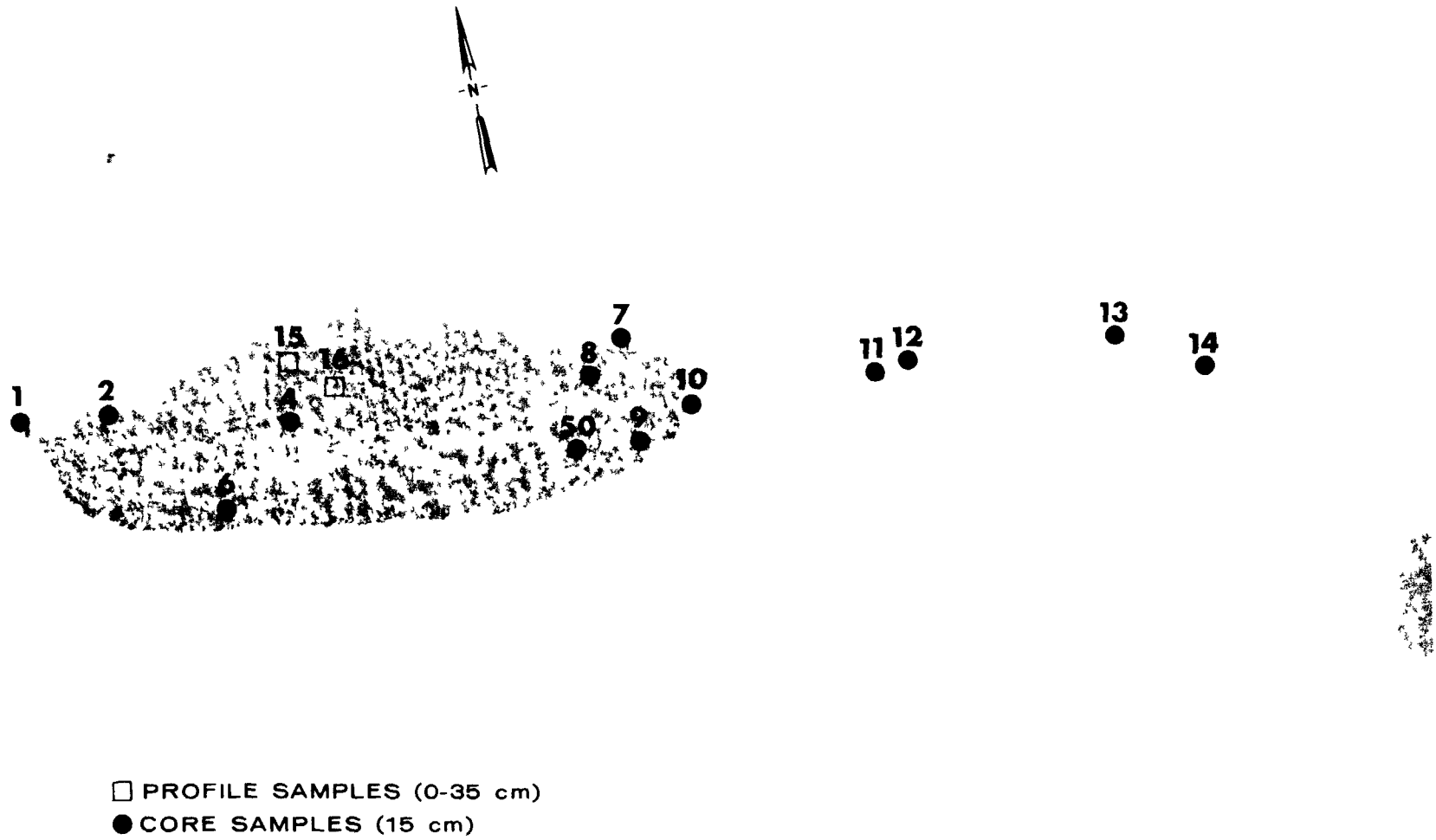
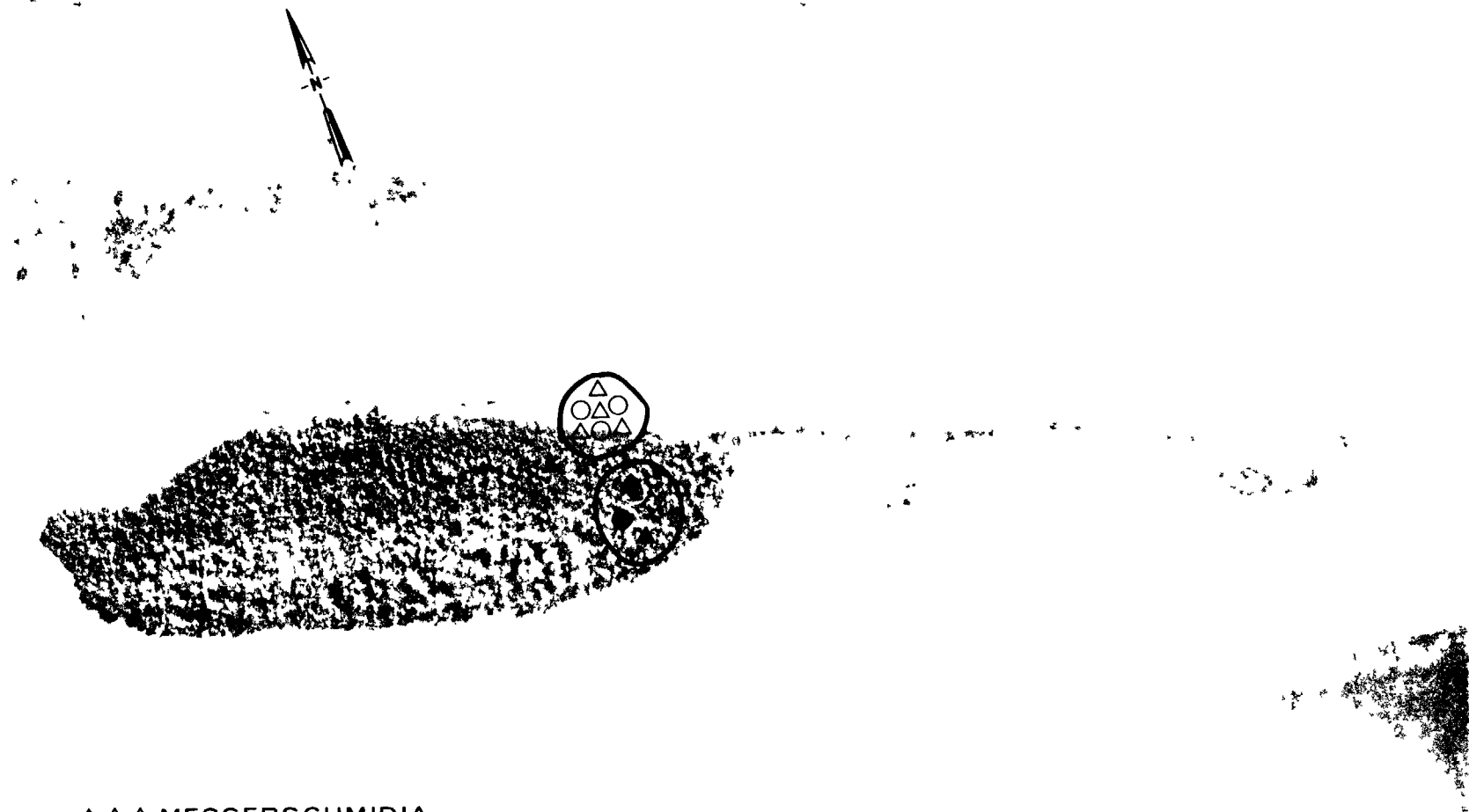


Fig. B.49.1.f. Soil-sample locations.



- △△△ MESSERSCHMIDIA
- SCAEVOLA
- ◇ PISONIA
- ◆ MORINDA
- COCONUT
- ▲ TACCA

Fig. B.49.1.g. Vegetation sample locations.

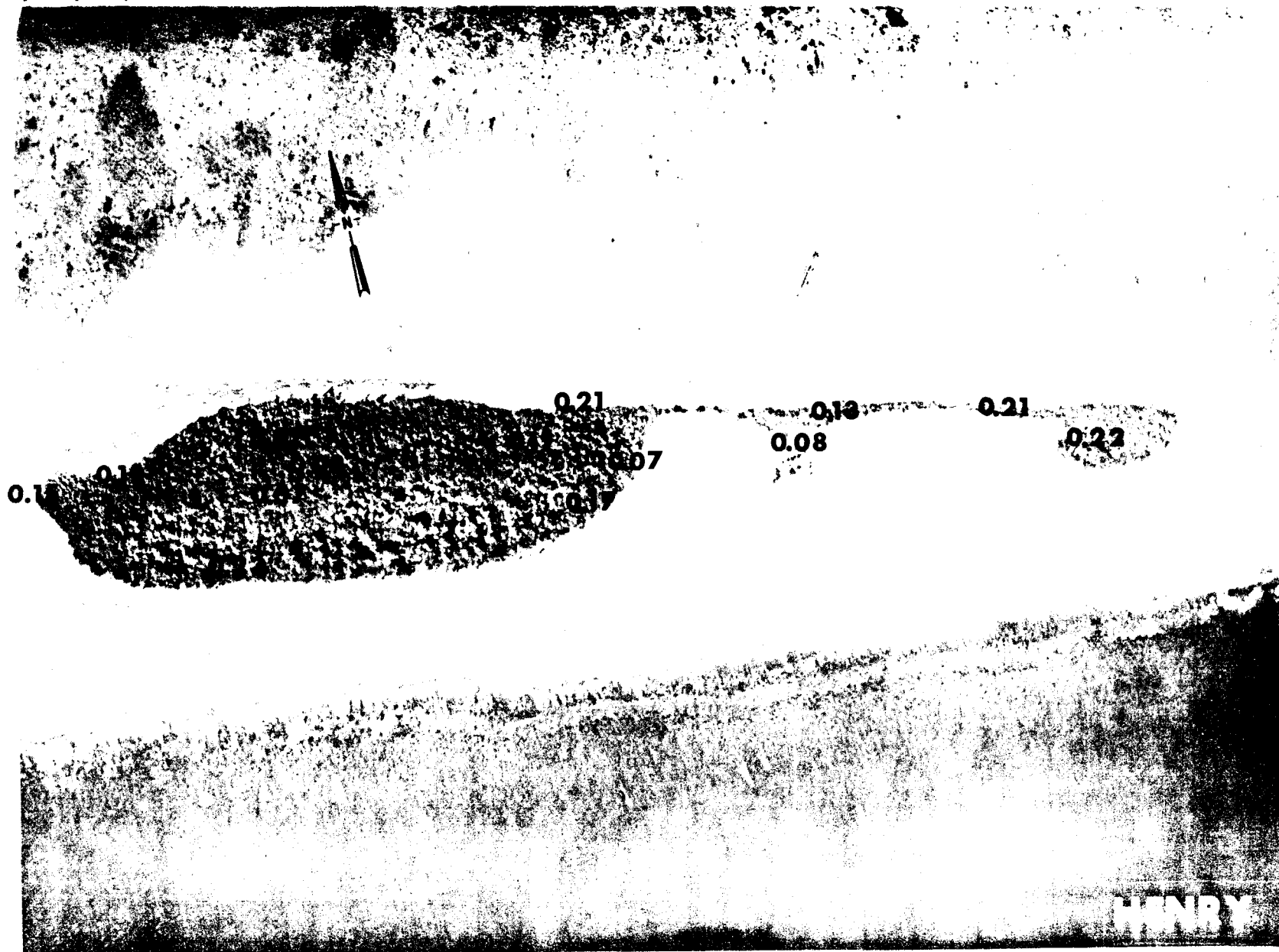


Fig. B.49.1.i. The average  $^{239}\text{Pu}$  activities (pCi/g) in soil samples collected to a depth of 15 cm.



Fig. B.49.1.j. The average  $^{90}\text{Sr}$  activities (pCi/g) in soil samples collected to a depth of 15 cm.



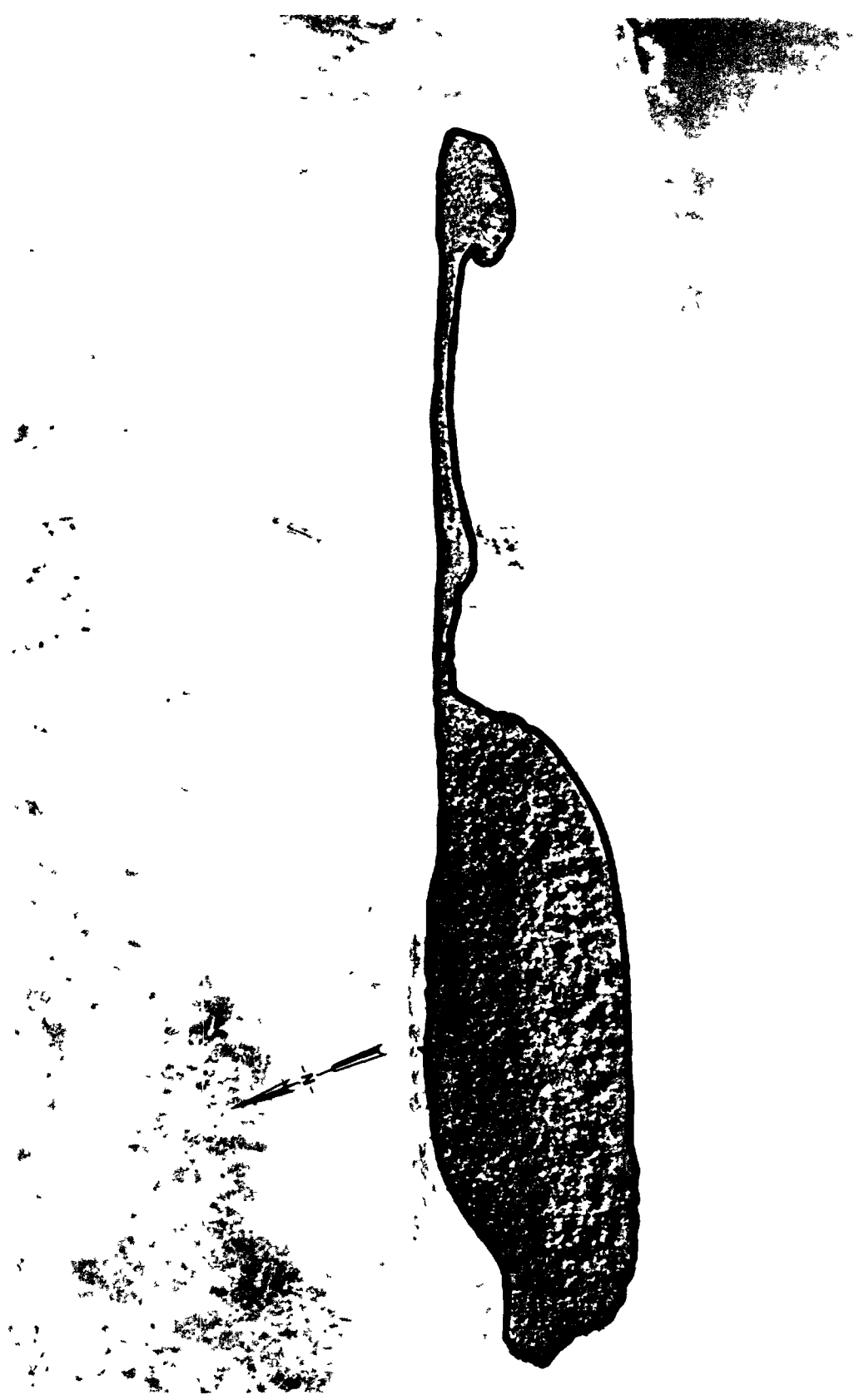


Fig. B.49.1.k.  $^{137}\text{Cs}$  isoexposure and isoconcentration contours. (Refer to alphabetic symbol key in this appendix.)



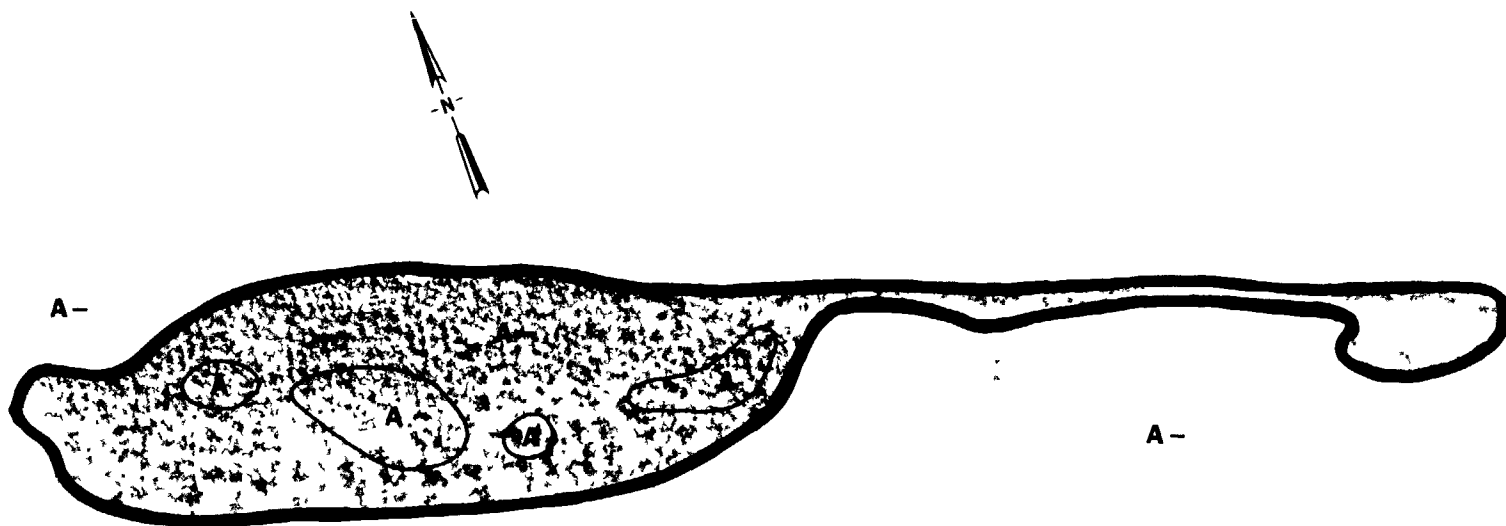


Fig. B.49.1.m.  $^{60}\text{Co}$  isoexposure and isoconcentration contours. (Refer to alphabetic symbol key in this appendix.)



Fig. B.49.1.n. The average  $^{60}\text{Co}$  activities (pCi/g) in soil samples collected to a depth of 15 cm.

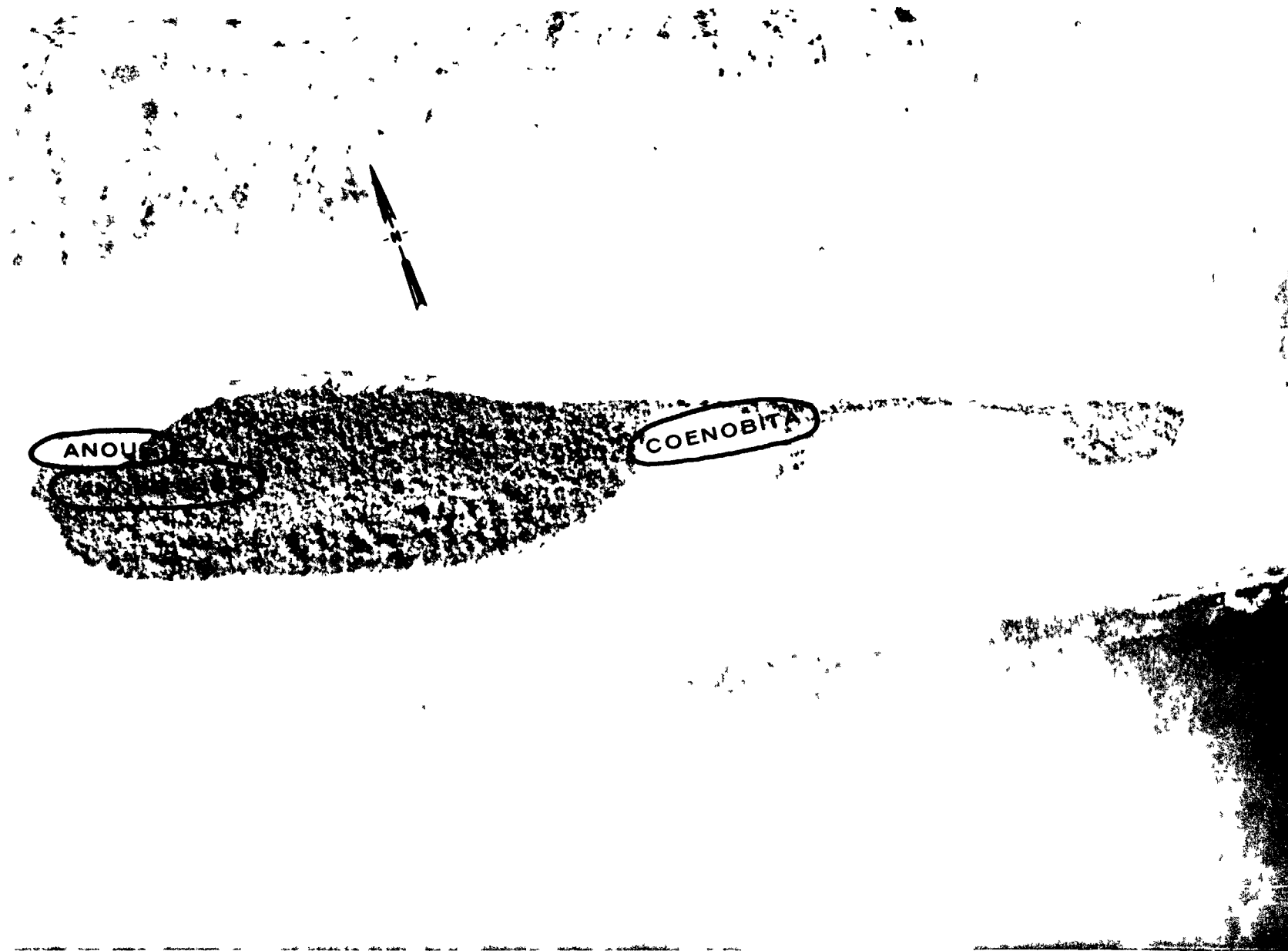


Fig. B.49.1.o. Terrestrial animal sample locations.

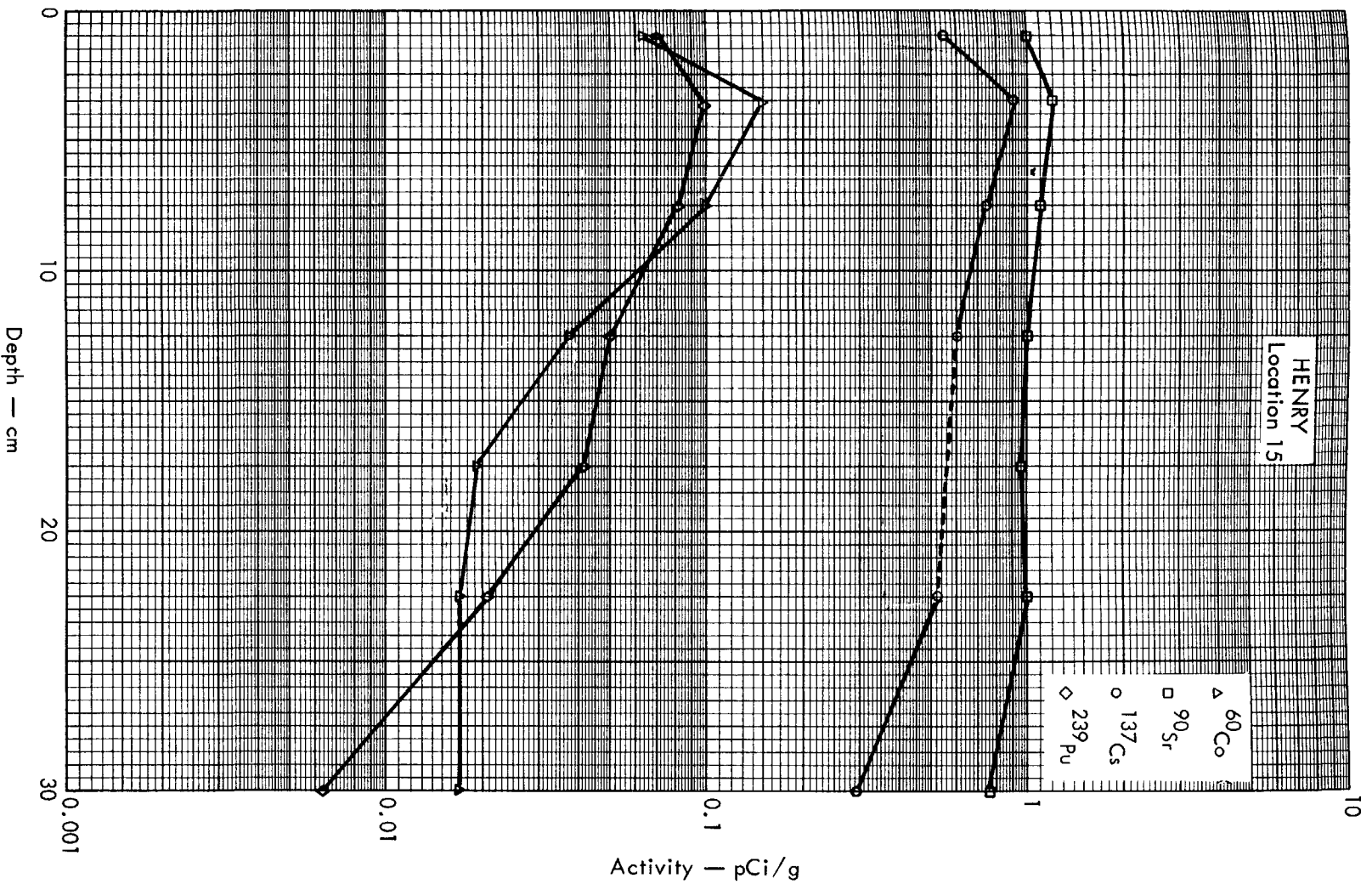


Fig. B. 49. 2a. Activities of selected radionuclides as a function of soil depth.

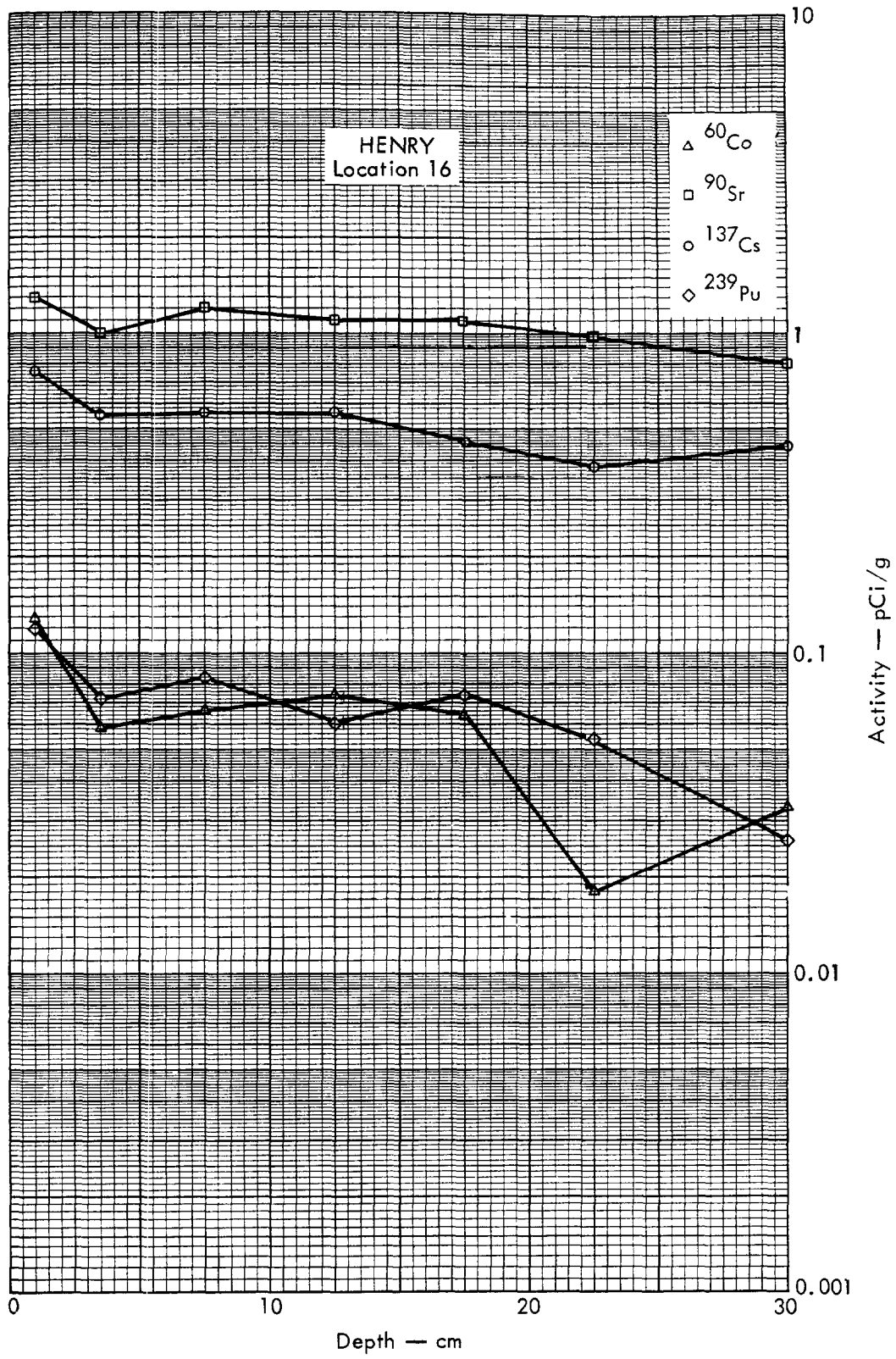


Fig. B.49.2b. Activities of selected radionuclides as a function of soil depth.



Fig. B.50.1.a.



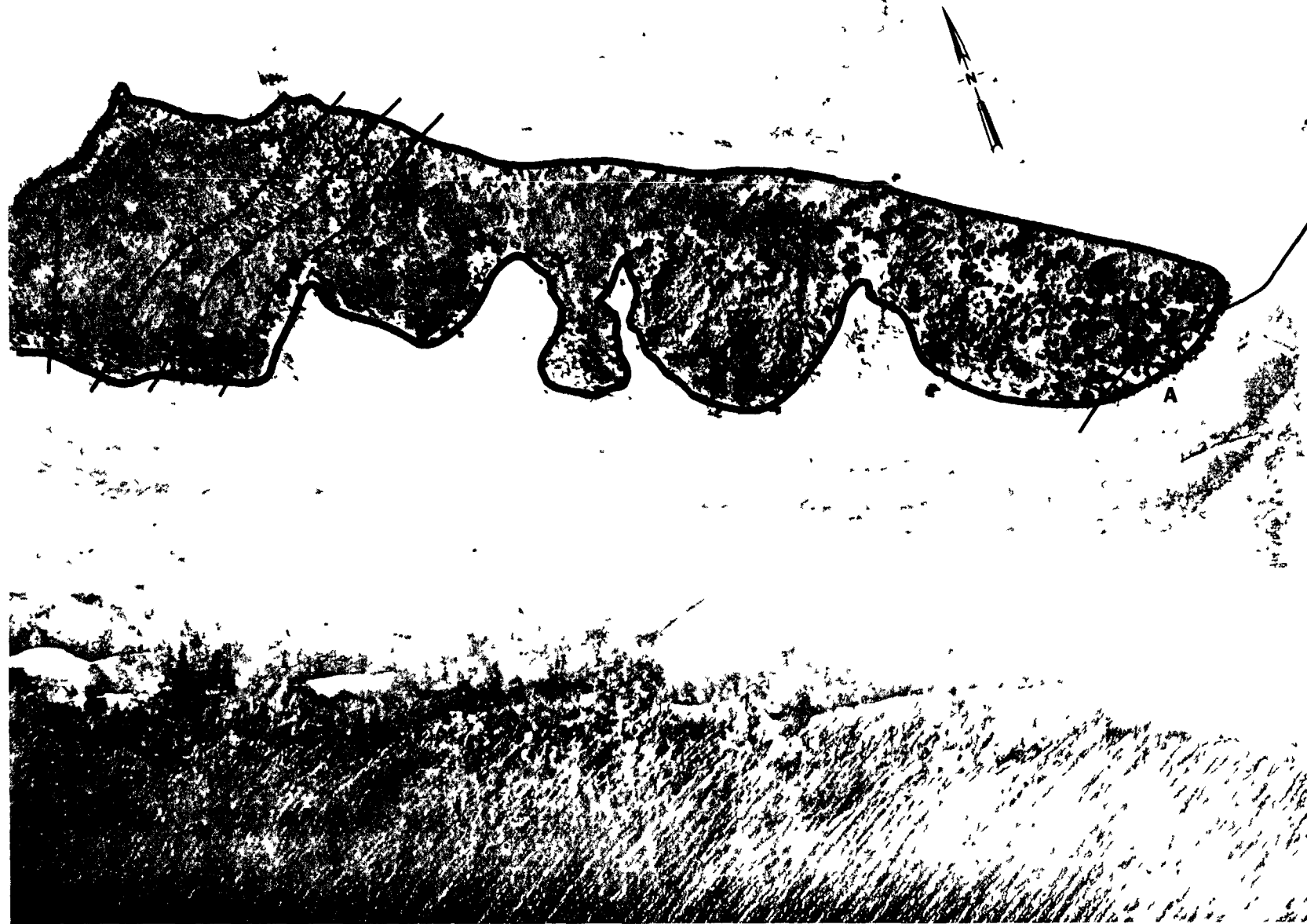


Fig. B.50.1.b. Gross count isoexposure contours. (Refer to alphabetic symbol key in this appendix.)



Fig. B.50.1.d. The gamma background exposure rate ( $\mu\text{R}/\text{hr}$ ) at 1 m above the ground, measured with a portable NaI scintillation counter.

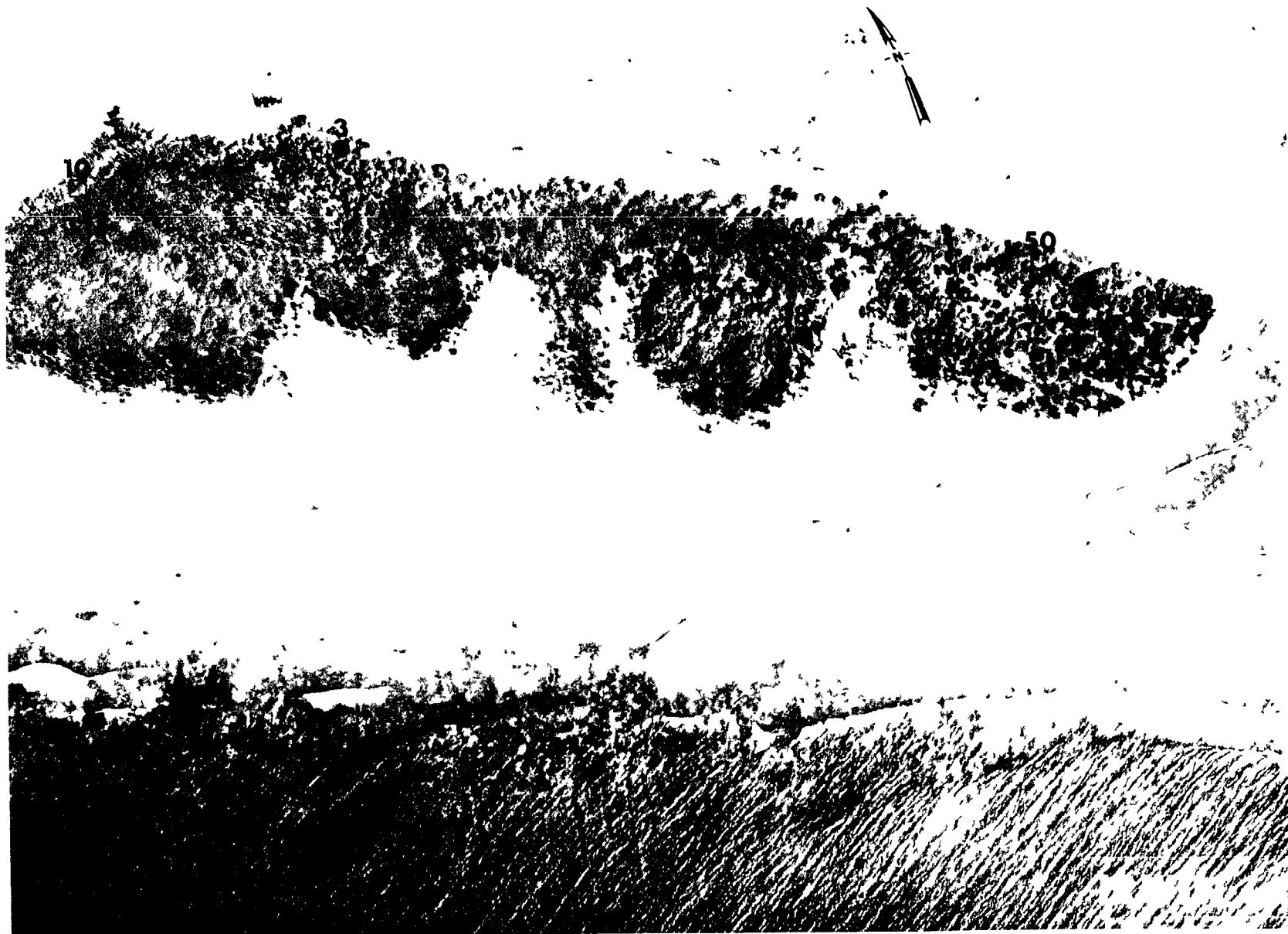


Fig. B.50.1.f. Soil-sample locations.

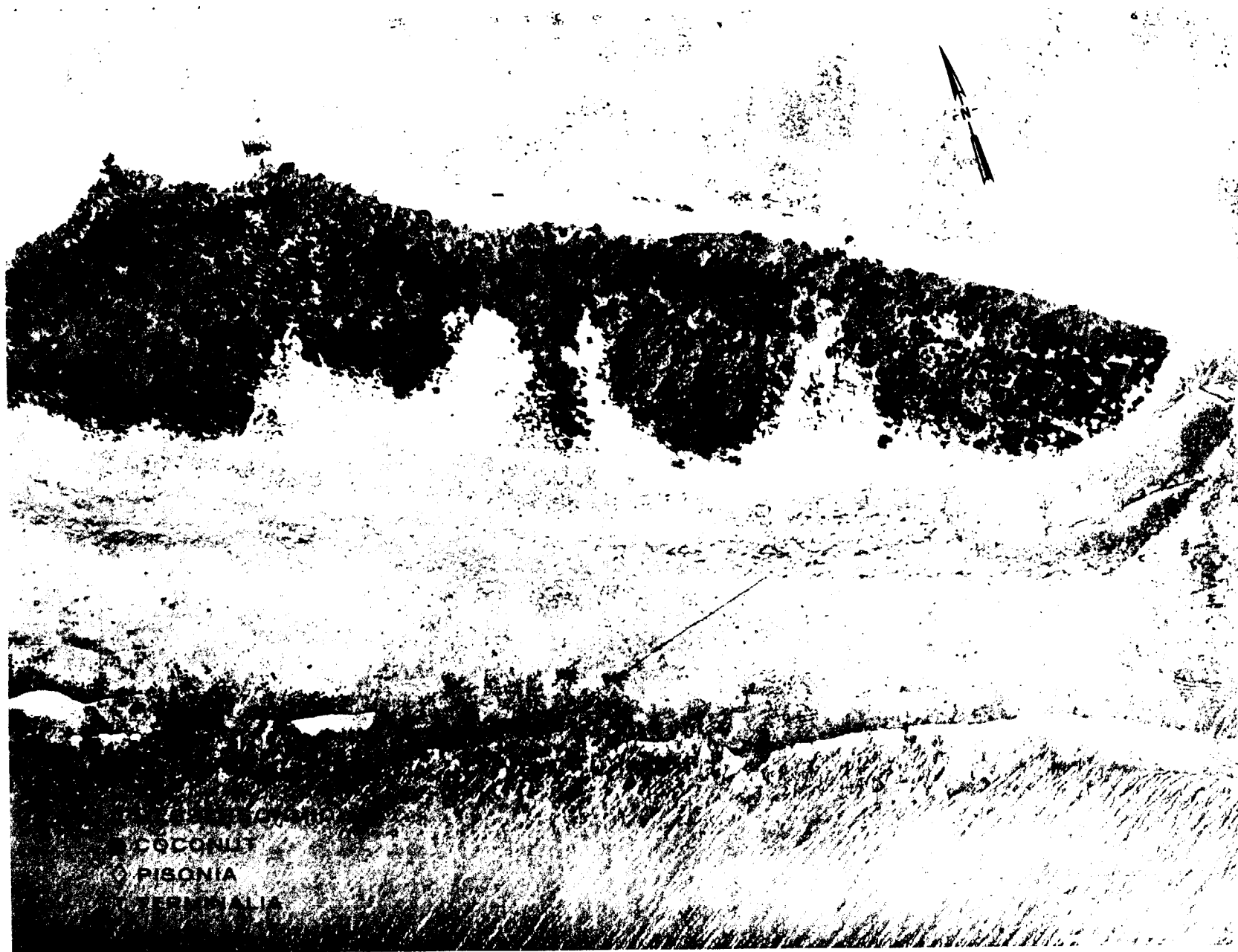


Fig. B.50.1.g. Vegetation sample locations.

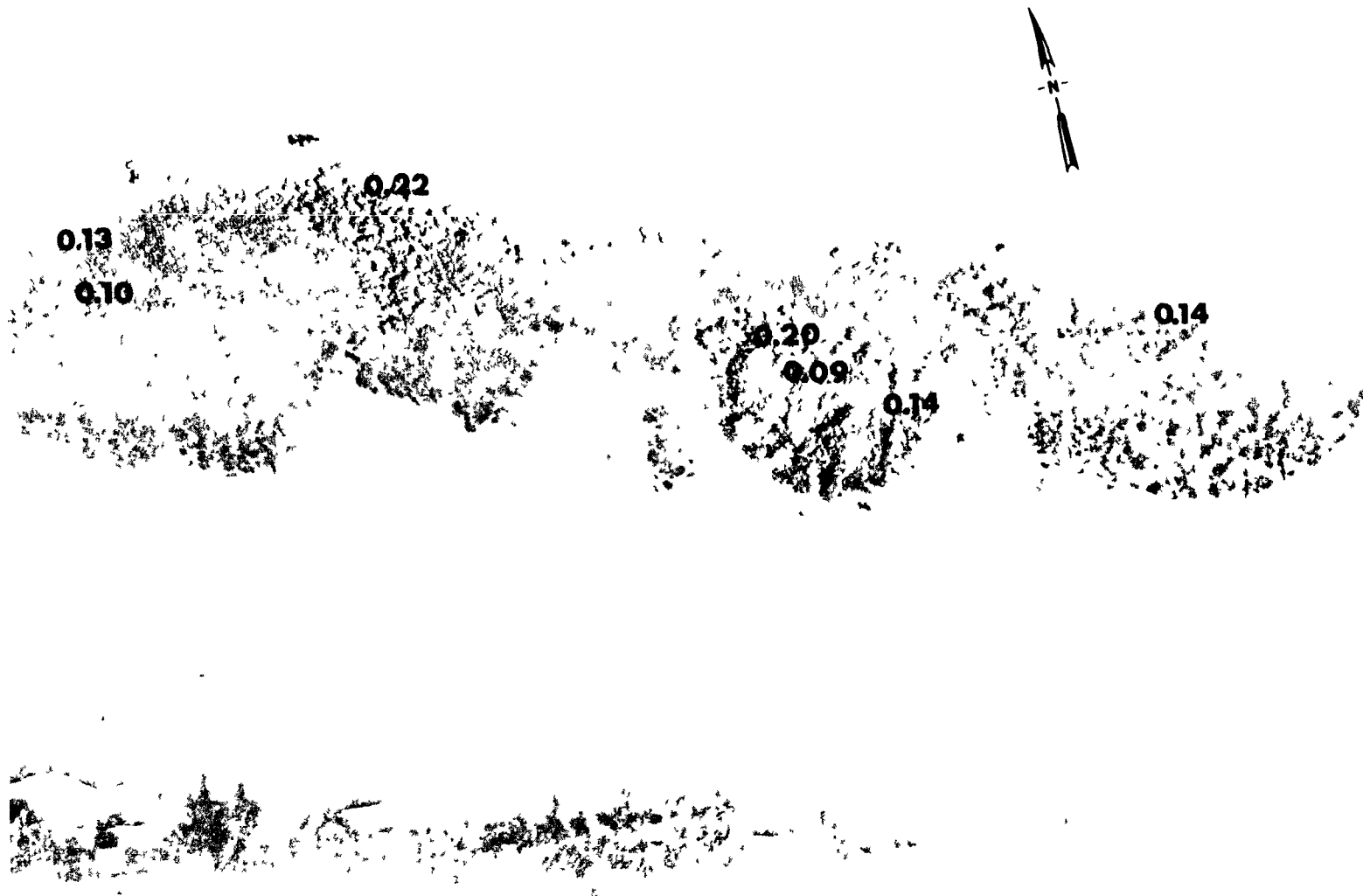


Fig. B.50.1.i. The average  $^{239}\text{Pu}$  activities (pCi/gm) in soil samples collected to a depth of 15 cm.



Fig. B.50. 1. J. The average  $^{90}\text{Sr}$  activities (pCi/gm) in soil samples collected to a depth of 15 cm.

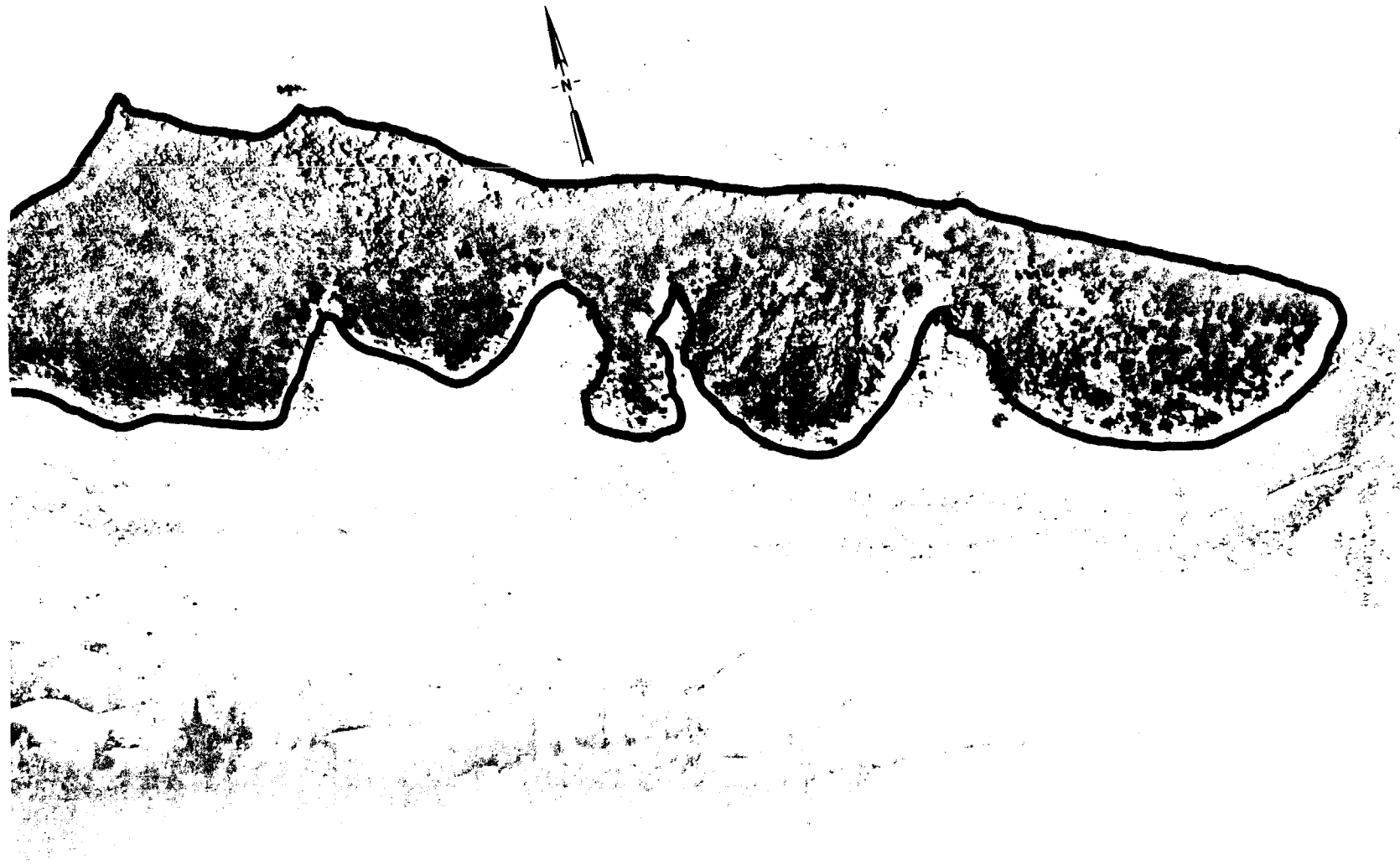


Fig. B.50.1.k. <sup>137</sup>Cs isosexposure and isoconcentration contours. (Refer to alphabetic symbol key in this appendix.)

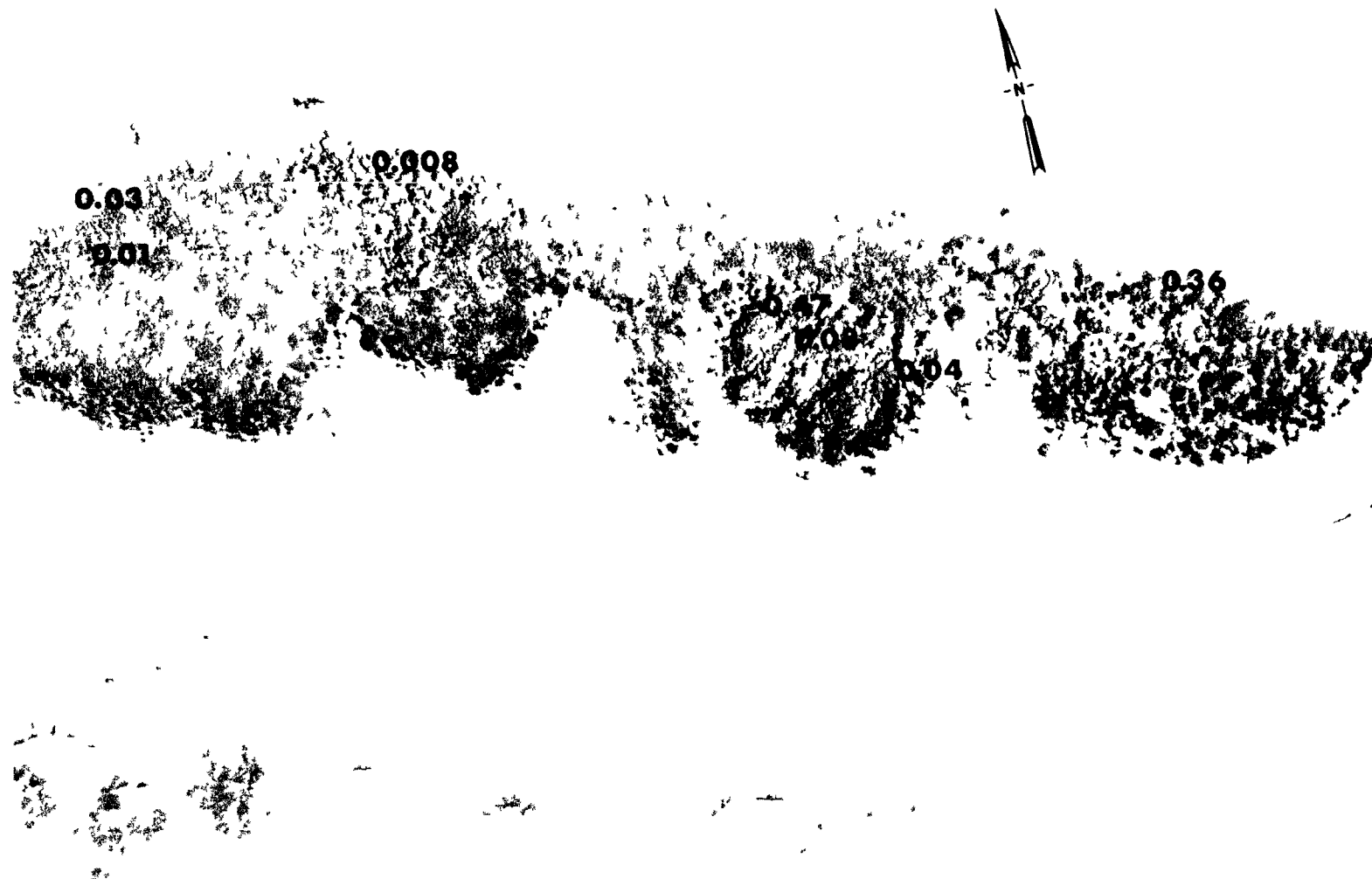


Fig. B.50.1.1. The average  $^{137}\text{Cs}$  activities (pCi/gm) in soil samples collected to a depth of 15 cm.



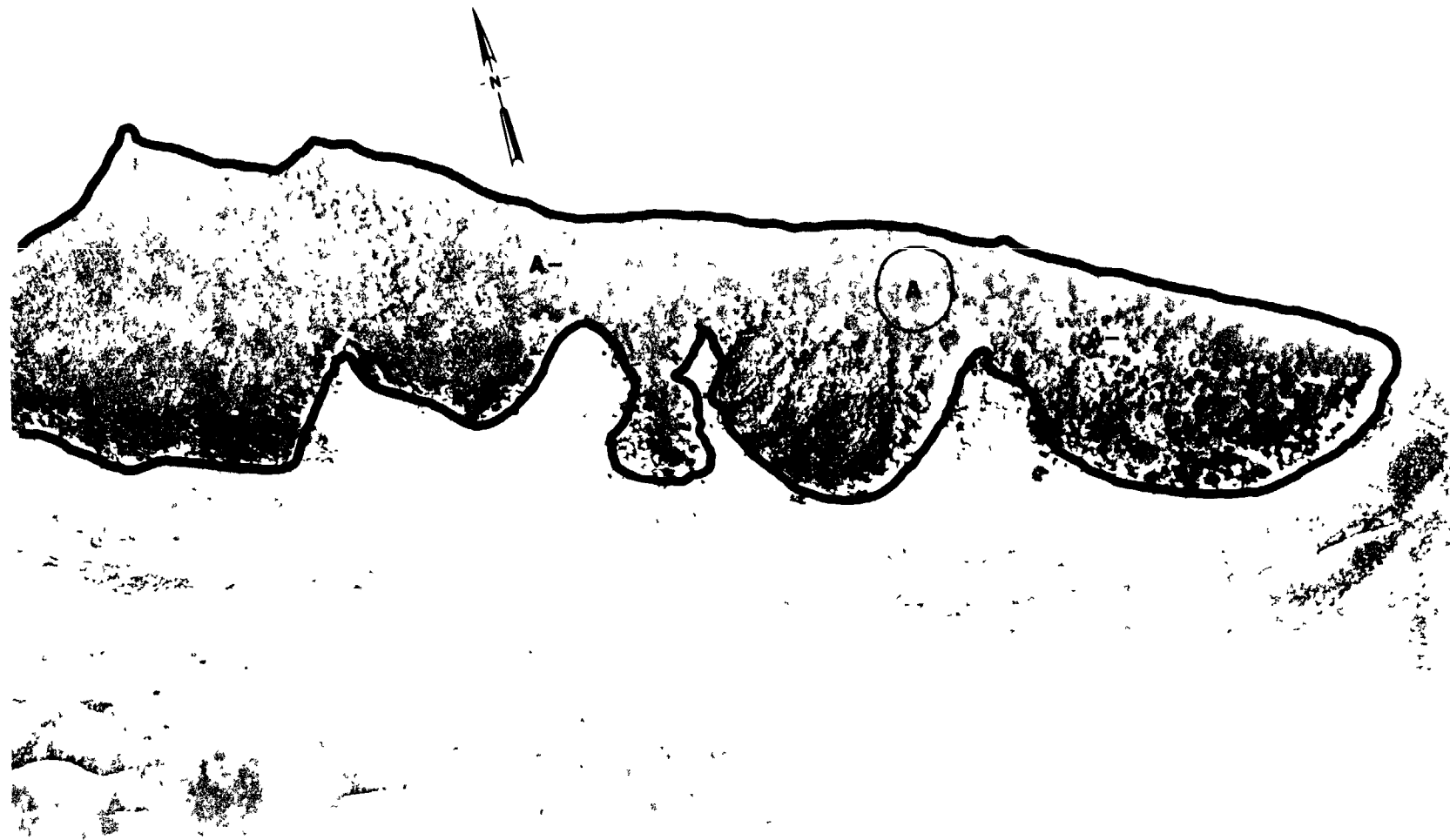


Fig. B.50.1.m.  $^{60}\text{Co}$  isosexposure and isoconcentration contours. (Refer to alphabetic symbol key in this appendix.)

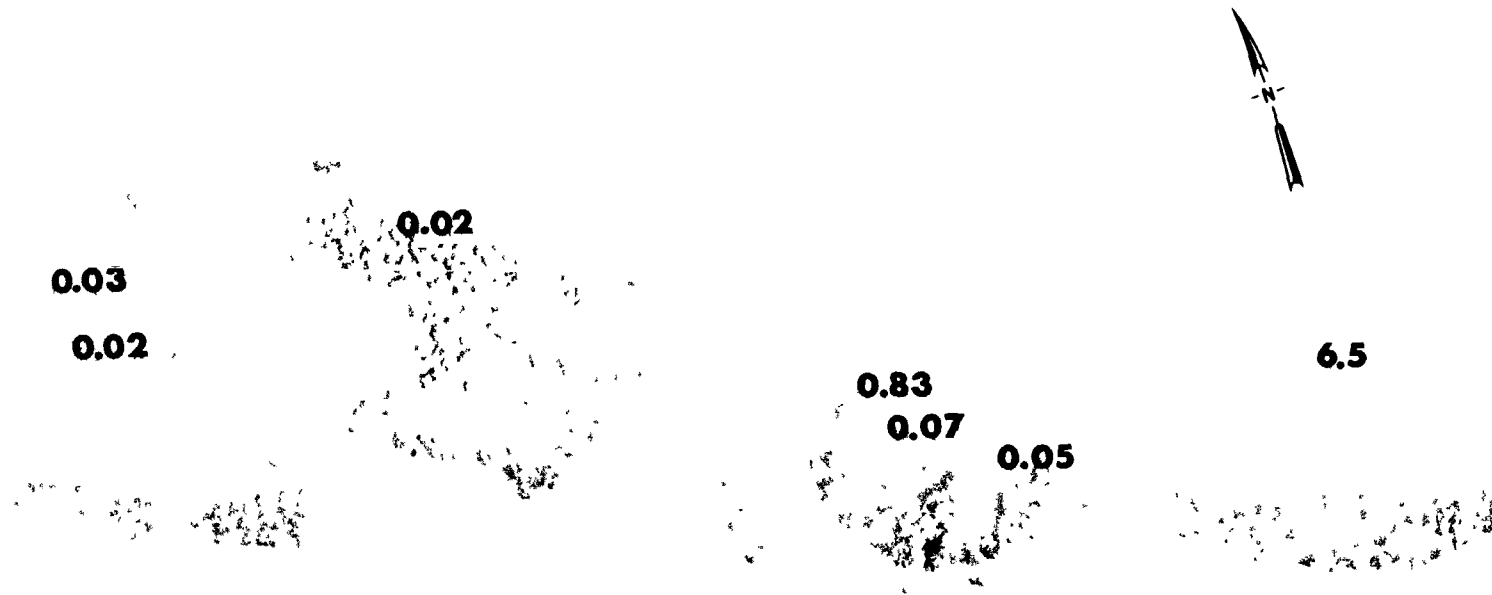


Fig. B.50.1.n. The average  $^{60}\text{Co}$  activities (pCi/gm) in soil samples collected to a depth of 15 cm.



Fig. B.50.1.o. Terrestrial animal sample locations.



Fig. B.51.1.a.

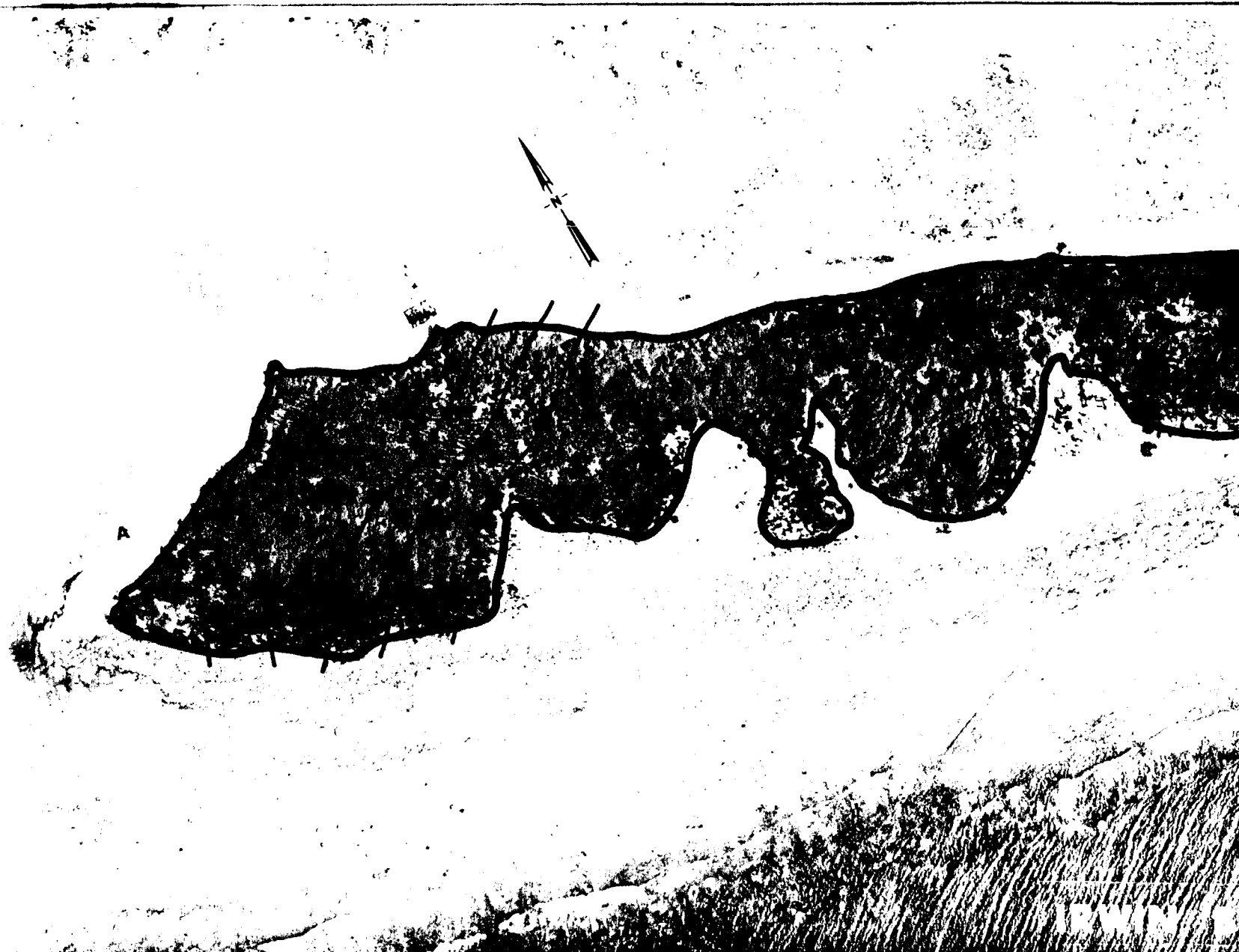


Fig. B.51.1.b. Gross count isoexposure contours. (Refer to alphabetic symbol key in this appendix.)

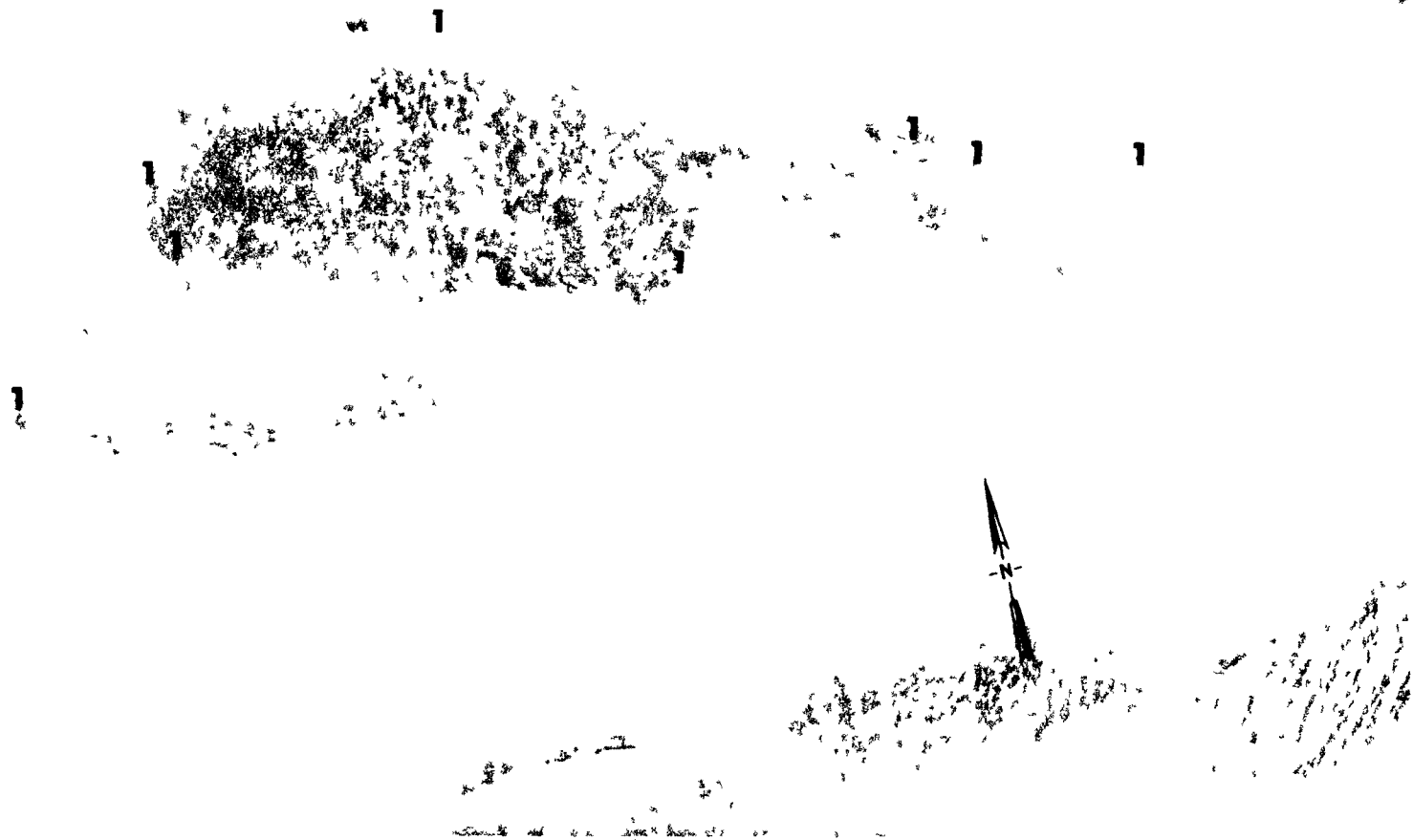


Fig. B.51.1.d. The gamma background exposure rate ( $\mu\text{R/hr}$ ) at 1 m above the ground, measured with a portable NaI scintillation counter.

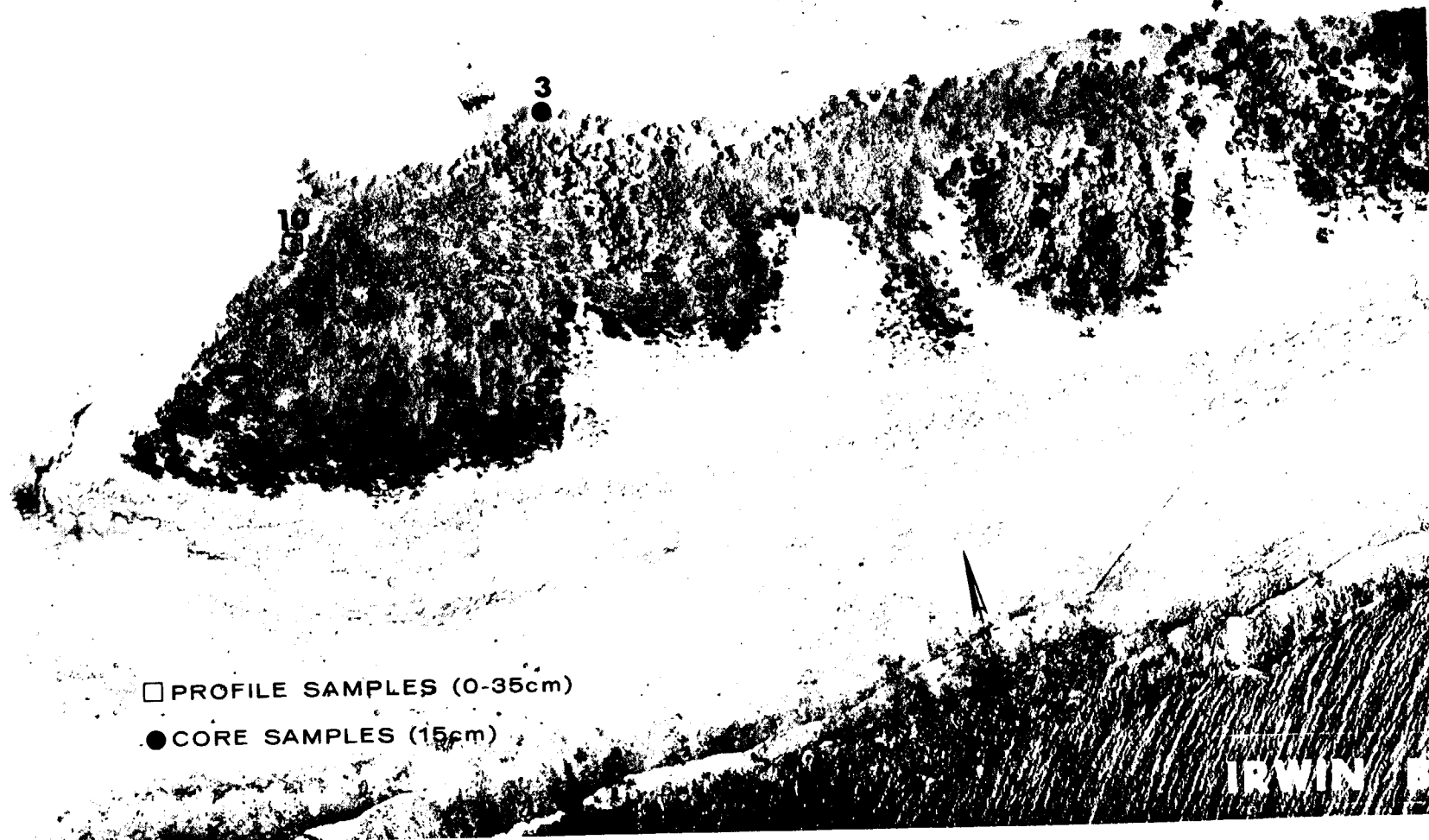


Fig. B.51.1.f. Soil-sample locations.



Fig. B.51.1.i. The average  $^{239}\text{Pu}$  activities (pCi/g) in soil samples collected to a depth of 15 cm.





Fig. B.51.1.j. The average  $^{90}\text{Sr}$  activities (pCi/g) in soil samples collected to a depth of 15 cm.



Fig. B.51.1.k,  $^{137}\text{Cs}$  isoexposure and isoconcentration contours. (Refer to alphabetic symbol key in this appendix.)





Fig. B.51.1.m.  $^{60}\text{Co}$  isoexposure and isoconcentration contours. (Refer to alphabetic symbol key in this appendix.)



Fig. B.51.1.n. The average  $^{60}\text{Co}$  activities (pCi/g) in soil samples collected to a depth of 15 cm.

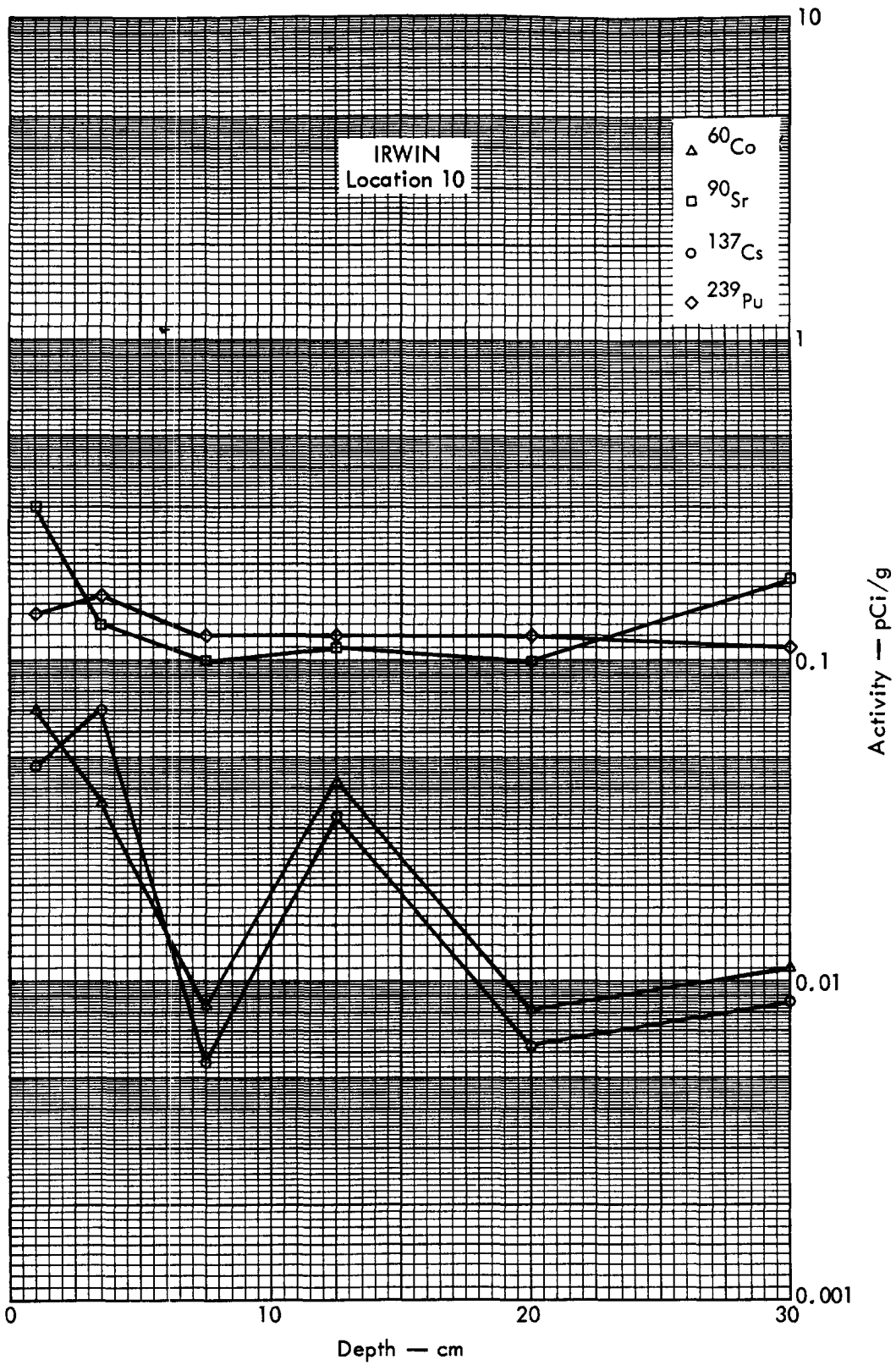


Fig. B. 51. 2a. Activities of selected radionuclides as a function of soil depth.

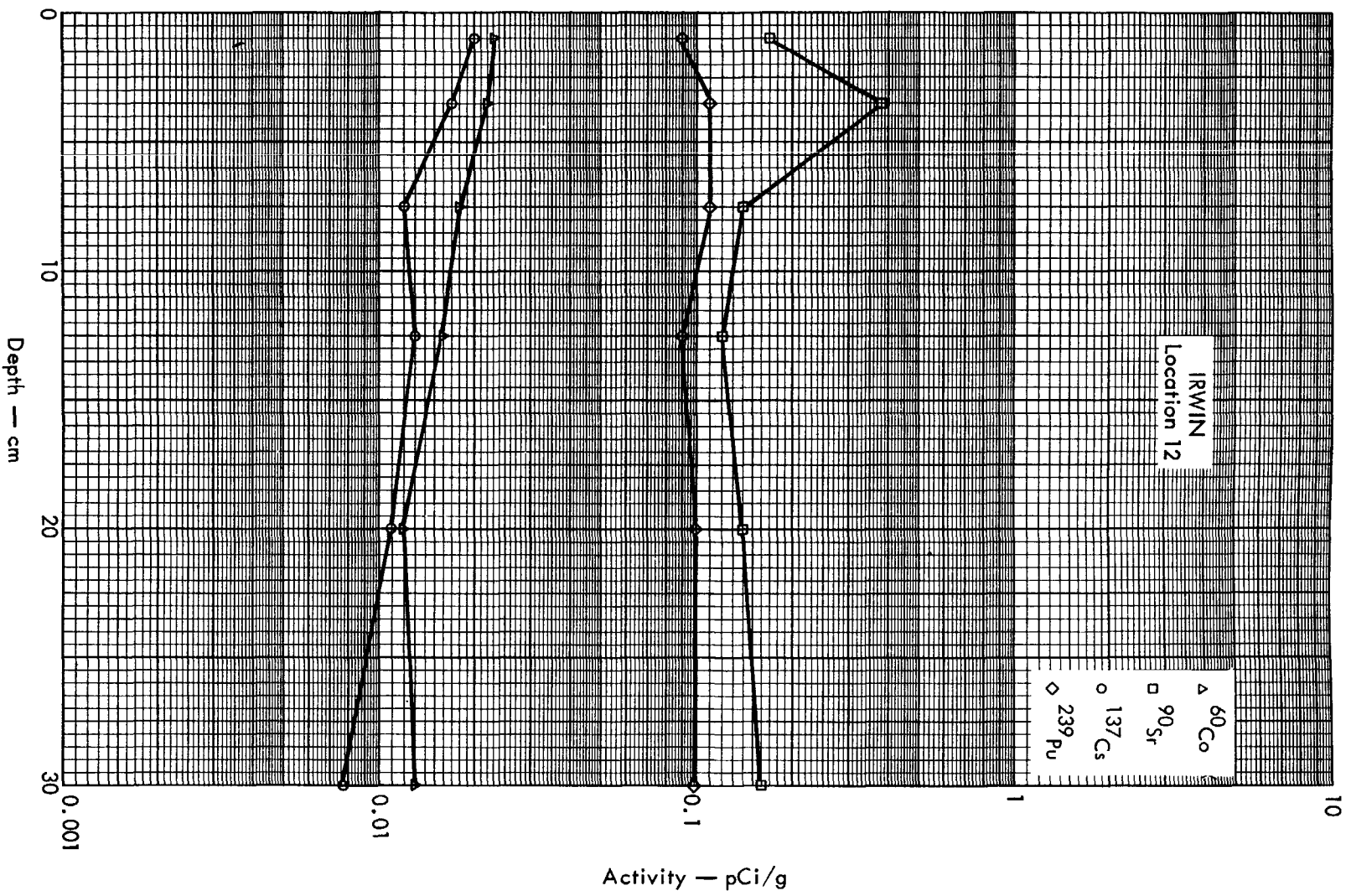


Fig. B. 51. 2b. Activities of selected radionuclides as a function of soil depth.



Fig. B.52.1.a.





Fig. B.52.1.b. Gross count isosexposure contours. (Refer to alphabetic symbol key in this appendix.)

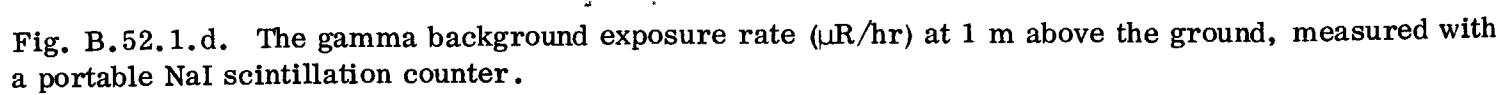


Fig. B.52.1.d. The gamma background exposure rate ( $\mu\text{R/hr}$ ) at 1 m above the ground, measured with a portable NaI scintillation counter.



Fig. B.52.1.f. Soil-sample locations.



Fig. B.52.1.g. Vegetation sample locations.

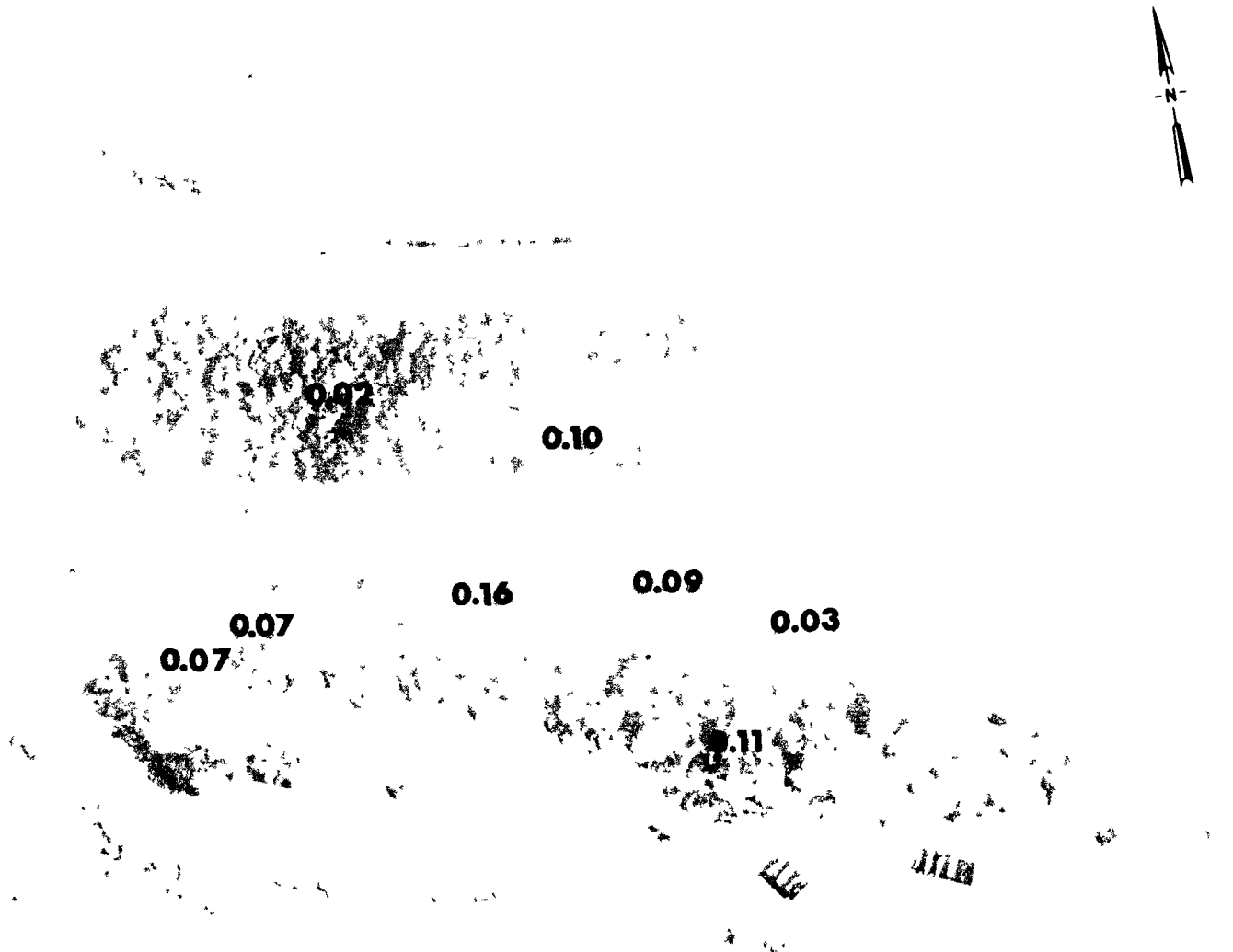


Fig. B.52.1.i. The average  $^{239}\text{Pu}$  activities (pCi/gm) in soil samples collected to a depth of 15 cm.

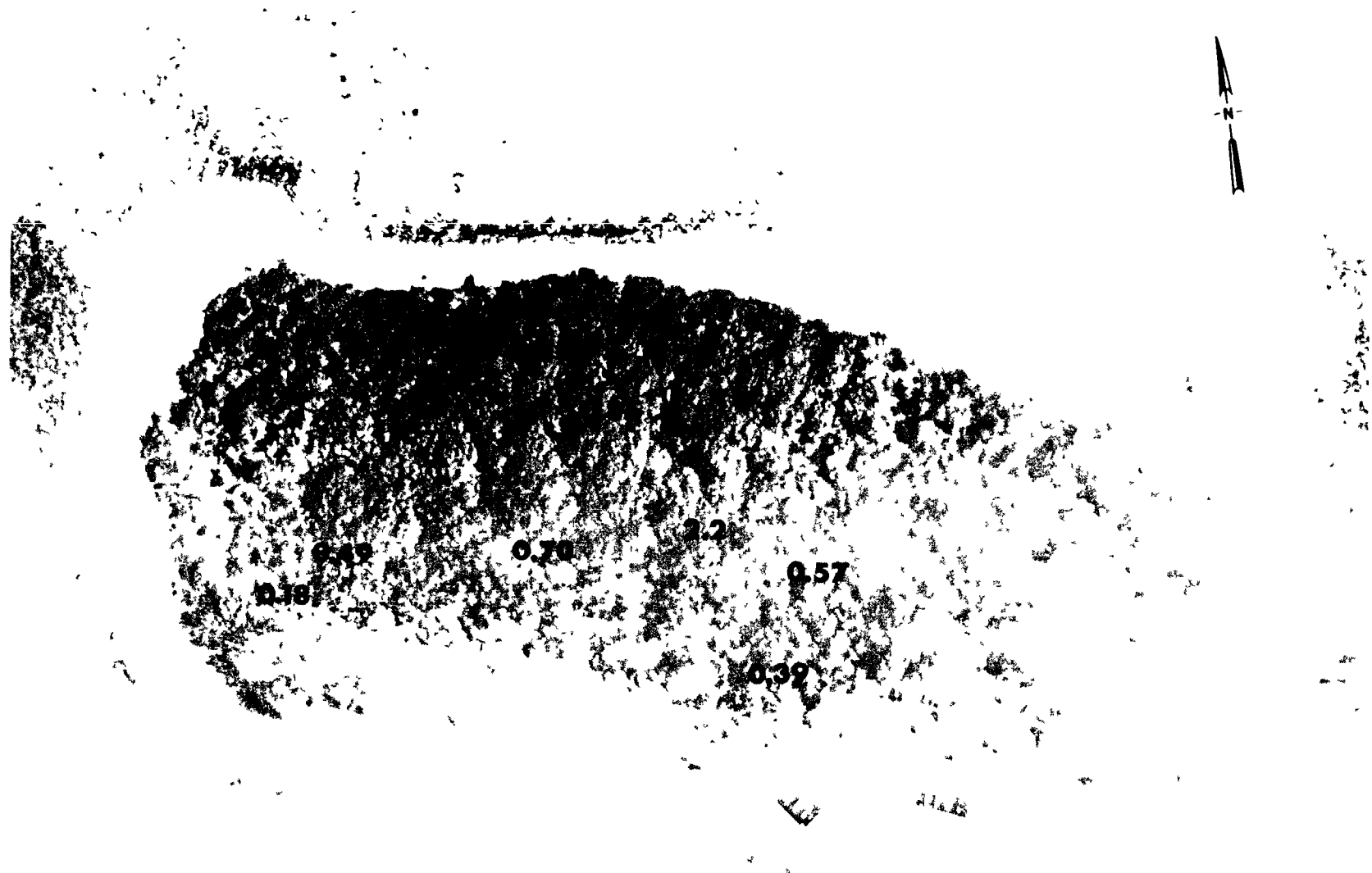


Fig. B.52.1.j. The average <sup>90</sup>Sr activities (pCi/gm) in soil samples collected to a depth of 15 cm.



Fig. B.52.1.k.  $^{137}\text{Cs}$  isoexposure and isoconcentration contours. (Refer to alphabetic symbol key in this appendix.)



Fig. B.52.1.1. The average <sup>137</sup>Cs activities (pCi/gm) in soil samples collected to a depth of 15 cm.



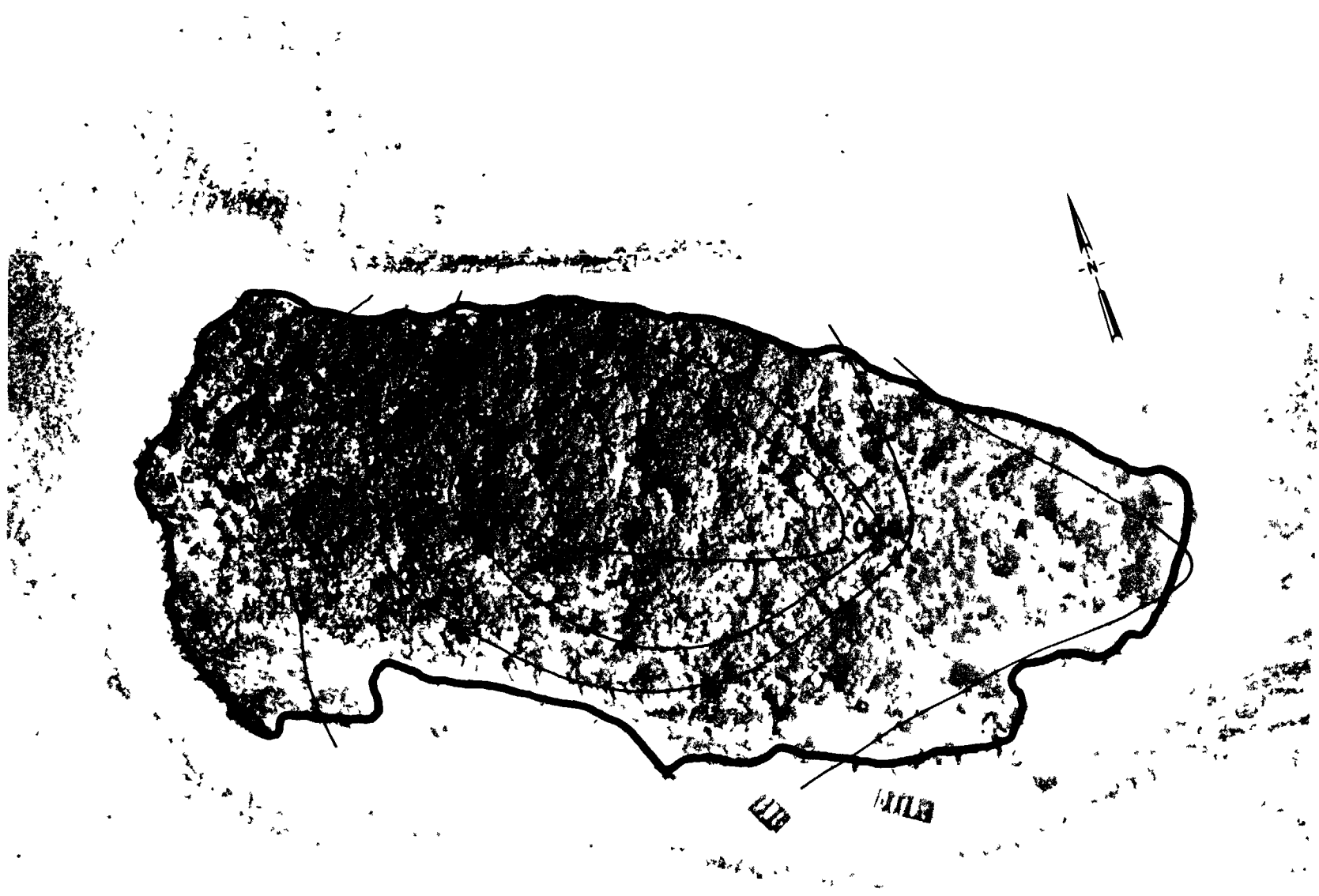


Fig. B.52.1.m.  $^{60}\text{Co}$  isosexposure and isoconcentration contours. (Refer to alphabetic symbol key in this appendix.)



Fig. B.52.1.n. The average  $^{60}\text{Co}$  activities (pCi/gm) in soil samples collected to a depth of 15 cm.

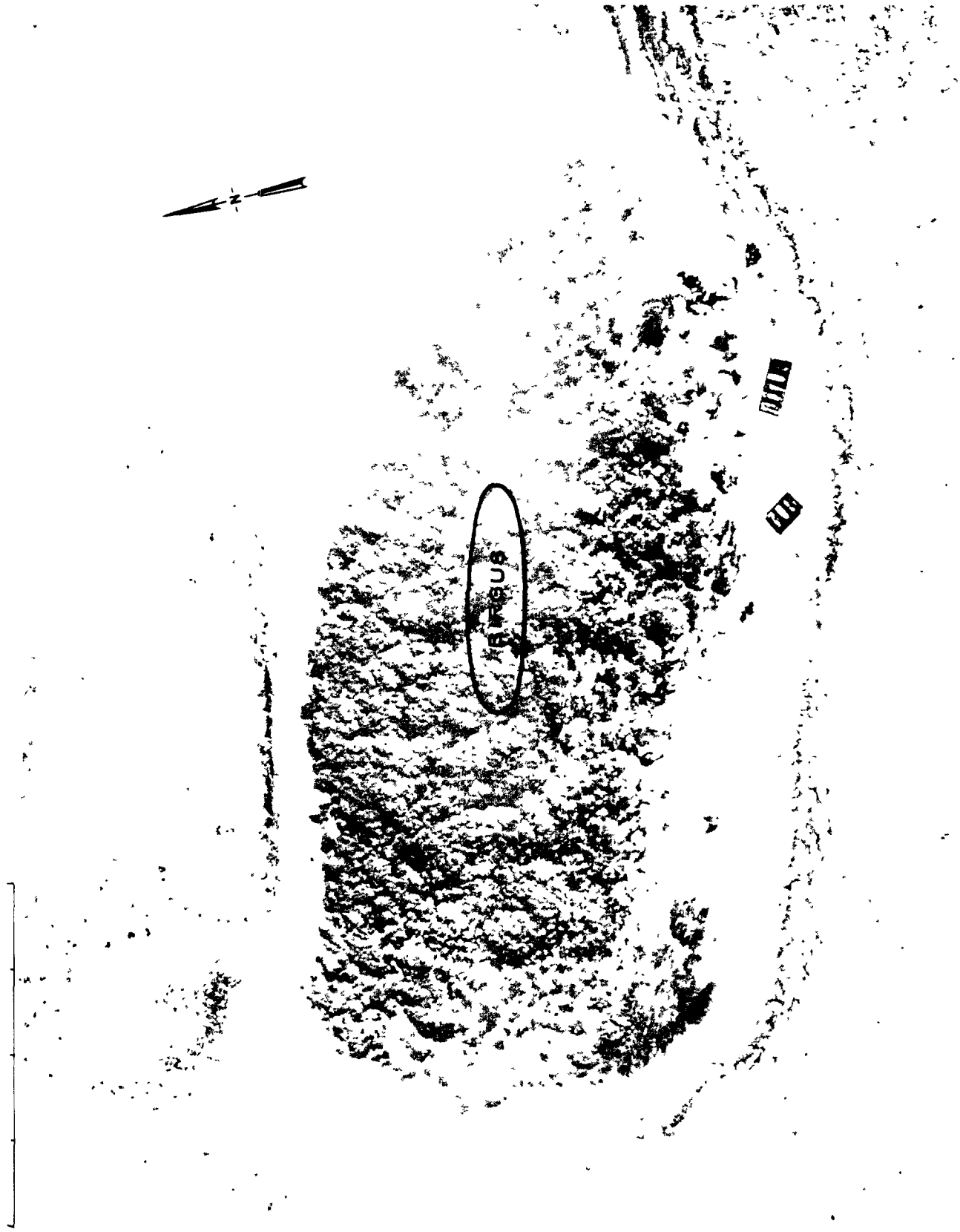


Fig. B.52.1.o. Terrestrial animal sample locations.

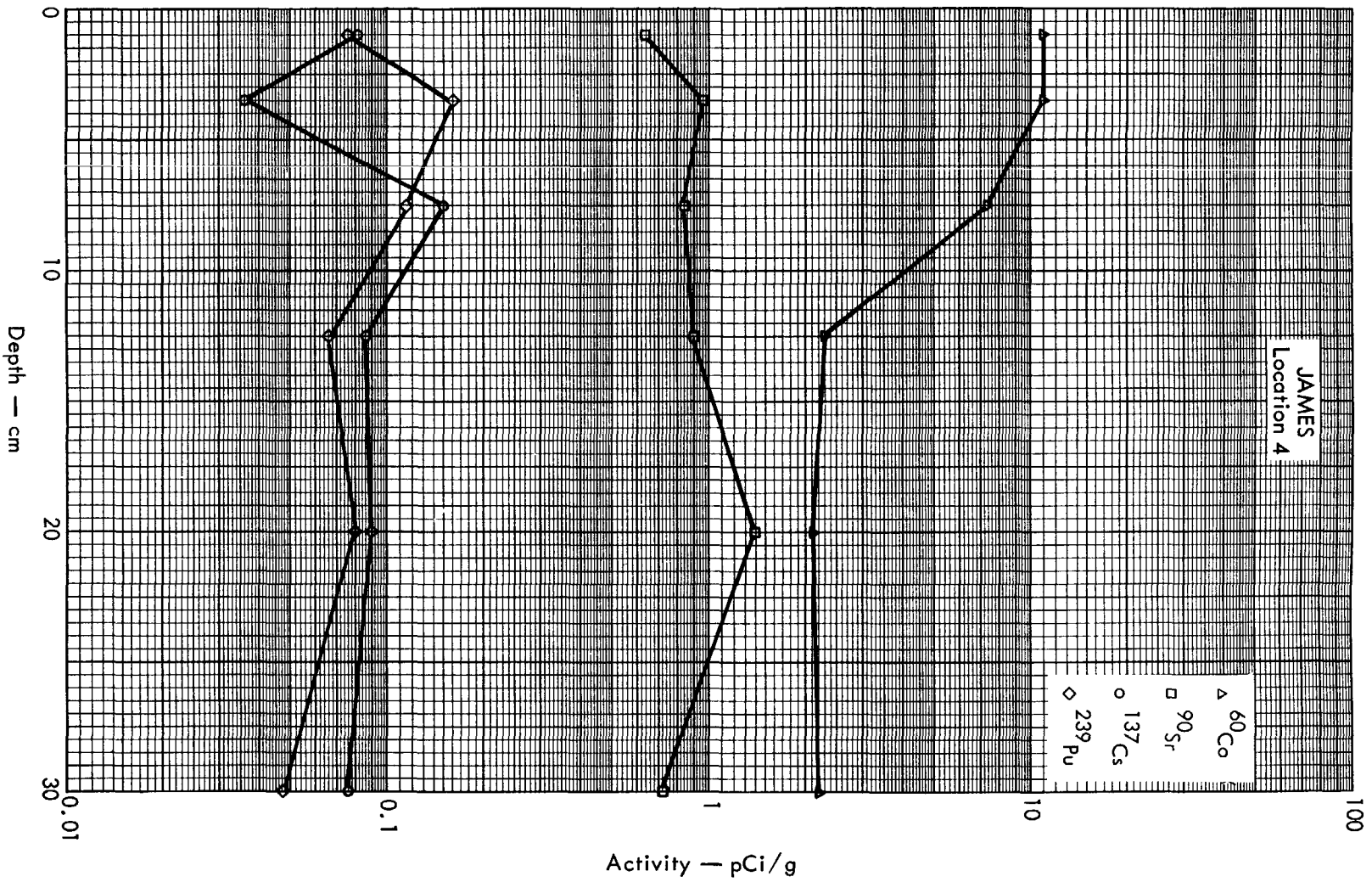


Fig. B. 52: 2a. Activities of selected radionuclides as a function of soil depth.

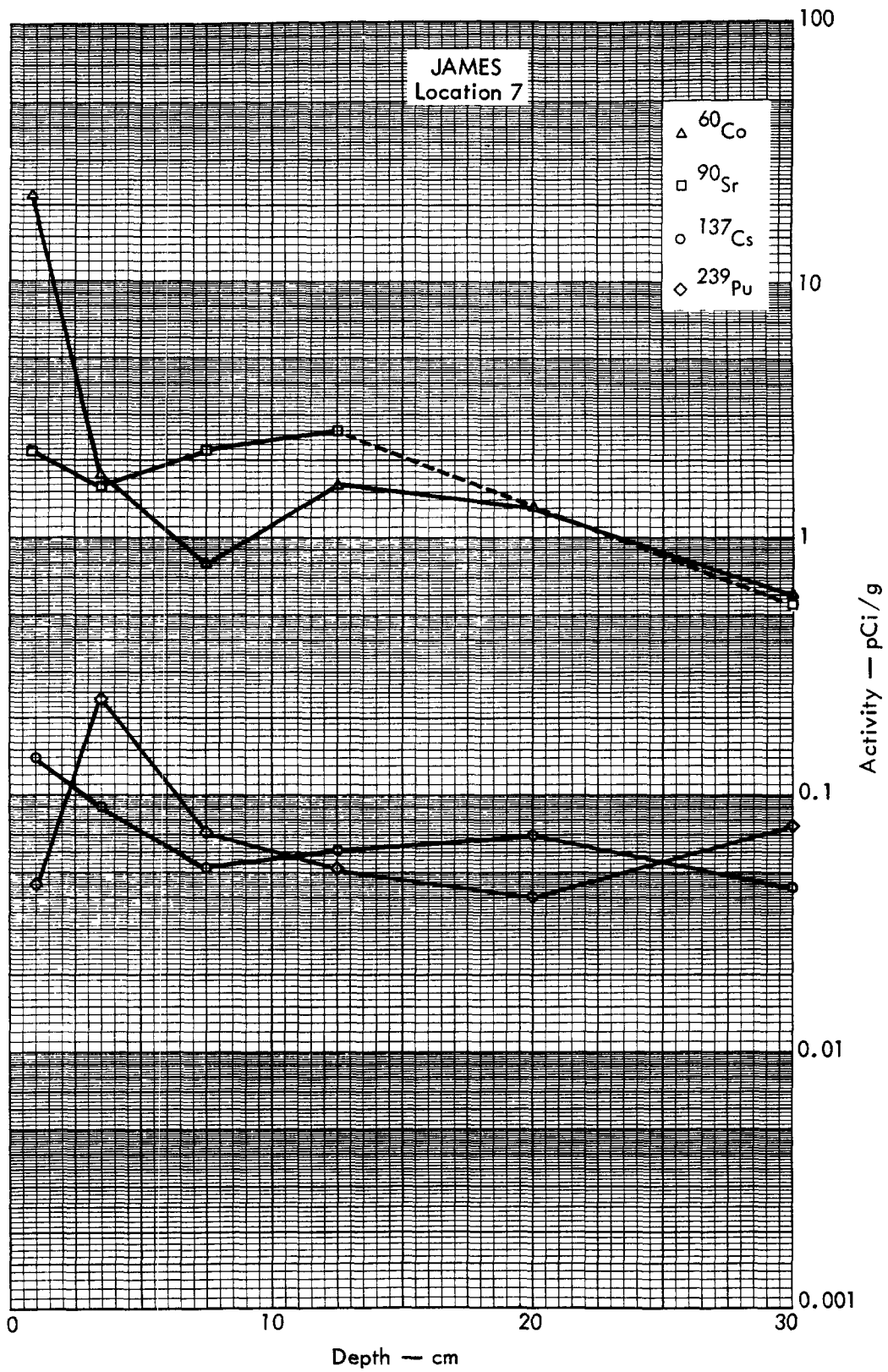


Fig. B. 52. 2b. Activities of selected radionuclides as a function of soil depth.

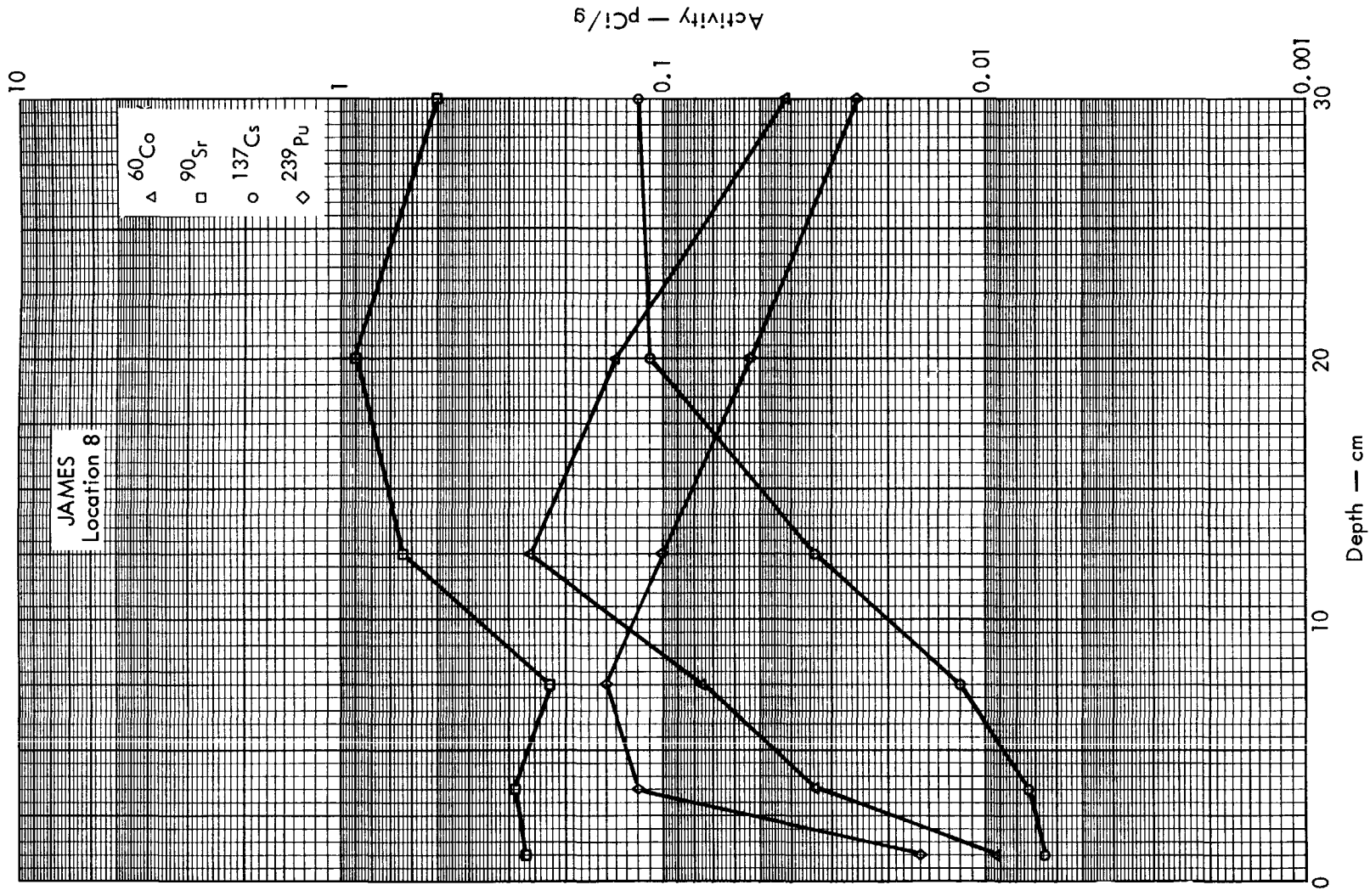


Fig. B. 52. 2c. Activities of selected radionuclides as a function of soil depth.

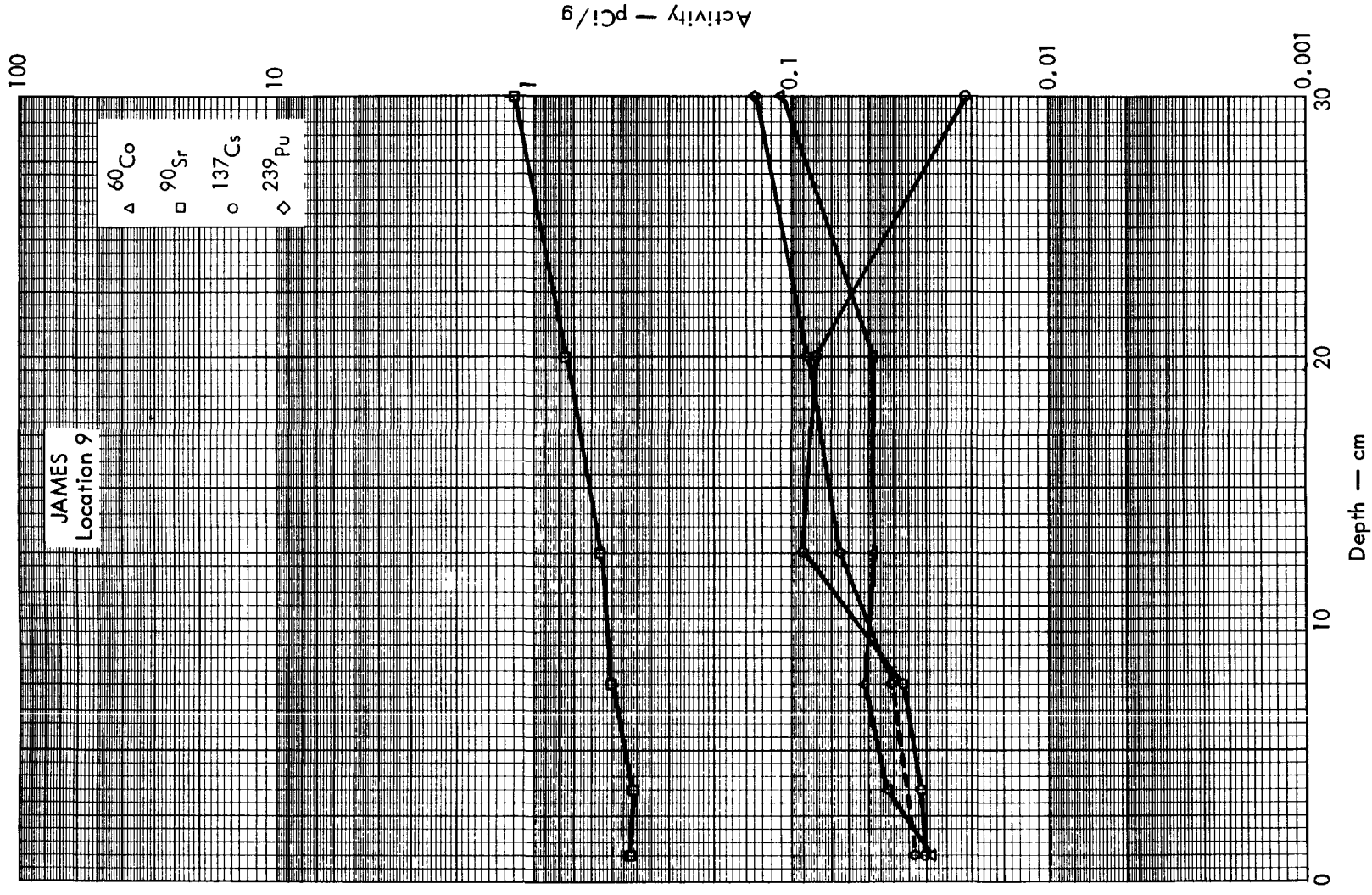


Fig. B. 52.2d. Activities of selected radionuclides as a function of soil depth.



Fig. B.53.1.a.



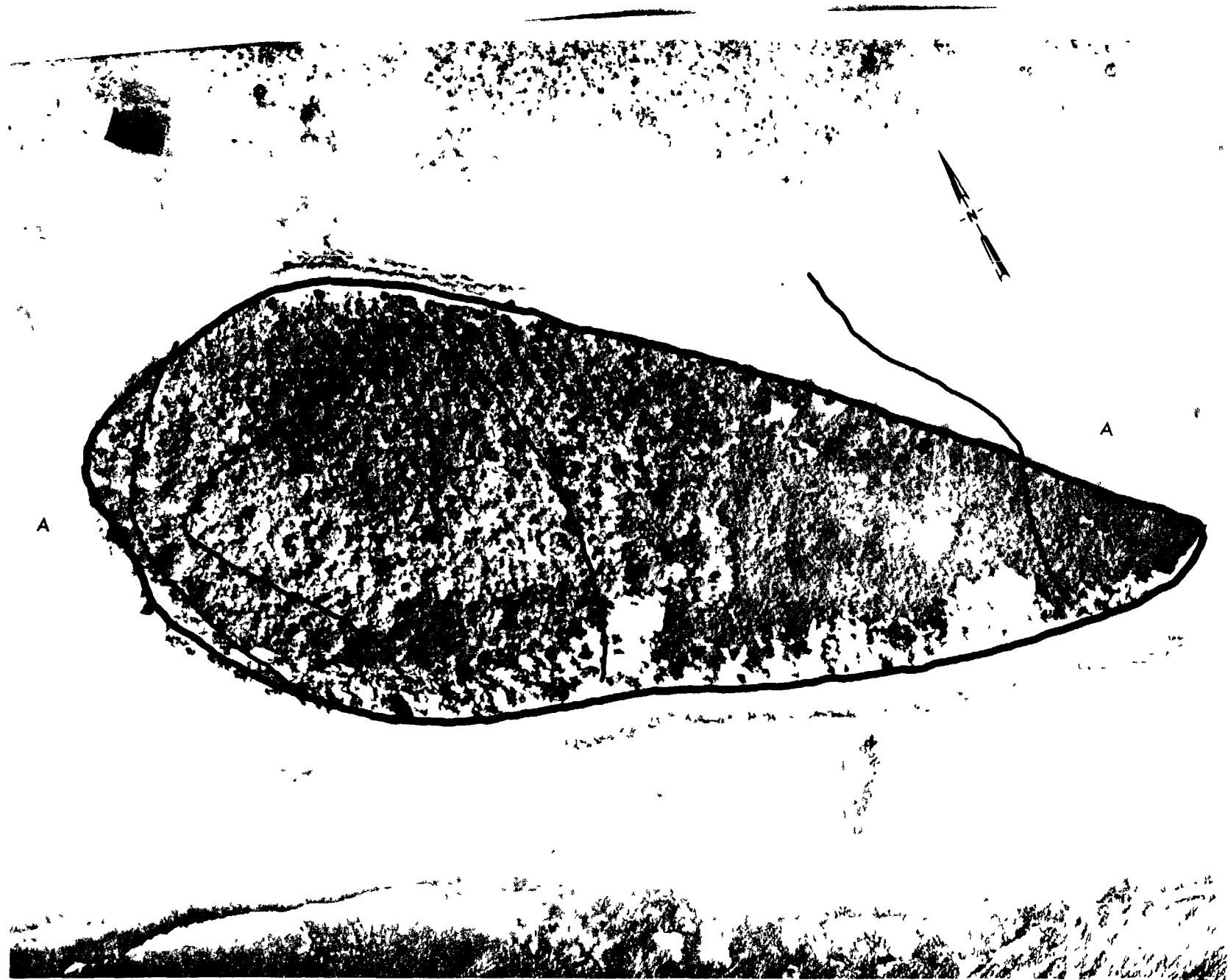


Fig. B.53.1.b. Gross count isoexposure contours. (Refer to alphabetic symbol key in this appendix.)

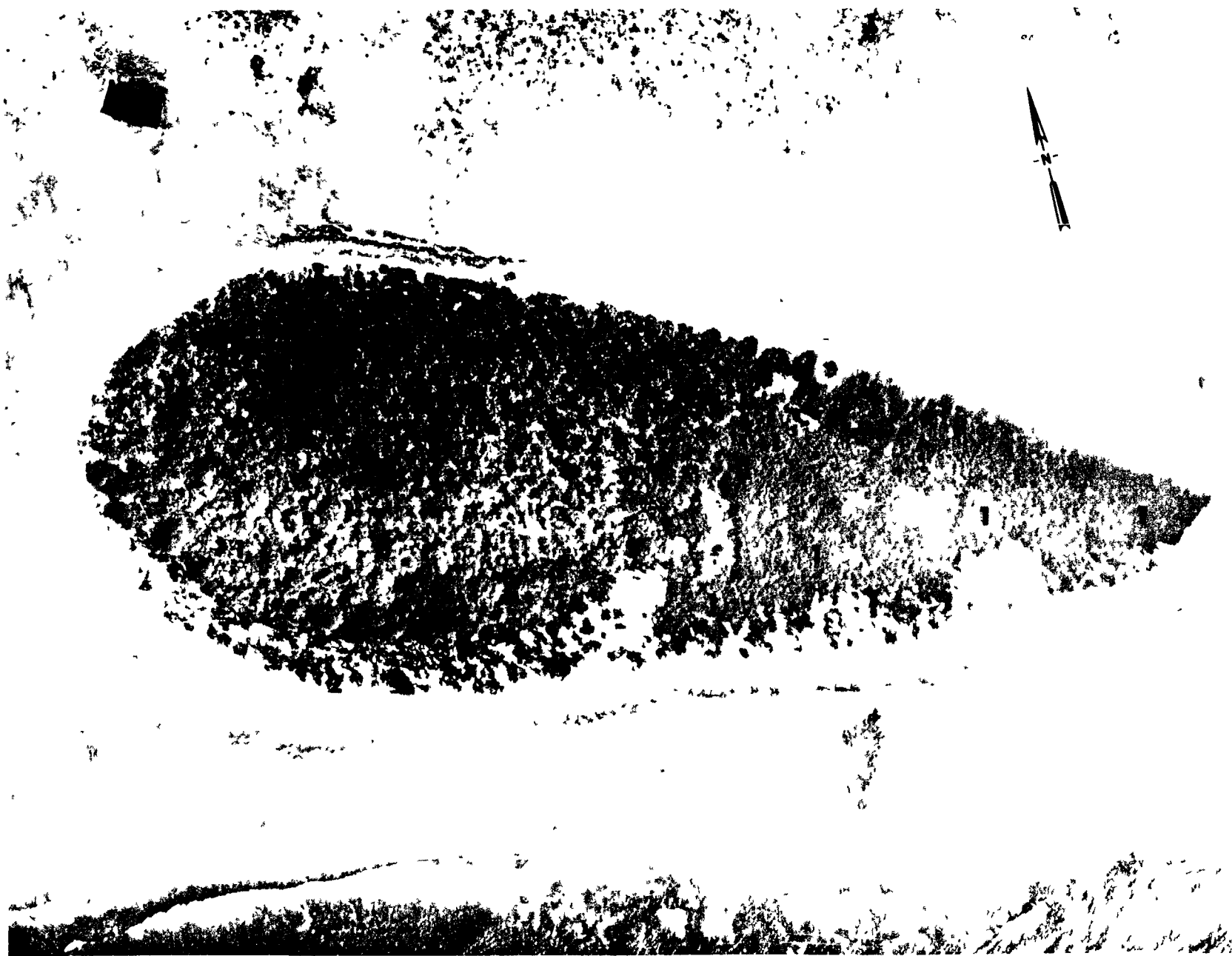


Fig. B.53.1.d. The gamma background exposure rate ( $\mu\text{R/hr}$ ) at 1 m above the ground, measured with a portable NaI scintillation counter.

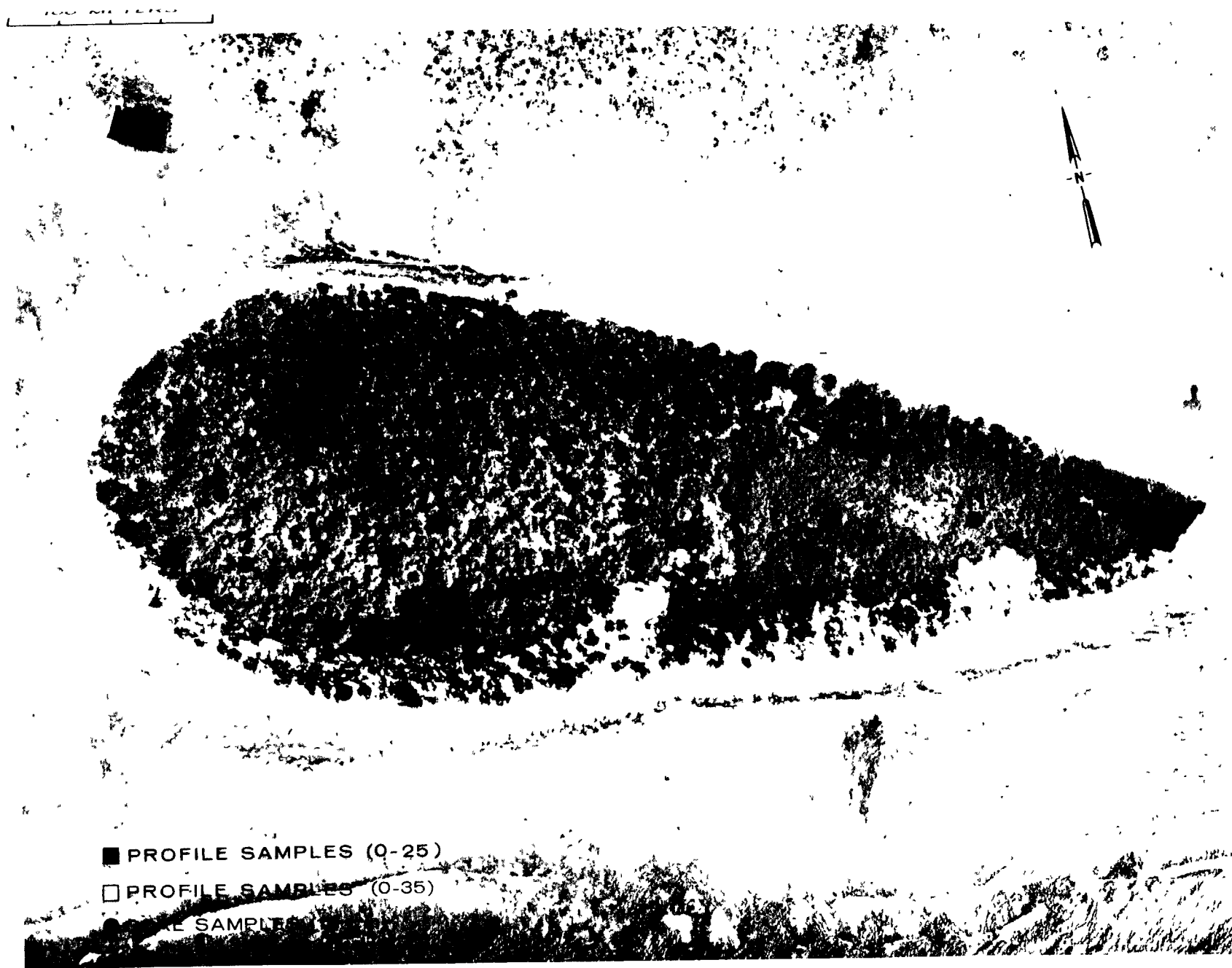


Fig. B.53.1.f. Soil-sample locations.

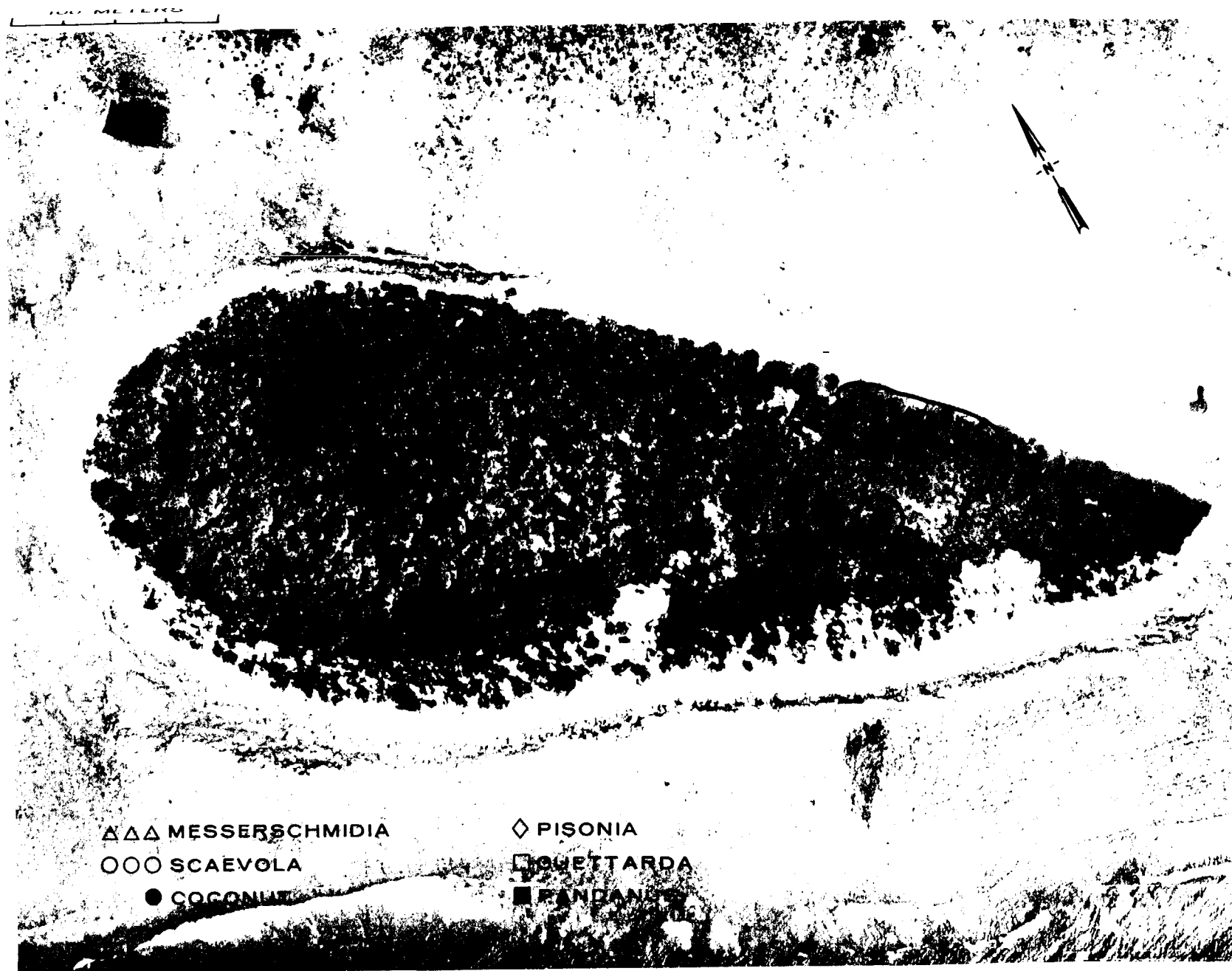


Fig. B.53.1.g. Vegetation sample locations.



Fig. B.53.1.i. The average  $^{239}\text{Pu}$  activities (pCi/gm) in soil samples collected to a depth of 15 cm.



Fig. B.53.1.J. The average  $^{90}\text{Sr}$  activities (pCi/gm) in soil samples collected to a depth of 15 cm.

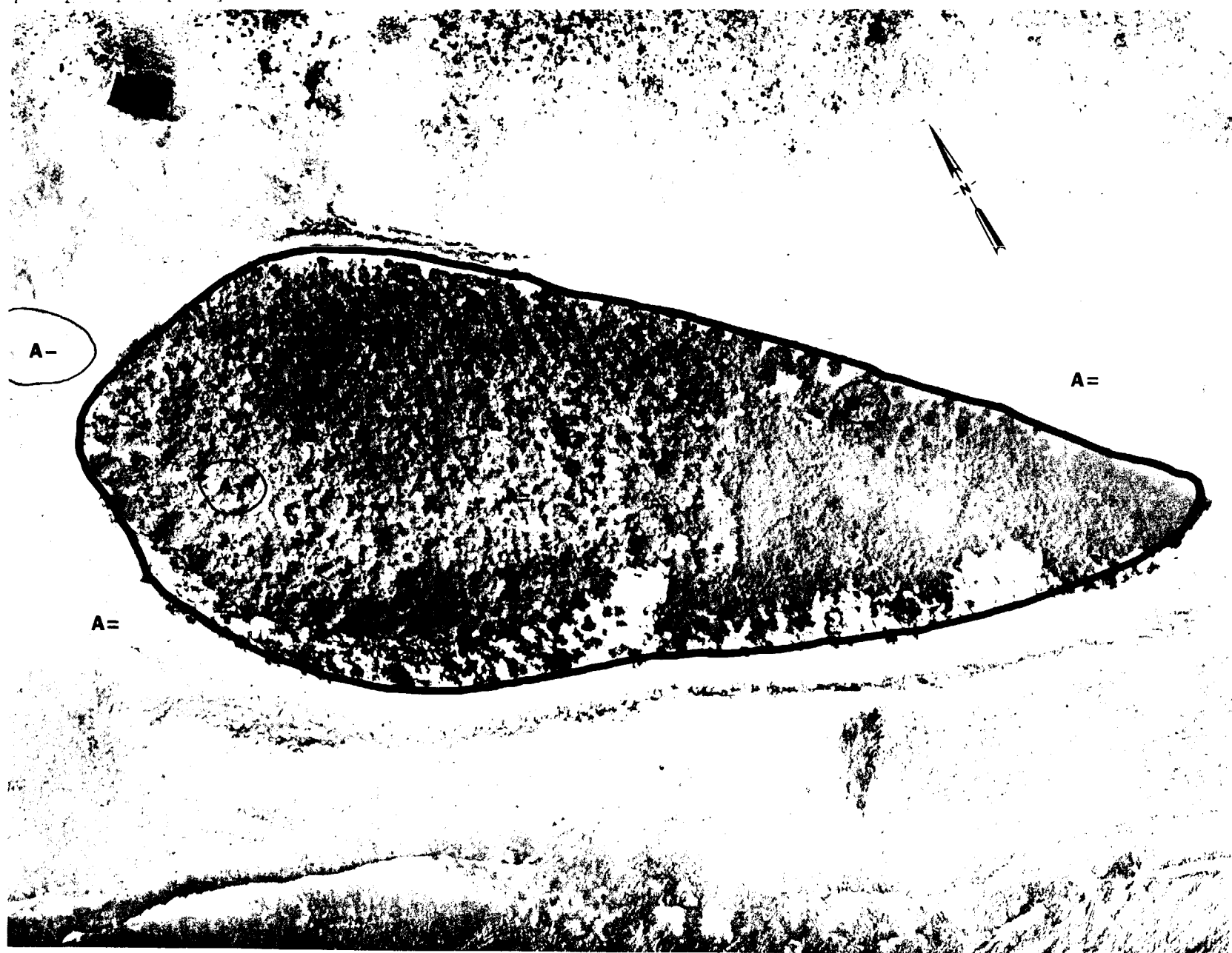


Fig. B.53.1.k.  $^{137}\text{Cs}$  isoexposure and isoconcentration contours. (Refer to alphabetic symbol key in this appendix.)

100 METERS



Fig. B.53.1.1. The average  $^{137}\text{Cs}$  activities (pCi/gm) in soil samples collected to a depth of 15 cm.





Fig. B.53.1.m.  $^{60}\text{Co}$  isosexposure and isoconcentration contours. (Refer to alphabetic symbol key in this appendix.)

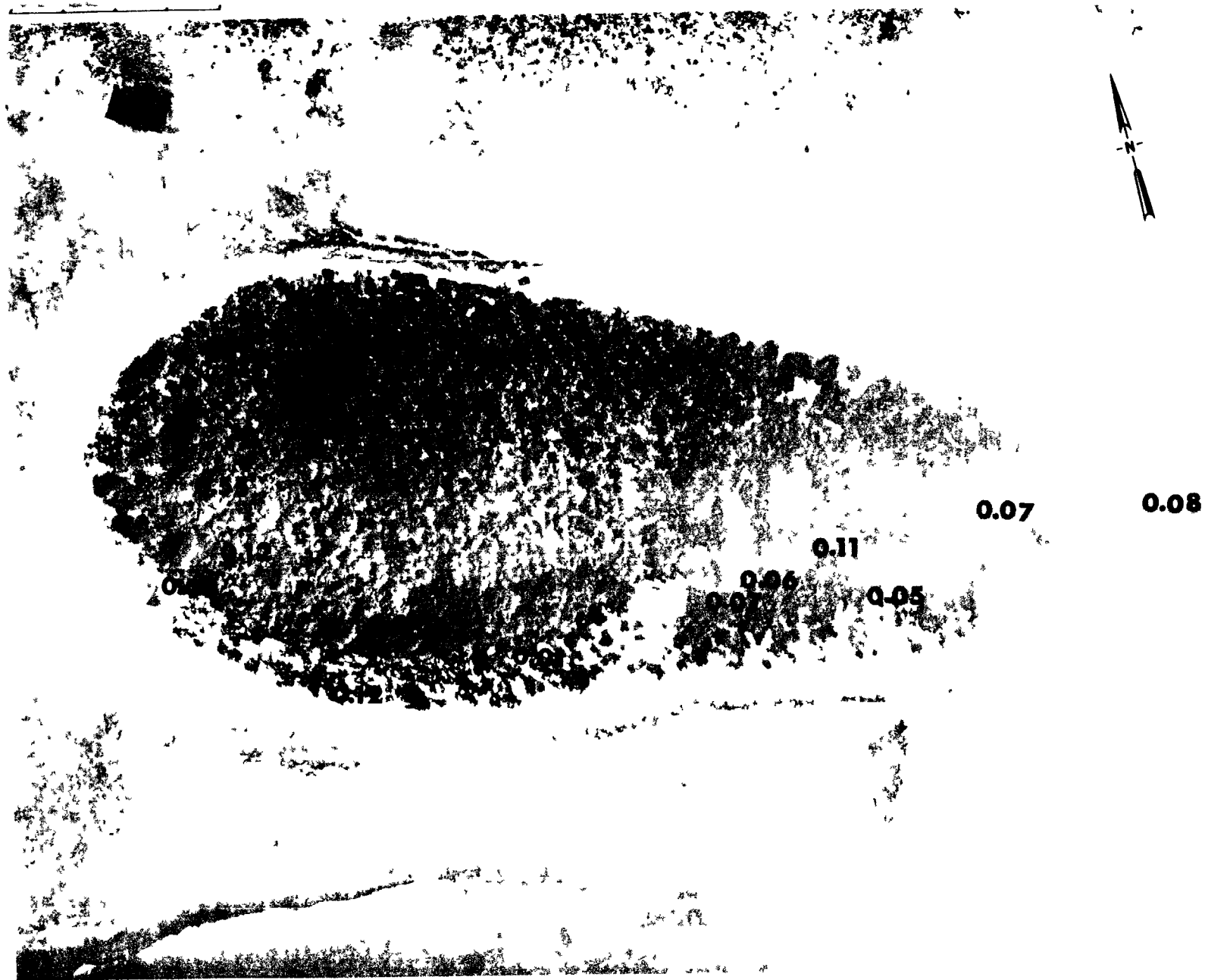


Fig. B.53.1.n. The average  $^{60}\text{Co}$  activities (pCi/gm) in soil samples collected to a depth of 15 cm.



Fig. B.53.1.o. Terrestrial animal sample locations.

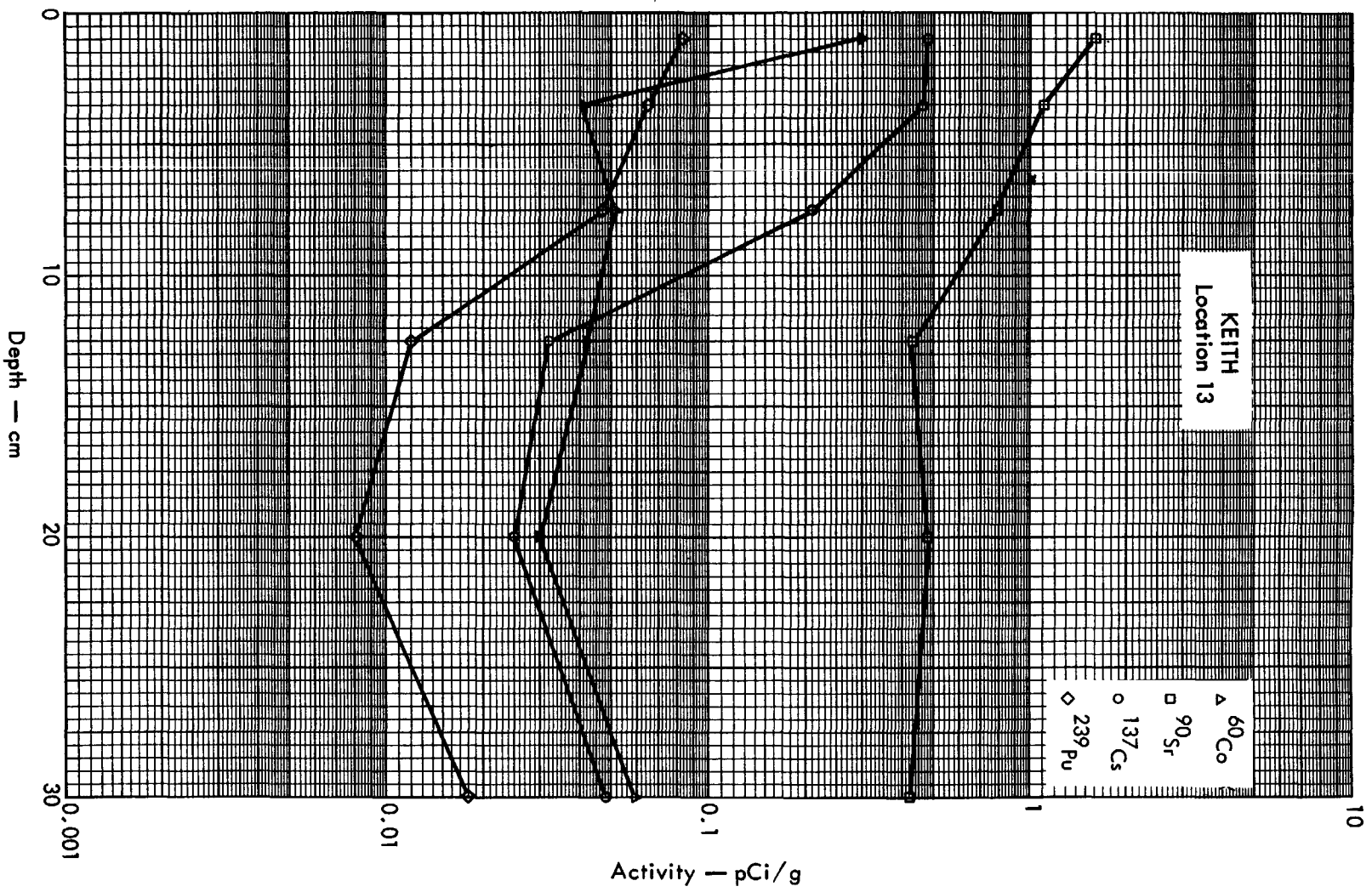


Fig. B. 53. 2a. Activities of selected radionuclides as a function of soil depth.

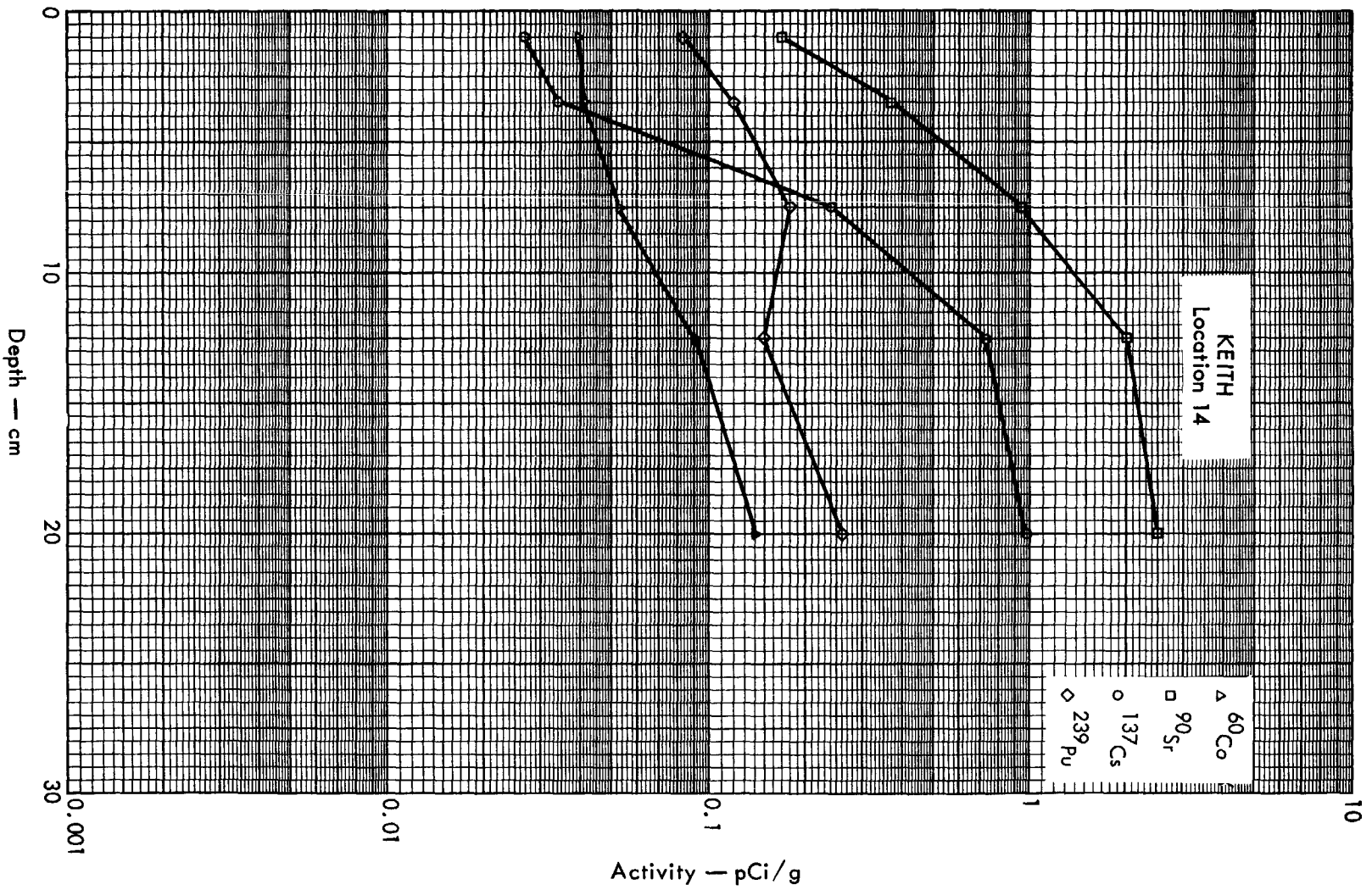


Fig. B. 53. 2b. Activities of selected radionuclides as a function of soil depth.

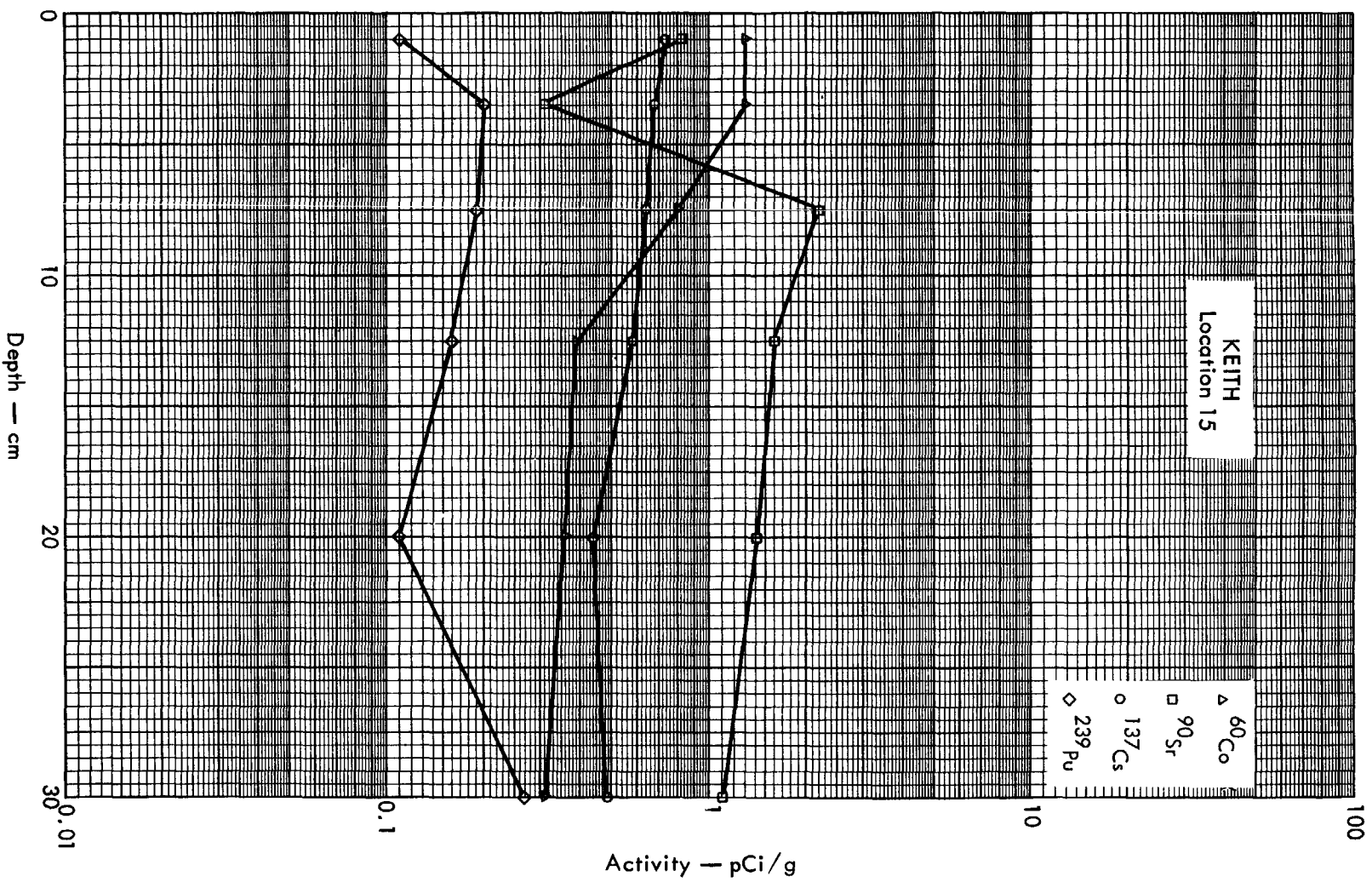


Fig. B. 53. 2c. Activities of selected radionuclides as a function of soil depth.



Fig. B. 54. 1. a.

100 METERS



Fig. B.54.1.b. Gross count isoexposure contours. (Refer to alphabetic symbol key in this appendix.)



100 METERS

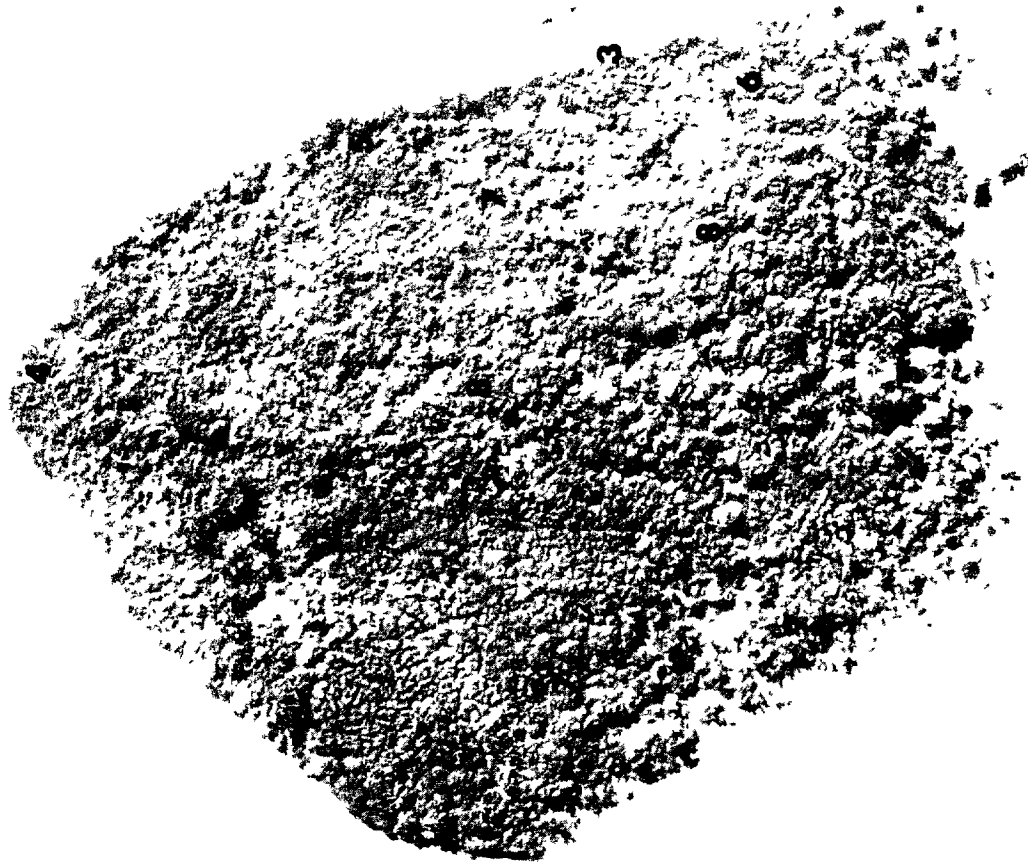
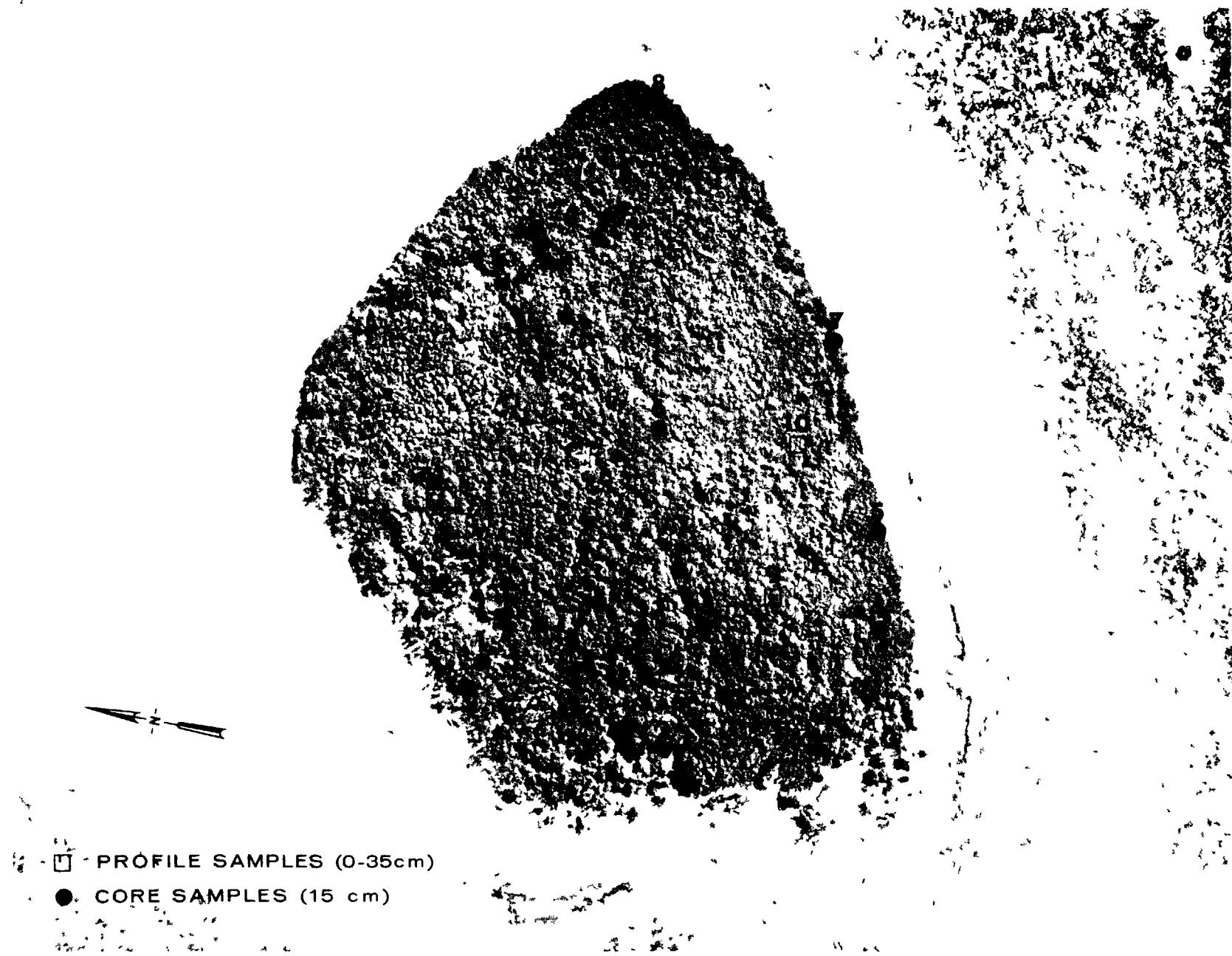


Fig. B.54.1.d. The gamma background exposure rate ( $\mu\text{R/hr}$ ) at 1 m above the ground, measured with a portable NaI scintillation counter.



□ - PROFILE SAMPLES (0-35cm)  
● CORE SAMPLES (15 cm)

Fig. B.54.1.f. Soil-sample locations.

100 METERS

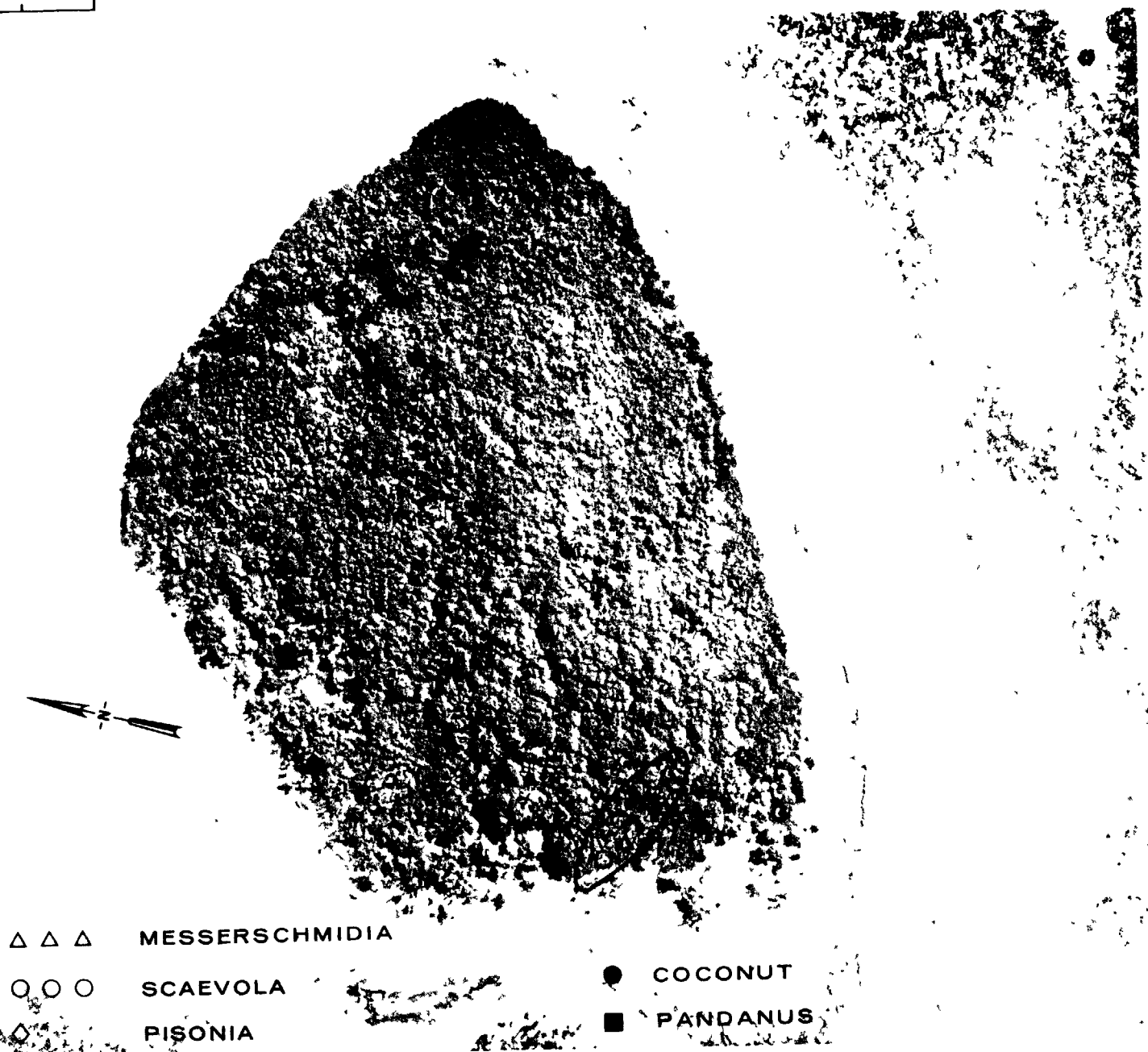


Fig. B.54.1.g. Vegetation sample locations.

100 METERS



Fig. B.54.1.i. The average  $^{239}\text{Pu}$  activities (pCi/gm) in soil samples collected to a depth of 15 cm.

100 METERS



Fig. B.54.1.j. The average  $^{90}\text{Sr}$  activities (pCi/gm) in soil samples collected to a depth of 15 cm.

100 METERS



Fig. B.54.1.k.  $^{137}\text{Cs}$  isoexposure and isoconcentration contours. (Refer to alphabetic symbol key in this appendix.)

100 METERS

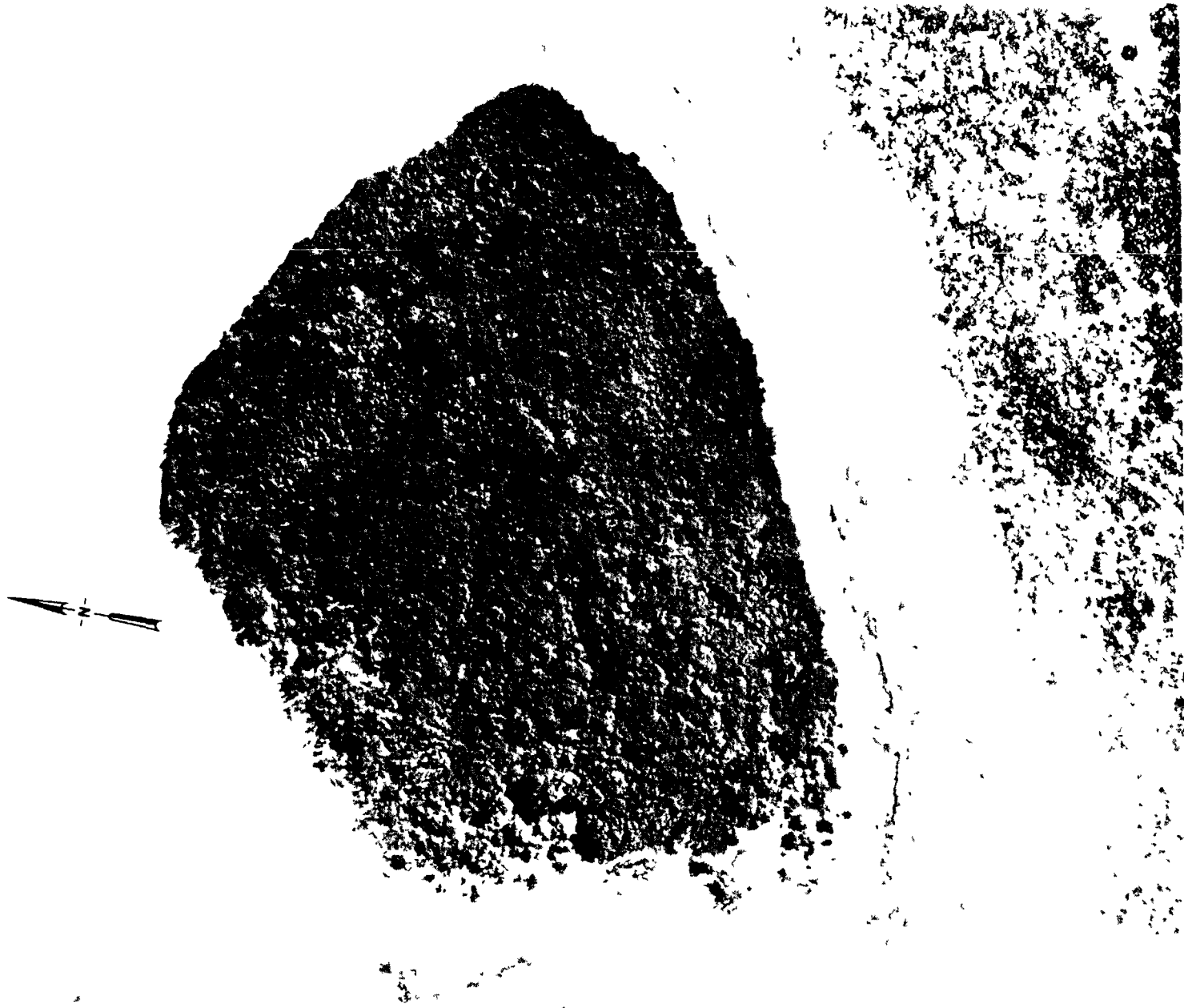


Fig. B.54.1.1. The average  $^{137}\text{Cs}$  activities (pCi/gm) in soil samples collected to a depth of 15 cm.

100 METERS

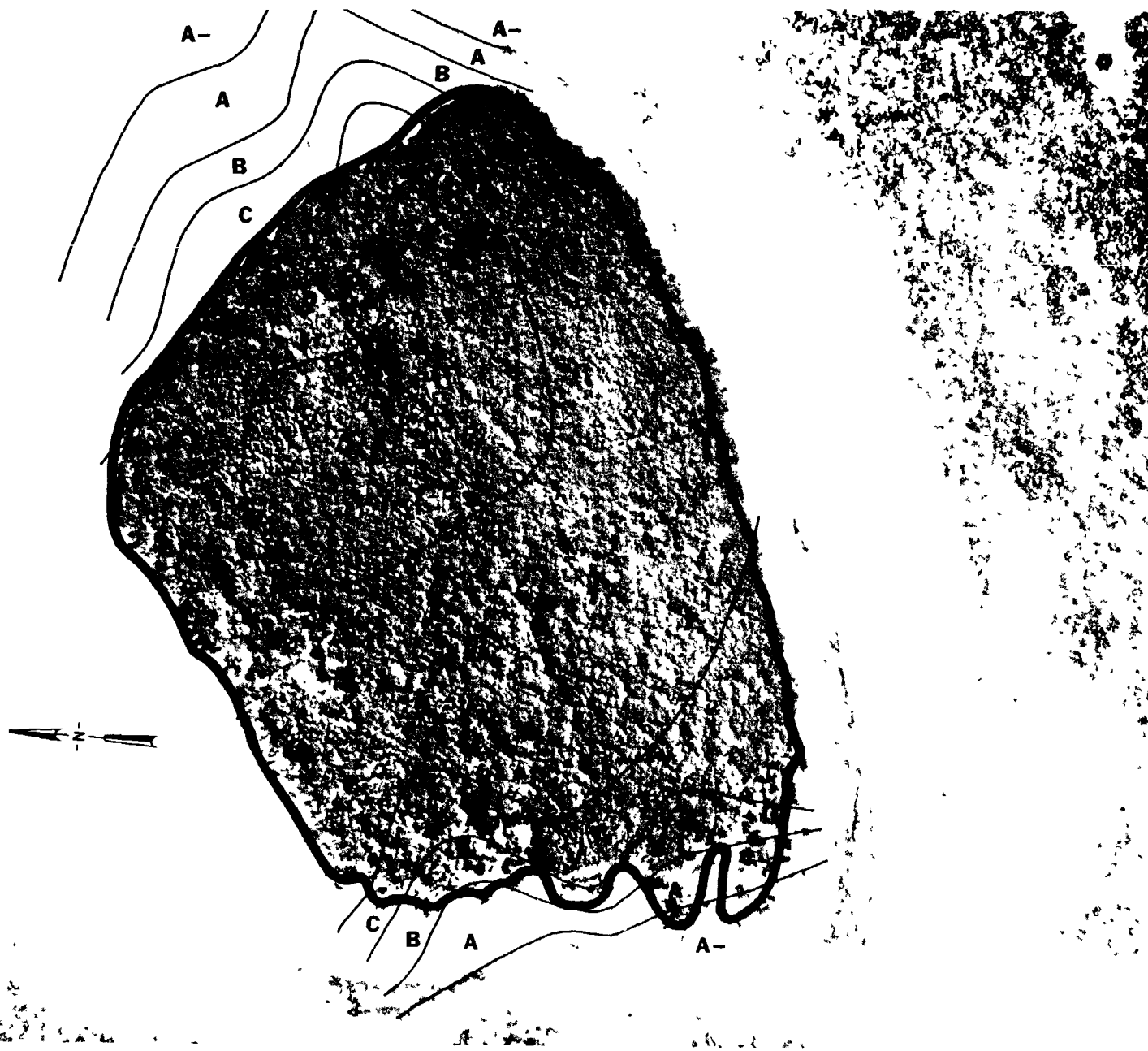


Fig. B.54.1.m.  $^{60}\text{Co}$  isoexposure and isoconcentration contours. (Refer to alphabetic symbol key in this appendix.)



100 METERS

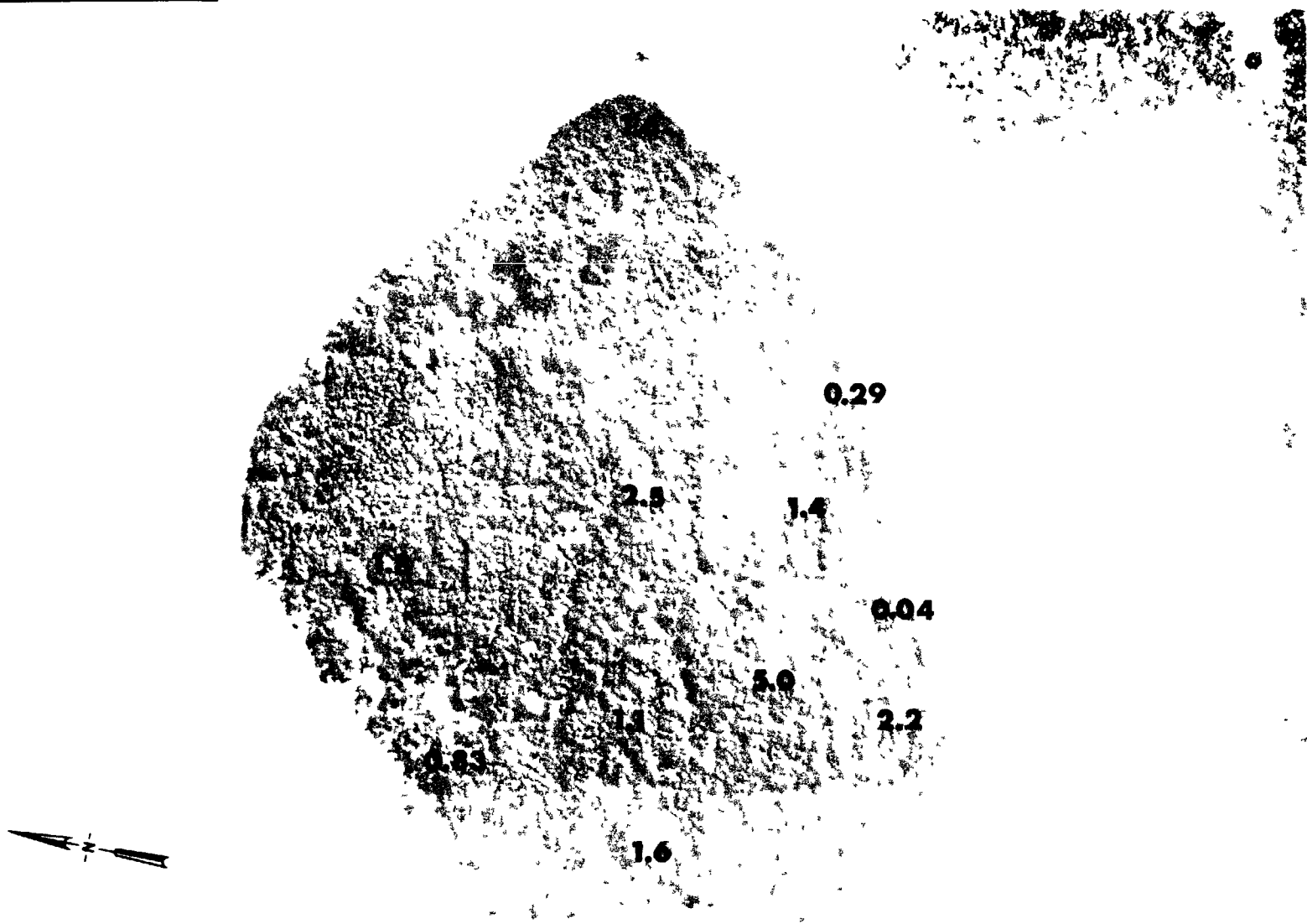


Fig. B.54.1.n. The average  $^{60}\text{Co}$  activities (pCi/gm) in soil samples collected to a depth of 15 cm.

100 METERS



Fig. B.54.1.o. Terrestrial animal sample locations.

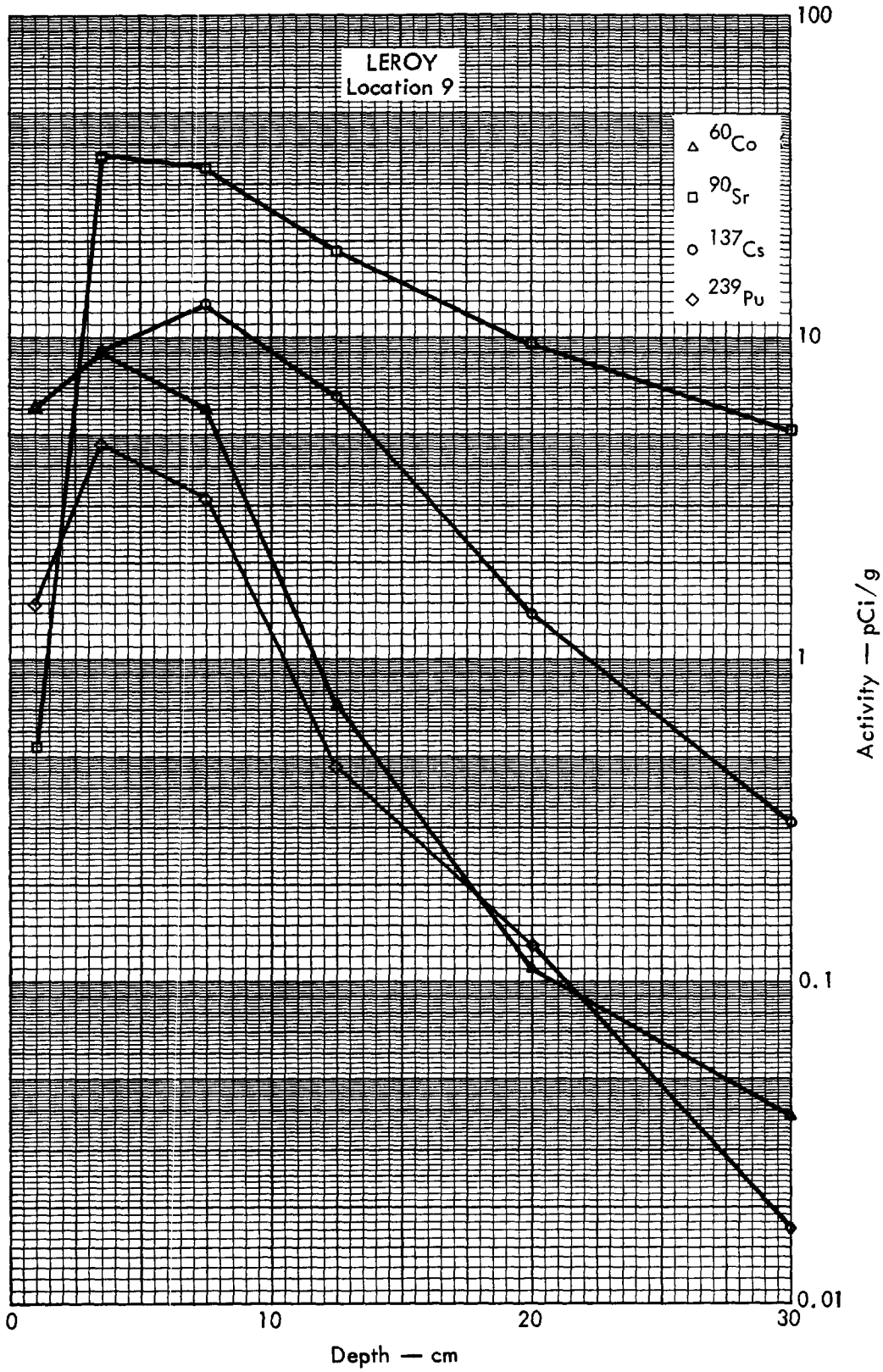


Fig. B. 54. 2a. Activities of selected radionuclides as a function of soil depth.

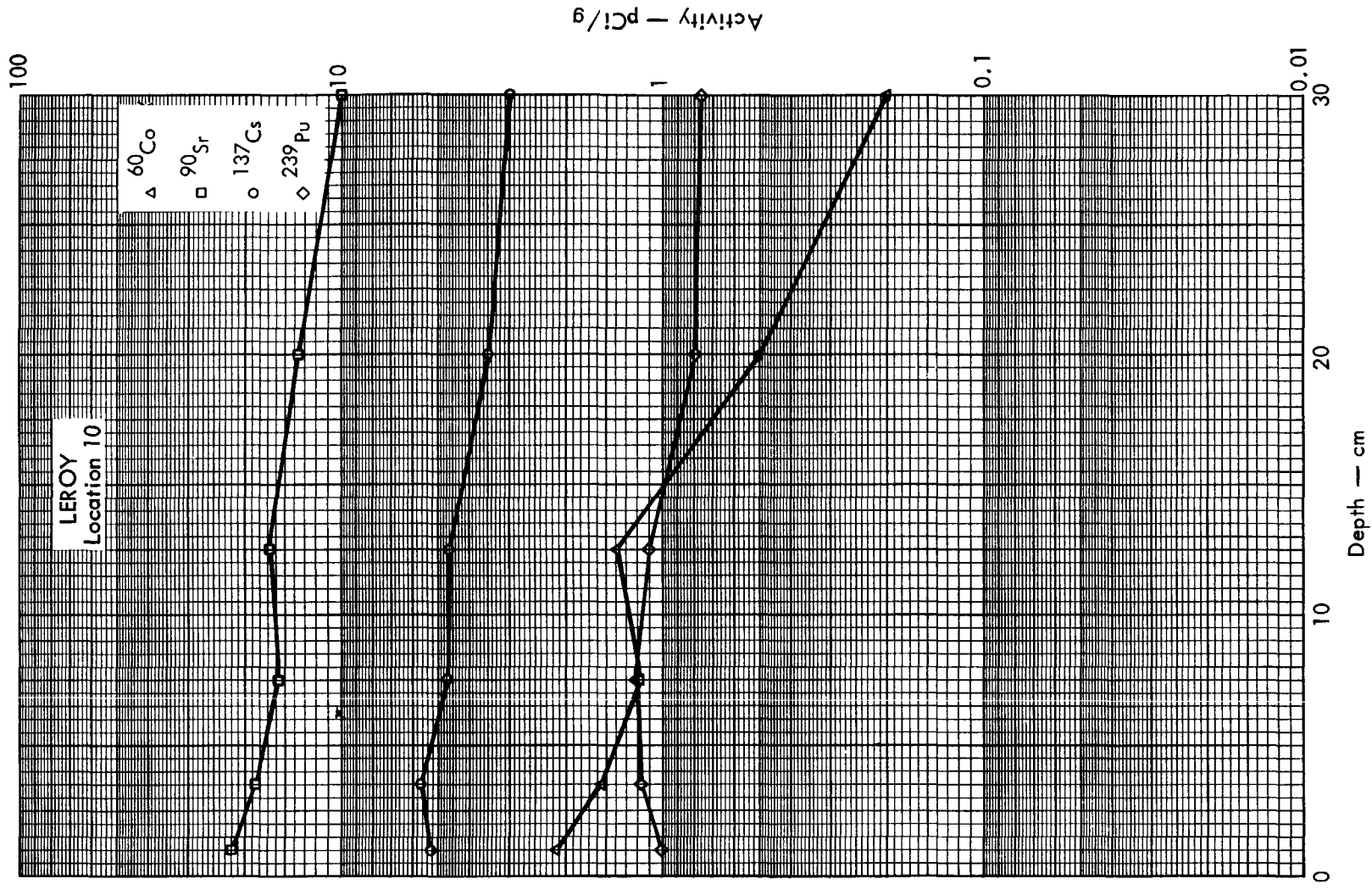


Fig. B. 54. 2b. Activities of selected radionuclides as a function of soil depth.

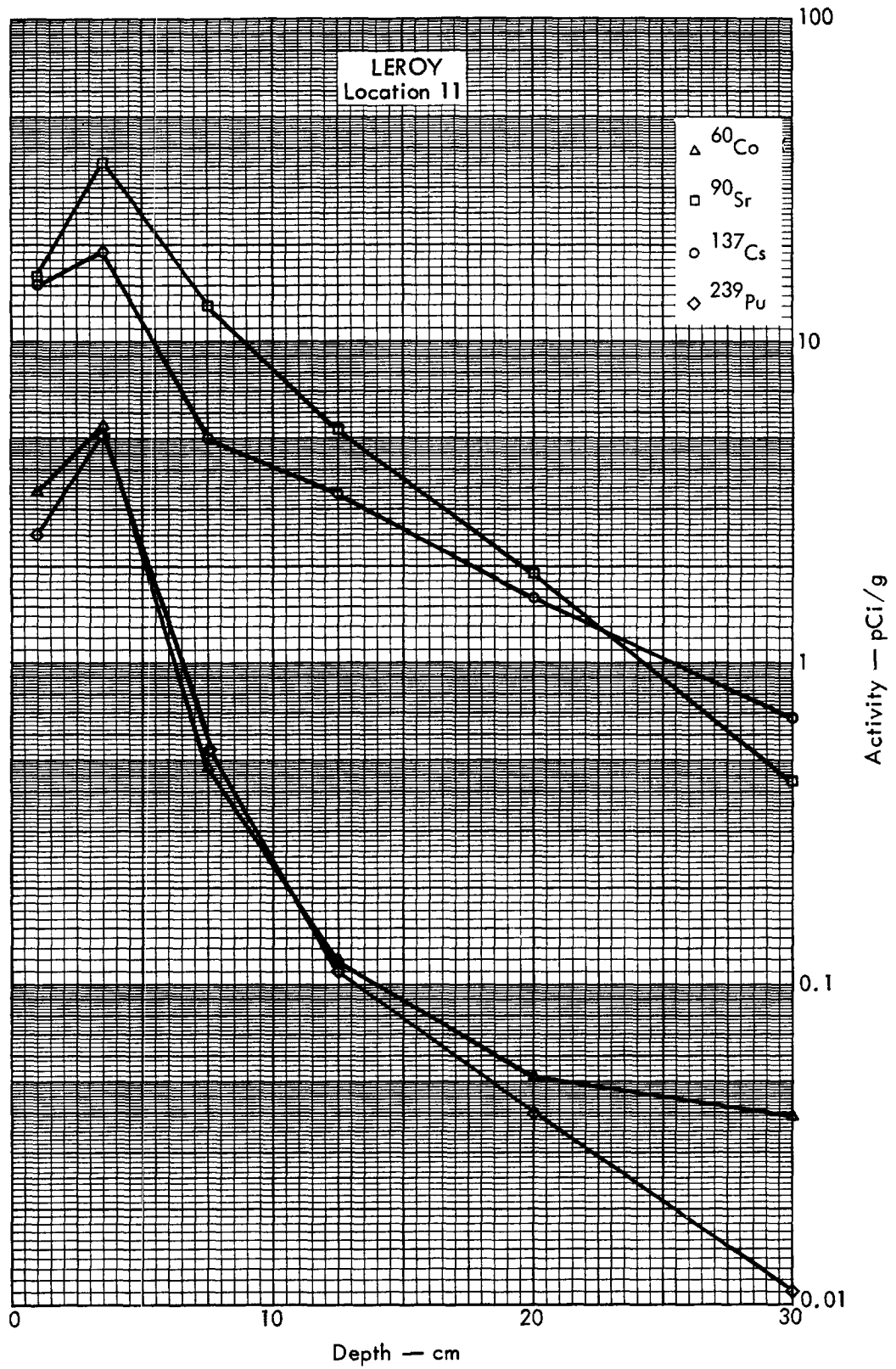


Fig. B. 54. 2c. Activities of selected radionuclides as a function of soil depth.

### C. SUMMARY OF EXPERIMENTAL DATA

Measurements of radionuclides in each sample resulted in activity concentration values which were entered on IBM cards, one nuclide per card and sample, along with sample identification, spectrum and detector designation, time of measurement, and replicate number. The data on a given card were designated as being in one of three categories, "first wild guess," preliminary, or final. As the measurements were made, data cards were prepared and submitted to a CDC-7600 computer program which ordered the data and printed a summary.

During the analytical measurement phase of this survey, the data summary was updated on a regular weekly basis; copies of the summary were provided to the scientists for evaluation of the data. At the end of each week, all new data cards were sorted and merged into the master data file in a CDC-7600. Use of an IBM photostore device for massive data storage enabled us to avoid the handling problems usually encountered in continuous updating and storage of data on magnetic tape. All replicate information was presented in the weekly data reports. Only the highest category of data was listed for any given nuclide. For example, if "final" data were available, no "first wild guess" or "preliminary" data were listed; if "preliminary" data were available, no "first wild guess" were listed.

For inclusion in this final report, the data bank was processed so as to provide one best set of concentration values for nuclides measured in each sample. These data are listed on microfiche in

Table C.3. Replicate measurements were reduced to a weighted mean by conventional averaging techniques. Where more than one upper limit was set for any nuclide, the lowest limit is listed.

All samples were assigned an identification number which identifies the sample uniquely and includes digits designating the type of sample and the location where the sample was collected. Format for this identification number and for designating sample type and location is listed in Table C.1.

In Table C.3 the data are ordered initially according to sample type as listed in Table C.2 (sample type is designated by the first two digits of the sample identification number). Within a given sample category, e.g. soils, the data are listed according to island designator, beginning with Alice and proceeding clockwise around the atoll (the island designation is given by the last two digits of the sample identification number). This island sequence is given in the last part of Table C.1.

Soil data from a single island are ordered in the following way:

1. Biota soil samples—these samples were taken from locations which relate directly to certain vegetation samples.
2. Soil survey samples—these samples are numbered sequentially for each island. Sample locations are shown on maps (Section B, "f" series), keyed according to the sequential location number. Both surface samples and profile sets are included.
3. TLD soil samples—samples taken for gamma spectrum measurements which are of use in understanding results of TLD measurements.

Soil survey samples (item 2) were taken from every island; biota and TLD soil samples were taken only from selected islands.

Many of the samples taken in the marine studies are designated according to the island which was nearest to the sample location. Such is the case for plankton, sediment, seawater, coral, and fish samples. Of course, more precise records of locations where samples were collected were made and used in evaluating these samples. Designation of island location for the vegetation, terrestrial animal, and air filter samples is unambiguous.

For each sample, the following information is given:

<u>Sample number</u>	Identification number whose format is discussed in Table C.1.
<u>Logbook number</u>	Assigned by field collection team; this number is usually used in referring to the location where the sample was collected. Not all samples were assigned logbook numbers.
<u>Location</u>	Island name
<u>Sample type</u>	Soil, sediments, vertebrates or invertebrates (aquatic), vegetation, animals (land), etc.
<u>Description</u>	Examples: goatfish, eviscerated whole; tridacna, viscera and kidney; common noddy, eggshell. Soil samples do not have any further descriptive information listed here.

Participating laboratories

Three-letter designators showing which laboratories made wet-chemistry determinations, principally for  $^{90}\text{Sr}$  and  $^{239,240}\text{Pu}$ . Other nuclides determined in this manner were  $^3\text{H}$ ,  $^{14}\text{C}$ ,  $^{55}\text{Fe}$ ,  $^{63}\text{Ni}$ ,  $^{113\text{m}}\text{Cd}$ ,  $^{147}\text{Pm}$ ,  $^{151}\text{Sm}$ , and  $^{238}\text{Pu}$ . This designation is for wet chemistry determinations only; all gamma assays were made at LLL. Gamma emitters determined routinely were  $^{60}\text{Co}$ ,  $^{106}\text{Ru}$ ,  $^{102\text{m}}\text{Rh}$ ,  $^{125}\text{Sb}$ ,  $^{137}\text{Cs}$ ,  $^{133}\text{Ba}$ ,  $^{152}\text{Eu}$ ,  $^{155}\text{Eu}$ ,  $^{207}\text{Bi}$ ,  $^{235}\text{U}$ , and  $^{241}\text{Am}$ .

The remaining information given for each sample is a table listing radioactive concentration of various nuclides determined in that sample.

The designation PU 3940 refers to total alpha activity from  $^{239}\text{Pu}$  plus  $^{240}\text{Pu}$ ; these nuclides are reported together because their most abundant alpha group energies are almost identical. Radioactive concentrations are reported in picocuries per gram of dry sample. Samples were dried in various ways; the reader is referred to Chapters III-E, -F, -G, and -I for details of sample preparation. All of the activity concentrations in Appendix II are reported as of an arbitrary single time, January 1, 1972. Thus, measured values were corrected for decay between January 1, 1972 and time of measurement; for some of the shorter-lived nuclides, these corrections may be appreciable. When making use of the

data in Table C.3, activity levels must be corrected for decay to appropriate times. For example, one may wish to know  $^{55}\text{Fe}$  levels in various fish samples at time of collection; in making dose estimates to future population on Enewetak, one calculates activity levels at some starting time and takes into account decay over the

period of the dose estimate. Percentage uncertainties are listed for each determination. When certain nuclides were not detected in a sample, upper limits were calculated. These limits are indicated by a "less-than" sign, <, preceding the value and by a NDET (not detected) in the error column.

Table C.1. Survey ID number scheme.

General form: AB-XXXX-CD

where AB are two digits which indicate sample type,  
 XXXX are four digits which were assigned sequentially and which identify the sample uniquely, and  
 CD are two digits which indicate location of sample collection.

Specific example: 09-0577-20

where 09 indicates a marine sample, vertebrate (in fact, the sample is bone from a snapper fish),  
 0577 identifies this sample, and  
 20 indicates collection in proximity of TILDA.

Sample-type identifier, first two digits:

01 General soil classification, used where depth information is not known or for biota soil samples.

Soil samples, classified according to depth:

29	0-10 cm	44	75-85 cm	74	40-50 cm
30	0-2 cm	45	85-95 cm	75	50-60 cm
31	0-5 cm	46	95-105 cm	76	60-70 cm
32	0-15 cm	47	105-115 cm	77	70-80 cm
33	2-5 cm	48	115-125 cm	78	80-90 cm
34	5-10 cm	49	125-135 cm	79	90-100 cm
35	10-15 cm	50	135-145 cm	80	100-110 cm
36	15-20 cm	51	145-155 cm	81	110-120 cm
37	15-25 cm	52	155-165 cm	82	120-130 cm
38	20-25 cm	53	165-175 cm	83	130-140 cm
39	25-35 cm	54	175-185 cm	84	140-150 cm
40	35-45 cm	70	0-10 cm	85	150-160 cm
41	45-55 cm	71	10-20 cm	86	160-170 cm
42	55-65 cm	72	20-30 cm	87	170-180 cm
43	65-75 cm	73	30-40 cm	88	180-190 cm



Table C.1 (continued)

---

02	Algae
03	(Designation not in use)
04	Plankton
05	Samples from lagoon floor, sediments, cores, dredge samples, etc.
06	Seawater
07	Coral (pieces broken from living coral heads)
08	Marine, invertebrate
09	Marine, vertebrate
10	Vegetation
11	Animal, terrestrial
12	Potable water
13	Air, high-volume sampler
14	Air, low-volume sampler
15	Air, Anderson cascade impactor

## Location identifier, last two digits:

01	ALICE	19	SALLY	38	GLENN
02	BELLE	20	TILDA	39	HENRY
03	CLARA	21	URSULA	40	IRWIN
04	DAISY	22	VERA	41	JAMES
05	EDNA	23	WILMA	42	KEITH
06	FLORA (Mike Crater)	24	YVONNE	43	LEROY
		25	(note in use)	44	MACK
07	GENE	26	SAM	45	OSCAR
08	HENRY	27	TOM	46	LLL Whaler
09	IRENE	28	URIAH	47	LCU, Navy vessel
10	JANET	29	VAN	48-51	(not in use)
11	KATE	30	ALVIN	52	<u>Palumbo</u> , AEC research vessel
12	LUCY	31	BRUCE		
13	PERCY	32	CLYDE	53	Wide passage
14	MARY	33	DAVID	54	Deep passage
15	NANCY	34	REX	60	Kwajalein
16	OLIVE	35	ELMER	61	Meck-Kwajalein
17	PEARL	36	WALT	62	Enewetak-Kwajalein
18	RUBY	37	FRED	70	Midway

---

Table C.2. Order in which sample data are listed in Table C.3.

Designator	Sample type	Microfiche film number
01, 29-88	Soils	1 ALICE-JANET
		2 JANET-VERA
		3 VERA-URIAH
		4 URIAH-Ujilang
02	Algae	5
03	(Designation not in use)	—
04	Plankton	5
05	Samples from lagoon floor	5
06	Seawater	5
07	Coral (solid pieces)	5
08	Marine, invertebrate	5
09	Marine, vertebrate	5,6
10	Vegetation	6
11	Animal, terrestrial	6
12	Potable water	6
13	Air, high-volume sampler	6
14	Air, low-volume sampler	6
15	Air, Anderson cascade impactor	6